EUR 4842 e

COMMISSION OF THE EUROPEAN COMMUNITIES

Joint Research Centre

ISPRA ESTABLISHMENT _ ITALY

ANNUAL REPORT 1971

LEGAL NOTICE

This report is on sale at the addresses listed on cover page 4

at the price of B.Fr. 500.—

Commission of the
European Communities
D.G. XIII - C.I.D.
29, rue Aldringen
L u x e m b o u r g

October 1972

EUR 4842 e

COMMISSION OF THE EUROPEAN COMMUNITIES

JOINT RESEARCH CENTRE

ISPRA ESTABLISHMENT-ITALY

ANNUAL REPORT 1971

ABSTRACT

This report is a comprehensive review of the work carried out during 1971 in the Ispra establishment of the Joint Research Centre. The first part is devoted to a description of the activity carried-out in the frame of the so-called "objectives" of the 1971 research programme. In the second part are described, from the viewpoint of the Scientific Divisions of the Centre, some the most relevant scientific and technical achievements. In the third part the operation of the big installations is reported. The fourth part treats both the technical and administrative support activities. A bibliography of reports, contributions to conferences, seminars and meetings etc. is given at the end.

1971 Ispra — J.R.C. — Annual Report
Edited by the scientific directorate
scientific supervisor: G. *Casini*
Composition and graphics supervisors:
G. Bonnet, D. Nicolay
Ispra, August 1972

Grateful acknowledgements are made to the many people who have contributed to the preparation of this report, in particular, the typing team of the Ispra publications office, the draughtsmen and the photographers of the Ispra design service.

Foreword

P. Caprioglio

The present report contains a general description of the work performed at the Ispra Establishment of the Joint Research Centre of the Community during the year 1971.

As will be shown, this has been a transition year of great importance in the scientific and technical evolution of the Establishment, in so far as during this period, not withstanding the general political crisis of our Community, new objectives and new fields of work have been identified and pursued.

The development of an original type of nuclear power reactor, which has been for many years the focus of interest for a large portion of the Establishment's work, is now forgotten. Emphasis is being now put on public service work, such as reactor safety or fissile materials safeguards, and a diversification process has been initiated towards new fields of research, such as environment protection or reference materials.

On the administrative and organizational side as well, the year 1971 has been very important, since this has been the first year of a new conception in the management of the Joint Research Centre. A much larger autonomy has been granted to the local management, a new and more modern budgeting system has been essayed, new forms of link-up with the research activities in the Member countries have been introduced through the establishment of specialized Committees for the management of various programmes and through the work of a General Consultative Committee as far as the preparation of future programmes is concerned.

The technical and administrative burden has borne heavily on the staff at all levels, but the challenge was met with devotion and enthusiasm in spite of a concurrent dwindling of the number of employees, which created additional difficulties.

General Director

Table of contents

Introduction

S. Finzi

This 1971 Annual Report represents an attempt to make the situation with regard to the research activities currently being carried out at Ispra more easily understood by the outside world. At this moment there would seem to be a particular need for comprehensive information in some concise form, because the 1971 programme, as fixed for the Centre by the Council of Ministers of the Community, does not appear to be focussed upon subjects of interrelated interest. Quite the contrary, it is spread over number of relatively dissimilar items. This is due to its having been conceived, as were the programmes of the two preceding years also, to fill a transition phase which extended from a period in which the majority of our work was concentrated upon one single reactor project, and the next multiannual plan, which is expressed to concentrate upon work of a basic and public-service character, and to be expanded to include non-nuclear activities.

As this report goes to press, the problems relevant to the J.R.C. in general, and to the Ispra Establishment in particular, have not yet been solved: up to the end of 1971 the Council of Ministers still had not established a satisfactory definition of the general scope of the Centre on consequent plans for possible activities within the framework of a multiannual programme. The programme proposed for 1972 is therefore still within this transition phase.

The general policy of the 1971 programme for the Ispra Establishment was drawn up by the Council of Ministers in January 1971. The main actions of the programme – called objectives – are listed in Table 1, together with their allocated budgets and manpower. The number of people given for each objective covers the scientific and technical staff directly involved in research, as well as the people engaged in the technical support (electronics, chemistry, work-shop, etc), general services operation, and administrative work.

Table 1 – JRC-Ispra Budget Programme 1971.

Objectif	Budget UC	Man power (men year)	Partecipant Countries
Fast Breeders	830.000	55	B/G/I/L/H
Heavy Water Reactors	4.950.000	296	G/F/I/L/H
Essor	5.850.000	262	G/F/I/L/H
High Temperature Gas Reactors	456.000	25	B/G/I/L/H
Reactor Safety	1.200.000	73	B/G/I/L/H
Fissile Material Control	700.000	42	B/G/I/L/H
Reactor Physics	680.000	42	B/G/I/L/H
Physics of condensed Matter *	2.400.000	169	B/G/I/L/H
Nuclear Material Research	1.505.000	93	B/G/I/L/H
Direct Conversion of Energy	710.000	42	B/G/I/L/H
CETIS - Informatics	4.100.000	161	B/G/I/L/H
Training and Education	580.000	6	Common
Overnumber **	2.560.000	184	Common
Total	26.521.000	1.450	

* including SORA design studies.

** the total number of people engaged in Ispra exceded the total number of people allocated by the approuved research programme of 184 men-year. The corresponding man power has been oriented partly to support researches in the different objectifs, partly to new actions for the future.

Table 2 summarises the total number of scientific and technical people involved directly in each of the objectives of the 1971 programme. Approximately 300 scientific graduates were directly involved in research work during 1971.

Table 2 also summarises the specific sums allocated in the budget for laboratory work. The remainder, if this figure is subtracted from the total indicated in Table 1, covers salaries and the general cost of operating the Establishment. From Table 2 we can see that the total specific research budget in 1971 was of about 6.650.000 UC, including the cost of operation of the large installations of the Establishment.

Table 2 – JRC-Ispra Research Budget Programme 1971.

Objectif	Budget* UC	Man power (men year)
Fast Breeders	144.500	32
Essor	1.417.400	154
Heavy Water Reactors	829.500	105
High Temperature Gas Reactors	63.000	32
Reactor Safety	169.700	45
Control of Fissil Materials	124.800	23
Reactor Physics	134.500	44
Physics of Condensed Matter**	1.215.700	111
CETIS-Informatics	2.017.500	67
Direct Conversion of Energy	139.200	21
Nuclear Materials	227.400	74
Technical Support		
– Chemistry	101.400	34
– Hot Laboratories	20.000	6
– Electronics	40.000	23
Total	6.644.600	771

* excluding personnel charges

** including SORA design studies

Within the framework of the programme given, the Scientific Directorate devoted its efforts both to strengthening ties as far as possible with European organisations involved in reactor projects, in order to discover the real requirements for basic support in this sector; and also to giving priority to activities which might become important in the future should the J.R.C. assume the role of the public-service establishment. Thirdly, preparatory work was begun on the development of research in new areas, namely in pollution, and in the fields of standardisation of methods and substance purities.

The work has taken the following main directions:

- As far as the heavy water programme is concerned we concentrated, whever possible, on research activities which might be of equal interest for light water reactor development. This appeared to be feasible mainly in the field of materials (zircaloy studies) and thermohydraulics;
- In the field of fast breeders and high temperature gas reactors, a number of cooperation agreements were established with European laboratories and industries to select likely areas for development. Preparatory work was started for HTGR's on a possible extension of activity at Ispra to include the field of non-electrical applications. In particular, exploratory research on direct hydrogen production, already begun in 1970, was stepped up during the year so that we would be in a position to judge whether or not consistent development of this activity would be of interest for the next multiannual plan.
- A special effort was made to exploit know-how already existing at Ispra in investigations into the safety problems of fast breeders and water reactors, and at the same time we considerably extended basic activities aimed at increasing our understanding of the phenomena occurring in nuclear plants during accidents;

- Studies covered by the "Nuclear Materials" objective have taken on a more basic characters, from the point of view of fuel element behaviour and from that of new materials for reactor components;
- Reactor physics studies not immediately related to reactor projects have been oriented towards the assessment of two information services, where the need for a public support of the development of the reactor industry is recognised. At the same time nuclear strategy studies already begun in 1970 have been pursued with a view to a possible extension of system- analysis work to support the future needs of the EEC-Brussels Services;
- CETIS (Centre Européen de Traitement de l'Information Scientifique) has concentrated its research activity on informatics: i.e. a tool for access to information. This has led, on the one hand, to a considerable amount of methodological work for the creation of basic software for automatic processing of information inatural language, and on the other hand, to an increase in computer networks know-how. Practical results have been achieved in the organisation of program libraries, and the foundation has been laid for future activity in these fields. These activities will be developed further in connection with COST (Cooperation europeenne dans le domaine de la recherche Scientifique et Technique);
- The work on direct energy conversion has been brought forward to its final stage, since no extension of this project at the J.R.C. is foreseen in the coming years. Meanwhile we are trying to decide upon the best way of applying the experience acquired in this area (namely on heat pipes and thermodynamics of surfaces) to other possible future activities;
- In the field of the physics of condensed matter, we have in particular tried to achieve a more efficient integration of the different techniques (neutron diffraction, X-rays and magnetic resonance) used in basic research;
- An effort was also made to give to the work carried out in support of the Commission in Safeguards the form of a real project, in the hope of making a positive contribution to their ultimate goal, which is the systematic control of the circulation of fissile material in various types of plant.
- As far as the SORA facility is concerned, the Council of Ministers decided in January 1971 to allocate 800.000 UC to carry out a detailed study of the reactor and subsequently to obtain offers from industries within the Community. Following the work done by these industries, a great effort was made in the Establishment to prepare specifications and to evaluate the safety requirements of the facility.

The next section of the annual report summarises the principle results of work carried out during 1971 within the framework of the various programme objectives. The third section presents the organisation of the Scientific Divisions anddetails results of a number of sections representative of the year's work which achieved a sufficient degree of maturity.

Although reference to these sections will give a complete picture of the scientific work performed at Ispra during 1971. I should like to select for mention here a few activities which were, in my opinion, of particular interest:

- The development of sophisticated calculation models for the analysis of thermohydraulic phenomena in the fuel assemblies of fast breeders has established the usefulness of these tools for checking the application limits of current design methods.
- Work on the pyrochemical head-end of spent fuel in fast breeders has confirmed the great potential of this approach as applied to the various stages of fuel reprocessing: fuel transport, decanning, disintegration and uranium-plutonium separation.
- The experience accumulated with ECO on measurements in hot conditions, by using water circuits at temperatures of up to 200°C and organic liquid up to 350°C, has proved to be very satisfactory. Reactivity temperature coefficient measurements of a high degree of accuracy can be obtained with a limited amount of fuel (from one to nine heated fuel channels). In view of the very few facilities available in the world for this kind of experiment, it would obviously be advantageous to exploit the ECO facility in this direction in the future.

- Very faithful comparisons have been made between experiment and theory in water reactor depressurization studies. In view of the present concern over the behaviour of the primary circuit during blowdown, we intend to persevere with these studies and even to extend them to include the study of emergency core-cooling systems.
- Work on the UO_2 /Na thermal interactions in the case of fuel melting is approaching the completion of the necessary installation. Although no extensive interactions have as yet been conducted, this effort is nevertheless being given the highest priority.
- A significant contribution has been made to improving the EURATOM Nuclear Safeguards System, both from the point of view of efficiency and of economics. In particular, instruments for the non-destructive measurement of fissile materials have been developed and installed in nuclear plants. At the same time work on solutions to the problems of using tamper-proof seals for the identification of fuel elements has advanced satisfactorily.
- The EURACOS converter system associated with the ISPRA-1 reactor has been confirmed as a powerful tool for carrying out mock-up shielding experiments. Measurements performed for the CIRENE and SNR projects have demonstrated that the methods in use at Ispra can be employed for design purposes. Here again, as in the case of fuel element thermohydraulics, the development of sophisticated methods, in particular those based on Monte-Carlo techniques, has proved to be of primary importance.
- In the field of the structure and properties of solids, a new effect of dynamic spin polarization has been discovered, and quasi-elastic neutron scattering experiments on hydrogen in transition metals have been carried out for the first time on single crystals.
- A new type of fast rotating crystal spectrometer for neutron scattering using the time focussing technique has been constructed. In collaboration with the Institute Max von Laue – Paul Langevin of Grenoble, studies on the dynamic diffraction of neutrons have led to the development of Cu-Ge crystal monochromators with a gradient of the lattice parameter.
- From amongst the different applications of Informatics. I can mention the realization of an Automatic Conversational Information Retrieval System (SIMAS) applied to the management of the computer JRC program library; the completion of an Integrated Library System (ILS) for the automatic management of a library and the implementation of the modular calculational system CARONTE for an automatic execution of a sequence of correlated programs.
- The research on decomposition of water in chemical cycles for hydrogen production has led to interesting results. The cycle Mark 1, the first one patented for this purpose, can now be considered sufficiently known as far as the most important chemical parameters are concerned: other chemical cycles, which have been defined on the basis of thermodynamic calculations, seem attractive. The related reactions are now under investigation.
- In the field of fiber reinforced composite materials, we have performed the characterization of the mechanical behaviour of the unidirectional solidified eutectic Ni-Ni/3 Ta. Tensile properties at room and at elevated temperatures have been correlated to the morphology of the composite.
- In the field of fracture mechanics studies, the measurements of differential density variation carried out on creep specimens of an austenitic stainless steel have demonstrated that the total void volume of the microcracks formed during deformation is the main parameter controlling the fracture mode of this material.

I will not persist any longer with this review of studies or results which I myself consider to be significant, but will invite the reader to judge for himself the selected papers which follow.

And finally I would just like to emphasise the fact that in spite of the difficult situation in which the Ispra research establishment was called upon to operate during tha past year, a number of researchers tried sincerely to make an honest contribution to the increase of scientific and technological knowledge within the Community.

Organisation

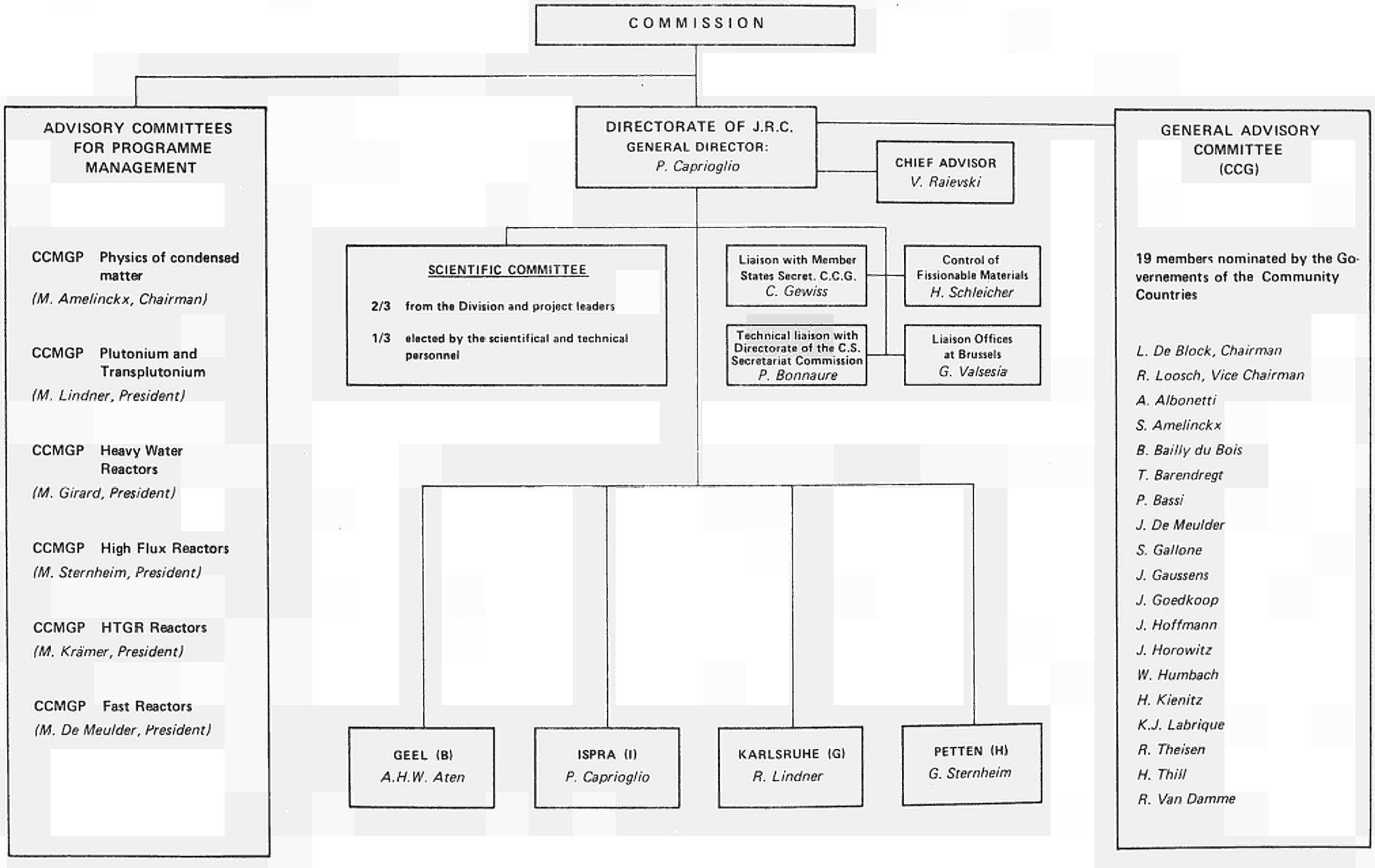

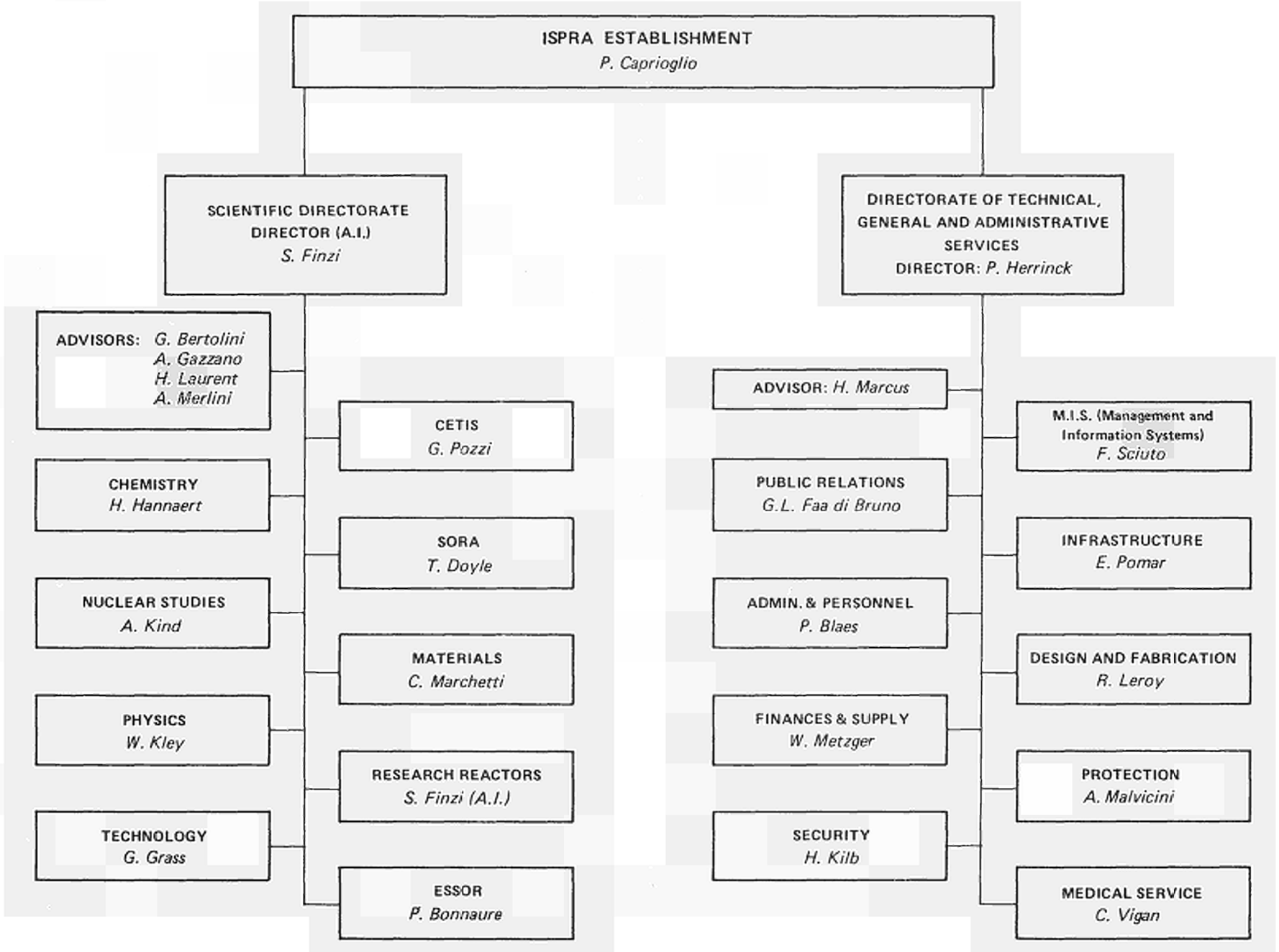
ISPRA ESTABLISHMENT
P. Caprioglio
SCIENTIFIC DIRECTORATE
DIRECTOR (A.I.)
S. Finzi
DIRECTORATE OF TECHNICAL, GENERAL AND ADMINISTRATIVE SERVICES
DIRECTOR: P. Herrinck
ADVISORS: G. Bertolini
A. Gazzano
H. Laurent
A. Merlini
CETIS
G. Pozzi
CHEMISTRY
H. Hannaert
SORA
T. Doyle
NUCLEAR STUDIES
A. Kind
MATERIALS
C. Marchetti
PHYSICS
W. Kley
RESEARCH REACTORS
S. Finzi (A.I.)
TECHNOLOGY
G. Grass
ESSOR
P. Bonnaure
ADVISOR: H. Marcus
M.I.S. (Management and Information Systems)
F. Sciuto
PUBLIC RELATIONS
G.L. Faa di Bruno
INFRASTRUCTURE
E. Pomar
ADMIN. & PERSONNEL
P. Blaes
DESIGN AND FABRICATION
R. Leroy
FINANCES & SUPPLY
W. Metzger
PROTECTION
A. Malvicini
SECURITY
H. Kilb
MEDICAL SERVICE
C. Vigan

SUMMARY OF THE RESULTS

IN THE VARIOUS PROGRAMMES

FAST BREEDERS

HEAVY WATER REACTORS

HIGH TEMPERATURE GAS COOLED REACTORS

REACTOR SAFETY

SAFEGUARDS

REACTOR PHYSICS

PHYSICS OF CONDENSED MATTER

SORA REACTOR PROJECT

DATA PROCESSING

NUCLEAR MATERIALS

COMMUNITY BUREAU OF STANDARD

ECOLOGY

FAST BREEDER PROGRAMME

G. Casini

The resources allocated for this program being limited as compared to the effort made in the area of fast breeders by the centres and industries of the Community, activity was concentrated on a limited number of subjects, with particular attention focused on the basic aspects of the problems investigated in order to provide results of general interest for the various national projects.

The main part of the work lay in the following fields:

- thermohydraulics
- fuel reprocessing
- safety
- physics.

A limited effort was devoted to fuel element technology. The safety aspects of the work are discussed in the context of the Safety programme. For physics, see Reactor Physies Programme.

A layout of the budget (excluded personnel charges) and of the manpower allocated for the different actions of the programme is given in the following table.

Action	Budget (U.C.)	Man power (man year)
– safety	17.000	8
– fuel element technology	8.700	3
– fuel reprocessing	17.500	4
– thermohydraulics	67.200	17
Total	110.400*	32

* plus 34.100 U.C. for big apparatus

Thermohydraulics

Fuel Element Thermohydraulics

A substantial part of the work consisted in a combined theoretical and experimental analysis of two-dimensional velocity and temperature fields in an assembly of smooth rods. Satisfactory calculation methods were developed for the case of a single sub-channel of an infinite rod array. The theoretical work was supported by experiments aimed at determining detailed temperature fields in compact rod arrays. These measurements are now being evaluated. At the same time an extensive theoretical study was done on friction factors and momentum mixing coefficients in fuel rod assemblies (e.g., hexagonal bundles). From these studies the following conclusions can be derived:

- the friction factor depends on rod-rod spacing, rod-wall spacing, and the number of rods in the channel;
- the mixing coefficient depends on both the configuration and the dimensions of the subchannels. This proves in particular that caution must be taken in applying the subchannel mixing coefficient concept for rod bundle calculations.

Three-dimensional studies were started in experiments to investigate the hydrodynamic entrance effect in a compact assembly of smooth rods.

The information obtained from these basic studies was used to improve the HERA code intended for design purposes.

More details on these activities are given in the frame of the Technology Division contributions.

Boiling and Superheating

In the course of the studies investigating the parameters which influence boiling and superheating of liquid metals, the following points were experimentally analysed:

- influence of surface conditions and impurity on the superheat of sodium;
- liquid layer left behind on the wall after ejection of coolant;
- hydrodynamic behaviour of argon bubbles in the liquid metal flow through narrow channels.

At the same time we completed the analysis of experiments, started in 1970, for the determination of the influence of oxygen impurities and operation history on incipient superheating.

Concerning the first point, various boiling surfaces have been used, prepared by acid etching or by mechanical treatment. The test results show that the scattering of the superheating is much smaller for the first case than for the second one. An influence on the mean value of superheating could not be clearly detected. The analysis is continuing.

The second type of experiment was done on a capillary tube, the film thickness being measured by voltage tamps welded on the tube. Two values for the pressure difference between the inlet and outlet vessel were considered. The results showed clearly that the film thickness increases with the velocity of the ejected liquid.

The third investigation, done in collaboration with BELGONUCLEAIRE and the University of Louvain, centered on the following points: bubble rise velocity as a function of the bubble volume under isothermal conditions; blockage conditions for the plug regime (filling-out of the channel hole cross-section by the gas plug). These results were compared with those of simulation measurements with water and air performed at the University of Louvain.

The results of the measurements at Ispra (Na-argon) indicated a channel blockage in tubes up to higher diameters than those performed at Louvain (water-air). Bubble rise velocities in water with air and in Na-K with argon show the same trend. The evaluation of these experiments is still under way.

Concerning the analysis of the influence of oxygen impurities and operating conditions on incipient superheating, details are given in the framework of the Technology Division contributions. The main results can be summarized as follows: although the strong influence of oxygen on the superheat was confirmed, no definitive influence of time or pressure-temperature-history process was observed, either on the mean value or on the scattering range of the individual measuring values.

Vibrations

An analytical model describing the vibrations of a rod under axis-parallel fluid flow in response to the driving-pressure fluctuations was experimentally investigated. The first part of the study, involving tests on a single-rod arrangement, has been completed. The main conclusions of these studies are as follows.

a) The analytical model describes satisfactorily the flow-induced vibrations of the rod, under both ideal and perturbed (pumps, etc.) flow conditions.

b) Comparing the two investigated forms of the analytical model, the simpler one, using the pressure fluctuations at a single point only to describe the driving forces, seems preferable for practical purposes, but does not take into account the inhomogeneities of the pressure field (e.g., entrance effect).

c) The spectral density of the pressure-fluctuation field, which is an input for the vibration calculation, is similar to a broad-band noise with a Root-Mean-Square value of about 1% of the dynamic pressure. This value was found to be nearly the double in non-established flow conditions and dependent as well as the spectral structure on flow disturbances (pumps, valves, etc.).

d) The proportionality factor between pressure difference fluctuations and resulting driving forces seems to depend on the flow velocity. This point together with the effect of flow geometry will be further investigated.

Secondly measurements were done with a three-rod test facility. Early results seem to confirm the expected influence of the flow geometry.

Fuel Reprocessing

This activity has been carried on at the JRC for some years, with the aim of investigating the feasibility of pyrochemical methods for head-end treatment of spent fuels in fast breeders.

During 1971 the studies principally concerned the oxidative breakdown of fuel and the extraction of plutonium through the use of molten salts (nitrates). This activity, carried out in collaboration with BELGONUCLEAIRE and CEN-Mol, centred on the following investigation

- thermal and radiolytic decomposition of alkali nitrates. The experiments were performed with a 2 MeV Van de Graaff accelerator with samples heated to temperatures of up to 500°C;
- formation of uranates, fission-product behaviour and corrosion studies, in order to obtain a better knowledge of the process of attack on uranium, oxyde attack by nitrates and of parameters necessary for passing from laboratory scale to a pilot plant;
- design of a furnace for a technological demonstration of the process; the furnace offers the possibility of making several heterogeneous reactions (gas/liquid, liquid/liquid) with molten salts followed by filtration and recycling of the salts.

A comprehensive description of this activity is given in the frame of the Chemistry Division contributions.

Explosion Welding of Fuel Pins

The explosive welding technique, developped at Ispra, has proved well suited for welding end-plugs of fast breeder fuel pins. In this technique the energy of chemical explosives is used to produce an impact of one work piece on another with sufficient velocity to allow metallurgical bonding. The method is particularly attractive for welding fuel-pin end-plugs owing to its high reproducibility, simplicity of inspection (by ultrasonic testing) and low cost. Furthermore, it permits the welding of materials which cannot be welded by conventional methods, such as dispersed-phase materials.

During the year the construction of a prototype machine which can automatically perform the ultrasonic testing and give a map of the welded area for each pin was almost completed.

At the same time, in extension of the tests already done on stainless steel, the possibility of welding sinterized ferritic steel cans of fuel pins was investigated in cooperation with CEN-Mol.

HEAVY WATER REACTOR PROGRAMME

N. Cadelli

Both polyvalent and specific researches have been included under the same objective, the difference between the two items having progressively lost its meaning.

The tendency of the 1971 activity has been to include, besides the study of peculiar heavy water reactor phenomena (such as reactor core physics), also studies interesting both the heavy and light water reactor fields (such as Zirconium alloy studies and water chemistry).

An effort has been made to concentrate the activity on some major items, dropping what could be considered a dispersing work. For this reason, all work related to organic cooled reactors having been stopped in preceeding years, during 1971 studies related to fuel fabrication, fuel vibration, welding of fuel rods, fretting corrosion, concrete vessel thermal insulation and stress analysis, were also excluded from the program. At the same time activity was accelerated in the field of pressure tubes and their joints to bring this work to a definite conclusion, since there is a tendency to direct water reactor material studies towards the characterization of canning materials.

The main part of the work has been carried out in the following fields:

- Reactor Core Physics
- Studies on Zirconium Alloys
- Thermohydraulics
- Water Chemistry.

A certain effort has also been devoted to problems of more general interest such as noise analysis, liquid rod shut-down systems, instrumentation.

The program and its progress has been discussed extensively during 1971 with delegates of the member states during the meetings of the "Consulting Committee for Heavy Water Reactor Program Management" and within some groups of national experts in specific fields (as for Reactor Physics and Water Chemistry studies).

A layout of the budget (excluded personnel charges) and of the manpower allocated for the different actions of the programme is given in the following table.

Action	Budget (U.C.)	Man power (man year)
– core physics and dynamics	64.400	32
– thermohydraulics	74.000	21
– zirconium alloys	168.900	22
– fouling studies	42.000	11
– complementary studies	85.100	19
Total	434.400*	105

* plus 310.900 for ECO-heavy water and 84.200 for big apparatus

Reactor Physics

The aim of these studies has been research on the different factors which play an important role on the neutronic behaviour of a reactor under operating conditions. Nearly all the activity covered by this item has been spent to prepare and perform experiments in ECO and to analyse and interpret the results. The subjects which have been treated during the year were:

a. Temperature coefficient measurements on MZFR type fuel elements. The work done with the progressive substitution method investigated the influence of such parameters as lattice pitches, moderator temperature, and coolant temperature. Since the experimental results should represent standards for the test of calculation techniques, particular effort has also been made to know their accuracy.
   A comparison of the measurements with theoretical results showed that:
   - All temperature coefficients have negative sign.
   - Their magnitude varies between $3 \cdot 10^{-3}$ and 10^{-3} $m^2/°C$.
   - Theory describes correctly the influence of the considered parameters but provides a systematic overestimation of their effects.
   - The overall error involved in experimental temperature coefficient lies between 10 and 30%.

b. Temperature coefficient measurements on Pu- bearing fuel elements.
   Measurements have been made on three-rod and single-rod fuel elements having U-nat and U-Pu as fuel. Three lattice pitches have been investigated with D_2O and H_2O as coolant at a temperature of 20° to 200°C. The first interpretation of experimental results showed a much smaller absolute value of the buckling temperature coefficients as compared to those obtained with MZFR type fuel elements, but the sign of the coefficient changes with the temperature.

c. Void coefficient measurements on Pu bearing fuel.
   The experiments utilize a loop especially conceived to allow, in a section of the central fuel element under test, the introduction of N_2 bubbles which simulate void fractions between 0% to 50%.

d. Spectral indices measurements in hot Pu-lattices.
   First measurements, under cold conditions, have been made essentially to test the reproducibility of data in view of the more complete experiments foreseen for 1972 to determine the fine structure of thermal spectrum indices.

e. Properties of irradiated fuel elements.
   The aim of the study is the investigation of the reactivity effects of irradiated fuel elements, performed by the oscillation technique. The activity has been devoted to the preparation of the experiment to be performed during 1972.

In addition to this activity mention has to be made of shielding studies. A mock-up has been built of the CIRENE reactor shielding to measure shielding efficiency of different geometries. Total attenuation factor has been measured for a Fe-H_2O laminar structure, possibly penetrated by an iron channel, and perhaps an iron and polystirol channel simulating the discharge tube configuration.

Zirconium Alloys

Studies on zirconium alloys were oriented principally towards the characterisation of classical alloys for claddings. The main activity has been devoted to prepare in-pile creep measurements and to study mechanical properties of Zr-2 and Zr-4.

An in-pile device for creep measurements in the ISPRA-I reactor has been constructed and a dummy has been tested to assess environment conditions. Meanwhile transducers were developed to measure in-pile displacements and creep specimens prepared from pressure tubes were studied so that their original metallurgical condition can be preserved. In parallel, to assist in-pile experiments, a set out-of-pile creep machines has been adapted to permit inert atmosphere operation for high temperature tests.

Fatigue tests on ring samples taken from Zr-4 canning tubes allowed the Wöhler curve for transverse pulsating tension to be traced.

A basic study on Zr-2 has been made to analyse microvoid formation during deformation. It has been possible to plot as a function of the temperature, up to 400°C, the total porosity of specimens ruptured by tension and prehydrurated at different H_2 contents up to 3000 ppm.

Mechanical properties of zirconium alloys for pressure tubes have been studied for

practical application, i.e., the experimental determination of data allowing the control of fractures and the life under operating conditions (sub-critical crack propagation, length of critical defect).

Corrosion studies have been oriented in two directions. Previous work on new zirconium alloys (Zr-Cu-Fe, Zr-Cu-Fe, Zr-Fe-V) has been pursued in order to find a compromise between mechanical properties and corrosion resistance, taking into account such parameters as cold work and anneal conditions. On the other hand an activity has been started to study classical zirconium alloys behaviour (corrosion and mechanical properties) in connection with their fabrication history.

In order to characterize conveniently zirconium alloys from the chemical point of view an optical spectroscopy method has been set up to detect the presence of different impurities at the ppm level. Attempts have also been made to determine Hf content.

LMA activity has been devoted to irradiated fuel examination, including CIRENE and Trino Vercellese fuel, as well as UO_2/SS fuel elements containing burnable poisons.

Thermodynamic Studies

The work included in this item has been developed following two major activities: studies on Boiling Crisis and Emergency cooling experiments.

Boiling Crisis

The influence of different parameters on the generation and development of a boiling crisis has been extensively studied.

Experiments have been completed at high pressure to determine the influence of entrance conditions. They showed a definite effect of the flow history both for thermal and hydraulic behaviour of the coolant.

Increasing entrance enthalpy showed:

- a dislocation of the onset of the crisis in the direction of growing qualities;
- a diminution of the wall temperature step in the region of the crisis.

The influence of the entrance enthalpy on the critical quality could be observed only above a certain threshold.

The effect of the nature of the heating wall (rugosity, as well as physical properties) has also been investigated and its influence on the wall temperature beyond which steam bubbles are reabsorbed.

Emergency Coolings

An experimental apparatus has been utilized to measure heat transfer coefficient and temperature evolution in a steel wall simulating a pressure vessel during flooding. Measurements have been made taking initial temperature (between 150° and 300°C) and water temperature (30° to 90°C) as parameters.

An other experiment was completed to determine the efficiency of radiation cooling in a 37 rod cluster. It could be shown that, under the choosen experimental conditions, pure cooling by heat radiation offers small benefit. Typical measured values were: 0,9 ÷ 1,2 W/cm^2 heat flux under 800°C wall temperature.

Water Chemistry

This action was started in 1970 already, in order to clarify some basic phenomena related to wall-coolant ion exchanges and mass transport in high temperature water loops. Parallel to this activity, methods have been developed to detect element traces in water.

The loop for mass transport studies has been tested and adjusted and is now ready to be operated in connection with the particles counter, which has also been set up meanwhile. The samples collection devices are ready to be tested in the mass transport loop. Some basic experiments have also started to measure the flow potential under laminar and turbulent conditions.

A second loop has been designed to study the corrosion of activated samples in circulating water up to 350° at 200 bar and to measure the concentration of radioactively marked corrosion products transported and deposited in the circuit. The equipment for the loop has been ordered.

In connection with this experiment an activity has been developed to analyse the impurity content of water. Quantitative determination, at ppb level, of dissolved and undissolved impurities has been extended to Ni, Cr, Fe utilizing the X-fluorescence method following a preconcentration by an ions exchange technique. Spectral analysis has also been employed to determine element traces in water and a special device has been set up permitting the detection of Fe, Ni, Cr at levels lower than 1 μg/l, and of Mn at less than 0,1 μg/l. For more details see later.

Complementary Studies

The items mentioned under this action refer to studies representing the conclusion of preceeding activity or whose interest extends beyond the field of water reactors.

Under the first type of activity are included the studies on pressure tube joints, junctions and explosion welding.

Thermal shock experiments on conventional and sandwich type joints showed a satisfactory behaviour of the junctions after more than 40 shocks between 420 and 150°. Creep tests have been made on sandwich joints and indicated that their behaviour could be of some concern. Tests are in progress to clarify the problem of the inner tube.

Destructive tests on explosion welds in pressure tube geometries showed a good shear resistance (higher than 32 kg/mm). The pressure cycling indicated no weakness in the weld after 1000 cycles. Creep behaviour and hydration velocity have also been studied and showed promising results. A study has also been undertaken to coordinate the theory of the welding mechanism with the experimental results.

Studies of general interest include liquid rod shut-down systems, noise analysis and instrumentation.

CECILE project involves the study of the corrosion behaviour (in a boric acid solution) of junctions between inpile and out-of-pile sections of a liquid shut-down system. An experimental loop was constructed and its coupling with ISPRA-I reactor is under way. A second loop for a multirod shut-down system was operating throughout the year following different operation cycles to control the behaviour of its components. More details on this subject are included later.

Measurements have been made in ECO reactor on fuel element vibrations in order to establish a coordination with neutron fuel oscillations. It could be demonstrated that a tight dependence exists between the two phenomena, and the ECO reactor showed itself to be an excellent tool for detecting and investigating malfunctions in nuclear reactors by methods of neutron noise and vibration analysis.

The activity under the item "instrumentation" included fabrication of thermocouples, collectrons and strain gages. Corrosion tests in autoclave have been made on collectrons; irradiations in ESSOR, to test and calibrate different emitters (Co, V, Ag, Cd), have been terminated.

HIGH TEMPERATURE GAS COOLED REACTOR PROGRAMME

G. Angelini

The research subjects have been divided, similarly to the 1970 activity, as follows:

- Physics
- Fuel Elements
- Graphite
- Plant Components
- Materials for Turbines
- HTGR for chemical processes.

Concerning Physics, the work is described in the context of the Reactor Physics Programme Some research on materials for turbines have been done and reported in the frame of the Nuclear Material Programmes.

A layout of the budget (excluded personnel charges) and of the manpower allocated for the different actions of the programme is given in the following table.

Action	Budget (U.C.)	Man power (man year)
– fuel elements	23.300	10
– technology studies	20.800	9
– graphite studies	5.500	4
– HTGR for chemical processes	11.100	7
– turbine materials	2.300	2
Total	63.000	32

Physics Studies

Fuel Cycles

A new version of the RACE computer code for one-dimensional equilibrium fuel cycle calculations was written, including a two-group treatment of the neutron distribution.

Concerning the running-in problem, some preliminary work was done for the study of the best approach to a code for the authomatic search of the running-in procedure.

A special version of the space-dependent dynamics computer code COSTANZA was written. This version treats the two-dimensional two-group neutron distribution in HTR cores with the reactivity feedback calculated by a thermohydraulic routine.

Shielding Activity

In the ESIC (European Shielding Information Centre) context, the MORSE program study was continued; its application to some sample problems enabled several features of the code, and in particular the geometry routines, to be checked. The 100-group DL C-2B library (from ENDF/B) was used with success. A subroutine was written, by which the trajectories of a certain number of particles can be drawn with the Calcomp device.

Fuel Elements

Materials Research

Silicon carbide samples with different microstructres and different density were prepared for the diffusion studies. The samples were heat-treated in a cesium atmosphere and were examined with the ion-microanalyser.

A method was developed for the determination of the I^{127} concentration in SIC with a sensitivity of 10^{-7} of iodine.

Irradiated compacts with a burnup in the range of 50-80% FIFA were annealed and the released fission gas was measured.

The irradiation of two rigs was started, to determine the relation between the fission-product release and the number of defective particles under irradiation.

Out-of-pile heat treatments of different batches of coated particles under a thermal gradient were continued.

Fluidized Beds

Room-temperature model studies were continued concerning:

- gas residence-time distribution measurements in a single-inlet column, diameter 125 mm;
- solid transport measurements in the same 125 mm column, using an activated particle as track tracer;
- exploratory experiments on temperature profile determination inside the bed.

Experimental high-temperature fluidized bed coater components were manufactured to adapt to the existing furnace unit. The principle of a "directly heated bed" is employed and a new gas injector system is incorporated for testing.

Graphite

Stress Analysis

Three digital codes based on the finite-element technique were developed for the stress analysis of irradiated graphite structures.

The stress analysis work for graphite fuel pins during 1971 concentrated on the development of FEM codes, with special reference to input preparation and representation of results.

An application of the interacting type of fuel pin was studied, using the visco-elastic approach.

Characterization and Model Studies

Specimens for standard fracture toughness on irradiated graphite were determined.

Fifty specimens taken from three different graphite bars were irradiated at HFR, Petten at a fluence of $2 \cdot 10^{21}$ (ncm^{-2}) at 1100°C.

Tests on 70 non-irradiated specimens, of the same dimensions as above, are in course.

An investigation of the fracture toughness of 10 various types of graphite with grain size from 0.4 to 6 mm was started.

A four-point bending test, measuring the load deflection curve, was performed on these specimens.

A series of tensile and compression tests were conducted, using a normal nuclear grade Pechiney graphite, in order to define the volume effect, if any.

Since the density of the graphite has a very strong influence on the mechanical resistance, the ultimate strength varies considerably. For this reason all the studies on the geometrical effects were done on samples standardized to the same density on the basis of a linear relation.

The geometrical parameters affecting the strength are the volume, surface and beam depth of the specimen A sensitivity analysis, by multilinear regression, showed that the

three parameters affect the resistance in a rather complex manner. To clarify the influence of these parameters separately, a digital computer program is being developed.

The series of experimental results concerning the influence of various factors on strength has suggested the development of a cumulative stochastic model rather than a simple weakest-link model. According to the cumulative model the failure of the "structure" needs a certain minimum number of connected injuries. A set of connected injuries is a stochastic process controlled by a transition probability. A complete development of this cumulative damage model taking all the relevant functional relationship into consideration would be a matter for further theoretical and experimental investigation. The experimental investigations have started in two directions: study of the effect of surface conditions on the strength, and evaluation of the damage with the help of various techniques: strain measurement in bending and stress-wave-emission.

Plant Components

Thermal Insulation

The second part of a programme of rapid depressurization tests on DARCHEM insulation coils has been terminated. Depressurization rates up to 20 atm/sec were reached with Δp in the bobbins up to 2 kg/cm^2.

Thermal tests with a special view to local temperature effects were started on the special insulation which has been developed at the JRC.

Sealings

The activity can be divided into two parts:

- Further characterization of the four-lip seal.

  A material was chosen with an elastic limit (0.2%) of 120 kg/mm^2. This was Armco 17-4-PH, usable up to 500°C, and seals of diameters 72 and 89 mm were constructed.

  A small high-temperature valve was designed and two prototypes are under construction. The sealing of the valve is based on the four-lip-seal system.

- Construction of large diameter seals.

  The design of an installation for the production of large-diameter seals was achieved. Electron bombardment welds were carried out on specimens of AISI 304, 310 and Inconel 600 of different thicknesses.

Materials for Turbines

The work done up to now consists mainly in determining the mechanical properties of the composite material Ni-Ni_3-Ta previously elaborated. Tensile fracture tests at different temperatures have been performed on specimens obtained from rods of Ni-Ta-Alloy previously submitted to unidirectional solidification in order to obtain fibrous structures.

The results are interesting since stress values of 84, 67, 49 kg/mm^2 at 800°C, 900°C, 1000°C respectively have been reached. All specimens have been previously subjected to a 1000 hours heat treatment at the temperature corresponding to the tensile test.

HTGR for Chemical Processes

HTGR for Iron Production

A reference study has been accomplished, concerning the use of a HTGR with prismatic fuel elements coupled with a steam reforming plant.

Other chemical processes to be coupled with an HTGR have been considered and a draft of possible chemical cycles has been made.

Diffusion studies are under way, dealing with the penetration of He and Pb into graphite, as basic research for a He/Pb-heat exchanger which is provided in one of the alternative proposals in the HTGR project.

For the measurement of the diffusion of He through a graphite tubing a test sample of the tubing closed at both ends by brazed graphite plugs is to be prepared.

The activity during recent months has been concentrated on developing brazing methods and investigating various brazing materials for brazing graphite to graphite and graphite to refractory metals.

Hydrogen Production from Water

Search for new chemical cycles.

Studies are in progress on the conditions which must be satisfied by the compounds which might be used in a water decomposition cycle in three or four stages, as well as experimental tests on some chemical reactions.

Chemical studies for the Mark 1 cycle.

The studies now in progress are principally related to the following: hydrolysis reaction of calcium bromide; reaction of mercury with hydrobromic acid; tests of solubility of mercury bromide in hydrobromide acid solutions under pressure at different temperatures; boiling points of $CaBr_2$ solutions in water as a function of concentration and pressure.

REACTOR SAFETY PROGRAMME

J. Randles

Research during 1971 in support of reactor safety was carried out in eleven problem areas: depressurization, UO_2/Na thermal interaction, dynamic properties, design basis accident containment, fracture mechanics, reactor dynamics, criticality, reliability, early failure detection, ultrasonic probing, noise analysis.

A layout of the budget (excluded personnel charges) and of the manpower allocated for the different actions of the programme is given in the following table.

Action	Budget (U.C.)	Man power (man year)
– coolant thermohydraulics	58.800	16
– dynamic behaviour of reactor materials and structures	83.300	15
– reactor physic and dynamics	–	5
– realiability, etc.	27.600	9
Total	169.700	45

Depressurization

Depressurization tests simulating the blowdown of a water reactor core and primary circuit due to hot leg ruptures (using the DHT-1 loop) were completed and analysed. The qualitative results are: (1) Reproducibility of the tests is good. (2) With increasing rupture size, the increases in the initial heat flux to coolant and its subsequent rate of fall are such that the total heat transferred during ejection is roughly constant and equal to about 2 full power seconds. These tests were used by the French firm GAAA to check a blowdown computer code. From this comparison between theory and experiment, the following useful conclusions were drawn: (a) the assumption of a unit slip ratio in the calculations gives better results than all the well-known steam slip correlations;(b) the assumption of thermodynamic equilibrium is reasonable; (c) Moody's critical mass flow correlation is valid up to about 50% steam quality and thereafter underestimates the mass flow rate; (d) heat transfer in post-crisis conditions can be satisfactorily obtained from the film boiling formula of Tong with Miropolsky's correction term. The above studies were accompanied by some interesting work on a new statistical method of measuring two-phase flow rates and the installation of a data handling unit for digitalizing and processing the output signals from the experiments.

UO_2/Na Thermal Interaction

Effort aimed towards an understanding of the UO_2/Na thermal interaction has been concerned mostly with the final preparation of the two test installations. One has a channel and the other a tank geometry. As yet, no controlled UO_2/Na interactions have been accomplished in these systems because of UO_2 handling problems in the channel experiments (UO_2 "creeping" and destruction of the crucible) and because the development schedule of the tank experiment has not yet arrived at this stage. However, several useful experiments were done with other materials (tin/water in the tank and Al_2O_3 in the channel system) and, with the present high priority given to these studies, it seems certain that a wide range of UO_2/Na interactions will be realized in 1972.

Dynamic Properties

Studies of certain basic dynamic properties of certain materials or structures followed four lines. First, the embrittlement of Zircaloy-2 due to hydriding was studied by means of explosive rupture tests on rings. These tests have now been performed for various H_2 levels and temperatures, but attempts to measure the detailed stress/strain/strain-rate relation using high speed photography have so far failed. Secondly, the behaviour of model reinforced concrete shields under internal explosive loading was studied with a view to establishing criteria to suppress "scabbing". Thirdly in close connection with the latter studies, some effort was directed towards a more basic understanding of shock propagation and dissipation in concrete. To this end, instrumentation was developed and tested on explosively loaded bars of Al 24 ST (because of its precisely known Hugoniot) and a powerful shock tube was built allowing shock pressures up to about 8000 atm. Tests on concrete bars will start in 1972. Fourthly , with the object of measuring the detailed stress/strain/strain-rate relation for the steels used in reactor containment systems, a split Hopkinson bar assembly was designed and built and is undergoing optimization tests.

Design Basis Accident Containment

Considerable priority is given in the programme to design basis accident (DBA) containment studies, using model reactor vessels and chemical explosives to simulate the internal loading caused by the DBA. Though carried out for specific projects, it is felt strongly that these studies are of very general interest because the containment problem is essentially the same for all LMFBR's. Model tests have been performed for two systems: the DeBeNeLux SNR and the CNEN PEC reactor. The tests for the SNR reactor employed a 1: 12 scale model of the vessel and made use of a slow-burning explosive developed by Belgonucléaire for a better simulation of the DBA than TNT. The sodium coolant of the SNR is replaced in the model by water and, as elsewhere, it was observed that one of the main hazards in a DBA is the impact ("water hammer") of a slug of this coolant against the roof of the vessel. Hence much time was spent in testing perforated plate devices which disperse this slug and reduce the impact. In addition, the effect of a relatively thin steel liner placed just inside the vessel for the purpose of absorbing energy in large plastic strains was investigated and found capable of greatly reducing plastic strains in the vessel. Thus it was shown that a relatively light perforated plate/liner combination is very strongly protective of vessel integrity in DBA conditions. For the theoretical analysis of the experiments, the Belgonucléaire SOURBOUM II, Argonne REXCO-H and ASPRIN codes are being prepared. In the studies for the PEC reactor, the DBA has been simulated only with TNT. Tests were performed in 1: 10 scale models. The 1: 20 scale tests concentrated on the behaviour of the vessel plug and its bolts. The energy absorption and plastic deformation of these components were measured and shown to be acceptable. The 1: 10 scale tests simulated the core, primary circuit and vessel multilayer structures in some detail and the effect of these structures was to restrict plastic deformations in the vessel to below 1%, a gratifying result.

Fracture Mechanics

In 1971, preparations were started for the study of failure of fast reactor structures by the methodology of fracture mechanics. In LMFBR conditions, fatigue is likely to be the failure mode and effort is therefore being placed in this field. Instrumentation is being prepared for fatigue crack growth studies of steel (in sodium). Compact tension specimens and burst test tubes (containing suitable cracks) of a type of steel (AISI 304) used in fast reactor pipes etc have been fabricated and a Losen-Hausen high force fatigue machine is being prepared. Fatigue crack testing on the compact tension specimens growth (in air) has been started using the Schenk 2-T machine, crack growth being monitored optically. The crack growth per cycle appears to have a Parris-type correlation with the stress intensity factor within the range measured. Burst tests have been performed on the cracked-tube speciments to check certain basic rules of fracture mechanics when applied to the steel and dimensions of interest (e.g., the crack opening displacement criterion for crack instability and the amplifying effects of pipe curvature).

Reactor Dynamics

In the field of reactor dynamics, work was done on some new extensions to the COSTANZA code series. First, the main two-dimensional (r,z) two-energy-group neutronics program was coupled to the two-phase hydrodynamics routine FRANCESCA for a fuller spatial description of excursions involving coolant boiling (BWR and PWR) and the treatment of steam slip in this routine was improved. Secondly, the number of energy groups in the main one-dimensional (z) neutronics program was extended from 2 to 4 so as to be able to compute fast reactor transients, and the coupling of this new main program with the sodium thermohydraulic (including boiling) code CARMEN of Belgonucléaire is under way. Thirdly, the two-dimensional (r, z) two-group version of COSTANZA with one-phase coolant thermohydraulics was adapted to HTGC reactors (a) of the Dragon type with hollow fuel elements and (b) of the pebble bed type. In addition to this effort on reactor dynamic methods, ideas were developed for the inclusion in the FRANCESCA code of the mass, momentum and enthalpy exchanges among the subchannels of a fuel bundle which occur during boiling two-phase flow (static and dynamic). Lastly, a code was developed for the spectral analysis of digitalized experimental signals recorded in dynamic experiments. This code is intended as a tool for noise and acoustic analysis in connection with research on early failure detection.

Criticality

On the subject of criticality of fissile assemblies, the Monte Carlo code GRANT-3 for the calculation of the reactivity of complicated geometries was verified against some well-known fast neutron assemblies (ZP3, Jezebel). Some practical calculations on annular U and Pu containers were performed for CNEN, with their assistance. Studies of pulsed source methods of measuring criticality were restricted to attempts at numerical simulation of existing experimental results.

Reliability

Activities in the field of reliability followed a number of directions. Three methods of reliability computation, based on different logical schemes, were assessed by a comparison of their ability to treat a typical nuclear power station electrical supply system. Differences of handling, flexibility, and computer time indicated a clear advantage for the fault-tree representation which forms the basis of the Ispra code CADI, now tested. Given the failure and repair laws of the elements of the tree, CADI computes the availability of each element and the whole system. This code was used to assess the availability of the PEC system using a fault tree of primary events with exponential failure laws and constant repair times. Development work has also started on another code (REMO) which will performe fault tree analysis by a Monte-Carlo technique. For the analysis of the reliability of structures, some work was done to evaluate the statistical distribution of the failure stress of steel and graphite. To this end a failure model, which assumes that rupture is the cumulative result of a sequence of independent steps of material "damage" was used to justify the correlation of failure stress data by means of functional-gamma distributions.

Early Failure Detection

Some work was done in support of early failure detection. As a preliminary to the study of ultrasonic emission from stressed vessels (as a means of detecting dangerous crack formation and propagation), tests were performed on small specimens of AISI 310 and 304 stainless steel. The number of ultrasonic pulses was measured as a function of the strain and strain-rate and a theoretical model suggested as a possible framework for correlating the results. A technique for incipient boiling detection and triangulation using the ultrasonic signals emitted by bubble nucleation and collapse was completed and new related studies on the detection of erosion were started.

Ultrasonic Probing

Work in support of ultrasonic probing was concerned exclusively with the sort of transducers proposed for fault surveillance in reactor vessel (samples provided by Kernkraftwerke Stade). The problem of interest regarding these transducers is their reliability in the environment next to the vessel, in particular the effect of irradiation and temperature. During the year, a test system was built for the accurate measurement of transducer characteristics (frequency, symmetry, focal distance, damping) by means of which the performance of the transducers before and after exposure to irradiation and temperature will be compared. Pre-irradiation tests were completed and irradiation in the Ispra-1 reactor started.

Noise Analysis

A special test system was built for the calibration of transducers employed in the above-described ultrasonic emission studies and for other noise analysis studies carried out in the water reactor programme (to be continued in the 1972 safety programme). The main function of this system is to measure the detailed frequency response of transducers, and several external bodies have asked to make use of it. A users' instruction manual is being prepared.

SAFEGUARDS PROGRAMME

H.W. Schleicher, M. Bresesti

The problem of safeguarding fissile material from diversion to non-peaceful uses has attracted continuously-growing interest during recent years, which have been characterized by impressive growth in the nuclear industry and thus of the amount of fissile material in operation. The conclusion of the Non-Proliferation Treaty was an outcome of this development which also attracted the attention of the general public.

The Commission of the European Community is already charged by the Rome Treaty of 1957 to "satisfy itself that in the territories of the Member States ores, source materials and special fissionable materials are not diverted from their intended use as stated by the users". This task is assigned to the Safeguards Directorate, in Luxembourg. Since 1969 the JRC has taken active part in R & D for nuclear safeguards, with the main objective of giving scientific and technical support to the Safeguards Directorate and with the further aim of providing methods for more efficient fuel management by the nuclear industry.

Although the activity of the JRC is thus based on close collaboration with the control body of the Commission, it needed direct contact and coordination with other research groups working in the Community in the same field, and this was achieved through an association contract which now comprises CEN, Mol (Belgium), CNEN, Rome (Italy), GfK, Karlsruhe (Germany) and RCN, Petten (Netherlands).

Apart from this, direct collaboration in special fields has been established between the JRC and industrial firms. In this connection, the work done with Nukem on the development of safeguards techniques in fabrication plants for highly enriched uranium, and that with ENEL, concerning the use of isotopic correlations and a number of other techniques, are worth mentioning. With both these partners a formal agreement is to be signed in the near future.

The main effort on the JRC's safeguards R & D programme is furnished by the Ispra Establishment, but Geel, Karlsruhe and Petten have also produced a number of valuable contributions.

A layout of the budget (excluded personnel charges) and of the manpower allocated for the different actions of the programme is given in the following table.

Action	Budget (U.C.)	Man power (man year)
– system analysis	–	2
– control experiments on reprocessing plants	8.100	4
– analysis of fissile material evolution in reactors	–	2
– techniques for fissile material measurements	93.700	13
– containement studies	23.000	2
Total	124.800	23

Main items of the programme

A general safeguards programme calls for the collaboration of scientists from different disciplines, e.g., mathematicians, physicists, chemists, and engineers. Consequently, at the Ispra Establishment, the programme is executed by people from different divisions, and is

coordinated at the level of the Directorate. A number of special topics concerning the safeguards programme are therefore dealt with in detail under the heading of the respective divisions. In this chapter only a very short review will be given.

The activity in 1971 mainly concerned the following areas:

- system analysis;
- control exercises in reprocessing plants;
- development of measurement techniques;
- development of identification techniques.

System analysis

In the context of safeguards, system-analytical studies are mainly intended to determine, on the basis of the fuel cycle, what strategy will most efficiently detect a possible diversion, taking into account the flow of the material, the feasibility and precision of measurements, and various restrictions such as inaccessibility of special areas.

Special studies have been done at Ispra in this field, concerning the safeguarding of reactors, reprocessing and fabrication plants. For fabrication plants a study has been started for the determination of a continuous inventory on the basis of several material balance areas; this work will be continued with simulation techniques. Another subject tackled has been the implementation of verification procedures, as they will possibly be applied by the IAEA safeguards department.

Lastly it should be mentioned that studies have begun on the use – for safeguards purposes – of correlations between different isotopes in irradiated fuel.

Control exercises in reprocessing plants

The best way to get a realistic estimate of the feasibility of safeguards procedures and their precision is by carrying out control exercises under practical conditions. In 1971 Ispra was concerned with two such exercises at reprocessing plants, the Jex-70 integral experiment applied to Eurochemic, Mol (Belgium), now completed, and the ECE exercise applied to EUREX, Saluggia (Italy).

In the JEX-70 experiment, promoted in 1970 by GfK in cooperation with Euratom, several laboratories of different countries and the IAEA collaborated. Its main purpose was the study of the possibility of applying a method for in-process inventory determination.

The Ispra contribution mainly concerned the following items:

- system analysis studies by numerical simulation;
- data processing for the inventory measurements;
- analyses to determine the concentrations and isotopic compositions of fissile materials;
- participation in an interlaboratory comparison of analytical techniques for assaying uranium and plutonium.

The final report on this experiment (EUR-4576 e and KFK-1100) was issued during the 4th Geneva Conference in September 1971. For a special article see A. Rota: "Critical Evaluation of a New Technique for Inventory Taking in Reprocessing Plants" in the frame of CETIS contribution.

The main objective of the ECE experiment is the verification of the material balance declared by the operator and the study of isotope correlations. This experiment will be continued in 1972.

Development of measurement techniques

The main effort in this field was expended on non-destructive techniques, using neutrons and gamma-rays.

Concerning the neutron techniques, three developments are worth mentioning: the determination and analysis of spontaneous fission neutrons, as described by G. Birkhoff and L. Bondar in their contribution: "Computerized System for the Application of Fission Neutron Correlation Techniques in Nuclear Safeguards" reported in the frame of Physics Division topics; the determination of U^{235} and Pu^{239} in mixed fuels by measuring the ratio of prompt to delayed neutrons emitted upon irradiation by a Sb/Be neutron source; and the

determination of the U^{235} content in fuel balls of the pebble-bed HTR by measuring the delayed neutrons emitted after irradiation by a Cf^{252} neutron source.

In the field of gamma spectrometry the studies for the determination of highly-enriched uranium in MTR fuel elements were continued. A gamma-scanning apparatus was developed and installed in the Nukem fabrication plant. This apparatus is utilized for routine measurements by the inspectors of the Safeguards Directorate for control operations on MTR type fuel elements.

Studies for the utilization in safeguards of gamma-ray measurements on irradiated fuels were started. Experiments have been planned in collaboration with ENEL on spent fuel elements of the Trino Vercellese reactor.

The non-destructive techniques require considerable support work from Electronics, including original developments. Two examples of such work are given in this report by M. Bernede, and L. Stanchi: "Derandomizer for Fast Acquisition into a Small Computer" (Development linked to the neutron correlation technique), and A. Bret, N. Coppo, A. Pedrini, and L. Stanchi: "Portable Multichannel Analyser" (256 channels especially designed for use by safeguards inspectors presented in the frame of the Electronics Unit contributions).

In the field of destructive measurements, a considerable number of analyses were done at the request of the Safeguards Directorate. However, the development was rather limited and was oriented mainly towards the amelioration and adaptation of X-ray fluorescence and emission spectroscopy techniques.

Identification techniques

The application of these techniques allows, through the use of tamperproof seals, a considerable reduction in the inspection effort. The development at Ispra is based on the determination, by ultrasonic investigation, of randomly distributed particles in a matrix of metal or plastic. P. Jehenson and S. Crutzen describe it in detail in a separate contribution to this report: "Identification Techniques in Safeguards presented in the frame of the Materials Division selected topics". MTR and LWR fuel elements with seals developed at Ispra will be introduced in the coming months in some reactors.

Final remarks

The effort spent on the safeguards programme in the Ispra Establishment is a relatively modest one compared to the overall activity. However, the programme takes full advantage of the different specialities and competences of the Centre's staff, and the fact that it is linked as well to the activity of the Safeguards Directorate of the Commission as to that of other European Institutions working in the field has helped to make it successful. Some of the work was reported in ten papers given at the "International Meeting on Non-Destructive Measurement and Identification Techniques in Nuclear Safeguards" held at Ispra in September 1971 and earned international recognition. Furthermore at the Fourth International Conference on the Peaceful Uses of Atomic Energy at Geneva, S. Finzi gave a review on the safeguards activities of the JRC.

Future programmes envisage a continuation of the work on generally similar lines, but with the activities mainly slanted towards problems of practical application of the methods developed so far. Thus, for instance, implementation of non-destructive techniques in the plant, application of seals to specific cases and elaboration of control systems for existing installations will be given special attention in order to help the operator as well as the inspector to organize and optimize the fuel management and safeguards activities.

REACTOR PHYSICS PROGRAMME

G. Casini

The Reactor Physics activities were oriented in the following directions:

- basic research on neutron phenomena;
- work in supoort of specific types of reactors;
- definition of areas where an Information Analysis Service can be provided to the Community;
- survey studies of technical and economic type.

A layout of the budget (excluded personnel changes) and of the manpower allocated for the different actions of the programme is given in the following table.

Action	Budget (U.C.)	Man power (man year)
– nuclear data and mathematical methods	76.100	19
– core physics and fuel cycles	16.400	16
– shielding	42.000	9
Total	134.500	44

Basic Studies

In the context of the studies on neutron thermalisation which have been carried out for some years at Ispra, a contribution was made to the study of the evolution of the neutron pulses in non-multiplying finite media. Measurements of the decay constant of a neutron pulse as a function of time were performed in beryllium blocks at low temperatures (from room temperature to 90°K). The pulsed fast neutron source was obtained by a 1.2 MeV deuteron burst accelerated by a 1 MeV Van de Graaff accelerator and impinging on a thick beryllium target. A critical analysis showed the necessity of allowing, in the theoretical model, for the interpretation of the spatial dependence of the problem. A detailed illustration of these results is given in the frame of the Nuclear Study Division contributions.

A new method of reducing the variance in Monte Carlo problems was investigated. This approach starts by using the solution of the adjoint Boltzmann-equation (importance function) to transform the normal Monte Carlo game into another one which guarantees the same mean value but with smaller variances. The estimation of the importance function is done through an each-collision-collimator game. The contribution of each collision can be interpreted as a point-wise estimation of the importance function. During the year the feasibility of the method (called ISEMOC, Importance Function Self Producing Monte Carlo Code) was assessed and the possibility of introducing it as a subroutine in the Ispra Monte Carlo code TIMOC was evaluated.

Support to Reactor Studies

This activity consisted in support work for the power reactor development studies. Two types of action were carried out:

a) setting up and refinement of calculation methods with the aim of obtaining general and flexible tools for the analysis of similar problems in different reactor types;
b) execution of measurements and calculations on specific problems in collaboration with the Community bodies involved in reactor projects.

Core Physics

A set of burnup codes was developed for equilibrium and approach to equilibrium fuel-cycle analyses for the first type of study; the nodal technique was employed to deal with the spatial treatment of the problem, with a saving of computer time as compared to the standard techniques for solving the diffusion equation. One and two-dimensional codes (RACE and TRACE) in one-energy-group approximation are in operation. The extension of RACE to two groups is at the debugging stage. For non-equilibrium studies a zero-dimensional code (RINO) is under test. It uses multigroup libraries with the self-shielding factor technique and an analytical burnup routine.

These codes have been extensively checked and used during the year to study problems related to HTR fuel cycles (in collaboration with the DRAGON Project and BELGONUCLEAIRE) as well as for preliminary evaluations of fast breeder fuel depletion problems.

In the context of the HTGR reactor studies, a number of experimental investigations were carried out:

- measurement of resonance integrals and Doppler effect for coated particle fuel elements;
- experimental determination of the temperature coefficient of fuel;
- feasibility studies on burnup measurement by the inverse kinetic technique.

The first study has been completed: the results compare well with the ZUT-TUZ codes (General Atomics Library). The measurement of the temperature coefficient of the fuel (with and without plutonium, to study the effect of burnup) will be carried out during 1972 in the RB-2 reactor at Bologna, in collaboration with AGIP-Nucleare.

The third analysis, with Brown Boveri Krupp, was intended to clarify some points relating to the interpretation of reactivity measurements for burnup evaluation in HTGR pebble-bed reactors. Attention has been focalised to the following points:

- interpretation of measurements in order to determine the "importance functions" of each of the fuel components;
- checking, the validity of the methods intended for the routine experimental analysis by the use of transport two-dimensional multigroup codes.

Shielding

The EURACOS facility was operated for investigations related to the SNR and CIRENE projects.

In the case of SNR (collaboration with GfK Karlsruhe), the object of the experiment was to study the radiation streaming along a twice-bent sodium-filled duct through graphite and concrete walls similar to a cooling tube section of the reactor. During the year the SNR mock-up facility was mounted in the EURACOS area and measurements on the first configuration (without borate graphite diaphragm at the upper duct exit) were started. Threshold detectors and sandwich foils are used for fast and intermediate neutron detection. Supporting calculations are carried out by the Monte Carlo TIMOC code.

Information Analysis Service

During 1972 preparations were made to organize a service for systematic analysis and distribution of the information in two selected areas, namely,

- integral nuclear data for reactor calculation (INDAC);
- shielding (ESIS).

INDAC

In the INDAC area, the following work was done:

a) Processing and testing of multigroup libraries from ENDF/B data files. Libraries were prepared for TIMOC (26 groups) by the CODAC code and for GAM (99 groups) by SUPERTOG. Work to put in operation the GAND-GAF-GAR chain, particularly suitable for fast breeder calculations, is well advanced.
b) Test of multigroup libraries on integral experiments. Preliminary tests were run on the U.S. Benchmark Experiments for fast breeders using various code chains such as

CODAC-TIMOC, SUPERTOG-ANISN and GAM-GATHER-ANISN. A first evaluation of the SORA critical experiment showed the important role played by the structural materials in the neutron balance of such configurations.

c) Definition in collaboration with CNEN and AGIP-Nucleare, of the main parameters of an integral measurement of the capture cross-section of iron in epithermal and fast neutron spectra. The experiments are scheduled to start at the beginning of 1972 in the RB-2 reactor of AGIP-Nucleare (Bologna), converted into a coupled thermal-fast facility. The test zone will be formed by a mixture of microspheres of fuel (U^{235}), graphite and iron. The neutron balance will be determined by the zero reactivity technique together with the measurement by activation of capture rates and spectrum indices.

ESIS

In the ESIS area, the following work was done:

Code Assessment

A number of codes were analysed, put into operation and tested on practical cases:

CINNA, based on the integral form of the transport equation, developed at the JRC, Ispra. Work in 1972 has been devoted to the refinement of the code from the operational point of view (computing-time saving, flexibility, checking on operational problems, etc.);

ANISN, based on the S_n approximation of the transport equation;

MORSE, dealing with the Monte Carlo technique.

These three codes were used, in the case of neutrons, with a library taken from ENDF/B by which up to 100 energy groups can be attained. The preparation of a gamma library starting from the code GAMLEG is almost completed. Alongside the code testing, in the case of MORSE, efforts were made to refine the methods for variance reduction.

Benchmark Experiments

An experiment with a clean geometry (multilayer plane arrangement) was prepared, for execution in EURACOS during 1972. The aim of the measurements is the integral evaluation of the iron and sodium cross-sections of interest for shielding calculations.

Technical and Economical Studies

Strategy studies have been started as a support to the EEC Directory for Energy (Brussels), to evaluate the criteria of penetration of the nuclear power installations in the Community network during the coming years.

Survey studies concerning strategies with conventional stations, light water reactors with and without plutonium recycle and fast reactors were first carried out, using the Interatom code INTAT. Input data for fuel cycle costs were taken for the TRACE burnup code. The analysis was subsequently extended to the case of plant combinations including HTR-systems. Details of the work performed are given below. (Nuclear Studies Division contribution).

In the last part of the year a new type of evaluation of the results of the strategies elaborated during 1971 was started, with a view of the production of pollutants (SO_2, heat, radioactive disposal),

Under a joint arrangement with RCN-Petten a program was developed for the evaluation of the fuel cost for a nuclear reactor to be used in marine propulsion. In this code the concept of "cycle" which is currently used for this type of calculation was not retained but the whole fuel history of the nuclear plant was represented by a sequence of individual events occurring at predetermined dates and associated with an equal number of financial commitments. Details of the method and its application to practical cases are given in the frame of the Nuclear Studies Division contributions.

PHYSICS OF CONDENSED MATTER PROGRAMME

G. Fraysse

In 1971 the work on the Physics of Condensed Matter followed three lines:

a) Fundamental, experimental and theoretical research on solids (crystalline and amorphous), liquids and liquid crystals.
b) Development of new instruments for fundamental research
c) Studies on materials (applied physics) with a view to possible future applications.

The program consisted of eight projects, together with the maintenance and operation of the ISPRA-I reactor which was under the budgetary control of the Physics Programme.

A layout of the budget (excluded personnel charges) and of the manpower allocated for the different actions of the programme is given in the following table.

Action	Budget (U.C.)	Man power (man year)
– magnetic resonance	27.400	13
– solids	44.400	12
– theoretical physics	13.600	5
– instrumentation development	29.300	6
– neutron scattering	54.200	8
– neutron properties	6.700	3
– preparation and properties of special materials	18.100	8
– structure and lattice defects	9.500	2
Total	203.200*	57

* plus 212.500 U.C. and 33 men for ISPRA-I operation

Magnetic Resonance

NMR and ESR Studies in Solids

The investigations concerned the motional behaviour in amorphous and crystalline solids, the effect of strong radiofrequency fields, and magnetic properties of organic materials. In glasses, Zeeman and dipolar relaxation times of ^{7}Li and electric field gradient distributions were measured. The field distribution in glasses has been found broader than in crystals, indicating less regularity in the symmetry of the environment of the atoms or ions. In organic solids, a new effect of induced dynamic polarization by temperature variation leading to enhancements greater than 100 (see detailed description in this annual report) was found.

Studies on the effect of ratio frequency irradiation on the wings of NMR lines were completed by observing and explaining the dynamics of the equilibrium approach.

Relaxation and magnetic phenomena were studied in crystalline free radicals between 300°K and 1,3°K. Spin lattice and spin-spin relaxation mechanisms are greatly determined by exchange interactions.

Relaxation and Polarization Studies in Liquids, Adsorbed Liquids, and Solutions

The investigations concerned relaxation and dynamic nuclear polarization in liquids, adsorbed liquids and solutions. Enhancement factors were measured in solutions of free radicals in trimethylthallium at various temperatures and magnetic fields. Structural studies were done on metal-ammonia solutions. No important differences between solutions of Li, Na, K, and Ca were observed.

Electron spin relaxation time T_1 and T_2 were measured in a considerable number of different solutions. T_1 has been found in all cases proportional to the radical concentration, and T_2 independent. The relaxation was explained in terms of scalar and dipolar interactions modulated by electron exchange, translational and rotational molecular motion.

NMR Studies in Liquid Crystals

A new apparatus with pulsed gradient coils has been constructed in order to measure the anisotropy of self-diffusion coefficients D in liquid crystals. Preliminary measurements on tetramethyl-silane in a nematic liquid have shown that D values parallel and perpendicular to the magnetic field differ by 15-20%.

Within a larger study on the limitations in the determination of geometrical structure, the ^{13}C-NMR of acetylene and the ^{1}H-NMR of 1,4-dioxadiene were investigated in nematic solvents.

Radicals Produced by High-Energy Irradiation

As described in detail in this annual report, the purpose of this study is to determine molecular structures from ESR spectra of free radicals during irradiation of organic materials.

Solids

Radiation Damage in Metals and Alloys

Neutron irradiations of C-25% Au alloys and electron irradiation of αCu-Zn alloys were done at the ISPRA-I reactor and at the 2 MeV Van de Graaff accelerator to study radiation-enhanced diffusion in f.c.c. alloys. A large increase of the long-range order was observed in the Cu-25%Au alloys; this increase was strongly dependent on the irradiation temperature. A decrease of the electrical resistivity was observed with increasing short-range order of Au-15% Ag alloys. This result supports the point of view that static crowdions are created in these alloys during electron irradiation (see the paper in the annex).

Imperfections and Radiation Damage in Ionic Solids

The main activity was devoted to the studies of colour-centre formation in deformed alkali halides, discussed in one of the annex papers. The investigations on thermal stability and reactions of excess colour centres were also continued.

Determination of Fundamental Optical Properties

Developments in this fields include:

a) extension of ellipsometric techniques and computing methods to the study of the optical response of anisotropic absorbing solids. In this line, work on the lamellar semiconductor WSe_2 was continued;

b) application of thermomodulation techniques in ellipsometry. Experiments have been started on $BaTiO_3$ to study the variations of the optical response in the vicinity of transition points.

Studies on the Dynamical Diffraction of X-Rays and Neutrons

A work of the effect of temperature on the anomalous transmission of X-rays in single crystals of copper and zinc was completed. The investigation concerning the effect of Compton scattering on the dynamical diffraction through thick, perfect crystals of silicon was continued and a precise determination of the Debye-Waller factor of Si at room and liquid nitrogen temperatures was completed.

In collaboration with the Institut Max von Laue - Paul Langevin of Grenoble, diffraction line profiles were calculated by applying the dynamical diffraction theory of neutrons to elastically bent crystals. These results were used for the development of new types of neutron monochromators. More specifically, single crystals of Cu-Ge which were grown with a gradient of the lattice parameter were investigated by neutron, X-ray and α-ray diffraction.

Single crystals of silicon which were elastically bent by growing a silicon nitride layer on one face of the crystals were investigated by neutron diffraction. Lastly a theoretical investigation concerned the phenomenon of dynamical diffraction in the strongly asymmetric Bragg case.

Application of the Mössbauer Effect to the Investigation of γ-scattering by Crystals

The 14.4 keV γ-rays from Co^{57} sources were scattered on different crystallographic planes of various Si and Al crystals. By using nuclear resonance absorption it was possible to separate the elastic and inelastic components of the scattered beams. An analysis of the temperature diffuse scattering at the Bragg reflection of Si and Al showed that there is good agreement between the experimental results and the wave theory of the lattice vibrations.

Theoretical Physics

Atomic Interactions

To conclude the jump diffusion studies, a computer code "JUMP" was written which allows the calculation of the parameters of the quasi-elastic neutron scattering for several models. A subroutine allows the calculation of scattering curves.

Some investigations were done on the effects of impurities in the dynamic scattering of neutrons.

Lattice Dynamics of Metals

Using the PSAF computer program, the model parameters for Li, Na, K, Rb, and Al were obtained. On the basis of the pseudo-ion model, binding energies were calculated showing remarkable agreement with experiment.

Stability and Migration of Point Defects in CaF_2, UO_2, ZrO_2 and transition metals

The studies, done by computer simulation, concerned the determination of interatomic potential, the diffusion of anion vacancies, the anionic interstitial configuration and the interstitial site of hydrogen in metals. The saddle point and the configurational energies were determined in ZrO_2.

Statistical Thermodynamics and Dynamics of N-Particle Systems

The studies on non-linear mechanics of a classical anharmonic chain were developed in several directions: computational program for 2-dimensional model, discovery of the existence of one-dimensional systems, Planck-like distributions, and Monte Carlo calculations for the research on quantized vortex lines in liquid He^4.

Instrumentation Development

The construction of a time-focusing spectrometer (ITFS) and the design of a double-crystal-X-ray spectrometer were completed. Preliminary tests of the ITFS were done.

Neutron Scattering

Several spectrometers already installed at the ISPRA-I reactor were operated and improved: a slow-chopper facility, a rotating crystal spectrometer, a double chopper, and a water scatterer for the slow chopper. The improvements essentially concern: background reduction, a computer program MEANVAL and a code TOFCOR for the slow chopper, an adjustable time-of-flight sector, reduction of parasitic reflections, and new counting chains for the rotating crystal spectrometer; a new detector bank of He^3 counters, background reduction and a computer program DOCHAP for the double chopper.

Density Fluctuations in Liquids by Small Angle Scattering

This study was done to investigate the feasibility of experiments on liquid rotating helium, and the coherent scattering by deutoride liquid crystals in an electric field.

Preliminary measurements at the slow chopper verified the necessary experimental resolutions.

Measurements on Liquid Crystals

At the slow chopper, inelastic scattering measurements have been started on para-azoxyanisole in order to establish the existence of a soft mode. At the double chopper other quasi-elastic scattering measurements were performed on 2 room-temperature liquid crystals in the presence of magnetic and electric orientation fields.

Neutron Scattering by NbH in the Temperature Range from 350 to 800°C

Preliminary data concerning the determination of the Lorentz-width of quasi-elastically scattered neutrons were obtained at the slow chopper facility.

Low Energy Modes in Amorphous Selenium

Measurements of the specific heat indicate the existence of such a mode. An amorphous sample of Se was prepared by quenching liquid selenium at 250°C in liquid nitrogen or water. The sample was demonstrated to be amorphous by means of X-ray analysis.

Inelastic neutron scattering measurements at $E_i = 6$ meV at the double chopper facility and at 15 meV at the RCS facility were performed and showed characteristic inelastic scattering at small energy transfers.

Neutron Scattering Experiments with the Rotating Crystal Spectrometer

As detailed in this annual report, measurements were done on NbH single crystals to obtain information about the mobility of the hydrogen atoms.

Study of the Ferroelectric Phase transition in KDP

A cryostat with a temperature stability of 1/100° was built for this experiment. The first part of the work was concerned with the identification of soft ferroelectric modes by means of incoherent inelastic scattering at the slow chopper.

Neutron Properties

Fission Fragment Properties

The experiments concerning ionization laws of fission fragments showed the quasi-independence of the energy per ion pair/fragment mass.

Data handling is being continued to complete the results.

An experiment was built for measuring the time-of-flight of fragments, in the subnano-second range of accuracy. This experiment, combined with X-ray experiments, would lead to the nuclear charge determination for each fragment.

Neutron Electric Dipole Moment and Spin Interactions

The investigation concerned the possibility of a neutron spin precession in a gravitational field. The difficulties encountered in the measurement of the residual fields in the magnetic shielding led to the construction of a milli-gauss sensitive magnetic probe.

Preparation and Properties of Special Materials

Preparation of Li-Nb-O_3 crystals and isomorphous compounds

In order to obtain well characterized crystals, an improved CZOCHRALSKI system was set up. The improvements essentially concern the absence of vibrations, constancy of pulling forces by avoidance of friction (rolling movements instead of sliding) and a more uniform temperature profile.

Satisfactory crystals (transparency, absence of small fractures) have been obtained.

Ion Range Measurements and Atom Location in Implanted Layers

The investigations concerned two types of studies: measurement of concentration distribution profiles of implanted atoms, and atom location studies.

Electrical profiles of As implanted in Si were studied by sheet conductibility and sheet Hall effect measurements. An automated system was set up for determining physical profiles in silicon, using a radiotracer technique with anodic oxidation sectioning.

A scattering chamber for atom location to be associated with the 1 MeV accelerator has been completed. The sample can be cooled (100°K) or heated (800°K) while in position in the goniometer.

Structural and Lattice Defects

Observation by Internal Friction of H and D in Nb, Va, Ta, Zr

Measurements on the Ta-H system confirmed the existence of a relaxation peak in the temperature range of 100°K. Measurements on the Nb single crystals showed the orientation dependence of the Snock peak for oxygen in interstitial solution and for hydrogen.

The installation has been improved towards an automation of the measurements.

Diffusion Studies in U Compounds by Internal Friction

For the measurements of internal friction in the range 20°-1000°C in UC, UO_2 ZrO_2, new sample holders have improved the existing facility. First measurements were done on a UC specimen to detect split vacancy defects predicted by the theory.

Electron Microscope Study of Deformation and Ions in Ni-Mo

The investigations concerned two types of studies on (a) the effects of ion bombardment on the order-disorder of Ni-Mo alloys (with 100 kV ion accelerator) and (b) deformation and corrosion behaviour of the same alloys, by electron diffraction and transmission microscopy, scanning microscopy, microprobe X-ray analysis.

The first study has yielded only preliminary results, in the absence of sufficiently clean vacuum conditions, the second one gave remarkable results as illustrated by the corrosion of Ni-Mo alloys exposed to hydrobromide-acid: a combination of all the different observation techniques allows an unambiguous interpretation of the phenomena.

SORA REACTOR PROJECT

T. Doyle

The SORA (SOrgente RApida = Fast Source) reactor project was begun in 1962 at the Ispra JRC. It is a periodically pulsed fast reactor designed as a source for neutron beam research in the physics of condensed matter and neutron physics in general, using time-of-flight measurement techniques.

Since a comparison of experimental methods shows a general equivalence between pulsed and stationary techniques for the same source flux, the pulsed reactor proves extremely attractive as its cooling power and fuel burnup is about 200 times less than that of an equivalent steady state reactor.

This basic cost advantage and development potential led to the choice of a pulsed fast reactor.

A fast spectrum is necessary to maintain pulse at an acceptably low value, the pulse being generated by super-prompt-critical multiplication of the delayed neutrons. This fast pulse is tailored to the specific needs of the experimenters in various moderating substances, and the consequent sub-thermal, thermal or epithermal pulse is led through beam channels to the experiments. This tailoring possibility is a further advantage of the fast pulsed reactor.

In 1962 the first studies started on kinetics and dynamic behaviour of fast pulsed reactors. The initial concept elaborated was a 100-250 kWt, NaK cooled system enlarged in 1962-1964 to a 600 kWt system. Then followed a detailed study and cost estimate by an industrial consortium of the 600 kWt reactor. In 1965-68 critical experiments and analyses were made, and were followed in 1969-1970 by some optimization work. In late 1970 the Council of Ministers approved a design study by industry, and in 1971 the Consortium was chosen. Work started in mid-1971 and led to freezing of major design options by the end of September 1971, and a new reference design by the end of 1971.

Present Project

The present phase of the project can be defined as the final design to which a fixed-price will be attached. It is characterized by a fixed-price design study leading to a fixed price for reactor construction. It started essentially in early 1971 in the form of an information meeting to which interested Community firms were invited.

At that meeting the design that emerged from the previous industrial contract in 1965 was presented. However, the following major modifications were given as essential features of the new design:

Reactor power

Increased to 1 MW from 600 kWt. Core design consequently modified by increasing the pitch diameter ratio of fuel rods from 1 to 1.08, and by increasing coolant flow rate.

Moderator

The two cold sources were moved from an asymmetrical position (required because of beam tube layout) to a symmetrical position around the reactor vessel. They were also increased in size (about 5 times larger volume) and the later use of liquid hydrogen was foreseen.

Accelerator

It was decided to provide for the later addition of an accelerator. As far as the reactor and buildings are concerned, space is simply being provided for the accelerator bending magnets and targets.

Pu Fuel

It was decided to make provisions for later use of Pu fuel, i.e., to ensure that the design of reactor components allows the use of Pu.

Beam Channels

Their number was increased from 15 to 22, their orientation was modified, and their beam section made 6 times larger.

Pulsation Frequency

The possibility of lowering the frequency from 50 c/s to perhaps 5 c/s was foreseen. A double rotor solution should therefore be provided for, even though the first rotor will be the single solution for a limited time.

The industrial companies interested in SORA then bid for the design study contract. A consortium of five companies was chosen for the study, and the work started in mid-71. The contract which covers the design study foresees the following work break down between the Consortium and the JRC.

Consortium

- Preparation of plant design containing details needed to take a decision on construction;
- submission of a turn-key price for the construction and start-up of the reactor;
- a detailed planning schedule for reactor fabrication, construction and start-up;
- a basis study of reactor safety.

C.C.R.

- participation in plant design studies for items of JRC competence e.g., reactor physics;
- safety evaluation as needed for reactor licensing;
- experimental studies related mainly to safety;
- contacts and formal discussions with Italian licensing authorities.

It should be noted that the design study concerns only the reactor itself and essential supporting services; the particular experimental neutron research equipment, in particular the flight channels together with associated movable equipment and instrumentation, are not included in the contract.

Technical Progress

Basic Design Choices

In the introduction above a brief desciption is given of the design that emerged from the mid-60's collaboration with industry. The re-orientation of this design after five years had to take account of the following significant differences, compared to the mid-60's effort:

a) a relatively new type of research tool, such as SORA, must take account of considerable evolution in the type of experiments contemplated. In fact, the work done at the JRC in the period 1966-1971 resulted in the modifications noted in the previous section in order to keep the reactor better aligned on the experimental use.
b) The industrial Consortium is now required to give a fixed-price bid valid for a certain time. Considering the rapid rate of price increase, especially in the nuclear sector, and the considerable strain imposed on companies engaged in advanced R & D, the Consortium feels obliged to take a conservative approach. In fact, proven solutions are required by the Consortium in order to give a fixed price; the resulting changes in the SORA design, especially in the core region, are not always consistent with optimum reactor use.
c) Fast reactor technology has progressed considerably in the past five years. Solutions favoured then by industry or the JRC are not always favoured now, and again further change is required.
d) In parallel the approach of licensing authorities has evolved. In some respects an increasing conservatism is characteristic of the national bodies charged with the final assessment of nuclear safety. For example, seismic criteria are now applied to the SORA design, whereas in 1965 this was not done.

In general, licensing considerations bulked large in the 1971 re-orientation of the design, particularly since a fixed price would be meaningful only for a design with good licensing prospects.

The above four factors were important in the collaboration between the Consortium and the JRC in 1971, especially on the following points:

- the pulsation device;
- the core and fuel element;
- the core cooling circuits.

The interplay between the JRC and the Consortium to establish a new reference design fomed a large part of the 1971 effort, a reference design being proposed by the JRC in mid-1971, then modified to allow for the above points and finally agreed upon in late 1971 as the final reference design. Only a summary of the most important results of these exchanges is given below.

Reactor Physics

Over the years a special competence has been acquired at the JRC in the physics of repetitively pulsed fast reactors. This is recognised in the contract with the Consortium, where reactor physics work is done entirely by the JRC. During 1971 the major activities in this field were:

- improvement and transfer of various codes;
- design calculation for reactor design.

These activities are treated in detail in the frame of the Nuclear Study Division contributions, and are therefore not repeated here in detail.

The core proposed to the Consortium in mid-1971 had a volume of about 7.5 litres, a height of 24 cm, and 201 fuel elements spaced with 0.5 mm diameter spiral wire and arranged into three concentric subassemblies. The Consortium preferred a spiral wire diameter closer to 1 mm and more structural material in the wrapper cans. To achieve sufficient reactivity, the number of fuel elements was increased to 228 and the core height up to 30 cm. The significant physics comparisons of these cores was investigated in a parameter study of which the main results are given in Table 1.

The target k_{eff} is 1.06 using fuel in all positions, i.e., with no dummy elements. This reduces to 1.02 with about 10% dummy elements, regarded as a realistic margin in the operating reactor. It can be see from Table 1 that the final core will be between Core IV and Core I, as far as spiral wire diameter is concerned, in order to reach the target k_{eff} of 1.06.

Table 1 – Possible Sora core arrangements and physics results.

Core Designation	Core	Element No.	Wire ϕ mm.	Element pitch Inner SA 1	Middle SA 2	Outer SA 3	Sections Total cm^2	1 cm^2 (cm ϕ)	2 cm^2 (cm ϕ)	Height mm.	Mean Volume fractions $f_{fuel}/f_{steel}/f_{na}$	K_{eff}
Mid. 71 Reference Design	Core II	201	0,5	13,0	13,0	13,0	301,1	29,0 (6,08)	107,0 (13,2)	240	72/8,0/20,0	1.04
Conservative Design	1	228	1	10,27	12,12	13,0	342,8	21,5 (5,22)	105,5 (12,7)	300	57,9/8,7/33,4	1.03
End 71 Reference Design	Core IV	228	0,5	10,6	12,22	13,0	341,1	22,4 (5,34)	105,6 (12,77)	300	64,4/9,2/26,4	1.09

Safety and licensing

During the report period the major activity in this field was the development and improvement of dynamics codes.

In periodically pulsed fast reactors, the time scale of the perturbations investigated determines the degree of detail in which the kinetic equations have to be established.

Therefore two approaches are possible.

a) For a time scale long enough with respect to the pulsation period, the kinetic equations can be solved outside the "discrete points" given by the pulses, taking into account the pulse characteristics as boundary values.
b) For a short time scale, the kinetic equations have to include a detailed description of the single pulse shape and of the reactivity variations during the pulse.

SORASI

This program makes use of the discrete time kinetics equations. The pulse period is divided into two parts: during and between pulses.

During the pulse any reactivity feedback effect is ignored and only the increase in precursor concentration is computed. Between two pulses a general integration of the precursor equation is used.

The reactivity feedback effects are computed through a core average channel and include prompt effects, like Doppler and axial expansion, and delayed effects like Na expansion and radial core expansion.

SORDYN

This program makes use of the kinetics equations in their general form. Owing to the small size of the core, a one point model and three energy groups have been used.

The "pulse function", representing the reactivity variation due to the moving reflector, is calculated by Monte Carlo method and approximated by a linear plus a parabolic function, symmetrical with respect to the core window centreline.

Reactivity feedback effects, like those of the other program, have been included.

This second approach is of general validity but requires longer computer time; the first can be considered in general more flexible for long-time problems.

For SORA dynamics, both approaches have been used and two computer programs, SORDYN and SORASI, have been developed.

Loop Dynamics

A loop dynamics code was already prepared to allow study of regulation and accident behaviour of the loops. This code will be coupled with SORASI for complete reactor dynamic analysis. Although some test runs were made with these codes, production cases will not start until early 1972 when the necessary Consortium input data are available.

Reactor Block

Fig. 1 shows a horizontal section of the overall reactor block layout and Fig. 2 that of the core and reflector region.

Core Design

Section above illustrates the changes in core design, especially fuel element spacing and wrapper can material. The reference design will probably be 30 cm high, with 228 fuel rods (of which about 10% will be dummies) spaced by a spiral wire of about 0.7 mm diameter in three subassemblies with wrapper can of 0.5 mm thickness.

The thermal hydraulics of these cores were investigated. The nominal fuel temperature of the probable reference case is ~ 400°C, with a nominal axial ΔT of 50°C, and a Δp of ~ 110 g/cm^2. Discussions were held with specialists on the probable burnup of this core.

The 3-subassembly core gives a compact arrangement, and thus favourable physics characteristics. However, it has some major disadvantages: difficulties in fuel handling (the outer SA has a k_{eff} of ~ 1.0 in water); inflexibility for fuel testing; difficulty of detecting failed fuel. The control rod worths, proved higher than expected or needed. The flexibility of core design thereby achieved led to the conclusion that a modular core study should be undertaken. The criteria for this study of ~ 16 hexagonal subassemblies were fixed. The work will be done by Euratom, because the limited scope of the Consortium contract does not allow alternative solutions.

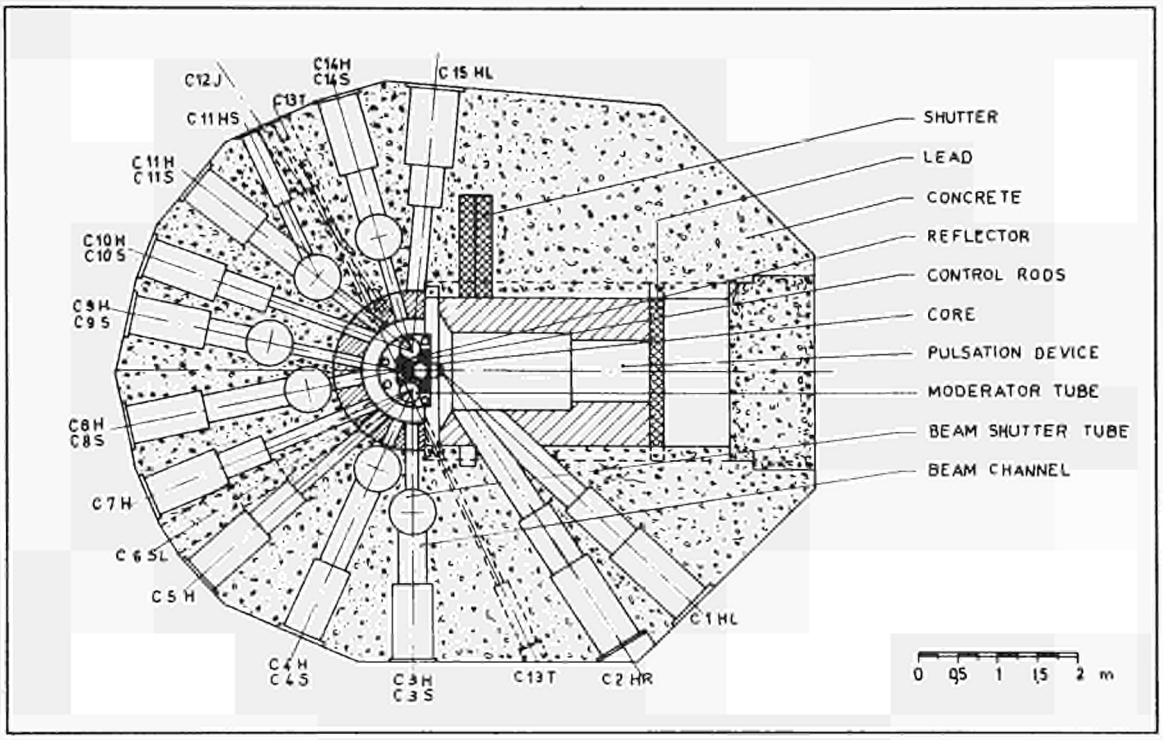

Fig. 1: SORA – Reactor block horizontal cross section.

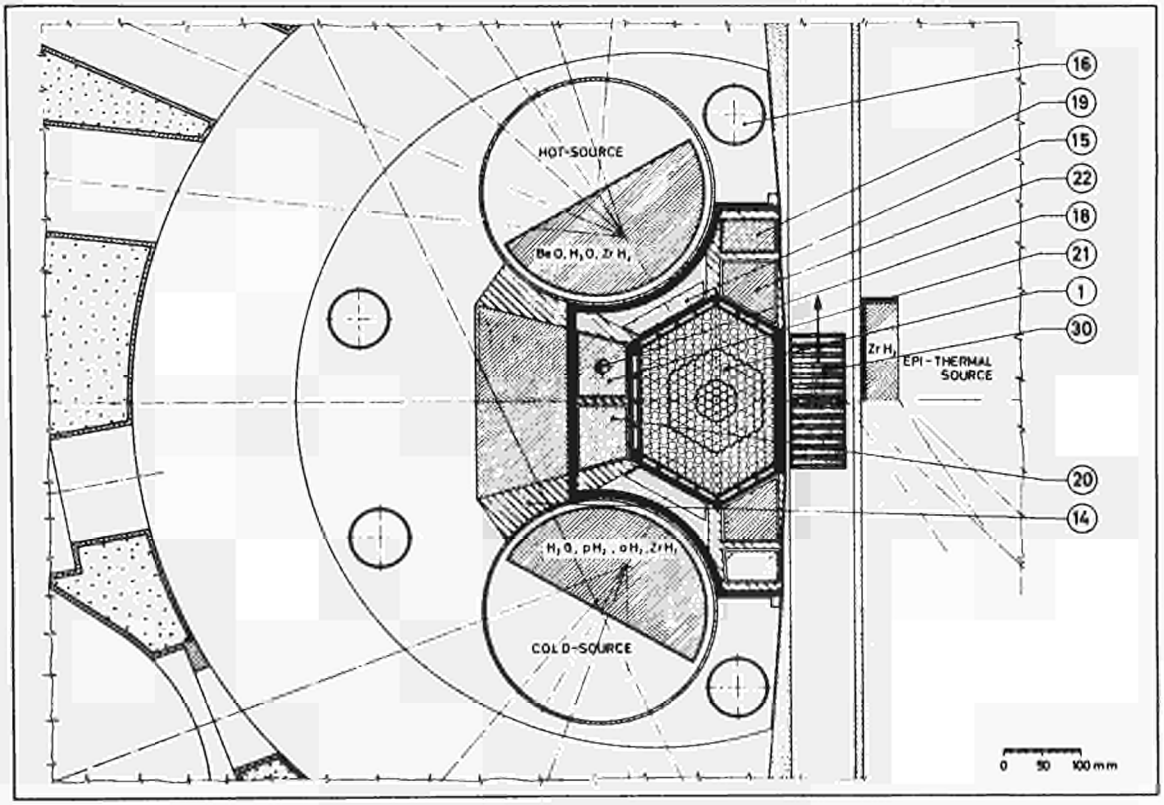

Fig. 2: SORA – Core and reflector horizontal section.

Reactor Vessel

The Euratom reference design was modified by the industry to take account of the circuit layoutt and to provide adequate support.

Pulsation Device

The preliminary study of a horizontal-axis pulsation device was completed by the Consortium. The study showed that the technology needed for the application of such a device to SORA was now available. In particular the large diameter bearings, the shaft rigidity needed for dimensional stability, the layout from the neutron irradiation viewpoint, and other major considerations all proved feasible. Although some points remained for further investigation (end-plate deflections, choice of cooling system etc.) it was decided that the horizontal-axis device could satisfy the requirements for SORA.

In view of the more dilute core (see above), the safety aspects of the vertical-axis device became more intolerable. The potential for energy release, and the possible assumptions needed for licensing were both moving in an unfavourable direction.

Therefore it was decided by late September to adopt the horizontal-axis device as the reference solution. By the end of the year a reference design was established, incorporating a double-rotor solution to allow pulsation frequency from 5 to 50 c/s; direct He cooling, graphite shielding. The shaft was overhung to protect the end bearing from excessive radiation and was located directly below the core.

Control Rods

The physics work on the control rods, reported in Section above, gave more favourable results than expected. The rods in general were worth 15 to 100% more than necessary, giving considerable freedom to possible changes in core design. In fact, this favourable circumstance cleared the way for the modular core study, mentioned above.

The drives for the rods were proposed by the Consortium. A rack-and-pinion solution already used by them has several advantages. Euratom comments on this led to rearrangement of some parts but basically the layout is fixed.

It was decided to insert addiational backup safety rods between the core and the moderators, for additional control, especially during the initial approach to critical, and also in case an accident barrier were to be required.

Beam Tubes and Shutters

The layout of beam tubes and shutters was re-arranged at the Consortium's request. The former arrangement left too little space between tubes and between shutters at their closest points for satisfactory concrete pouring. The shutters were consequently displaced back from the core. However, the number and basic orientation of the beam tubes remained unchanged.

Biological Shield

At Consortium request, a thermal shield (steel plates was inserted between the reactor and the concrete. This shield would protect the concrete from fast neutrons, and gammas, and would be gas-cooled.

Preliminary shield calculations by the Consortium and Euratom led to the conclusion that an additional 100 cm would be required in the biological shield thickness for the type of concrete proposed by the Consortium.

Moderators

The two large moderators were maintained unchanged. Provision was made for a third source between these two, but the Consortium work will merely deal with the space requirements. A fourth source of epithermal neutrons will be provided by the reflector block of the pulsation device.

Cooling System

The reference coolant was changed from NaK to Na mainly because of better heat transfer properties in fast reactors and because the industry is more familiar with Na than with NaK techniques (especially purification). The only disadvantage – preheating to keep it liquid – is not judged a problem by the Consortium.

The coolant circuit layout was maintained as a main and auxiliary system. The auxiliary loop removes only about 5% of the heat, and is intended to cover decay heat removal on loss of pumping power in the main loop.

Natural circulation was also adopted for ultimate backup cooling in the case of complete electrical blackout. This involved considerable rearrngement of the circuits since the heat exchangers were formerly located below the core. The new layout provided for the IHX about 2 m above core level, and located in the reactor block. The secondary coolant lines then lead to the Technical Annex and cover a very short path.

On this basis the main data for the Na cooling systems were defined. The auxiliary systems – cover gas, purification, tilling, etc. – were also tentatively defined. Fig. 3 shows the main layout scheme.

The gas cooling systems – for control rods, thermal shield, graphite column, shutter tubes, biological shield, pulsation device – were tentatively laid out.

Handling

The handling of the 3-subassembly core gave various difficulties:

a) the outer subassembly immersed in water has a k_{eff} of ~ 1. Criticality control of subassemblies in handling was therefore a problem;
b) the Reactor Building (RB) could not provide space for handling and hot cells, which had to be moved outside the RB.

A new handling scheme for fuel was defined:

– the subassemblies are removed on rails by Transfer Flask I (TF 1) from core to an Intermediate Storage (IS) located inside the RB. Gas cooling (Argon) is used both in TF-1 and in IS;
– after decay in IS they are removed by TF-3 through the Truck lock to the Handling Cell and Washing Station outside the RB;
– after cutting, cleaning and packing the fuel rods are shipped off-site for reprocessing.

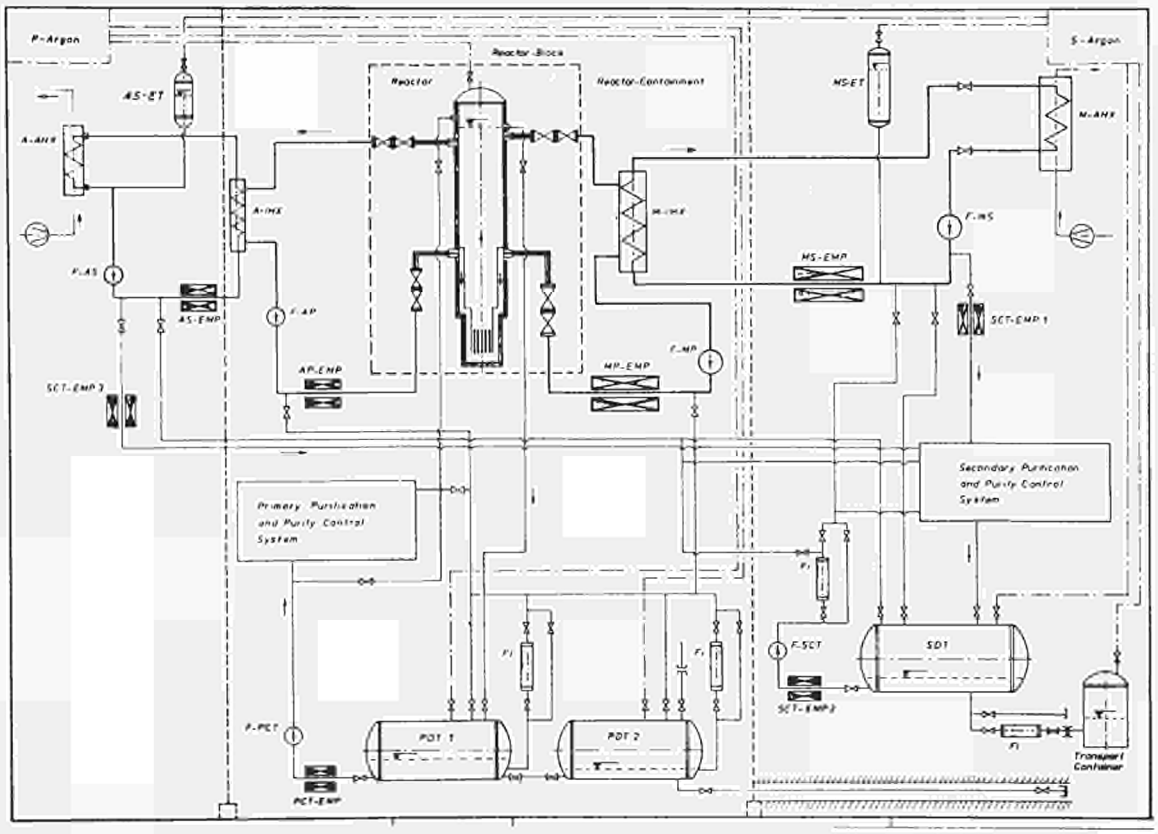

Fig. 3: SORA – Liquid-metal cooling-system flow-sheet.

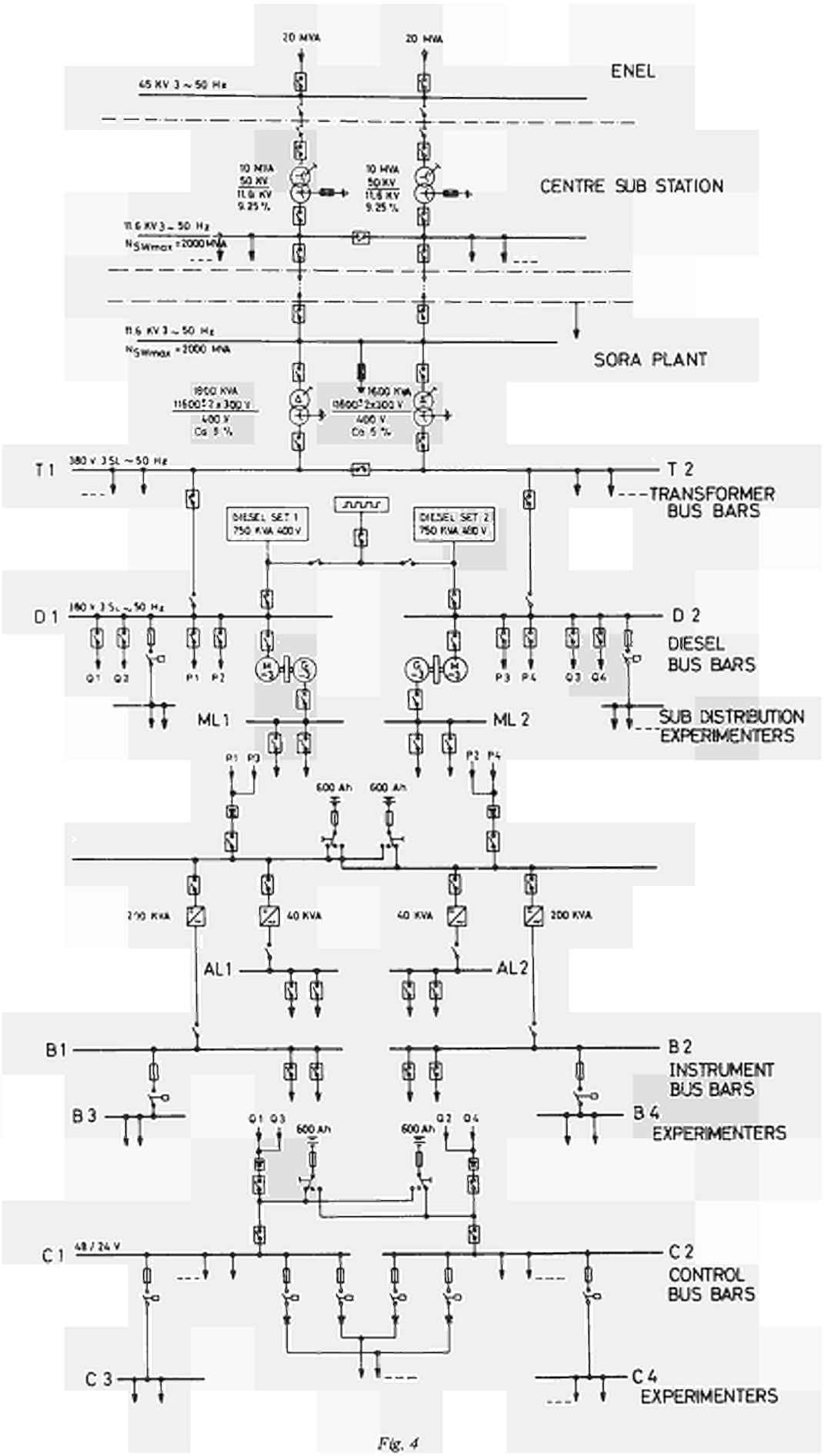
20 MVA
20 MVA
ENEL
45 KV 3 ~ 50 Hz
10 MVA
50 KV
11.6 KV
9.25 %
10 MVA
50 KV
11.6 KV
9.25 %
CENTRE SUB STATION
11.6 KV 3 ~ 50 Hz
N_{SWmax} = 2000 MVA
11.6 KV 3 ~ 50 Hz
N_{SWmax} = 2000 MVA
SORA PLANT
1600 KVA
11600/2x300 V
400 V
Cc 5 %
1600 KVA
11600/2x300 V
400 V
Cc 5 %
T 1
380 V 3 SL ~ 50 Hz
T 2
TRANSFORMER BUS BARS
DIESEL SET 1
750 KVA 400 V
DIESEL SET 2
750 KVA 400 V
D 1
380 V 3 SL ~ 50 Hz
D 2
DIESEL BUS BARS
Q1 Q2
P1 P2
P3 P4
Q3 Q4
ML 1
ML 2
SUB DISTRIBUTION EXPERIMENTERS
P1 P3
P2 P4
600 Ah
600 Ah
200 KVA
40 KVA
40 KVA
200 KVA
AL1
AL2
B1
B2
INSTRUMENT BUS BARS
B3
B4
EXPERIMENTERS
Q1 Q3
600 Ah
600 Ah
Q2 Q4
C 1
48 / 24 V
C 2
CONTROL BUS BARS
C 3
C 4
EXPERIMENTERS

Fig. 4

Absorbing material may be necessary in some operations, especially in TF-3, to avoid criticality on immersion in water.

The pulsation device would be handled through the same Truck Lock, using the crane to put it on a special truck.

Handling of the control rods and moderators will be done by means of a special transport container lifted by the main building crane through a hatch on the main floor and into the truck and brought to the outside handling cell or warm workshop.

Instrumentation and Electricity

Neutron Flux Instrumentation

A reference design has been elaborated. Work has started on the calculation of the overall behaviour and of the single components.

The Consortium has started the mechanical design of the plugs, containing the detectors.

An uncertainty is the total range to be covered by the flux instrumentation, since this depends on the start-up source, which has still to be defined.

Scram System

A preliminary document has been prepared with four alternative solutions, which are being subjected to a reliability study. The final system will be selected in the light of the study finding and other considerations.

Rod Control

A reference document was prepared but now needs to be adjusted, since the mechanical design of the rods actually adopted is widely different from the design on which the interblock system was based.

Sodium Circuit

A proposal for the sodium temperature control system was made to the Consortium.
Health Physics.

A proposal for the instrumentation to be installed to control stack activity was made to the Consortium.

Electrical Energy Supply

A detailed reference design for the total Energy Supply System has been elaborated and the work on the specifications of the single subsystems has just started. Fig. 4 shows schematically the reference design.

Buildings Installations

The Euratom reference design was presented to the Consortium. It consisted of a Reactor Building (RB) with Operation Building (OB) and Technical Annex (TA) located in a ~ 130° sector and bounded to the south by the Technical Gallery. The RB contained the active primary coolant system, part of the secondary system, the purification systems, the gas loops, the moderator loop rooms, and in addition hot cells for examination and handling of fuel after irradiation.

The Consortium claimed that such hot cells would be better located outside the RB. There would not be sufficient space or flexibility within the RB. It was decided to modify the fuel handling so that subassemblies would be simply stored inside the RB in an intermediate storage, and moved after a suitable decay time to the Handling Cell located outside the RB. In spite of those modifications it was necessary to increase the RB diameter from 30 to 33 m.

The RB was also modified to place the electrical rooms closer to it to give a more rational layout of control room, and to provide a suitable decontamination and controlled area. The TA was modified slightly.

The present SORA site is ~ 130 m a way from the site where test drillings were made in 1966. For this reason, and to answer more stringent requirements regarding earthquakes, the technical aspects of a new drilling program were agreed with outside contractors.

A study made by an outside consultant showed that the seismic characteristics of the site could be represented by a horizontal ground acceleration of 0.2 g, as far as the Design Basis Earthquake is concerned.

APPLIED INFORMATICS PROGRAMME

A. Gazzano

Starting at Brussels in 1959 with the creation of a research group on scientific information processing, the JRC has developed its activities in the informatics field since that time around relatively powerful computing facilities. Right from the beginning, the research workers had to face the necessity of generalizing particular methods and techniques and improving the means of communicating with the computers in order to facilitate their access to non-specialists. Having to face these necessities led to CETIS (Centre Européen de Traitement de l'Information Scientifique) in its present form. CETIS carries out the research program, in informatics and is also entrusted with managing the computing installations as well as the permanent task of general support and advice in computing methods and automatic data processing for the scientific and administrative units of the JRC.

Users' reaction to some of the CETIS teams' results in basic and applied software gave rise to the following general guidelines for the informatics activities to be developed at the JRC:

- public service activities which are of interest for all the countries of the Community;
- development of special programming systems and of software oriented towards general applications.

The topics are chosen in the light of such factors as: existence at the JRC of sufficient knowledge; direct needs of the institution; multinational character of the studies or activities; studies corresponding to a general interest in a specific field and whose nature or complexity justify a common effort and financing; studies corresponding to the needs of a considerable number of users and neglected by the software industry because of the relatively high capital cost and the difficulty of protecting the know-how; possibility of acquiring know-how in less exploited fields.

A layout of the budget (excluded personnel charges) and of the manpower allocated for the different actions of the programme is given in the following table.

Action	Budget (U.C.)	Man power (man year)
– computer program library	60.000	9
– data communication systems	9.000	2
– information science	51.500	5
– computerized management	96.000	6
– numerical mathematics	–	5
– programming systems	51.000	4
	267.500	31
– computing centre	1.750.000	36
Total	2.017.500	67

The staff employed on the 1971 activities was smaller than that approved by the Council of Ministers, the reasons being the numerous tempting posts available elsewhere in the Market and the cessation of recruiting at J.R.C. to replace posts left vacant by departures.

Apart from support activities, during 1971 work was done in the following fields: computer program library, data communication systems, information science, computerized management, numerical mathematics, programming systems.

Computer Program Library

Setting up of an automatic conversational system (called SIMAS) operated by video terminals, for the retrieval of information on programs and automatic printing of bulletins, newsletters and statistics. A first version of this system was already in operation at CETIS in 1971; an implemented version has been realized in collaboration with the software company SYNTAX Ltd.

Participation in the Study Group, Project 12 of the COST (Scientific and Technical Cooperation) Working Party on informatics; this Study Group was responsible for preparing a detailed project for a European Information Centre on Computer Programs which it is planned to set up at Ispra.

Data Communication Systems

Completion of the network for low-speed data transmission within the Joint Research Centre, consisting of terminals for Remote Batch as well as of conversational type and stations for automatic control of experiments, connected with the central computer in "time-sharing" mode.

Extension of the teleprocessing system controlling various types of terminals from the IBM 360/65 central computer. This system, which had been conceived by CETIS in 1967 and became operational in 1969, was improved in 1970 principally with regard to reliability and the number of terminals to be accepted. The extensions made in 1971 concerned the introduction of new types of terminals (including small computers), greater flexibility in using terminals, facilities for writing application programs, the aim being to extend the number of persons able to write programs.

Completion and installation of a concentrator allowing on-line connection of several automatic stations with the IBM 360/65 by means of only one "line adapter". This equipment, called system 130, was designed by the Electronics department at Ispra.

Preliminary study concerning an internal high-speed network (50000 baud) to be set up in 1972.

Contribution towards the planning and setting-up of a pilot experiment, with a view to building up a European network of large-scale computers. Ispra is envisaged as one of the nodes. The work has been done in the contex of COST (Project 11).

Information Science

The ultimate aim is to achieve an integrated system of automatic indexing translation, and interactive information retrieval; this entails a series of single studies which have a complementary function. The 1971 work included the following:

Completion of SLC-II system (Simulated Linguistic Computer). SLC-II is a special-purpose basic software for automatic natural language processing. Starting from a primary version used at CETIS for several years in connection with the Russian-English automatic translation system, the overall approach and methodology were completely redesigned to take into account the progress made in the last ten years both in computational linguistics and in computer science. The version of SLC-II for batch-processing was implemented and became operational by the beginning of 1972. The next step will be to produce the conversational version of the system.

Completion of the automatic indexing system, which assigns keywords of the Euratom Thesaurus to English abstracts of the nuclear literature. The system is in the second phase of development. In 1966-1969 an experimental system had been developed which showed that automatic indexing quality can be at least equivalent to that of human routine work. In 1970 a second version of the automatic indexing system was designed and then implemented in 1971; it uses a subset of the SLC-II, and will permit an evaluation of the indexing algorithms in a real-life environment with large collections. This system will be compatible with the Euratom Nuclear Documentation Systems (ENDS).

Computerized Management

Analysis of the procedures currently used at the JRC in the sectors having a general, technical or administrative service character, with special regard to the interaction between these services and the scientific divisions, as well as to the type of information which is generated, transformed and transmitted, and to its flow. This work was done in collaboration with "Metra International Co", Paris.

Completion and use of the ILS (Integrated Library System). ILS is an integrated system gathering into a single automatic procedure all the administrative work required by a library (renewal of subcriptions, control orders, control and recording of arrivals, lending services, budgetary control, editing of catalogues). ILS is operated in a time-sharing environment by means of video type terminals (CRT displays).

Completion of an integrated system for the JRC workshop.

This system was conceived in 1968 and a first simplified version has functioned since the second half of 1969.

The notion of integration is applied to the various technical and administrative functions of the workshop as well as to the connections with the other JRC procedures (accounting, inventory, etc.). The final version was put in operation at the end of 1971.

Numerical Mathematics

The aim of this action is study and research in various domains of mathematics and numerical analysis concerning theoretical problems, numerical methods of approximation and the development of algorithms and polyalgorithms, taking into account the possibility of interactive computer applications. The work done in 1971 included the following items.

In the field of partial differential equations, research was started on a class of free-boundary hydrodynamic problems in collaboration with Pavia University. A particular problem relating to the seepage of a fluid through a homogeneous porous medium was solved both theoretically (existence, uniqueness and regularity) and numerically.

In the field of linear algebra, algorithms were developed well suited for the solution of linear systems with large sparse matrices and band matrices. These algorithms optimize both computing time and memory occupation. They are of particular interest for solving elasticity problems by finite-elements methods.

In the field of numerical integration several algorithms were developed for multidimensional quadrature in regions such as cubes, spheres, simplexes, half-spaces. By using reduced points integration formulas, economies of up to 30 % CPU time were obtained in running complex programs in the field of engineering.

Several algorithms for data analysis (smoothing, numerical integration and derivation, fitting, minimization etc.) were developed and applied to γ-spectrometry, X-ray difraction, and neutron spectrometry problems. An interactive system was set up which permits analysis of experimental data with CRT graphic displays.

Programming Systems

The aim of this action is to devise flexible tools of general interest in order to facilitate communication between users and computers. The following work was done during 1971.

Implementation of LICE (Little Compiler and Executor). LICE is a single-user interactive programming system especially designed for research groups, which can solve small scientific or technical problems whilst shortening the compile-debug-edit-compile cycle. The system includes a FORTRAN-like language for algorithm description, a typical time-sharing command language, an incremental compiler and an interpretive executor. LICE is accessible from a remote terminal station, within the context of an existing time-sharing subsystem supporting a number of remote terminal stations. Conceived by CETIS, LICE was developed in collaboration with ITALSIEL Ltd. It has been operational since December 1971.

Implementation of CARONTE: The Euratom Modular Calculational System. In the middle of 1967, CETIS started to develop the CARONTE system, which had to be capable of controlling the automatic execution of a group of modules (taken from existing programs) and exchanging data between them. Though initially designed for reactor calculations, the system may be used with programs from different fields. The system, in its first version, was finished in 1969. The implementation made in 1971 concerns the extension of the library of code modules of CARONTE relevant to the nuclear field; the introduction into the system of a library of code modules for chemical molecular properties calculations; some developments in the organization of the system and in the control language in order to increase the execution speed and to make input data preparation easier. This work was done in collaboration with the software company PRAXIS Calcolo Ltd.

The next step will be the development of the interactive version of CARONTE. This work is planned for 1972.

Computer graphics. This activity was coordinated by a EURATOM-CNEN working group. The work done at Ispra in 1971 includes the analysis and evaluation of some existing systems, packages and languages for graphic processing; the design and realization of a graphic interactive version of CSMP (Continous Systems Modeling Program) on the IBM 360/65; and the design and implementation of a package (GRAF) offering Fortran programmers a powerful tool for communicating with the CRT graphic display 2250.

NUCLEAR MATERIALS PROGRAMME

N. Cadelli

The program has been developed partly on applied research in the field of reactor technology and partly on oriented basic studies.

The activity was grouped in the following actions:

- Fuel element behaviour
- High performance materials
- Radiation damage
- Fracture studies
- Direct hydrogen production.

A layout of the budget (excluded personnel charges) and of the manpower allocated for the different actions of the programme is given in the following table.

Action	Budget (U.C.)	Man power (man year)
– fuel elements	50.300	24
– direct production of H_2	49.900	14
– high temperature materials	35.000	13
– radiation damage	23.500	9
– deformation and fracture	6.500	10
– tribology	11.000	4
Total	176.200*	74

* plus 51.200 for big apparatus

Fuel Element Behaviour

An important part of the activity has been devoted to studying the behaviour of coated particles. Two irradiations of capsules have been made in the ISPRA-1 reactor to investigate the influence on the "amoeba effect" of parameters such as: surface temperature of the coated particles, temperature gradient, heat rating of the kernels. Post-irradiation examination of the capsules is in progress. A third irradiation has been prepared.

Two rigs containing 4 capsules each have also been irradiated in ISPRA-1 to obtain a correlation between fission product release and the number of defective particles. The capsules contained compacts with different amounts of defective coated particles. Burn-ups have been: 6140 MWd/tU at an average temperature of 1000°C, and 7000 MWd/tU at 850°C.

In the field of diffusion barriers an extensive investigation has been made to clarify the influence of the deposition conditions on the characteristics of pyrolytic silicon carbides. Temperature and linear deposition rate have been the two main parameters investigated. At the same time measurements of the physical properties of SiC have progressed.

Studies oriented towards Fast Reactor applications included irradiation, in the pool side facility of H.F.R. in Petten, of a two fuel pins capsule (of vibro-compacted UC powder and of pellets with a hole) to study swelling accomodation of UC under a heat flux of 800 w/cm^2 at 650°C and 1500°C respectively for sheath and central temperature. The burn-up reached at the end of the year has been 25.600 MWd/tU (the target being 50.000 MWd/tU for July 1972). The work to determine the influence of various fission products on the thermodynamic activities of U and C in UC as a function of temperature, has been pursued. Progress has been accomplished both for the preparation of samples and to improve the experimental device.

Studies on impact welding by use of variable magnetic field have been pursued and applied to welding stainless steel cannings for fast reactors in order to determine the best welding parameters and assess the applicability of the method.

In the frame of this action mention has to be made of the analytical support for burn-up measurements. After the isotopic determination on samples of Trino Vercellese fuel, already completed, measurements on enriched UO_2 are in progress.

High Performance Materials

An extensive work has been developed in the field of the alloys reinforced with Ni based fibers as materials for high temperature. Unidirectional solidification has been employed and showed promising results for the Ni-Ta system. Ternary eutectics have been examined during the year and their mechanical properties tested. Fracture modes have been analysed after cold and hot tension tests with the help of the scanning microscope. The examinations allowed a positive evaluation of the mechanical characteristics of Ni-Ni_3 Ta at high temperature. Similar analysis of other complex systems is in progress.

Studies on Va-Nb-Si alloys were limited, during the year, to the examination of their mechanical properties. Varying the aging temperature of the alloys mechanical resistance has been measured at 800°C and a heat treatment has been found which resulted in a slightly better mechanical resistance while maintaining a good ductility.

The studies on impregnated graphites have been pursued to find a composite advanced material as a potential cladding for fuel elements. Samples were prepared with different ceramics and impregnation and submitted to tightness measurements, thermal annealing and thermal cycling. The experiments allowed the choice of the most promising impregnation materials as, for instance, the SiO_2-MgO, Al_2O_3-CaO-ZrO_2 glasses which kept their tightness after 100 cycles from 900°C (and 1000°C) to room temperature.

Corrosion resistance of glass impregnated graphites has been tested in water and superheated steam (at 350°C and 600°C respectively). Measurements have been made of weight and dimension changes and of the tightness.

A rig has been prepared and tested to perform an irradiation of impregnated graphite samples in the HFR reactor at Petten. Other samples in capsules for high temperature applications have been irradiated in ISPRA-1 DIRCE loop. Post-irradiation examinations are in progress.

Together with these basic works the ability of impregnated graphite to act as fuel canning has been tested. Two fuel rods with UO_2 pellets, clad with impregnated graphite were irradiated in ISPRA-1 reactor, under water cooling. One rod could maintain its tightness up to a linear power of 250 w/cm. The planned post-irradiation analysis should allow definitive conclusions to be drawn.

Radiation Damage

The study of the behaviour of small inert-gas bubbles in irradiation environment was continued. A series of re-irradiated experiments was performed with Al foils. α-particles were used in successive irradiations of the Al foils and the same areas have been examined at different exposures. The contrast study of He bubbles in Al was extended to non-focused image conditions and it could be shown that under these conditions the bubbles' study was also possible in thick foil regions.

This technique will be applied to a final set of experiments, now in preparation, where thin as well as thick foil regions will be examined.

Fracture Studies

Dynamic in-situ studies of the deformation and fracture behaviour of metals such as Al, Al alloys and Zircaloy were initiated with the help of the scanning microscope. The tensile

straining device has been tested. Some modifications are planned to improve its performance.

Another activity has been pursued in the field of graphite mechanical behaviour to test the influence of geometrical parameters and to define what statistical distribution best fits the experimental results. Beside the well known influence of the volume, the results confirmed the importance of the surface of the samples.

Direct Hydrogen Production

The activity in this field covered studies on chemical cycles, on materials, on process engineering and on the development of analytical methods.

Concerning MARK-1 process, two phenomena have been studied: solubility of mercury bromide and decomposition of mercury oxide. Apparatus for both experiments has been designed and partly assembled. Moreover equilibrium measurements of the reaction of $CaBr_2$ with water have been carried out at 1000°K under 20 ata steam, making use of the quenching technique. The determination of K_p showed that equilibrium was not reached after a 4 h reaction. Kinetics measurements have been started at atmospheric pressure using a micropump and a preheater for direct injection of water in the furnace. Experiments varying the different parameters affecting the reaction rate are in progress.

Searching for chemical cycles for water decomposition, a simple cycle for the hydrogen sulphide decomposition has been found, which could be interesting in connection with the oil desulphuration processes. Studies on a new process based on chlorine, sulphur and iron chlorides have been started and experiments are in progress to find optimal reaction conditions.

Screening tests on potentially corrosion resistent materials have been made in hydrobromic acid. Static and dynamic tests have been carried out on Ta, Mo, Zircaloy-2 and Zr-Nb samples up to 3000 h. Non-metallic materials such as Al_2O_3, enamelled steels, or Teflon have also been tested for corrosion at 200°C.

As for process engineering, the reactor model which has been worked out for further test, is an hydrolysis reactor in adiabatic counter-current. The system should offer an almost complete change of $CaBr_2$ causing any major technological problem due to the use of a solution of $CaBr_2$ and ceramic material coating in the reaction column. At the same time the work on the $CaBr_2$-CaO phase diagram is progressing.

In view of the control of the different steps of the MARK-1 cycle, electrochemical methods for the analytical determination of $CaBr_2$ (in saturated $Ca(OH)_2$ solutions) HBr (eventually in presence of $HgBr_2$) $HgBr_2$ (in presence of $CaBr_2$ or HBr,) have been studied and led, in almost all cases, to satisfactory results. In order to determine the mercury concentration, an electrochemical method has also been tested. It appeared possible to measure concentrations of Hg lower than 10^{-4} in $CaBr_2$ by directly dipping an electrode into the solution.

Tribology

As a complement to the activity on materials some studies have been made on wear. Two lines have been followed. Firstly, two apparatus have been built to study wear effects under hot water and under high temperature gas or vacuum environment. The set-up of these apparatus included the construction of a special system for angular measurements.

On the other hand studies were carried out to measure vibration induced wear in fuel bundle assemblies. A special rig was used which permits operation in a hot water environment.

COMMUNITY BUREAU OF STANDARDS

H. Laurent

Preparatory Work in 1971

As a consequence of the Council Resolutions of 13 October and 17 December a temporary team was formed to list, with the aid of the national experts' "Advisory Group", the requirements and potential in the field of reference methods and substances. An initial survey was launched on two fronts:

a) to list the requirements for standard substances (chiefly of certified purity and/or composition);

b) to compile an initial draft for a European catalogue of the uses and availability of such substances, on the basis of information sent in by the national experts.

The Ispra team's work centred mainly on the first of these two tasks, and on the drafting of the Establishment's programme on standard substances and methods.

In the first quarter of 1971 numerous contracts were established with the Community firms and bodies concerned in this field, in order to decide how the survey should be conducted. Certain national oil, chemicals, metallurgy and pharmaceutical federations contributed their aid. Also in this first period, a joint study was begun, with CETIS, on computer programs to enable the results to be automatically analysed.

The definitive version of the questionnaire was approved by the Advisory Group at its second meeting, on 2 March 1971, and from then until mid-May some 3,000 questionnaires were sent out to 1556 bodies and firms.

Most of the replies come back between June and September, although a trickle continued to flow in up to the end of the year. By the end of July there were already enough replies to enable a partial report to be prepared, and its conclusions were submitted to the Advisory Group on 28 September 1971.

In view of the encouraging results obtained, it was decided to set up three Working Parties specializing in ferrous, non-ferrous and inorganic substances. These Working Parties, drawn from the Advisory Group and consisting of four or five national experts, with a secretariat of Ispra JRC personnel, were formed in the last quarter of 1971.

During the same period the Ispra team compiled the first version of a catalogue of the certified standard substances (CSS) available in the Community countries, together with a working paper summarizing the ideas on the production of a general catalogue and the possible creation of an Information Office in this field. In December a questionnaire was prepared and sent out, seeking supplementary information from the branches concerning the Working Parties, and meanwhile the final report on the survey was begun.

The more significant findings of this survey are summarized below.

The questionnaires were sent out to laboratories in the following industrial sectors: metallurgy, processing, chemicals, oil, pharmaceuticals, foodstuffs, hospitals and research institutes. The replies totalled 680 including 555 questionnaires, an average reply rate of 44%. The highest percentages were among the processing (61%), metallurgy (49%) and oil (50%) industries.

The laboratories that replied are basically concerned with quality control (288 replies), manufacturing control (272) and applied research (210); they purchase most of their standards from the USA. Of the 245 laboratories that are dissatisfied for some reason (supply difficulties, inadequate range of available CSS, lack of pressure, accuracy, purity etc.) 215 prepare their own standard substances.

The 364 laboratories who expressed CSS requirements did so as follows:

- 137 need CSS for metallurgical substances (usual ferrous and non-ferrous, light, refractory, ores);
- 123 need CSS for inorganic substances (pure substances, ceramics, gases);
- 147 need CSS for organic substances (pure substances, petroleum products, pesticides);
- 73 need CSS for pharmaceuticals (enzymes, vitamins, steroids, antibiotics);
- 57 need CSS for foodstuffs (colouring agents, preservatives);
- 63 need CSS for medical analyses (CSS for biological substances particularly need to be improved).

The methods of analysis most frequently mentioned as meeting new standard substances are spectrophotometry, gravimetry, titrimetry, followed by chromatography for organic substances and emission spectrography for metallurgical substances.

In the questionnaire the issue of standards for physical and mechanical properties was only touched on lightly, as a lead-in to a survey at a later date. Nevertheless 259 laboratories showed interest in this type of standard substance, thus expressing a definite lack in this field.

Numerous (256) laboratories said that they would be willing to help, within a coordinated project, in analyses and comparative measurements, or in preparing standard samples of certified composition, or substances with standard physical or mechanical properties.

PREPARATION OF A RESEARCH PROGRAMME ON ENVIRONMENTAL PROTECTION

Ph. Bourdeau, F. Geiss

In May 1969 a draft proposal for a research programme on environmental protection was submitted to the Council of Ministers as part of the 5-year programme of the Commission· (Document 350, Appendix 20). The Council did not take any decision concerning this document, but it granted 50.000 units of account to enable the Commission to make an inventory of certain non-nuclear activities in Europe. The Commission decided to explore the two fields: Environmental Protection and Standard Reference Materials.

As far as Environmental Protection is concerned, the mandate was carried out in two ways:

1) setting up an advisory group, whose members were selected jointly by the Commission's services, and by the official representatives of the member states of the European Communities;
2) by making a preliminary inventory of the research activities in the member states and other countries. This was done by visits to laboratories, interviews (about 40 of them) with scientists and research administrators, examination of reports and publications.

At first the list of laboratories and their activities in air and water pollution was presented as an annex to the 1st Communications of the Commission on "Environmental Policy" (Sec. (71) 2616, July 22).

The experiments of the Advisory Groups are:

Belgium:	Dr. A. Lafontaine, Institut d'Hygiène et d'Epidémiologie, Brussels, (Chairman).
France:	M.J.A. Ternisien, DGRST, Paris. M. Bovard, CEA (Paris).
Germany:	Dr. M. Buck, LIB, Essen. Prof. F. Korte, Universität Boon. Dr. U. Marckwordt, BMBW, Bonn.
Italy:	Prof. A. Liberti, Lab. Inquin. Atmosferico CNRN Roma. Prof. R. Passino, Inst. Ricerca sulle Acque CNRN Roma.
Luxembourg:	Dr. Keyser.
Netherlands:	Dr. M.F. Hartogensis MSZV Leidscheudam. Dr. P. Gootjes, RIV, Utrecht.

The group met on the following dates: 19 Jan.1971 (Brussels), 2 March 1971 (Brussels), 24/25 May 1971 (Ispra), 27 July 1971 (Brussels), 14 Feb. 1972 (Ispra).

It helped to prepare and finally approved a proposal for a 3-years programme in environmental research which became part of the official C.C.R. programme submitted in 1971. It initially covered some 150 scientific and technical workers, but was later reduced to 60 by the Commission.

At its meeting on December 21, 1971, the Council decided to extend for one year the 1971 programme with some modifications, including non-nuclear activities (in the form of "contracts" in the fields of Environmental Protection and Standard Reference Materials for a total of at least three and possibly four million units of account and a total of 215 people.

A detailed 1-year programme in Environmental Protection was then prepared on the basis of the three-year programme proposed for submission to the Advisory Group on Feb. 14, 1972. It includes a number of "studies" under the following headings:

1) Analysis and Measurement of pollutants.
2) Rathway of pollutants in the environment.
3) Effect of pollutants on man and his environment.
4) Pollution abatement technology.

5) System Analysis applied to pollution problems.
6) Data Centre on environmental chemicals (Data bank and "Registry" of environmenta chemicals, their fates and effects).

Two of the studies will be the Commission's contribution to Cost Projects 61a and 64b (Physico-chemical behaviour of SO_2 in the atmosphere and analysis of organic micropollutants in water), in the preparation of which we have taken an active part.

RESEARCH IN THE VARIOUS DIVISIONS

CETIS DIVISION

NUCLEAR STUDIES DIVISION

PHYSICS DIVISION

TECHNOLOGY DIVISION

ELECTRONICS UNIT

MATERIALS DIVISION

CHEMISTRY DIVISION

BIOLOGY DIVISION

COMPUTER GRAPHICS

INCREMENTAL COMPILERS

INTERACTIVE INFORMATION SYSTEMS

METHODS IN INFORMATION SCIENCE

SYSTEM ANALYSIS

INTEGRATED MANAGEMENT SYSTEMS

NUMERICAL ANALYSIS

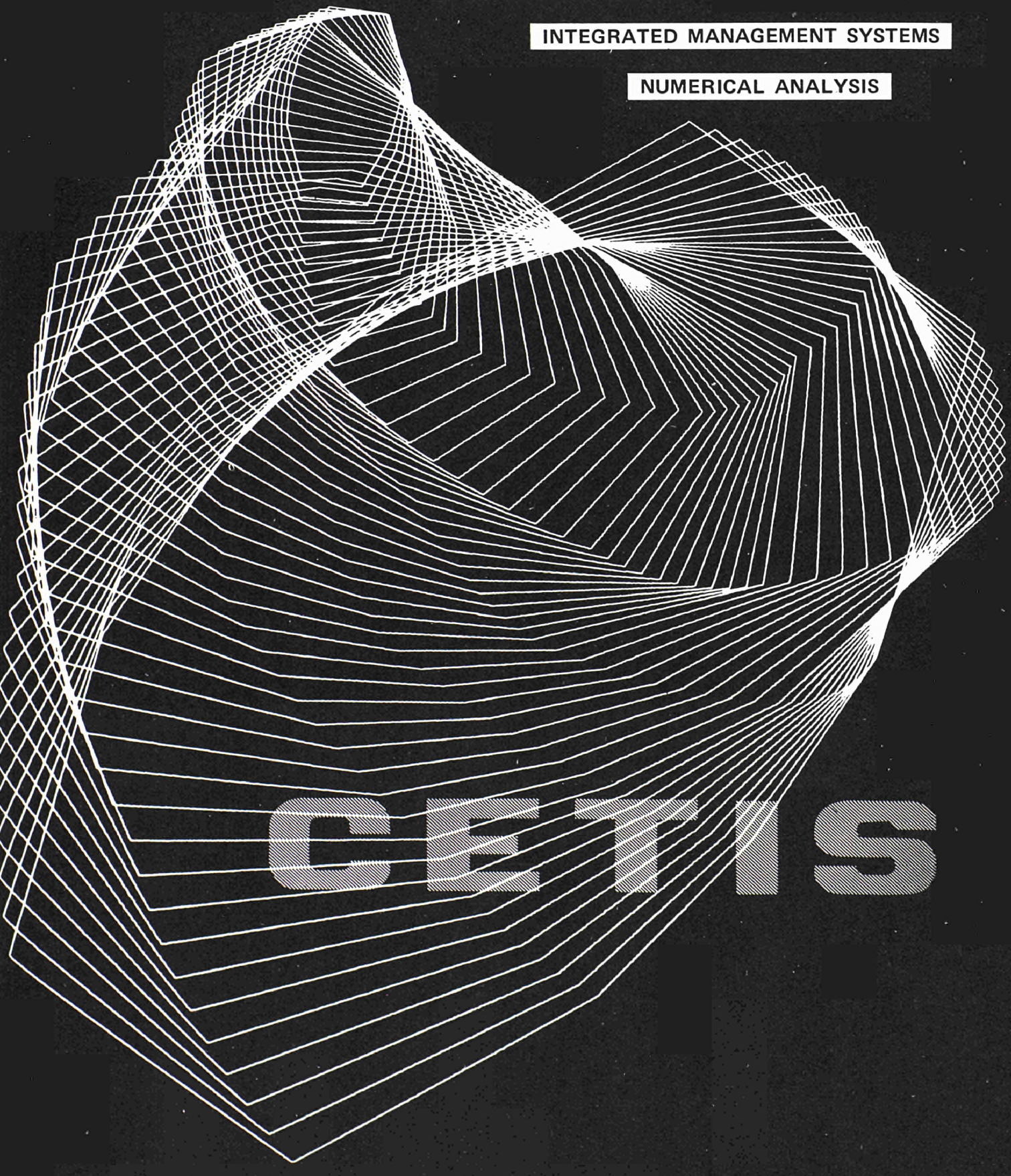

CETIS DIVISION

G. Pozzi

CETIS is concerned with the methods and techniques of automatic information processing, together with their applications to fields of activity of the various Commission departments.

This implies two complementary activities:

a) placing its skills and computing equipment at user's disposal for the solution of scientific and administrative problems. This involves management of the computing installations, maintenance of the available application software and analysis and programming work on request;
b) research into informatics in order to extend the range of methods and techniques for improving the man-computer interaction.

A certain amount of CETIS potential can also be made accessible, on request, to universities, organizations and enterprises of the Community by means of service-rendering contracts.

The present activity covers the following fields of applied informatics:

- Numerical Mathematics: development and application of numerical methods and algorithms concerning: linear algebra (in particular band matrices and high order matrices), multidimensional integration, ordinary differential equations, partial differential equations, function approximation. Work in the field of applied mathematics and statistics, strictly connected with the Institution's research programme, essentially covers the fields of fluid dynamics, magnetohydro-dynamics, structural analysis, experimental data analysis, process simulation.
- Information Science: the present activity in this field aims to employ the existing know-how for the creation of operational systems. Three such systems are being implemented: a generalized software package and programming language for natural-language processing (SLC-II Simulated Linguistic Computer), a fully automatic information storage and retrieval system (FAIRS), a Russian-to-English machine translation system.
- Administrative Data Processing: development of integrated systems for the management of certain general services of the Ispra Establishment (Workshop, Library, etc.).
- Programming languages and systems: definition and development of specialized languages and systems, to be used in particular in an interactive context.
- Program Library and Information Centre (COPIC): collection, study and distribution of computer programs in various scientific fields, advising on program utilization. A special effort has been devoted to improving the service by automating certain procedures. Information on programs is given by means of an automatic retrieval system (SYMAS) implemented on IBM 360/65 and using CRT displays. The storage and reproduction of programs are fully automatized.

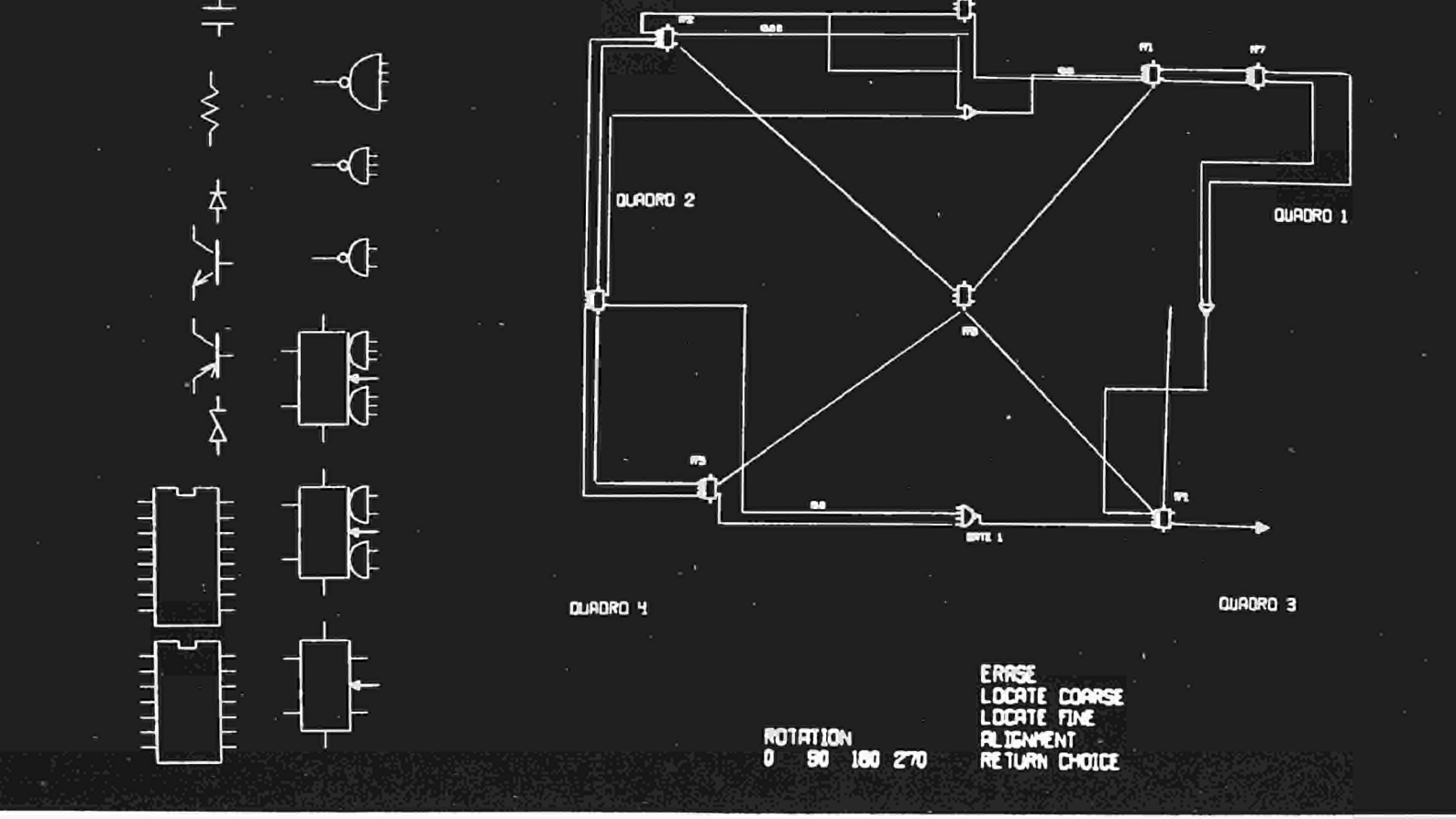

Interactive design of a logical circuit on 2250 IBM display.

SOME INTERACTIVE APPLICATION OF COMPUTER GRAPHICS

G. Di Cola, A. Endrizzi, L. Mongini

Introduction

The advent of the CRT graphical terminals has made a new dimension available in the field of interactive problem-solving.

They provide a means of displaying data and graphic forms at a very high speed which makes interaction quite efficient particularly in those cases where decisions can be taken only after the evaluation of a great amount of data in tabular or plotted form.

The user interacts with the digital computer by keying information at the keyboard or by touching elements of the drawing with a light-pen.

When using the light-pen each part of the displayed picture may be associated with a particular path which establishes the flow of the program.

The light-pen makes decision-making straightforward and accelerates human intervention enormously. It also provides a psychological advantage, for self-explanatory menus of options can be displayed, and correct actions may be performed even by an unexperienced user.

The existing graphic hardware is by no means satisfactory from the purely graphic point of view: quite simple graphic operations, such as insertion, deletion, line drawing and picture handling must be heavily supported by software.

The installation of graphical equipment based on an IBM 2250 display unit attached to the S/360 configuration of CETIS stimulated a certain research activity in the domain of computer graphic software and development efforts were made in a limited range of applications dealing with large numbers of users. Because of the advantages offered by this kind of interactive computing, general-purpose graphic software has been developed by CETIS system-programmers. This general software, accessible from high level languages, speeds up the programming of application problems and facilitates the management of data and programs, and information structure handling.

The application programs were developed keeping in mind the characteristics of the above-mentioned CRT graphic terminal use. To make efficient use of both man and machine the programs running on the computer graphic system were designed to have the following capabilities:

- rapid response;
- appropriate internal organization by means of built-in mathematical and graphic operators;
- simple on-line programming;
- easy data accessibility;
- direct user control;
- modularity;
- graphic I/O facilities.

In our own experience we have designed programs using the graphic facilities which may be quoted as examples of interactive computer graphics, in the following fields:

- continuous simulation
- circuit design
- experimental data analysis
- spectra simulation.

Interactive graphic version of S/360 continuous-system modeling program

In the field of the simulation of continuous dynamic systems, S/360 CSMP is a well established tool for investigating henomena that are the usual concern of engineers and scientists. S/360 CSMP is intended to satisfy the need for a problem-oriented program designed to prepare problems for solution on large-scale digital machines. It provided a basic set of functional blocks with which the components of a continuous system may be represented, and it accepts application oriented statements for defining the connections between these functional blocks. S/360 CSMP also accepts FORTRAN statements, thereby allowing the user to handle problems of considerable complexity.

Input and output are facilitated by means of user-oriented control statements. A fixed format is provided ffor printing selected variables in tabular form.

CSMP has been designed for batch-mode operation, which introduces some difficulties in the communications between the user and his problem. This interactive graphic version of S/360 CSMP provides the features for a flexible man-machine interface. Convenient means are available for maipulating the equations describing the model and for controlling the integrating process, by operation at a IBM 2250 display unit attached to a S/360 configuration.

To use this program the user should be well acquainted with S/360 CSMP but no further background is required. The grammar controlling the CSMP language has not been modified so that the programmer should not find any difficulty in communicating with his model.

The I.G. CSMP program starts by giving control to the CSMP translator which converts the CSMP model contained in the job deck into a FORTRAN subroutine. FORTRAN G compiler is called next to compile the output of the CSMP translator and all user's subroutines. Finally the linkedit program is called to generate an executable program. Messages appear on the screen signaling the execution of the three phases above.

If any error is encountered during these steps, control is given to the 2250 operator. He may look for the produced diagnosis, by page down page up operation at the displayed output, and he may update the input deck from the keyboard accordingly.

If no error is detected, I.G. CSMP enters the execution of the user's model. It displays the data decks contained in the input stream and the operator can update them, copy and generate new ones. In this way he defines one or a series of data containing different values for parameters, initial conditions, integration method, etc. and then he selects among them the runs to be executed.

The first time the integration processus is attached, the operator has to select the variable to be plotted against the x-axis and the variables to be plotted against the y-axis, and to define their lower and upper bounds.

While integrating, the program scales and plots the selected variables on the screen. At any instant the operator may stop the integration process by light-pen detect on the HOLD option, which enables him to request detailed information about the evolution of his problem and to modify the problem itself.

The following options are at his disposal for better analysis of the results:

- change the y-axis;
- make selected curves disappear and reappear;
- request the coordinates of displayed or blanked points and cancel them;

- change the variables to be plotted against the x-y directions;
- modify lower and upper bounds for better scaling of curves;
- display the history of the run in tabular format;
- display the minimum and maximum values of the variables;
- display the current values of the variables and parameters of the problem.

The user may also:

- modify the values of the parameters and variables,
- stop the execution of the current run,
- resume integration at the point it was interrupted.

At the end of each run the user is asked whether the program should keep the information relative to the executed run on a secondary storage for later display and comparison with other runs. Therefore the operator has to decide what to do next. There are the following possibilities at his disposal:

a) Execute a new run. In this case the program goes back to the definition and selection of the data to be processed.
b) Display previously stored runs.
c) Change the CSMP and FORTRAN statements describing the model and start a new analysis of the problem.
d) End of job.

At the end of the job a listing is produced that contains the CSMP output relative to all the executed cases.

The I.G. CSMP program communicates with the operator by means of messages and menus of options. It runs through its path automatically and only requires operator's intervention if essential. At any instant all options at disposal are displayed on the screen and decision is taken by light-pen detect on the selected option.

The text of the options is self explanatory, and the user should have no doubt as to procedure.

Alphanumeric information is introduced by keyboard operation. Numeric values can be written inside the specified fields in any of the I, F, E Fortran formats.

The following remarks outline some general information about the program. I.G. CSMP was programmed by introducing the graphic interactive facilities into the S/360 CSMP program by modifying its monitor-control routine and some subroutines of the execution phase.

Graphic forms and communications between the program and the operator are generated and controlled by the IBM Graphic Subroutine Package and by the GRAFI package that has been developed by the author to simplify the 2250's programming. Execution of the sample problem takes 176 K of the core memory but occupation may be further reduced if requested.

The facility that allows display of the results of the stored runs can also be used as a separate job to display and plot the results of previously executed S/360 CSMP runs.

Logical circuit layout

This program is intended to be the first step of a more ambitious project for interactive design of logical circuits. The aim is to create an interactive technique so that computer aid can become a working tool for the circuit engineer.

Some interactive techniques have been used for the drawing of logical circuit schematics in preparation for circuit analysis.

The system provides a large range of graphical operations oriented to the layout of logical elements and their connection. The position of all elements in the drawing can be freely chosen by the user to give the greatest clarity or the most pleasing appearence. This freedom is achieved by positioning nodes and components in isolation and then together.

The design of the data structure which contains the pictorial and the electrical description of the schematic is a most important consideration in meeting the objectives of the system. To achieve the high quality of display which is required, a large amount of pictorial information must be stored so that the user is free to arrange the elements of the schematic with the minimum of restriction. A data structure with good cross-referencing capabilities is needed, such as a ring structure.

To allow the greatest flexibility, the drawing process has been regarded as an editing operation instead of just the incremental addition of a new material, so that the user is free to go back and modify his earlier work.

The user builds up the schematics by using the light-pen to move symbols appearing in the menu (and, or, flip-flop, nand, etc.) to the selected positions. The positions may not be defined exactly: there is always the possibility of displacing an element by a certain amount, of rotating it and aligning it with other elements.

The connections are drawn by identifying the terminals of the elements to be connected by light-pen. Connections can be drawn in any direction, but special means are provided for rapid definition of a sequence of vertical and horizontal line segments. Such a sequence may be drawn by light-pen operations only.

Any point of the existing line may be the starting point of a connection.

The picture is usually redrawn completely for each addition of new material or for each deletion. Pictures appear almost instantaneously, the momentary flicker of the display serving as an acknowledgement of the user's latest request. Storing and retrieving pictures on secondary storage is also an important feature of this program, that allows circuits to be designed and/or updated in many work sessions.

The basic feature of the supporting file is that it should be easily interpreted by the program which performs the circuit analysis.

The program is composed of three parts: the first one is related to the library of symbols and to the displacement of elements; the second part refers to the connections between the elements of the circuit, the third part is devoted to the printing of titles and texts.

The library is composed of a maximum of twenty elements such as and, or, flip-flop, transistors, npn, pnp, etc.

Each element or graphic group (symbol, connection or text) may be identified by light-pen. The fundamental graphic operations on the symbols are: identification, translation and rotation, horizontal and vertical alignment, delete, derivation.

Thus the operator by means of keyboard, light-pen and macrooperations only, is able to construct the desired logical circuit on the screen.

Gamma spectrometry interactive data analysis

The most common gamma detectors such as the semiconductor or scintillator device are normally used in connection with multichannel analysers, which permit a great amount of data to be stored. Such data must be reduced and evaluated conveniently. For this purpose analysis techniques have followed a continuing development, in particular concerning possible applications in the typical problems of the gamma scanning of spent fuel elements, of the fission products measured after fuel dissolution, of the sample activation analysis, or, more generally of neutron activation data interpretation.

Interactive graphic data analysis allows a convenient and effective communication between the computer and the experimenter-user, in such a way that the latter always has control of the computational flow and may interact with the computer at decisive points of the program; this interaction has become possible by means of proper use of hardware and software, in particular by taking profit of graphic display, of keyboard and light-pen, and of specially studied (well suited) class of algorithms and computer subroutines.

The main features of a program for gamma spectrum data analysis are the photopeaks search, the computation of their characteristics (area, full width at half maximum, background, and uncertainty limits), and the determination of all the parameters necessary for any successive qualitative and quantitative requirements.

The GASIA (Gamma Spectrum Interactive Analysis) program allows analysis of a gamma spectrum and provides:

a) an interacting library of procedures which embody the analytical and computational techniques;
b) facilities in a conversational environment which permit maximum interaction between the user and the analysis mechanism;
c) interactive display subroutine with various graphical operations;
d) retrieval gamma spectra from a data-set library.

A GASIA user, seated at the console of an IBM 2250 video unit, may retrieve his spetrum data. He easily specifies a sequence of options by graphical operations, which allow different ways of attacking the problem, e.g., simple control calculation, choice of the model in the least squares fit, immediate graphical display and so on.

The design of this program is modular in the sense that additional capabilities can be easily added. Also the inclusion of more options and additional display modes is possible.

The subroutine library is based on well chosen numerical algorithms.

They perform:

- local smoothing by means of a least squares polynomial of low order (2 or 3) on a small segment (5, 7, 9 points) and/or global smoothing by cubic spline functions; computation of first few derivatives;
- peak location by means of channel grouping or by the method of the derivatives;
- peak characteristics computation;
- linear and non-linear least squares fitting of peaks with several algorithms.

Basic operation procedures of the GASIA program are as follows. At the beginning of each computation, by means of data supplied through the first display, GASIA retrieves the requested spectrum from the direct access data-set on a disk. The user may fix the display mode (log or linear), the limits of the spectrum range, its expansion. Procedures may be chosen according to the following sections:

I. automatic peak finding, which produces the smoothed spectrum, its derivatives and a list of the peaks and their characteristic parameters; if this list is not adequate, it could then be rejected and another attempt made to improve the results;

II. step-by-step peak finding; a few orders of derivative are displayed which allow the user to recognize the form of peaks (simple or composite) and to estimate visually the peak parameters; by light-pen detection it is possible to indicate the peaks which are of interest for the user;

III. peak data fitting; each peak may be fitted by means of gaussians with a polynomial and/or exponential background. The first step of data fitting process is the display which allows the selection of the appropriate form of the peak (single or doublet), the initial estimates of peak parameters; these may be chosen by the user by means of keyboard or identified with the results of section I. It is possible to analyse the same peak many times, utilizing the previous computations for improving the fitting.

IV. flow of program; the user may transfer the control of program by simple interaction and ask for intermediate or final results when he wishes.

Spectra simulation

The existing programs, related to the spectra simulation problem, are at the moment mostly concerned with the theoretical reconstruction of magnetic resonance spectra, that is Nuclear Magnetic Resonance (NMR) and Electron Spin Resonance (ESR) Spectra.

These existing programs are, to our knowledge, non-interactive and the display of the spectrum is obtained on some data plotter. We believe that an interactive method with utilisation of a display unit can be very useful and suitable for both NMR and ESR spectroscopy, although for the moment we have only been interested in the problem of the theoretical reconstruction of ESR spectra obtained in liquid phase.

In this case the input data have to be modified until the theoretical spectrum becomes equal to the experimental one. The process requires for every iteration the examination of the obtained theoretical spectrum, followed by the formulation of new hypotheses about the radical. For these hypotheses it is necessary to take into account the previously obtained results. A good level of chemical intuition together with a knowledge of many experimental facets of spectroscopy is required of the operator, whose intervention is hence always necessary.

In view of these considerations, and in order to give those interested in ESR spectroscopy in liquid phase a powerful tool for their job, we have developed an interactive system of programs, MOLP, which starting from a very small set of data about the paramagnetic molecule, is able to calculate the coordinates of the molecule, hence the isotropic hyperfine coupling constants and, from these constants, the theoretical ESR spectrum. CARONTE [1], a processor able to control the automatic execution of a sequence of interdependent programs, supervises the entire described job and allows for data transmission between the programs of the sequence, every of which can be also executed independently.

In this system, all input data for the execution of the sequence of calculations may be given from the keyboard of an IBM 2250 Unit and at nearly every step the operator can intervene to correct data or restart from the beginning of the sequence.

There are at the moment six modules included in the system. In the more complete case their sequence is the following:

(MB2250 – PLOTMOL – CNINDOV – SPIN – ESR2250) CALPLOT

The parentheses indicate that the first five programs are executed, in sequence, several times, until the obtained spectrum is satisfactory. At this moment the operator can obtain the exit from the loop and a copy of the spectra stored on disk on another unit for the Calcomp Data Plotter. Obviously the operator can choose some other sequence of programs. For instance it is possible to eliminate the first program if the coordinates are known. Also if some idea exists, with sufficient approximation, of the distance between the peaks of the spectrum and their relative intensities, only the last program ESR2250 need be utilized.

Fig. 1: An experimental E.S.R. spectrum of Ethyl Radical (second derivative).

Let us now consider the different programs of the system is some detail.

MB2250 is the program MBLD (standard Geometric Models and Cartesian Coordinates of Molecules) [2] deeply modified for utilisation with the IBM 2250 display unit and insertion in the system.

This program, from a minimal set of data, which in the present version may be completely given by the 2250 unit, calculates the Cartesian coordinates of all atoms in the molecules. All the bonding information necessary for the definition of a molecule is given by drawing the structure of the molecule on the cathode ray tube.

Once calculated, the coordinates are utilized by the programs PLOTMOL (for the display of the molecules on the screen of the CRT) and CNINDOV. This program is the CNINDO [3] program with minor modifications for its inclusion in the system. The program calculates, among other things, the unpaired valence S electron on the different atoms of the molecule or s orbital spin densities.

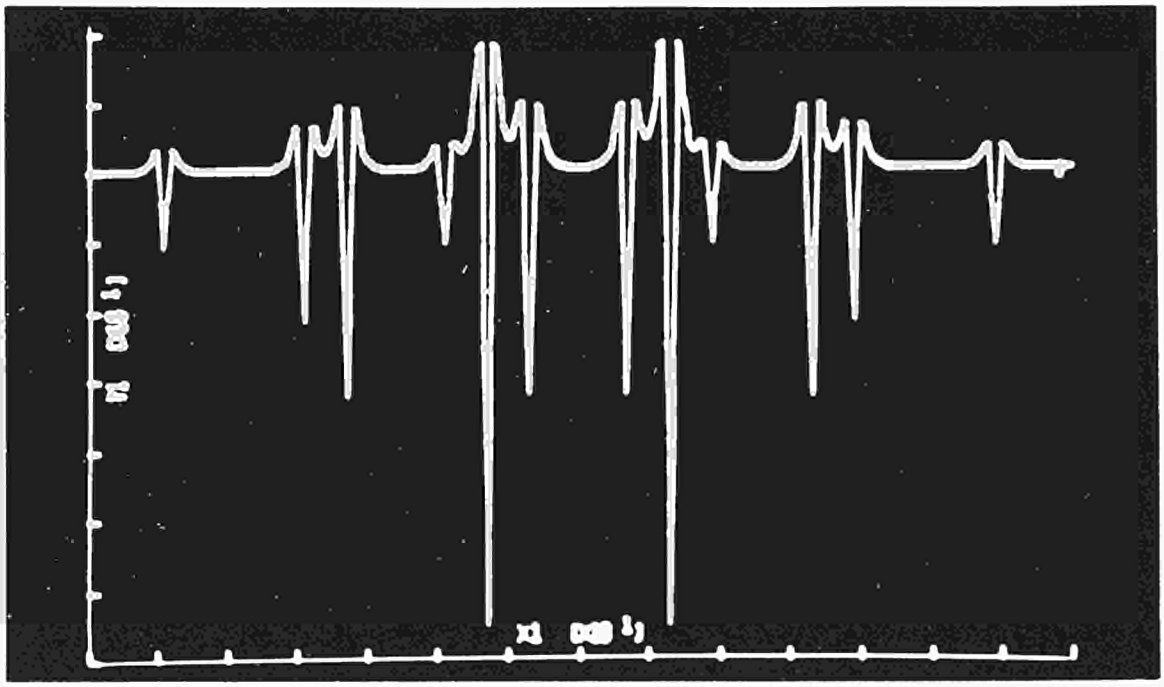

Fig. 2: Theoretical reconstruction of the E.S.R. spectrum Ethyl Radical (second derivative) on the IBM 2250 Display Unit.

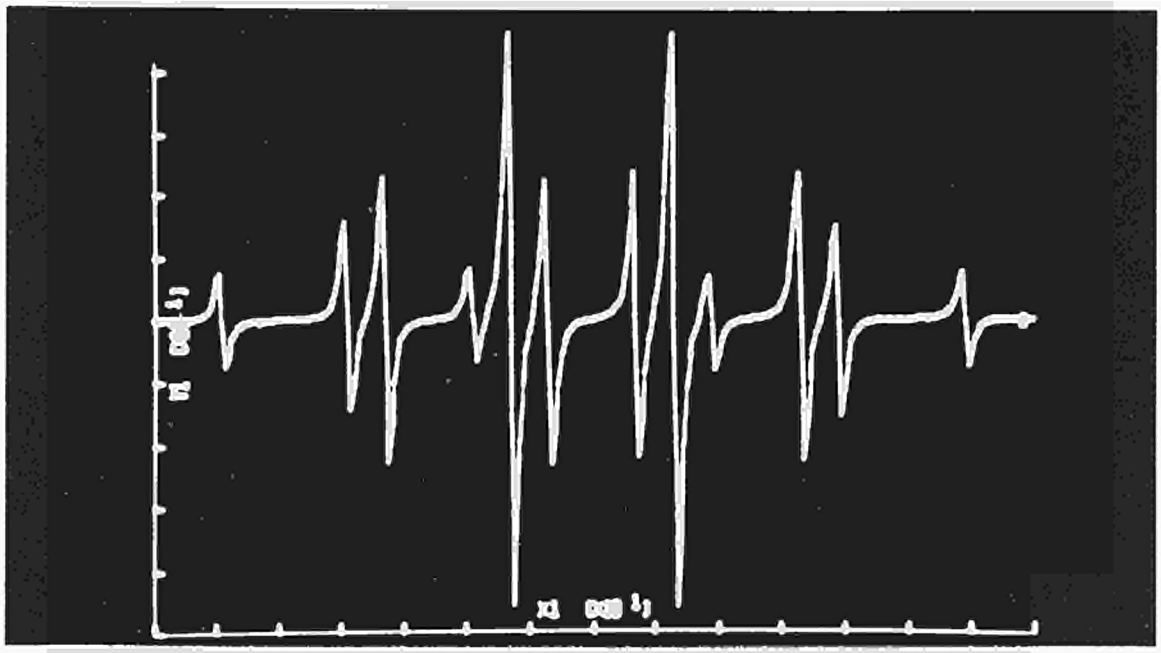

Fig. 3: Theoretical reconstruction of the E.S.R. spectrum of Ethyl Radical (first derivative) on the IBM 2250 Display Unit.

The spin densities are used by the next program SPIN for the calculation [4] of the hyperfine coupling constants, determining the distances in gauss between the peaks of the ESR spectrum. SPIN also prepares other input data for the subsequent program ESR2250 which calculates and displays the ESR spectrum [5].

The display of the theoretical spectrum can be obtained on the screen as a delta function, or as a Lorentzian or Gaussian absorption curve, or as the first or second derivative. Figs. 1 and 2 show respectively an experimental ESR spectrum of ethyl radical [6] and the CRT theoretical reconstruction (second derivative). The experimental spectrum is obtained by electron irradiation of ethyl ether and the theoretical reconstruction is obtained with Lorentz line shape. As one can see, a satisfactory agreement is reached concerning distances between peaks and relative intensities.

In Fig. 3 the CRT image of theoretical reconstruction of the ethyl radical spectrum (first derivative – Lorentz shape) is shown.

The above described system can of course, be extended by addition of more programs. By this means the computation of other atomic and molecular properties and also the choice between different computational methods will become possible. Modifications are planned in order to run the entire system with a different type of display unit in time sharing mode.

References

1) G. Buccari, G. Fattori and C. Mongini-Tamagnini, CARONTE – The Euratom System for Automatic Control of Linked Calculations, *Proceedings of Conference of the Effective Use of Computers in the Nuclear Industry*, April 21-23, 1969, Knoxville, Tennessee – U.S.A.E.C., Report CONF-690401, pp. 297-303

2) M.S. Gordon and J.A. Pople, MLBD – Standard Geometric Models and Cartesian Coordinates of Molecules, Program 135, *Quantum Chemistry Program Exchange*, Indiana University, Bloomington, Indiana

3) Paul A. Dobosh, CNINDO: CNDO and INDO Molecular Orbital Program, Program 141, *Quantum Chemistry Program Exchange* Indiana University, Bloomington, Indiana

4) According to John A. Pople, David L. Beveridge, Approximate Molecular Orbital Theory, McGraw-Hill Book Company, New York 1970, Chapter 4.3.

5) L. Mongini, C. Thonet, A program for theoretical reconstruction of ESR spectra, EUR Report (to be published)

6) G. Juppe, R. Fantechi, G.A. Helke, Elektron-Spin-Resonanz-Untersuchungen von durch Elektronenbestrahlung erzeugten Radikalen aus organischen Einschlussverbindungen, EUR 4223, 1969.

7) A. Endrizzi, GRAFI, A package for programming the IBM 2250 display unit, EUR 4789 (1972)

8) A. Endrizzi, Interactive graphic version of S/360 continous system modeling program. To be published EUR

9) L.B. Smith, PEG, An Interactive Least Squares Data Fitting Program

10) J.W. Frazer, L.R. Carlson, A.M. Kray, and M.R. Bertoglio, On-Line Interactive Data Processing.

LICE – AN INCREMENTAL COMPILER AND EXECUTOR

J. Pire

Introduction

Definition of the language and tests of the programs were done by the CETIS. The compiler-executor was developed by a software company (ITALSIEL S.p.A., Rome) under contract. The exhaustive tests were done with the aid of Mr. Buccari and Mr. Daolio.

LICE is a single-user interactive programming system especially designed for research groups, who can solve small scientific or technical problems whilst shortening the compile-debug-edit-compile cycle. The system includes a FORTRAN-like language for describing algorithms, a typical time-sharing command language, an incremental compiler and an interactive executor. LICE is accessible from a remote terminal station, within the context of the time-sharing subsystem developed by CETIS to support remote terminal stations connected to the IBM 360/65. Special emphasis has been given to optimization of the edit-debug cycle. Statement deletion or modification, label insertion, variable or procedure redefinition, monitoring of variables and execution of transient statement are amongst the various features. The status of a problem, interpretive string, variable storage and tables, can be saved for subsequent use in a two-level file-system. Source language strings are not saved, but may be reconstructed, upon command, from the interpretative string. LICE was completed in 1971 and now is normally used by IBM 2741 terminals available to several of the Ispra JRC divisions.

Design criteria

The system was designed to facilitate the debugging and execution of small scientific programs submitted by non-experienced programmers optimizing the response time and giving the user the opportunity to follow the logical steps of a computation.

Particular attention has been dedicated to this kind of user. He requires an easy flexible programming language, a "natural" command language and facilities for storing problems in a file system, which is accessible for further execution, redefinition or deletion and protected against unauthorised use.

Also, the user requires to redefine simple variables, arrays, strings and statements at any stage of the computation without re-compilation of the text previously compiled and executed. In addition he requires to link and execute with his program external procedures written in other programming language, which is a more flexible approach than having complex operators.

The limited amount of code space (18 k bytes for the system and the user area) dictated many of the design decisions.

The design criteria are the following:

a) compilation is incremental (in particular, syntax errors are noted as soon as the line is entered);
b) redefinition of variables, arrays or strings is allowed at any instant;
c) compilation time has to be short because correction of declaratives may require symbol table manipulation;
d) the execution of the program does not require heavy "linking" in order to facilitate rearrangements of the memory, closing gaps, removing deleted lines, etc.;
e) extensive run-time diagnostic aids are available;
f) shorthand notation is adopted when possible;
g) language specifications are "open" to fit new requirements. For this reason the grammar of the language is described in list structure form.

The environment

A time-sharing subsystem which has the ability to handle several remote terminals (model 2740 and 2741 teletype writers, IBM 1050's, etc.) has been designed and developed by CETIS. Within this system programs do not interface directly with the partitioned static version of OS 360. They are "time-sliced" and "swapped" within a particular partition dedicated to conversational programs. LICE system allocates 18 k bytes of this partition and uses overlays to perform less urgent functions (like diagnostic message emission).

In the current version, LICE is a single-user programming system, but provisions are made to extend its capabilities to serve many users.

Also, LICE design is largely invariant with respect to the environment. As previously stated, LICE is designed to work under the control of the EURATOM time sharing system but may be introduced into any system provided with the correct interface.

The file-system used by LICE has a directory of headers. Each header describes a permanent file containing the status of a computation previously stored at user's request.

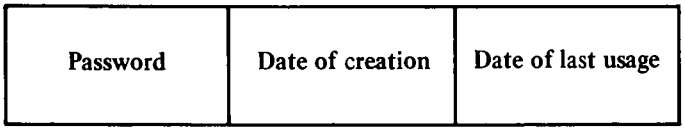

Fig. 1: Header of a file-system program.

The password is composed of two keys. The relative position of the header in the directory allows the system access to the subfile which allocates the stored program.

The first key of the password is necessary to execute the program, but storing, deletion and replacement require the complete password.

Processor Characteristics

When a user gains control of LICE, he gets the following question back:

EXEC FILE ?

and a working file is allocated to the remote terminal station. From this point on, the user can enter an old problem previously stored in the working file or in the permanent file system or can create a new program, typing in statements of the programming language. Each statement is preceded by an asterisk followed by a line number and a space. These characters are automatically printed by the system.

Unless otherwise specified, the system compiles and executes directly, statement by statement answering with diagnostics or results. This feature allows the user to enter complicated arithmetic expressions for immediate execution. Also statements can be typed in for deferred execution. In this case only compilation occurs.

Corrections are allowed at any level of computation. This implies that, when the execution phase terminates, the state of variable storage is preserved as well as the object code and symbolic tables.

The programming language

The source language is a FORTRAN IV dialect with the addition of some string manipulation capabilities. All the statements, except assigment statements, are preceded by a special character ($) followed by a keyword. During syntax analysis, backup is not required, which allows considerable economy of core space. The main difference between LICE and FORTRAN IV are described in the following paragraphs.

Program Structure

A LICE program is a set of data and procedure declarations plus a set of executable statements (Main Program). Procedure declarations may not be nested and do not necessarily precede their use. Array declaration must precede the use. The scope of declaration is the LICE program, except for dummy arguments and statement labels. The Main Program must be considered open, in the sense that a new executable statement is appended to it, even if it is preceded by procedure declarations.

Declarative Statements

They associate explicit attributes to variables, dummy arguments, array and procedures. LICE features are: type declaration, INT, FLOAT, LOG, STR, statements, dimension declaration, DIM statement, procedure declaration, FUN, SUB, EXT statements. The arithmetic statement processor considers integer and floating variables as a unique type variable. Thus mixed arithmetic is allowed, wherever an arithmetic expression can appear. Also, type matching between arguments is valid if they are respectively integer and floating or vice-versa. One, two, and three-dimensional arrays are accepted. Subscripts can be generalised arithmetic expressions. Implicit FORTRAN-like declarations are allowed.

Substring designators

The name of the string is followed by two arithmetic expressions; the former specifies the relative positions of the substring into the string., the latter specifies the substring length (in characters).

Assignment Statements

The logical and arithmetic assignment statements are quite similar to the corresponding FORTRAN statements. The string assignment statement operates catenating strings or substrings specified at the right of the equal sign and assigning the resulting string to the left member of the statement. A special type of assignment statement results in an integer value after searching for a substring into a string. This value assigned to an integer variable is the position of the first character of the substring in the string if the substring is found and 0 otherwise.

Execution Control Statement

Execution control statements are FORTRAN-like. Thus, we have GOTO (unconditional and computed), IF (arithmetic and logical), CALL, RETURN, DO, CONTINUE.

Input-Output Statement

Unformatted READ and WRITE provide the system with input-out capabilities. Data are converted into the type of corresponding list element. The output report is in standard format.

The Command Language

The command language is very simple and mnemonic. Its grammar is based on key-words which give a distinctive character to each command. Many commands require some dialogue between the systems and the user before producing their actions. This dialogue is typical of a time-sharing environment.

Execution Control Commands

Specific imperative statements are:

WAIT: delays the execution of the statements following in chronological order. The normal mode of execution is "direct". The "wait" status is forced automatically by the system in the following circumstances:

a. when the user enters program modifications;
b. during procedure definition, when a specific call is not active;
c. when statements like GOTO or IF require an undefined statement label;
d. after a call of a not yet defined procedure.

The automatic "wait" status is reset when the condition which caused it is no longer active.

RESUME: commands the execution of the piece of program types in after the WAIT command.

RUN: activates the execution of a set of program lines. This command permits of executing parts of a program in an order which has no relation to normal execution of the whole program, or executing blocks of program with no programmed interconnection (no IF, no GOTO) taking every time a decision on what is to be done now, depending upon the results just in hand.

File-System Command

These commands require some dialogue with the user. He must declare the password to the system in order to store, delete or replace a program file.

If he requires the execution of a program file, the first key of the password combined with the file number is necessary. This file number is given back by the system at storage-time.

The principal commands are the following:

NEW: clears working space and prepares the system to accept a definition of a new problem;

OLD: valid only as an answer to the request "EXEC FILE? " is useful for recovery purposes. This command loads the program into the core together with its status from the working file associated with the station;

USE: enters the file-system to retrieve a program of a given identification code.

The commands SAVE, DELETE, and REPLACE have obvious meaning.

Debugging Facilities

The user has at his disposal a set of debugging facilities capable of giving him a complete check on the problem program. He can use special operator's commands and correction procedures.

In addition he can obtain a list of his source program, preceded by a dictionary of referenced variables.

Special operators are slash and asterisk which can be typed in before any executable statement.

Specially, slash is allowed only before assignment statements and produces the effect of displaying the assigned value. Asterisk specifies a statement which must be executed and then deleted from the program file. It could be used for variables initialization, procedure calls, etc.

Special commands are:

TRACE: This command is generally followed by a list of line number specifications. It assigns a monitor operator to any statement of the list.

TRACE has the same effect as if a slash has been typed before the statements specified in the list.

UNTRACE: has the opposite effect.

An important facility is the LIST command. It produces two separate listings. From the symbol table it generates a dictionary of referenced variables, from the interpretative string and the symbolic tables it produces a resequenced source program listing.

This report reproduces the source text with the following changes:

- variable declarations and transient statements are not listed.
- two consecutive tokens are separated by one space.

Finally, the text can be modified by insertion or deletion of statements, by insertion of labels, by removal of pieces of text. New declarations replace previous declarations of the same quantities. Where ambiguity is possible the dummy arguments must be qualified with the corresponding procedure name. Declarative corrections imply that a recompiling activity must be activated especially when the correction regards procedures. This is because the system even allows modification of the header or the tail of the procedure only.

SIMAS – AN INTERACTIVE INFORMATION AND MANAGEMENT SYSTEM FOR A COMPUTER PROGRAM LIBRARY

G. Gaggero, C. Mongini-Tamagnini

Introduction

The tasks involving a Computer Program Library can be summarized as follows:

- the various programs have to be collected, together with an exhaustive description of their scope, characteristics, performances and acquisition conditions;
- bulletins containing the lists and selected information of the programs contained in the library, subdivided according to convenient categories, have to be prepared and distributed to the users in a selective way;
- on request more refined information has to be supplied to the users: this can consist of detailed information concerning a given program, or in the list and description of the programs having given characteristics;
- statistical analyses concerning the various programs contained in the library have to be performed and distributed periodically;
- the program(s) requested by a user have to be reproduced and dispatched, whenever it has been checked that the user may in fact have access to the program(s) he asks for. Appropriate letters to the requestors must be prepared, whether the program(s) are available or not;
- all the requests made to the library concerning information on programs and reproduction of programs have to be recorded, so that periodical statistical analyses of the actual functioning of the library can be prepared: such analyses will later provide an important feedback to the management staff.

As soon as the number of programs dealt with becomes rather high, the performance of the various processes in which a library is daily involved for handling the above tasks and coping with different customers requests can become quite a burden.

To automate and speed up such processes an automatic system, called SIMAS (Software Information Management System) was planned and implemented [1] at CETIS, with the aid of Mr. H.I. de Wolde, and backed up with contract work by a software company (Syntax S.p.A., Milan). The system, written in Fortran IV and Assembler language, is operative on the CETIS IBM 360/65 computer, and is utilized at the CETIS Application Program Library. In the following paragraphs we describe the overall structure of the SIMAS system, the files on which it acts, and finally the flow of operations of a library through the automatic SIMAS system.

The automation of the procedures

The first step towards the automation of all the processes described in the introduction consists in setting up an automatic tool capable of memorizing and updating on a suitable support directly accessible by the computer (disks, tapes) the programs collected by the library (source program, input data, etc.), their descriptions (program abstract, computing characteristics, etc.) and the reception information (name and establishment of the supplier, date, name of the program, availability conditions, etc.).

The second step consists in setting up an efficient automatic system that can retrieve and reproduce the requested programs after a check on the availability, retrieve and edit (periodically or on request) the program descriptions, and record on a convenient support information on the various requests (name and establishment of the requestor, date, type of request, etc.).

Finally, the last step is the setting up of a program that can do a statistical analysis of the receptions and request details.

The following scheme summarizes the ensemble of operations:

Reception of programs and program descriptions	– Memorization and updating of reception information – Memorization and updating of program descriptions – Memorization and updating of programs
Request of programs and program descriptions	– Memorization of request information – Retrieval and editing of program descriptions – Availability check and retrieval-reproduction of programs
Library management	– Analyses of statistical type on reception and requests

The SIMAS system provides for the automation of all the described operations.

The files of the system

The information to be recorded on peripheral storage in order to set up an automatic management system concern the following subjects:

a) description of the associates (i.e. the establishments which supply and/or request library material;
b) information on reception and requests;
c) description of the programs;
d) the programs themselves.

Let us now describe in some detail the structure of the above information and the related files (stored on disk memory).

Concerning point a) three files are created (and updated) called Associate Alphabetical File (AAF), Associate Master File (AMF) and Associate Inverted File (AIF).

The AAF contains the names (acronyms) of the associates (in full characters and codified), each followed by a pointer to the corresponding location on the AMF.

The AMF contains for each associate the corresponding full address.

The AIF contains a list of keywords, relating to the type of establishment (private company, research laboratory, etc.), the countries of location, the application domains of special interest, each followed by the pointers to the corresponding associates in AAF.

Concerning point b) two files are created (and updated), called Reception File (RECF) and Request File (REQF).

The RECF contains, in codified form, the following information: acronym of the supplier, date of reception, name of the program, type of material supplied (program and/or program description), restrictions concerning the distribution of the program.

The REQF contains, in codified form, the following information: acronym of the requestor, date of request, type of request (a program, the description of a program, the list of the programs matching given characteristics, i.e. characterized by given keywords), name of the requested program or the list of keywords, whichever is pertinent.

Concerning point c) five files are created (and updated), called Program Alphabetical File (PAF), Program Master File (PMF), Codified Master File (CMF), Program Inverted File (PIF), and Thesaurus File (TF). The PAF contains the names (acronyms) of the programs (in full characters and codified) each followed by a pointer to the corresponding location on PMF or CMF, and a pointer to the corresponding location on PDF (see point d).

The PMF contains for each program the description in full characters, i.e.

Source	author date of development . . . . .
Purpose	problem solved limitations . . . . .
Software Information	operative computer programming language . . . . .
Availability	acquisition conditions, use conditions

The CMF contains the same information items as the PMF, but given in codified form,i.e., through the use of pointers to the pertinent keywords in TF. The PIF contains the list of the keywords, each followed by the pointers to the corresponding programs in PAF.

The TF contains the list of the keywords in full characters, each followed by a pointer to the corresponding location on PIF.

It must be noted that the reasons for which the creation of a TF was felt to be useful is that whenever a conversational mode is used to gain access to the files, the possibility of selectively consulting the thesaurus of keywords must be considered.

Clearly the conversational use of SIMAS requires the pertinent files to be on-line. No problem arises in keeping the files on-line except for PMF, which can exceed the available on-line memory capacity. For this reason it was decided to create a CMF to be always on-line. The information on a given program will be obtained, when working in conversational mode, by a decodification of CMF through the use of TF.

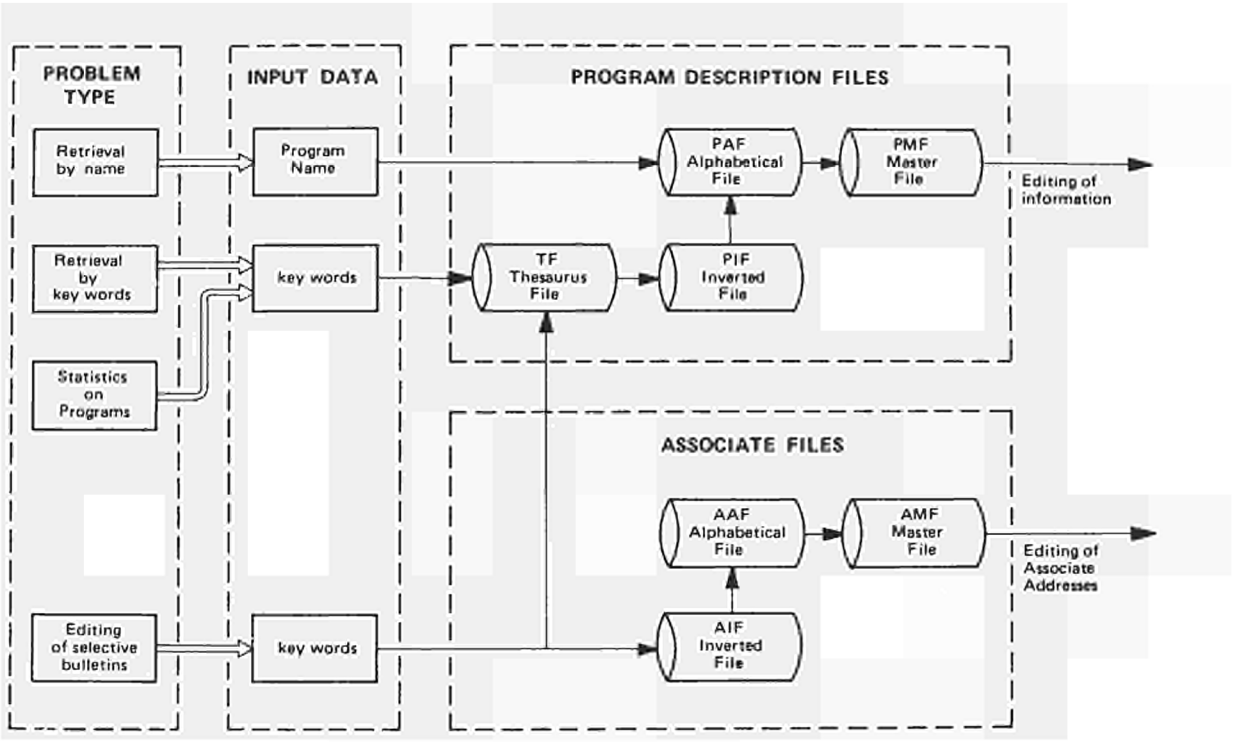

Fig. 1: Flow of retrieval operations.

Concerning point d) two files are created (and updated), called Program Directory File (PDF) and Program Deck File (PDKF).

The PDF contains for each program the description of the corresponding package which may consist of the following components: write-up(s), source deck, object deck, overlay structure, sample case(s), sample output(s). In the PDF, for each component, an indicator specifies the presence or not of the corresponding material, followed whenever pertinent by a pointer to the corresponding location on PDKF.

The PDKF is a partitioned data set whose members contain the various components of the package, with the exception of the write-up(s) and output(s).

In addition to the above-described files, the system uses some other work files, whose description is omitted for the sake of simplicity.

The System SIMAS

The information concerning points a), b) and c) of the previous paragraph is supposed to be supplied to the library through the use of convenient form-sheets to be filled in by the supplier/requestor. Such sheets are in a form ready for punching.

The SIMAS system is capable of creating and updating the described files starting from both this information and the programs themselves (cards or tapes).

We shall now describe the ways in which the system operates to retrieve the various information stored on the files.

The processes of retrieving and editing information from program description files are described first. The files containing the description of programs are addressed for retrieving purposes in the following circumstances:

1) answering specific questions concerning the description of one given program;
2) answering questions concerning the list and description of programs characterized by given keywords;
3) editing certain types of statistics concerning the collected programs;
4) editing of periodical selective bulletins containing the list and a short description of the programs.

In diagram 1 the flow of retrieval operations is shown in detail; it is to be noted that in cases 1) and 2) SIMAS can operate both in batch and in conversational mode by using CRT terminals (IBM 2260). This part of SIMAS is derived from an experimental system (SIRIUS) [2) 3)] developed at CETIS, only capable of acting on a very limited number of programs (4000), and much less flexible.

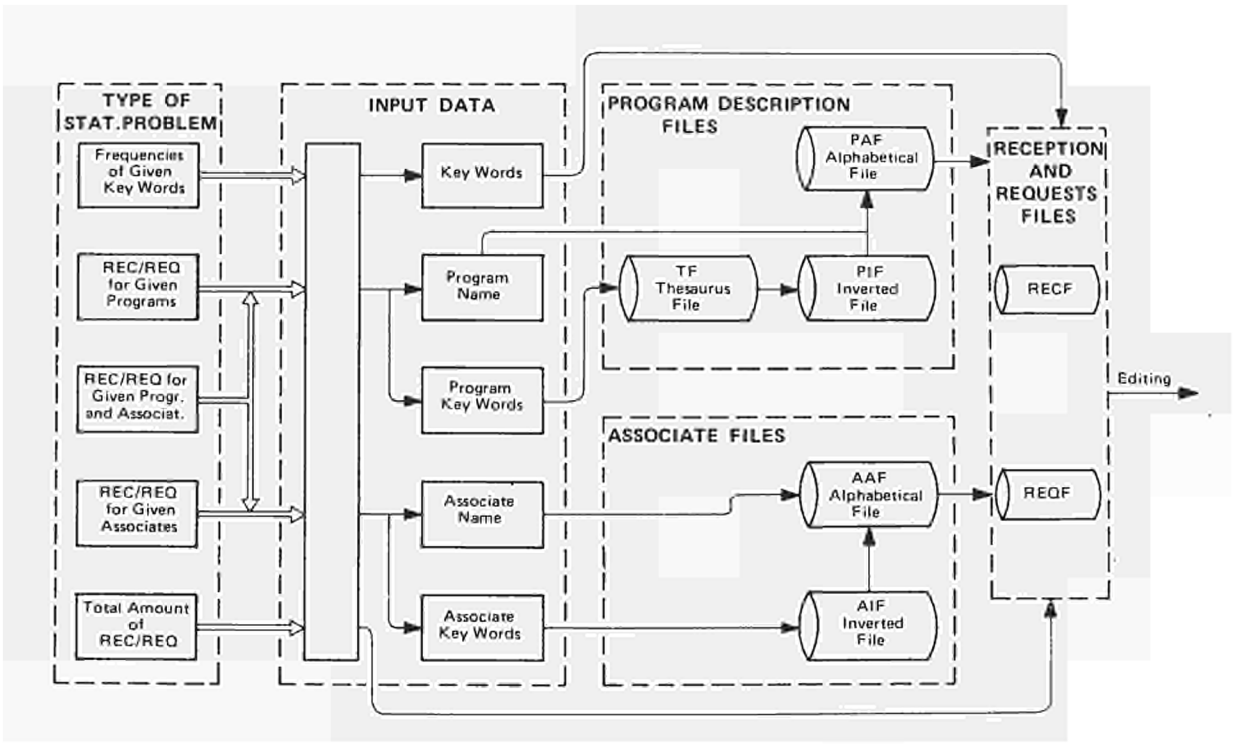

Fig. 2: Flow of analysis of statistical type concerning reception and requests.

Let us now consider the processes of retrieval and reproduction of the programs themselves. In this case the name of the requested program, together with the requested components, is indicated. The system provides through the sequential use of PAF, PDF and PDKF for reproduction of the material. Letters are automatically prepared, addressed to the requestor, and are dispatched with the material itself.

As concerns the statistical analyses regarding the management of the library itself, the kinds of analyses envisaged, over a given period of time, are the following:

a) total amounts of reception/requests;
b) reception/requests for a given program or for programs characterized by given keywords (e.g. programs in engineering);
c) reception/requests for a given associate or for the associates characterized by given keywords (e.g. belonging to a given country);
d) reception/requests in which points b) and c) are mixed;
e) frequencies of given keywords in the request by keywords.

All the results obtained by such statistical analyses are felt to be of the highest importance for enabling the library management staff to orientate the policy of the library and to improve the efficiency of the SIMAS system itself. The SIMAS provides for the requested analyses in batch mode, operating on RECF, REQF, PAF, PIF, TF, AAF, AIF. In diagram 2 the flow of such statistical analyses is shown.

References

1) G. Gaggero, C. Mongini-Tamagnini, G. Lunghi (Syntax S.p.A. - Milan): *"SIMAS - An Interactive Information System for a Library of Software Packages"*. International Computing Symposium - Venice, 12-14 April 1972

2) Aledi, (Syntax S.p.A. - Milan), G. Gaggero: *"Il Sistema Conversazionale d'Information Retrieval della Programmoteca del CETIS"*. Comunicazione al Convegno "Interazione Uomo-Macchina" A.I.C.A., Sorrento 31 May, 1-2 June 1971

3) G. Gaggero, J. Pire: *"Type of Applications of the Conversational Extension of HASP"* Part II - "An Information Retrieval System" Paper presented to SEAS XVI, Pisa (Italy), Sept. 29 - Oct. 1, 1971.

METHODOLOGY AND SOFTWARE DEVELOPMENT FOR APPLICATION IN INFORMATION SCIENCE

S. Perschke, H. Fangmeyer

Introduction

The present activity of CETIS in the field of scientific information and documentation is directed towards using experience in information science to create operational systems.

By 1970 three such systems appeared to be well enough defined to warrant starting intensive implementation:

1. A generalized software package and programming language for natural-language processing (SLC-II).
2. A fully automatic information storage and retrieval system (FAIRS).
3. A Russian-to-English machine translation system.

A valuable contribution to the realization of the projects was given by the group's staff, in particular Mr. Fassone and Mr. Geoffrion. Some of the computer programs were prepared under contract by a computer software company (ITALSIEL, Rome). At present, these projects are at various stages of completion, and naturally every effort was made to accelerate the first of them, which should become the software basis for the others.

SLC-II

It was possible to conceive a generalized software for applications which appear to be widely different (such as translation and information retrieval) by treating all the processes involved as problems of translation and communication of natural and artificial languages. Further, it was possible to break down all these processes into a series of recurrent basic functions. Each one of these basic functions employs an algorithm, a dictionary and a grammar. For some of the functions, the algorithm could be defined as invariant with respect to the different source data, grammars and dictionaries, and in this case the SLC programming language is non-procedural and is used for coding the grammars and dictionaries, while in other phases the algorithms vary depending on the application and the methodology employed, and in this case the SLC programming language is algorithmic.

If one considers a few characteristic applications in automatic information and documentation, the similarity of functions becomes striking: automatic language translation; automatic indexing, information retrieval for SDI and updating of the data base; automatic query formulation and information retrieval.

In all applications, the first part of the operation is basically the same.

A1) Source text input: The source text – some foreign-language text to be translated for MT, a new document for indexing or a query for retrieval – is scanned and those character sequences which are elements of the source language ("word item") according to the associated dictionary and grammar (D_1, G_1) constitute the arguments for the subsequent phase (A2). The algorithm is invariant.

A2) The word items are looked up in the source language morphological dictionary (D_2). In parallel, if the source language has inflections, a morphological analysis of the words and, optionally, the segmentation of compound words are performed. Each word item is represented by a lexical code and a morphological classification. Using the lexical code, the source language dictionary entry containing all information about the word, relevant for a given task, is located. Phase A2 is invariable.

A3) In principle, the object of this phase is to give a formalized description of the contents of the source text according to the grammar and the dictionary entries associated with the words. Largely, it covers syntactic and semantic analysis and the resolution of lexical and structural homographs. The objectives, the methods applied and the degree of sophistication are quite different from application to application. Therefore, no invariant algorithms for A3 (or for A4 and A5) could be defined and the programs are written in SLC (optionally, one also can use PL/1 for these phases).

A4) The transfer, in principle, has the function of substituting target language features for source language features in all instances where a metalinguistic description is not achieved and one has to take the equivalence between two languages as a basis.

A5) The target text generation is the inversion of step A3, i.e., one starts from a metalinguistic description of the target text and produces a string of items consisting of a lexical code and the definition of the inflectional form.

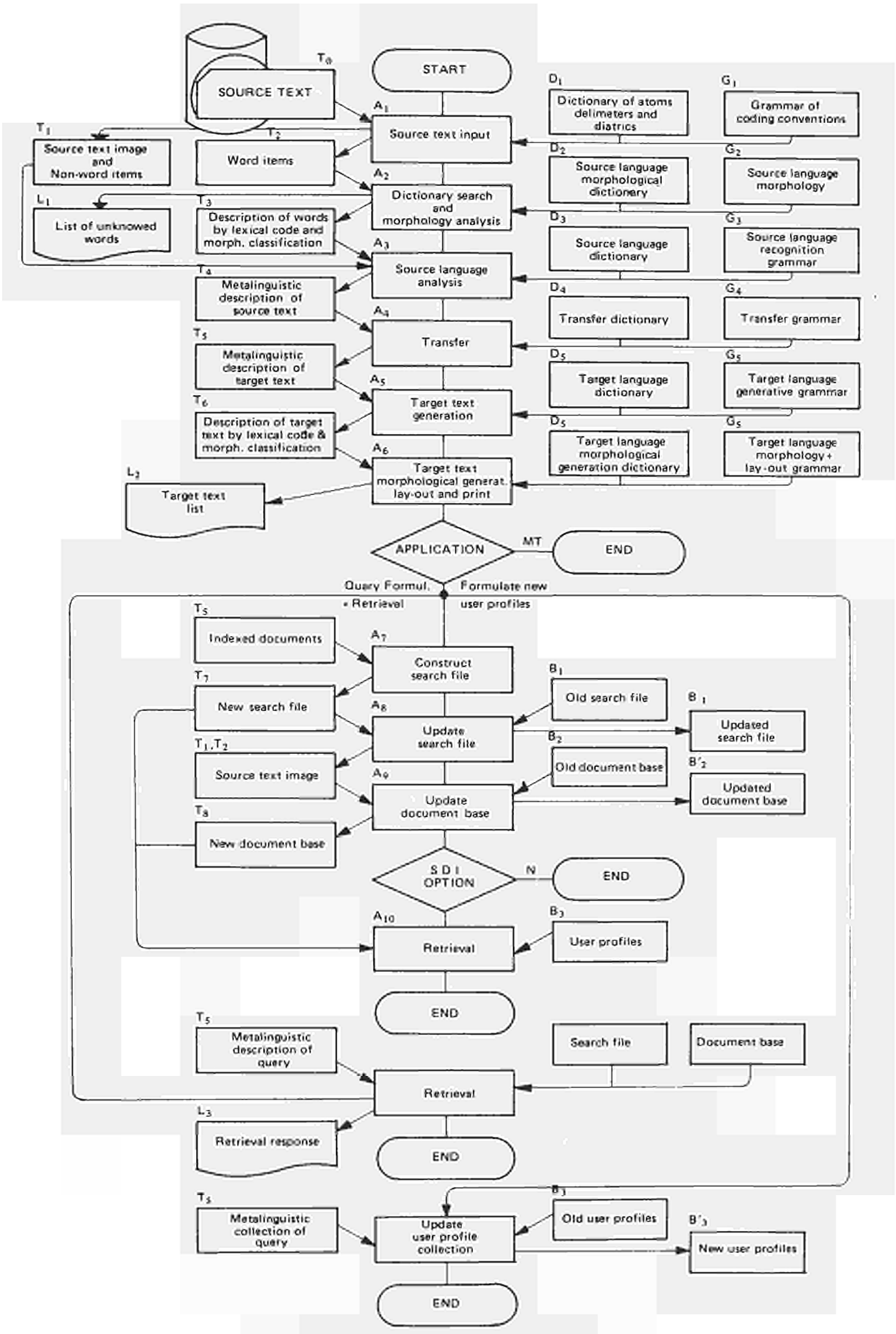

Diagram of the logical flow of data in SLC II.

A6) This phase is the inversion of phases A1 and A2 and is applied only if the target text is to be used by man (always in the case of translation, and for the visualization of the indexing and query formulation results).

The subsequent phases are specific in an IR environment and include, basically, the IR data base management and retrieval functions.

A7) The indexing output is converted into the form required by the search algorithms. It consists either in file inversion, if an inverted file strategy is used, or in the construction of a search directory (by means of automatic classification) if a direct file strategy is chosen.

A8) Updating the search file is a merge procedure between the new search file (built in phase A7) and an old search file.

A9) The new document units are added to the document base and linked to the search file.

A10) The retrieval, in principle, consists in the comparison of a query (formulated by the phases A1 through A4) and the document collection (indexed in the same way). The strategy itself depends on the information retrieval language and the data base organization (e.g., direct or inverted file).

A11) This is an auxiliary module for the maintenance of the collection of user profiles (processed by phases A1 through A6) for SDI.

Further, the system is equipped with a series of modules for creating and maintaining the various dictionaries and grammars involved in the process.

In summer 1971 a set of modules (covering principally the phases A1 and A2 and the interface to PL/1 for programming phases A3 through A6) became operational with all the housekeeping modules and has been largely used for automatic indexing. The SLC programming language which is to replace PL/1 with the relative compiler and control modules had been defined and implemented by the end of 1971 and at present is undergoing the final system test. The modules involving IR are in an advanced state of completion and should all become operational in mid-1972.

The first version implemented operates in a complex overlay structure with static storage management in batch mode. An interactive version of SLC-II, to provide access from a network of terminals, is planned for 1973, and as a first step the transformation of all programs into re-entrant recursive modules with dynamic storage and task management has started and will be terminated in summer 1972. These modules will constitute the basis of the conversational SLC without major modifications.

FAIRS

Historically, the interest of CETIS in automatic documentation has been focussed on the EURATOM Nuclear Documentation system (ENDS) developed and used at Luxemburg by CID. ENDS is the classical solution of a semi-automatic information retrieval system in that the analysis and indexing of the source documents, the construction of the Information Retrieval Language (IRL) vocabulary (thesaurus) and the formulation of queries are performed intellectually, while the computer only does the matching of queries and document descriptions (i.e. its function is limited to the mechanical portion of the retrieval process). Furthermore, both indexing and retrieval are performed on a purely binary base so that the answer is given in such a form that a system specialist must scan it and select those documents which he considers to be most pertinent to the query (screening).

The objectives of FAIRS can be summarized as the elimination of human intervention from the process, and are to be achieved gradually.

In the first stage, the most costly and time-consuming operation – indexing – was mechanized, maintaining unchanged the thesaurus, the query formulation and retrieval strategy. In 1968 an experimental indexing program was introduced, and a collection of some 100 documents were indexed. With such a small collection, the only acceptable method of evaluation was by checking the human and computer consistency. As a term of comparison an inter-indexer consistency investigation was used, which had been performed with a collection indexed by two distinct indexer teams. The results showed that the values are more or less equivalent (Ref. [1]). However, as the indexing quality can only be judged from the retrieval results, in 1969 a new collection containing some 500 documents was indexed and some 20 queries were processed both with the CETIS and the ENDS system. Again the quality of the automatic indexing turned out to be equivalent or even somewhat better than manual indexing (Ref. [1]). These results encouraged the implementation of a fully automatic operational indexing program on the basis of SLC-II, which was finished by the end of 1971 (Ref. [3]). As the new program has a very high performance and enables large document collections to be indexed, a new evaluation series on a semi-operational basis was

prepared in cooperation with CID. It is planned to process documentation queries against the two systems in parallel, and to obtain in this way a practical assessment of the indexing quality in terms of Recall and Precision. This investigation is to be conducted through 1972.

The results described above were obtained in spite of the fact that the IRL has been maintained unchanged (i.e. presented all of the disadvantages of an empirically compiled thesaurus for manual usage), and the queries had been formulated manually. It is evident that the maximum possible consistency between the indexing on one hand and the query formulation on the other must be aimed at in order to obtain optimum employment of the system. This objective can only be achieved through query formulation with the same parameters as used for the indexing of documents. The algorithms of query formulation are basically those of indexing with two additional features:

a) a more complex syntax (with the logical operators AND, OR, NOT)
b) the assignment of weighting factors at the start.

With automatic query formulation it is also possible to abandon the binary logic in favour of a probabilistic evaluation of the similarity of queries and documents and, thus, to present the answers in order of decreasing pertinence.

A last point is the replacement of the Euratom thesaurus, which was compiled empirically and tries to reduce the number of descriptor terms for more efficient use by man. The method of automatic thesaurus construction is based chiefly on the research and experimental work of Salton (Ref. [5]) the principles being as follows:

- the vocabulary of the source language is divided into significant and non-significant words;
- non-significant words are defined on one hand through a given list which basically contains the "function words"; on the other hand they are defined statistically, and comprehend all the words whose frequency of usage in the overall collection exceeds a certain threshold.
- the remaining words represent, in principle, the IRL vocabulary. It presents, however, two sorts of error: 1. synonyms, 2. homographs;
- homographs are detected automatically during dictionary search and are resolved either intellectually or statistically;
- synonyms must be recognized intellectually or statistically;
- since the IRL envisaged is of the syntax-free class, for major precision, it is advisable to include in the IRL vocabulary not only single words but also compound expressions. Here again, the methods to be applied are intellectual (with a given list of expressions), or statistical.

The statistical methods to be applied for the resolution of all of these problems are those of automatic classification based on the co-occurrence and the context of words in the source texts. In principle, an expression is a group of words which occur together with a certain frequency. Synonyms are two words which are rarely used together in the same text, but have a very similar context. Homographs are resolved by the classification of the contexts of each occurence. If the meanings of a homograph are not too close to each other, the contexts of the word through automatic classification are grouped into highly distinctive clusters. All known methods of automatic classification require a heavy load of data processing and it is therefore advisable to resolve the problems by combined automatic and intellectual work and to avoid using statistics if the only aim is to confirm well-known facts.

All methods and necessary software will be defined and tested during 1972 in connection with a large-scale IR project of an Italian public institution. This project is also to use SLC-II as the basic software.

Automatic language translation

Machine translation was originally one of the principle interests of CETIS. At the beginning of the sixties the in-house research work on linguistics turned out not to coincide with the CETIS objective, which was to produce an operational translation system. As a consequence, external relations were re-inforced and by 1963 CETIS acquired, through a research contract, the Russian-to-English translation system developed by Georgetown University. In spite of the evident inadequacies and the unsatisfactory linguistic basis of the system, it was possible to adapt it to the needs of the scientific community of the JRC and to organize a valuable translation service all over Europe, producing over 100 translations a year. This translation service for the Community institutions and the member countries is still expanding (Ref. [4]).

As the hardware (IBM 7090) used has meanwhile grown obsolete, it was decided not to reprogram the system in a conventional way for a third generation computer, but to design a new system which should if possible integrate all the progress achieved in linguistics in the last decade, and use the new SLC-II system as basic software, so as to raise considerably both the quality and the economy of translation.

The development of the system started with the transformation of the existent data bases into the form required by SLC-II. Work was particularly slowed down owing to the impossibility of obtaining

personnel qualified for this task. Meanwhile, all the phases of the system were defined, and a strategy for the resolution of the problems involved was developed. In particular, the translation process was subdivided into three principal phases, source text analysis, transfer and target text generation, of which two, basically, are self-sufficient, i.e., can be developed and checked independently of the others.

In order to characterize the difference with respect to the old translation system, the following points must be emphasized:

- the source text analysis is syntax and semantics oriented;
- the transfer function is no longer the principle task of the translation, but is considered as an auxiliary function in those cases where the analysis does not permit a full metalinguistic formalization:
- the text generation in the target language is performed independently of the source language, being based on the metalinguistic description of the text.

It is accepted that the final objective, the FAHQMT (Fully Automatic High Quality Machine Translation) dreamt of by Bar-Hillel, will still not be achieved with this approach. But as far as one can estimate the future translation quality, it should more or less be equivalent to that of a man-made translation where the translator knows the source and target languages, but does not know and understand the subject matter of the text he is translating.

This level of translation quality should satisfy to a considerable extent the information needs of the scientific community, but it should also introduce machine translation into a far wider field of international communication. Further, the system has been explicitely designed to allow the addition of new source and target languages with the final objective of a multilingual reversible translation system.

The development of the translation system has been seriously impeded by staff shortage over the past years. Nevertheless, thanks to the personal sacrifices of the staff, some results were achieved. However it is evident that the schedule proposed in 1967 for the 3rd research programme 1968-72, which included the realization of the project, fell very short of its target.

References

1) H. Fangmeyer, G. Lustig, The EURATOM Automatic Indexing Project. I.F.I.P. Conference 1968, Edingburgh.

2) H. Fangmeyer, G. Lustig, Experiments with the CETIS automatic indexing system. Symposium on the Handling of Nuclear Information, Vienna, 1970

3) H. Fangmeyer, Stand der Entwicklungsarbeiten für die automatische Indexierung bei der europäischen Forschungsanstalt Ispra. Jahrestagung der Deutschen Gesellschaft für Dokumentation, Bad Herrenalb, Oktober 1971

4) S. Capobianchi, G. Lustig, S. Perschke, A. Petrucci, W. Rittberger, Vernimb, Proceedings 5th Euratom Sponsored Meeting of Librarians Working in the Nuclear Field. - The Use of Machine Translation in Documentation. EUR 4256.e (1968)

5) G. Salton, Information Storage and Retrieval. Scientific Reports to the National Science Foundation.

CRITICAL EVALUATION OF A NEW TECHNIQUE FOR INVENTORY TAKING IN REPROCESSING PLANTS

A. Rota

The present work is the result of a close cooperation between the JRC, Ispra, and the GfK, Karlsruhe. It is due also to E. Drosselmeyer and R. Kraemer (both of GfK) and it has been published, in more detail, as chapters 4 and 5 of the report EUR 4576.e/KFK 1100.

Introduction

One of the objectives of the MOL III experiment was to determine the physical inventory of the fissile elements Pu and U, in the process area of a reprocessing installation (EUROCHEMIC plant) during the normal running of the plant. The method chosen for this determination uses the usual tracer technique, and may be called a self-tracer method, because it is based on the different isotopic composition of the fuels to be reprocessed.

Let c_1 and c_2 ($c_1 \neq c_2$) be the values of the relative abundance of an isotope in two groups of fuel elements, which are reprocessed in sequence. If the fuel quantity which composes each group is sufficiently large, the hold-up of the plant at the initial moment of the reprocessing of the second group is simply expressed by the formula:

$$H = \sum_i M_i \frac{x_i - c_2}{c_1 - c_2} \qquad (1)$$

where the summing is done on all the outputs, subsequent (in time) to the first input of the second group, for which x_i, the relative abundance of the tracer isotope in the output batch i, is different from c_2 ; M_i is the total quantity of Pu or U in the i-th output batch.

The correct use of (1) requires the numerical definition of the "sufficiently large" quantities of fuel mentioned above as a limiting condition. Moreover the theory requires that the relative concentrations c_1 and c_2 are strictly constant. In practice this condition may not be completely fulfilled.

This part of the MOL-III experiment had a dual purpose:

1. the study of the conditions governing reliable use of the method;
2. the field test of the technique.

Thus it was possible to define both theoretically and experimentally the advantages and limitations of the self-tracer technique for the main safeguard requirement, namely the MUF (Material Unaccounted For) assessment.

Practical problems and constraints

The problems which arise when the method of inventory-taking is to be implemented, relate mainly to the following points:

1) determination of the minimum amount of material necessary to attain the object (taking into account, when possible, the characteristic features of the plant in question);
2) estimation, on the basis of the available data on the spent fuels, of the statistical uncertainty that can be expected for the measured inventory;
3) suggestions regarding the optimum batch sequence arrangement within the superbatches.

The complicated operating steps necessary to recover both U and Pu from the spent fuels cannot be described in a sufficiently accurate way by algebraic relationships. The process is carried out through a sequence of continuous and batchwise operations. For this reason the above-mentioned problems were solved by means of the simulation technique. A numerical model of the Eurochemic plant was set up and "ad hoc" features were generated. The relevant code was written in FORTRAN language and run on the IBM/360-65 computer.

The proper use of simulation would require the identification of the model with the real system. Strictly speaking identification means that the model parameters have been adjusted in such a way that both model and real system have the same response function. At the present time such an identification is possible because the normal operation procedures do not allow the definition of a response function: the range of choice left to the operator is too wide. At most, a sort of identification can be obtained "a posteriori", when all the operator's decisions are known. This kind of comparison is important because it

shows whether the model is able to produce realistic results, that is a series of outputs, related to prescribed inputs, which could be the actual data of a real plant. This type of identification was achieved in the case examined. The results summarized below concern a specific plant (Eurochemic) and a specific reprocessing campaign (LEU-71/1); nevertheless they can be regarded as indicative for similar experimental situations. The most important indications obtained from this introductory study may be shortly resumed as follows.

a) Total quantity of fissile material inside the superbatches which define the step. A recovery of more than 99% can be reached with superbatches of 19.8 and 8.5 kg Pu before and after the step signal. For U the corresponding figures are 4000 and 800 kg in runs without recycling; with recycles one needs 6000 and 3200 kg for the two superbatches.

b) Advance estimation of the physical inventory (H) precision. The results depend on the way in which the plant is operated. In the simulated experiments described above the assumption of a regular operation procedure was made. It was taken for granted that enough material was available. For every type of plant management strategy, the relative standard error σH-A/A is the difference between the measured and book inventories and was given as a function of r, the ratio between the batch-to-batch variation of the tracer concentrations within the superbatches and the step size.
As a general conclusion we found that for both Pu and U cases a relation of the following type holds good:

$$\frac{\sigma_{H\text{-}A}}{\bar{A}} = \text{r. const.}$$

The values of this constant prove to be independent of the different strategies investigated, except in the cases where the feed of each superbatch is mixed up in the head-end of the plant.

c) Ordering of single input batches within a superbatch. It was shown that the best results for the inventory determination are obtained if the batches are ordered in such a way that the straight lines drawn through the single concentration values according to linear regression remain horizontal.
When these conditions are fulfilled the hold-up of the plant can be calculated to within a few percent.

Field test or the technique

Five physical inventories were measured by means of the technique described during the safeguard experiment. The table gives an overall view of the main experimental results obtained. It may be remarked that, within a confidence interval of 95%, the evaluated MUF (material unaccounted for = book inventory minus physical inventory) is always compatible with the expected value of zero (no diversion).

The evaluation and error analysis was performed by means of Monte Carlo techniques providing distribution functions and confidence intervals. In particular the following accuracies were achieved:

i) physical Pu inventory ($\approx$ 12 kg) less than 5% RSD
ii) physical U inventory ($\approx$ 1800 kg) less than 2% RSD

It is interesting to notice that abnormal re-cyclings in the Pu purification line, did not allow the utilization of the tracer method in its simpler form. A more sophisticated data handling, that takes into account two isotopes as tracers and three, instead of two, superbatches has been used with satisfactory results. For lack of space this part of the work cannot be fully dealt with and as it is only an extension of the simpler approach, the reader is asked to refer to the previously-mentioned report.

AN INTEGRATED SYSTEM FOR THE MANAGEMENT OF TECHNICAL AND ADMINISTRATIVE PROCEDURES IN A WORKSHOP FOR PROTOTYPE FABRICATION

A. Fasoli

The "Informatics in Management" unit attaches great importance to the proper development of administrative data-processing logics and techniques. Consequently more and more ample families of events and procedures in the Centre are considered in their mutual connections, in order to obtain a more integrated treatment of information.

The set of programs designed and implemented for the "Design and Fabrication" Division is an interesting example of integrated management system, and it applies useful data-collection techniques.

The "Design and Fabrication" Division, at the request of users, design and/or constructs various kinds of apparatus or special parts.

The basic needs in its management - in terms of information treatment - are the following.

1) To associate every task with a cost centre (= a debtor).
2) To be acquainted with the overall resources (work-time and materials) expected or allocated for the different tasks, in order to keep an up-to-date financial account for each user and cost centre. Furthermore the comparison of foreseen and allocated resources shows the progress state of each job.
3) To keep the stock situation in view and to be promptly warned whenever a purchase of materials is required: that is, if the remaining stock of some material is less than the critical amount or the foreseen necessities for requested jobs.
4) To get a daily review of the work orders, required and available resources: this situation varies continuously owing to new work requests, new entries of materials, unexpected consumption and delays. Therefore a frequent feed-back is needed to verify and adapt the planning of work. The connection must be noted between this problem and the different aspects of management. For instance, the feasibility of every job depends on both the stock situation and the load on each machine-tool.
5) To represent and summarize the position by means of periodical reviews and statistics.
6) Lastly we would like to mention the great importance of rigorous checks of all data validity.

The above summary points out the main technical problems:

- the collection of data, especially considering that a lot of information is furnished by people not trained in coded data handling;
- the organisation of output sets, to provide better understanding of situations with their connections, alternatives and consequences;
- the logical structure of the programs, which are to be conceived as integrated in an organic whole, since good automation of each separate branch would solve only a part of the management problems, losing sight of the interrelations. In an integrated procedure it may be especially difficult to modify something, because of the possible effect on the logical coherence of the whole. On the other hand, the Division is not an independent system, but a subset in the Research Centre with its variable management needs and regulations, to which it is necessary to adapt certain administrative procedures.

As far as possible, we endeavoured to work out expedients allowing the outside connections to vary without forcing the internal flow and structure of data to change.

All programs were written in COBOL language.

The foundation stage lasted about three years, running through two intermediate steps and a final one. We had to solve not only designing and programming problems, but also logistic ones. The entire Division came from a purely manual data collection and accounting system. Then it was necessary:

a) to introduce a set of new practices without causing a shock in the entire previously-functioning organisation;
b) to build step by step the reserve of coded and stored information the computer was going to process;
c) to verify, in the field and for the most important sectors, the validity of our analysis.

As a first step, automated accounting of the work-time was started.

As a second intermediate step, the stock management procedure was introduced.

During this initial period, even though the other parts of the whole system (programs and data) where lacking, both the first and the second procedure proved able to supply useful and effective support in their own sector, removing the burden of manual updating and accounting.

The integrated system considers the whole information set according to three logical directions. In other words, there are three files sharing and interchanging information. Their own key-codes are the work-order, the material and the personal identification code. The data permanently applying to each of these codes are stored once and for all – for example, expected work times, needed materials, cost centre, description for a work order; measurement unit, price per unit, critical stock level for materials; names of individuals.

We simplified the perusal and manipulation of data by abolishing the previously-used double reference to a work request number and a work execution number for the same task. A single work-order code is now given to a task on reception of the user's work request: coding rules were established in order to allow a common identification term inside the Division and outside with the users, as well as rational criteria for efficient document filing at the end of each job.

The different functions are also codified, since for the description and planning of a task, either expected or allocated work-times have meaning only if characterized as project time, weld time, turn time and so on.

Every employee has a personal badge giving his identification code and his function code. Employees who have more than one function therefore use differently coloured badges, with the same personal identification number but distinct function codes. The code of each material in stock is punched on a card which the storeman keeps in his card-file.

When a job is to be done, the corresponding code is punched on work order cards which are passed on to the workshop department heads.

Badges, material cards and work cards are not directly processed by the computer; their function is the automatic generation of input cards which the computer will process.

Traditional work-timing clocks have been replaced by an IBM 357 data collection system, consisting of terminals cable-connected with a timer and a card punching machine.

The 357 system is hired and its monthly cost is about Lit. 400,000.

When a man starts working for a period of time on a given task, he inserts in a terminal his own badge and the appropriate work card the department head has given him.

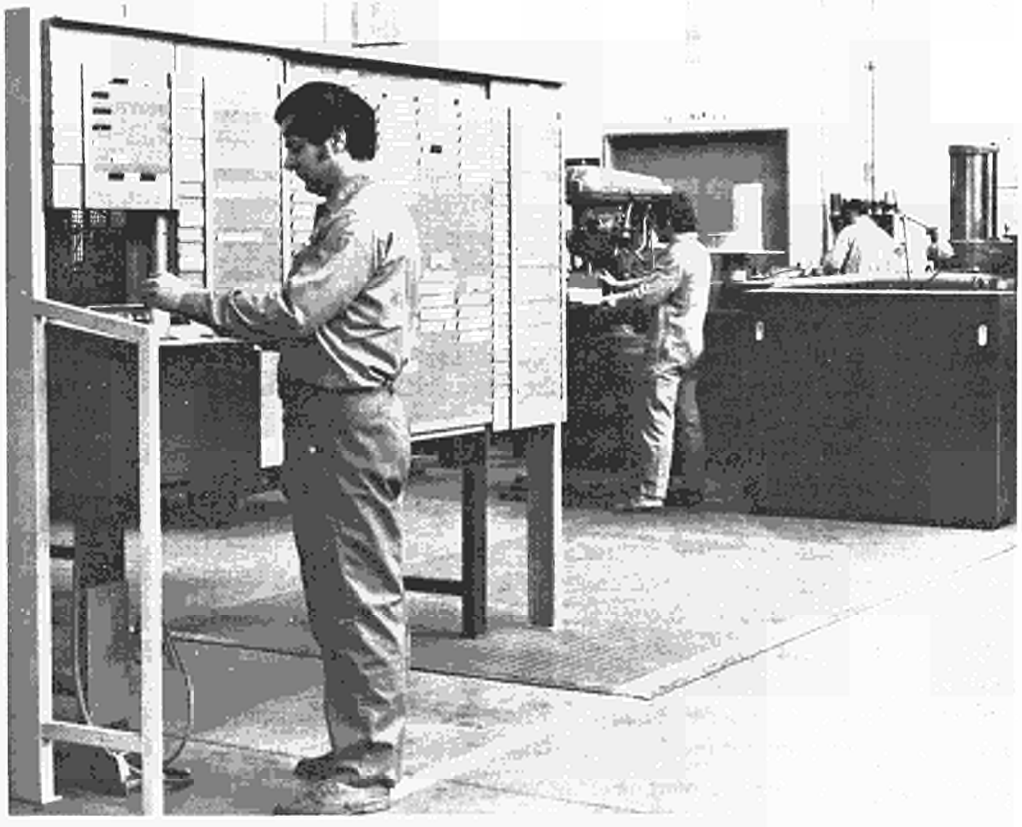

This simple operation causes an input work-time card to be punched and stored with the other similar ones. Its contents are the following: beginning date and time (from the timer); personal and function codes (from the badge); work order code (from the work card).

At the end of a day, the set of cards punched in such a way holds in an implicit form the work-time history and distribution. The computer, following a rather sophisticated deductive method, reconstructs the activity of each man as a chronological sequence of time segments, each segment referring to a work order code. The beginning time of a segment is given by the input card. The stop time corresponds to the beginning time of the next segment or the end of the daily work time. The real duration in hours and minutes is computed taking into account (i.e., subtracting) the normal break time if it falls within the start and the stop time of a segment.

The absence of input cards for an employee means that he is going on to work on the same task as the day before.

We devised this deductive logic in order to reduce the number of requisite punching operations: no punching at the end of job segments, no punching to give information the computer already knows.

In order to keep account of maintenance times, sickness absences, vacations, etc, a conventional work order code has been assigned to each of these occurrences.

The individual work-time segments, as soon as computed, are automatically sorted and assigned to their own work order records.

Material exit cards are similary generated by matching a material card and a work card inserted in the stock terminal; the quantity of material supplied is added by means of a digit manual entry unit which complements the stock terminal.

Punched cards of this kind, containing a material code, an amount and a work order code, allow the updating of both the stock and work order situation; the stock file in its turn enriches the material exit information by adding the previously stored price per unit, which allows a more complete updating of the work order situation.

In this way, by means of IBM 357 system, we get an automated data collection for the most important and copious data flows. The other data mentioned, such as descriptions, names, expected work-times and material needs and so on, which need less frequent introduction and modification occurences, are punched in the normal manual way. The programs work on this variable data set, applying different criteria and logical connections to produce the different kinds of request ouptut: control lists, estimates, warning for material shortages, work order feasibility situation, progress state in work execution, time burden for the different kinds of machine-tools and functions, debit lists for each cost centre (Division, Service, activity fiche), and so on.

It may be interesting to note that the data collection terminals could be directly connected to the computer, without involving any change in store and workshop departments behaviour. Completing the direct data communication by means of an appropriate set of TP terminals would then eliminate the need for intermediate punched input cards and allow automated real-time management.

This possibility could prove interesting and effective in the context of a computerized integrated management system for the entire Centre.

VARIATIONAL AND FINITE DIFFERENCE METHODS IN THE SOLUTION OF PARTIAL DIFFERENTIAL EQUATIONS

A. Benuzzi, L. Guerri, P. Fasoli-Stella

The actual solution of the partial differential equations of physics and engineering must, as a rule, be obtained by approximate numerical methods. Even when an exact method is available, for instance the method of variables separation, its implementation may be unpractical or less convenient than a numerical procedure.

For the same problem different methods may be considered and the choice may depend on various factors, such as the shape of the domain of the integration, the presence of moving boundaries, particular features of the equation or of the expected solution, computer time and memory availability. In the setting up of numerical schemes different approaches may be followed. For instance numerical methods may be derived from the analysis of discretized models of the physical problem. This approach is at the origin of the finite elements method as it has been developed by the engineers in the study of structural analysis and elasticity problems. Another domain where efficient methods have been derived from the analysis of discrete models is that of fluid dynamics and more generally magnetohydrodynamics.

A different and more classical way of deriving numerical schemes is by finite difference approximation of partial derivatives in the nodes of a mesh of coordinate lines. These methods constitute the core of classical numerical analysis applied to the solution of partial differential equations. In connection with finite difference methods various important questions arise such as the consistency, precision order and stability of the scheme.

It is also possible to apply the methods of funtional analysis in the setting up of numerical methods and this is the trend of modern numerical analysis. The adequate treatment of existence and uniqueness of solution for partial differential equations requires the use of function spaces with a suitable norm. But also the problems concerning the approximation of solutions, the convergence of approximate solutions to exact solutions, error propagation and stability can be treated in a more general and systematic way by means of the functional analysis methods.

Among these methods, of particular importance is the variational method which consists in the determination of the extremum values or generally of the stationary values of a functional defined on a domain of a function space. The importance of the method for the applications is due to the fact that many problems in elasticity, electricity, magnetism, hydraulics etc. can be put in a variational form and in this way it is possible to prove existence and uniqueness theorems and to develop approximation methods. The finite elements method mentioned above represents a variational approximation for a particular functional.

In the following, two problems are described as instances of the activities of CETIS in the field of applied mathematics.

The first problem is related to fluid flow through a porous medium and gives rise to a free boundary roblem for the Laplace equation. The existence and uniqueness of the solution and the numerical method for the computation of the approximate solution have been established by means of variational techniques. The second problem is related to plasma physics and is described by a system of nonlinear partial differential equations of mixed hyperbolic-parabolic type. It has been solved with a finite difference scheme. These problems are indicated below as problems A and B.

Problem A

In the context of a cooperative arrangement between CETIS and the "Laboratorio di Analisi Numerica" (LAN) of Comitato Nazionale per la Ricerca (CNR), Pavia, the study was undertaken of a class of free boundary problems, with a twofold aim: first, a theoretical investigation concerning questions of existence and uniqueness of solution; secondly, the establishment of rigorous and effective computational procedures.

The class of problems under investigation is related to fluid flow through porous media. Problems of this kind are encountered in hydraulics engineering and in geology and may concern fluids of various kind like water, salt water, oil, gas etc. The setting up of the equations of the problems, the formulation of boundary conditions, the physical interpretation of these conditions and of the quantities appearing in the equations and the solution were carried out in cooperation with the Hydraulics Institute of Pavia University. The first problem studied and solved is related to the steady flow of water through a homogeneous porous medium (for instance an earth dam) which separates two reservoirs of different

surface level. The basic law of the flow through porous media is Darcy's law which states that there exists a velocity potential u given (apart from a multiplying constant) by

$$u = z - p/\gamma$$

z is the vertical coordinate (the z-axis being oriented upwards), p,γ are the pressure and the specific weight of the fluid. The velocity potential satisfies Laplace's equation:

$$\Delta^2 u = 0$$

For the mathematical formulation of these problems and of the boundary conditions we refer to the specialised literature [1)2)].

Let us now consider the case of a dam with a horizontal impermeable boundary and vertical parallel walls and let us make the assumption that the flow is stationary and does not depend on the longitudinal direction of the dam. We refer now to Fig. 1 where the rectangle is a vertical cross-section of the dam; a the width of the dam; H, h the water levels; the curve C is the upper boundary of the flow region. This curve is called "free surface". Its form is not known in advance and its determination is part of the solution of the problem. The curve C starts at level C at the left wall and meets the right wall at level $h_s > h$. The right vertical boundary between h and h_s is known as "seepage surface". Since the flow is a gravity flow the curve C decreases monotonically. If G is the flow region, i.d., the portion of the rectangle bounded from above by C,

x, y are the independent variables,

$u = u(x,y)$ the velocity potential (without loss of generality the constant κ of the flow can be set equal to 1)

u_x, u_y, u_n are the partial and normal derivatives, then the problem is:

$\Delta^2 u = 0$	$(x,y) \in G$	
$u_y = 0$	$0 \leqslant x \leqslant a$	$y = 0$
$u = H$	$x = 0$	$0 \leqslant y \leqslant H$
$u = h$	$x = a$	$0 \leqslant y \leqslant h$
$u = y$	$x = a$	$h \leqslant y \leqslant h_s$
$u = y$	$u_n = 0$	on C

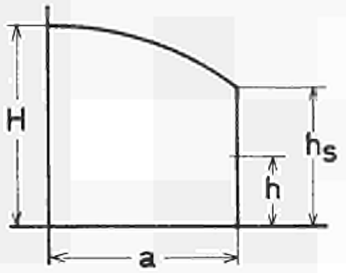

Fig. 1

The pressure along the free surface and the seepage surface is constant and can be set equal to zero.

This problem and other more general formulations of it have been extensively studied in the specialised literature and various numerical procedures of an iterative character have been worked out and successfully applied. Thus, as far as the numerical determination of the solution is concerned, it may be said that the problem has been solved.

However as was pointed out earlier the complete and rigorous treatment of a problem requires first a proof of existence, uniqueness and possibly regularity of the solution; secondly, proof of the existence of the numerical solution and its convergence to the exact solution. Moreover, since the numerical methods which have been proposed for the solution of the above mentioned problem are of the iterative type, i.e., the curve C is the result of successive modifications of a first guess C_0, the convergence of the iterative process is particularly important. It happens that these procedures are convergent and on physical grounds it is possible that it is so, but there is no proof of it. When one is working with an iterative method it is definitely better to know in advance that it is convergent and still better to have an idea of the rate of convergence. None of these questions has been settled with regard to our problem. In the specialized literature the assumption is made that the solution exists and is regular.

Now we give a brief idea of these iterative procedures which are very versatile and can be adapted to similar situations. One starts with a trial curve C_0 and the corresponding region G_0. On C_0 only one of the two boundary conditions is considered, for instance $u = y$ and the corresponding mixed boundary value problem on G_0 is solved. The solution is interpolated or extrapolated so to obtain a curve C_1 along which the second boundary condition is satisfied. The process is repeated with C_1 and G_1 and so on. If there is convergence on the limit curve C both boundary conditions are satisfied and the solution of the problem is obtained.

It may be observed that the solution of the mixed boundary problem for a given region G is obtained numerically by an iterative procedure but in this case there are theorems which prove the convergence of the procedure. Thus actually the entire process is doubly interative. Some techniques of this kind were developed and applied at the L.A.N. in the first phase of the research.

The question of existence, uniqueness and regularity of the solution is a difficult question which has been solved recently by C. Baiocchi of Pavia University [3].

The result was obtained by means of a variational formulation of the problem and the application of theorems concerning variational inequalities on convex sets in function spaces. We refer to the paper of Baiocchi for full details.

A wide class of variational inequalities on convex sets to which Baiocchi's inequality belong has been extensively studied in recent years and a rigorous and general approximation theory has been developed. Thus in our case we have at our disposal various methods for finding approximate solutions for which the questions of existence and convergence have been settled.

A great advantage of the variational approach is that the problem has been reduced to a fixed boundary problem which must be solved not in the unknown region G but in a rectangle of base a and a given height greater than or equal to H, and the region G coincides with the domain where the solution of the variational problem is positive.

This fact allows a great simplification in the numerical computation since we do not have to search for the curve C by means of an iterative procedure. Consequently the programming effort and the computer time are cut down and the application of functional analysis has proved advantageous also on the practical level.

For an account of the computational procedure we refer to [4].

Problem B

The researches on plasma physics and controlled thermonuclear fusion carried out jointly by EURATOM and CNEN at the Ionized Gases Laboratory in Frascati (Rome) require the development and application of mathematical models and of computational techniques for solving the related problems. This part of the work is carried out in cooperation with CETIS. The main problems in thermonuclear research are the containment of a plasma by means of magnetic fields or electrical discharges so that the rate of fusion reactions is high enough to produce a positive energy balance and the control of plasma instabilities.

Various experimental approaches are possible to these problems and are being tried out in laboratories all over the world.

A plasma, depending on the experimental conditions, may be studied according to the methods of statistical or continuum mechanics. The continuum model (known as MHD model) is best suited when the time and length scale of the phenomenon are greater than the characteristic time and mean free path of the plasma particles.

At CETIS the problems so far studied have been of the continuum type of model, which is described by a set of nonlinear partial differential equations of mixed hyperbolic-parabolic type.

One-, two-, or three-dimensional models can be considered. In relation to the experiment to be described below a two-dimensional model was used. Even with two dimensions the mathematical, computational and programming difficulties are quite considerable and much effort is devoted to the development of efficient numerical techniques. The methods currently used for the solution of MHD problems are finite difference methods and these can be of eulerian, lagrangean or mixed type. While for the one-dimensional problems the lagrangean methods are preferred because of their greater simplicity and precision, in the case of two-dimensional problems the eulerian or mixed type methods are preferred since the possibility of large distorsions of the fluid may cause difficulties and loss of precision in the use of lagrangean methods.

We now give a brief description of the experiment which is carried on at Frascati, in relation to which an MHD code has been developed. This experiment is concerned with the production of a "plasma focus" of high density and is known under the name of "MIRAPI FOCUS".

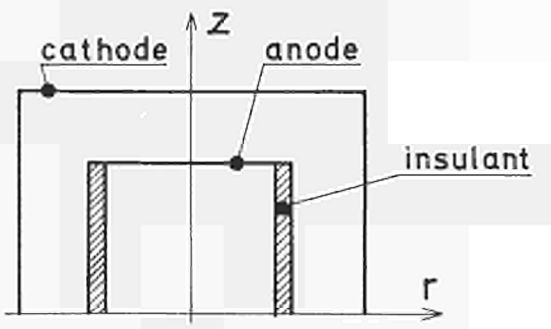

Fig. 2

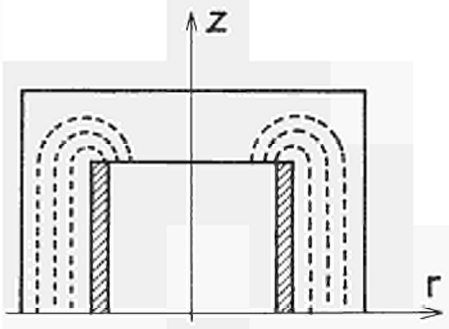

Fig. 3

The experimental apparatus consists of a hollow cylindrical electrode (cathode) inside which is placed a coaxial cylinder of smaller radius, whose lateral surface is insulated and whose upper surface is the anode (see Fig.2). The interspace between the two cylinders is filled with gas at uniform pressure and temperature. A condenser bank generates a high potential difference (40 kV) between the electrodes; the circuit is closed through the gas in the interspace. The sheet-like current discharge propagates at the beginning parallel to the lateral cylinder wall; afterwards it bends and converges towards the axis in the way shown in Fig. 3, generating an azimuthal magnetic field $B_0 \sim 1/r$.

The discharge drives the gas ahead generating a wave front.

The motion of the front may be represented in the early phase by a "snowplough" model since the gas is compressed in a thin layer near the discharge front, being otherwise undisturbed, while behind it there is practically a vacuum. When the discharge front reaches the axis a plasma implosion occurs with the consequent formation of a "plasma focus", i.e., a small region of high density and temperature. The forces generating the plasma focus are the wave front and the magnetic field pressure.

The focus phase is characterized by a kinetic energy for the plasma, with a high rate of neutron production as well as of hard and soft x-rays. For the mathematical and computational study of the problem use was made of the model and of the computer program of D.E. Potter of the Imperial College, London. Both the mathematical problem and the program were modified to suit the different requirements of the MIRAPI FOCUS experiment. The plasma is represented by a two fully ionized fluids model (electrons and ions).

For the description of this mathematical model see for instance [5]. The equations are in eulerian form and, because of axial symmetry, are considered in a cylindrical (r,z) geometry. Whenever possible the equations are set in conservative form since the adopted finite difference scheme is of the conservative type.

At the initial time the gas is at rest and an LC circuit sets up a potential difference between the electrodes.

The boundary conditions on the electrodes are derived from the assumption that the electrodes are rigid, perfectly conducting walls, hence the normal component of the velocity v and the tangential component of the electric field E are zero; on the insulated wall the normal components of v and j (current density) are zero; on the z-axis symmetry conditions are imposed and moreover the walls are adiabatic.

At any successive time t the initial plasma region is divided in two parts (see Fig.4): the first, which has been swept by the discharge with density $\rho < \rho_{min}$, is assumed to be a vacuum; consequently the magnetic field is that generated by the LC circuit; the second part, separated from the first by the discharge front, contains the plasma and it is in this region that the system of partial differential equations is solved.

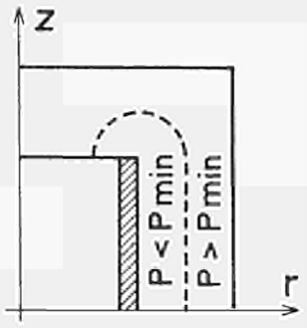

Fig. 4

For the numerical solution of the "MIRAPI FOCUS" problem, a code has been written and put into operation. This code has been developed taking as a basis the code of D.E. Potter for a similar experiment. The region in which the partial differential equations are considered is discretized by means of an (r,z) mesh.

The hyperbolic part of the system is approximated with a second-order Lax-Wendroff scheme; the diffusion terms are approximated with an explicit first-order scheme. The explicit treatment of the parabolic terms is made possible by the fact that for most of the time the hyperbolic character of the equations is prevalent. Ignoring momentarily the non-conservative terms the system may be put into the form:

$$\frac{\partial \vec{u}}{\partial t} + \Delta \cdot H = 0$$

where $\vec{u}$ is taken as a row vector and H is a two row matrix with as many columns; the components of $\vec{u}$ are the unknown of the problem in conservative form.

In the Lax-Wendroff scheme two superimposed uncoupled meshes are used and the computation is carried out in two time steps. To advance from time level $n\Delta t$ a set of provisional values is computed in the mesh points with odd sum of the space indices at time $(n+1)\Delta t$ in the mesh points with even sum of the space indices. For details see for instance [6].

The computation of the amplification matrix for these equations in linearized form gives a stability condition of the Courant-Friedrichs-Lewy type:

$$C_M \frac{\Delta t}{\Delta} < \frac{1}{\sqrt{2}}$$

where Δ is the smaller of Δr and Δz, and C_M is the local magnetosonic speed.

The non-conservative terms are computed only at time $(n+2)\Delta t$ together with the diffusion terms. A special treatment, however, is reserved for the equipartition term.

The choice of time step must take account of the diffusion terms. A rigorous stability analysis is not possible since the system is of mixed type. For the parabolic parts a stability is carried out on simplified equations of the form

$$\frac{\partial u}{\partial t} - \Delta \cdot (\sigma \Delta u) = 0$$

which gives an upper limit on Δt. Of the two limits on Δt given by the hyperbolic and parabolic stability analysis the smallest is chosen. To avoid instabilities due to wave lengths smaller than the mesh dimensions a smoothing mechanism is introduced in the Lax-Wendroff scheme. In the Potter code a small correction of all quantities is introduced according to an idea of Lapidus (1967); it is equivalent to the addition of a small diffusive term.

As has already been said, the code set up at CETIS was derived from a code by Potter. The modifications particularly concern the boundary treatment, since the MIRAPI FOCUS geometry is different from that of the "plasma focus" considered by Potter, also the numerical approximation of the boundary conditions has been improved. On the boundary the direct computation of divergence leads to non-centred approximation of space derivatives. For this reason it has been found preferable to compute the corresponding flux through a surface and the circulation around a line, thus achieving a higher order of precision.

A similar improvement of precision was introduced concerning the computation of second derivatives near the boundary.

With regard to the general scheme of computation, the treatment of the stability condition was simplified and chec s were introduced to signal the occurrence of anomalies, such as negative pressures and temperatures or densities, oscillations and so on. The analysis of such anomalies made it possible to detect some errors in the program, particularly concerning the boundary treatment.

Particular attention must be paid to the treatment of the equipartition term. This is of the form $(\epsilon_\ell - \epsilon_i)/\tau_{eq}$ and with small values for τ_{eq}, i.e., of the order of Δt, numerical instabilities may arise.

In Potter's code an implicit scheme is used in the treatment of this term and since the corresponding equations are nonlinear an iterative technique is used to solve them. In the MIRAPI FOCUS code it has been remarked that in the phase preceding the implosion an explicit treatment of the equipartition term is equally satisfactory and thus a saving in computation time may be obtained.

In the present version of the code overall checks of the computation process have been introduced which are related to the mass and energy conservation. The mass conservation should be automatically assured since the corresponding equation is in conservative form. The check on the mass is still a useful one, however, since it represents an initial check of the program and, besides, enables one to assess the soundness of the assumption that the region where $\rho < \rho_{min}$ can be treated as a vacuum. The check on the total energy conservation is a fundamental one since the electron and ion internal energy equations are not in conservative form.

References

1) M. Muskat, The Flow of Homogeneous Fluids through Porous Media, McGraw Hill, N.Y., 1937

2) M.E. Harr, Groundwater and Seepage, McGraw Hill, N.Y., 1962

3) C. Baiocchi, Su un problema a frontiera libera connesso a questioni di idraulica, (to appear on *Annali di Matematica Pura e Applicata*

4) V. Comincioli, L. Guerri, G. Volpi, Analisi numerica di un problema a frontiera libera connesso col moto di un fluido attraverso un mezzo poroso, Laboratorio di Analisi Numerica del C.N..R., Pavia, 1972

5) D.E. Potter, Numerical Studies of the Plasma Focus, *The Physics of Fluids*, vol. 14, n.9, 1071

6) Richtmyer Morton, Difference Methods for Initial Value Problems, *Interscience Publishers*

STRATEGY STUDIES

SHIP PROPULSION

DYNAMICS

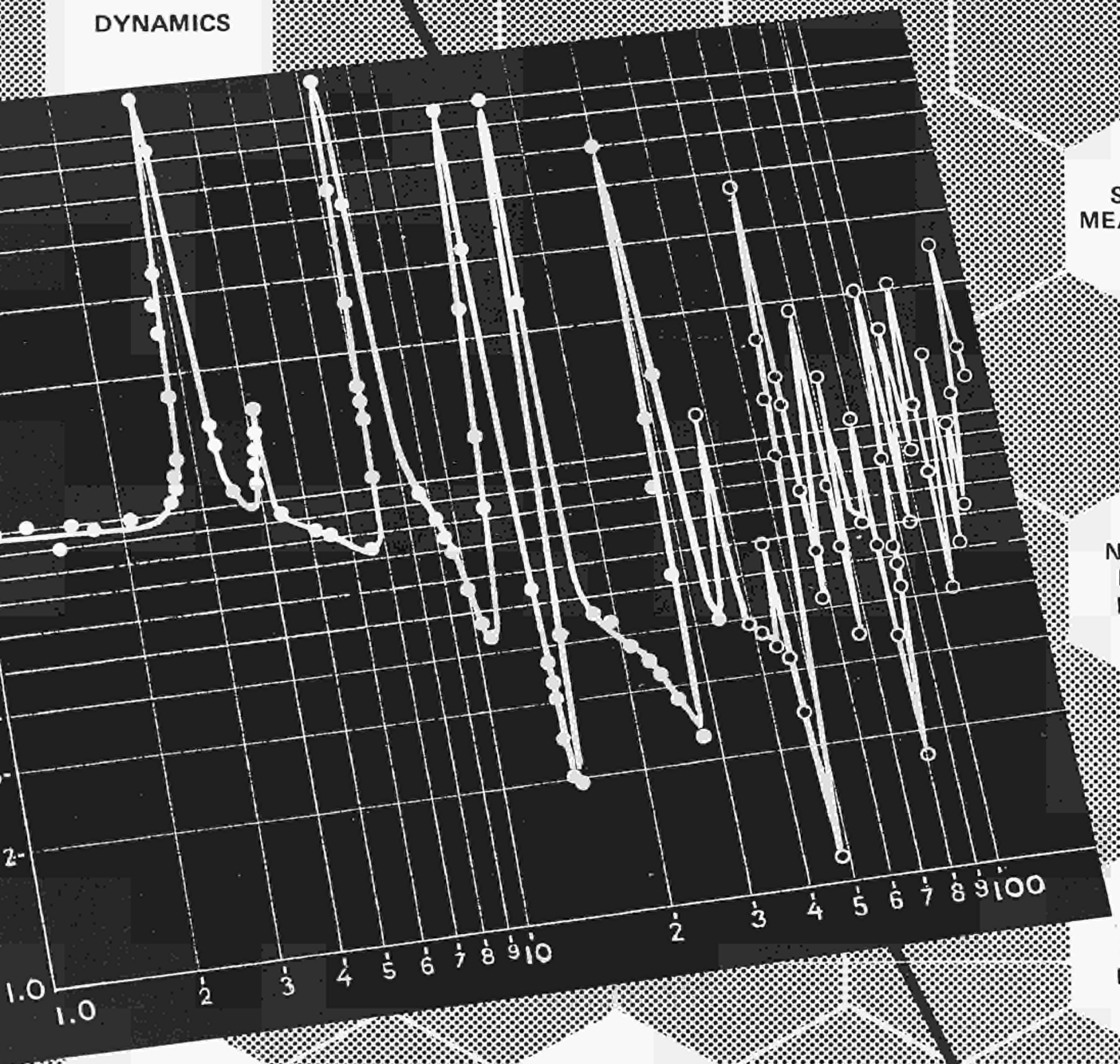

SHIELDING MEASUREMENT

NEUTRONIC METHODS FOR SORA

PULSED NEUTRON RESEARCH

STATISTICAL THERMO DYNAMICS

CROSS SECTION INTEGRAL MEASUREMENT

NUCLEAR STUDIES

NUCLEAR STUDIES DIVISION

A. Kind

The activities of the Nuclear Studies Division include:
- theoretical physics;
- theoretical reactor core physics;
- radiation and shielding physics;
- reactor analysis.

The main lines of the work performed during 1971 are as follows:

Theoretical Physics

Activity in this domain was mainly devoted to problems of condensed state physics. Some of this work was carried out as experimental research and a certain amount of it was of a fundamental nature.

Theoretical Reactor Core Physics

This activity was to support experimental core physics work carried out in the Centre, and was related both to the preparation and analysis of experiments performed in the ECO facility and to the design of a fast/thermal experiment in the RB 2 reactor at Monte Cuccolino (collaboration with A.N.) for integral cross section measurements of structural materials for fast reactors.

Radiation and Shielding Physics

This activity includes all the work carried out in the Centre on shielding. Its target is to provide Industry and the Research Centres of the Community with specific support in this field.

Theoretical work has been devoted both to the elaboration of shielding programmes for neutrons and gammas and to the evaluation and debugging of programmes established by other organizations. Experiments have been performed in the EURACOS facility to provide control of computer programmes and supporting specific design work. In addition, other design work has been carried out in collaboration with industrial firms and research centres.

Reactor Analysis

For many years now the Nuclear Studies Division has been active in this field, which covers problems connected with reactor physics and the elaboration of computer programmes. This activity also includes technical-economical studies for reactor fuel cycles and prospections for nuclear power plant installations. During 1971 work was mainly focussed on the following points:
- evaluation and debugging of processing programmes for the preparation of cross-section sets and elaboration of some of these sets for specific applications.
- improvements of computer programmes for the calculation of power distribution and of fuel evolution in light water reactors and the use of these programmes both for research on safeguard techniques and for the assessment of ship propulsion reactors;
- Reactor safety studies, including the elaboration of spatial dynamics computer programmes, with thermo-hydraulic routines for light water and for high temperature reactors, and of programmes for criticality calculations and reliability analysis;
- fuel cycle studies on HTGR's and fast reactors and strategy studies of the penetration of the various nuclear power plants in the energy market of the Community.

The work above was largely conducted in collaboration with external organisations; in addition, several industries signed a number of contracts for handling specific problems.

The general trend was to do research aimed at providing a public service. This will be followed up either by setting up specific information centres or by a regular system analysis support to the Commission Serives.

During 1971 the Nuclear Studies Division gave specific support to the SORA-Project, especially for core physics, dynamics and shielding studies.

Several particular activities of the Division have been selected and described here in detail.

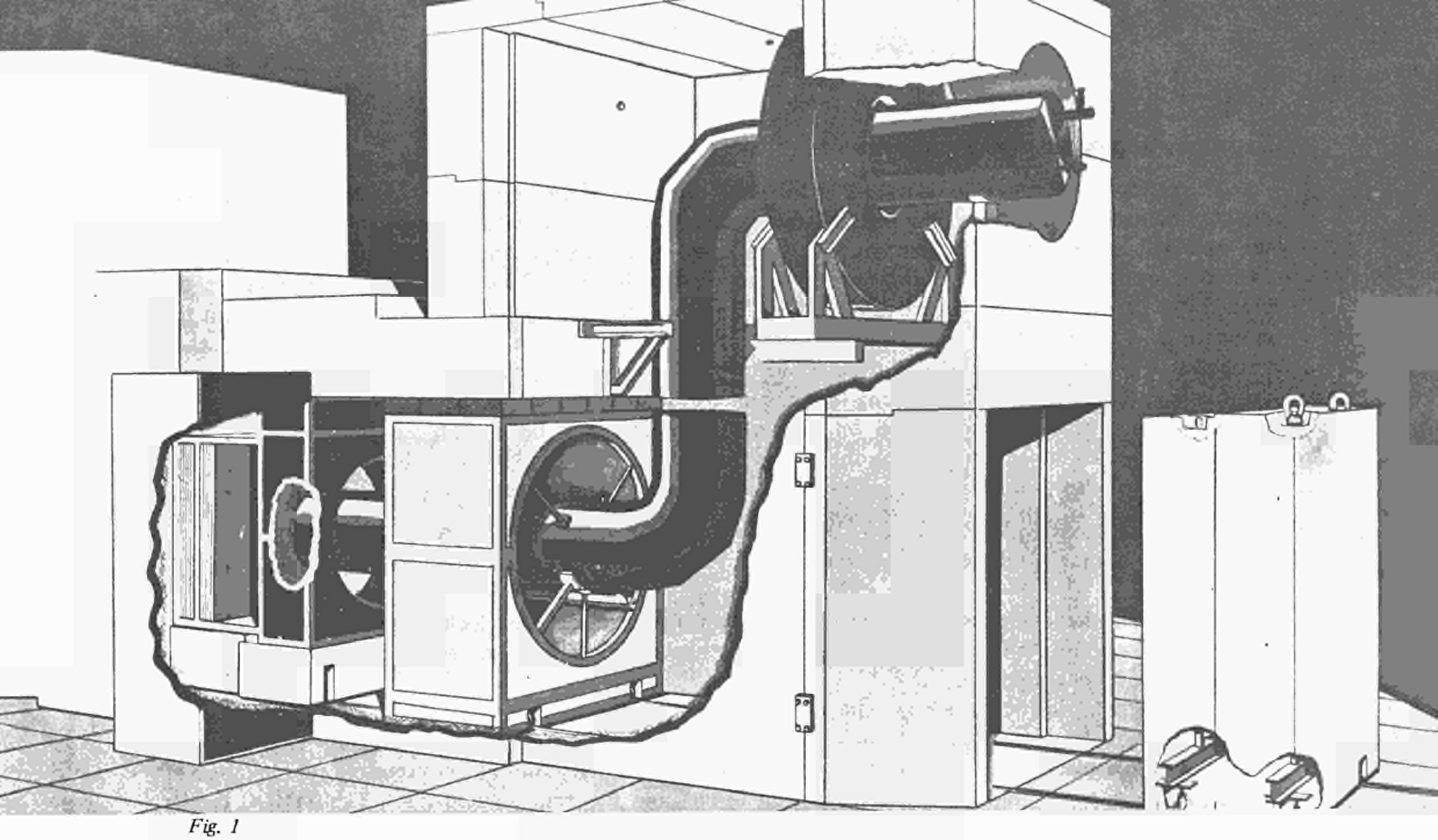

Fig. 1

SHIELDING EXPERIMENTS

U. Canali, O. Diettrich, G. Gonano,
A. Marchal, R. Nicks, G. Perlini

The SNR-sodium pipe shield penetration

Introduction

Neutron streaming along primary sodium pipes represents a characteristic problem in sodium-cooled fast reactors. Large annular gaps are provided between the penetration void and the pipe to allow for movements due to temperature changes and to accommodate the thermal insulation.

As these annuli are filled with low-density materials they give rise to radiation streaming. During the conceptual and preliminary design of the SNR fast reactor, one of the typical shielding problems identified was that of neutron streaming through these unavoidable passages. An experimental and theoretical development programme has been set up in the frame of a cooperative effort shared by Interatom, GFK and JRC Ispra.

Lay-out of the mock-up

The immediate aim of the experimental part was the study of radiation streaming along a twice-bent duct filled with sodium, similar to a cooling tube section of the SNR project. The duct penetrates through different graphite and concrete walls, so that the resulting geometrical configuration is rather complicated. A shield mock-up reproducing the design situation in one-to-one scale was erected at the Euracos shielding irradiation facility, which essentially consists of a disc emitting isotropically 10^{14} fission neutrons per second.

In order to soften the neutron spectrum incident on the shield mock-up, an iron-aluminium filter, 60 cm thick, was interposed between the converter and the front of the sodium tube. The existing irradiation tunnel (length 4 metres) was completed by a third vertical cell housing the sodium pipe and the diaphrams. The pipe has a diameter of 60 cm and is 7 metres long. It penetrates through a graphite diaphragm and two concrete walls, the penetration holes having a diameter of 120 cm. (Fig. 1).

Safety devices monitor the sodium temperature and the internal pressure in the tube. A gas injection system floods the cell's interior with argon and nitrogen in the case of temperature rise.

Experimental programme and measurements

The mock-up was put into operation in July 1971. Because of the upper pipe penetration there exists a direct communication between the cell and the reactor hall. Neutron leakage out of this penetration into the hall and subsequent reflection on the walls raises the radiation on the operating floor above the tolerance level; the mean total dose in the operating area is about 7 mrem/hr and corresponds to the predictions of the mock-up design calculations. Moreover, preliminary measurements confirmed that the radiation level inside the cell is sufficiently high to permit everywhere a sufficient activation of the set of resonance detector foils established during the planning phase of the experiment.

Since July, the neutron fields along the tube have been explored by the use of threshold and resonance activation foils. Spectral information on intermediate neutrons is being deduced from a set of seven resonance sandwich detectors covering the energy range from 2 eV to 3000 eV. (In, Au, W, Mn, Mo, Cu, Na). Figure 2 shows the measured profiles, along the lower horizontal tube, of a triple foil gold detector, together with the resulting activity differences of the outer and inner foils.

Interpretation

Because of the complicated layout the interpretation can only be tackled by fairly sophisticated three-dimensional Monte Carlo codes, which are now becoming available and which need to be assessed by comparison with measurements.

Two Monte Carlo codes are being checked with the experimental results obtained: the TIMOC code set up at Ispra and the Interatom ALBEMO code. The new version of TIMOC contains some time-reducing features of particular interest for shielding applications. Its geometry routine permits close reproduction of the geometrical configuration of the irradiation tunnel and the bent sodium duct. The TIMOC results obtained so far give an acceptable agreement between the measured and calculated absolute resonance activation rates; errors are within a factor of two. Errors due to cross-section uncertainties, geometrical approximations and statistics in the stochastic process still have to be analysed.

The measurements were also intended to decide on the validity of a less time-consuming approach, namely the albedo concept used in the Interatom ALBEMO code. This code calculates the distribution of neutrons within empty spaces of large volume. To determine the slowing-down effect through the reflector, the code utilizes a library with energy-dependent reflection coefficients prepared by a special one-dimensional Monte Carlo code. The Interatom ALBEMO results agree sufficiently with the measured results, within the degree of accuracy required for the shield design phase.

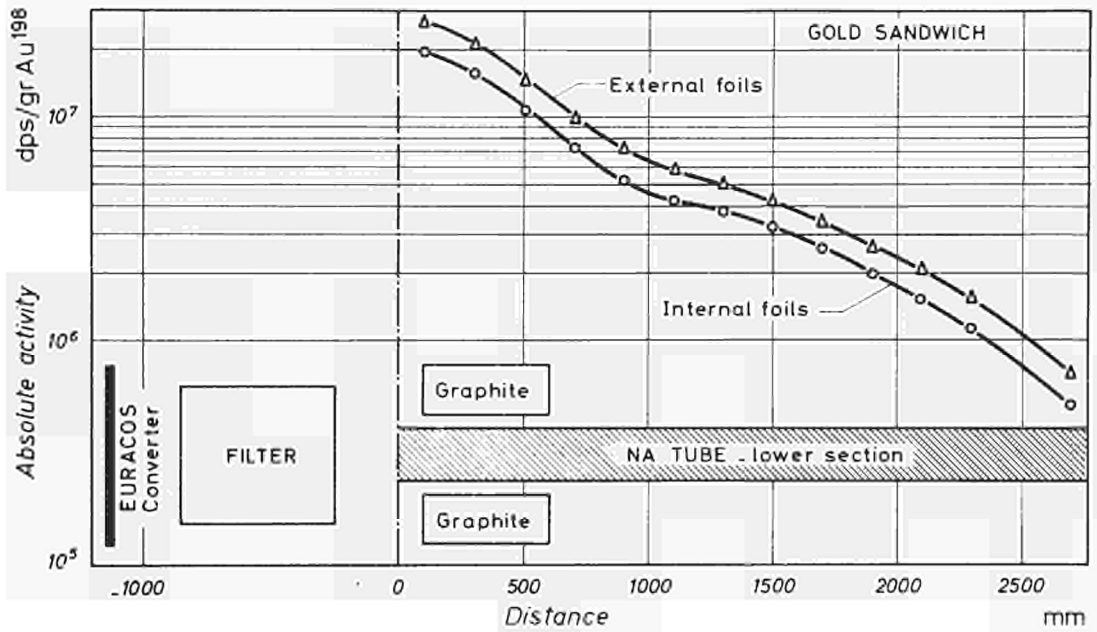

Fig. 2 – SNR Shield Mock-up. Single Foil activities for a Triple Au-Sandwich.

The CIRENE axial shield mock-up

Introduction

The aim of this study, performed jointly by the EURATOM JRC, Ispra, and the CISE, Milan, is to choose and implement a method of calculation for the design of a neutron shield of complicated geometry and containing considerable volume fractions of iron (varying between 50% and 75%), such as occurs in the CIRENE prototype reactor. This shield is composed of alternate slabs of iron and water perpendicularly traversed by cylindrical channels of iron; these are the end structures of power channels, scram rods and control rods. The configuration is thus remarkably heterogeneous in both the axial and the transversal direction; its detailed description would require a geometrical representation in three dimensions.

Among the available shielding codes, there exists no method of calculation that can be considered as proven for this type of shield. It was therefore decided to carry out an experiment with a mock-up similar to the shield, in order to check the codes in use at present and to devise a calculation method that will best meet the need for economy of computing time, ease of use, and accuracy of results.

Lay-out of the mock-up

The measurements were done on the EURACOS shielding irradiation facility, consisting essentially of a disc source emitting isotropically 10^{14} fission neutrons per second. The experimental programme comprised three phases: the first one is composed only of alternate slabs of iron and water, with the same thickness as planned for the real shield; the volume fraction of iron is 50% of the total volume; this mock-up may be studied with one-dimension codes.

The aim of this first experiment was to assess an experimental technique, to check one-dimension codes, particularly SABINE, for a medium with high iron content, and to test the cross-section libraries used.

The second mock-up was derived from the first one, by inserting iron cylinders perpendicularly between the iron slabs, arranged with the proper mesh in order to simulate the penetration of different channels (Fig. 3). The iron concentration of this configuration is about 75% in volume.

In a third phase, the real penetrations have been simulated in greater detail. The experimental study of this third mock-up, which is of specific interest to the CIRENE project, has not yet been concluded and will not be reported here.

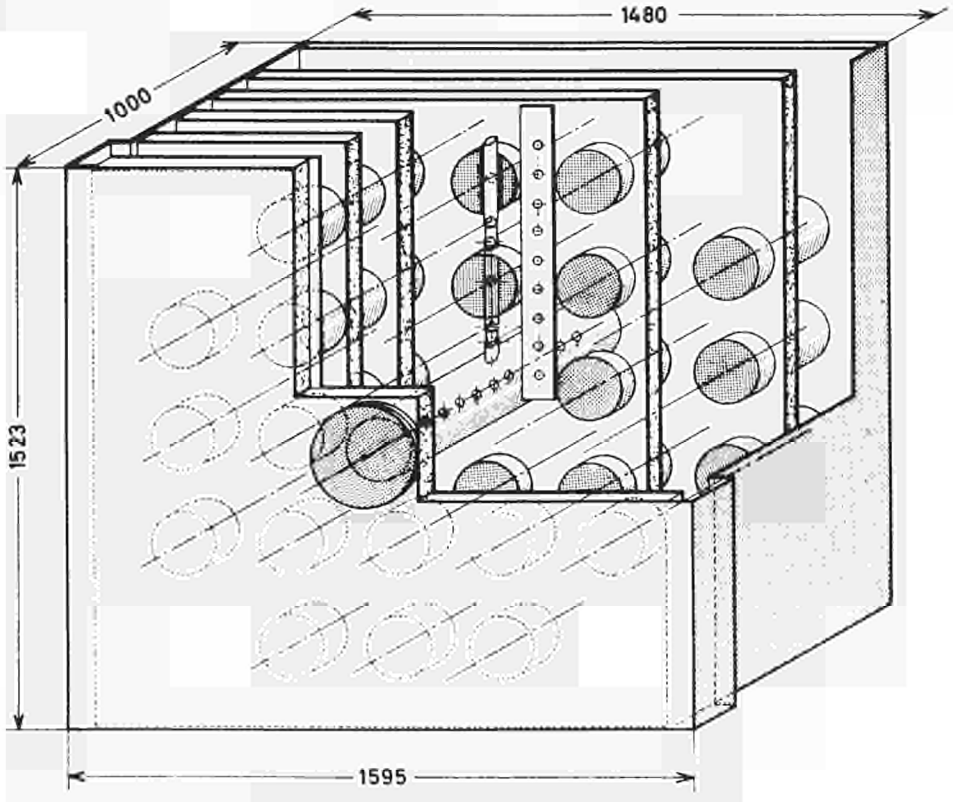

Fig. 3 – Geometrical Configuration on the Second Phase.

Measurements

The detectors used were activation foils, the response of which covered the energy range of interest to shielding research:

- thermal neutrons : dysprosium 1/v detector
- epithermal neutrons : gold (4,9 eV) and manganese (335 eV) resonance detectors
- fast neutrons : indium ($E_{th} \geqslant 0{,}8$ Mev), sulphur ($E_{th} \geqslant 1{,}5$ Mev) and Al ($E_{th} \geqslant 6$ Mev) thresold detectors

The measured neutron fluxes vary within a range which is eight to nine decades wide. Axial and radial profiles throughout the mock-up were recorded and compared with the calculations.

Interpretation

The comparison between the experimental results from the first and second mock-ups highlights the main features of the neutron penetration in iron, and in particular the amount of the epithermal neutron streaming.

One-dimension calculations to be compared with the results of the first experiment were performed with removal-diffusion (SABINE) (Fig. 4) and transport (ANISN, CINNA) codes. This comparison is quite satisfactory as to the data libraries employed and as to the codes, considered from the point of view of ease of use, computing time, and accuracy of the predictions. In particular the SABINE results have the same kind of accuracy as those given by the transport codes, and are obtained with significantly less machine time.

For the interpretation of the second experiment the following methods were applied: two-dimension diffusion (SQUID) and removal-diffusion (ATTOW), two-dimension discrete ordinates (DOT-2), and three-dimension Monte Carlo (MORSE). In ATTOW and SABINE the same cross-section library was used; for DOT-2 and MORSE the cross-section library and energy-group scheme were the same as for ANISN; finally a third library for SQUID was calculated with GGC II, using the group scheme and the self-shielding factors from the ABBN library.

The advantages and drawbacks of each method applied are being analysed in order to draw some conclusions about the present situation of multi-dimension shielding codes. The agreement between calculations and measurements, for the type of shield taken into account, is not generally satisfactory; computing times jump from a few minutes for the first mock-up to about one hour or more (IBM 360/65) for the second one. Furthermore each code exhibits some particular problem: convergence, amount of storage needed, adaptation to the particular problem, use of variance reduction techniques, interpretation of results.

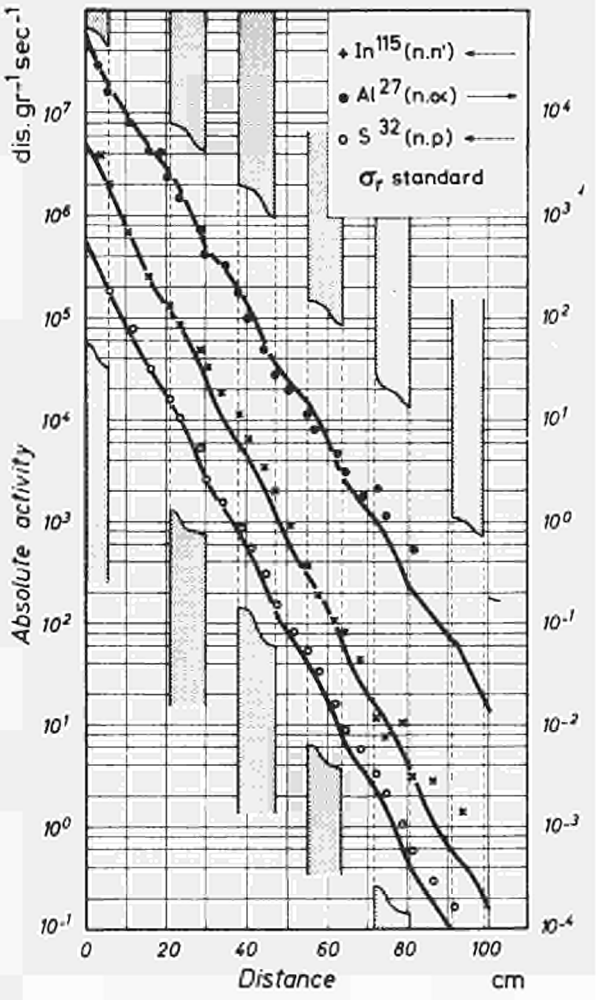

Fig. 4: CIRENE Axial Shield Mock-up: Comparison between Measurements and SABINE Calculations.

NON-EXPONENTIAL DECAY OF NEUTRON PULSES IN LOW TEMPERATURE BERYLLIUM

V. Ardente, G. Rossi (Nuclear Studies Division)
P. Pierini, G. Riccobono (Physics Division)*

Introduction

It is well known that a non-exponential decay of neutron pulses in finite coherent moderators has been put in evidence experimentally through the so-called "drift" of the log N(t) curve [6] i.e., a sort of slowing-down of the decay process has been observed in beryllium blocks at a time of the order of 1 ms (depending on the dimensions) after the pulse injection.

The theoretical interpretation of the phenomenon generally accepted is based on the concept of "trapping" [5] i.e., the effect of the elastic coherent scattering which retains the neutrons in an energy region of very low diffusion coefficient and consequently of minimum leakage probability. The influence of elastic coherent scattering on the time evolution of the neutron pulse in a finite moderator is enhanced in low temperature moderators, owing to the fact that it remains practically unaffected by the change of temperature; on the other hand the inelastic contribution to the total scattering cross-section decreases sharply with temperature in such a way that, eventually, the "KT" of the moderator could have no more significance in characterizing the asymptotic behaviour of the pulse.

Furthermore the average neutron velocities in the block at low temperature are smaller (after a short initial period) than at room temperature, consequently the experimental situation is certainly better, i.e., the time interval in which the process is observable is longer than at room temperature. An experimental investigation at low temperature allows a more precise and more reliable study of the time evolution of the neutron pulse, in a situation in which the effects of the various dynamical processes in the moderator are better separated.

Difficulties of the theoretical interpretation in the case of low temperature moderators

In order to introduce into the theoretical analysis of the problem as many of the details of the moderator dynamics as possible and to study the evolution of the pulse over sufficiently long times, a simplified mathematical scheme was needed for the treatment of the time, space and energy-dependent Boltzmann equation.

The following line of approach appeared very promising [1]: the time-moments of the neutron density are obtained from the solution of stationary Boltzmann neutron transport equations with high accuracy as regards the energy-exchange processes (101 energy groups from 0.5 eV down to $0.5 \cdot 10^{-4}$ eV) and increasing order of approximation as regards the leakage process (diffusion, S_n, etc.). To utilize this informations a time-energy dependence of the neutron flux of the type $\varphi(E,t) = f(E) \cdot \exp[-\lambda(E)t]$ was guessed, and this function was required to have the same time-moments $m_0(E)$ and $m_1(E)$ of order 0 and 1 respectively, as the exact solution of the neutron transport equation. As a consequence one obtains:

$$f(E) = \frac{m_0^2(E)}{m_1(E)} \equiv \frac{m_0(E)}{\tau(E)} \; ; \; \lambda(E) = \frac{m_0(E)}{m_1(E)} \equiv \frac{1}{\tau(E)} .$$

The calculations performed with the code GATHER-2 ("$D(E)B^2$" approximation) and compared with sophisticated methods of solution of the Boltzmann equation and with experiments in beryllium and graphite at room temperature gave sufficient confidence in the reliability of the model [2]. In the same ref. the difficulty of correctly introducing a source spectrum in the calculation method is mentioned.

This difficulty was overcome by utilizing the Monte Carlo code [3] MCT 2 to evaluate the life history of the pulse during the first stage of the thermalization process. The space averaged energy distribution of the neutron density at $t = 50\,\mu s$ in a beryllium sphere ($r = 7 \div 8$ cm) at 90°K turns out to be a more or less Maxwellian distribution with an average velocity corresponding to a temperature of the order of 425°K.

A second difficulty arises in considering the so-called transport effects, i.e., treating the leakage term in the Boltzmann operator. The great majority of the theoretical analyses of the pulsed neutron problem were performed in terms of the diffusion approximation (from the simple "DB^2" approximation to the "asymptotic reactor theory"). The interpretation of the experiments requires in this case the determination

* Postgraduate Fellow. Now of IBM, Florence.

----- GATHER 2 results for $B^2 = 0.1\ cm^{-2}$
—— average values in the 8.18 cm radius equivalent sphere by DTF IV

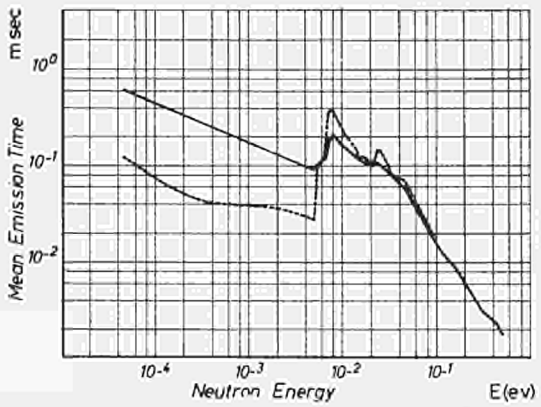

Fig. 1: Mean emission time in the 15x15x20 cm³ beryllium block at 90°K as a function of energy.

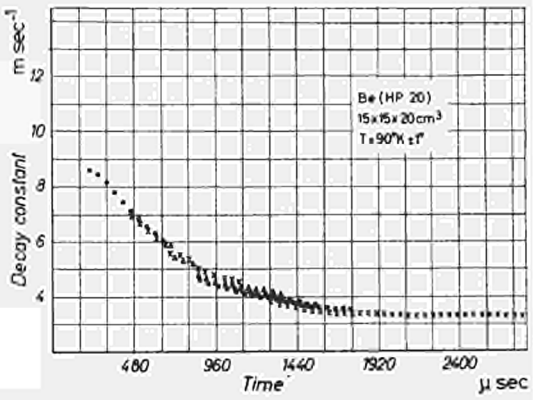

Fig. 3: Decay constant as a function of time: experimental results for the 15x15x20 cm³ berylium block at 90°K.

of a buckling value, i.e. of an extrapolation length for the considered moderator. To give an idea of this, it will be sufficient to list the following values of the transport mean-free-path for Be at 90°K:

$\bar{\lambda}_{tr}$ (Maxwellian average, T = 300°K) = 5 cm
$\bar{\lambda}_{tr}$ (Maxwellian average, T = 90°K) = 35 cm
$\bar{\lambda}_{tr}$ (E = energy of the main Bragg peak) = 0.6 cm.

We therefore utilized, for the evaluation of the time moments of the neutron density to be introduced in our model, the transport code DTF IV [8] in a particular version. Some peculiar modifications of the results in the "$D(E)B^2$" approximation, due to the improved DTF IV treatment of the leakage process, are shown in Fig. 1, where the emission time as a function of energy (average values in a sphere, r = 8,182 cm) and the same quantity calculated with GATHER-2 ($B^2 = 0{,}1\ cm^{-2}$ corresponding to $\bar{\lambda}_{tr} = 0{,}6$ cm) are given for beryllium at 90°K.

The effects of the leakage appear sharply overestimated in the "DB^2" approximation.

The one-dimensional geometry to which the multigroup version of DTF IV is restricted requires nevertheless the adoption of a criterion for the equivalence between sphere and parallelepiped. In applying the model to the evaluation of the decay constant in a Be block of large dimensions, for which the decay constant is well established, we adopted the criterion of equal volume to surface ratio, but it is clear that this point represents a considerable source of uncertainty in the comparison between theory and experiments.

Low temperature die-away experiments performed at Ispra

The measurements were performed on two blocks (15x15x20 cm^3 and 10x15x20 cm^3) at room temperature 20°C, at 153°K and at 90°K.

For the purpose of discussion in this paper only the result for the larger Be block at 90°K will be given, together with the essentials regarding the experimental set-up and the data reduction. As a matter of fact

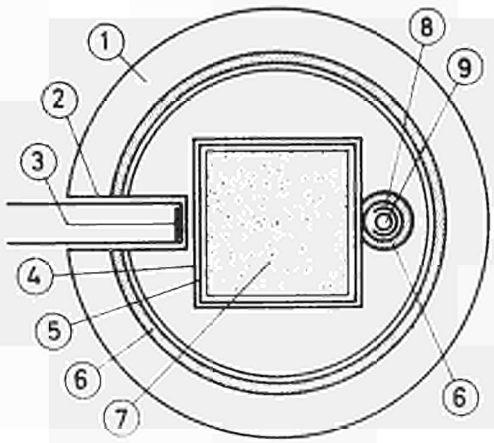

1 – Borated paraffin
2 – Cryostat walls 3 mm Al.
3 – Thick target of Be
4 – Thermal shield of 1 mm Al.
5 – Shield of 1 mm Cd.
6 – Shielding of 6 mm borated rubber
7 – Be block
8 – Lining of Cd with window of 115x10 mm^2
9 – He^3 counter

Fig. 2: Sketch of the experimental set up.

the larger Be block at the lowest of these temperatures allows one to follow accurately the time evolution of the neutron population, within the intensity limitations of our experimental means, for the longest time (~ 3 ms) after the fast neutron injection pulse and also to draw most of the conclusions given in the following paragraph. Other experimental results will be given in a more complete account of the present work.

The experimental set-up is sketched in Fig. 2. The beryllium block, placed in a cryostat by which the temperature can be regulated and controlled to within 1°C from room temperature down to 90°K, is located in front of the pulsed fast neutron source obtained by a 1.2 MeV deuteron burst (accelerated by a VDG) impinging on a thick Be target. The pulse length used for these measurements was 50 μs and the deuteron current during the pulse (of square shape) 2.5 mA, giving a neutron source strength of $\sim 2.5 \cdot 10^7$ neutrons per pulse.

Obviously this is a weak source when compared to the source strength used for similar measurements in other laboratories (e.g., at the Rensselaer Polytechnic Institute or the Kurchatov Institute of Atomic Energy).

The lack of intensity therefore would not permit of following the time evolution of the neutron density for a significant time after the pulse injection as is done by means of a 1/v detector.

With a black detector one can increase the efficiency by a factor of $\sim 10^5$ and therefore overcome the intensity limitations just mentioned. In this case one measures the decay constant of the neutron flux. A He_3 counter (1 inch dia, 6 inches effective length, filled at 4 atm), was available and was for the measurements reported here.

The counter faces (see sketch) the side of the Be block opposite to the side facing the target. In the geometry used and for the neutron spectral region of interest here the counter is not effectively black; its efficiency can be estimated, in those conditions, to be $\sim 99\%$. The entire Be block is covered by 1 mm thick Cd sheet except for a window 1 cm wide, 11.5 cm long in front of the counter. The entire cryostat (see drawing) is heavily shielded to minimize background from room returns. The working temperature of the counter during the measurements was ~ 0°C. In the worst case (i.e., in the last channel included in the graph) the signal to background ratio was about 16. The most severe requirement is obviously imposed on the counting chain, for since one wants to follow the decay process over such a long time, the counting rate covers 6 decades. During the accelerator pulse, moreover, a counter of such high efficiency will be paralysed and the counting chain overloaded.

It was therefore mandatory to perform the measurements with different waiting times to get the complete $\lambda(t)$ curve shown in Fig. 3, by adjusting the pulsed source strength (i.e., the accelerator voltage and current) so as to obtain a count rate in the first useful channel of the time analyser such that the dead-time correction was of the order of 5%. Furthermore a network of delayed gates was used to avoid the above-mentioned overload on the counting chain and to feed the time analyser only during the useful portion of the time for each measurement.

To obtain the λ versus t curve from the raw data the following procedure was adopted.

After correcting for dead-time losses and subtracting the appropriate background for each measurement, a least-squares fitting of the counting rate in each channel was performed on ten channels (each 48 μs long) with a single exponential. The value of λ found was assigned to the time corresponding to the first channel (this is suggested by statistical considerations). Then the first channel was taken out and the eleventh added in the best fitting calculation was repeated and so on up to the end. In the given graph full circles, crosses, triangles etc. refer to different measurements carried out with the criterion given above. The consistency of the results in the region where they overlap is inherently a further check of their reliability and accuracy.

Theoretical results, comparison with the experiments, and concluding remarks

The comparison between measurements and calculations concerns the $\lambda(t)$ curves, in the time interval ($0 < t < 2.5$ ms) in wich experimental results can be considered as sufficiently accurate. The calculations give $\lambda(t)$ as $(1/N)(dN/dt)$ (t) (1/v detector) or $(1/\varphi)\cdot(d\varphi/dt)$ t ("black" detector). The DTF IV time-moment calculation were performed in spherical geometry, the radii (determined on the basis of the above mentioned equivalence criterion between parallelepiped and sphere) being respectively 8.182 and 6.923 cm for the two blocks. The GATHER-2 calculations were related to the buckling values 0.10 and 0.14 cm^{-2} respectively, which correspond to the value of the transport mean-free-path in beryllium at the energy of the main Bragg peak.

The energy spectrum of the source for the zero-moment equation was evaluated with the code MCT 2 in a sphere at t = 50 μs after the pulse injection, the source for this preliminary calculation being monoenergetic (at 1 eV) and placed at the centre of the sphere. As for the space distribution of the thermal

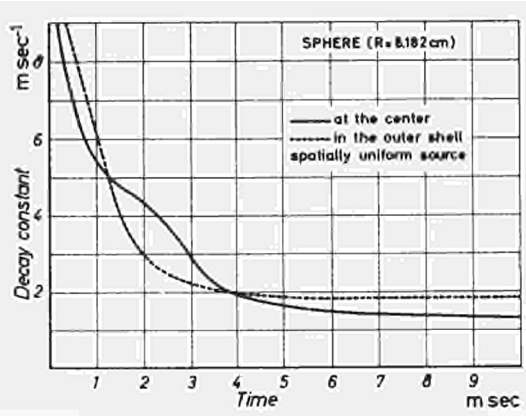

Fig. 4: Decay constant in a belyllium sphere (T = 90°K, r=8.18 cm) as a function of time.

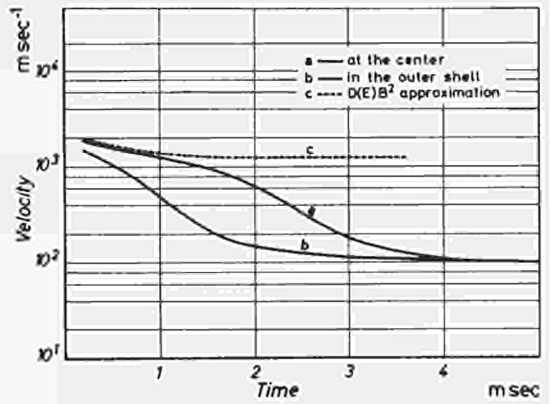

Fig. 5: Average Neutron Velocity in a beryllium sphere (T = 90°K, r = 8.18 cm) as a function of time.

source, two possibilities can be considered: a) uniform distribution, b) energy-averaged space distribution at $t = 50\,\mu s$ as given by MCT 2. The assumptions on the space distribution of the source seem to have a rather strong influence mainly on the results at the boundary. As a matter of fact the measurements were performed out of the block, at a distance of about one centimetre from the centre of one side (necessary for thermal insulation of the counter) i.e., in a situation which could not exactly be reproduced in the calculations. On the other hand, the whole theoretical effort for the interpretation of pulsed experiments has neglected until now such details of the experimental set-up.

Independently of any comparison with experiments we can observe (Figs. 4,5) that the $\lambda(t)$ curves in the centre of the sphere, related to a "black detector", exhibit clearly the transition from the region of the "elastic" continuum to the region of the "sub-Bragg" continuum of the λ-plane (in the sense of [4]).

The same behaviour is confirmed by the curve of the average neutron velocity in the centre of the sphere as a function of time, which has a sort of plateau for a value ($\sim 1200\ ms^{-1}$) corresponding to the main Bragg peaks in a time interval corresponding to the "plateau" of the $\lambda(t)$ curve.

The corresponding results in the outer shell show how differently such dynamical details affect the behaviour of $\lambda(t)$ depending on the position.

The average neutron velocity calculated in the "$D(E)B^2$" approximation tends asymptotically to the velocity corresponding to the main Bragg peak, the constant B^2 value at energies with a high diffusion coefficient producing a sharp underestimation of the effects due to sub-Bragg neutrons, and consequently a pseudo-fundamental energy mode peaked at the energy of the main Bragg peak.

The results given in Figs. 4,5 were obtained with a spatially uniform source.

The comparison with the experiments is presented in Fig. 6 in regard to the block of $15x15x20\ cm^3$. The situation for the smaller one is completely analogous. Since the detector was to be considered as nearly black, we give the $\lambda(t)$ curves in the time interval of the measurements ($0 < t < 2.5$ ms) only for a black detector. The curves refer to the external shell of the sphere and to an energy-averaged space distribution of the source as given by MCT 2, i.e., to the situation which appears as the most closely related to the experimental one. We also show the curve obtained with GATHER-2 for the same block ($B^2 = 0.1\ cm^{-2}$).

We can observe first of all that the theoretical curve $\lambda(t)$ in the external shell of the sphere is not so sharply characterized by elastic scattering as the curve $\lambda(t)$ in the centre. This is due to the very important role that is played in this shell by inelastically scattered neutrons, which arrive here earlier from the internal region, while elastic scattering (or "trapping") effects are clearly less important than in the internal regions. In general the theoretical curve rather largely overestimates the decay constant with respect to the measurements. Experimental points present a well-defined plateau for $t > 1$ ms, which extends until the end of the time-interval accessible to the experimental investigation. Such a behaviour is characteristic also of the GATHER-2 calculations ($D(E)B^2$ approximation) for the above-mentioned reasons, while it is practically absent in the DTF IV results.

It is beyond the aim of this paper to analyse the possible influence on the theoretical $\lambda(t)$ curve either of the scattering model, or of the possible limits of the numerical solution of the transport equation as carried out by the code DTF IV. Hence, when the simplification included in our model is also taken into account, we cannot exclude some doubts on the reliability of the curve $\lambda(t)$, as far as its details are concerned. As for the mentioned discrepancy, we simply suggest the following interpretation in the light of certain physical considerations.

A small beryllium block at low temperature determines a physical situation in which the fact that the measurements are performed outside the block cannot be neglected. The neutrons with energy smaller than the Bragg cut-off energy E_B predominate in the leakage flux from the block for many hundred μs. As a matter of fact the RPI results (see [7], Fig.6) show the relevance of such neutrons in the surface spectrum of a block of rather large dimensions ($B^2 = 0.026$ cm^{-2}) even at room temperature. We recall that at 100°K the discontinuity between Bragg and sub-Bragg σ_s is ~ 10 times greater. It is then presumable that the time evolution of the pulse as registered by the measurements performed at Ispra up to ~ 1 ms is due principally to inelastically scattered neutrons. Whereas at the time when the experimental $\lambda(t)$ curve shows the well-defined plateau, the elastically scattered neutrons (already trapped inside the block) are those significantly measured out of the block.

An attempt has been made to put in evidence qualitatively this interpretation. We tried to simulate the physical situation outside the block in the framework of our calculation model by introducing a counter sensitivity step function, defined as follows:

$$\begin{aligned} &S(E,t) = 1 \quad (E < E_B) \\ &S(E,t) = 0 \quad (E > E_B) \end{aligned} \qquad t < 1.2 \text{ ms}$$

$$\begin{aligned} &S(E,t) = 0 \quad (E < E_B) \\ &S(E,t) = 1 \quad (E > E_B) \end{aligned} \qquad t > 1.2 \text{ ms}$$

Altough in this way the situation was clearly oversimplified, the results confirm the proposed interpretation for $t < 1.2$ ms, while for $t > 1.2$ ms only the shape of the experimental $\lambda(t)$ curve was exactly reproduced (the experiments seem to lose any effects due to sub-Bragg neutrons after 1.2 ms). The fact that the λ-value is overestimated shows how differently the elastic coherent scattering effects appear inside and outside the moderator (see the comments on Figs. 4-5).

A more detailed and quantitative research is in progress. As a matter of fact a correct comparison between theory and experiments must take into account the spatial problems we have stressed in this paper. Thus, our aim is to simulate the actual experimental situation in a realistic way by means of a multiregion transport code.

A new series of low temperature measurements is now programmed, in which the die-away process will be observed at the centre of the block as well. The experiment will also be repeated on a block of larger dimensions in order to observe the pulse evolution up to later times.

In any case, even at this early stage, the critical analysis of the experiment shows how careful one should be in drawing conclusions about the existence of decay or pseudo-decay constants even from experimental λ (t)-curves, the direct inspection of N(t) curves being certainly inadequate to this purpose.

References

1) Ardente, V. and Rossi, G (1967) J. Nucl. Energy (Parts A/B), *21*, 559.

2) Ardente, V. and Rossi, G. (1968) Proceedings of the IAEA Symposium on Neutron Thermalization and Reactor Spectra, Ann. Arbor, vol. I, pag. 169.

3) Ardente, V., Cupini, E. and Molinari, V.G. (1970) CNEN Report RT/FI (70) 49.

4) Conn, R. and Corngold, N. (1969) Nucl. Sci. Engng. *37*, 85.

5) Corngold, N. (1965) Nucl. Sci. Engng. *23*, 403.

6) Fullwood, R.R. et al. (1964) Nucl. Sci. Engng. *18*, 138.

7) Gaertner, E.R. et al. (1965) Proceedings of the IAEA Symposium on Pulsed Neutron Research, Karlsruhe, vol. I, pag. 483.

8) Lathrop, K.D. (1965) Los Alamos Report LA-3373.

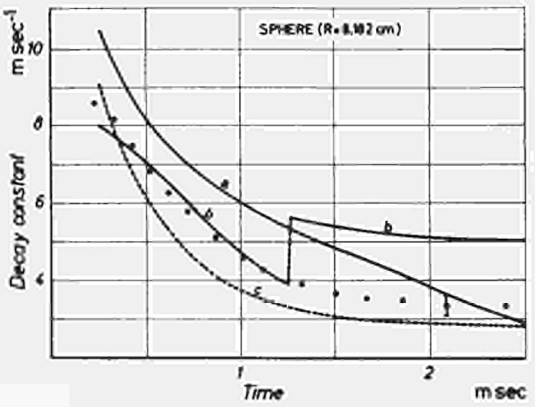

Fig. 6: Comparison between experimental results and theory.

a – without sensitivity step function (DTF IV results in the outer shell of the equivalent sphere)

b – with sensitivity step function (id.)

----- GATHER-2 results for $B^2 = 0.1$ cm^{-2}

STATISTICAL THERMODYNAMICS AND DYNAMICS OF N PARTICLES SYSTEMS

A. Scotti

Introduction

The foundations of classical statistical mechanics and their connections with the foundations of quantum statistical mechanics have been studied. The guiding motivation of this research is the realization, based on recent mathematical and numerical computations, that the fundamental hypothesis on which classical statistical mechanics was based, i.e. ergodicity, does not have the generality that was up to now assumed. This lack of ergodic behaviour shows up in systems constitued of particles interacting via potential having a minimum, such, as, typically, molecular potentials, and for energies near this minimum. This feature should then, be relevant for solids at extremely low energies. Since it is exactly for these systems that classical mechanics was supposed to fail, the study of what is in fact the correct behaviour according to classical laws, and its comparison with the quantum one, is of very great theoretical interest.

Recent progress in classical nonlinear dynamics

In classical mechanics there have recently been two great achievements, i.e., the Kolmogorov, Arnol'd and Moser (KAM) theorem [1] and Sinai's theorem [2], which can be considered as related to different aspects of one and the same problem. The problem is the behaviour of a system of particles interacting, for example, with a pair potential of molecular type, characterized by the presence of both a repulsive and an attractive part. Indeed, in this case, for high values of the energy the system can be considered essentially as a system of hard spheres, while for energies slightly above the minimun of the total potential energy it is equivalent to a system of perturbed harmonic oscillators. Now, harmonic oscillators have quite ordered motions and KAM theorem guarantees that essentially the same happens in the presence of a small perturbation; on the other hand, hard spheres have quite stochastic motions, as guaranteed by Sinai's theorem, and it is expected that essentially the same should happen in the presence of a perturbation.

The problem can now be stated as that of understanding what happens in an intermediate situation. Indeed one expects this to be a very complicated one, as can be seen by analogy with the three-body problem with gravitational interaction, where all possible kinds of final motions have been classified [3]. The traditional answer given by physicists was very simple, however, namely that there was no intermediate behaviour at all, every motion being stochastic. The support to this statement was presumably a theorem of Fermi [4], essentially based on a theorem of Poincaré [5], according to which for generic systems there are no analytic constants of motion besides energy. This theorem was misunderstood, however, and the problem of the constants of motion is much more complicated.

The question of greatest interest is the existence of invariant surfaces constituted by trajectories, and their total measure. If these surfaces constitute continuous families filling the whole phase space they correspond to constants of motion such as energy. This, however, is not the general case. In general one can find formal expressions for constants of motion (Birkhoff, Whittaker, Von Zeipel, Contopoulos), but the related families of surfaces correspond to actual invariant surfaces only in limited regions of space [6][7][8]. The first examples of such a situation were found by astronomers [9] in connection with the observed distribution of stars in our galaxy. The picture which now prevails is the following. For low energies the motions are of ordered type, as if there actually were other constants of motion besides energy, which can indeed be computed (region of KAM stability); above a certain threshold energy the system becomes stochastic.

Such a picture constitutes the general framework in which many different problems have been understood which can be reduced to the study of non-integrable systems of two degrees of freedom as for example: the motion of a star in an axially symmetric galaxy [6]; the trajectories of particles in an accelerator [10]; the oscillations of an artificial satellite [11]; the magnetic fields at zero Lorentz force [12]; the restricted three body problem [13].

The question is now whether such a picture is valid and relevant for atomic and molecular systems. Here the interesting fact is that such a picture stands at variance with the commonly accepted one, according to which it is clear that, in classical mechanics, the specific heat of solids does not vanish at low energies. This belief is based on the assumption of equipartition of energy among the degrees of freedom of the solid, a property which can be easily proved, at least for low energies, if there are only stochastic

motions on each energy surface. Moreover, the asserted nonvanishing of the specific heat of solids at low energies is just one of the first examples quoted in books on quantum mechanics [14] to point out the failure of classical mechanics; KAM theorem could then have a role in understanding the foundations of quantum mechanics. An analogous situation obtains in the case of the electromagnetic field, considered as an infinite system of oscillators; indeed, the classical Rayleigh-Jeans law is deduced by assuming equipartition [15].

Things could be settled in agreement with the traditional belief if one could prove that the threshold energy for stochasticity vanishes with increasing number of particles. KAM theorem would then be irrelevant for atomic physics. This has indeed been conjectured [16]. Things, however, are not so clear and nothing definitive can be said on this point at present [17],

The possibility that KAM theorem is indeed quite meaningful for physics, particularly in understanding the foundations of quantum mechanics, can then be investigated. Some supports are given by numerical computations on the Fermi, Pasta and Ulam (FPU) model [18] in the version of Bocchieri, Scotti, Bearzi and Loinger (BSBL) [19], which is the most natural one-dimensional model of a solid. On this model, contrary to the expectations based on Fermi theorem, FPU proved numerically the existence of ordered motions. Stochastic motions were found by Izrailev, Khisamutdinov and Chirikov [20] and, independently, the threshold energy for stochasticity was evaluated by BSBL [19] for numbers of particles from 10 to 100. It has been found that, for physical values of the parameters in the problem, this threshold energy is of the order of magnitude of the quantum zero-point energy [21]. Correspondingly, it had already been found [22], for many initial conditions, that the final distributions of energy among the oscillators are of Planck-like shape and are well fitted by a Planck distribution with an action which is of the order of magnitude of Planck constant. To understand these facts an old paper by Nernst [23] on the interpretation of Planck law is of interest; this paper, strangely enough, had been almost completely forgotten, and gives instead a physical basis to the picture described above. According to Nernst, at zero temperature it is not energy that vanishes, but entropy. In other words, at zero temperature there still has to be present some energy which however, like every kind of energy at zero temperature, i.e., at zero entropy, has to be of ordered type. In the picture described above, the ordered motions are just the stable KAM motions, and the motions above zero temperature are the stochastic motions above the threshold energy. The interesting fact is that the presence of a nonvanishing threshold, in the opinion of Nernst, influences the stochastic motions making them of quantum type. An argument supporting this opinion has been given [21]. A review article on recent progress in classical non-linear dynamics is in preparation [24].

References

1) A.N. Kolmogorov, Dokl. Akad. Nank SSSR *98*, 527 (1954);
V.I. Arnol'd, Dokl. Akad. Nak SSSR *1377*, 255 (1961);
J. Moser, Nachr. Akad. Wiss. Göttingen: *Math. Phys. Kl. IIa, 1*, 1 (1962)
2) Ya. Sinai, Russian Math. Surveys 25 137 (1970)
3) Alexeyev, Actes Congrès Intern. des Mathémat., Nice (1970), Tome 2, 893
4) E. Fermi, *Z. Physik* 24, 261 (1923)
5) H. Poincaré, Méthodes Nouvelles de la Mécanique Céleste (Gauthier-Villars, Paris), 1892
6) M. Hénon and C. Heiles, *Astron. Journal 69*, 73 (1964)
7) F.G. Gustavson, *Astron. Journal 71*, 670 (1966)
8) J. Roels and M. Hénon, *Bull. Astron. 2*, 267 (1967)
9) G. Contopulos, *Astron. Journal 68*, 1 (1963)
10) L.J. Laslett and K.L. Symon, C.R. Symp. CERN, Geneva, 287 (1956)
11) V.A. Zlatonsov, D.E. Okhotsiniski, V.A. Sarichev and A.P. Torjevski, *Kosmicheskie Issledovania 2*, 657
12) M. Hénon, C.R. Acad. Sci. *262*, 312 (1966)
13) V.I. Arnol'd, *Russian Math. Surveyes 18*, 85 (1963)
14) P.A.M. Dirac, Quantum Mechanics
15) For a modern discussion on this point see for example P. Bocchieri and A. Loinger, *Lett. Nuovo Cim. 4*, 310 (1970); ibid. *1*, 709 (1971); ibid. *2*, 41 (1971)
16) J. Ford, *J. Math. Phys.*, in press
17) J. Moser and M. Hénon, private communications
18) E. Fermi, J. Pasta and S. Ulam, in E. Fermi, *Collected Papers* (Univ. of Chicago Press, Chicago 1965), p. 978
19) P. Bocchieri, A. Scotti, B. Bearzi and A. Loinger, *Phys. Rev. A2*, 2013 (1970)
20) F.M. Izrailev, A.I. Khisamutdinov and B.V. Chirikov, Preprint 252, Inst. of Nucl. Phys., Novosibirsk (1968)
21) C. Cercignani, L. Galgani and A. Scotti, *Phys. Lett., 38A* 403 (1972)
22) L. Galgani and A. Scotti, *Phys. Rev. Lett.*
23) W. Nernst, *Ver. D. Phys. Ges. 4*, 83 (1916)
24) L. Galgani and A. Scotti, *La Rivista del Nuovo Cimento*, to appear

DEVELOPMENT OF METHODS FOR THE SORA DESIGN CALCULATIONS

T. Asaoka, E. Caglioti, J. Hartman, R. Jaarsma,
W. Matthes, K.H. Müller, H. Rief, E. Sartori

Quasi-Stationary Design Calculations

The behaviour of the neutron population in a pulsed reactor with short superprompt critical phases and long periods of subcriticality is a rather complex dynamical process. A quantitative analysis of such fast systems shows, however, that the neutron generation time of 30 nsec is very short compared to the pulse length of 60–80 μsec. It corresponds to ~ 2000 neutron generations during a pulse. One can therefore with good reasons assume that at each time moment a stationary neutron distribution in space and energy is reached. This allows, as far as core calculations are concerned, the application of the stationary neutron transport equation and the definition of the static eigenvalues. Neutron spectra, flux distributions and the reactivity worth of control devices and the pulsation can therefore be expressed in the classical way.

The methods used to perform these semistatic design calculations are the Carlson S_N codes and Monte Carlo.

The two methods have been applied in a complementary manner, making full use of their particular potentials. The two-dimensional S_N program DOT2 and the one-dimensional ANISN code proved to be particularly useful to perform all kind of parametric studies dealing with relatively small changes of cross-sections and geometrical compositions. Furthermore they were used to generate mappings of neutron fluxes and their adjoints, power distributions in the core, reactivity changes, and finally input parameters for kinetic, dynamic and Doppler calculations.

The Monte Carlo method on the other hand served for the analysis of problems requiring a real three-dimensional treatment such as the reactivity value of the pulsation, the control devices and the neutron scatterers feeding the experimental facilities. In addition this method is used for problems where a more detailed cross-section description is required. For this purpose the TIMOC code (originally written in FAP for the use of the IBM 7090/94, see EUR 45193, 1970) has been rewritten in Fortran IV and improved. In this version the procedure for calculating small effects has been ameliorated. It is based on an iteration model to approximate an adjoint function and the possibility of splitting in the "perturbed region". In addition, a different calculational scheme makes small effect calculations less time consuming than previously [7].

In another more general approach a Monte Carlo procedure for the calculation of perturbations in a multiplying system due to changes in system parameters (e.g. temperature, control rod positions etc) was elaborated. The procedure is based on the perturbation-theory formula which gives the reactivity change exactly up to terms of second order if the fission density distribution and/or the corresponding adjoint function are known up to first order. As this formula makes full use of the properties of the importance-(adjoint) function a Monte Carlo procedure for the evaluation of the adjoint function was developed too [4].

Finally a new approach has been shown to arrive at the simulation of the adjoint transport equation. Usually one starts from the adjoint equation and constructs a Monte Carlo game for its simulation. This procedure requires sophisticated reasoning to find out which quantity of the game is adjoint to what. Contrary to this point of view, we start from the beginning with two independent games of two different kinds of particles and put the condition that the expectation value of some estimator in the two games should be equal. This leads directly to the Monte Carlo game for the adjoint flux and provides a large arbitrariness for the adjoint games. This arbitrariness can be used to find adjoint games with smaller variances [6].

Stationary Pulse Kinetics Studies

The power pulse shape can be determined by solving the prompt neutron kinetics equation through knowing the shape of the reactivity pulse in the region near and above prompt critical and the maximum reactivity level. Owing to the steady-state operating condition, that is, time-independent pulse characteristics for periodically pulsed reactors, there is one value for the maximum reactivity level k_m for given reactor kinetics parameters, and a reactivity pulse shape which is approximated by a parabola: $k_m - \alpha(vt)^2$.

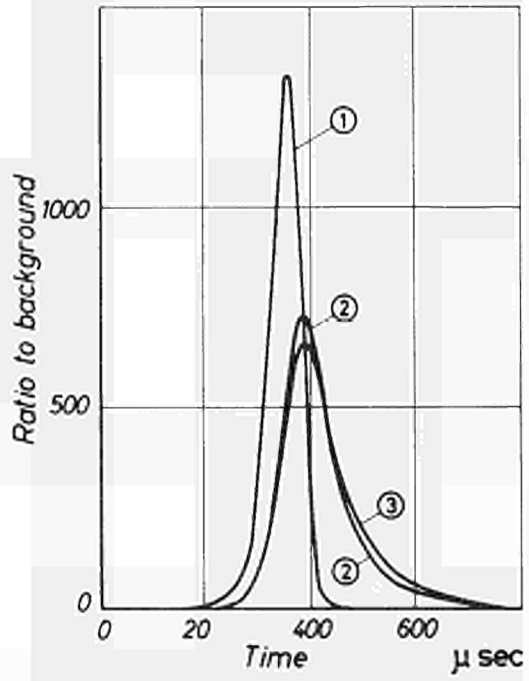

Fig. 1: Stationary fast and thermal neutron pulses.

1 – Fast flux in core-region
2 – Thermal flux in central moderator
3 – Thermal flux in side moderator

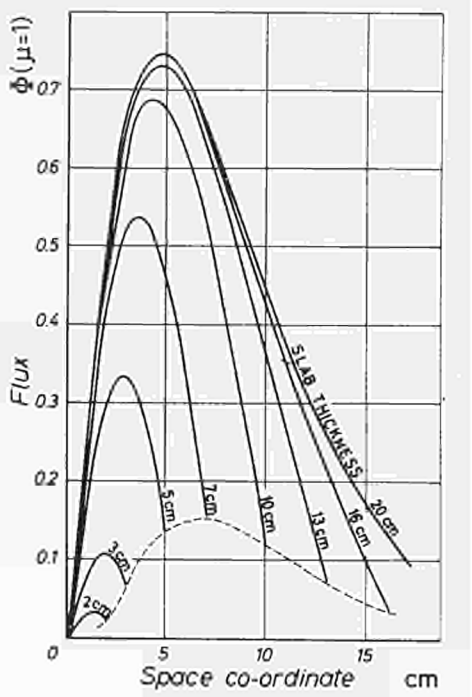

Fig. 2 – The angular flux (below 0,15 eV) in the normal direction in 300°K water slabs.

The stationary power pulse characteristics as well as the pulse characteristics of low-energy neutrons originated from the external moderators can thus be estimated from the few-space-point kinetics equation in a few-energy-group model (T. Asaoka and R. Misenta, EUR-2273e, 1965). Fig. 1 shows a typical stationary pulse shape obtained with the values $\alpha = 6\ m^{-2}$, $v = 283$ m/sec and the background k_{eff} (between the reactivity pulses) = 0.967. The required maximum prompt reactivity for achieving the stationary pulse is about 150 pcm or $k_m = 1.0084$.

The Optimization of Low Energy Neutron Moderators

In the SORA reactor, some of the neutrons produced in periodic pulses in the core are converted in the external hydrogenous moderators into pulsed beams of low-energy neutrons for time-of-flight measurements. From the experimental viewpoint, the important characteristics of a neutron source are the intensity of the neutrons reaching the target and the relation between time distribution and energy resolution. Therefore, when there is no collimation between the source and the target, an overall figure-of-merit as a basis for optimization of pulsed reactors is $E_p P\phi_s/\sigma^2$ where P is the mean reactor power, E_p the fraction of power generated during the pulses, ϕ_s the fictitious isotropic leakage flux produced per unit power [$\phi_s = 4\pi S \int_0^\infty dt\ G(t)$ in which S = fast neutron intensity incident on the moderator surface and G(t) = time distribution of neutron leakage due to an incident unit delta function source] and σ^2 the source pulse variance which is equal to the sum of power pulse variance σ_p^2 and the variance of G(t) σ_m^2. In experiments where the dependence of the source-target distance is less than the inverse square, a suitable figure-of-merit will be $E_p P\phi_s/\sigma$ or $E_p P\phi_s$ (T. Asaoka and J.A. Larrimore, J. Nucl. Energy, 24, 439, 1970).

For performing optimization studies in terms of the figure-of-merit the computer code JN-METD1 (see 1) was developed. It is based on the j_N method developed at Ispra. The calculations were performed for moderator slabs [water at 300°K, para-hydrogen at 20°K or liquid hydrogen (75% ortho + 25% para) at 20°K] with various thicknesses for eight energy-groups and a j_7 approximation. Fig. 2 shows a typical result: the ϕ_s ($\mu = 1$) of the lowest energy group (below 0.15 eV) as a function of space inside water slabs of various thicknesses. The ϕ_s at the boundary (leakage flux) peaks at a slab thickness of around 7 cm, though the spatial maximum value of ϕ_s increases as the slab thickness goes up to about 15 cm.

After establishing the optimum slab size of a moderator by JN-METD1 calculations, the full time-dependence of the moderator leakage flux and the absolute flux values are calculated by Monte Carlo (TIMOC 71). For this purpose the time-dependent moderator response function G(t) of a $\delta(t)$ burst in the core is calculated and convoluted with the power pulse usually approximated by a Gaussian representation

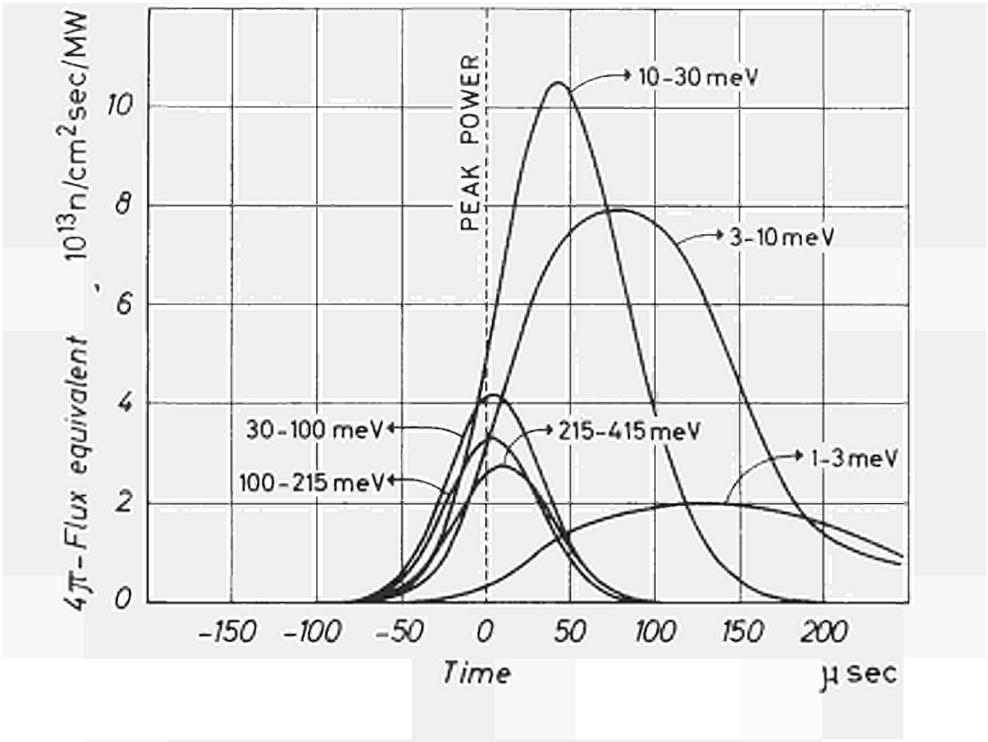

Fig. 3: Time dependent leakage flux out of a Para-Hydrogen scatterer.

Fig. 3 shows as a typical example of such a convolution, $\phi_S(t) = S \times \int_{-\infty}^{t} d\tau G(t-\tau) \exp[-\tau^2/(2\sigma_p^2)]$, the time-dependent leakage flux out of a para-hydrogen moderator (half cylinder of 13 cm radius).

In addition, with the use of another jN computer code JN-METD2 (T. Asaoka and E. Caglioti, EUR report under preparation), heterogeneous poisoning has been studied with the aim of reducing σ_m^2 by inserting a cadmium sheet inside a water slab in order to increase the figure-of-merit. The results will be given in a separate publication [3].

Power Pulse Fluctuations in the SORA Reactor

Fluctuations of the power pulses in periodically (reactivity-) pulsed reactors were confirmed experimentally. The necessary analytical methods to describe such phenomena were established in Ref. 5. It turns out that the variance to mean ratio of some fluctuating quantities (e.g. the number of neutron counts in an absorption counter integrated over the power pulse) is power-independent and only a function of the criticality of the reactor. These quantities can therefore be used to determine the criticality of the reactor experimentally.

A New Macro Random Walk Approach to Analyse Shock Wave Propagation and Shielding Problems

A sudden evaporation of a reactor core creates shock waves in the surrounding vessel and containment. The superimposition of these waves is strongly dependent on the geometry and accumulates at local tension spots which become starting points for fracture and fragmentation.

A stochastic model was developed, based upon Huygens' principle and describing the expansion and superimposition of elastic waves inside complex bounded media.

For the computation of the space-time dependent pressure distribution in a finite shear-free medium, created by a point-impact, $p(0,t) = P_0\,\delta(r)f(t)$, a computer code has been written and applied to a liquid in a prismatic containment (publication, K.H. Müller, in preparation).

A more generalized code version suitable for elastic wave fields in solids is now being prepared. It uses the 05R-geometry routine of ORNL.

The transmission of neutrons emitted by a fast reactor core through layers of strong neutron attenuation was likewise treated. For this purpose a new random-walk approach was developped and applied to thick Fe-layers. This method interprets the leakage probability $W(V_0/R, \theta, S, V)$ of a neutron starting at the centre of Fe-spheres (R = 1,2,3,4,5 cm) as cross-sections of the spheres and constructs with

them a (macro-) random walk, MMC.

The W-functions of the Fe-spheres were calculated with 200,000 neutron histories of the starting energies

$$E_0 = 0.01 - 1.4 \text{ MeV (16 groups)}$$

by the usual analog Monte Carlo approach AMC and stored on tape.

A MMC-calculation extended the W-library to Fe-spheres with $R > 5$ cm.

The computation of the transmission of 10,000 (1 MeV) source neutrons through a Fe-prism (20x20x10 cm) required a calculation time of about 70 sec. on an IBM 360/65 (publication, K.H. Müller, in preparation).

A Critical Analysis of Statistical Choppers applied to Periodically Pulsed Neutron Beams

In time-of-flight experiments using periodically pulsed reactors as a neutron source, the neutron beam falling on the sample shows an inherent periodical structure. The intensity and spectrum of the input beam at the position of the sample vary periodically in time. A pseudo-statistical modulation of the input beam just before the sample will lead to an improvement of the efficiency (resolution duty cycle) of the experiment. We give a procedure for performing the cross-correlation function between the neutron input beam and the output beam of scattered neutrons and describe a method by which the scattering function of the sample material can be evaluated from the measured cross-correlation functions.

The accuracy of the method depends on the detailed time pattern of the incoming intensity. This allows one to characterize each time pattern by a gain factor, which gives greater accuracy than the conventional time-of-flight experiment. It turns out that for short input pulses a local, gliding average value of the scattering function, taken over a small interval (twice the input pulse length) around the point of measurement, is responsible for the accuracy. This work will be presented at the "Fifth IAEA Symposium on Inelastic Neutron Scattering", Grenoble 1972 by W. Matthes, Statistical Chopper for Periodically Pulsed Neutron Beams. Paper/SM-155/F-7.

References

1) T. Asaoka *JN-METD1, A Fortran-IV Programme for Solving Neutron Transport Problems with Isotropic Scattering in Bare Spheres and Homogeneous Slabs by the j_N Method,* EUR 4601e (1971)

2) T. Asaoka, *Analysis of Critical Experiments on the SORA Mockup by the S_N Method,* EUR 4676e (1971)

3) T. Asaoka and E. Caglioti, *The j_N Method for Neutron Transport Problems in Multilayer Slab Systems and its Application to the Optimization of Medorator in Pulsed Reactors,* in preparation.

4) W. Matthes, *Some Applications of the Monte Carlo Method at the Euratom Research Centre Ispra,* ANS-Meeting, March 27, 1971, Idaho Falls, invited paper.

5) W. Matthes, *Power pulse fluctuations in the SORA reactor,* external report EUR 4679e (1971)

6) W. Matthes, *Monte Carlo simulation of the adjoint transport equation,* external report 4678e (1971)

7) H. Rief, W. Matthes, *Monte Carlo Störungsrechnungen in multiplizierenden Medien,* Dt. Atomforum, Tagungsbericht, 1971.

INTEGRAL CAPTURE CROSS SECTION MEASUREMENTS OF STRUCTURAL MATERIALS IN THE FAST-THERMAL RB-2 FACILITY BY THE VOID-NULL REACTIVITY METHOD

G. Casini, G. Cordani, R. Cuniberti, M. Dubujadoux, S. Guardini, B. Sturm, S. Tassan, P. Varekamp

Introduction

In recent years considerable attention has been devoted to the assessment and use of integral measurements as a check of nuclear data playing an important role in the design and operation of power reactors. The capture cross sections of the structural materials used in fast breeders are among the nuclear data where the uncertainties existing to-day are still significantly higher than acceptable for an economical design.

In order to contribute to fill this gap AGIP NUCLEARE, CNEN-Bologna and EURATOM, Ispra JRC have set up a joint experimental program for the determination of average capture cross sections of structural materials, such as iron, nickel and chromium, in "tailored" epithermal and fast spectra, the maximum of neutron events being in the 1 keV - 100 keV energy region.

The experiments will be carried out in the RB-2 reactor of Bologna, modified into a coupled fast-thermal facility, with a central test-zone consisting of mixtures of coated fuel particles (highly enriched in U^{235}), particles of graphite and of the material under investigation. The void-null reactivity method associated with the reactor oscillation technique will be used, poisoning the test-medium to k-inf = 1 by loading the graphite particles with boron.

Definition of the problem

The last improvements in the cross section data for fissile and fertile materials contrast strongly with the large variations among the results of different measurements of the absorption cross sections of some of the elements used for the fuel cladding and in the structure of fast reactors, as iron, nickel and cobalt. In fact, the recent high-resolution capture measurements [1) 2) 3)] have shown some large discrepancies, when compared to the previous measurements using the lead slowing-down time spectrometer, putting into evidence a much more complex resonance structure. Narrow capturing resonances are superimposed on the underlying capture cross section due to the broad s-wave structure that is observed in total cross section measurements. The presence of these narrow resonances makes analysis, interpretation and correction of the observed data from differential experiments particularly difficult.

A picture of the actual situation (MOXON, 1970) concerning the capture cross section of iron versus energy, is given in Fig. 1 [4)]. A calculation of the mean value of the different sets of measured points in the 1 keV – 100 keV energy range, gives an uncertainty of + 65 %, – 45 %.

These values are slightly more pessimistic than the estimate of ± 30 %, as given by Moxon. In the energy region from 100 keV to 1 MeV, the Moxon indication is for an uncertainty of (± 50 %.) For nickel and chromium a similar situation is observed.

These uncertainties are still too high for the economical design of a fast breeder reactor, as shown in an analysis by Greebler (1968) on the significance of neutron data in fast power plant design [5)], where an accuracy of ± 10 % was required for the capture of structural materials, as nickel, iron and chromium, in the energy range between 100 eV and 10 MeV.

In order to improve this situation integral experiments seem necessary, together with additional effort on the evaluation of the existing differential measurements. However, to be effectively useful, integral experiments must meet a number of requirements:

- clean geometry of the test-medium (preferentially homogeneous medium), in order to substantially reduce or eliminate the uncertainties associated with the evaluation of heterogeneity effects;
- minimization of the net leakage from the test-zone;
- use of materials with known nuclear properties (apart from the material under investigation) and in well defined proportions, so as to obtain a "tailored" neutron distribution in the energy range of interest;
- possibility of easily varying the ratio between fuel and moderator in the test-zone, in order to produce a significant set of different energy spectra over which the measured captures are averaged.

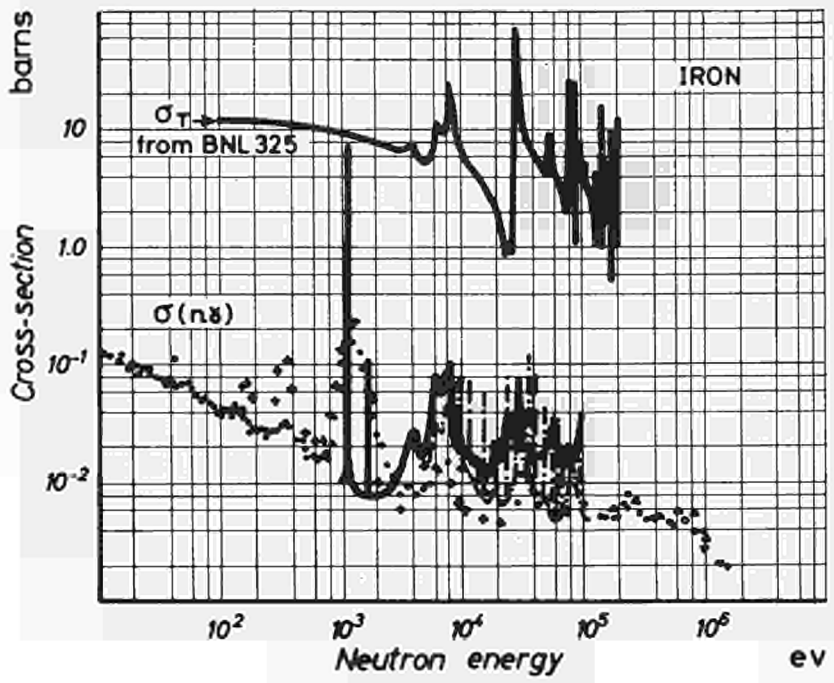

Fig. 1: Capture cross-section of iron versus energy.

Type of Experiment Selected

To satisfy the above requirements, the experiment makes use of:

- test media consisting of mixtures of particles of fuel, moderator and test-material;
- the void-null reactivity technique for neutron balance measurements;
- a multi-region reactor with a thermal driver region (external), a buffer region and a fast region (test-medium, central).

The sequence of the measurements is:

A. A mixture of fissile (U^{235}) and moderating (C) microspheres, in a suitable proportion to generate the required neutron energy spectrum, is poisoned by boron to k-inf = 1.
The basic balance equation is

$$\text{k-inf}_1 = (\nu_1^5 F_1^5 + \nu_1^8 F_1^8) / (F_1^5 + C_1^5 + F_1^8 + C_1^8 + C_1^C + C_1^B) = 1 \qquad (1)$$

where F,C indicate fission, resp. capture rates, and the indices 5, 8, C, B refer to U^{235}, U^{238}, graphite and boron.

B. A proper amount of the structural material under investigation is homogeneously added to the test-medium (maintaining the same fissile-to-moderator ratio) which is poisoned again by boron to k-inf = 1. The balance equation is:

$$\text{k-inf}_2 = (\nu_2^5 F_2^5 + \nu_2^8 F_2^8) / (F_2^5 + C_2^5 + F_2^8 + C_2^8 + C_2^C + C_2^B + C_2^S) = 1 \qquad (2)$$

The above equations are simultaneously solved (the capture by graphite, as well as the U^{238} fission, are ignored), yielding

$$R^S = XN(1 + \alpha_1^5 + R_1^8 + R_1^B) - (1 + \alpha_2^5 + R_2^8 + R_2^B)$$
$$\text{where } R = C^{(8,5,S)}/F^5,\ X = \frac{\text{k-inf}_1}{\text{k-inf}_2},\ N = \frac{\nu_2^5}{\nu_1^5},\ \alpha^5 = \frac{C^5}{F^5} \qquad (3)$$

and the subscripts 1, 2 refer to the values relative to measurements A and B, respectively.

The directly measured quantities are:

- k-inf_1 and k-inf_2;
- the composition of the null reactivity test-medium expressed in terms of the atomic ratios $C/U^{235}/B$ and $C/U^{235}/S/B$ for measurements A and B, respectively);
- the ratios of B capture to U^{235} fission (C^B/F^5) and U^{238} capture to U^{235} fission (C^8/F^5) in the null reactivity test-medium.

The quantities $N = \nu_2^5/\nu_1^5$ and $\Delta\alpha_5 = \alpha_1^5 - \alpha_2^5$ are calculated. The variation in the values of ν^5, α^5 from measurement A to B is due to the energy spectrum softening caused by neutron scattering in the structural material. This variation being in general of little magnitude, its theoretical evaluation in the simultaneous solution of the equations related to the two measurements does not introduce a significant error in the experiment.

Criteria for the definition of the main parameters of the test-medium

The main parameters of the test-zone are:

- the ratio "moderator/fuel" = C/U^{235} (or C/U);
- the ratio "structural material/moderator" = S/C.

In order to proceed with the definition of these parameters a detailed analysis of the error associated with the experiment is necessary. Starting from the expression (3) (ignoring the effect of the uncertainty in R^8), one obtains for the error in the capture rate of the structural material:

$$\frac{dR^S}{R^S} = f_X \frac{\delta X}{X} + f_N \frac{\delta N}{N} + f_{\Delta\alpha^5} \frac{\delta\Delta\alpha^5}{\Delta\alpha^5} + f_{R_1^B} \frac{\delta R_1^B}{R_1^B} + f_{R_2^B} \frac{\delta R_2^B}{R_2^B} \qquad (4)$$

where f are the error transmission factors.

Let us consider as an example the measurement of the capture in iron, assuming the following values for the partial errors (as inferred from conservative estimates based on previous experience):

$$\frac{\delta X}{X} = 0.35\,\%, \frac{\delta N}{N} = 0.05\,\%, \frac{\delta\Delta\alpha^5}{\Delta\alpha^5} = 15\,\%, \frac{\delta R^B}{R^B} = 1.6\,\%.$$

One obtains for the error in R^{Fe} (iron capture/U^{235} fission) the results given in Fig. 2, over the C/U^{235} and Fe/C ranges $100 \div 250$ and $0.4 \div 1.25$, respectively.

From the curves of Fig. 2 it appears that the error in R^{Fe} (Fe capture/U^{235} fission) rapidly decreases with the increase of both the C/U^{235} and Fe/C values. This dependence is obviously due to the relative increase of the Fe total capture at softer spectra and at higher Fe contents in the test-medium, respectively. The less pronounced reduction of the overall error towards the higher values of Fe/C is due to the contrasting effect of the increase of the error component relative to $\Delta\alpha^5$ (4), following the uncertainty associated with the evaluation of the scattering by Fe.

Clearly, the corresponding error in the mean capture cross section of the structural material in the energy range from 1 keV to 100 keV (i.e. where the uncertainty in the cross sections is highest) depends on the relative importance of the captures of the material in this energy range. These data are plotted in Fig. 3 for iron, as a function of the moderator-to-fuel ratio (C/U^{235}) and the fraction of the overall capture which is Fe capture (Cr(Fe)%). The significant decrease of the percent capture by iron in the energy range of interest with the increase in the values of both parameters, follows the spectrum softening due to moderation by carbon and (less pronounced) by Fe scattering.

The opposite trends evidenced by Figs. 2 and 3 indicate that a compromise solution must be sought for the values of the main parameters defining the test-zone: C/U^{235} and S/C, respectively.

Significantly different curves than shown in Figs. 2 and 3 are obtained when using the various evaluated sets of group cross sections for iron, due to the large uncertainty of these data. This analysis is underway, but one will rely also on the large flexibility of composition of the test-medium, due to the particular solution adopted and based on the use of mixtures of microspheres [5] to adjust the above parameters as evidenced by direct experimentation.

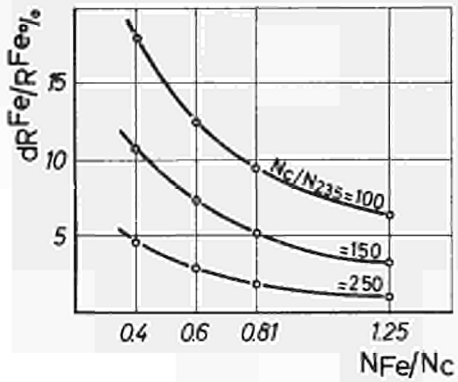

Fig. 2

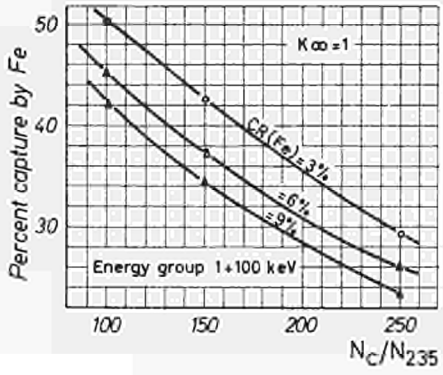

Fig. 3

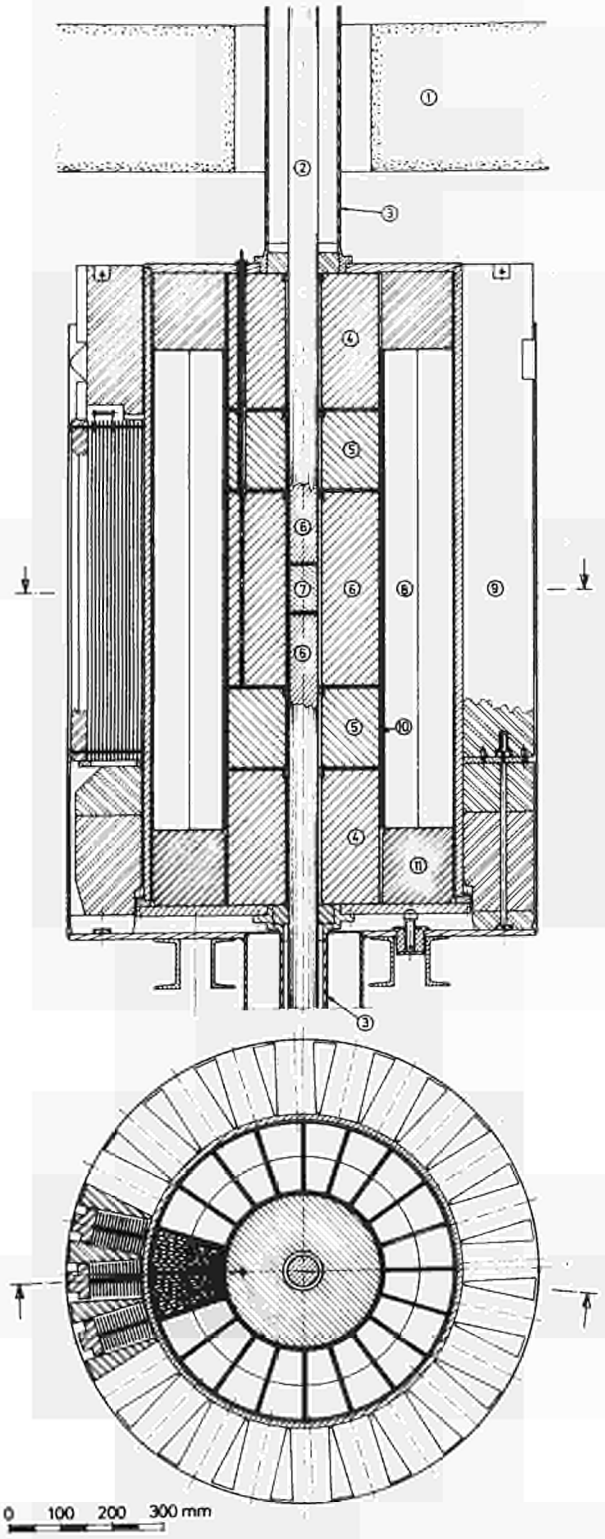

Fig. 4: Reactor RB-2/TV (fast-thermal version). Preliminary design.

1 – Concrete shield
2 – Oscillating column
3 – Cadmium
4 – Flux flattener
5 – Unpoisoned microspheres (U235, C)
6 – Poisoned microspheres (U235, C, B)
7 – Test sample
8 – Buffer zone (mtr plates, graphite)
9 – Termal zone (mtr plates in H_2O)
10 – Boron-steel shield
11 – Graphite
12 – Empty sample

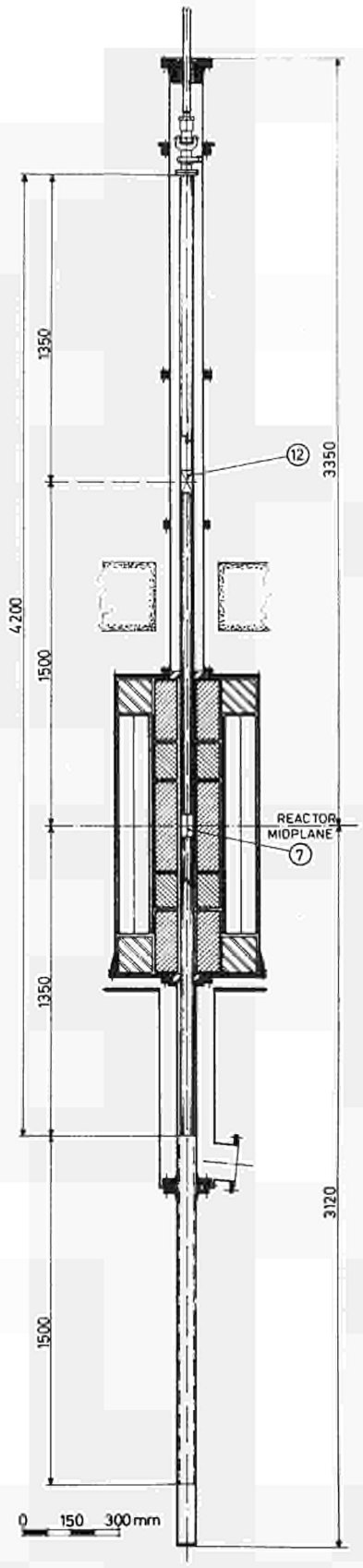

Fig. 5: Reactor RB-2/TV. Oscillating column view.

Test-medium composition

The test-media will consist of mixtures of microspheres (about 1 mm diameter) of graphite coated fuel (UO_2 enriched to 93% U^{235}), nuclear grade graphite (poisoned by natural B so as to reduce the k-inf of the test-medium to unity), structural material. High purity materials will be used (e.g. very low H_2 impurities).

Such a solution offers, in principle, several important advantages:

- quasi-homogeneous medium conditions, thus minimizing heterogeneity corrections and associated uncertainties. It is reminded that heterogeneous media require elaborate neutron transport treatments which are one of the main sources of uncertainty in this kind of experiments.
- clean medium conditions, due to the limited number of high-purity materials present, with well known cross sections (except for the material under study). This allows accurate calculations from the point of view of nuclear data.
- low inventory of expensive fuel, due to the possibility of using the same fuel particles (after separation of the mixture components) for generating test-media with varying composition and neutron energy spectrum.
- operating flexibility, associated to the easiness of composition and separation of the particle mixtures.
- quasi-fluid medium, which can fill volumes of varying shape and size, according to the experimental requirements.
- very low hazard of contamination, assured by the pyrolytic graphite coating of the fuel, allowing a safe and rapid handling of the particle mixtures.

The main problems related to this solution regard:

- fabrication of boron loaded graphite microspheres with adequate properties;
- obtaining homogeneous two and three components mixtures in the test-zone;
- producing highly pure microspheres of the structural material under investigation.

Preliminary design of the experimental facility

As mentioned, the experiments will be performed in the ARGONAUT reactor RB-2 of AGIP NUCLEARE, Bologna [6], which has lately been modified to carry out k-inf measurements of HTR lattices following the null reactivity-void principle, by the reactor oscillation technique. The feasibility and orientative design studies so far completed, have led to a preliminary arrangement of the facility for the integral measurement of the capture cross section of iron in the 1 keV – 100 keV energy range as shown in Figs. 4 and 5.

The preliminary design of the experimental facility includes:

- a central test-zone, 30 cm diameter and 70 cm height, filled with a mixture of 1 mm diameter graphite coated UO_2 particles (93% enriched U^{235}) and borated graphite particles, with atomic ratio C/U = 150, and void coefficient 0.37. A proper amount of Fe microspheres is included in the mixture when performing the experiment type B previously described.
- a boron loaded steel liner
- a buffer zone (32 cm inner diameter, 60 cm outer diameter, 90 cm height), consisting of a modular arrangement of 90% enriched uranium plates and graphite slabs, with the same atomic ratio C/U = 150.
- axial flatteners around the test- and buffer zones
- an oscillating column on the axis of the test-zone, containing the test sample filled with the same particle mixture of the test-zone (see below). The facility is contained in the 61 cm diameter aluminium tank of the reactor, surrounded by the driver zone (MTR plates in light water).

This design meets the requirement to produce around the central test-sample a space-energy neutron distribution very near to that of an infinite medium with the same composition. The analysis has involved one-dimensional and two-dimensional calculations. The one-dimensional calculations have been carried out in a 26 energy-group structure by the diffusion and transport (S_4 for flux anisotropy) approximations. The two-dimensional calculations have been performed in a 6 energy-group structure by diffusion approximation. The group-averaged cross sections have been generated by the code GAM.

In Table 1 some calculated parameters characterizing the space-energy distribution of neutrons in the test-zone are presented, for different buffer configurations. The parameters are: neutron production-to-absorption ratio versus the radial distance from the test-zone axis; boron, respectively iron, absorption-to-U^{235} fission neutron production ratios at the center of the test-sample. The buffer configurations compared are: completely poisoned (homogeneously), partially poisoned (homogeneously), not poisoned but with boron-loaded steel liner around the test-zone. From the data in the Table, it appears that boron poison must be present in the buffer; however, a boron-steel liner seems to be as effective as a homogeneous dispersion of boron in the buffer-zone. In Fig. 6 the neutron energy spectrum at the centre of the test-sample (configuration 5 of Table 1) is compared to that of the infinite medium with the same composition poisoned to k-inf = 1.

Table 1

Case	Buffer zone characteristics	k_{eff} reactor	production absorption			CR (Fe) ν FR(235)	CR (B) ν FR(235)
			r = 0	r = 5cm	r = 12	r = 0	r = 0
1	Infinite medium	–	1.000	–	–	$2.923 \cdot 10^{-9}$	0.393
2	Buffer completely poisoned	0.929	0.997	0.997	0.992	2.990	0.396
3	Buffer not poisoned	1.053	0.933	0.984	0.944	3.027	0.405
4	Buffer not poisoned boron-steel liner	1.0446	0.998	0.996	0.978	3.016	0.397

Some remarks on the experimental method

Basically, the experiment will consist of:

- verifying the neutron space-energy distribution and matching in the zone of the test-sample;
- null reactivity measurement;
- measurement of B, resp. U^{238} capture, and U^{235} fission rates in the test-sample;
- determination of the test-sample and test-medium compositions.

The space-energy neutron distribution in the test-zone will be measured by miniaturized fission chambers (1.5 mm diameter) with energy sensitive deposits, as U^{238}, Pu^{240}, Np^{237}, Pu^{239}, as well as U^{235}. The spectral indices obtained (as U^{238}/U^{235} fission) will be normalized with a measurement performed at the same time in the thermal column of the RB-2 reactor.

The matching to the infinite medium conditions will be verified by the asymptotic flattening of these indices about the central portion of the test-zone, as well as by comparison with the corresponding calculated values for the infinite medium (the quasi-homogeneous and clean configuration of the test-zone should allow accurate theoretical evaluations).

Other techniques, such as activation of spectrum sensitive detectors, proton recoil chambers, etc., are also envisaged to supplement the information deduced from the fission chambers data.

The null reactivity measurement will be performed by the reactor oscillation technique. A 6 cm diameter, 4 m long column (ref. Fig. 5) filled with the same particles mixture as the test-medium, is periodically oscillated through the test-zone axis. The column contains a 10 cm high sample (with varying boron content or voided) which during the oscillation is transferred from the test-medium center to outside the reactor. The length of the column is such that during the oscillation the active part of the reactor is always filled with test-mixture, so that the neutron density modulation in the reactor is essentially due to the transfer of the test-sample only. This reduces spurious signals thus improving the accuracy of the measurement.

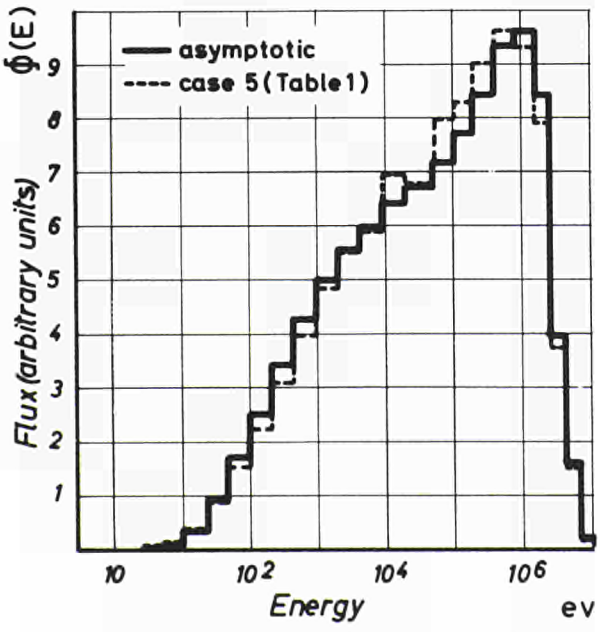

Fig. 6

The neutron density modulation will be interpreted in terms of a Fourier analysis or by other reactor kinetics techniques. The use of a calibrated auto-rod, to compensate the power modulation, is also being considered.

The "B capture/U^{235} fission" ratio in the test-sample will be measured by 4 mm diameter chambers with B, respectively U^{235}, deposits and normalized to the corresponding ratio determined in the thermal column. The U^{238} capture in the test-sample will be measured by foil activation and normalized to the thermal column data.

The test-samples and test-medium compositions will be determined by high precision chemical and isotopic analysis.

, A detailed evaluation of the uncertainties involved in the various steps of the experiment has been introduced in the error analysis previously outlined.

References

1) Spitz, L.M. et al., Nucl. Phys. A 121, 655 (1968)

2) Hockembury, R.W. et al., Phys. Rev. 178, 1846 (1969)

3) Stieglitz, R.G., Rep. RPI-328-171

4) Moxon, M.C., IAEA-CN 26/32 (1970)

5) Greebler, P. et al., Nucl. Appl. 4 (1968)

6) AGIP Nucleare, FNU/112 (1971)

SPACE-DEPENDENT REACTOR DYNAMICS

E. Vincenti, G. Forti, A. Clusaz, S. Dal Ben

Introduction

In the year 1971 the work on the space dynamics codes of the Costanza series was oriented to produce a two-dimensional (RZ) code for either boiling or single-phase coolant reactors. These codes consist of a neutronics part simulating the whole reactor, and of a thermohydraulics part (code of the Francesca series) simulating the cooling channels.

Neutronics [1) 2)]

This is the short description of two codes one of which is used to calculate dynamic transients whilst the other is used for xenon operational transient and xenon stability research. The geometry is cylindrical and two dimensions R and Z are considered. The time-dependent diffusion equations in the two-energy-group approximation are solved with the finite difference method.

The method

The vertical section of the reactor is subdivided with a Cartesian point lattice. To each point (i, j) corresponds a part of the space Aij delimited by four points of the lattice, within which the physical magnitudes are constant.

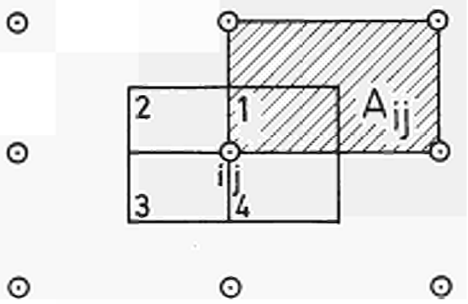

The two diffusion equations and the six precursor equations are integrated over the volume corresponding to the point (i, j); this volume is divided into four subvolumes belonging to different part of the space. Taking an average over the surrpunding space, we obtain the same formulas at the interfaces of the regions and within the regions and we can consider a pointwise temperature feedback.

The time step is constant. In the diffusion equations the time discretization is treated by the semi-implicit method, which is numerically stable and has a much smaller error than the usual implicit method for the same ratio of the time step to the reactor period $\Delta t/T$. The precursor equations are solved explicitly at every time step.

After integration the general form of the two group diffusion equations is:

$$-\alpha_{ij}\cdot\varphi_{i-1,j} - \beta_{ij}\cdot\varphi_{i,j-1} - \gamma_{ij}\cdot\varphi_{i+1,j} - \delta_{ij}\cdot\varphi_{i,j+1} + \epsilon_{ij}\cdot\varphi_{ij} = \delta_{ij}\cdot\psi_{ij} + C_{ij} \qquad \text{thermal}$$

$$-\alpha'_{ij}\cdot\psi_{i-1,j} - \beta'_{ij}\cdot\psi_{i,j-1} - \gamma'_{ij}\cdot\psi_{i+1,j} - \delta'_{ij}\cdot\psi_{i,j+1} + \epsilon'_{ij}\cdot\psi_{ij} = \delta'_{ij}\delta_{ij} + C'_{ij} \qquad \text{fast}$$

We have a system of 2 x n equations, where n is the number of points of the lattice. For solving this we use a direct method in the radial direction and an iterative method in the axial direction. The fluxes at the points on the upper and lower radii are considered as already known from the preceding iteration. The terms with α and γ are known and may be incorporated in the known term C. Let r be the number of points of the radius. If we intercalate the r equations of the fast group with the r eq. of the thermal group we have for each radius a system of 2r equations. This system has a coefficient matrix which is pentadiagonal, the matrix can however be partitioned into (2x2) submatrices.

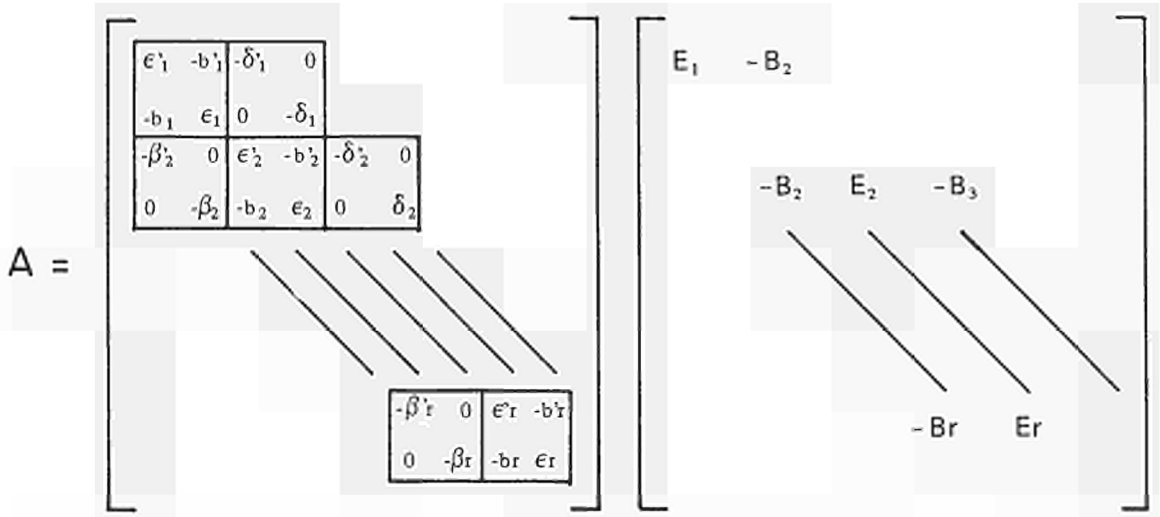

It can be considered as a tridiagonal matrix with entries consisting of (2x2) submatrices. As $\beta_{j+1} = \delta_j$ the matrix is symmetrical. It operates on the two component vectors of the fast and thermal flux on each point (i,j). The known terms are also two component vectors:

$$\overline{\lambda}_j = \begin{pmatrix} \psi_j \\ \varphi_j \end{pmatrix} \qquad \overline{C}_j = \begin{pmatrix} C'_j \\ C_j \end{pmatrix}$$

To solve the resulting system we can use the direct method of forward eliminations and backward substitutions with the recurrent formula:

$$\overline{X}_{j-1} = A_j \overline{X}_j + \overline{b}_j$$

where $A_j = (E_j - B_j * A_{j-1})^{-1} * B_{j-1}$ is a (2x2) matrix

and $\overline{b}_j = (E_j - B_j * A_{j-1})^{-1} * (\overline{C}_j + B_j * \overline{b}_{j-1})$ is a two-term vector

The direct calculation is repeated at each radius scanning the point lattice in Z direction until convergence is reached. This partly direct and partly iterative method reduced the computing time by a factor of approx. 3 compared to the usual Gauss-Seidel iterative method. It is justified by the fact that there are no more iterations between the groups and that the inversion of the (2x2) submatrix $(E_j - B_j * A_{j-1})$ is not very time-consuming and is required only where and when the nuclear constants change for temperature reaction or rod movement.

The core may be subdivided into regions (up to 30) with different compositions. The poison concentration in any wanted region may be varied to obtain criticality. The core may also be subdivided into vertical zones (up to 10). In each zone the control rods move independently and may be used to reach criticality. Each zone contains cooling channels of the same type. Thermohydraulics calculations are made for the typical channel in each zone. The temperatures of fuel and moderator and the corresponding feedback on any wanted physical constant are calculated pointwise in the axial direction and zonewise in the radial direction.

During the procedure for criticality search the thermal calculations are made at every iteration to have the initial conditions in equilibrium with the temperature and void feedback.

The criticality search is made using the time-dependent diffusion equations. The poison concentration or rod insertion are varied in order to render the time derivative zero.

Afterheat calculation

The code makes a distinction between prompt heat (fission) and delayed heat (decay of fission products), in different proportion in fuel and moderator. This permits a more accurate evaluation of the temperature feed back when important variations of power level take place during the transient, and also enables the afterheat after shut down to be evaluated.

Xenon transients

In the program for Xenon operational transient the initial criticality is obtained, with a given fixed value of poison concentration and rod insertion, by varying pointwise the reactivity in the core. This is obtained by acting on the ν of $\nu\Sigma f$. At every iteration the temperature feedback and xenon asymptotic

concentration are calculated for a given initial power level. At the subsequent time steps the power will be varied according to a tabulated schedule. Criticality calculations are repeated at every time step at the new level of power. The xenon concentrations in every point are calculated analytically, using the values of the fluxes at the beginning of the time step. Contrary wise the temperature feedbacks are iterated for criticality and they are consistent with the value of fluxes at the end of the time interval.

After a shutdown period the program calculates analytically the point xenon concentration at the end of the period without intermediate steps.

After shutdown or restarting after a period of reduced power, the program calculates automatically the maximum attainable power at every time step.

Spatial xenon stability is analysed by introducing any wanted perturbation into the initial equilibrium and repeating the criticality calculation at every time step at a given power level.

In case of divergence the program can calculate automatically a strategy of compensating rods in order to dump the divergent oscillations.

Thermohydraulics

Description of problem

A number of parallel channels are considered, which are all identical in geometry and composition. Each channel is considered to be composed of a cylindrical fuel rod, a cladding, and the water cooling the outer surface of the cladding pertaining to the fuel element. Local restrictions to the coolant flow may exist over the length of the channels, these restrictions being identical in all the channels. The only exception to this rule are the inlet orificing coefficients, which may be different for different groups of channels.

In the steady-state problem, a power distribution is given for each group of parallel channels (up to 10 groups with different power distribution). The coolant flow distribution among the different groups of channels is obtained by an iterative procedure, varying the initial guessed distribution until the calculated pressure drops in each group of channels agree within 1%. Alternatively the pressure drop across channels may be imposed as the flow distribution, and the inlet gagging for each group of channels is adjusted in such a way as to obtain the prescribed pressure drop. In the latter case no iteration is necessary; instead of fixing the pressure drop, it is also possible to determine it as the average among the different channel groups, weighted on coolant flows.

In the dynamic part of the code the total inlet mass flow and the inlet enthalpy of the coolant water are varied according to independent time tables. The program calculates at each time step Δt the new flow distribution among groups of channels in the dynamic situation, as well as the temperatures inside the fuel rod, the cladding, the cooling water, and the void fractions at each axial level of the different channel groups. No DNB correlation is considered, and no special provision for calculation after DNB is made. The code in the present version is intended to foresee the occurring of boiling crisis, rather than predicting the evolution of a transient after this occurrence.

The Two-Phase Flow Model of the Single Channel

We shall give here the equations of the model as obtained directly in the finite difference formulation.

Let us consider a segment of channel of height ΔZ during the time interval Δt; we shall assume that the liquid and vapour flowing out of the segment are representative of the whole space and time interval. (This corresponds physically to an infinite turbulent mixing in the interval, and from an analytical point of view to a backward difference scheme in space and time for the corresponding differential equations). With this assumption and indicating by a star the quantities at the beginning of the time interval, the continuity equations read as follows:

a) Vapour Continuity Equation

$$\Delta Z\, \rho_v \alpha + \Delta t\, \rho_v q_v = \Delta Z \rho_v^* \alpha^* + \Delta t \rho_{v_{inlet}}\, q_{v_{inlet}} + \Delta Z\, \Delta t\, \psi$$

where ψ is the vapour volumetric source, α is the void fraction, ρ_v is the vapour density and q_v is the vapour volume flow-rate.

Taking into account the "kinematic constitutive equation":

$$a = \frac{k q_v}{w + k V_{drift}} + \frac{Z_e \psi_S}{w + k V_{drift}}$$

it may be written as:

$$q_v = \frac{w + k\bar{V}_{drift}}{w + k\bar{V}_{drift} + k\,\frac{\Delta Z}{\Delta t}} \left(q_{v_{inlet}} + \psi \Delta Z - \frac{\Delta Z}{\Delta t} \frac{\rho_v^*}{\rho_v} \alpha^* - \frac{\Delta Z}{\Delta t} \frac{Z_e\, \psi_S}{w + k V_{drift}} \right)$$

b) Total Mass Continuity Equation

$$\Delta Z \left(\rho_v \alpha + \rho_\ell (1-\alpha) - \rho_v^* \alpha^* - \rho_\ell^* (1-\alpha^*)\right) + \Delta t \left(\rho_\ell q_\ell + \rho_v q_v - \rho_\ell q_{\ell_{inlet}} - \rho_v q_{v_{inlet}}\right) = 0$$

Taking $\rho_\ell^* = \rho_\ell$ since the liquid density variation with pressure is negligible, remembering that $w = q_v + q_\ell$, and making use of the vapour continuity equation, this gives:

$$w = w_{inlet} + \Delta Z (1-\gamma)\, \psi - \frac{\Delta Z}{\Delta t} \left(1 - \frac{\rho_v^*}{\rho_v}\right)$$

c) Energy Continuity Equation

In terms of enthalpy, the energy continuity equation gives the total enthalpy change in the segment during the time interval as equal to the heat added, plus the pressure variation term $V \Delta p$, minus the net enthalpy flow out of the segment.

Referred to the unit cross-section this gives:

$$\Delta Z \left(H_v \rho_v \alpha + H_\ell \rho_\ell (1-\alpha) - H_v^* \rho_v^* \alpha^* - H_\ell^* \rho_\ell (1-\alpha^*)\right) = =$$

$$= Q \Delta t \Delta Z + \Delta p \Delta Z - \Delta t \left(\rho_\ell H_\ell q_\ell + \rho_v H_v q_v - \rho_\ell H_{\ell_{inlet}} q_{\ell_{inlet}} - \rho_v q_{v_{inlet}} H_{v_{inlet}}\right)$$

Taking into account the other continuity equations this gives for the liquid enthalpy the following equation:

$$H = \frac{\left(Q + \frac{\Delta p}{\Delta t}\right) \frac{\Delta Z}{\rho} + q_{\ell_{inlet}} H_{inlet} - \gamma H_v \Delta Z \psi}{q_\ell + \frac{\Delta Z}{\Delta t} (1-\alpha)} +$$

$$- \frac{\gamma (H_v - H_v^*) \frac{\Delta Z}{\Delta t} \frac{\rho_v^*}{\rho_v} \alpha^* + \frac{\Delta Z}{\Delta t} (1-\alpha^*) H^*}{q_\ell + \frac{\Delta Z}{\Delta t} (1-\alpha)}$$

This equation is useful when $H < H_{sat}$; if the liquid enthalpy reaches saturation, assuming thermodynamic equilibrium, the energy equation enables the vapour source ψ to be calculated as follows:

$$\psi = \frac{1}{\gamma \lambda \Delta Z} \left(\left(Q + \frac{\Delta p}{\Delta t}\right) \frac{\Delta Z}{\rho} - \frac{\Delta Z}{\Delta t} (1-\alpha^*) (H_{sat} - H^*) + \right.$$

$$\left. - \frac{\Delta Z}{\Delta t} \gamma \frac{\rho_v^*}{\rho_v} \alpha^* (H_v - H_v^*) - q_{\ell_{inlet}} (H_{sat} - H_{inlet})\right)$$

These are the continuity equations used; the momentum equation is disconnected from the others in our assumptions as has been explained in the previous reports. It is employed only to evaluate the pressure drops in the channel.

The correlations employed in the model to describe the heat flux from cladding to coolant and the vapour source in the subcooled region were established in the original FRANCESCA model [3] and will not be described in detail here. We shall only mention the recondensation correlation $\psi_b = R\alpha(T - T_{sat})$ for which a comparison with experiments and other calculations showed the value of the free recondensation constant R = 5 to be a well-fitting one. These data which were elaborated by AEG and presented at the "Two-Phase-Flow" meeting in RISO in June 1971 are shown in the figure below [4].

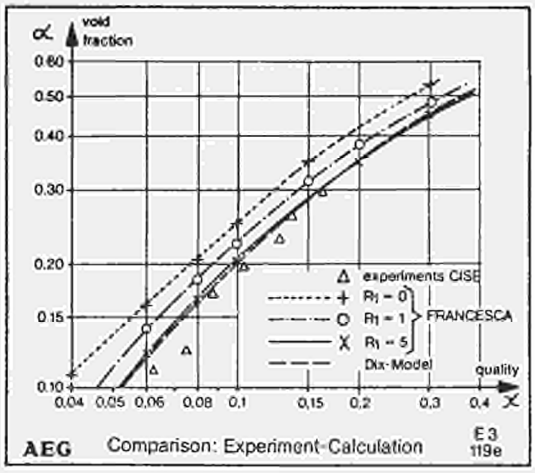

d) The Flow Redistribution Calculation

During a heat transient, the coolant mass flows into the different groups of channels satisfy the following equations

1) $A \sum_i n_i G_{o_i} = Q$

where n_i is the number of identical channels in each group i, A the flow area of the channels, G_{o_i} the inlet mass flow rate in each channel of group i, and Q the total mass flow into the system.

2) $\Delta p = \frac{d}{dt} \int_O^L G_i(z)\, dz + \Delta p_{fi} + \Delta p_{gi} + \Delta p_{si}$

Δp is the pressure drop (common to all parallel channels) across the channels; Δp_{fi}, Δg_i, Δs_i are respectively the frictional pressure drop, the gravity head, and the space acceleration pressure drop across the channels i, which are evaluated each time t according to the single channel model. The momentum derivative term may be written as

$$\frac{d}{dt}\int_O^L G_i(z)\, dz = L \frac{d G_{oi}}{dt} + \frac{d}{dt}\int_O^L (G_i(z) - G_o)\, dz$$

The second term in the right-hand side is very small in all practical cases (see [3] for a discussion). It is therefore ignored in the model, but it is calculated and printed as a check term in the output, to control the validity of the assumption.

Equation 2) is therefore rewritten

$$L \frac{d G_{oi}}{dt} = \Delta p - \Delta p_{fi} - \Delta p_{gi} - \Delta p_{si} = \Delta p - \Delta p_i$$

Δp is evaluated at each time t as the average value (weighted over the inlet mass flows) of the Δp_i. Writing $\Delta p1_i$ for $\Delta p - \Delta p_{gi} - \Delta p_i$ the equation for each of the channel groups is transformed into:

$$L \frac{dG_{oj}}{dt} = \Delta p1_i - \frac{\Delta p_{fi}}{G_{o_i}^2} G_{o_i}^2$$

which is in the form of the Riccati equation and may be integrated analytically in the time interval Δt, giving the solution

$$G_{o_i}(t+\Delta t) = G_{o_i}(t)\, R \frac{(1+R^{-1}) - (1-R^{-1})\, e^{-2k\Delta t}}{(1+R^{-1}) + (1-R^{-1})\, e^{-2k\Delta t}}$$

in which $R = \sqrt{\frac{\Delta p1_i}{\Delta p_{fi}}}$ and $K = \frac{L}{G_{o_i}(t)} \sqrt{\frac{\Delta p_{fi}}{\Delta p1_i}}$

The values obtained for $G_{o_i}(t+\Delta t)$ for all i are then renormalized to yeld the prescribed total mass flow according to equation 1).

This method of solution offers the following advantages:

- The method is explicit and therefore very quick, but always stable, because of the braking term dependent on $G_{o_i}^2$.
- The effect of the dynamic redistribution of flow among the different channel groups is separated from the total mass flow variation, which depends essentially on the external loop. The total mass flow is given in input in the code, but a representation of the external loop may easily be implemented into the code, adding a routine for the recirculation loop in the place of the tabulation.
- Whenever R is very near to 1 in any channel group the redistribution calculation may be automatically skipped for that group, and the error is automatically compensated in the further time steps if the tendency to pressure unbalance is continuing in time.

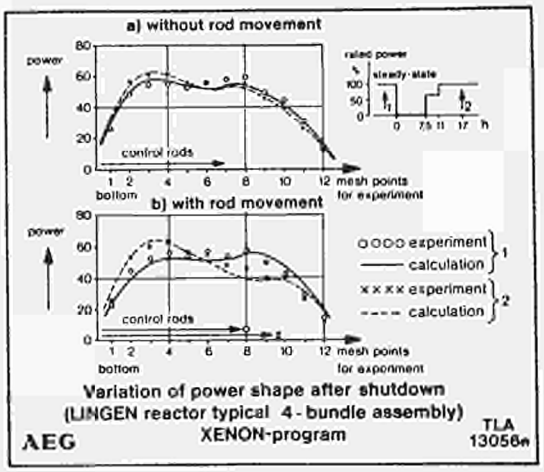

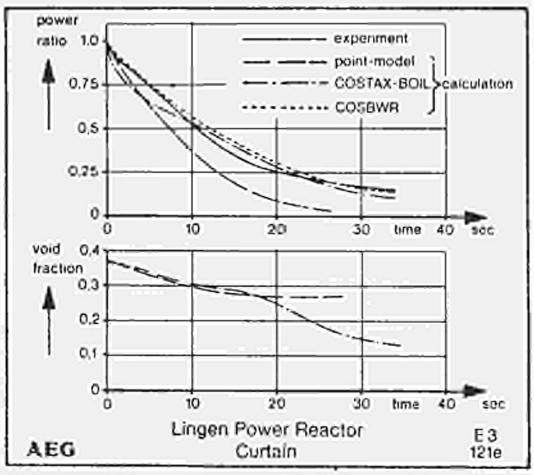

One-Dimensional Codes

This (RZ) code results from a preceding work on one-dimensional codes which were further physically tested and completed in 1971.

In the figures are illustrated some results obtained with the model by AEG for the BWR Lingen reactor [4].

The first figure illustrates the Xenon spatial deformation in a typical transient, the second the curtain rod insertion case; in the latter the COSBWR curve corresponds to the last version of the code, which includes pressure variation.

The one-dimensional code COSTAX-BWR is the subject of an external report which is in course of printing.

The (RZ) code is operating and tested but still requires comparison with measurements taken in power reactors, which is planned for 1972 by AEG.

References

1) E. Vincenti and A. Clusaz, Euratom JRC, COSTANZA (RZ), EUR 4673.

2) E. Vincenti, A two-dimension code COSTANZA (RZ) for the study of dynamics transients, xenon operational transients and xenon stability, Deutsches Atomforum HI 161, Reaktortagung 1971

3) G. Forti, A Dynamic Model for the Cooling Channels of a Boiling Nuclear Reactor with Forced Circulation and High Pressure Level, EUR 4052 (1968)

4) J. Lockau (AEG), The Axial Dynamics Code COSBWR, paper presented at the European Two-Phase Flow Meeting in Riso, 9-11 June, 1971

STRATEGY STUDIES FOR ELECTRIC POWER GENERATION IN THE COMMUNITY

F. Conti, C. Zanantoni

Introduction

The problem of energy resources and energy production is common to all the Community countries, and is therefore typically an issue for the Commission to deal with. In support, the JRC has done an analytical study of the possible power plant building strategies. In this study only electric energy was considered; in particular, attention was focused on the penetration of fast breeders into the market, as the assumptions concerning fast reactors have a strong influence on the optimum policy and carry considerable uncertainties.

The problem of electric power production can be approached from many angles; the one taken here was to optimize the installation rate of various types of power plant in such a way as to obtain a minimum integrated discounted cost of the total energy production over a given period.

However, the total cost is not the only variable that should be considered when deciding which is the "optimum" policy. Other aspects like fuel consumption, investment in fuel-processing and separation plants, availability of capital etc. should be considered. Moreover, even accepting the minimum integrated cost as the goal to be pursued, care should be taken to investigate other policies which may lead in theory to slightly higher costs, but be much more practical from many points of view, e.g. installation of one type of plant instead of two, lower capital investment, slow variation of the installation rate with time etc., not to mention political considerations.

It is because of this, and the uncertainty of some input data, that the results gathered during this year give only preliminary indications, as is stressed again below. This does not mean that strategy studies should not be made before taking decisions, for these decisions should be based on a sound evaluation of the physical and economical quantities involved. It simply means that our calculation facilities should be made more flexible and the study should be much wider than the one presented here.

The Assessment Method

The work was performed by choosing a number of cases, defined by a set of assumptions such as:

- rate of growth of the electric energy requirements;
- load diagram;
- types of power stations and year of their introductions;
- economic and physical characteristics of the various power stations;
- maximum rate of growth of the power installed with each type of plant;
- actualization rate;

and searching for the installation policy corresponding to the minimum cost of energy production between the years 1970 and 2020. All costs are converted to the 1970 actual value.

This job is automatically performed, using the linear programming technique, by the INTAT code, developed under EURATOM contract by INTERATOM and modified at Ispra.

This code, as it stands, does not perform any "sensitivity analysis", i.e. it does not allow any appreciation of whether the minimum is sharp or not. In other words, it does not allow an assessment of the penalty resulting from not following the code's prescriptions.

There are three ways round this inconvenience; one can

- try to make better use of the facilities of the IBM routine MPS incorporated into INTAT, so as to let the code investigate a range around the minimum;
- associate with INTAT a much simpler code which takes a given installation policy as an input and evaluates the effect of different physical and economical assumptions;
- run a large number of INTAT cases corresponding to parametric variations of the most important assumptions and take only the reasonable suggestions common to this lot.

All three ways were tried, but only the third one was used for the results presented here; it should, however, be mentioned that this procedure alone cannot be considered satisfactory and must be followed with caution because "a statement common to a lot of foolish speeches is not necessarily wise".

In any case the variation of input was not only done in order to assess the sensitivity of the system to various input data: it was necessary in order to assess the uncertainties in the advisable policy due to the considerable uncertainties in the basic input data.

Main Assumptions

Type of plant

Three types of power plant are considered – conventional plants, light water reactors and fast breeder reactors.

The conventional power plants (introduced in the following with the symbol C) represent the oil-fired stations. Neither hydroelectric nor coal-fired stations are considered because their penetration is strongly limited by natural resources and economic reasons. Therefore the significant competition is between the oil-fired and the nuclear power plants.

The light water reactors have been split into two types of stations, the LWR fuelled with enriched uranium and producing plutonium (symbol L) and the LWR with plutonium-enriched fuel (symbol LB). This in our case is the easiest way to simulate the recycling of the plutonium produced by light water reactors in the same reactor. LMFBR fuelled with plutonium are considered here (symbol F). No fast reactor using enriched uranium has been taken into account up to now in view of its bad economy, as generally stated in the literature.

The optimization period

The period chosen for the optimization is 50 years, from 1970 to 2020. The interest of the strategy is focused on the first 20 to 30 years, but a longer period was considered in order to free the first part from the perturbations due to the discontinuity found at the end of the optimization period (horizon effect).

Assumptions concerning plutonium

The optimization of the strategy is performed by the program in two steps; first a short-term optimization is made by choosing for each year the policy which makes the unit cost of energy minimum for that year; then the system is improved to provide a minimum of the unit cost of energy integrated over the whole period. The difference between the two is due to the stocking and recycling of plutonium, the economic impact of which is properly taken into account in the long-term optimization.

The various isotopic compositions of the plutonium produced and recycled are taken into account by considering the Pu^{239} equivalent to each of them. A closed market has been assumed for the artificial isotopes like plutonium. This seems reasonable because as the share of nuclear power in energy production becomes important the producers will tend more and more to use the Pu in their own systems. The hypothesis of the closed market implies that the expenditues (fuel cycles and inventory costs) for power generation must not include the cost of Pu, which is put equal to zero. This does not mean that Pu has no value: it is determined by the code as "marginal value" or "shadow price", which is the value by which a gram of Pu added to the system will reduce the total cost.

Power demand curve

Four power growth assumptions are chosen (Fig. 1). The higher growth assumption (curve A) is assumed in all our calculations, unless otherwise mentioned; it has a constant 7% per year growth rate and may be considered an extrapolation of the past trend.

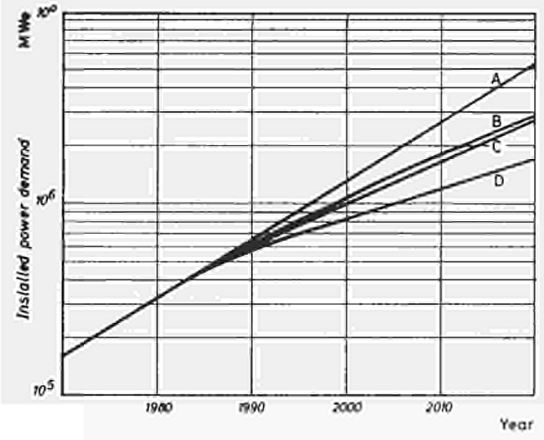

Fig. 1: Four power growth assumptions.

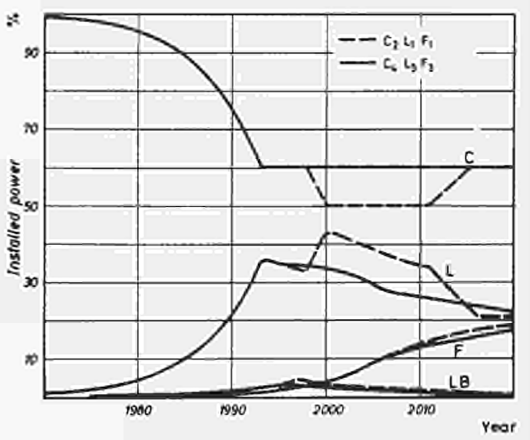

Fig. 2: Installed power of the two reference cases. Min. doubling time = 3 years.

Load Diagram 1		Load diag. Zone No.	Load Diagram 2	
Yearly utilization hours	Installed power fraction (%)		Yearly utilization hours	Installed power fraction (%)
7884	30.0	1	7750	23.37
7314	10.0	2	7250	23.38
5168	10.0	3	6000	6.37
3153	10.0	4	4000	6.38
1752	12.5	5	1750	12.75
876	12.5	6	350	12.75
0	15.0	7	0	15.0
4257		Average	4427	

Table 1 – The two load diagrams.

Curve B is a "weak" hypothesis assumed for the European Community. Curve B is very similar to C and was obtained from a projection of electric utilities generation in the USA, as quoted in WASH 1098, and shifted in time.

Curve D shows a power increase of 4% per year from 1990 and was used to demonstrate the effect of power demand saturation.

Load diagram and load factor assignment

Two load diagrams are considered (Table 1); they are split into load steps, as required by the linear programming technique used by the code. The load diagram No. 1 is assumed in all our calculations, unless otherwise stated.

The assignment of each plant to a load step is performed automatically by the code.

Costs

The economic assumptions and the identification key for the various cases are given in Table 2.

Table 2 – Economic assumption for various strategies.

		1	2	3	4
Fixed costs	high			•	•
	low	•	•		
Proportional costs	high		•		•
	low	•		•	

	C		L		LB		F	
	Plant cost ($/KW$_e$)	Oil price ($/Ton)	Plant ($/KW$_e$)	Fuel cycle (mills) KWh	Plant ($/KW$_e$)	Fuel cycle (mills) KWh	Plant ($/KW$_e$)	Fuel cycle (mills) KWh
1	100	10	140	1.4	140	0.63	140	0.7
2	100	14	140	1.9	140	1.13	140	1.2
3	125	10	180	1.4	180	0.63	180	0.7
4	125	14	180	1.9	180	1.13	180	1.2
First core value at boro Pu value ($/KW$_e$)			28.8		19.6		8.9	

The fixed costs have been split into plant cost and first core charge which includes the fuel inventory in the "recycle line" to reactor-out reactor-in and in the "feed line" mine-out to reactor-in. The plant cost is intended to be comprehensive of direct and indirect costs, but does not include the interests during construction which are taken into account separately in the calculations in the following way:

22% for nuclear stations
18% for oil stations

The plant cost for fast reactors has been assumed to be the same as for thermal reactors as this may be the trend in the long range. However, several cases have been run where the pessimistic assumption for the fast reactor plant cost is coupled with the optimistic one for thermal reactors.

All the costs shown in Table 2 are now subject to strong criticism in view of the new sets of calculations.

Date of introduction of fast breeders

Two dates of introduction of fast breeder reactors were alternatively considered, namely, 1985 and 1990.

Limits on the installation rate.

To make allowance for the industrial difficulties in coping with over-rapid growth of the reactor builing potential, limits have to be imposed on the growth of the installation rate of each type of station. With the currently available codes the limitations can be set only on the growth of the installed capacity and not on the rate. The values chosen are alternatively a doubling time DT = 2 years and a DT = 3 years.

Physical data

The reactor physical data such as fuel enrichment, charge and discharge rate, inventory and consumption, separative work requirements, etc. are omitted here to save space. These data were ereviously calculated on the basis of a fuel cycle optimization for each reactor type.

The penetration of various plants

Definition – general remarks

The word "penetration" is taken here to mean the percentage of the total installed capacity covered by a certain type of plant in a given year.

The penetrations are evaluated at the year 2000, unless otherwise stated. Figs. 2, 3 and 4 allow an appreciation of the penetration for two typical sets of assumptions (C_2 L_1 F_1 and C_4 L_3 F_4, see Table 2), two different minimum doubling times of the installed capacity (2 and 3 years) and two different demand curves (Figs. 4 and 1). The derivative of the installed capacity is too high in places, because the code does not allow of putting a limit on it, but the results are not much affected by this, as the variation could be staggered over a larger number of years without a noticeable change in the total cost.

It is interesting to note that the penetration by conventional power stations which can be seen in Figs. 2 and 3 is typical of most of the cases considered.

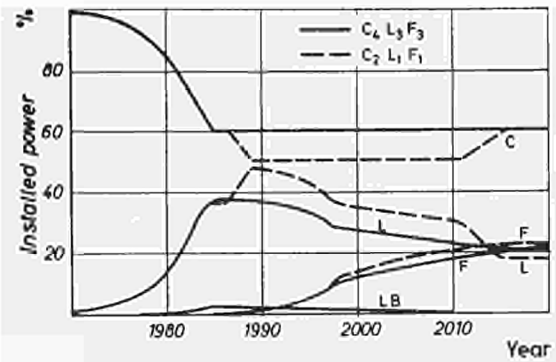

Fig. 3: Installed power for the reference cases with min. doubling time = 2 years.

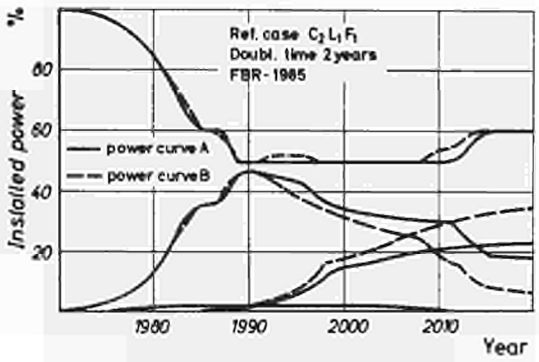

Fig. 4: Effect of power demand growth.

There is an economic incentive (to be better assessed, as already stated above) towards a penetration by the conventional station of some 60–50% and by the thermal reactors of some 30–40%.

The penetration by the conventional stations is assured, with our economic assumptions, by their competitivity for peak-load operation. The penetration by the thermal reactors is assured by their competitivity with the conventional stations for base-load operation and by the need to produce plutonium for future fast reactor capacity. Even with a slow demand growth (Fig. 4) the fuel inventory of the fast breeders is too large and their plutonium production too small to satisfy their plutonium requirement.

The penetration by light water reactors would be large even if other thermal reactors like the HTR were present, according to our preliminary evaluations, because the LWR is the best plutonium producer.

Considerable differences can be found on this point if one compares these preliminary indications with some of the literature. Let us take as an example the results of strategy evaluations done at Battelle NWL for the US Task Forces. The model used, still based on the LP, adopted a plant "load history" instead of a load diagram subdivision. This means that all new plants run in the base load for the early years of their life, and therefore nuclear plants get a higher installation rate and hence wider penetration. Other differences are:

- Power demand curve shows saturation (growth rate 5% per year in 1993 to 4% at 2020).
- Lower present-worth conversion rate (7%) which enhances FBR savings after year 2000.
- Optimistic values for FBR inventory.
- Increasing cost for yellow cake depending on reactor consumption.

All these differences in favour of the FBR can explain its much wider penetration and a negative slope in the separative work demand curve.

Effect of plant and fuel costs

These data are quite uncertain, particularly the plant costs. The effects of all possible variations from the data of Table 2 are far from being evaluated, but a typical example is given by Figs. 2 and 3, where the dotted line corresponds to a plants cost reduction of 25 \$/kWe for the conventional plants and 40 \$/kWe for the nuclear plants.

The result is a considerable increase in the LWR's, both because they are more competitive and because their plutonium is used in the cheaper FBR's.

The effect of the variation of the plant cost for the fast reactors only can be appreciated from Figs. 5 and 6. The penetration by fast reactors and the amount of plutonium recycle can be strongly affected, but the penetration of conventional and light water stations remains in the range mentioned above.

The effect of an increase of the fabrication cost for fast reactors from 250 to 300 \$/kg and of the reprocessing cost from 150 to 180 \$/kg can be appreciated in Fig. 7.

Effect of power demand growth

The uncertainties on this point are particularly large, as we assume, in the second half of the optimization period. Therefore they do not much affect the penetrations at year 2000, as can be seen from Fig. 4.

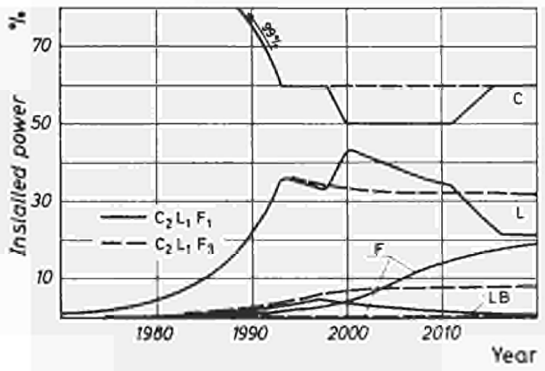

Fig. 5: Effect of higher F plant cost.

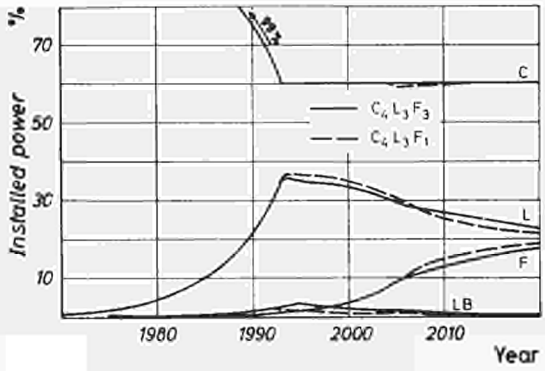

Fig. 6: Effect of lower F plant cost.

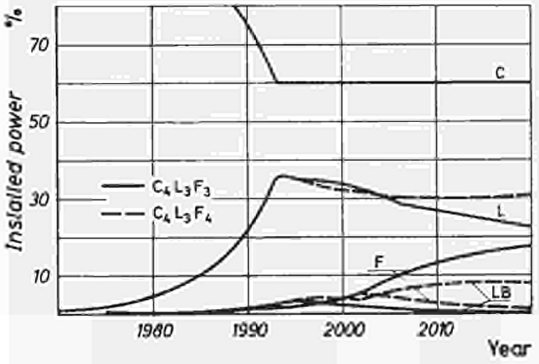

Fig. 7: Effect of higher F fabrication + reprocessing cost.

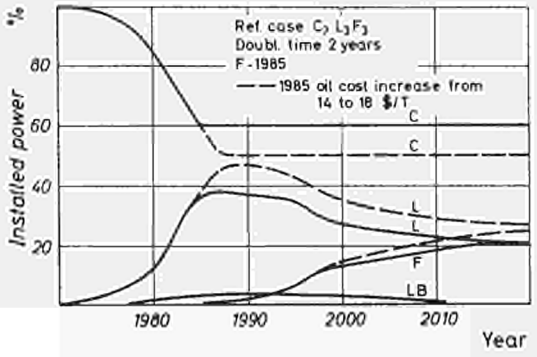

Fig. 8: Effect of an oil cost increase.

Looking as far as 2010 (after this date the results have no meaning) there is a marked increase of fast reactors and corresponding decrease of light water reactors with the lower growth curve, due to the fact that the plutonium procurement is a less urgent need. The penetration by conventional stations is unaltered, always assured by the shape of the load diagram.

Effect of the load diagram shape

This effect is remarkable, even for a small variation such as assumed in Table 1. The slight increase of average load factor from diagram 1 to diagram 2 leads to a 4% increase in the penetration by LWR's, with a corresponding decrease of the conventional stations. The fast reactor penetration is practically unaffected. Much larger variations of the load diagram should be investigated.

Effect of a limitation of the installation rate

The effect of increasing the possible installation rate from doubling time = 3 years to doubling time = 2 years can be appreciated from Figs. 2 and 3.

The FBR penetration increases by more than a factor of 3, thus affecting the LWR penetration, while the conventional stations are unaffected because their competitivity for peak load operation is not affected.

Nor, indeed, is the competitivity of the LWR's affected, but the maximum of their penetration occurs at an earlier date, due to the need to accumulate a larger plutonium stock for the start of the breeders.

Effect of an increase of the oil cost

The effect of an oil-cost increase from 14 to 18 $/t was evaluated (see Fig. 8). Again, this does not very much affect the fast reactor penetration, but it does affect the light water competitivity for operation in the intermediate ranges of the load diagram. Variations of 10% of the conventional power fraction are caused. It should be noted that a variation from 14 to 18 $/t is not large, it is of the order of the difference that can be found between the oil prices at European ports.

Remarks about sensitivity

As said, an evaluation of the economic incentive to follow the code prescriptions has not been fully performed and is fairly difficult with the tools available at the moment. However, an appreciation of the cost of departing from the optimum installation policy can be obtained in several ways, e.g. by evaluating the cost of not introducing the fast breeders.

Taking the case $C_2L_1F_1$ with high growth rate we get:

Total Present-work cost (10 $) until year:	standard case	no breeders	no plutonium recycle	no nuclear construction
2000	83.17	83.14	83.39	86.12
2020	108.7	109.6	108.8	114.6

The relative variation of the total cost is fairly small, i.e. less than 1%, unless the case is considered where no nuclear reactors at all are installed. However, some attention should be given to the absolute figures, which are of the order of 1 million (present-worth) $ over 50 years. Moreover, it should be recalled that our assumptions (Table 2) were purposely cautious as to the difference of costs between various types of plant.

Finally, other consequences of the policy should be considered, such as separative work requirements and fuel consumption (see below).

Plutonium recycle and stocks. Plutonium value

The amount of plutonium recycle is represented in our scheme by the installation of light water plutonium burners (LB). Their penetration is typically of a few %, to be compared with the typical 30% of uranium-fuelled LWR's.

The stockpiling of plutonium starts only a few years before the introduction of the fast breeders, reaches a maximum in typically 5–7 years and goes to zero again in another 3–5 years. The plutonium value also varies quite widely and sharply and has a maximum when the stock reaches the zero value.

Typical values (case $C_2 L_1 F_1$, high growth rate) are as follows

	Standard case	No plutonium recycle in LWR's
max Pu stock (tonnes)	232	403
at year	1994	1995
fissile Pu value ($/g)	9.2	8.8
at the same date		
max Pu value	13.5	13.1

Separative work requirements

Apart from extreme cases where only conventional stations are installed the separative work required from 1970 to 2020 is of the order of $3–5 \cdot 10^6$ tons.

The capacity of the American separation plant is of the order of $20 \cdot 10^3$ tons SW/year, and it could be increased to 26. Even if we assume that it can work at 26 from 1970 and that it works full time, i.e., that preproduction is preferred to investment in new plants, its production of 50 years is $1.3 \cdot 10^6$ tons. If the European needs are multiplied by 1.3 to account for the UK and EFTA and by 2.5 to account for the USA, we get about $1.3 \cdot 10^7$ tons. That means that the USA separative work capacity is about 10 times too small to cope with world demands up to 2020. Of course a much lower figure for the SW would be obtained with more optimistic assumptions concerning the doubling time and inventory of fast reactors. One could get curves of SW requirements which exhibit a maximum, instead of a steady increase as in our cases. This point will be further investigated. The separative work requirement is one of the typical figures which should be considered in estimating the merits of any installation policy. The following data, relative to the $C_2 L_1 F_1$ case with high growth rate, can be considered as typical.

at year	standard	no breeders	% increase
2000	78.4	82.8	5.4
2020	177.2	331.4	87.0

Fuel consumption

Another interesting parameter is the ore consumption. Typical values and an appreciation of their variation due to the assumption of non-introduction of fast breeders are given in the following table (case $C_2 L_1 F_1$).

growth curve (Fig. 1)	from 1970 until:	standard case	no fast breeders	% variation
D	2000	0.888	0.856	− 3.6
	2020	1.253	2.420	+93.6
A	2000	1.288	1.196	− 7
	2020	3.660	5.47	+49

The uranium requirements without fast breeders are smaller at year 2000 because when FBR's come into the strategy (standard case) a higher number of thermal reactors are to be installed to supply the Pu needed. But the considerable savings produced by FBR can be seen at the end of the optimization period in 2020.

Final remarks

The work carried out during this year has given a number of useful indications on the penetration by the various types of plant, but has also allowed us to clarify the following points:

1) means for an easier sensitivity analysis have to be provided, as explained in the first section of the paper.
2) a much larger range of variation of physical and economic hypotheses has to be considered.

Moreover, the need to extend our consideration to strategies including High Temperature Reactors has been recognized, as well as the need to take into account the constraints imposed by pollution abatement.

FUEL COST FOR NUCLEAR SHIP PROPULSION

*C. Foggi, G. Giacomazzi**

Introduction

The work performed at the JRC Ispra in this field is divided into two main parts. The first is concerned with the fuel-cycle cost calculations for a nuclear container-ship powered with a high-power PWR. The second part is the preparation of a general program for the IBM 360/65 computer, able to calculate the fuel costs for a marine reactor taking into account any possible variation or accident in the course of the whole life of the ship. A point deserving note is the importance of having performed the first part of the work, that consisted in studying a specific case, in order to be able to understand the complexity of the problem in all its aspects and, consequently, to write the computer program. Indeed for this type of problem it is imperative to have some reference calculations involving the knowledge of realistic cost values and practical sequences of the possible operations.

Fuel Cycle Cost Calculation for a 120,000 SHP Reactor Plant for Ship Propulsion

In connection with a study being performed in the Netherlands on nuclear propulsion for large high-speed container ships, a series of fuel-cycle cost calculations for a 120,000 SHP PWR reactor plant has been carried out by the JRC Ispra (European Community Commission) and RCN (Netherlands). The fixed parameters for these calculations were the thermal power for the reactor, 320 MWth, and a load factor of 70%. Several parameters were varied in the course of the calculations, for instance the fuel rod diameter, the water/uranium ratio in the core and the length of the refuelling cycle.

Refuelling cycles with single-batch loading for 1000 equivalent full power operating days between refuelling, as well as two-batch cores with partial reloading after 500 equivalent full power operating tion of the physical and economicaldays, have been studied. The results of these calculations are considered to be relevant for a fairly wide range of reactor power above approximately 100,000 SHP.

For the comparison of the different core configurations the average heat flux through the cladding of the fuel rods was kept constant (47,2 W/cm^2) throughout the main set of calculations. Additional calculations were performed to compare core configurations with a constant burn-out ratio (1,64).

Two different refuelling schemes were calculated:

Single-batch core (4-year operation without refuelling)
Two-batch core (refuelling every 2 years by replacement of one batch and repositioning of the order)

The fuel pellet diameters considered for the single batch core were: 0.9 - 1.0 - 1.1 cm; the moderating ratio (water/fuel volume ratio) was varied in the range 1.075 - 3.25. For the two-batch core a fuel pellet diameter of 1.0 cm only was taken, and the moderating ratio was varied between 1.55 and 2.63.

The thermohydraulic calculations were performed by RCN.; the reactor physics and the economics calculations were done at the JRC Ispra in collaboration with RCN.

Reactor physics calculations

Case "a" (constant average heat flux through the cladding)

The lifetime of the fuel was assumed to be 1000 days at full power in both cases (single-batch and two-batch cores). With the two-batchcore, each batch stays in the outer zone for the first half of its life; it is then moved to the inner zone where it stays until the end of its life (out-in refuelling scheme).

All the core burnup calculations were done with the two-dimensional code CONDOR-3 [1]. The variation of the neutron spectrum during lifetime was taken into account by using different libraries of average cross-sections. In the calculations, the excess reactivity of the core was compensated for by a homogeneous poisoning of the moderator. For the two-batch core, calculations were done for the initial core and for the equilibrium core. In the case of the single-batch core, some of reactivity coefficients of importance were calculated with the LASER cell-code [2]. The one-dimensional code SQUIRREL [3] was

---

* Coauthors for the first part of the work, performed in collaboration with R.C.N.: N.H. Dekker, D. Nolson, J. Slobben.

Table 1 – Core characteristics

Thermal power (MW)	320		
Fuel	UO_2		
Fuel smear density (gr/cm^3)	9.8		
Cladding	Zircaloy-4		
Number of fuel rods	9512		
Fuel pellet diameter (cm)	0.9	1.0	1.1
Cladding thickness (cm)	.063	.070	.077
Core height (m)	2.09	1.88	1.71
Moderating ratio, minimum	1.075	1.075	1.075
Moderating ratio, maximum	3.250	3.250	3.250
Circomscribed core diameter (m)			
min. moderating ratio	1.43	1.58	1.74
max. moderating ratio	1.97	2.19	2.41
Height/diameter of the core			
min. moderating ratio	1.460	1.19	0.98
max. moderating ratio	1.060	0.86	0.71
Weight of UO_2 in the core (t)	12.400	13.8	15.1
Weight of fuel elements (t)	14.900	16.6	18.2
Power density in the fuel (W/cm^3)	239.000	215	196
Linear power density in the fuel (W/cm)	152	169	186
Power density in the uranium (W/g of U)	27.6	24.8	22.7
Average moderator temperature in the core (°C)	302	302	302

used for the two-batch core.

The main characteristics of the cores are given in table I. The results of the physics calculations show that:

- The enrichment of the fuel strongly depends on the moderating ratio (Fig. 1).
- The smaller fuel pins require higher enrichments (Fig. 1).
- In the event of the reactor being controlled by soluble poison, the temperature coefficient of reactivity and the hot-cold effect are strongly influenced by the quantity of poison used and by the moderating ratio (Figs. 3 and 4). Positive temperature coefficients can be expected with large moderating ratios and heavy poisonings.
- In the event of the reactor not being controlled by soluble poison, the temperature coefficient of reactivity is always strongly negative (Fig. 3).
- The core power factor decreases as the irradiation proceeds, leading to a progressive flattening of the power distribution. For the case with moderating ratio 1.55 and fuel pellet diameter 10 mm, a maximum power factor of 2.6 for the single-batch and 1.7 for the two-batch core was found.

A comparison between single and two-batch cores shows that:

- The enrichment needed for the two-batch core is much lower than for the single-batch core (Fig. 2).
- The initial k_{eff} is correspondingly lower; a lower concentration of soluble poison is, therefore, required for control of the reactor.
- In the two-batch core nearly all the excess reactivity can be controlled by the use of soluble poison without danger of a positive temperature coefficient. This is not the case with the single-batch core.
- The power distribution is more favourable in the case of the two-batch cores.

Case "b" (constant burn-out ratio)

As already mentioned, a separate set of calculations was made in order to compare different core configurations with constant burn-out ratio.

The results of the thermohydraulics calculations (Fig. 4) for an integral-type reactor, show that the height of the core increases considerably with the moderating ratio (it will be remembered that the height remains constant when assuming constant average heat flux). For this reason, the dimensions of the core and the initial enrichment of the fuel are higher than in case "a" for moderating ratios greater than 2.1 and pellet diameters greater than 10 mm. (Fig. 5).

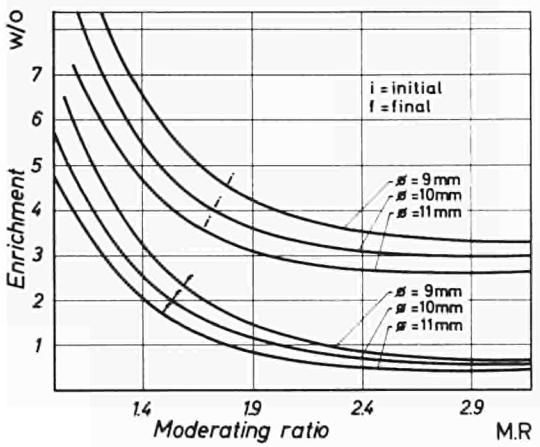

Fig. 1: Initial and final enrichment. Single batch cores.

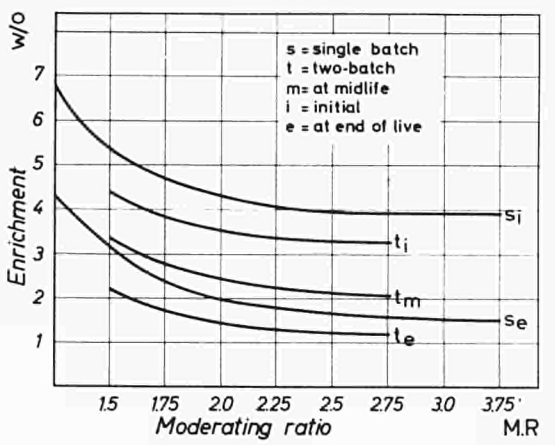

Fig. 2: Initial and final enrichment. Comparison of single batch and two-batch cores. Fuel pellet diameter 1.0 cm.

Fig. 3: Reactivity temperature coefficient of the moderator at power. Comparison between single and two-batch (equilibrium) cores. Pellet diameter 1.0 cm.

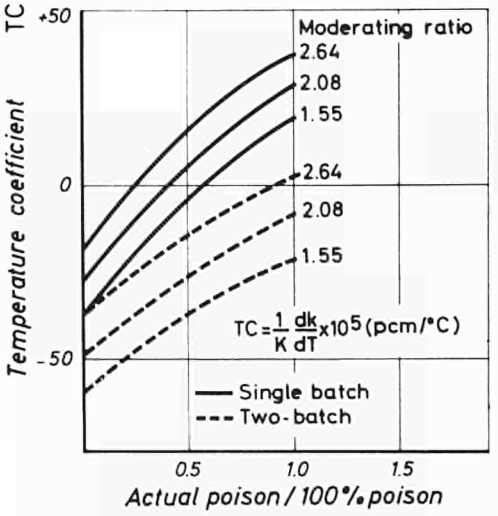

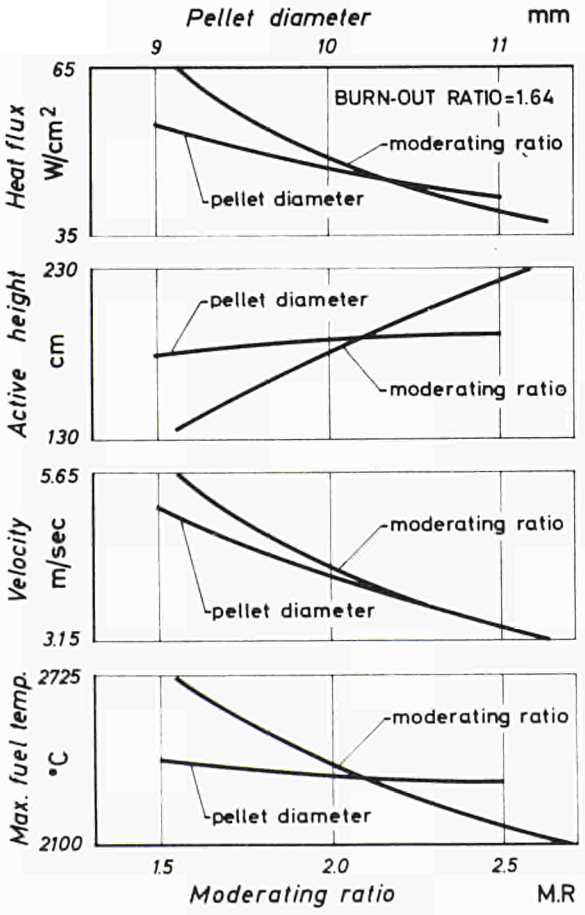

Fig. 4: Integral types. Some parameter variation with constant burn-out ratio.

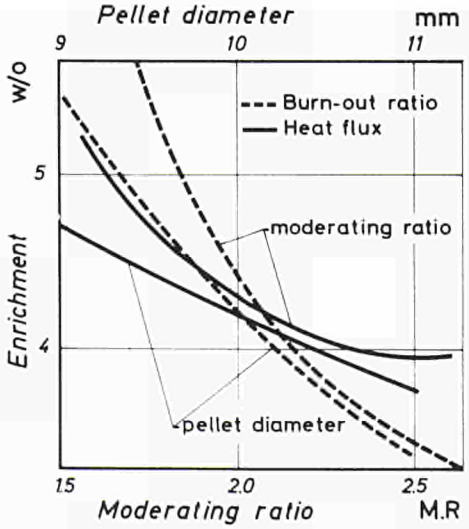

Fig. 5: Burn-out ratio and heat flux as constant values during initial enrichment calculations. Integral type.

Economic calculations

The economic analysis concerns the cost of the fuel cycle at equilibrium; therefore all the costs deriving from the tests required by a new nuclear ship are left out of account.

Yet in the case of the two-batch core the first fuel charge and the last charge are different from the equilibrium charge, i.e., they are "anomalous"; since the influence of these anomalies on the cost of the energy is not negligible, they have been considered explicitly.

The economic calculations were based on the following prices and on the assumption that fabrication, reprocessing and reactor fuelling take place in Europe.

Price of U_3O_8	8.0	\$/lb	
Conversion to UF_6	2.7	\$/kg	
Separative work	28.7	\$/kg	
Fabrication cost (including cladding)[4) 6)]	122.2; 106.7; 95.3	\$/kg U	(0.9 - 1.0 - 1.1 cm pellets respectively)
Transport cost (handling and insurance included)[4) 5)]	0.65	\$/kg U	(fresh fuel)
	7.5	\$/kg U	(irradiated fuel)
Cost of the refuelling[7)]	170,000	\$	
Storage of the fuel at the shipyard (per fuel batch)	5,000	\$	(fresh fuel)
	30,000	\$	(irradiated fuel)
Reprocessing and conversion to UF_6[6)]	32.1	\$/kg U	
Price of fissile Pu	9	\$/g	

The assumed tail assay at the enrichment plant is 0.248 wt.%[8)]; the losses at the reprocessing plant are fixed at 1.3% for U and 1% for Pu[9)]. An interest rate of 8% was used throughout the calculations although, in some instances, the effect of the increase to 10% was examined.

The time needed to fabricate a complete charge of fuel elements is assumed to be six months for the single-batch core and four months for the two-batch core (one charge is only half of the core). The irradiated fuel elements are cooled in a pool for four months. Transport delay from the fabrication plants to the refuelling facility is assumed to be one month; the same period applies for transportation to the reprocessing plant. Reprocessing will take one month. The residual fissile material will be sold immediately after recovery.

In the case of the single-batch core, the refuelling of the reactor is performed every four years during the overhaul of the ship required for the Register Special Survey; in the case of the two-batch core, refuelling is performed every two years during the overhaul for either the Register Special Survey or the Biennial Survey. The time required for the refuelling and the survey is assumed to be 1.5 months.

For the single-batch core a financial commitment is needed every four years for refuelling the reactor. For the two-batch core this is required every two years when only half a core is being replaced; however, at the beginning of the reactor life when a complete core has to be loaded, an extra investment is required.

The cost of a single fuelling operation is the sum total of all the expenses incurred for the purchase of uranium, fabrication of fuel elements, fuelling operations, reprocessing of these same fuel elements after irradiation, their storage and transportation. The price of the materials recovered at the reprocessing plant (uranium and plutonium) has to be subtracted from this amount.

The present value for the above credit and costs was calculated with the usual financial formulas as at the beginning of the lifetime of each fuel batch. The cost of the SHPh (shaft-horse-power-hour) is given by

$$p = \frac{\bar{A} \cdot 10^3}{\text{SHPh/years}} \quad \left(\frac{\text{mills}}{\text{SHPh}}\right)$$

$\bar{A}$ is the yearly instalment (\$/years) to be paid by the shipowner over the period between two successive fuelling operations. In the case of two-batch cores the cost of the first fuelling is higher than that of the subsequent fuellings (two half-cores have to be purchased). This extra cost is distributed over the whole life of the reactor (20 years, approximately) and results in an increase of 10-15% of the fuel cycle cost over the equilibrium value (Fig. 6). This procedure leads to a constant cost of the SHPh for all but the last of the fuel cycles in the life of the reactor. The last fuel batch is operated for a shorter period than the equilibrium batch; this means that the price of the enriched uranium recovered at the reprocessing plant will be higher and the credit for this material larger.

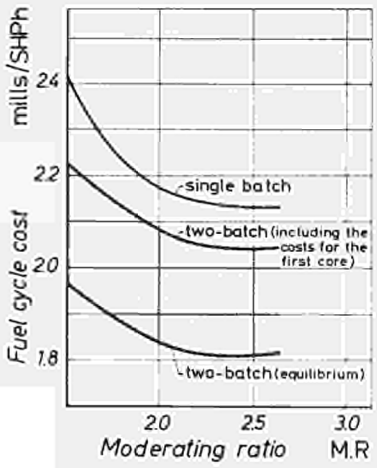

Fig. 6: Single and two-batch cores. Comparison between fuel cycle costs $\phi = 10$ mm, $i = 8\%$ and minimum time length.

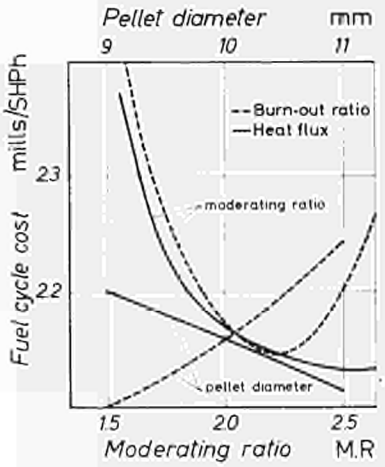

Fig. 7: Burn-out ratio and heat flux as constant values during fuel cycle cost calculations. Integral type, $i = 8\%$.

Case "a" (constant average heat flux through the cladding)

The results of the calculations show that:

- The investment needed every two or four years for refuelling the reactor is strongly influenced by the moderating ratio; this is to be expected as it is closely related to the enrichment of the fuel.
- Similar results are obtained for the fuel cycle cost (Fig. 6).
- The choice of the fuel pin diameter scarcely influences the fuel cycle cost (less than 5% between 0.9 cm and 1.1 cm pellet diameter in the considered range of moderating ratios).
- The interest rate also influences the costs. A one-point increase in the interest rate causes an increase of 2-3% in the fuel cycle cost and of less than 1% in the investment.

The comparison between single and two-batch cores in the considered range of moderating ratios shows that:

- The fuel cycle cost of the two-batch core at equilibrium is lower than that of the single-batch core by 15%. However, compared with the standard refuelling every two years, the extra commitment for the first fuelling is between 1.5 and 1.8 million dollars; this means either an addition of \$ 150-180·10^3 per year to the cost of operation of the ship over 20 years or an increase of 0.22-0.26 mills to the equilibrium cost of the SHPh (Fig. 6). On the other hand, the fuel cycle cost is approximately 20% less during the last two years of operation of the ship.
- The financial commitment for refuelling the reactor with a single-batch core is 2.3 times as large as that with a two-batch core.

It can be concluded that a two-batch core is more attractive than a single-batch core because the fuel cycle cost (including the extra investment for the first fuel charge) and the financial commitment needed for each fuelling operation are lower.

It also appears that a very low moderating ratio is not economical if a low fuel cycle cost has to be obtained. The increase in the core dimensions associated with higher moderating ratios (approximately 30 cm on the diameter) results in a higher investment for the reactor installation, but this will probably be largely compensated by the reduction of the fuel cycle cost.

It is conceivable that the use of a multiple-batch core with moore frequent refuelling (e.g. once per year) could lead to even lower costs provided that the refuelling time is not too long.

Case "b" (constant burn-out ratio)

In Fig. 7 the calculated fuel cycle cost for the case of constant burn-out ratio is compared with the corresponding result for the constant heat flux case; the comparison is given for the case of a single-batch core, 8% interest. Two sets of curves are given, one for a constant pellet diameter of 10 mm, the other for a constant moderating ratio.

Fig. 7 clearly shows that in the case of a constant burn-out ratio there is a pronounced minimum in the fuel cycle costs at a moderating ratio of about 2.2, whereas with a constant heat flux through the cladding the fuel cycle costs appear to decrease continously as a function of the moderating ratio.

A New Computer Program for Fuel Cost Calculation for Ship Propulsion

The method currently used to calculate the fuel cost in a nuclear reactor makes use of the "cycle" concept. The operation of fuelling the reactor usually takes place after fixed and equal time intervals, and it is easy to plan a scheme of events that is repeated identically at every time interval. This basic scheme, whose repetition describes the overall fuel history during the reactor life, is the "cycle" of the fuel. The economic calculations are therefore performed over a single cycle and the result ("fuel cycle cost") is intended to be valid for all the cycles of the reactor lifetime.

This philosophy is useful as long as the "cycle" is really repetitive. In actual fact many factors are likely to modify this ideal condition; for instance:

- in a multiregion core the fuel elements which are loaded at the beginning of the reactor life have different characteristics from the standard fuel elements; they are also irradiated to a lesser extent.
- the same situation occurs at the end of the reactor life.
- the design of the fuel elements may be changed during the life of the reactor.
- costs and other parameters of economic concern may change owing to market conditions or tecnological progress.
- unexpected events may alter the sequence of events of a given cycle.

Some of these factors cannot be avoided, others are only occasional; nevertheless it can be of some interest to investigate what type of consequences we may expect from these occasional events.

When taking into account such factors, the calculation of the fuel cost with a "cycle" method becomes a real headache since many successive and cumbersome corrections must be carried out on the basic "fuel cycle cost". It seemed therefore reasonable to abandon the concept of "cycle" where the complete history of a nuclear plant has to be studied. This is particularly true in the case of the analysis of a nuclear plant for ship propulsion, since many of the aforementioned factors have to be considered.

If the concept of "cycle" is rejected, the whole fuel history of the nuclear plant will simply be represented by a sequence of individual events occurring at predetermined dates and associated with an equal number of financial commitments. The usual methods of financial mathematics can be applied to these data to derive the fuel cost per annum (or per unit energy). This method is quite simple, and allows any variation or accident in the course of the events to be taken into account. Yet it entails handling a large amount of data; the use of a digital computer therefore becomes at least recommendable.

A program for calculating the fuel cost for a nuclear reactor to be used in ship propulsion, based on the criteria described above, is now in preparation.

Any scheme of reactor fuelling can be treated, and all the relevant parameters concerning the fuel, the costs, and the time schedule of the various events can be varied at will during the reactor life. Special facilities incorporated into the code allow the treatment of some typical fuel histories (which can be assimilated to "cycles") with a minimum of input data. The trend of certain costs to increase or decrease, due to predictable market behaviour, can also be simulated by the code. Differential calculations, in which only one parameter is varied, can be performed.

References

1) E. Salina: CONDOR-3, a two-dimensional reactor lifetime program with local and spectrum-dependent depletion. EUR 4539 (1970).

2) C.G. Poncelet: LASER, a depletion program for lattice calculations based on MUFT and THERMOS. WCAP 6073 (1966).

3) E. Salina: SQUIRREL, a FORTRAN-IV one-dimensional few-group diffusion depletion code which includes the effect of local power and water density. EUR 4490 (1970).

4) "Future trends in fuel cycle costs for medium-size light-water reactors" by D. Hundt. IAEA: Proceedings of the Symposium on Nuclear Energy Cost and Economic Development – Istambul, October 1969.

5) An evaluation of advanced converter reactors, April 1969, WASH 1087.

6) "The economics of nuclear fuel in maritime applications" by N.B. Mc Leod et al., July 1968. PB. 179222.

7) "The economics of nuclear fuel for maritime applications", PB – 174 – 219.

8) "The cost of enriched uranium" by Pelser. January 1971. (New version of the reports R.C.N. – Int.-67-117 and R.C.N. – Int.-67-118, considering the new price of 28.70 $/kg for separative work).

9) "Factors affecting the cost of nuclear fuels and the selection of reactor fuel cycles in the developing countries" by A.O. Wordsworth, S.J. Cowherd. IAEA – Proceedings of the Symposium on Nuclear Energy Cost and Economic Development – Istambul, October 1969.

PHYSICS

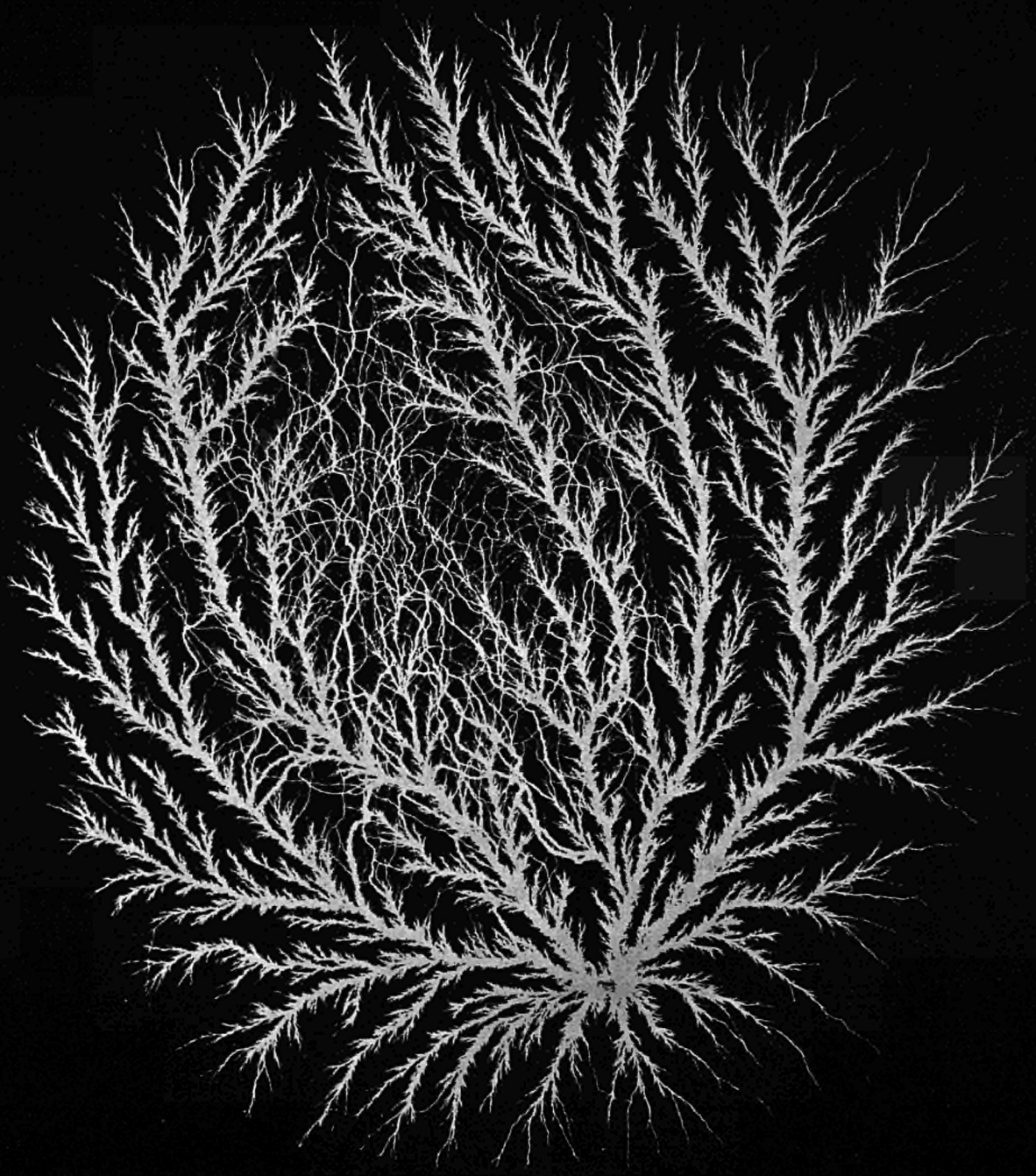

STRUCTURE OF IRRADIATED ORGANIC MOLECULES

CROWDIONS IN IRRADIATED Au-Ag ALLOYS

HYDROGEN IN Nb SINGLE CRYSTALS

COLOUR CENTRES IN ALKALI HALIDES

NEUTRON CORRELATION TECHNIQUES IN NUCLEAR SAFEGUARDS

TIME FOCUSSING SPECTROMETER

CH_3 ROTATORS IN MOLECULAR CRYSTALS

COOLANT VOID COEFFICIENT IN D_2O LATTICES

PHYSICS DIVISION

Helmut Warmuth

The Physics Division consists of five sections which are in alphabetic order:
- Experimental Neutron Physcis
- Magnetic Resonance
- Reactor Physics
- Solid State Physics
- Theoretical Physics

With the exception of Reactor Physics all efforts of the Division are concentrated on the Physics of Condensed Matter Programme.

The Experimental Neutron Physics Laboratory

has slow chopper, double chopper and rotating crystal spectrometer facilities in the ISPRA-I reactor. The installation of a new time focusing spectrometer which is in principle a very fast rotating crystal spectrometer has been finished. The laboratory is furthermore equipped with a 1 MeV-Van de Graaff accelerator. The main activities include the investigation of ferroelectricity, measurements of the quasieleastic scattering on NbH in single crystals and quasielastic scattering on liquid crystals. Further work concerns fission experiments and experimental investigations on the neutron spin precession in the gravitational field. The laboratory participates greatly in the preparation of the SORA experimental programme.

The Magnetic Resonance Laboratory

is equipped with various spectrometers for high-resolution NMR, relaxation and dynamic polarization studies, and electron spin resonance. Special features of the facilities are the relatively large frequency and temperature ranges which are aceessible for the study of solid and liquid samples. Of particular importance is the combined installation of a 2 MeV Van de Graaff with an ESR spectrometer for the study of radicals during fast electron irradiations. The activity of the laboratory includes the investigation of molecular motions in liquids, adsorbed liquids, liquid crystals, glasses and crystals; dynamical polarization studies and the determination of the structure of molecules and free radicals. In addition some fundamental problems of nuclear magnetism and magnetic phenomena in organic materials are studied.

The Solid State Physics Laboratory

is equipped with fast neutron and electron irradiation facilities, X-ray diffraction equipment, two Mössbauer spectrometers, optical spectrometers, a spectrophotometer and various installations for the study of mechanical, optical and electrical properties of solids. The main activity comprises the study of radiation damage and imperfections in preferably metallic solids, the determination of optical properties in order to study the electric structure of ferroelectric crystals, dynamical diffraction studies of X-rays and neutrons, and applications of the Mössbauer effect.

The Theoretical Physics Group

during 1971, worked mainly on lattice dynamics, on the effect of impurities on dynamical scattering of neutrons, and on the diffusion of vacancies and interstitials.

The Experimental Reactor Physics Group

has the competence and instrumentation to carry out work in various fields of reactor physics. Its activity is greatly governed by a close cooperation with other divisions and by requests from experts of the Community. During 1971 the main activities were
- D_2O reactor physics, mainly carried out in the critical assembly ECO.
- Experiments in the field of HTGR reactors (resonance capture and Doppler coefficients of coated particles, burnup measurements by the inverse kinetic technique)
- Nuclear safeguards (new measuring techniques for non destructive assay of fuel elements, spontaneous fission by autocorrelation techniques etc.).

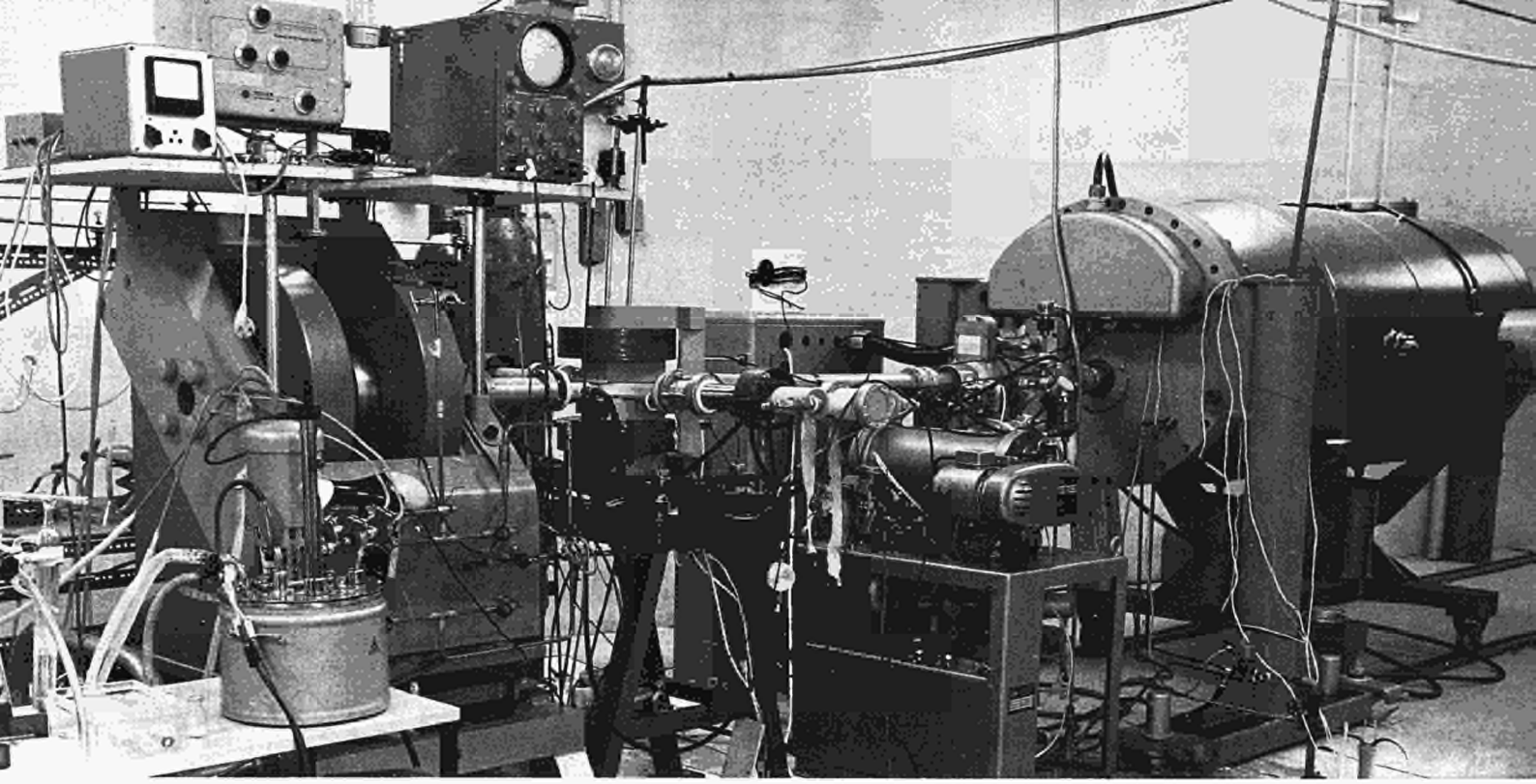

Fig. 1: General view of apparatus.

STRUCTURE OF RADICALS IN IRRADIATED ORGANIC MATERIALS AS REVEALED BY MOLECULAR ORBITAL THEORY AND ELECTRON SPIN RESONANCE

R. Fantechi, G.A. Helcké

Introduction

The radical species produced in organic materials by ionizing radiation are, in general, highly reactive and consequently short lived. This makes their study difficult and ways have had to be found of getting round this problem.

Since diffusion rates are lower in solids than in liquids, it is common to freeze liquids and study them at low temperatures. Restricted translational diffusion reduces radical recombination and increases lifetimes. Unfortunately, however, the lower rotational diffusion rates of the radicals prevent the complete averaging out of anisotropic terms in the electron spin Hamiltonian. This leads to a broadening of the spectral lines and a loss of resolution.

Anisotropic effects are large or small according to whether the majority of the unpaired spin density is in p- or s-orbitals. Since most radicals are of the π-type, low temperature studies are usually not ideal.

An alternative, adopted in this work, is to irradiate the substance under study whilst the ESR spectrum is recorded. If the rate of production of radicals can be made at least equal to the rate of recombination, an observable concentration of radicals can be built up even when lifetimes are short.

The radiation source used is a High Voltage Engineering, 2MeV Van de Graaff, the beam tube of which passes through an axial hole in one of the pole faces of a Varian 9" magnet. The ESR sample cavity has stainless steel walls which are made very thin in the vicinity of the sample so that there is minimum retardation of the electrons on entering. The interior of the cavity is gold-plated to present a highly conducting surface to the microwave radiation employed by the ESR spectrometer. The layout of the apparatus is shown in Figs. 1 and 2.

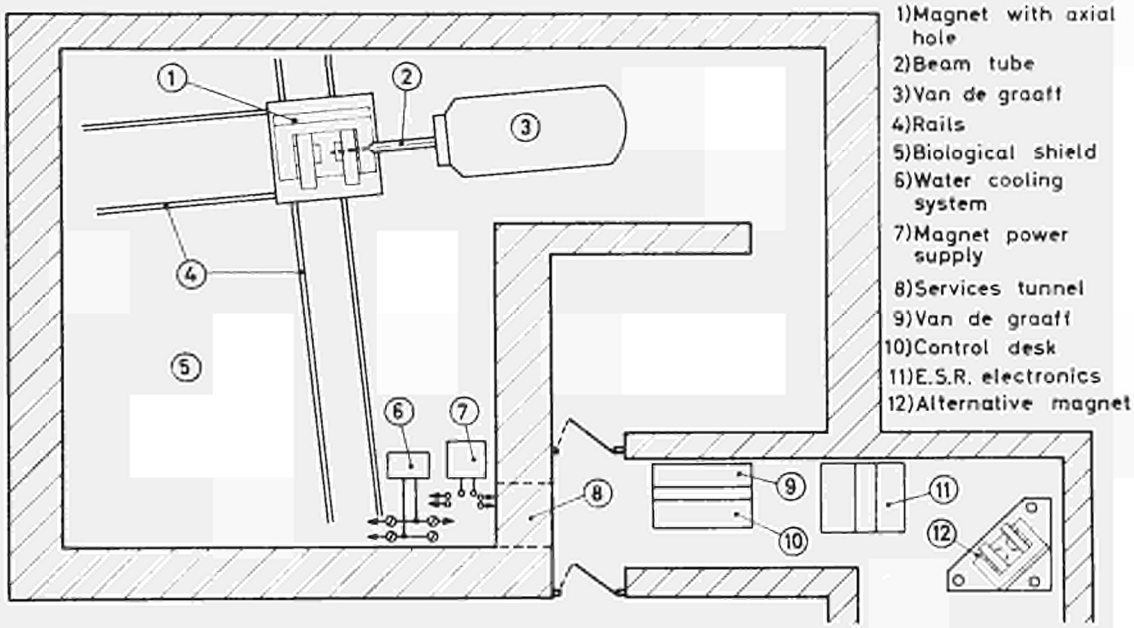

Fig. 2: Layout of apparatus.

Fessenden and Schuler [1], who were the first to use this method, examined transient radicals formed in a whole range of liquid aliphatic hydrocarbons. In attempting, at Ispra, to extend the method to other types of compounds, several difficulties were met with. Non-aliphatic compounds were often more radiation-resistant or had faster recombination rates, so that radical concentrations were frequently too low. More serious still, many substances had high dielectric absorptions in the microwave region which caused severe damping of the resonant cavity. Decreasing the amount of sample reduced the dielectric losses but also the total number of radicals which could be produced. In this case, moreover, ionization of the vapour phase caused noise in the ESR output.

To overcome these difficulties a new technique [2,3,4] was developed here which involves adsorbing the substance to be studied in the pores of zeolite "molecular sieves". These are crystalline substances whose lattices contain a regular three-dimensional array of interconnecting cells of molecular dimensions into which substances can be adsorbed. The space available is about 50% of the total volume.

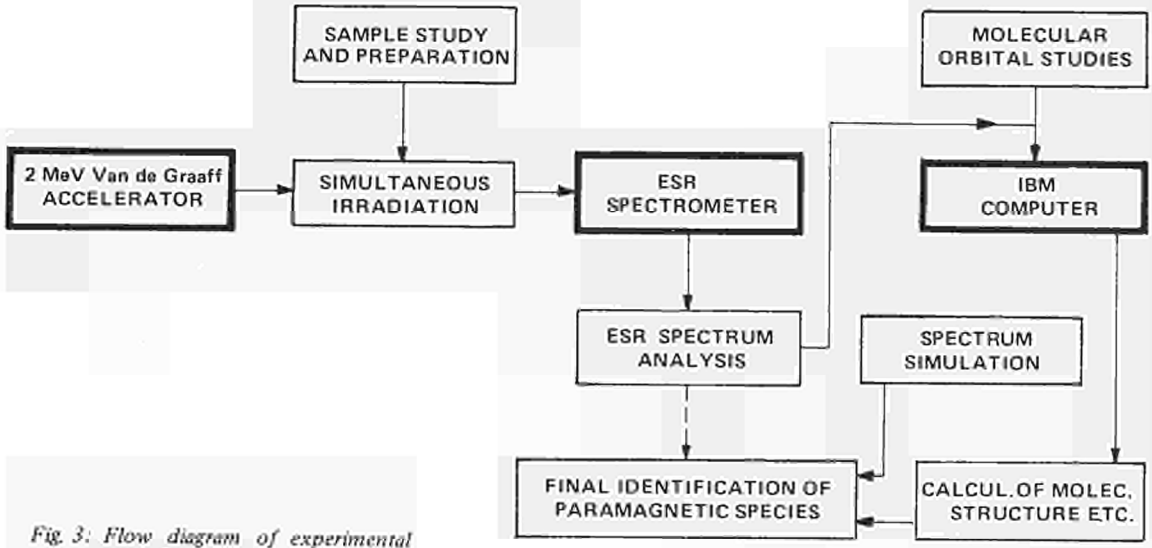

Fig. 3: Flow diagram of experimental procedure.

With careful preparation, samples can be obtained in which there is, on average, only one molecule adsorbed per cell. The nature of the sieve channels hinders translational but not rotational diffusion, so that whilst recombination rates are reduced, anisotropic effects are averaged out almost as in a liquid. The resulting spectra are essentially isotropic and resolution good, especially when high temperatures are used. Since the higher the temperature used the faster the recombination rate becomes, simultaneous irradiation of increasing intensity is required for the best-resolved spectra.

In early experiments, carried out to test the practicability of the method, we were able to obtain well-resolved spectra from the ethyl radical at temperatures as high as +150°C. This illustrates how very effective the isolation of individual radicals is and how inert the walls of the cells are to radical attack.

The two studies described in this paper illustrate both the molecular sieve technique and the more common technique of irradiating the solid phase. In the latter case the radical studied is of σ-type so that the anisotropic effects do not hinder interpretation of the spectra.

It will be seen that, together with the tentative identification of the radical from its ESR spectrum, molecular orbital calculations, employing this Centre's IBM 360 computer, are made which predict the ESR splittings that the supposed radical should have.

The first step is a systematic minimization of the total energy of the molecule with respect to all independent geometrical variables (bond length and bond angles). This gives the absolute minimum of the total energy corresponding to the *equilibrium* geometry of the radical under study. The calculated ESR splittings for this geometry should then correspond to those observed. In practice it is found that a geometry near to but slightly different from the equilibrium geometry is required for a best fit of calculated and observed splittings. This reflects a combination of two factors, one that the calculation of minimum energy by approximate molecular orbital methods is itself approximate and the other that the radicals, if trapped, are not likely to be able to adopt their fully unconstrained geometry.

Fig. 3 shows schematically the various steps and procedures involved in this work.

The Radical $OCNH_2$ found in irradiated formamide, urea and biuret

Fig. 4 shows the spectrum obtained on irradiating urea at room temperature. A similar spectrum can also be obtained by irradiating solid formamide, or biuret [5]. The spectrum is clearly due to the interaction between the unpaired electron, a single hydrogen atom and a nitrogen atom. The hydrogen splitting is approximately 30 G and the nitrogen splitting 20 G. The irradiation of these amides might be expected to cause either or both of the reactions

$$1.\ RCONH_2 \longrightarrow O\dot{C}NH_2 + \dot{R}$$

$$2.\ RCONH_2 \longrightarrow RC\dot{O}NH + \dot{H}$$

so that the observed spectrum could be due to one of the two radicals $O\dot{C}NH_2$ and $RC\dot{O}NH$.

In order to know which radical would be most likely to show the observed splittings, molecular orbital calculations have been carried out using the CNDO/2 method of Pople and Segal [6] via a computer program due to Dobosh [7]. Structural information was taken from Chemical Society Tables [8].

The CNDO/2 calculations give the unpaired spin density in each orbital on atom of the radical. It has been found, from a study of many radicals, that these spin densities can be converted into the corresponding ESR hyperfine coupling constants by use of formulae whose general form is

$$a^i = A\rho^i_{ss} + B\rho^i_p + \sum_j c^j \rho^j_p \text{ Gauss}$$

where j refers to any adjacent atom.

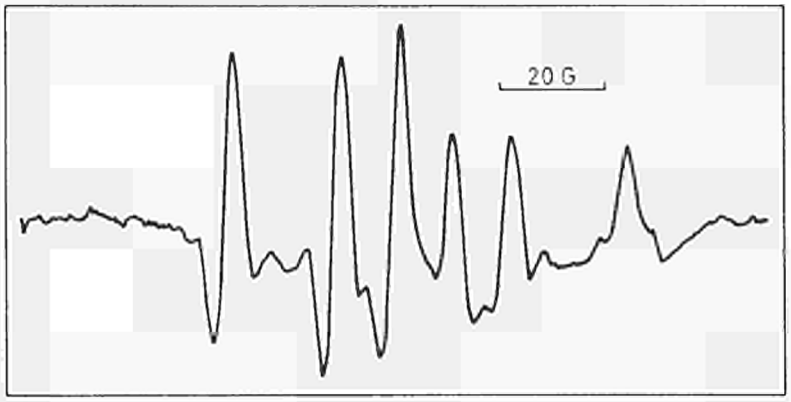

Fig. 4: Spectrum seen during irradiation of urea at room temperature with electron beam current of 0.1 μA.

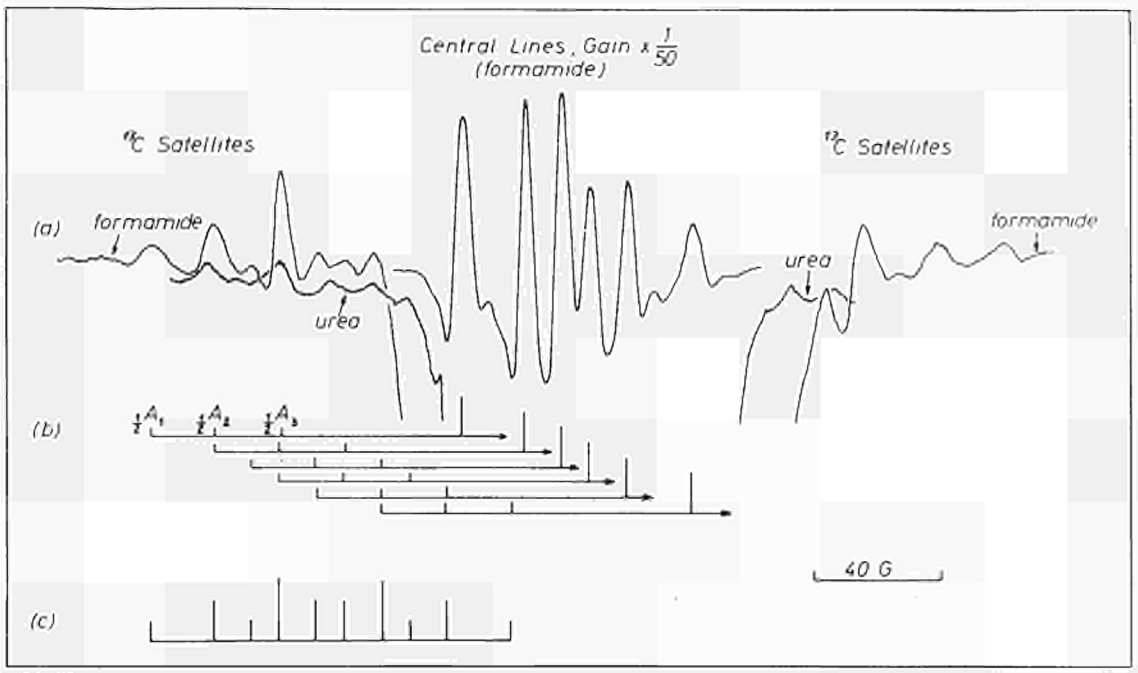

Fig. 5: ^{13}C satellite lines seen during high intensity irradiation of formamide at − 80°C. Electron beam current 1.0 μA.

For hydrogen splittings, the constants are found to be A = 506.8 G, B = 0 and C = −22.5 G, whilst for nitrogen, A = 768.5 G, B = 14.5 G and C = 0, and for ^{13}C, A = 1057.9 G, B = 42.6 G and C = 0.

The calculations show that the radical $O\dot{C}NH_2$ should be of σ-type, whilst the radical RCONH should be of π-type when R = NH_2 but of σ-type when R = H. Since the radical in question is seen in both urea and formamide, RCONH can thus be ruled out.

The radical $O\dot{C}NH_2$ is predicted to show two hydrogen splittings which, with an OCN angle of 132°, have the values of 32.7 G and 1.5 G. The smaller splitting would not be observed in Fig. 3 since the line widths are around 4 G. The same radical has, however, been produced chemically in the liquid state [9,10] and a small splitting of 1.3 G is in fact seen. The 20 G nitrogen splitting observed in the spectrum assigned to the $O\dot{C}NH_2$ radical, with OCN = 132°C, was used to calculate the A constant given above. Since this constant gives good results for other radicals, the assignment must be correct.

In addition to the hydrogen and nitrogen splittings, the calculations also predict a ^{13}C splitting of 138 G. Since the natural abundance of ^{13}C is only a little over 1%, ^{13}C lines are usually very weak. In this case, however, it was found possible to create very large radical concentrations with simultaneous irradiation, and unusually intense ^{13}C satellites were observed (Fig. 5). The ^{13}C spectrum can be analysed, as shown in the figure, to give not only the isotropic component of the splitting but also the anisotropic components. The isotropic splitting is found to be 153 G which is in reasonable agreement with the predicted value. The various splittings are collected in the table.

The calculations also predict that the anisotropy in the hydrogen and nitrogen splittings should be less than 1 G so that the satellite lines seen in Fig. 3 must be due to g-value anisotropy. The principal values of the g tensor obtained are very similar to those of another σ radical, formly, as seen below.

this radical:	$g_1 = 2.0054$	$g_2 = 2.0018$	$g_3 = 1.9979$
formyl:	$g_1 = 2.0041$	$g_2 = 2.0027$	$g_3 = 1.9960$

From the table it can be seen that the ratio a_H/a_N of the large hydrogen splitting to the nitrogen splitting is temperature dependent. The CNDO/2 calculations show that this variation of a_H/a_H corresponds to the average value of OCN, being smaller at high than at low temperatures. For formamide, the total change in a_H/a_N between −80°C and room temperature corresponds to an angular change of about 2.5°.

CNDO/2 calculations thus provide very clear proof that the radical formed in formamide, urea and biuret is $O\dot{C}NH_2$. Close correspondence is found between the calculated and observed values of the hydrogen and ^{13}C coupling constants. The prediction that the radical should be of σ type is borne out by the close similarity between the g values measured for this radical and those of formyl. In addition to this, the calculations provide a value for the OCN angle and show that variations in $\hat{OCN}$ can account for temperature-dependent effects in the observed spectrum.

Parent Substance	Temp.	a^N ±0.2G*	a^H ±0.2G*	^{13}C tensor ± 2 gauss *		g tensor ± 0.0002*		a^H/a^N	Ref.
				A^C	a^C	g_1, g_2, g_3	isotropic		
Formamide				194		2.0052			
(solid)	− 80°C	19.9	32.4	154	153	2.0012	2.0007	1.63	*
				112		1.9958			
(solution)	+ 20°C	21.65	30.55				2.0016	1.41	9
			1.22						
	+ 9°C	21.62	30.47				2.00154	1.41	10
			1.31						
	+ 32.5	21.69	30.41				2.00155	1.40	10
			1.27						
Urea	− 80°C	20.7	33.1	193		2.0054		1.60	*
(solid)	+ 20°C	21.1	32.4	153	152	2.0018	2.0017	1.53	*
	+ 75°C	21.6	32.5	105		1.9979		1.50	*
	+ 110°C	21.7	32.4					1.49	*
Biuret cis	+ 20°C	21.8	32.9			2.0018		1.51	*
(solid) trans	+ 20°C	22.8	33.6			2.0018		1.47	*

*) This work

The hydrazyl radical found in irradiated hydrazine

During irradiation by 2MeV electrons of liquid hydrazine ($H_2N\text{-}NH_2$) adsorbed in Linde 4A molecular sieves, the spectrum (Fig. 6) of the hydrazyl radical ($H_2N\text{-}\dot{N}H$) was observed [3]. The attribution of the observed spectrum to that radical was made on the basis of the presence in the spectrum of a large doublet of 18.8 G, which must correspond to a single hydrogen atom, and of three triplets of 11.7, 8.8 and 2.3 G, respectively, which must be due to two nitrogen atoms and two equivalent hydrogen atoms. For the radical $H_2N\text{-}\dot{N}H$ there are no *a priori* reasons for deciding the angles which the various hydrogen atoms should form with the nitrogen atoms. From the planar structure of the trigonal nitrogen ($\widehat{HNH} = 120°$) to the pyramidal structure ($\widehat{HNH} = 109.5°$) all conformations are possible. Also, for the N-H bond in the $\text{-}\dot{N}H$ group, the angle formed with the N-N bond can take any value from 120° to 180° A third variable is the angle between the xz-plane (see below) and the N-N-H plane, and a fourth is the N-N bond length. The N-H bond lengths, on the other hand, can be safely assigned standards values.

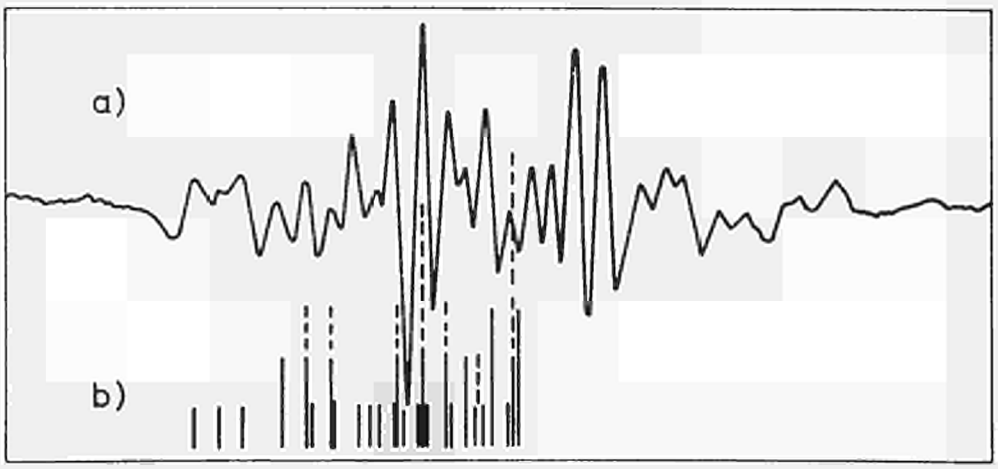

Fig. 6: (a) Spectrum observed from hydrazine, adsorbed in a zeolite, during irradiation at + 90°C with a beam current 0.3 μA. (b) reconstructed stick spectrum.

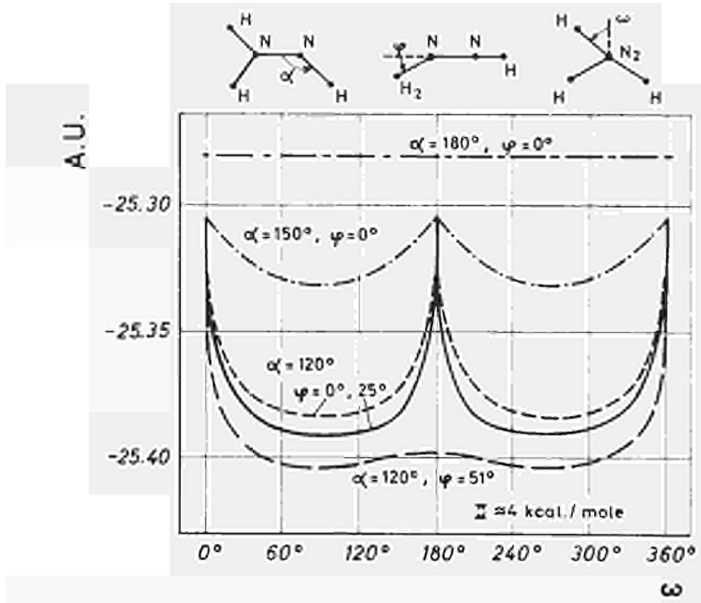

Fig. 7: Variation with ω, of the calculated total energy of hydrazil for several values of α and φ.

A whole series of guesses is therefore necessary in the present case. The various geometrical variables are shown at the top of Fig. 7. φ is the angle ($< 90^\circ$) formed by the bisector of the HNH angle, in the H_2N-group, with the x-axis, which is taken to coincide with the N-N bond. This bisector and the N-N bond are contained in the xz-plane. The two hydrogens in the H_2N-group lie symmetrically at either side of this plane. α is the angle ($\leqslant 120^\circ$) formed by the N-N bond and the N-H bond. The latter can rotate around the x-axis, and ω is the angle of rotation. $\omega = 0^\circ$ when the N-H bond lies on the xz-plane with $z > 0$.

First, a study of the total energy of the radical was made for several conformations. Although, as already mentioned, this cannot give an absolutely reliable answer, it can nevertheless help in deciding which geometries are more likely to be assumed by the radical. Fig. 7 shows that conformations are favoured for which $\omega = 90^\circ$, and increasingly so with smaller α and larger φ values. Fig. 8 shows that, for $\alpha = 120^\circ$ and $\omega = 90^\circ$, large values of φ and small values of the N-N bond length are favoured, but also that the system is much more sensitive to changes in the N-N bond length than in φ. Similar indications can be obtained from a study of the variation of the hyperfine coupling constants, with the various geometrical variables. Fig. 9 shows the variation of the five a^i-values with α, when $\varphi = 25^\circ$ and $\omega = 90^\circ$. Two regions of acceptability are

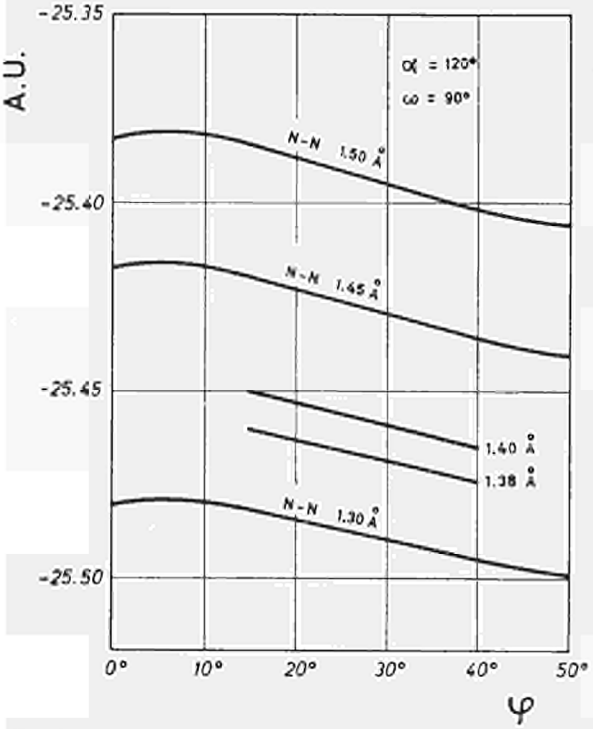

Fig. 8: Variation with φ, of the calculated total energy of hydrazil for several N-N bond lengths.

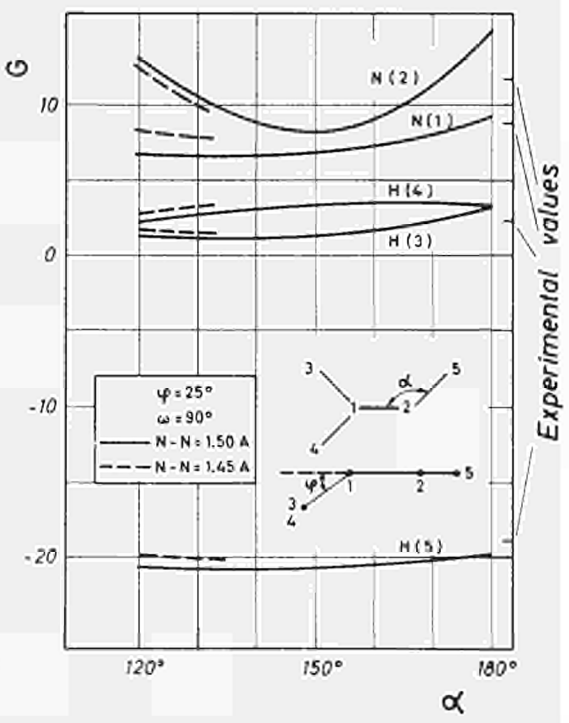

Fig. 9: Variation of the calculated hyperfine coupling constants with α for $\varphi = 25^\circ$ and $\omega = 90^\circ$.

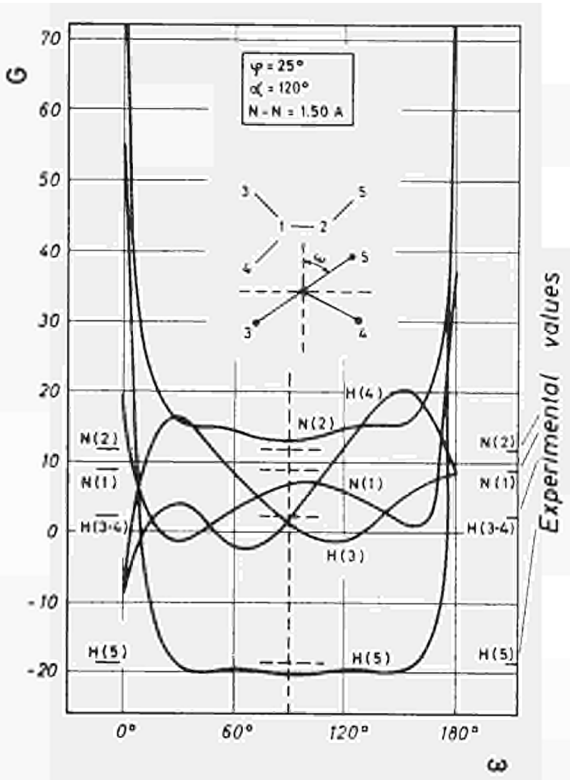

Fig. 10: Variation of the calculated hyperfine coupling constants with ω for $\alpha = 120°$ and $\varphi = 25°$.

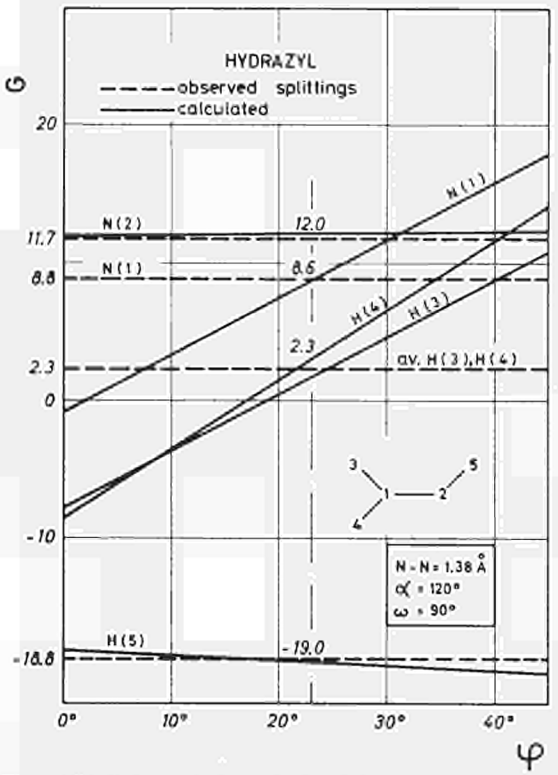

Fig. 11: Variation of the calculated hyperfine coupling constants with φ for $\omega = 90°$, $\alpha = 120°$ and N-N = 1.38 Å.

present here, one with $\alpha = 180°$, which must be discharged on energy grounds, and the other with $\alpha = 120°$. Shortening the N-N bond length makes the calculated a^1-values approach the observed ones more closely.

A more dramatic change is shown in Fig. 10 where the a^1-values are plotted as a function of ω, for $\alpha = 120°$ and $\varphi = 25°$. Here, only one region of acceptability is present, namely when $\omega = 90°$, in agreement with the energy predictions. A complete study along these lines led to the conclusion that $\omega = 90°$ and $\alpha = 120°$, with N-N = 1.38 Å. These are the values that allow the best reproduction of the observed hyperfine coupling constants. The final choice of φ is shown in Fig. 11, where it can be seen that $\varphi = 23°$ gives almost perfect agreement with experiment.

In this case, besides confirming the identity of the radical, a careful comparison of the observed hyperfine splitting constants with those calculated by CNDO/2 provides detailed information on the geometry of the radical under the conditions of study.

The two studies described in this paper, taken in conjunction with previous work on a hitherto unknown radical observed in irradiated mesitylene [2,11] show that the combined use of Electron Spin Resonance techniques and Molecular Orbital Theory provides a most powerful tool for the study of radical or ion species produced by ionizing radiation. The amount and the precision of the information thus gained is much greater than either ESR or MO theory could supply separately.

References

1) R.W. Fessenden and R.H. Schuler, *J. Chem. Phys., 39* (1963) 2147
2) G.A. Helcké and R. Fantechi, *Mol. Phys., 17* (1969), 65
3) R. Fantechi and G.A. Helcké, *J. Chem. Soc.* Faraday Transactions), 68 (1972) 924
4) G.A. Helcké and R. Fantechi, to be published (Uses of Sieves in ESR Studies: full description of technique)
5) G.A. Helcké and R. Fantechi, *J. Chem. Soc.* Faraday Transactions, 68 (1972) 912
6) J.A. Pople and G.A. Segal, *J. Chem. Phys. 44* (1966) 3289
7) P.A. Dobosh, Quantum Chemistry Program Exchange, Program No. 141, Indiana University Chemistry Dept.
8) Tables of Interatomic Distances and Configurations in Molecules and Ions. Special Publication Nos. 11 and 18. The Chemical Society London (1958 and 1965)
9) P. Smith and P.B. Wood, *Canad. J. Chem., 44* (1966) 3085
10) R. Livingston and H. Zeldes, *J. Chem. Phys. 47* (1967) 4173
11) R. Fantechi and G.A. Helcké, *Mol. Phys. 22* (1971) 737

EVIDENCE FOR STATIC CROWDIONS IN ELECTRON-IRRADIATED Au-15 at.%Ag ALLOYS

*W. Schüle**
and
W. Frank and A. Seeger
Max-Planck-Institut für Metallforschung, Institut für Physik, and
Institut für theoretische und angewandte Physik, Universität Stuttgart, Germany

Introduction

In spite of large research efforts during the last two decades, agreement on the configurations and basic properties (e.g., activation energies of migration) of the simple point defects in f.c.c. metals has not yet been achieved. For a brief survey of the outstanding questions the reader is referred to the panel discussion in [1]. The main problems centre around the nature of self-interstitials, in particular on the question whether in addition to the mechanically stable configuration, which the majority of the authors believe to be the <100>-dumbbell, self-interstitials in f.c.c. metals may also have a mechanically metastable configuration. In the 'one-interstitial model' the interstitial is assumed to migrate freely at low temperatures (in the case of copper with a migration energy of 0.12 eV, in the so-called annealing stage I_E). In the 'two-interstitial model' the stable configuration is thought to migrate at high temperatures (in copper with a migration energy of 0.69 eV, in the so-called annealing stage III). The two-interstitial model ascribes to the metastable interstitial configuration those phenomena that the one-interstitial model attributes to interstitial migration (for further details see below).

Rather direct evidence has been obtained in support of the view that the stage-III defect is indeed an isolated self-interstitial and that, at least in copper and nickel, it has the <100>-dumbbell configuration [2]. Recently, considerable evidence has also been found for the most striking feature of the two-interstitial model, namely the possibility that, by thermal activation, the metastable interstitial configuration may be converted into the stable configuration (thermal conversion). [2-4]

The question concerning the nature of the metastable (i.e., stage-I_E) interstitial is more difficult to decide for reasons that will become apparent presently. Two different views have been presented (they are presumably the only possible ones, once the <100>-dumbbell configuration has been accepted for the stable configuration):

1) The metastable configuration migrates three-dimensionally. Its configuration must then be either the tetrahedral interstitial or the <111>-dumbbell, or closely related to these two configurations. This is the view-point of Simpson and Sosin [5], who are of the opinion that the annealing kinetics of stage I_E in copper can only be accounted for in terms of three-dimensional defect migration.
2) The metastable configuration migrates one-dimensionally [6-8]. A natural extension of the concept of the 'dynamic crowdions' [9] is that the metastable interstitial has the crowdion configuration, i.e., one preferred <110>-direction in which it is able to migrate by thermal activation. Such a crowdion may either be an 'on-line' crowdion or an 'off-line' crowdion, depending on whether or not the line of migration of the crowdion passes through the annihilation volume of the vacant site from which it originated [10,11]. The distinction between on-line and off-line crowdions is important in the discussion of recovery processes, as emphasized by Schilling and coworkers [12]. The on-line crowdions have a very high chance to find back to their 'own' vacancies and will thus annihilate with vacancies after a relatively small number of jumps [13]-[15]. By contrast, off-line crowdions cannot annihilate with their own vacancies. If we disregard other sinks, such as dislocations or surfaces, they can only disappear by conversion to the stable configuration or by finding a 'foreign' vacancy. The latter process requires a much larger number of jumps than would on the average be required for a three-dimensionally migrating interstitial in order to annihilate with one of the 'foreign' vacancies [8].

In model 2) the correlated recovery within stage I of electron-irradiated f.c.c. metals is attributed to the recombination of on-line crowdions with their own vacancies. If free defect migration takes place at the high-temperature side of stage I, as is the case, e.g., for copper, silver, and nickel, this is ascribed to the annihilation of off-line crowdions with foreign vacancies.

The probability that crowdions produced during electron or γ-irradiation are off-line crowdions increases with increasing transferred energy. The existence of off-line crowdions makes it virtually impossible to decide between one-dimensional and three-dimensional migration on the basis of a simple

kinetic analysis, since the recombination of off-line crowdions with vacancies has many features in common with the corresponding reaction of three-dimensionally migrating interstitials [8-11]. Evidence that at least in nickel the stage-I_E defect migrates one-dimensionally has recently been obtained from recovery studies of the magnetic after-effect [16, 17].

The present paper investigates the question whether by studying alloys rather than pure f.c.c. metals evidence for or against one-dimensional migration in stage I may be obtained. This seems indeed feasible on account of the following argument: Whereas three-dimensionally migrating self-interstitials (which are assumed to migrate by the interstitialcy mechanism) may choose such a path that the degree of order in the alloy increases significantly over that prevailing before the introduction of the interstitials, (in the case of copper base alloys it has been established that not only vacancy migration but also interstitial migration may be accompanied by an increase of atomic order. This is particularly true if the lattice parameter of the alloy does not change appreciably with composition [18,19]. For the Au-Ag alloys to be discussed in this paper this condition is fulfilled.), this is obviously not possible for a one-dimensionally migrating defect, whose path is largely determined by geometry. If a crowdion recombines with its own vacancy, the atomic order prior to the production of the pair of defects is restored. Annihilition of a crowdion with a foreign vacancy may result in a slight decrease of the degree of order if the crowdion path goes through regions with relatively high degrees of order. An increase of the degree of order as a consequence of crowdion migration does not seem feasible.

Sprusil, Haas, and Wollenberger [20] have recently reported on the low-temperature electron-irradiation and the recovery of the electrical resistivity of Au-Ag alloys of several compositions. Taken together with the analogous experiments on gold [21,22] these alloys are particularly interesting, since with respect to the resistivity recovery at low temperatures irradiated gold does not appear to follow the usual pattern of the other f.c.c. metals investigated [23].

In the crowdion picture an explanation of this apparent exception is that in pure gold the energy barrier for the conversion of crowdions to the <100>-dumbbells, E_C^c, is lower than or comparable with the activation energy of crowdion migration, E_C^M, so that crowdions in gold are not able to migrate over significant distances by thermal activation. A striking confirmation of this picture would be obtained if a suitable alloying addition to gold could be found that stabilizes the crowdion configuration to the extent that thermal crowdion migration becomes observable. It is the principal aim of this paper to demonstrate that the Au-15 at.% Ag alloy investigated by Sprusil et al. is such a 'suitable' alloy, whereas in the Au-0.2 at.% Ag and Au-5 at.% Ag alloys also investigated by Sprusil et al. the condition of pure gold still prevails, i.e., the crowdion is sufficiently unstable and not detectable by its thermal migration. The Au-Ag system is indeed a good candidate for the search for such a change-over, since in pure Ag the conversion energy E_C^C of the crowdion is large enough for the thermally activated migration of crowdions to be detectable [24]. We shall see that in addition the study of the recovery of the Au-15 at.% alloy provides rather direct evidence that the stage-I_E defect migrates in one dimension and not in three dimensions.

Crowdions in gold and gold alloys

In this section we shall deduce a number of conclusions from the ideas outlined in the above section that may be tested experimentally.

In electron-irradiated pure gold an almost continuous isochronal recovery is observed from stage I through stage II up to stage III [21,22]. This is interpreted in terms of a spectrum of annealing stages of dumbbell-vacancy pairs of various separations [23]. This spectrum is limited on its high-temperature side by the free migration of dumbbells. There is no evidence for a low-temperature annealing involving the free migration of a radiation-induced defect.

In electron-irradiated pure copper the annealing spectrum associated with crowdion-vacancy pairs is terminated by the free migration of the off-line crowdions in stage I_E. There is practically no stage II [25] (provided that the specimen is 'pure' and that the irradiation dose has been kept sufficiently low in order to prevent the production of secondary dumbbell-vacancy close pairs [26,27]. Nevertheless, a marked stage III is observed. This is attributed to the migration of dumbbells that were produced with little or no correlation to vacancies by the conversion of crowdions that had migrated in stage I_E. If we can find an alloying addition to gold that stabilizes the crowdion configuration sufficiently (such an alloy will be called a 'suitable' alloy), then, in analogy to copper, stage II recovery should be suppressed (*Conclusion 1*).

In gold with a suitable alloying addition stage I should increase, since the annihilation of dumbbell-vacancy close paired in stage II of gold is in the alloy at least partly replaced by crowdion-vacancy annihilation in stage I (*Conclusion 2*).

Au-15 at.% Ag specimens show short-range order when slowly cooled or when quenched from high temperatures and subsequently annealed [28-30]. In analogy to the results known from many other alloys [31-37] the increase of the electrical resistivity found after quenching may be attributed to the formation of small ordered regions formed during the quench. (An interpretation of the quenched-in resistivity in terms of scattering of conduction electrons at vacancies must be ruled out on account of Schulze's results [28]. They indicate that even during a quench from 450°C to 150°C with a quenching rate of 40,000°C/sec almost all vacancies should have annealed out.).

Let us assume that Au-15 at.% Ag is a suitable alloy from the point of view of crowdion stabilization. For a specimen that is furnace-cooled from 650°C to room temperature and subsequently electron-irradiated at 25°K, the following predictions may then be made on the basis of the two-interstitial model:

In addition to the effects due to the generation of point defects the electrical resistivity is increased by dynamic crowdions, which, on their paths through locally ordered regions, leave behind disordered atomic rows. Hence, the resistivity increase per defect pair after low-temperature irradiation is expected to be enhanced in Au-Ag alloys in comparison with pure gold (*Conclusion 3*).

In isochronal recovery experiments the resistivity must decrease monotonically throughout stage I, since defects which, on account of their free migration in three dimensions, might be capable of increasing the degree of order and thus giving rise to an initial increase of the electrical resistivity are practically immobile up to the beginning of stage III (*Conclusion 4*).

During annealing in stages III and IV we expect the ordering effects associated with three-dimensional migration of interstitials and vacancies. Such effects have been observed by Beardmore and Bever [38] on an Au-27 at.% Ag alloy after low-temperature deformation. After an initial increase of the electrical resistivity a decrease was found. The same should be true after irradiation (*Conclusion 5*). (The initial increase is attributed to the growth of already existing ordered regions and the nucleation of additional ones, in agreement with the interpretation in [38]. The subsequent decrease of resistivity originates from the fact that coalescing ordered particles lose some of their effectiveness as scattering centres for conduction electrons. An additional reduction of the electrical resistivity results from the mutual annihilation of dumbbells and vacancies.).

Interpretation of the Experiments by Sprusil, Haas, and Wollenberger [20]

As mentioned above Sprusil et al. [20] have recently reported on the low-temperature electron irradiation and the isochronal recovery of the electrical resistivity of Au-Ag alloys of several compositions (0.2 at.% Ag, 5 at.% Ag, and 15 at.% Ag).

The Au-0.2 at.% Ag and Au-5 at.% Ag alloys resemble strongly pure gold with respect to their annealing behaviour. This means that the silver additions are too small to stabilize static crowdions. Even in these alloys with low Ag-contents an unambiguous resistivity increase per defect pair compared with pure gold is observed in accordance with Conclusion 3.

In the case of the Au-15 at.% Ag alloy there is strong evidence for the existence of static crowdions: This alloy shows all the characteristic features predicted by the two-interstitial model for suitable alloys in the preceding section (cf. Conclusions 1 to 5). Fig. 1 of [20] shows the verification of Conclusion 3, Fig. 2 that of Conclusions 1, 2, 4, and 5.

We conclude that the experimental results of Sprusil and coworkers demonstrate in a rather specific manner that in stage I one-dimensional migration of defects may take place. This rules out both the Simpson-Sosin version of the two-interstitial model and the one-interstitial model, which have in common that they attribute stage I_E to three-dimensional migration of an interstitial.

In particular the one-interstitial model would predict

- a gradual suppression of stage I_E with increasing Ag-content on account of an increasing trapping probability by Ag-atoms (contrary to our Conclusion 2).
- an enhancement of stage II (attributed to detrapping of interstitials from impurity sites) with increasing Ag-additions (contrary to our Conclusion 1), and
- the possibility of an increase of resistivity on the high-temperature side of stage I due to ordering by three-dimensional migration of interstitials (contrary to our Conclusion 4).

The experimental results obtained by Sprusil, Haas, and Wollenberger, bearing out the phenomena predicted by Conclusions 1, 2, and 4, are clearly incompatible with the preceding fundamental predictions of the one-interstitial model.

Conclusions

It is shown that recent investigations by Sprusil, Haas, and Wollenberger on the low-temperature electron irradiation and the recovery of the electrical resistivity of Au-15 at.% Ag alloys may be easily explained in terms of the two-interstitial model. These results indicate in a rather specific way that in this alloy defect migration in stage I takes place one-dimensionally. It is concluded that none of the models that assume three-dimensional migration for the interstitial migrating at low temperatures are capable of accounting for the recovery behaviour of Au-15 at.% Ag alloys.

Acknowledgement

The authors would like to express their appreciation to Dr.H. Warlimont for his contributions to the analysis of the ordering phenomena in alloys.

References

1) A. Seeger, D. Schumacher, W. Schilling, and J. Diehl, Vacancies and Interstitials North-Holland, Amsterdam (1970)
2) A. Seeger, in Ref. 1, p. 999
3) D.O. Thompson and O. Buck, *J. Appl. Phys. 38*, 3068 (1967)
4) D.O. Thompson and O. Buck, *Phys. Stat. Sol., 37*, 53 (1969)
5) H.M. Simpson and A. Sosin, *Rad. Effects,2*, 299 (1970)
6) C.J. Meechan, A. Sosin, and J. Brinkman, *Phys. Rev., 120*, 411 (1960)
7) A. Seeger, in 'Radiation Damage in Solids', *IAEA, 1*, Vienna (1962), p. 101
8) W. Frank, A. Seeger, and G. Schottky, *Phys. Stat. Sol., 8*, 345 (1965)
9) A. Seeger, Proc. 2nd UN Internat. Conf. PUAE, Geneva, 1958, *6*, UN, New York (1958), p. 250
10) A. Seeger, Verhandl. DPG (VI), *5*, 413 (1970)
11) W. Frank, *Rad. Effects*, in press
12) W. Schilling, G. Burger, K. Isebeck, and H. Wenzl, in: Ref. 1, p. 225
13) G. Polya, *Math. Ann., 84*, 149 (1921)
14) E. Montroll, *J. Soc. Ind. and Appl. Math., 4*, 241 (1956)
15) H.G. Vineyard, *J. Math. Phys., 4*, 1191 (1963)
16) G. Lampert, Dissertation, Universität Stuttgart (1971)
17) H.-E. Schaefer, Dissertation, Universtiät Stuttgart (1971)
18) W. Schüle, *Z. Naturforschg., 20a* 527 (1965)
19) W. Schüle, E. Lang, D. Donner, and H. Penkuhn, *Rad. Effects, 2*,151 (1970)
20) B. Sprusil, H. Haas, and H. Wollenberger, *Rad. Effects, 5*, 273 (1970)
21) J.B. Ward and J.W. Kauffman, *Phys.Rev., 123*, 90 (1961)
22) W. Bauer, J.W. DeFord, and J.S. Koehler, *Phys. Rev., 138*, 1497 (1962)
23) A. Seeger, *J. Phys. Soc. Jap., 18*, Supplement III, 260 (1963)
24) F.W. Wiffen, C.L. Snead, Jr., and J.W. Kauffman, *Phys. Stat. Sol., 32*, 459 (1969)
25) R.M.Walker, in:'Radiation Damage in Solids', *Scuola Intern. di Fisica,* E. Fermi, XVIII Corso, Academic Press, New York and London (1962), p. 594
26) R. von Jan, *Phys. Stat. Sol., 17*, 361 (1966)
27) R. von Jan, *Phys. Stat. Sol., 18*, 364 (1966)
28) H.A.Schulze, Jül.520-RW (1968)
29) K. Lücke and H.A. Schulze, *J. Appl. Phys., 39*, 4860 (1968)
30) G.P. Williams, Jr., B.J. Klein, and J. Everett, Jül-Conf-2,*1*(1968), p. 215
31) C. Panseri and T. Federighi, *Acta Met., 8*, 217 (1960)
32) S. Ceresara, T. Federighi, and I. Pieragostini, *Phil. Mag., 9*, 623 (1964)
33) T. Federighi, in:'Lattice in Quenched Metals', edited by R.M.J. Cotterill, M. Doyama, J.J. Jackson, and M. Mshii, Academic Press, New York (1965), p.217
34) H. Saito and H. Morita, *Sci. Rep. Inst. Tôhoku Univ., A18*, Suppl. 70 (1966)
35) H. Gleiter and E. Hornbogen, *Z. Metallkde. 58*, 157 (1967)
36) P. Wilkes, *Acta Met., 16*, 863 (1968)
37) W. Gaudig and H. Warlimont, *Z. Metallkde.; 60*, 488 (1969)
38) P. Beardmore and M. Bever, *Trans. Met. Soc.* AIME, *245*, 165 (1969)

QUASIELASTIC NEUTRON SCATTERING ON HYDROGEN IN NIOBIUM SINGLE CRYSTALS

W. Gissler, R. Rubin, N. Stump

Abstract

Quasielastic neutron scattering experiments on the system $NbH_{0.07}$ were performed with niobium single crystals at T = 235°C. To study the anisotropy, we measured the half-width of the quasielastic line dependent on $|\vec{K}|$, the K-vector being parallel to the (100), (110) and (111) crystal direction. The results were compared with theoretical half-widths corrected for experimental resolution. They exclude the octahedral and cubic interstitial site model assuming simple jump diffusion.

In two of the main symmetry directions the agreement with the simple tetrahedral model is fairly good, but in the third there are strong deviations.

Introduction

In recent years quasielastic neutron scattering investigations of the diffusive behaviour of hydrogen in transition metals have been performed on polycrystalline samples by several authors. In the case of the α-phase of palladium [1] the experimental results were compatible with a jump diffusion model (negligible jump time, only next nearest neighbour jumps, no self-restraint in the diffusion process), assuming octahedral sites as the position of the hydrogen atom. In all the other cases [2-6] the experimental data could not be fitted to such a model. Theoretical calculations [7 8 9] show that single-crystal measurements are much more sensitive to the interstice configuration. In this work we report on measurements on NbH single crystals. We measured the width of the quasielastic line for the main symmetry directions in the $|\vec{K}|$-range $1.3\ \text{Å}^{-1} \leqslant |\vec{K}| \leqslant 4.3\ \text{Å}^{-1}$. Single-crystal results were published recently [10 12].

Theory

Owing to the predominating incoherent scattering of the proton (bound scattering cross-section for incoherent scattering $\sigma = 79.6$ barn) the scattering function is given by the Fourier transform with respect to the energy $\hbar\omega$ and the momentum transfer $\hbar\vec{K}$ of the self-correlation function in space $\vec{r}$ and time t

$$S_{inc}(\vec{K},\omega) = \frac{1}{2\pi} \iint G_s(\vec{r},t)\, d\vec{\gamma}\, dt$$

Neglecting correlations between the oscillatory and diffusive motion [7] and starting from the assumptions for the simple jump diffusion model, $G_s(\vec{r},t)$ and $S_{inc}(\vec{K},\omega)$ respectively can be calculated by the method of Chudley and Elliot [7] for primitive lattices, which has been extended to non-primitive lattices [8 4], or by another method using a random flight technique [9]. This last method was used to calculate the full width at half maximum Δ_{res} of the convolution of the experimental resolution function of our spectrometer and the scattering function for three interstitial site configurations to compare with our experimental data. Fig. 1 shows Δ_{res} (full width at half maximum of the quasielastic line in the t.o.f. spectrum corresponding to the Ipsra spectrometer) for the simple cubic interstitial site lattice (interstitials at ± 1/4, ± 1/4, ± 1/4), the octahedral and the tetrahedral interstitial site lattice compared with the FWHM Δ_{the} without considering experimental resolution. From Fig. 1 one sees that the theoretically predicted vanishing FWHM Δ_{the} at $\vec{K} = 2\pi\vec{\tau}$ ($\vec{\tau}$ is a reciprocal lattice vector of the interstitial site lattice) do not reveal the resolution width for all these points. This is due to a strong non-Lorentzian shape of $S(\vec{K},\omega)$, especially for these momentum transfer regions. Therefore an unfolding procedure assuming Lorentzian-shaped $S(\vec{K},\omega)$ can lead to unreasonable interpretations. This procedure can only be applied in the simple cubic case because here $S(\vec{K},\omega)$ is always Lorentzian.

Fig. 1 shows that only in the tetrahedral case Δ_{res} of the (002) direction in the range $|\vec{K}| \leqslant 3.2\ \text{Å}^{-1}$ is larger than for the (110) direction, and only in this case the curves for the (110) and (111) directions have a cross point at $3.8\ \text{Å}^{-1}$. In the cubic case we expect at $|\vec{K}| = 3.8\ \text{Å}^{-1}$ a Δ_{res} equal to the resolution width for the (110) direction.

Experimental

The samples used were cylindrical single crystals (cylinder axis parallel to a (110) direction) of length 40 and diameter 12 mm and, for a few measurements, rectangular single crystals of size 10 x 10 x 3 mm^3 ((100) direction normal to the largest face). The single crystals were outgased at 2200°C at 10^{-10} torr before loading at about 700°C with purified hydrogen. The hydrogen content was determined from the weight increase by 7.0% and 7.5% respectively. The mosaic spread of the loaded samples was about 35 arcmin. The experiments were performed at the ISPRA-I reactor with a rotating crystal spectrometer [12] ($E_o = 14 \cdot 10^{-3}$ eV, $\Delta E/E_o = 5\%$, $\Delta\vartheta = 2.8°$).

The measurements were performed in a vacuum furnace at a temperature T = 235°C ± 2°C. For the measurements the width of the quasielastic line was determined by the difference of the intensities of the loaded and unloaded samples. A sample-holder was constructed for this purpose, allowing automatic rotation of both samples in the beam-position. For intensity reasons two pairs of cylindrical and five pairs of rectangular single crystals respectively have been used, the orientation of each to the other was better than ± 1 degree.

In order to avoid errors due to long-time background variations, the samples were interchanged every half an hour. This is advisable, since phonon and Bragg contributions from the host lattice as well as contributions from the sample holder can be detected immediately.

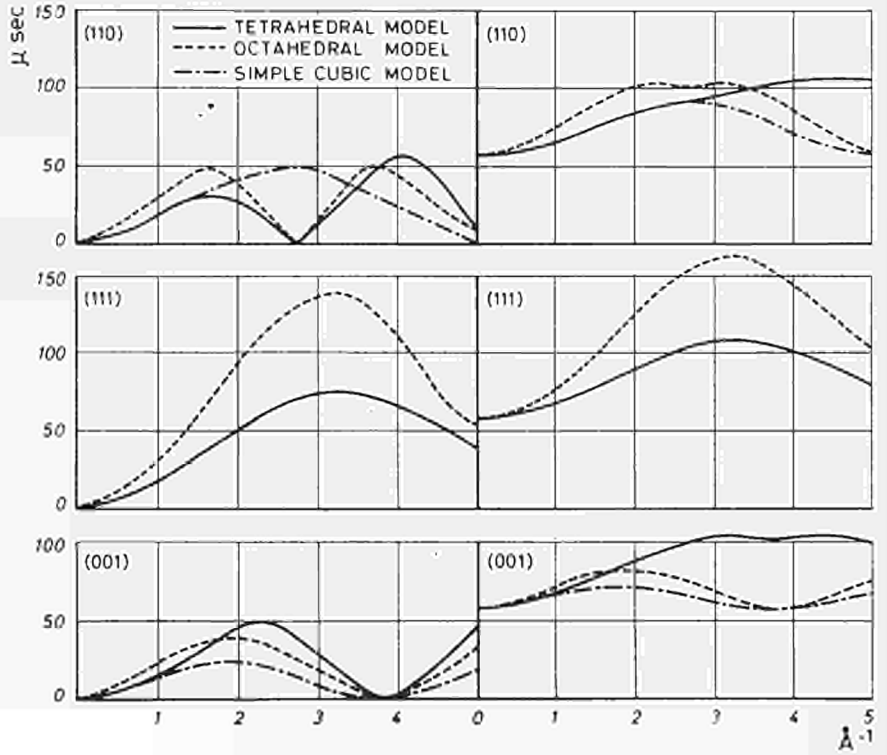

Fig. 1: Calculated full width of half maximum (FWHM) of the quasi-elastic line with (right) and without (left) the experimental resolution for the tetrahedral, octahedral and cubic interstitial site model of the b.c.c. Nb host lattice dependent on the momentum transfer $|\vec{K}|$. Δ_{res} has been calculated for the Ispra spectrometer resolution Δ_{the} is given in the same scale for comparison.

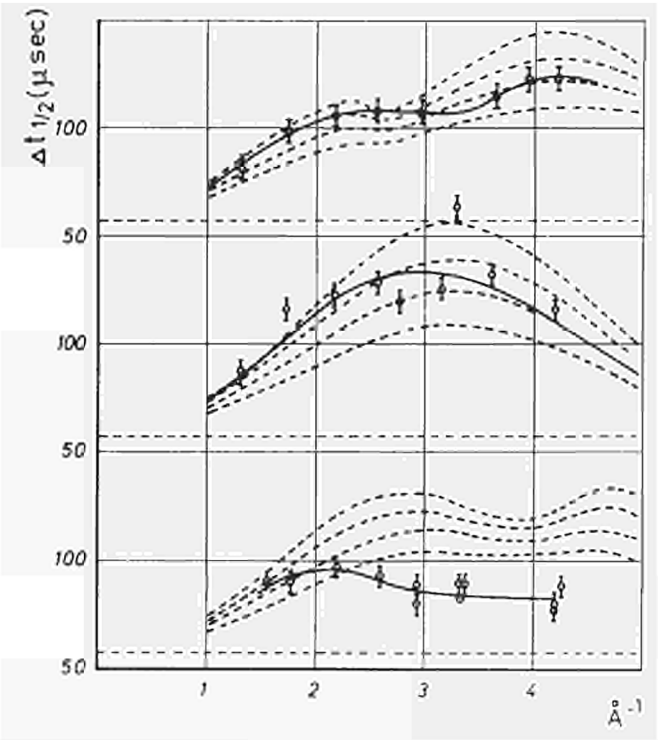

Fig. 2: Experimental FWHM of the quasi-elastic line for the three symmetry directions (001), (111), (110) are plotted vs. $|\vec{K}|$. The dashed lines are calculated from the tetrahedral model for the τ^{-1}-values indicated.

Results and Discussion

The measured intensities of the quasielastic line have been corrected only for counter efficiency and background. A rough estimation shows that the influence of multiphonon and multiple scattering is negligible. The errors of the presented half widths Δ_{exp} are only due to counting statistics and are given by bars.

Fig. 2 shows the results for the three directions parallel to the (002), (111) and (110) direction in the usual plot Δ_{exp} vs Π. The dashed lines are the theoretical half width Δ_{res} calculated for the tetrahedral model for four different τ^{-1} values, from 8.10^{11} sec^{-1} to 14.10^{11} sec^{-1}. A comparison with Fig. 1 shows that here also in agreement with the former results, the octahedral and cubic models can be excluded. The half-width curves for the (110) and (111) direction have a similar shape as in the tetrahedral model. More especially, the cross-point of these two curves is in good agreement with the theoretically predicted value at $K = 3.8$ $Å^{-1}$. Such a cross-point is not predicted by any other of the proposed models. Nevertheless these two curves cannot be fitted with one parameter τ^{-1}. The curve for (002) disagrees completely with the theoretical predictions, especially for $K = 2.5$ $Å^{-1}$.

The tetrahedral model being assumed, table 1 gives values for the reciprocal of the mean residence time, calculated from the experimental half widths at $|\vec{K}| = 2.2$ $Å^{-1}$ for all the main directions.

Table 1

	MEAN RESIDENCE TIME (10^{12} s^{-1})		
Direction of the momentum transfer K parallel to the direction	(100)	(110)	(111)
From neutron scattering at $T = 256°C$	0.8 ± 0.1	1.0 ± 0.1	1.0 ± 0.1
From neutron scattering at Ispra at $T = 235°C$	1.0 ± 0.1	1.2 ± 0.1	1.3 ± 0.1
From $D = 4.10^{-5}$ cm^2/s (Schaumann et al. (13)		0.5	

These values are compared with values derived from the measurements [12] and with $\tau = 4.5.10^{11}$ sec^{-1} at T = 250°C derived from the relation $D = a^2/(48\tau)$(a = 3.3 Å) taking $D = 4.10^{-5}$ cm^2/sec from Gorski measurements [13]. With the octahedral model a better agreement would have been achieved, but this model can be excluded, as shown above. This discrepancy cannot be explained on the basis of a simple jump diffusion model. An extension of the theory to finite jump times has recently been performed [14]. Results for the simple cubic model reveal larger half-width values for equal diffusion constants. Such an effect also tends to explain the observed discrepancies concerning the shape of the observed $\Delta_{exp} - |\vec{K}|$ curve. In contrast to measurements on polycrystalline VH_x (x = 0,2 and 0,4) [5] we have not observed any drastic increase of the width at large $|\vec{K}|$. The observed strong anisotropy does not allow by any means the use of a liquid-like model, as proposed for measurements at β-PdH_x [6].

Acknowledgement

The authors wish to tank G. Alefeld and W. Kley for their financial support and stimulating conversations, B. Jay for valuable technical assistance and P. Blanchard, A. Sieffert, R. Beyss and M. Bierfeld for the construction of the sample holder and the sample preparation.

References

1) K. Sköld and G. Nelin, J. Phys. Chem. Solids 28, 2369 (1967)..
2) G. Verdan, R. Rubin and W. Kley, Proc. IAEA-Symp. Neutron Inelastic Scattering, Vol. 1, 223 (1968), Vienna.
3) W. Gissler, G. Alefeld and T. Springer, J. Phys. Chem. Solids 31, 2361 (1970).
4) J.M. Rowe, K. Sköld, H.E. Flotow and J.J. Rush, J. Phys. Chem. Solids 32, 41 (1971).
5) L.A. de Graaf, J.J. Rush, H.E. Flotow and J.M. Rowe, Proc. Int. Conf. Hydrogen in Metals, KFA-Jülich, JÜL-CONF.-6(Vol I), p. 301 (1972)
6) M.M. Beg and D.K. Ross, J. Phys. C. 3, 2487 (1970).
7) C.T. Chudley and R.J. Elliott, Proc. Phys. Soc. 77, 353 (1961).
8) G. Blässer and J. Peretti, International Conference on Vacancies and Interstitials in Metals, KFA Jülich, Jül. Conf. 2 (1968).
9) W. Gissler and H. Rother, Physica 50, 380 (1970).
10) G. Kistner, R. Rubin and J. Sosnowska, Phys. Rev. Let. 27, 1576 (1971).
11) H. Meister, R, Haas, F. May, Ch. Schenk and B. Weckermann, Kerntech. Isotopen tech. Chem. 10, 145 (1968).
12) N. Stump, to be published.
13) G. Schaumann, J. Völkl and G. Alefeld, Phys. Rev. Let. 21, 891, (1968).
14) W. Gissler and N. Stump, to be published.

EFFECTS OF PLASTIC DEFORMATION ON THE PRODUCTION AND REACTIONS OF COLOUR CENTRES IN ALKALI HALIDES

M. Boni, P. Camagni

Introduction

The enhancement of X-ray colourability in deformed alkali halides raises a continued interest, owing to its connections with basic processes. Various efforts were made in the past to elucidate such connections, in particular: a) the nature of lattice imperfections introduced by plastic flow, and b) the way in which these imperfections are able to modify (possibly, to by-pass) the normal colouration mechanisms, based on a Frenkel type of damage. A good amount of this work was devoted to the study of F-centres which, for many reasons, constitute a sensitive probe of deformation effects. However, our knowledge remains unsatisfactory even in this particular area.

The first interpretation of the enhanced F-centre yield in deformed crystals was based on Seitz's idea of radiolytic vacancy formation at dislocation jogs [1]. This theory is now discarded, and the majority of authors agree that the sources of excess vacancies must reside on special products of dislocation processes, the so-called *debris*. Among the various possibilities, several authors suggest a specific role of dislocation dipoles [2-5], which are known to be a systematic product of cross-slip in alkali halides and are sufficiently stable to explain the annealing behaviour of extra colouration. However, plain vacancy clusters such as those created by dislocation crossing have also been proposed [6,7]. The available information is not sufficient to afford a direct choice between these two types of vacancy sources; as a consequence, little can be said about the mechanisms through which excess vacancies are released into the bulk during irradiation. It appears at present that any substantial progress will entail re-examination of neglected topics, such as the relationship of F-centre production to the details of deformation pattern.

It is worth noticing that past experiments were always based on pre-deformed samples: this gives limitations, which can be commented on briefly. The first is inherent to the fact that all vacancy sources are present from the beginning, i.e., prior to irradiation: in consequence one can only explore the operation of these sources, not the way in which they were originally produced. Another difficulty is the time-lag between deformation and irradiation, which allows unwanted annealing.

In view of the state of the subject, we undertook to study excess colouration in crystals that are irradiated *during* progressive deformation at controlled speed.

Results

Use was made of a special cryostat, linked to the mobile shaft of an Instron machine and containing the necessary features to allow simultaneous runs of irradiation and deformation *in vacuo*, as well as the subsequent optical measurements. Inside the cryostat the sample was mounted in a suitable compression cell, the drive to which was provided by mechanical coupling with the fixed shaft of the Instron.

The typical experiment consisted in applying a sequence of deformation-irradiation cycles to an individual crystal, and measuring the increments of colouration at the end of each cycle. During runs, a record was also taken of the load acting on the sample. A schematic illustration of the procedure is given in Fig. 1.

Time-growth of excess F-centres

The room temperature (RT) behaviour is illustrated in Fig. 2 for pure KCl. The figure shows the growth of colouration in identical samples of the given salt, as a result of irradiations with the same X-ray intensity, but subject to different conditions of plastic flow. The normal curve of the undeformed material is also plotted for comparison.

The figure demonstrates two main facts, namely, that (i) samples irradiated during plastic flow display a stimulated growth of F-centres, which is largely in excess (for equal dose increments) of that obtained in underformed crystals, and (ii) there is a direct dependence of this growth on deformation rates. Each curve shows a short induction period at the outset during which probably deformation is less effective in producing excess vacancies - followed by a smooth uniform growth in the rest of the history. The uniform stage extends over a substantial interval of strain and seems representative of steady-state conditions. The phenomena were essentially similar in NaCl, KBr and LiF, not shown here. The difference between various

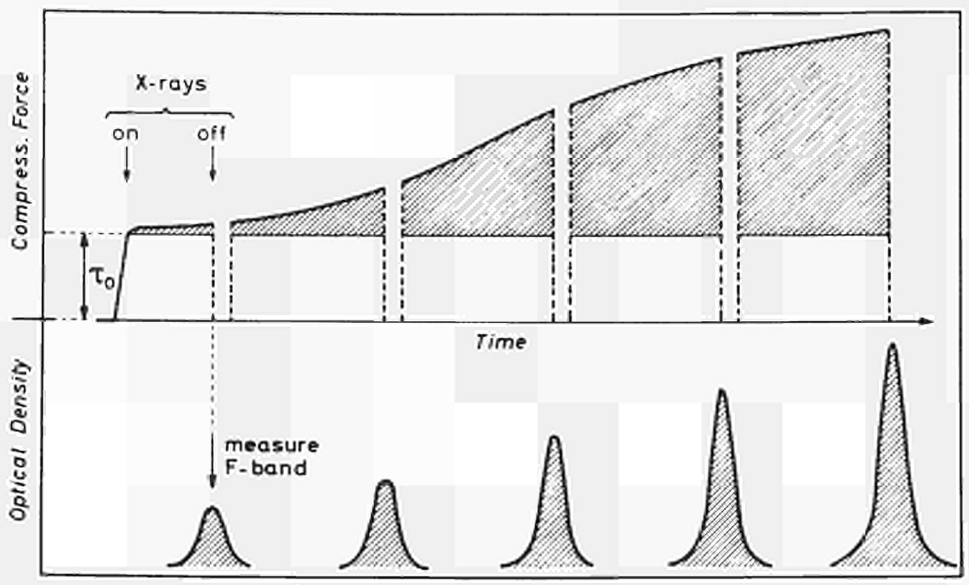

Fig. 1) : Scheme of the experiments on deformation-enhanced colouration. The partial sum of the shaded areas under the stress curve is the quantity X(t) defined in the text (eq. 1).

salts concerned the extent of the region over which the growth curves can be considered linear: for KCl this is about 7-8%, and in these limits one can approximately define a constant colouration rate (the slope of the curves) hence an average *excess colourability*. The dependence of this colourability on deformation parameters was first investigated by comparing the increments of slope (relative to the undeformed case, dotted line), with the corresponding strain-rates. The latter were by definition in the fixed ratio 1:2.5:5; it can be checked from the figure that the increments of colouration rates were instead as 1:1.6:2.4, i.e., something very near to the ratio of the square roots of the relative strain rates. This specific dependence on deformation speed was seen to hold generally in all the experiments performed on KCl, NaCl and LiF. The result seems rather important, in that it strengthens the idea of a quasi-stationary kinetics: in other words, it suggests that the accumulation of free excess vacancies is somehow rate-limited by the competition between primary production and annealing processes. However, the conclusions at this stage remained qualitative, owing to the approximate character of the above observations. In view of this, a systematic effort was made to analyse the phenomena in greater detail, so as to check whether a square-root relationship is intrinsic to the kinetics of growth.

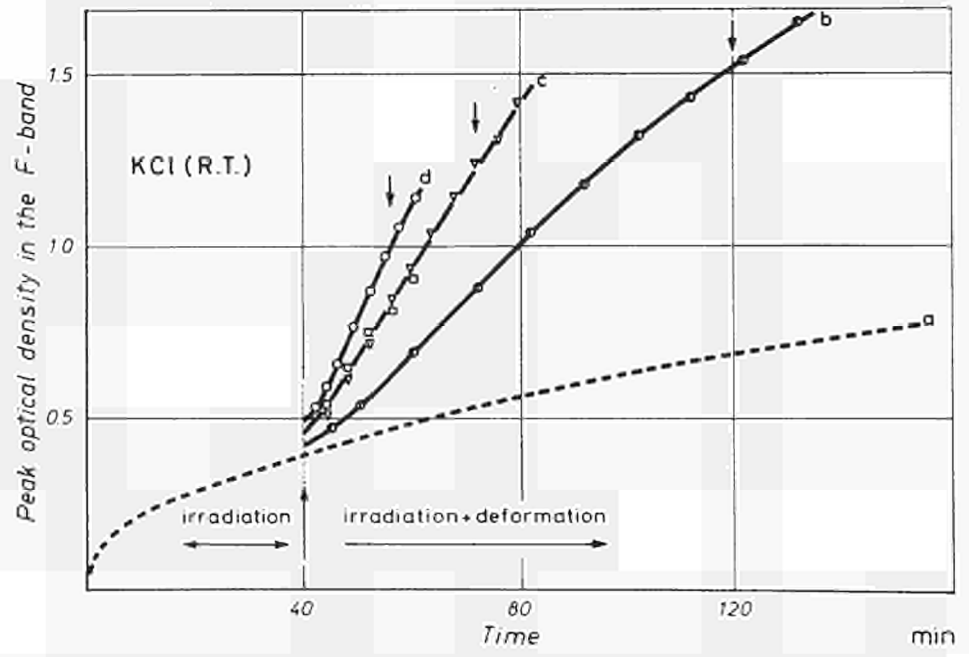

Fig. 2) : Time-growth of F-centres during deformation assisted irradiations. Same X-ray intensities, different conditions of plastic flow as follows:
a) no deformation
b) strain rate $2x10^{-5}$ /sec
c) strain rate $5x10^{-5}$/sec
d) strain rate $1x10^{-4}$/sec

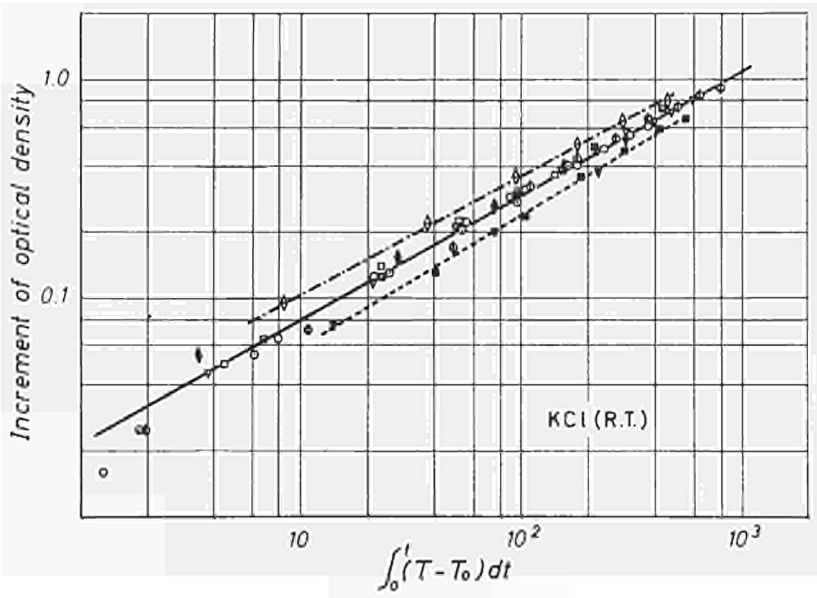

Fig. 3: Double-log plot of the increments of optical density in the F-band vs. the time integral of the flow stress. R.T. experiments. Different symbols for different specimens; deformation conditions as follows:

◇◆ϕ : strain rate 2×10^{-5}/sec
▽▼□■□ : strain rate 5×10^{-5}/sec
○○ : strain rate 1×10^{-4}/sec

Excess colouration vs. flow-stress

For the purpose of achieving a consistent analysis, the use of a time scale and the reference to nominal strain rates are unsatisfactory: in fact, the existence of bending in the curves of Fig. 2 is in itself a proof that te concept of an *average* colouration rate is only approximate. As an alternative, stimulated growth was studied in terms of the stress data, which were available from the records taken during each deformation run. The procedure was to work out possible correlations between the stress function and the corresponding increments of colouration. Fig. 3 summarizes the results of a number of independent measurements on KCl at RT, obtained by plotting D(t) (the net increase of optical density relative to the undeformed material) against a quantity which is defined as

$$X(t) \equiv \int_0^t (\tau - \tau_0)\,dt$$

where $\tau(t)$ is the instantaneous stress on the flowing sample, τ_0 is the initial yield stress. An easy and accurate evaluation of the quantity (1) is obtained graphically as shown in Fig. 1.

Fig. 3 shows the relationship between D(t) and X(t) in a double-log plot, for a number of measurements in various conditions. The results clearly indicate that $D(t) \propto X(t)^m$. The remarkable feature of this plot is that all data on stimulated growth now fit the same function, with a unique value of the exponent m, irrespective of the different deformation rates. This is all the more remarkable if one remembers the different slopes and the bending of the growth curves, when they were plotted against a time basis as in Fig. 2. It must be concluded that the choice of the parameter X(t) introduces the appropriate transformation, giving a unified form to the kinetics of excess colouration. From the slope of Fig. 3 one obtains $m = 0.53 \pm 5\%$. It is legitimate to interpret this as a proof of a simple square-root relationship, which we write explicitly:

$$D(t) = C\,[\int_0^t (\tau - \tau_0)\,dt]^{1/2}$$

Temperature dependence

The experiments on excess colouration were extended with similar criteria to a number of temperatures in the range from 25°C, to 110°C and the new data were subjected to the same type of analysis. Fig. 4 summarizes the results, showing that the correlation expressed in eq. (2) has a general validity even above RT. At the same time it is evident that the amount of excess colouration, for a fixed value of the abscissa X(t), is a decreasing function of temperature. Since the correlation is obtained in each case considering the actual values of $\tau(t)$, such a decrease cannot be due to the temperature dependence of the flow stress, and must be intrinsic to excess colouration. On this basis one assumes that the values of D(t) (at fixed X(t)) are a relative measure of the constant C appearing in eq. (2), and by plotting them against reciprocal temperature one can see whether the yield of the process is thermally activated. This was done with the results of our experiments (including those of Fig. 4) and it was concluded that C(t) is of the form exp(Q/kT), with $Q \cong 0.25$ eV.

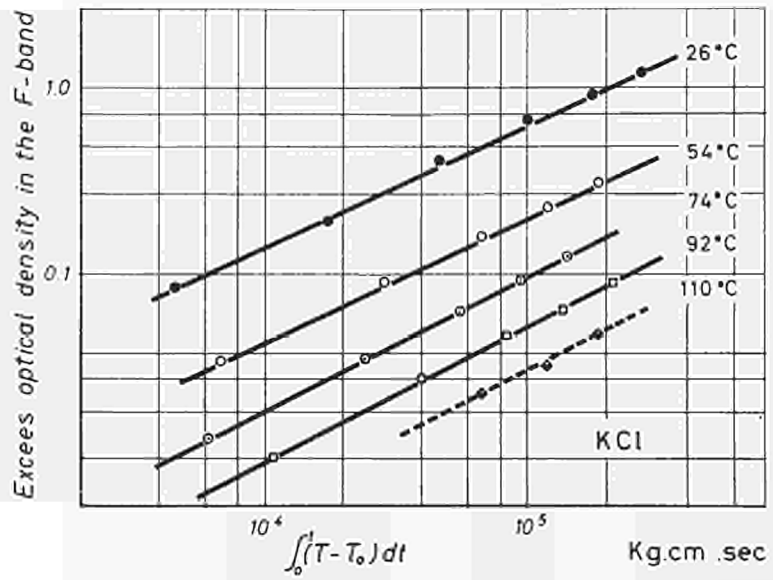

Fig. 4: Same as fig. 3, for a set of experiments at fixed strain rate 2 x 10^{-5}/sec and different temperatures.

Discussion

The most significant results obtained in the present work are:

1) the square-root correlation between the growth of excess F-centres and the time integral of flow-stress,
2) the negative effect of temperature on the yield of these centres. It is evident that such phenomena cannot be accidental, and must be considered systematic features of the production kinetics in the crystals as flowing.

In particular, point 1) suggests very strongly that the output of centres is the result of a dynamical equilibrium between production and annealing processes of bimolecular type, whereas point 2) hints that annealing must be involved with vacancy reactions. A simple interpretation, taking account of these observations, can be developed as follows.

Let us suppose that plastic deformation supplies vacancy sources of some kind, from which individual defects are immediately released under the action of X-rays, and made available for conversion into F-centres. We identify these sources with dislocation debris, without for the moment enquiring whether they are definite clusters, or other configurations. One then describes the stimulated growth of centres as a two-step process. The first step is the accumulation of the sources, controlled by the balance between the supply of debris (due to deformation) and the release of free vacancies (due to irradiation). The simplest way to analyse the phenomena is by an equation of the type

$$\frac{dN}{dt} = \gamma P(t) - \alpha N(t) \tag{3}$$

where P(t) is the total production rate of debris (which is time-dependent during plastic flow); γ is the fraction of debris able to act as vacancy sources, N(t) their actual population. The recovery term $\propto N(t)$ expresses the fact that the incipient vacancies are radiolyzed by X-rays at a rate which is proportional to concentration.

The second part of the process is the appearance of free vacancies, limited by pairing between opposite defects. This can be tentatively described by:

$$\left.\begin{matrix}\frac{dn}{dt} \\ \\ \frac{dp}{dt}\end{matrix}\right\} = \alpha N(t) - \beta n \cdot p \tag{4}$$

Here n(t) and p(t) are the concentrations of isolated vacancies of the negative and positive ions, respectively. The two species are assumed to be removed by combining into stabile pairs at a specific rate β.

The recovery terms of eqs. (3) and (4) cannot be specified a priori. However, it is reasonable to investigate the limiting cases in which only one of the equations is the controlling step. Of a particular interest is the case in which $\alpha N(t) \ll P(t)$, i.e., when the rate of radiolysis of the sources is negligible with respect to the primary production. Then eq. (3) gives simply $N(t) = \gamma \int P(t)dt$; substituting into eq. (4) one obtains the quasi-steady-state solution for negative-ion vacancies, hence for the final F-centres, in the form

$$n_s(t) \cong \left[\frac{\alpha\gamma}{\beta} \int_0^t P(t)\,dt\right]^{1/2} \tag{5}$$

This obviously holds when the bimolecular reaction of eq. (4) is sufficiently fast (i.e., temperature sufficiently high) to compensate for the slow time evolution of N(t). We suppose this to be true at RT and above.

It is soon appreciated that the above result has a striking similarity to the experimental relationship, eq. (2) linking the growth of the excess F-centres to the time integral of the stress function. The similarity is complete if P(t) is made proportional to the quantity $[\tau(t) - \tau_0]$. This allows specific conclusions, which are not entirely trivial. In the first place it confirms that a model based on a bimolecular reaction among vacancies is fully adequate to describe the kinetic of extra colouration; secondly it shows that the production rate P(t) of vacancy sources is directly proportional to the instantaneous stress.

Since the stress is a measure of the resistance to dislocation motion, the necessary deduction is that vacancy precursors are a systematic by-product of those events, which specifically determine such resistance. It has been proved [8] that plastic flow in alkali halides is accompanied by the appearance of a large number of dipoles of dominant edge character, coming from the intersection of orthogonal systems of screw dislocations. Recently, unified theories of work hardening were sucessfully built on this basis [9]. It is natural to think that the source of F-centre vacancies in deformed crystals must reside in this particular type of dipoles. Incidentally the argument excludes other mechanisms of vacancy generation, such as for instance the non-conservative motion of jogs, for which a one-to-one correspondence with hardening is difficult to realize.

A second test of the model discussed here comes from its coherence with the effects of temperature. As was seen, the experiments have shown that the empirical relationship (2) continues to hold even above RT and the yield of colouration decreases in this range with a heat of activation which is approximately Q = 0.25 eV. According to eq. (5) this can be explained by observing that the parameter β contains the mobility of the defects, which is thermally activated. It follows that the migration energy must be twice the value of Q, i.e. $\sim$ 0.5. This will be in any case a lower limit, owing to the fact that the parameters α and γ cannot be decreasing functions of the temperature. The quoted value is therefore of the correct magnitude to strengthen the role of vacancy reactions, as opposed to vacancy-interstitial recombination.

Conclusions

It was shown that the general features of vacancy growth during deformation-assisted irradiation are well consistent with a picture based on the presence of vacancy precursors, which are identified as dislocation dipoles. Deformation produces an increasing reservoir of these entities, acting as a source of defects in the subsequent irradiation; the kinetics and specific yield of extra colouration are controlled by the balance between radiolysis of these sources and the combination of free vacancies into stable pairs, which do not contribute to F-centres. The model automatically implies a negligible role of secondary reactions (interstitial trapping, impurity effects) on the deformation enhancement. At the same time it contains all the elements to account for the localized origin of the extra vacancies, as well as for the intrinsic stability of the sources in the absence of irradiation, in agreement with the observations of various authors [3] [8].

References

1) F. Seitz, Rev. Mod. Phys. 26, 7 (1954)
2) R. Chang, Phys. Rev. 138, A-839 (1965)
3) W.A. Sibley, J.R. Russell, Phys. Rev. 154, 831 (1967)
4) F. Fröhlich, P. Grau, phys. stat. sol. 8, 917 (1965)
5) J. Serughetti, H. Saucier, phys. stat. sol. 37, 381 (1970).
6) R.W. Davidge, P.L. Pratt, phys. stat. sol. 3, 665 (1963).
7) B.S.H. Royce, R. Smoluchowski, Discuss. Faraday Soc. 38, 218 (1964).
8) R.W. Davidge, P.L. Pratt, phys. stat. sol. 6, 759 (1964).
9) W. Frank, Material Science and Engineering 6, pp. 121 and 132 (1970).

COMPUTERIZED SYSTEM FOR THE APPLICATION OF FISSION NEUTRON CORRELATION TECHNIQUES IN NUCLEAR SAFEGUARDS

G. Birkhoff, L. Bondár

Introduction

Time correlation analysis among the neutron detection pulses is frequently applied in passive and active neutron assays of fissile materials, for distinguishing fission neutrons from others. For example for Pu-240 spontaneous fission neutron measurements in presence of (α, n) neutrons or discrimination of source neutrons by coincidence techniques. The application of this method is quite simple if restricted to small samples. The extension to larger samples becomes, very complex, however, owing to neutron multiplication. In the latter case it is rather difficult to elaborate a measuring routine for field applications which assures that measurements taken during an inspection will be useful and of optimum accuracy. For this purpose we set up a computerized system. It is based on an inspection concept as out-lined below.

a. *Planning of an inspection* (Chief Inspector)

- Find the optimum response of the detection system to be employed to a defined sample to be measured.
- Do calibration measurements and calculations with a standard having isotopic and geometrical data similar to those of the sample.
- Evaluate corrections of calibration factor to be applied to measurements with the actual sample.
- Set up measurement strategy (number of samples to be measured, time per measurement, etc.)

b. *Execution of inspection* (Inspector)

- Repeat measurements on the spot with standard sample.
- Take measurements with a sample.
- Compare results with planning data,
  if good agreement : go on measuring
  if significant discrepancy : call Chief Inspector.

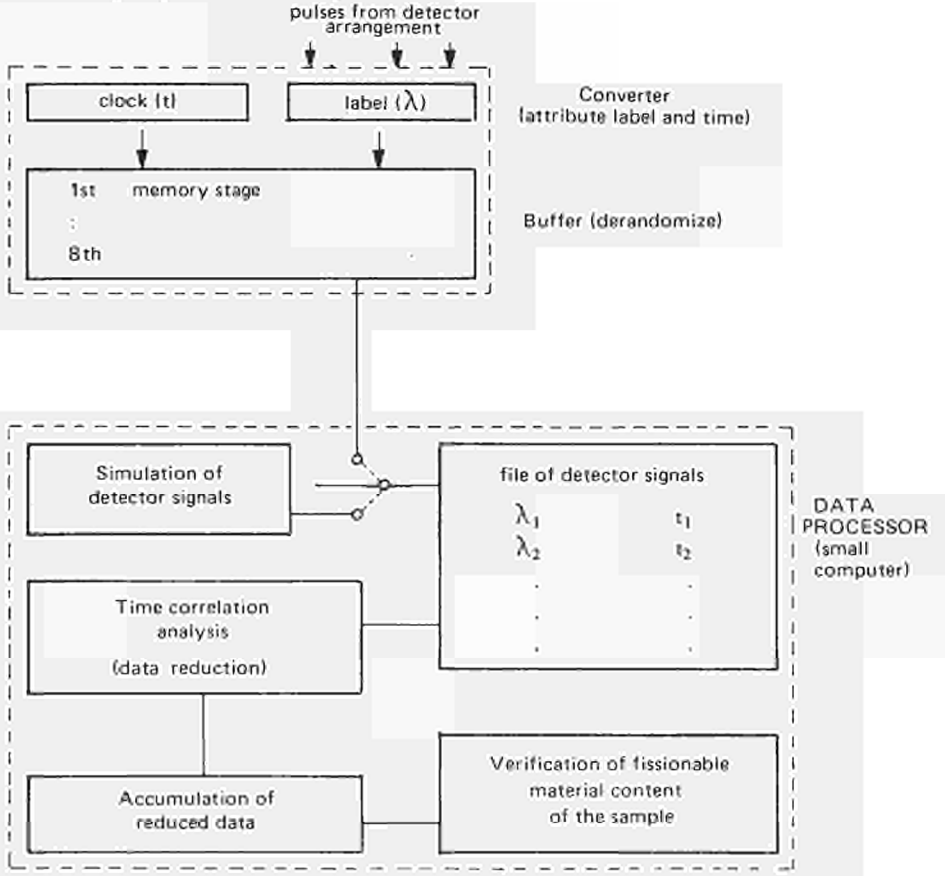

Fig. 1: Computerized system for time correlation analysis of neutron detection pulses (schematic).

General Description of the System

The operation principle of the computerized systems is explained in the schematic diagram Fig. 1. Detector pulses are produced physically or simulated by a computer program. In the computer a signal is formed by a data pair: a label (λ) corresponding to a specific detector (or detector group) and the real time (t) at which the signal appears in the detection system. After collecting nearly a thousand signals, time correlation analysis, that is, data reduction will be accomplished. In order to get sufficiently high statistics this procedure must be repeated periodically and the reduced data accumulated. These reduced data, as a response of the detection system to the sample, serve for the verification of the fissionable material content of the sample.

Detector Pulses from Counter Arrangement

In case of measurements a label (λ) and time (t) (as defined above) are to be attributed to each detector pulse and these data must be fed into the computer. An explanation of this procedure is given in the paper by M. Bernede, L. Stanchi: "Fast acquisition of neutron coincidences into a small computer", presented at the "International Meeting on Non-destructive Measurement and Identification Techniques in Nuclear Safeguards", Ispra, Sept. 20-22, 1971 (to be published)

Simulated Detector Signals

Simulation of detector pulses by computer program (Fig. 2) requires the preparation of some parameters and distribution functions. Spontaneous events follow Poisson distribution. n (number of fissions per second), ν (average number of neutrons per fission) and P (distribution function of fission neutrons) being pure isotopic properties can be found in any nuclear data book. The other parameters ϵ (detection probability), k (probability of provoking a fission) and l (mean lifetime) depend on the geometry and nuclear properties of the sample and detector assembly. Such parameters require complex calculations checked and adjusted by specific measurements. For calculation we use the Monte Carlo transport code TIMOC [1], which is capable of resolving the neutron transport problem in a complicated geometry such as that of fuel samples embedded in a detector arrangement. Numerous techniques are known for measuring ϵ, k and l. All these parameters are to be tabulated for typical sample geometries and isotopic compositions covering the range of most commonly used fissile materials. Intermediate sample parameters are obtained by interpolation.

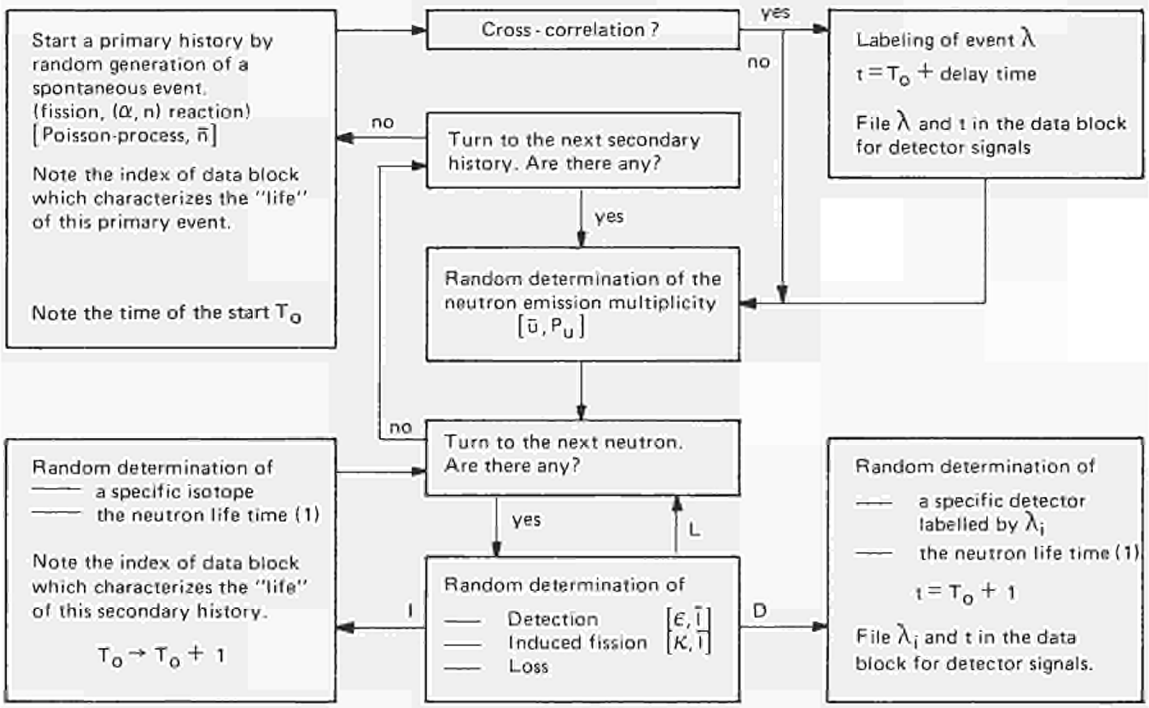

Fig. 2: Schematic flow diagram for the Monte-Carlo simulation of neutron history in a detector arrangement.

Time Correlation Analysis

There are different well-known methods for separating correlated signals from Poisson background. Usually special electronic instrumentation is employed for this purpose. If a small computer is available, it is more convenient to realize such electronics by software. Indeed, we programmed several coincidence circuits based on autocorrelation methods.

Verification

Verification of the fissionable materials is obtained through the interpretation of the results from correlation analysis in terms of emission rates and multiplicities of fission neutrons, confronting measured and nominal data (declaration of properties). The sensitivity of these signatures has been investigated from samples containing Pu^{240} and Cf^{252} with different background of (α,n) neutrons. The results are satisfactory.

Reference

1) Kschwendt, H. and Rief, H.: "TIMOC - A general purpose Monte Carlo code for stationary and time-dependent Neutron transport" EUR 4519.e (1970).

A HIGH RESOLUTION TIME FOCUSING SPECTROMETER FOR QUASI-ELASTIC NEUTRON SCATTERING

H. Meister, B. Weckermann

Introduction

The rotating crystal spectrometer has become a standard instrument in neutron time-of-flight spectrometry since it was first proposed by Brockhouse in 1958 [1]. Its lay-out principles and performance have been described in several articles [2] [3] [4]. Up till now it has always been recognized that the intensity and resolution of this device – at least for moderate neutron energies – are affected by the angular velocity of the spinning crystal due to Doppler effect. This causes the neutron velocity and the reflection time to become space-dependent over the crystal volume, which in practice improves the intensity as extinction is reduced, but at the cost of the resolution.

The basic idea of time-focusing slow neutrons by means of the Doppler effect in neutron reflection from moving crystals was introduced by Maier-Leibnitz in 1966 [5]. He demonstrated that if certain focusing conditions are observed, all neutrons reflected from a vibrating monochromator crystal during a period of constant acceleratiion meet at the sample and form a narrow and intense neutron pulse. This method seems particularly suitable for energy gain experiments in which the resolution is determined mainly by the pulse duration, while the velocity spread of neutrons before scattering is of limited importance.

From an analysis of the Doppler effect in the reflection of neutrons by fast-spinning crystals we deduced that the possibility of time-focusing is also inherent in these systems [6]. In the focal plane the influence on the burst width resulting from Doppler broadening of neutron velocity and reflection time merely cancel out those of the crystal dimensions. Apart from the above mentioned application, we proposed focusing onto the detectors [7] with the sample somewhere close to rotating crystal. This would permit high resolution work in the quasi-elastic range. Neutrons scattered elastically in the sample fall within the narrow line in the time-of-flight spectrum given by focusing, whereas neutrons undergoing a small energy change in the process of scattering will arrive at the detectors at different times. This method can also be adapted to phonon work [8], the resolution peaking around the discrete value of energy transfer for which the focusing arrangement is set.

In mid-1969 we started construction of such a time-focusing spectrometer, which is now installed and operating at the Ispra-I reactor. The underlying principles, some lay-out and design features of the instrument, and the results of performance tests will be described in the following sections.

Time Focusing of Neutrons Based on the Doppler Effect in Neutron Reflection by Rotating Crystals

Reflection Time and Neutron Velocity

Normally, a rotating crystal system consists of a collimator in the primary beam, a crystal with at least one set of crystallographic planes parallel to its axis of rotation, and a second collimator which is set at double the Bragg-angle Θ with respect to the primary beam. Neutron reflection along a certain section of the crystal is not influenced by its angular speed $2\pi\nu$. This section, which from now on will be called the "reference plane", contains the axis of rotation and is normal in crystallographic planes in the stationary reflection position as determined by the two collimators. In comparison with the reference plane, neutron reflection at any other point in the crystal occurs at a different time $t + \Delta t$ and yields neutrons of different velocity $v + \Delta v$. These differences depend linearly on a coordinate y which is normal to the reference plane [6]. With the coordinate system as indicated in Fig. 1, we obtain

$$\Delta t = (-1)^i \, y \cos\Theta / v$$

and

$$\Delta v = (-1)^i \, y \, 2\pi\nu \sin\Theta$$

where i = 1 stands for anticlockwise, and
i = 2 for clockwise rotation.

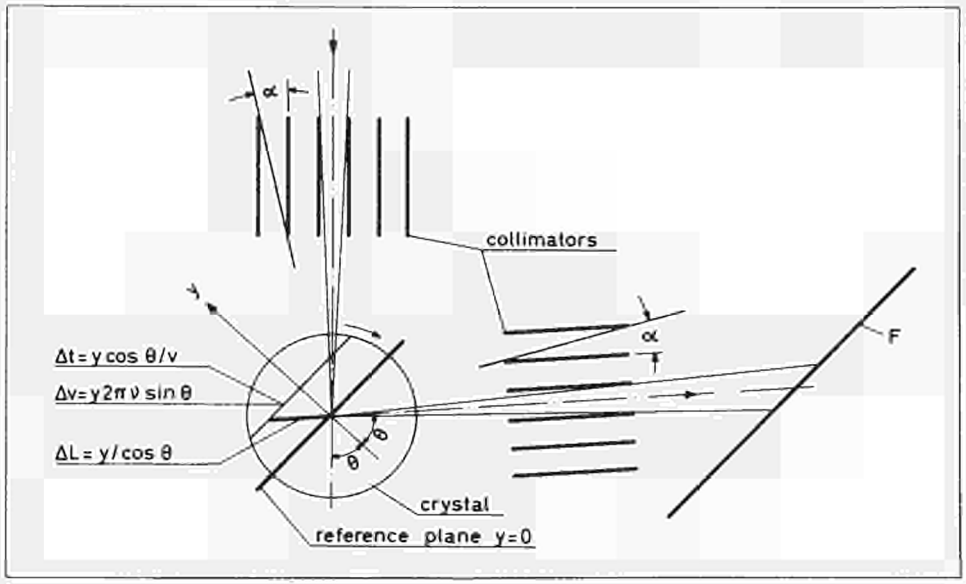

Fig. 1: Schematic sketch of the rotating crystal system. The plane which contains the axis of rotation and the bisector of the angle between the two collimator axes is called the reference plane since neutron reflection along this plane is not affected by the angular velocity of the crystal.

Time Focusing

Let us imagine a plane parallel to the reference plane at a distance L measured along the reflected beam and call it F. The difference in flight path with respect to F for neutrons reflected along the reference palne of the crystal and along other sections y = const is again proportional to y due to the second collimator:

$$\Delta L = y/\cos\Theta \tag{3}$$

With clockwise rotation of the crystal (i = 2), we can arrange things so that Δt and ΔL on one side and Δv on the other side will compensate each other as regards the arrival time of neutrons at the plane F, which then turns out to be the focal plane:

$$\Delta t + \Delta L/v = L.\Delta v/v^2 \tag{4}$$

With Eqs. (1), (2) and (3) we get the focusing condition

$$y\cos\Theta/v + y/v\cos\Theta = y.L.2\pi\nu\sin\Theta/v^2 \quad \text{or} \quad L = (1+\cos^2\Theta)\,v/2\pi\nu\cos\Theta\sin\Theta \tag{5}$$

which is valid for the whole crystal volume as the y-dependence of the individual terms cancels out.

Focusing can also be achieved for neutrons which, after the second collimator, are scattered in a sample with discrete energy transfer, provided that the flight path length from all points on the reference plane of the crystal via the sample t the new focus is equal. For elastic scattering this length is simply given by Eq. (5).

Although we shall not deal in the following paragraphs with the inelastic case, te respective focusing condition should be mentioned for the sake of completeness:

$$L_{inel} = (1+\cos^2\Theta)\,vV^3/2\pi\nu\cos\Theta\sin\Theta[(1-\rho)V^3 + \rho v^3]$$

ρ indicates the location of the sample in the sense that ρx L is the distance between sample and focus. The energy transfer to which focusing refers does not appear explicitly in Eq. (6) but is included in V. It gives the velocity after scattering for a neutron which previously had a velocity v.

For certain experimental applications one should note that there is also a focal plane in the primary beam. The focal planes in primary and reflected beams are symmetric with respect to the reference plane of the crystal. This is due to the fact that neutrons which appear after reflection with a velocity $v + \Delta v$ had a velocity $v - \Delta v$ previously. Applications for which the focus of the primary beam could be of interest are the use of a chopper for background reduction and for suppression of higher order reflections, successive neutron reflection by two fast spinning crystals or Doppler focusing in connection with a pulsed neutron source.

Burst Width at Focus

The half-width in time of the neutron burst as observed at the focal plane of the reflected beam is determined by the mosaic spread η of the crystal and by the finite collimation of primary and reflected beam. With the assumption that the angular divergencies of primary and reflected beam are equal to α and that the sweep of the reflected beam can be ignored, we obtain the following independent contributions to the burst width Γ (from now on "burst width" will always mean "full width at half maximum"):

– From the time interval of reflection at y = const.:

$$\Delta T_1 = \alpha\,(0.5^2 + m^2)^{1/2}/2\pi\nu \tag{7}$$

where $m = \eta/\alpha$

– From the stationary spread of neutron velocity for a distinct direction within the collimation of the reflected beam:

$$\Delta T_2 = \alpha\,.\,L\,\mathrm{ctg}\,\Theta/2v \tag{8}$$

– From the angular dependence of flight path length and of stationary neutron velocity within the collimation of the reflected beam:

$$\Delta T_3 = \alpha\,L\,\mathrm{tg}\,\Theta/v + \alpha\,L\,\mathrm{ctg}\,\Theta/2v \tag{9}$$

Since these contributions are not inter-correlated, we can sum them up quadratically to find the burst width:

$$\Gamma = \{(\alpha/2\pi\nu)^2(0.5^2 + m^2) + (\alpha L\,\mathrm{ctg}\,\Theta/2v)^2 + (\mathrm{tg}\Theta + \mathrm{ctg}\Theta/2)^2(\alpha L/v)^2\}^{1/2} \tag{10}$$

and with Eq. (5)

$$\Gamma = \alpha/\pi\nu\{(0.5^2 + m^2) + [(1 + \cos^2\Theta)/2\sin^2\Theta]^2 + [(1 + \cos^2\Theta)/\cos^2\Theta + (1 + \cos^2\Theta)/2\sin^2\Theta]^2\}^{1/2} \tag{11}$$

Γ can be measured directly by means of a very thin neutron detector such as a fission monitor with only one plane layer of fissile material. If larger detectors are used, the local distribution of neutron detection has of course to be taken into account separately.

The burst width Γ^{SC} at the focus of neutrons scattered elastically in the sample cannot be dealt with by means of a closed formula. It will depend very much on the specific geometry of the scattering experiment. In most cases Γ^{SC} will be smaller than Γ owing to the fact that the angular dependence of flight path length and of constant neutron velocity in the reflected beam are correlated only up to the sample.

Fig. 2 illustrates three of many possible scattering arrangements. Fig. 2a gives an example of how a number of detectors can be placed at different scattering angles Φaround the sample which covers a large portion of the reflected beam cross section. Sample and detectors are parallel to the reference plane. The use of collimators in front of the detectors is necessary at least for those which face the sample surface at angles which differ considerably from 90°. In this situation the first three contributions to Γ^{SC} are similar to Eq. (7), (8) and 9(0, with the only difference that L is replaced by $(1 - \rho)$ L. (For the definition of ρ see above).

Concerning the scattered neutrons we must take the full stationary velocity spread into account with $\alpha\rho$ L ctg$\Theta/\sqrt{2}$ v and the spread of the sample to detector flight-path with $\Delta(\rho L)/v$.

In the following paragraphs we formally include in $\Delta(\rho L)$ all flight path uncertainties caused by the geometrical extension of the sample. Consequently $\Delta(\rho L)$ in itself consists of three uncorrelated parts originating in the collimation of scattered neutrons and from sample and detector thicknesses, where at least the first two depend on Φ. Without splitting up $\Delta(\rho L)$ into its components, we obtain for configuration 2a.

$$\Gamma_a^{SC} = \Big\{(\alpha/2\pi\nu)^2(0.5^2 + m^2) + [(\mathrm{ctg}\Theta/2)^2 + (\mathrm{tg}\Theta + \mathrm{ctg}\Theta/2)^2]\,(\alpha L/v)^2(1-\rho)^2 + (\alpha\rho L\,\mathrm{ctg}\Theta/\sqrt{2}v)^2 + [\Delta(\rho L)/v]^2\Big\}^{1/2} \tag{12}$$

Fig. 2b shows an arrangement in which the sample is turned anticlock-wise from the position parallel to the reference plane by $\Theta + \beta$. The angles at which the two detectors are facing the sample are tuned to the value of β in such a way as to ensure that the flight-path length from the reference plane via sample to the detectors is equal to L. Additional collimators are not necessary since the detector surfaces are perpendicular to the direction of neutron incidence.

Special attention is paid to the reduction of burst width by the term which is analogous to Eq. (9) for the path between crystal and sample. With the geometry of Fig. 2b the correlated effects of flight path and stationary velocity spread compensate each other to a certain extent. With the definition of Δ (pL) as mentioned above we obtain:

$$\Gamma_b^{sc} = \{(\alpha/2\pi\nu)^2(0.5^2 + m^2) + [(\mathrm{ctg}\Theta/2)^2 + (\mathrm{ctg}\Theta/2 - \mathrm{tg}\beta)^2](\alpha L/v)^2(1-\rho)^2 + \\ + (\alpha\rho L\ \mathrm{ctg}\Theta/\sqrt{2}v)^2 + [\Delta(\rho L)/v]^2\}^{1/2} \quad (13)$$

Fig. 2c represents schematically a scattering experiment with a cylindrical sample surrounded by many detector tubes in a circle of radius ρL. The diameter of the detector tubes is about as small as that of the sample. Small, in the sense that it is used here, means that the burst width at the detectors should not be primarily determined by Δ (ρL) which includes the effects of both sample and detector size. Larger counting units can be assembled by a number of single detector tubes. This does not affect the burst width, which in this case is given by:

$$\Gamma_c^{sc} = \{(\alpha/2\pi\nu)^2(0.5^2 + m^2) + [(1-\rho)^2 + \rho^2](\alpha L\ \mathrm{ctg}\Theta/\sqrt{2}v)^2 + [\Delta(\rho L)/v]^2\}^{1/2} \quad (14)$$

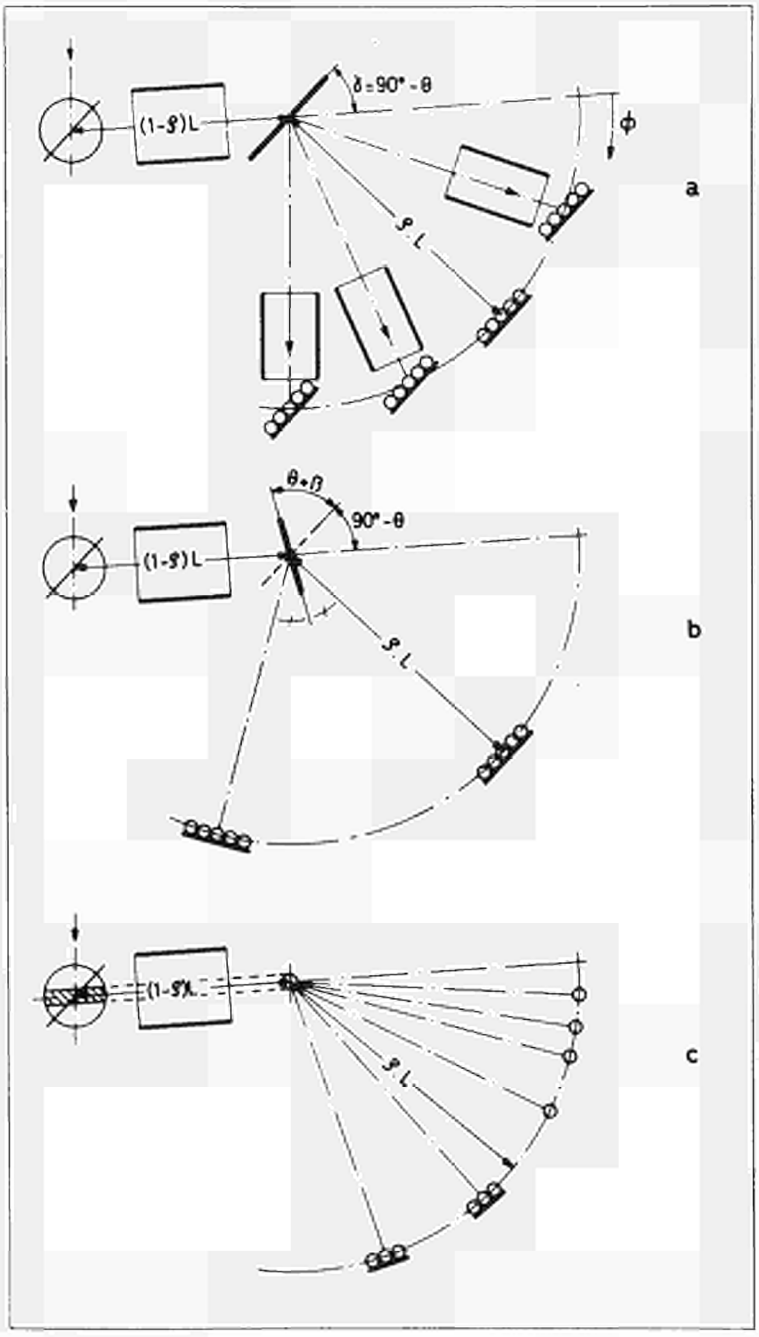

Fig. 2: Schematic sketch of three different neutron scattering arrangements with time focusing onto the detectors.

Quasi-Elastic Energy Resolution

The burst widths Γ^{SC} at the detectors, as calculated above for elastic scattering, are directly related to the energy resolution which can be obtained in a quasi-elastic neutron scattering experiment. If energy is exchanged during the scattering process between sample and neutron this causes the neutron to arrive at the detector at a different time than if it were scattered elastically. A discrete energy transfer corresponds to a discrete shift in arrival time for all neutrons within the Doppler-broadened velocity band. This is, of course, a simplification, but in most practical cases the errors remain small compared to Γ^{SC} if the energy transfer does not exceed a value of about ten times the resolution of the instrument. With the definition that an energy transfer ΔE can be resolved if it leads to a shift in arrival time at the detector equal to Γ^{SC} we obtain:

where E is the neutron energy corresponding to the mean velocity v of neutrons impinging upon the sample.

For experiments where discrete energy transfers or the fine structure of a quasi-elastic line have to be investigated, Eq. (15) certainly gives a good standard of what can be established. On the other hand, if one knows already from the beginning that the quasi-elastic broadening is described by a single Lorentzian, one should be able to analyse it even if its half-width is smaller than the value given by Eq. (15), which in its turn is equivalent to an effective line broadening of 40%.

Resolution of Momentum Transfer

As far as energy resolution is concerned, the time-focusing method offers a means to get rid of the influence of Doppler broadening on reflection time and neutron velocity, and of the influence of the geometrical extension of the rotating crystal. These influences are usually considered to be great obstacles in high-precision work with conventional rotating crystal spectrometers. However, the situation is different for the resolution of momentum transfer $\vec{\kappa}$. Unlike a conventional time-of-flight experiment, the neutrons used in a time-focusing experiment fill a velocity band Δv which is much wider than the one corresponding to energy resolution. The uncertainty $\Delta\vec{\kappa}$ of the observed momentum transfer as caused by Δv is parallel to $\vec{\kappa}$. It is given by:

$$(\Delta\kappa_{\parallel})_{1/2}/\kappa = (\Delta v)_{1/2}/v \tag{16}$$

The subscript 1/2, indicating that we are dealing with half widths of κ and v distribution, implies that $(\Delta v)_{1/2}$ is evaluated from $\Delta v(y)$ by weighting it with the differential crystal volume $\Delta V(y)$ which in effect contributes to the neutron intensity at the sample. With a cylindrical crystal of radius R the result is

$$(\Delta v)_{1/2} = \sqrt{3}\, R\, 2\pi\nu \sin\Theta \tag{17}$$

for a sample extended over the full cross-section of the reflected beam, and

$$(\Delta v)_{1/2} = R.4\pi\nu \sin\Theta\cos\Theta \tag{18}$$

for a sample width much smaller than R.

$\Delta\kappa_{\parallel}$ can be varied with the dimension of the rotating crystal in the direction of the reflected beam. It is therefore directly linked to intensity.

Intensity

From the many possible ways of calculating intensity we have chosen the one which explicitly contains the factor $(\Delta v)_{1/2}$ in order to demonstrate the inter-connection between intensity and momentum transfer resolution:

$$N_S = \Phi(v)\,(\Delta v)_{1/2}\,(\Omega/4\pi)\,A\,F_S\,r\,n\,\alpha\,(0.5^2 + m^2)^{1/2}/2\pi \tag{19}$$

with N_S = neutron current at sample,

$\Phi(V)$ = flux density distribution at neutron source,

Ω = solid angle of primary beam,

A = attenuation factor including collimator transmission and losses by air scattering, filters and windows,

F_S = area of crystal in reflection position as seen by the sample (through the second collimator),

r = crystal reflectivity

n = number of reflections per crystal revolution.

When estimating a value for r, it is reasonable to take the reflectivity of a crystal slab in transmission with mosaic spread $m\alpha$ and thickness $\alpha v \, ctg\Theta/2\pi\nu \sin\Theta$. This thickness corresponds to a step Δy for which the Doppler shift of neutron velocity proceeds by the value of the stationary velocity spread.

The intensity gain which can be achieved with the time-focusing method, as compared to that of the conventional time-of-flight technique, is expressed in Eq. (18) by $(\Delta v)_{1/2}$. If small samples are being used, this expression also includes the effect of the compression of a large primary beam cross-section into the smaller one of the reflected beam. The ratio of Doppler-broadened to stationary velocity spread, which gives the gain factor, usually lies around 10, depending upon the kind (absorption) and size of the crystal used.

In summarizing one can say that the time-focusing method offers advantages for the study of problems which need good energy resolution but can at the same time tolerate a more relaxed momentum resolution.

Lay-out of the Spectrometer

We plan to use the time-focusing spectrometer for investigation of quasi-elastic scattering in the cold and thermal neutron energy region. For the first version, presented here, its characteristic lay-out data are summarized in Table I.

With respect to the focal length L which defines the overall dimensions of the installation, we are restricted L = 250 cm by the free space available in the reactor hall. In view of the fact that time-focusing yields best resolution for Bragg angles around 45°, this results in a rather high crystal speed. For the nominal speed of 10,600 rpm, the diameter of the lead single-crystal cannot be larger than 5 cm without running the risk of it being destroyed.

Table 1 – Characteristic Lay-Out Data

Primary Beam

Radial beam tube of reactor Ispra-1 ($\Phi_{th} = 2.10^{13}$ n cm^{-2} sec^{-1})
Cross-section at position of rotating crystal 10 x 10 cm^2
Horizontal angular divergence α = 10 min of arc
Vertical angular divergence 1.5°

Rotating Crystal

Pb-single crystal, 5 cm dia x 11 cm
Cylinder axis vertical, parallel to the (110) crystallographic axis
Reflection by (111)-planes
Mosaic spread η = 30 min of arc (m = 3; the optimum with respect to resolution would be around m = 1.5)
Angular velocity $2\pi\nu$ = 1110 sec^{-1} (corresponds to 10,600 rpm)

Reflected Beam

Beam axis at 2Θ = 94.6° with respect to primary beam
Cross-section of beam channel 10 x 10 cm^2
Horizontal angular divergency α = 10 min of arc
Beam filtered by polycrystalline Be
Distance between crystal axis and focus L = 250 cm
Distance between crystal axis and sample $(1 - \rho)$ L = 80 cm
Mean neutron velocity v = 940 m sec^{-1}
Mean neutron wave length λ = 4.21 Å
Mean neutron energy E = 4.4 meV
Velocity spread $(\Delta v)_{1/2} = 3.8.10^{-2}$. v $\simeq$ 36 m sec^{-1}
Burst width at focal plane $\Gamma = 14.7.10^{-6}$ sec

Detectors

^{3}He-detectors, active volume 0.6 cm dia x 25 cm, filling pressure 15 atm
Range of scattering angle 100°

Since the mean neutron wave length is slightly larger than that of the Be cut-off, the use of a Be-filter suggests itself. This is useful not only for background reduction and suppression of higher order reflections, but because it stops all neutrons from higher index reflections, it also allows the crystal to rotate around the [110] crystallographic axis. By this means we can utilize four reflections from the (111) planes per crystal revolution and drive the duty cycle to its maximum possible value. With the (111) reflections coming along in a 70°-110° sequence, we already find frame overlap in the 70° interval, which means in fact that neutrons being scattered with energy gain can catch up with neutrons from the foregoing burst, scattered elastically before they reach the detector. If this inelastic background is really disturbing, however, it can be measured simultaneously in the overlap-free 110° interval.

A calculation of the burst width Γ in the focal plane of the reflected beam by means of Eq. (11) yields the value $\Gamma = 14.7.10^{-6}$ sec. For the geometrical arrangement of Fig. 2a we have estimated $\Delta(\rho L)$ to be 0.76 cm with a plane counterbank of 17 x 17 cm entrance window, facing the sample surface under 90°. Using this estimate in Eq. (12) we obtain $\Gamma^{SC} = 12.5.10^{-6}$ sec, a value which may be regarded as a standard for the burst width to be expected in a scattering experiment. The corresponding value of the energy resolution is $\Delta E/E = 1.4\%$.

In this case we find the neutron velocity spread to be $(\Delta v)_{1/2} = 36$ m sec^{-1} and the respective momentum transfer resolution $\Delta\kappa\|/\kappa = 3.8\%$. The maximum value of momentum transfer observable is $\kappa_{max} = 2.3$ A^{-1}.

Intensity calculation is based on the following assumptions and estimates:

- The flux density distribution of the neutron source (integral thermal neutron flux 2.10^{13} n cm^{-2} sec^{-1}) is Maxwellian.
- Attenuation due to collimator and filter transmissions, air scattering and windows amounts to A = 0.25.
- Reflectivity r = 0.2 (corresponding to crystal slab of thickness 0.3 cm and mosaic spread 30 min, see 2.6.)

The resulting neutron current at the sample is $N_S = 2.1 \cdot 10^3$ n sec^{-1}.

Construction Features of the Spectrometer

Fig. 3 represents a horizontal section through the spectrometer. The collimator of the primary beam is constructed of cadmiated steel plates 0.5 mm thick spaced by 1 cm. In total it is 3.40 m long. It consists of four adjacent subsections. The first one, as seen from the side of the reactor core, is embedded in the beam hole plug and starts from behind the main shutter of the reactor beam hole with an overall width of 10 cm and height of 18 cm. Its height narrows continuously down to 10 cm at the surface of the reactor block after which the beam cross-section remains a constant 10 x 10 cm^2. The next collimator subsection is incorporated in a revolving beam shutter. It is supported by springs, and because of special guides its plates line up exactly with those of its neighbouring subsections when the shutter is opened. Similar provisions were made for the connection between the third and fourth subsections in the course of their adjustment to the section in the beam hole plug, which was done by optical methods. The collimator, except for the part in the revolving shutter, and the adjoining open beam channel of 1 m length, can be filled with He gas.

The entire structure outside the beam hole rests on table-like containers filled with water, which serve as downward neutron shielding. The neutron shielding above and at the sides is in the form of paraffin blocks clad in sheet metal.γ-radiation shielding is provided by lead bricks arranged closely around both the collimator and the open beam channel. All the shielding can be dismantled by hand.

The same principle was applied to the construction of γ-and neutron shielding around the rotating crystal unit. The rotating crystal is supported by a pair of air bearings, a solution which was chosen in consideration of a possible future use at much higher crystal speed for work with another crystal and elevated neutron energy. The crystal part is coupled magnetically to a synchronous motor. The power supply of the motor [9] is controlled by a quartz-oscillator which provides a frequency stability of 5.10^{-5}. Every time the crystal turns through a reflection position a T_0 reference signal for the time-of-flight measurement is supplied by a magnetic pick-up coil. There are two such coils, one for each set of (111) planes used, which can be adjusted by gears and stepping motors independently, to a precision of 12 min. If neutrons scattered by the sample are recorded in only one time-of-flight spectrum, fine tuning of the T_0-signals from the two coils is required. This is done by an electronic delay.

The collimator between the crystal and the sample position combines the function of a collimator with that of a filter. Its central part consists of a close assembly of 120 Be sheets of 0.8 x 100 x 250 mm with a 0.03 mm thick layer of Cd, each applied electrolytically to one of the large surfaces [10]. This central part is kept at liquid nitrogen temperature. The container around it is filled up with B_4C granulate for shielding purposes, but there is enough free space left inside this material for it to serve also as a liquid nitrogen reservoir with capacity for one full day's operation. Thermal insulation is ensured by vacuum. This entire assembly, together with a curved lead shield at the side of the crystal, is placed in a tank and can revolve in it around the fixed axis of the sample which is intersected by the axis the collimator. Beam channels lead from this unit to the tank openings on both the crystal and the sample side. These channels have curved plates at their extremities. With pressurized rubber seals around the tank openings, these plates prevent water from leaking into the beam channels when the tank is filled, once the collimator has been set according to the Bragg angle desired.

The adjustment of the spectrometer to a certain Bragg angle necessitates subsequent positioning of the rotating crystal in the primary beam channel. This is facilitated by a special guiding device between the crystal and the filter-collimator unit. Bragg angles can be chosen within the range $39° \leqslant \Theta \leqslant 56°$

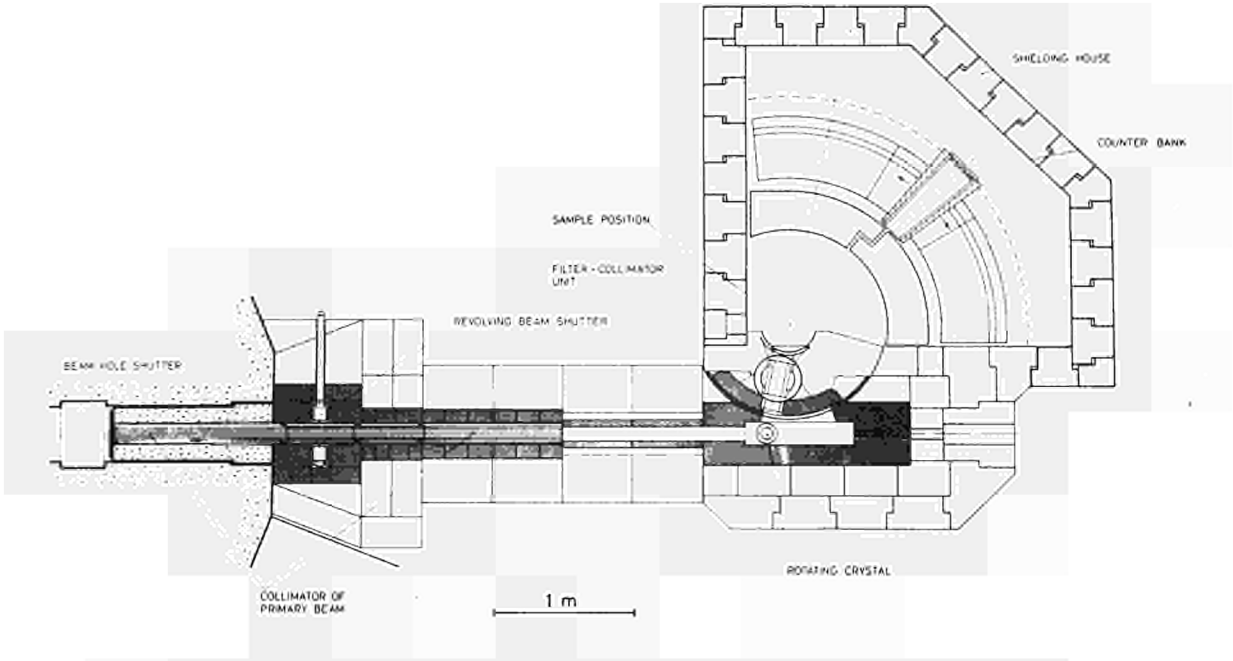

Fig. 3: Horizontal section through the time focusing spectrometer installed at the reactor ISPRA-I.

Sample and detectors are enclosed in a shielding house constructed of 30 cm thick water containers. At the circular opening in the roof of the shielding house the free space around the sample axis has its minimum diameter of 30 cm. The shielding house is divided into two compartments for sample and detectors respectively. They are separated from each other by a 30 cm thick curved shield which leaves only a 17 cm high slit free, through which the detectors are exposed to the sample. Detectors with or without collimators in front of them are mounted on carriages which run on a curved and precisely machined rail which is centred upon the sample.

In the near future a PDP 11 will be available for data acquisition. The measurements reported in the next chapter were carried out with an Intertechnique 1024 channel time-of-flight analyser.

Results of Performance Tests

Test measurements were carried out in the direct beam emerging from the filter-collimator unit and with neutrons scattered by a 6.6 cm thick sample of vanadium. In the direct beam the ^{3}He detectors (for specification see Table I) are used together with a multi-slit Cd-diaphragm for beam attenuation in order to avoid a distortion of the results by dead-time effects. The uncertainty of the measured half-widths quoted below is $\pm 0.5.10^{-6}$ sec.

With a single detector tube placed vertically in the centre of the direct beam, the burst width Γ has been measured as a function of the distance from the axis of the crystal which has been rotating with the nominal speed of 10,600 rpm. The result is shown in Fig. 4.

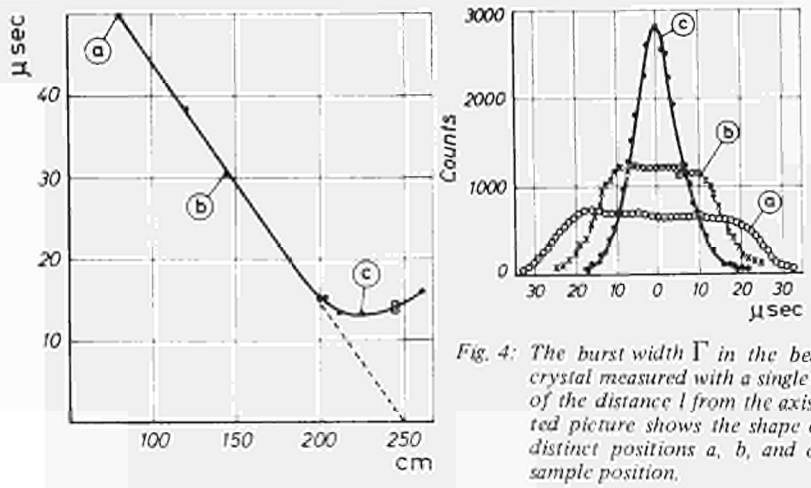

Fig. 4: The burst width Γ in the beam reflected by the rotating crystal measured with a single ^{3}He-detector tube as function of the distance l from the axis of crystal rotation. The inserted picture shows the shape of the neutron bursts at three distinct positions a, b, and c where a corresponds to the sample position.

The narrowing of Γ (1) in the linear region up to about l = 190 cm is due exclusively to focusing. An extrapolation to zero burst width gives the focal length l = L = 250 cm which is in full agreement with that calculated for the actual experimental arrangement using Eq. (5). The deviation of Γ (1) from its linear behaviour is caused by the effects which finally determine the burst width at the focus. At l = 225 cm, where we observe the minimum burst width of $13.0.10^{-6}$ sec, the fraction of the total burst width due to incomplete focusing has already become so small, that its further decrease with l is overcompensated by the effects of stationary velocity and flight-path spread which increase with l. The burst width at the focus amounts to $14.0.10^{-6}$ sec. The inserted picture of Fig. 4 plots the time-of-flight spectra measured at three distinct distances from the rotating crystal (a corresponds to the sample position). The trapezoid shape of the spectra a and b indicates that the full crystal volume contributes to the intensity of the reflected beam.

The measurement of the burst width as a function of crystal speed with a single detector tube at l = L = 250 cm results in no change of Γ upon reducing the speed to 9,000 rpm, but a rapid increase when the speed exceeds the nominal 10,600 rpm. This observation can be explained by arguments similar to those used for the interpretation of Γ (1) in the region around the focus, since reducing the crystal speed is equivalent to enlarging the focal length and vice versa.

With a plane counter bank at l = L = 250 cm consisting of 21 ^{3}He-detector tubes large enough to cover the full direct beam, we measured the burst width Γ as function of the angle γ between counter bank and beam axis. The results are illustrated in Fig. 5.

γ is equal to $90^\circ - \Theta = 42.7^\circ$ when the counter bank is parallel to the reference plane. The burst width measured in this position amounts to $16.0.10^{-6}$ sec, whereas the minimum value of $15.0.10^{-6}$ sec, is observed at $\gamma = 48^\circ$. (The corresponding numbers for a one-layer fission monitor are $15.5.10^{-6}$ sec and $14.5.10^{-6}$ sec respectively). This difference, surprising at a first glance, is reasonably explained by two effects: first, the major contribution to the burst width is ΔT_3 (see Eq. (9)) which is reduced by increasing γ. Secondly, and this is the main influence, the mean neutron energies on the slopes of the intensity profile of the beam are different, and so are the mean values of the recorded time-of-flight for off-centre detector tubes on either side of the beam axis. These different mean values come closer together as γ increases.

To demonstrate the angular dependence of the mean value of time-of-flight within the direct beam, we sampled it with another 10-min collimator. The counter bank behind it was set at $\gamma = 48^\circ$. The results are shown in Fig. 6. Between the two extreme collimator orientations $\Delta\alpha = +8.1$ min and $\Delta\alpha = -8.1$ min respectively, the mean values of time-of-flight differ by about 10.10^{-6} sec.

For a test of resolution and intensity obtainable in a scattering experiment, we have chosen the same arrangement to which the lay-out calculation refers (see section 3). The sample is a 6.6 mm thick plate of vanadium which completely covers the direct beam. When the geometry of the arrangement is taken into account, its effective scattering probability amounts to 11%. The monitor in the focus of the direct beam is set at $\gamma = 48^\circ$.

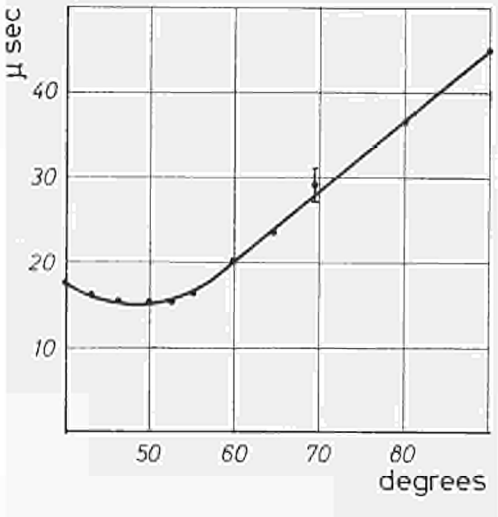

Fig. 5: The burst width Γ in the focus of the beam reflected by the rotating crystal measured with a plane counter bank as function of the angle γ between counter bank and beam axis.

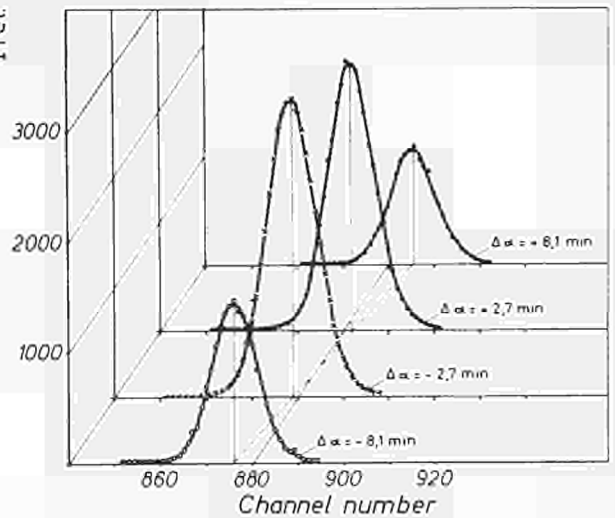

Fig. 6: Time-of-flight spectra recorded with a plane counter bank behind a second 10 min-collimator in the focus of the beam reflected by the rotating crystal. The parameter $\Delta\alpha$ indicates the angle between the axes of the second collimator and the filter-collimator unit. The channel width is 1 μsec.

Fig. 7: The plot on the right hand side represents the time-of-flight spectrum of neutrons scattered by a vanadium sample of 11 % effective scattering probability recorded within three days. Counter bank: 17 cm x 17 cm. The monitor spectrum on the left hand side refers to a one-layer fission monitor placed in the focus of the beam reflected by the rotating crystal. The channel width is 1 μsec.

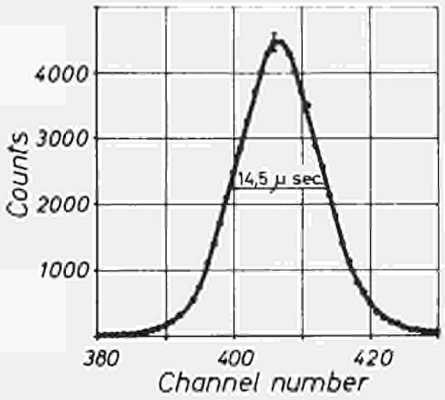

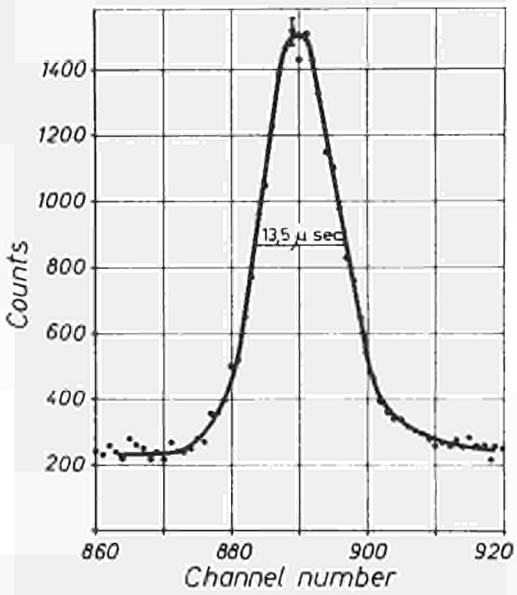

The result of the experiment, which lasted three days, is shown in Fig. 7. The elastic line recorded by the counter bank is fairly symmetric and has a half width of $\Gamma^{sc} = 13.5.10^{-6}$ sec. This corresponds to an energy resolution of $\Delta E/E = 1.5\%$. Γ^{sc} is reduced to $12.5.10^{-6}$ sec when the counter bank is subdivided into three leaves consisting of 7 detector tubes each, whereby the side leaves are inclined by 2° towards the sample in order to approximate the curvature of radius ρ.L .

The signal-to-background ratio is 5.5. This can be improved still further by putting the sample into vacuum or He-atmosphere (no background from Al construction material by single scattering) and by shielding the direct beam more effectively. Where background is concerned, the high filling pressure of the detector, specified in view of the planned future use of thermal neutrons, is another obstacle.

What has not been specified, but constitutes a drawback as regards intensity, is the fact that the detectors are constructed of steel tubes with 1.2 mm wall thickness. Consequently, we can obtain only a 50% detection probability with the plane counter bank owing to free cross-section and absorption. Taking this into consideration when evaluating the neutron current at the sample from the intensity observed in this experiment, we arrive at a value $N_{s,} = 1,6.10^{3}$ n sec^{-1} .

In contrast to measurements taken with the counter bank in the direct beam, a scattering experiment in which the sample is set at $\gamma = 48°$ and the counter bank is facing it under 90° yields a Γ^{sc}-value which is larger by $1.5.10^{-6}$ sec than the one reported above. This confirms that the angular dependence of neutron velocity and flight path length in the direct beam plays only a minor role in a scattering experiment.

Conclusion

The agreement obtained between the calculated and measured values of the focal length is excellent. As far as half widths of the neutron burst in the focal plane of the reflected beam and of the elastic line recorded in a scattering experiment with a vanadium sample are concerned, calculated and measured numbers differ by about 6 to 8%. The discrepancy of 25% between the predicted and the experimentally determined intensity we consider to be quite moderate in view of the large number of estimates used in the calculation.

The time-focusing spectrometer in its present version is installed at the reactor Ispra-1, which has an integrated thermal flux of 2.10^{13} n cm^{-2} sec^{-1}; quasi-elastic scattering experiments with an energy resolution of 1.4% at 4.4 meV neutron energy can be performed within one or a few days using counter banks of about 6°. acceptance angle.

The limit of the momentum transfer resolution is 3.8%. It is set by the spread of neutron velocity due to the Doppler effect in the rotating crystal and cannot be lowered, not even by reducing drastically the width of the counter banks. In return it results in an intensity advantage of a factor of 10 compared to a conventional time-of-flight spectrometer with an energy resolution as reported above.

References

1) Brockhouse, B.N., Bull. *Am. Phys. Soc.* 3 (1958) 233.
2) Brockhouse, B.N., Prc. IAEA Symposium Vienna, (19610 134.
3) Gläser, W., Proc. Symp. Neutr. T.o.F. Methods, Saclay, July (1961) 301.
4) Carvalho, F., Ehret, G., and Gläser, W., *Nucl. Instr. Meth. 49* (1967) 197.
5) Maier-Leibnitz, H., Mitteil. Bayerische Akademie der Wissenschaften, 16 (1966) 173.
6) Meister, H.,*Nuckleonik 10* (1967) 97.
7) Meister, H., *Nukleonik 10* (1967) 101.
8) Furrer, A., *Acta Cryst. A27* (1971) 461.
9) Eder, J., Roebbelen, D., External EUR-report in preparation.
10) Be-sheets supplied by Trefimetaux G.P., 95 Argenteuil, France.

QUANTUM EFFECTS OF HINDERED ROTATORS ON NUCLEAR MAGNETIC RELAXATION IN SOLIDS

J. Haupt

Introduction

It has been known for many years [1] that molecules or parts of molecules may undergo rapid reorientation in solids even at temperatures far below the melting point. Methyl groups, in particular, have high mobility around their threefold axis [2] - [5]. In principle, these phenomena can be observed with a variety of techniques, but up to now the predominant one has been magnetic resonance which has shown itself to be a powerful tool in this field. The type of molecular motion studied gives rise to a narrowing of the NMR lines and to relaxation via a modulation of the dipole-dipole interactions between the protons.

A "semi-classical" theory for the treatment of nuclear magnetic relaxation has been given in the pioneering work of Bloembergen, Purcell and Pound [6]. In this work the spin system is treated quantum-mechanically whilst, for the rotation, the classical Brownian diffusion model is used. This way of regarding the situation proved very fruitful for many investigations and has been used with only slight modifications up until now. The BPP theory seemed to describe all experiments quite well until studies of methyl-group rotation with small hindering barriers were done [3]-[5].

In general terms it can be stated that the semi-classical treatment is not applicable if the "tunneling splitting" of the rotational levels is comparable with the characteristic proton Zeeman frequencies of the spin system or the line width. In other words, one may say that owing to the incertainty principle, the position of the methyl group can no longer be determined sufficiently precisely with respect to the H-H distance, if the hindering barrier becomes too low. In consequence one can no longer treat the problem as a classical Bownian motion. A different way of describing the problem has therefore to be applied, which should contain as a limiting case the semi-classical model. We shall see that such a description not only explains the strong deviations in the relaxation behaviour [7] from the semi-classical theory but in addition a completely unexpected and unknown effect discussed briefly at the end of this paper [8].

Typical Experimental Data and Semi-Classical Theory

In Fig. 1 experimental data for the dependence of the longitudinal relaxation time measurements T_1 of toluene for two Zeeman frequencies (curves 3a, 3b) on the absolute reciprocal temperature are compared with the relaxation times predicted by the semi-classical theory for a high (curve 1a, 1b) and a low (curve 2a, 2b) hindering barrier. These experimental data are also representative of other measurements on materials with small hindering barriers. In the case of methyl-group rotation one expects a relaxation rate

$$\frac{1}{T_1} = 3.9 \cdot 10^9 \left[\frac{\tau_c}{1+\omega_0^2 \tau_c^2} + \frac{4\tau_c}{1+4\omega_0^2 \tau_c^2} \right] \qquad (1)$$

where ω_0 is the Zeeman frequency and τ_c the correlation time. τ_c usually follows an Arrhenius law.

For high activation energies the experimental data usually agree with formula (1) (compare also [2]). For low activation energies the following essential differences have been found:

i. the experimental curves have, on the high temperature side of the maxima, a greater slope than on the low temperature side.
ii. often two or more maxima are observed which are more or less pronounced (compare [3]-[5])
iii. the height of these maxima, which should be at a given Zeeman frequency independent of the activation energy, is too low by more than a factor of ten in the case of small activation energies.

These deviations are too large to be explained by more sophisticated models using, for example, a distribution of correlation times. At the same time the second moment of the proton line, in all materials with small activation energies, remains small down to very low temperatures (smaller than 1°K) although from the semi-classical theory one would expect an increase. An explanation of this result has been given elsewhere [9].

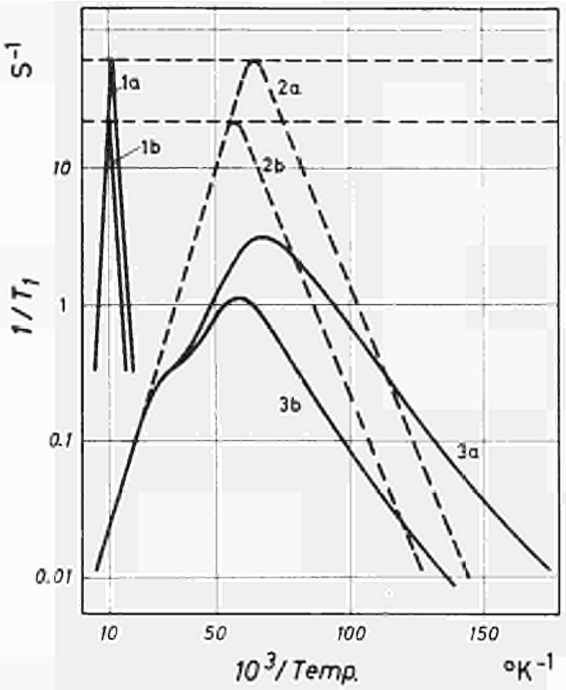

Fig. 1: Experimental and theoretical relaxation rates versus reciprocal temperature as explained in the text. The Zeeman frequency of the curves a is $\omega_0 = 9{,}1 \cdot 10^7\ s^{-1}$ and of b $\omega_0 = 25{,}6 \cdot 10^7\ s^{-1}$. The activation energy for 1a, 1b is 1,7 kcal/mole and for 2a, 2b 0,3 kcal/mole.

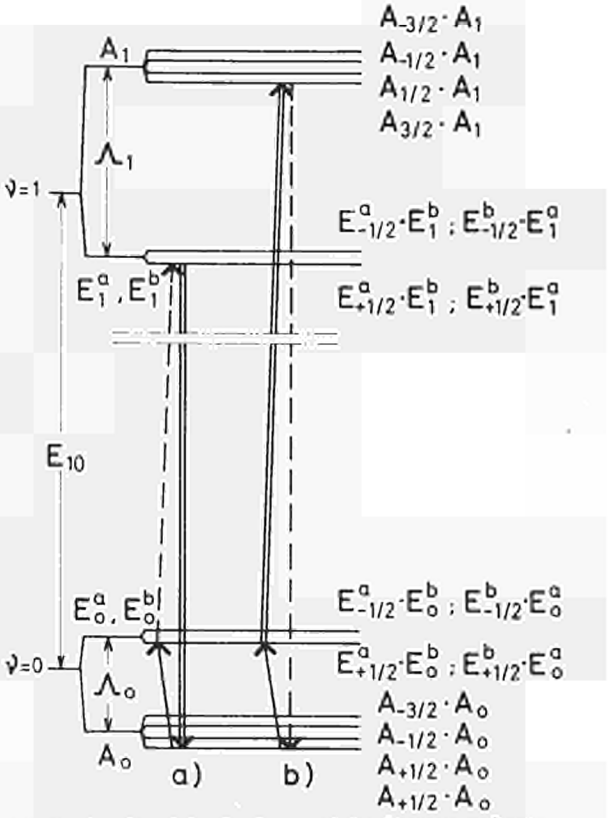

Fig. 2: Combined level scheme of the Zeeman and rotational states. The arrows indicate the matrix elements for the two essential contributions of the second order transition probability from $A_{+3/2}$ to $E^a_{+1/2}$.

Theoretical Considerations

In this chapter the principles of the theoretical description and the essential results will be given. An extended treatment is given in [7].

The Hamiltonian of the total system may be written in the following form

$$\mathcal{H} = H^Z + H^R + H^P + H^{DD} + H^{RP} \tag{2}$$

where H^Z is the zero-th order Zeeman Hamiltonian, and H^R and H^P are the zero-th order rotational and phonon Hamiltonians. The dipole-dipole Hamiltonian, H^{DD} couples the nuclear and torsional modes, and H^{RP} describes the coupling of the rotational and phonon modes. For H^{DD} only the dipole-dipole interactions between the three protons of the methyl group are treated and the interaction with the surrounding protons is qualitatively considered afterwards. For the applied magnetic fields $H^{DD} \ll H^Z$, H^R. H^{DD} may be treated as a perturbation. H^{RP} characterizes the modulation of the hindering barrier due to a phonon wave propagating through the crystal.

In Fig. 2 the combined Zeeman-rotational level system and the corresponding states are shown for the two lowest torsional states. From torsional states it is possible to construct the rotational states, whose levels lie below the barrier. Owing to the threefold symmetry each of the torsional levels splits into two rotational levels of A and E symmetry. The E-level is doubly degenerate. Λ_0 and Λ_1 are the tunneling splittings of the ground and first excited torsional states. As indicated in Fig. 2 the rotational levels combine with the magnetic levels (a quartet and doublet system) due to the Pauli exclusion principle.

Because of the simplicity of the problem the other operators can also be given and the matrix elements of interest for the low temperature approximation can be calculated. The transition probability between the Zeeman states m→ m' occurs in second order. Because of the diverse selection rules and the properties of the energy spacings, the sums and differences of matrix elements, weighted with Boltzmann factors and energy spacings, which appear in the second-order calculation for the transition probability between two magnetic states, can be reduced in the low temperature approximation for a fixed m and m' to only two essential terms.

The arrows in Fig. 2 represent the matrix elements for the two essential contributions to the second order transition probability between the Zeeman states $A_{3/2}$ and $E^a{}_{1/2}$ given in eq. 40 of [7]. Each of these contributions is proportional to the square of a product of two matrix elements, which are connected with a change either of the magnetic and tunneling state (solid line) or of the torsional and phonon state (dotted line). The resultant "transition" determining for instance the energy involved in this process is given by the double line. In case a) a phonon is emitted and in case b) a phonon is absorbed.

The results for all other magnetic transitions are similar. In the low temperature region, the relaxation behaviour is determined by quantum effects. A magnetic transition changing the magnetic quantum number is, in this region, always connected with a phonon transition of about the energy difference between the zero-th and first excited torsional states, and, simultaneously, with a change of the tunneling state.

The consequences of these properties explain the characteristic divergences of the experimental data from the predictions of the semi-classical theory. The apparent activation energy is therefore, at low temperature ($E_{10}/kT > 1$), the energy difference between the ground state and first excited state $-E_{10}$. This is typically two or three times smaller than the total barrier height for the range between 0.1 and 1 kcal/mole. At high temperatures one expects again the full barrier height as activation energy. A quantitative quantum-mechanical treatment of the last case has not been given up to now.

To explain the existence of two or even more maxima, we have to take account of the fact that under the simplifying assumptions of an isolated methyl group the magnetic transitions occur at frequencies $\Lambda_0 \pm 2\omega_0$. Since, in the interesting range of barrier height, $\Lambda_0 >> \omega_0$, one would expect a maximum of the relaxation rate for $1/\tau_c \approx \Lambda_0$. In addition, there should be another maximum, as in the semi-classical theory, at $1/\tau_c \approx \omega_0$ due to the neglected intermolecular dipolar interactions of the protons of the methyl group with the surrounding protons. For these interactions direct transitions within the quartet and doublet system are not forbidden since the symmetry is much lower than for the methyl-protons alone.

Point iii is explained in the same way. On the low temperature side, the relaxation rate is expected to be proportional to $1/\Lambda^2_0$, instead of $1/\omega^2_0$. This leads to a highly reduced relaxation efficiency. If the relaxation efficiency of the isolated methyl group is very low the relaxation rate will be determined by the intermolecular dipolar interactions which are proportional to $1/\omega^2_0$ as was observed in most experiments. Because of the reduced efficiency the relaxation maxima will be lower. An extended description of all these properties is given in [7].

New Polarization Effect

The considerations of the last chapter allow one to understand the principle of a new polarization effect, which was observed in γ-picolene. A jump in the temperature from 8 to 30°K caused a dynamic enhancement of the dipolar signal by a factor of 10^4. The build up of the polarization is given in Fig. 3. Fig. 4 shows the typical shape of a dipolar signal obtained after a temperature jump with a 45° pulse of a 15 MHz spectrometer.

To understand this effect qualitatively, we have to consider the two essential contributions to the second order transition in Fig. 2. Since the transition probability depends on the third power of the energy difference [7] of the resultant transition it will be larger for transition b) than for a). This tendency will be the stronger the smaller the barrier height.

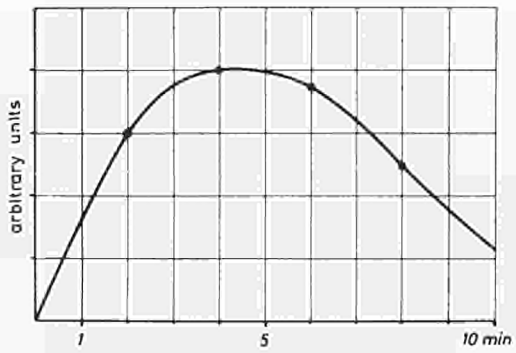

Fig. 3: Typical build up of the dynamic polarization with time. Ordinate arbitrary units.

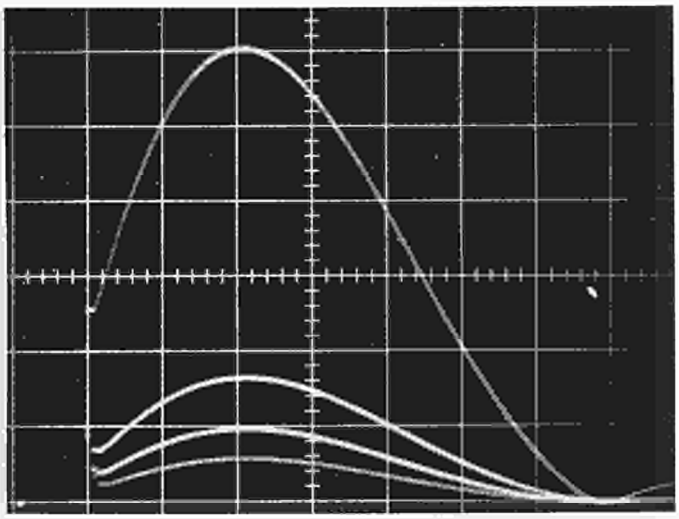

Fig. 4: Oscilloscope display of free induction decays after a temperature jump. The time scale is 5 μs/div. The curves have the typical shape of a "dipolar signal".

For the sake of simplicity we neglect case a) and obtain that transition $A_{3/2} \rightarrow E^a_{1/2}$, with $\Delta m = -1$, occurs on the absorption of a phonon. The reverse transition $E^a_{1/2} \rightarrow A_{3/2}$ ($\Delta m = +1$) is connected with the emission of a phonon. By changing the temperature to a higher value, more phonon absorption and fewer emission processes will occur until the new equilibrium is reached. A negative contribution to the Zeeman polarization is therefore obtained. By reversing the temperature jump, the sign of the effect is reversed too. In the most favourable case the populations of the rotator levels might be transferred to the magnetic levels.

In order to calculate the net effect, the contributions of all magnetic transitions have to be summed up. It turns out that the sum of the Zeeman polarization is zero, whilst it is not zero for the contributions of the dipolar polarization [8].

Since a transfer of the dipolar order to Zeeman order and vice-versa is easily possible, moderate absolute Zeeman polarizations can also be obtained by this method. γ-picolene seems to be a particularly favourable case because of its small hindering barrier and weak intermolecular interactions. There is some hope that similar effects may also be observed in other materials with "quantum motions".

References

1) Review article: E.R. Andrew and P.S. Allen, *J. Chim. Phys. 1* 85 (1966)
2) K. Grude, J. Haupt, W. Müller-Warmuth, *Z. Naturforschg., 21a*, 1231 (1966)
3) J. Haupt und W. Müller-Warmuth, *Z. Naturforschg. 23a,* 208 (1968)
4) J. Haupt, W. Müller-Warmut, *Naturf. 24a,* 1066 (1969)
5) P.S. Allen, A. Cowking, *J. Chem. Phys. 47*, 4286 (1967)
6) N. Bloembergen, E.M. Purcell, R.V. Pound, *Phys. Rev. 73,* 679 (1948)
7) J. Haupt, *Z. Naturforschg. 26a,* 1578 (1971)
8) J. Haupt, *Physics Letters* 38A, 389 (1972)
9) P.S. Allen, *J. Chem. Phys. 48*, 3031 (1968)

MEASUREMENT AND INTERPRETATION OF THE COOLANT VOID COEFFICIENT IN D_2O LATTICES

W. Hage, H. Hettinger, H. Hohmann, B. Sturm, F. Toselli

Introduction

Experimental determination of the void coefficient of the material buckling $1/B_M^2 \cdot \Delta B^2/\Delta\alpha$ and of the diffusion constant $1/D \cdot \Delta D/\Delta\alpha$ in fuel elements serves to check cell calculation methods of reactor lattices. In the ECO reactor of the JRC Ispra the void coefficients of UO_2 fuel elements were measured in connection with the D_2O reactor physics program of the European Community, in collaboration with the CEA (France), CISE (Italy) and Siemens AG (Germany).

Experimental Conditions

The ECO reactor was loaded with 97 U/19/12-diphyl fuel elements [1] in a square lattice arrangement. In this core the central zone was replaced by nine $UO_2/28/12\text{-}D_2O$ test elements (Fig. 1).

Each of these 28-rod UO_2 elements contained 45 aluminium tubes, arranged in four independent ring groups. By means of a N_2 pressure system the coolant could be displaced in axial steps in any ring combination of tubes in one, five and nine test elements. The void depth was measured using a U-tube manometer with ±0.3 cm accuracy. The tubes permitted a coolant displacement of maximum 27%. All experiments were performed in the lattice pitch range 20.5 cm $\leq d \leq$ 26.5 cm corresponding to a moderator-to-fuel volume ratio of $8.3 \leq V_M/V_F \leq 17.3$

Measurement Method

Voiding of the selected combination of tubes in one, five or nine test fuel elements was performed with the reactor near criticality. The axial voiding steps were about 20 cm. At each step the critical water level was measured by two methods:

1. Direct measurement of the critical water level with the D_2O level meter (accuracy ±0.1 mm);
2. Measurement of the pile reactivity variation between two coolant void conditions at constant water level with the inverse neutron kinetics technique [2]. The corresponding critical-height variation was derived from the reactivity coefficient $\Delta H/\Delta\rho$ of the moderator level. $\Delta H/\Delta\rho$ was determined in a separate experiment, measuring the reactivity difference between the critical and a supercritical moderator level with the same technique.

Method 2 has the advantage that very small variations of the critical height (10^{-2} mm $\leq \Delta H \leq$ 10 mm) are measured. The accuracy in the ΔH measurement is limited to small values by the reactor noise and was during the measurements about $4 \cdot 10^{-3}$ mm; at larger values the predominant source of error lies in the $\Delta H/\Delta\rho$ measurement (about 1%).

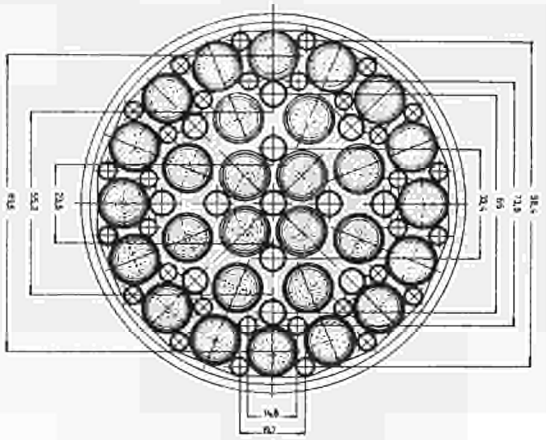

Fig. 1 FUEL ELEMENT $UO_2/28/12 - D_2O$

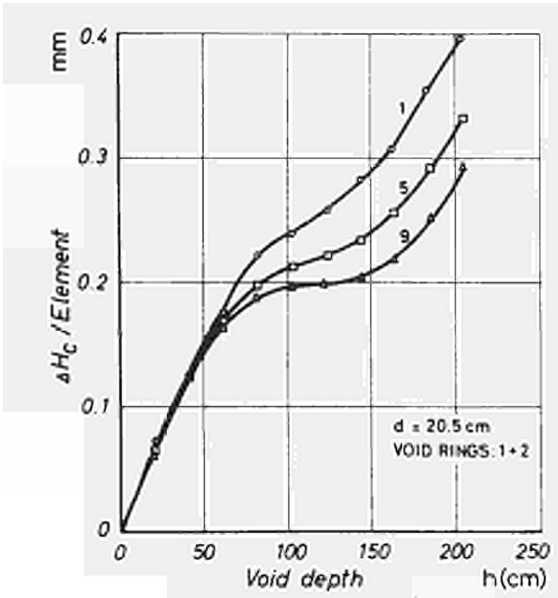

Fig. 2 Axial void effect

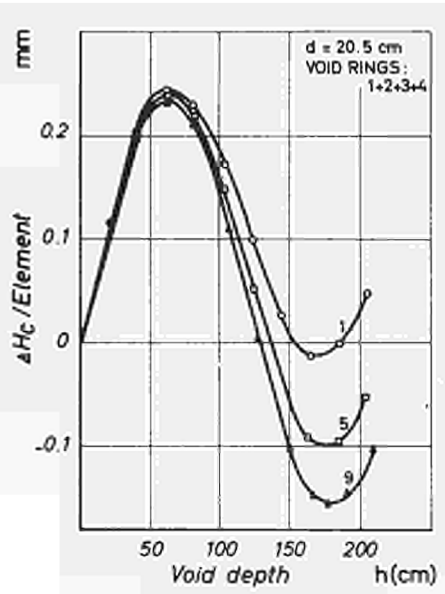

Fig. 3 Axial void effect

Analysis of the Experimental Results

Fig. 2 shows a typical result of a measurement. The variation of the critical moderator level ΔH per voided test element is plotted above the void depth h of the voided test elements. The data were obtained at the smallest lattice pitch, voiding the two outermost tube rings. In this case all critical height variations are positive with increasing h. The same measurement with a stepwise voiding of all tubes leads to a completely different behaviour, with first a positive then a negative variation of the ΔH/element (Fig. 3). In Fig. 4 the relative critical height variation $\Delta H/H$ is plotted above the relative void depth h/H (H ≡ extrapolated critical height) for different lattice pitches.

For the analysis of the experimental data a two-group perturbation theory was applied giving a relation between the relative critical height variation $\Delta H/H$ and the void depth h for one, five and nine elements voided.

$$-\left(\frac{\Delta H}{H}\right)_N = \frac{1}{2}\left[U_N C\left(\frac{h}{H}\right) + V_N S\left(\frac{h}{H}\right)\right] \quad N = 1,5,9,; \quad C\left(\frac{h}{H}\right) = \frac{h}{H} - \frac{\sin 2\pi\frac{h}{H}}{2\pi} \qquad (1)$$

$$S\left(\frac{h}{H}\right) = \frac{h}{H} - \frac{\sin 2\pi\frac{h}{H}}{2\pi}$$

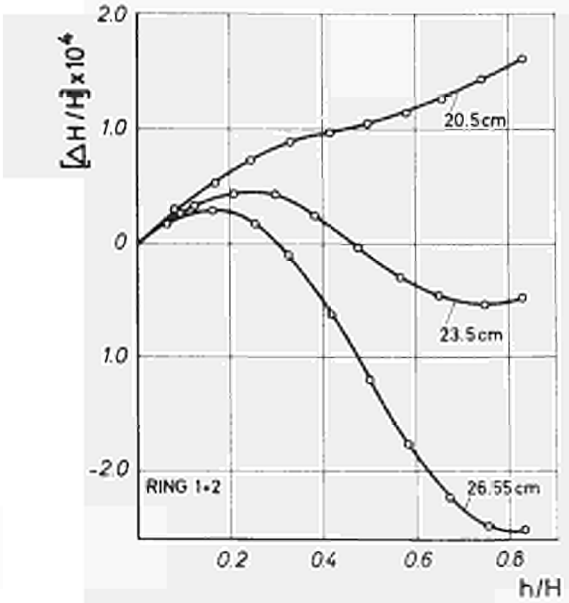

Fig. 4 Relative critical height variation

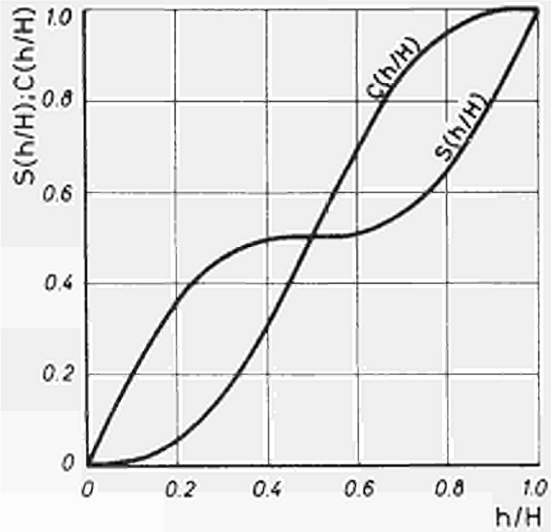

Fig. 5 The functions $S(\frac{h}{H})$ and $C(\frac{h}{H})$

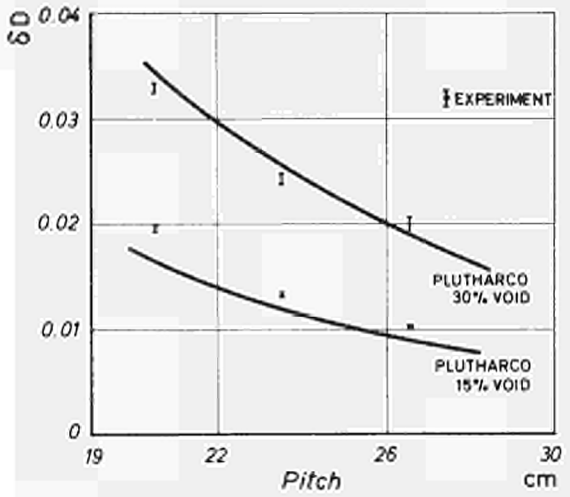

Fig. 6 Void coefficient of the diffusion constant as function of the lattice pitch.

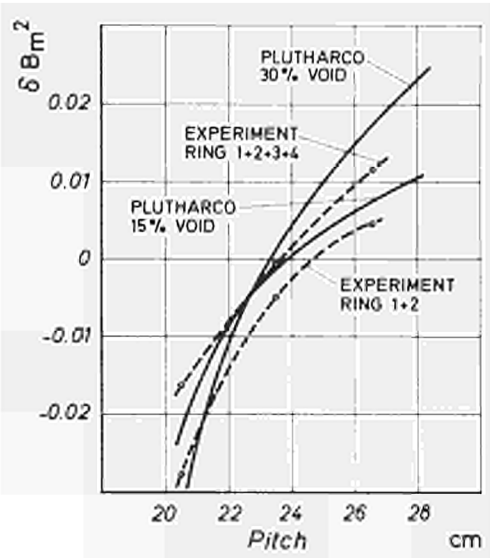

Fig. 7 Void coefficient of the material buckling as function of the lattice pitch.

The functions C(h/H) and S(h/H) are given in Fig. 5. The parameters U_N and V_N are obtained from a least-squares fit on the function $\Delta H/H = f(h/H)$. The theory gives a relation between U_N and the relative variations of the material bucklings $\delta B_M^2 = \Delta B_M^2/B_M^2$ and of the diffusion constants $\delta \bar{D} = \delta \bar{D}/\bar{D}$

$$\delta B_M^{2*}(U_N, V_N) = \delta B_M^2 + f(C_N^*) \tag{2}$$

$$\delta \bar{D}^*(V_N) = \delta \bar{D} + g(C_N^*) \tag{3}$$

$f(C_N^*)$ are functions which tend with C_N^* toward zero.

C_N^* is a parameter describing the perturbation of the teslattice spectrum by the reference lattice. This perturbation is most dominant for the outer elements of the test zone, increasing C_N^* with the number of elements voided.

From plots of $\delta B_M^{2*}(U_N\ V_N)$ and $\delta\bar{D}(V_N)$ above the abscissa C_N^* for one, five and nine elements, the extrapolated values to $C_N^* \Rightarrow 0$ lead to $\delta B^2{}_M$ and $\delta\bar{D}$ respectively. The results of this analysis are given in Figs. 6 and 7.

Theoretical values obtained with the lattice code PLUTHARCO [3] are included in these figures. The curves indicate that for small lattice pitches the increase of the leakage is larger than the corresponding increase of k_∞. For larger pitches, however, the positive contribution of k_∞ dominates the positive void coefficient.

The void effect as function of pitch is given by the used theory only qualitatively, possibly owing to the assumption of a homogeneous void. In a further study the effect of the heterogeneous void distribution will be taken into account by the cell lattice code used.

References

1) W. Hage et al., *ATKE 13-26* (1968) 133-138
2) L. Anselmi et al., *Nukleonik 11* (1968) 1-14
3) W. de Haan, R. Meelhuysen, EUR 3141.e (1966)

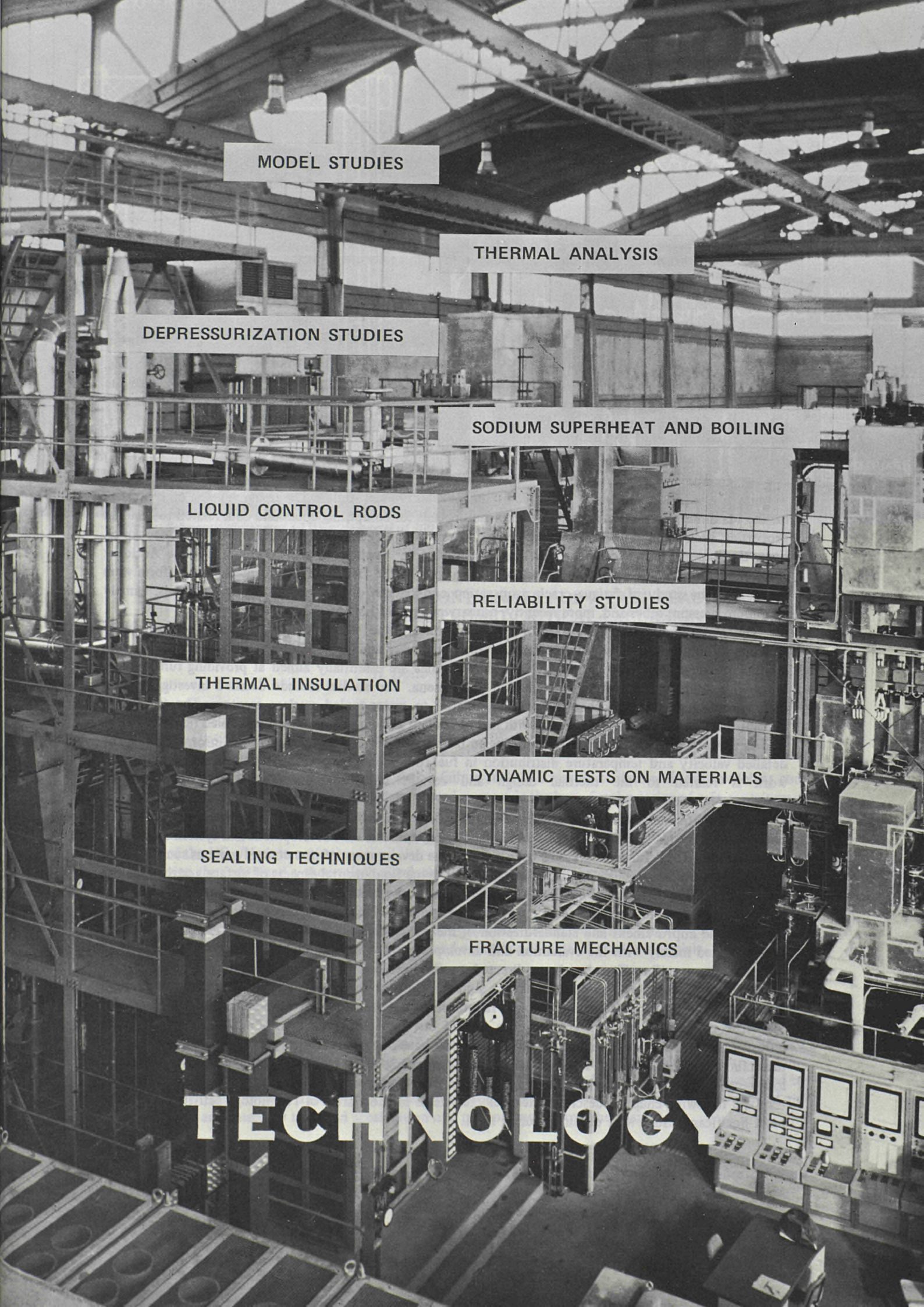
MODEL STUDIES
THERMAL ANALYSIS
DEPRESSURIZATION STUDIES
SODIUM SUPERHEAT AND BOILING
LIQUID CONTROL RODS
RELIABILITY STUDIES
THERMAL INSULATION
DYNAMIC TESTS ON MATERIALS
SEALING TECHNIQUES
FRACTURE MECHANICS
TECHNOLOGY

TECHNOLOGY DIVISION

G. Grass

Research work in the Technology Division, Ispra, principally concerns the three following branches of activity:

- Applied Mechanics
- Heat Transfer and Fluid Flow
- Process Engineering.

The structure of the Technology Division in 1971 was organized in accordance with these branches. The three activities mentioned form part of the various programmes mentioned in the first part of the report (Fast Breeders, HTGR, Reactor Safety etc.). On the other hand an endeavour has been made to give a fundamental basis to these activities in order that, apart from providing direct help to reactor projects, licensing authorities and others, they shall also be of long-term interest.

The *Applied Mechanics* activities include studies on stress analysis, material behaviour under dynamical stresses, fracture mechanics, studies related to the production and propagation of shock waves, explosion welding, investigations on tightness problems and Accident Model studies. The research going on in Europe on the Maximum Credible Accidents of fast reactors calls for computing codes and data related to material properties, such as experimental state equations, stress-strain diagrams in dynamics and fracture mechanics. Even the experimental Accident Modelling is designed for application to Maximum Credible Accident studies. The two items are treated in close association. In the field of fracture mechanics, efforts were devoted to the study of fatigue crack propagation and criteria of rupture in reactor structures, namely zirconium pressure tubes and, more recently, primary circuits of LMFBR.

The *Heat Transfer and Fluid Flow* activities concern the steady-state and transient behaviour of coolants in one or two-phase flow conditions (for both water and liquid metals) and heat transfer studies relating to fuel-rod bundles. The two-phase flow studies are essentially aimed at providing fundamental knowledge on burn-out and coolant ejection phenomena. The studies include detailed investigations on boiling mixing between subchannels and are related to water-cooled nuclear reactors. The studies on coolant ejection are directly connected with loss of coolant accidents in liquid-metal-cooled fast breeders as well as in water-cooled reactors. The research on heat transfer in rod bundles furnishes information on the detailed velocity and temperature distribution in fuel-rod assemblies cooled by a non boiling fluid. This work is related to the thermal design and certain safety aspects (subchannel blockages) of liquid-metal-cooled fast breeders.

The activities in the field of *process engineering* are primarily concerned with problems of surface phenomena, physical properties, liquid metal technology, process unit development and system evaluation. Considerable effort,, furthermore, has been given to the development of new control systems such as liquid control rods. Studies on surface phenomena deal with some fundamental aspects of surface activity, such as the relationship between work function and other physicochemical properties. Studies of more technological character are carried out on wear and friction. Physical properties evaluation activities are aimed at the improvement and standardization of measuring techniques. Liquid metal technology studies are concerned mainly with the evaluation and development of cooling circuit components. In the field of process units specific effort has been directed to fluidized-bed model studies and spray-drier reactor development. System evaluation studies are aimed mainly at the assessment of system safety through reliability analyses and detection of incipient failure through noise and stress wave emission techniques.

Most of the Technology activities are carried out in close contact with national organisms and industries. Thus they are always oriented towards problems of current interest. The Division endeavours to maintain a good equilibrium between new ideas (originating from technical problems put to us) and a long-range disciplinary philosophy ensuring scientific competence and a continuous progress of work.

The following chapters describe a few selected items in those areas of Technology activities where the most significant results were obtained during 1971.

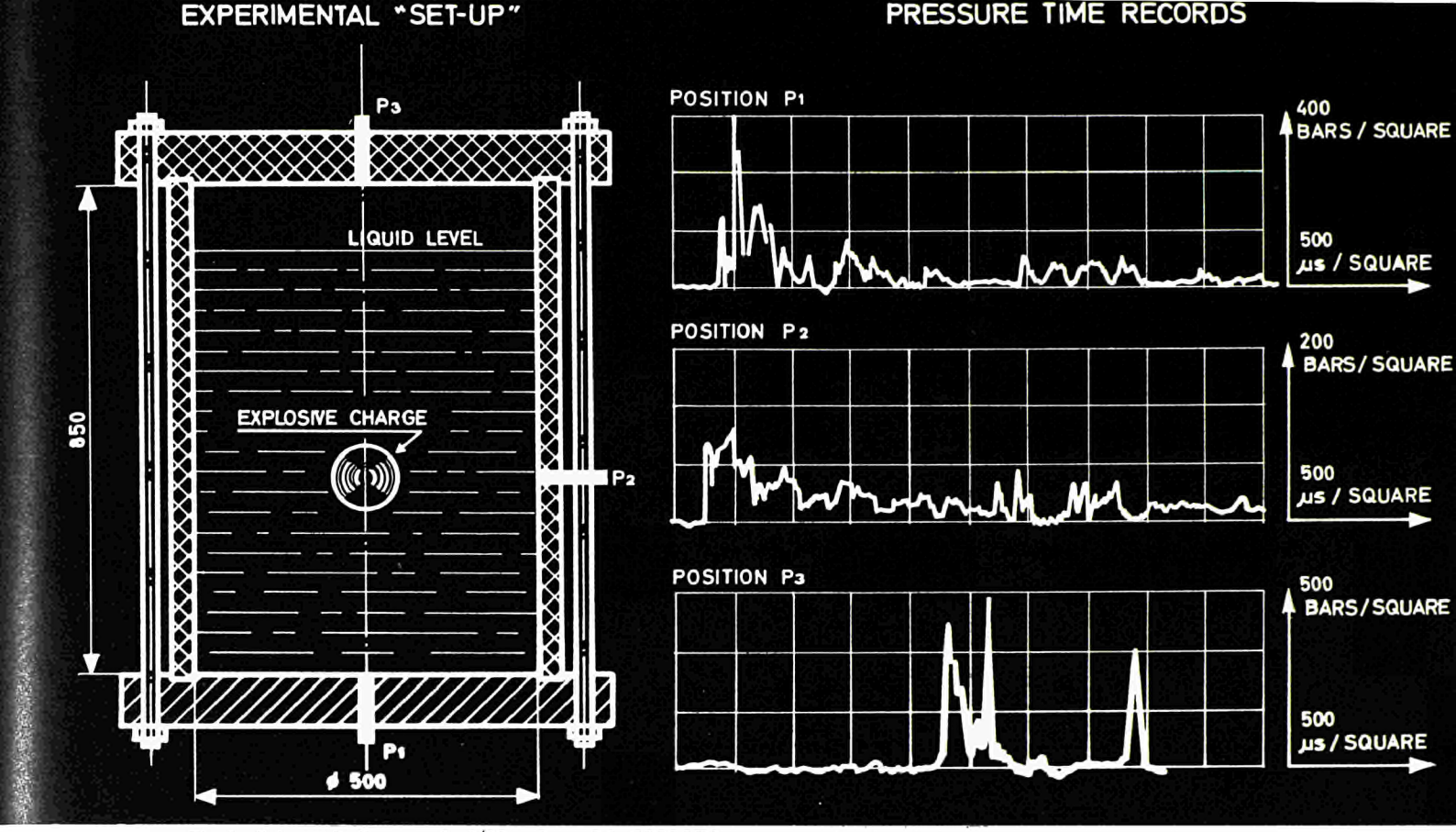

Fig. 1: Schematic diagram of a 1/12 scale model of 300 MW reactor vessel and typical pressure traces corresponding roughly to a DBA.

DYNAMIC LOADING OF THE CONTAINMENT OF A FAST REACTOR DUE TO AN ACCIDENTAL PROMPT CRITICAL EXCURSION

H. Holtbecker, G. Verzeletti

Introduction

Despite the extemely low probability that a failure such as a loss of coolant will lead to violent core destruction, such an accident is nevertheless studied to provide the basis for the design of safe containment systems. The magnitude of the energy release is evaluated by the well-known Bethe-Tait method. A further calculation establishes how much of this energy may be converted into mechanical work (including the effects of the UO_2/Na interaction).

Having thus obtained a theoretical calculation of the mechanical energy that the containment must be designed to withstand, the question arises: how do we demonstrate that the containment can in fact withstand it?

The answer to this is provided by carrying out explosion experiments and by performing calculations with codes using the equation of hydrodynamics and equations of state of reactor materials.

Experimental results

Pressure-time histories

To illustrate the experimental work Fig. 1 shows schematically a 1 : 12 scale rigid model of a 300 MW sodium cooled reactor and typical pressure traces measured for low burning explosive charge corresponding roughly to a "design basis accident" or maximum hypothetical accident. The liquid sodium is simulated by water. From the pressure traces it can be seen that the largest pressure pulses occur on the roof of the vessel. They are caused by the rapid acceleration of a plug of water above the charge.

Loading of the lid of the vessel

A basic parametric study was performed in order to analyse the lid behaviour under different experimental conditions.

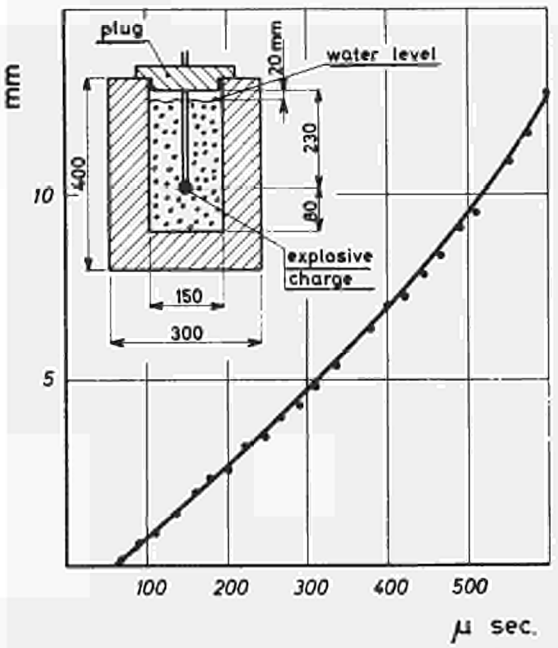

Fig. 2: Displacement versus time curve for an unfixed plug of 5 Kg. Charge weight: 5 gr TNT.

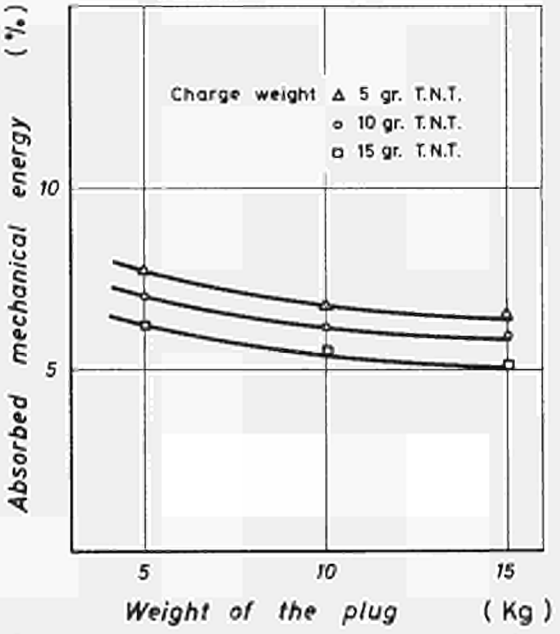

Fig. 3: Percentage of absorbed mechanical energy of an unfixed plug.

Fig. 2 shows a measured plug displacement versus time curve. The plug was not fixed on the vessel and a rigid walled vessel similar to that shown in Fig. 4 was used. TNT-type charges were used.

A rapid change of the slope of the displacement versus time curve reproduces the "bouncing" behaviour of the water plug indicated in the pressure versus time curves in position P 3 of Fig. 1.

The percentage of absorbed kinetic energies calculated from these velocity measurements are shown for three different charge weights and for various weights of the plug in Fig. 3. These energies reach 5 - 8% of the total mechanical energy released by the charge. With any given weight of charge, the amount of energy absorbed by the plug diminishes as the plug weight is increased.

Fig. 4 shows the results concerning the energies absorbed by the bolts with which the plug was fixed on the vessel. By comparison with the experiments performed with an unfixed plug the absorbed energies are lower. The absorbed energy further decreases when the number of bolts is increased. These results are explained by the fact that the quantity "force multiplied by velocity" decreases as the plug is more and more clamped to the vessel. The energy absorption with a free plug in the graph in Fig. 4 was obtained by catching the plug with bolts after a free displacement of about 60 mm. This value of absorbed deformation energy corresponds roughly to the results obtained for the kinetic energies in the series of tests with an unfixed plug as shown in Fig. 3.

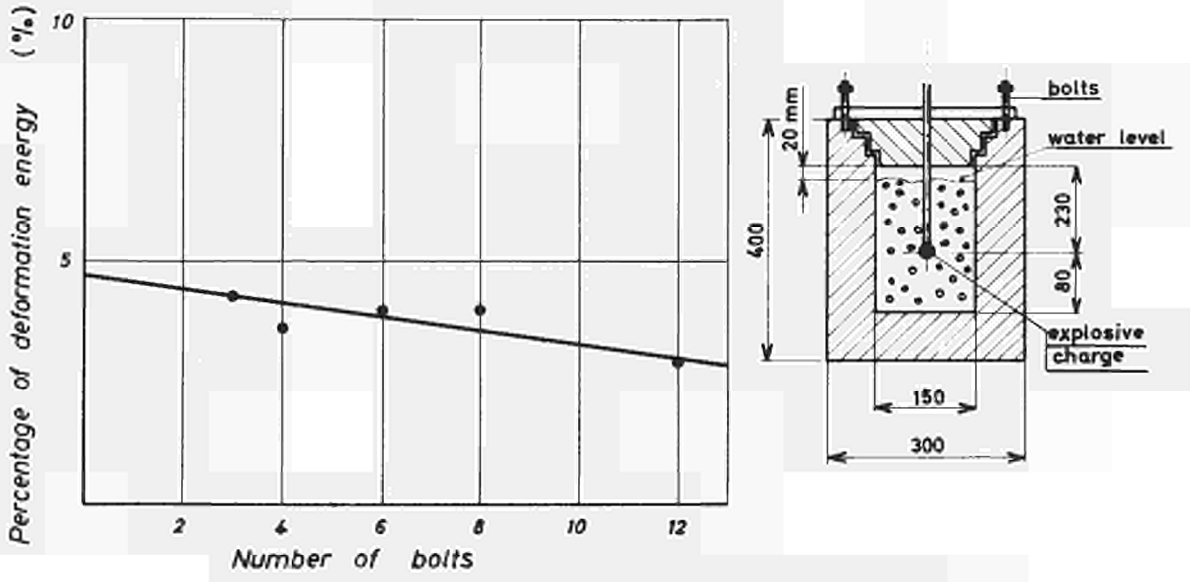

Fig. 4: Percentage of deformation energy versus number of fixation bolts.

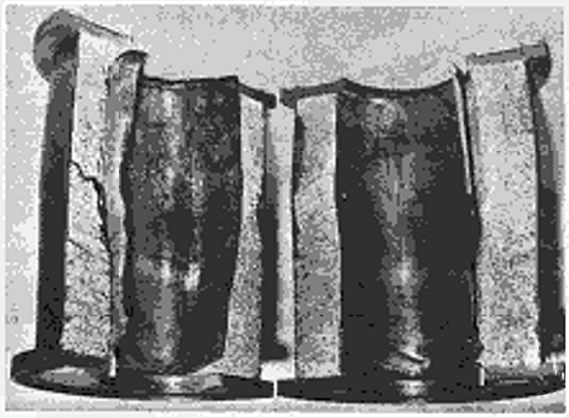

Fig. 5: Multilayer structure after explosion: 30 gr plastit; concrete interlayer.

Fig. 6: Multilayer structure after explosion: 30 gr plastit; sand interlayer.

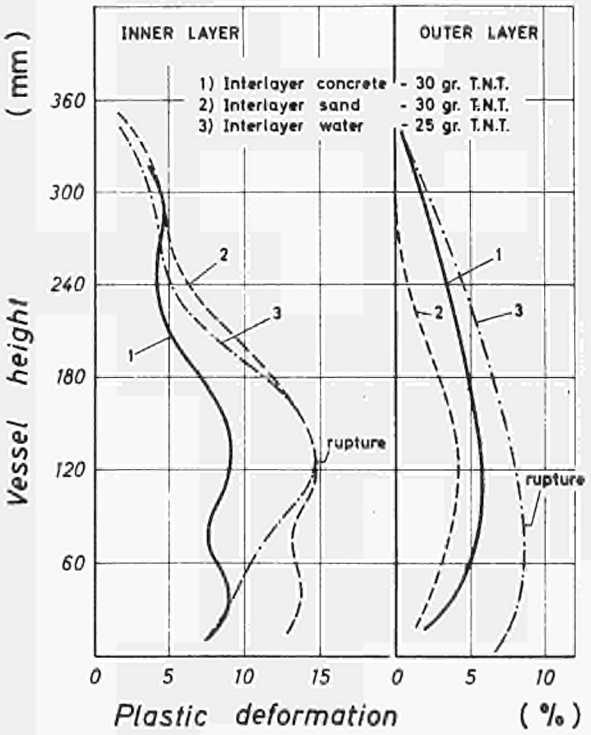

Fig. 7: Residual tangential deformations of a multilayer structure.

Additional parameters having an influence on the impulse on the plug after an explosion were investigated. First, experiments were performed comparing the effects of detonating with deflagrating explosives. The results show that the energy distribution in the vessel is directly related to the type of explosive used. Detonating explosives produce high energy shock waves which propagate in the coolant and cause large deformation on all low-inertia structures which are in contact with the liquid. The deflagration explosion produces low shock energies. A large amount of the energy released results in a fast-growing vapour and gas bubble inside the coolant (blast) which projects a piston of sodium against the lid. In our experiments by comparison with the values measured with dynamite the impulse on the lid is about 60 % higher with the deflagration explosive.

Secondly, tests were performed in which a perforated plate connected to the plug was mounted in the mock-up. The results show a strong reduction (about 40 %) in the impulse acting on the plug. Perforation ratios of 0,1; 0,2; 0,4 have been investigated.

Thirdly, the inpulse on the plug clearly depends on the rigidity off the reactor vessel. Tests performed in the geometry indicated in Fig. 1 with a 35 mm and a 3 mm thick vessel show that the plastic deformation of the thinner vessel reduces the energy absorbed by the bolts by a factor of 3.

Loading of the containment vessel walls.

A parametric study was performed on different methods of absorbing explosion energies in the containment.

As shown in Fig. 5 and 6, a multilayer structure was employed with concrete, sand and water used as filler materials.

In Fig. 7 the residual tangential strains are shown as a function of the height of the vessel for the three types of filler materials used. The concrete protects the internal shield better than sand. The low compressibility of concrete allows a transfer of the deformation of the internal shield to the external one. Sand is more compressible. The high deformation of the internal shield is only partially transferred to the external one. With water as filler material almost no energy is absorbed. With 25 gr of Plastit the vessel ruptures. The conclusions of this study were that with sand as filler material the external vessel could withstand a charge of 70 g of TNT; with concrete the weight of the charge should not be higher than 60 g; and with water the integrity of the vessel cannot be relied upon with more than 15 g of TNT.

A more detailed description of these tests and the explanation of the results by a theory similar to the "energy deformation" relation of WIN-Proctor is given in [1].

Another approach was attempted for the geometry of Fig. 1. Fig. 7 shows how the residual tangential strains of the vessel can progresively be equalized over its whole length by first introducing a skirt around the reactor core and then adding a perforated plate.

Analysis of the experimental results

A code for calculating the two-dimensional hydrodynamic response of a primary reactor containment system is applied in order to explain the experimental results and provide a means of extrapolating these results to real reactor conditions. One of these codes named Rexco was developed by ANL and was been slightly modified in order to take the properties and the equations of state of different types of explosive charges into account.

The code is able to describe the propagation of shock waves, the loads on the reactor components and the resulting deformations. The equations are expressed in lagrangian form.

Belgonucleaire (Belgium) developed a new two-dimensional code called SOURBOUM which cannot describe the propagation of pressure waves but because it is written in Eulerian form, it allows a detailed description of large fluid flows.

CNEN (Italy) contributed to the analysis of experimental results with the one-dimensional code ASPRIN.

The above two organizations signed contracts of cooperation with Euratom to solve specific problems for the SNR and PEC reactors. They collaborate in the defining of the experimental and theoretical programme performed at Ispra, and they have their own theoretical programme for the direct use of these results for the reactor design.

Fig. 8: Residual tangential deformations for vessel and inner skirt for three types of experiments.

BEHAVIOUR OF MATERIALS UNDER DYNAMIC LOADING

M. Montagnani, C. Albertini, V. Andrighetti,
G. Fratus, L. Verheyden

Introduction

A study of a reactor incident cannot exclude a study of the behaviour of materials in dynamics. The data collected in these experiments are in fact necessary to calculate the strength of structures subjected to a rapid mechanical transient. The data concerned are essentially the stress-strain diagram and the equation of state. Research done at Ispra in this field has been useful both to the techniques for measuring such data, and to gain deeper understanding of the basic mechanisms of deformation and rapid rupture. It will be useful at this point to describe briefly the research carried out so far, so as to give a full picture of the extent of our work.

Rapid Deformation of Zirconium Alloys

Although the effect of increasing embrittlement had been studied in the past by classical methods [1], it was still not known how materials would behave when subjected to very rapid and extensive deformations.

To provide this information Zircaloy-2 rings were deformed by detonating a charge of explosive placed in the symmetrical centre of the ring. The ring was placed in a shock resistant furnace, so that the experiment could be carried out at increasing temperatures, up to 300°C.

The rings were hydrated, before the tests, by means of an electrolytic system. The H_2 content of the ring varied from 120 to 220 and 500 ppm. After the test the deformation of the ring was measured over the three axes. The fact that Zr-2 becomes increasingly brittle was confirmed by these tests, the results of which have been assembled in a paper [2] prepared for the International Congress "Hydrogen in Metals", Paris, 29th May to 2nd June 1972. In this study one can see the considerable strains obtained in the tests owing to the high deformation speed. Nevertheless, it can also be seen that the large strains measured macroscopically on the test pieces, are not always matched by a similar strain in the grains. This suggests that there is a particular dislocation mechanism, which requires further investigation. To this end further microscopic examinations are in progress, including a statistical study of the deformation of the grains in areas far from and near to the fracture.

Dynamic Resistance of Reinforced Concrete to an Internal Explosion

Theoretical and experimental studies carried out in this field have been assembled in a report [3] presented at the "Structural Mechanics in Reactor Technology" Conference, Berlin, 20 - 24 September 1971.

These studies were preliminarily based on a series of experiments on a mock-up of the effect of an explosive wave on a concrete structure, reinforced or not. The most noticeable effect observed was the "scabbing", i.e., the detachment of an external layer of concrete, caused by the tension wave reflected off the wall periphery. It was observed that this phenomenon can be reduced, and more or less eliminated by inserting a shock absorber, e.g., of porous concrete, between the charge and the concrete shielding. The effect is completely eliminated by adding to the structure, on the external surface, a thin stainless steel sheet, which also stops the smallest fragments of the structure. This device has been the subject of a patent request, and has been suggested as a possible shielding for the SORA reactor. During the research carried out to achieve these findings, various phenomena were observed which are summarized briefly as follows:

a) damping of the pressure wave as it passes through the concrete structure, with conservation of the momentum (Fig. 1);
b) effect of the way in which the reinforcing steel is deployed: advantage of a minute distribution of the steel.

Using this latter piece of information, we planned an experiment, which is now being prepared, in which the metal reinforcements consist of capillary threads of steel (diam. 0.3 mm, length 25 mm), distributed throughout the concrete. Tests on this type of structure will be performed as before, always using the system of loading by explosive charge.

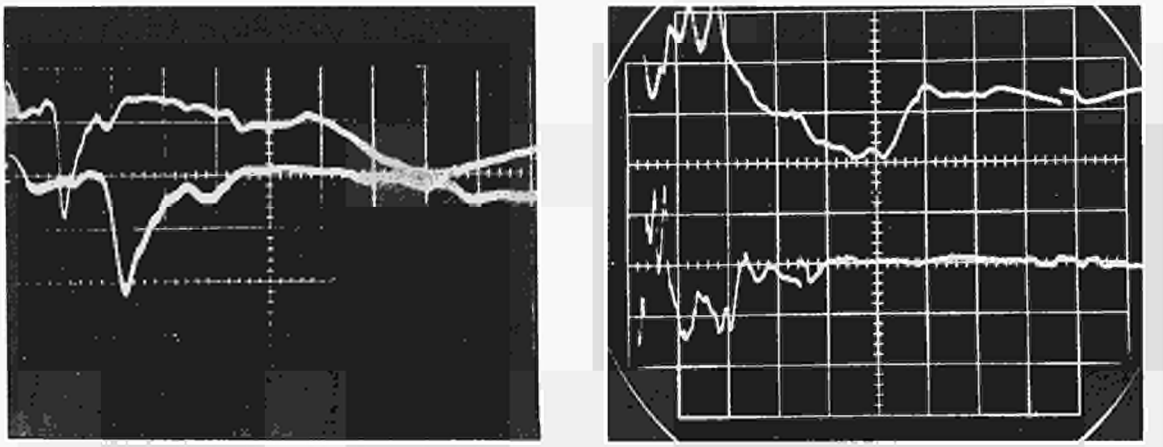

Fig. 1: Damping in the concrete.

Dynamic Stress-Strain Diagram of Metallic Material Subjected to Tensile Stress

For calculations on the deformability of a structure subjected to an impulsive load, one must know the dynamic stress-strain diagram of the material, above all under tensile stress. Diagrams of this type have been obtained by various research workers in the past, but one problem has not been dealt with in enough detail, and that is the measurement, instant by instant, of the "true" resistent section of the test-piece, given the difficulty of recording the section of a test piece in very limited times of the order of microseconds. In order to do this, we developed an apparatus which will permit the synchronization of the deformation measurements with a fast camera, which is able to photograph, precisely in the range of times desired, the resistent section of the test-piece. In order to synchronize the fast camera with the event, we used as loading system an explosive charge, detonated by an electric detonator with a known time delay. The principle of this apparatus is that described by Hopkinson [6]. The rod is used to transmit a wave of sufficient intensity to deform and break the test-piece which forms the connection between the two parts of the rod. The intensity and duration of the pulse must be such as to produce the desired deformation speed. On the two parts of the rod deformation measurements are carried out, by means of which the operative stress and the deformation speed can be calculated as shown in Fig. 2.

The wave of tension originating at extremity A reaches the measuring element 1, which consists of an electric semi-conductor strain-gauge. The level of the wave does not exceed the elastic limit in the rod, so that Hooke's law remains valid for the rod itself. Continuing the course, the wave reaches the extremity a) of the test-piece and is partially reflected, and the value of this reflected wave is recorded by the measuring element I.

The wave, deforming the test-piece, reaches extremity b) and subsequently the measuring element 2, and then continues along the rod. In element 2 the value of the operating force is measured, still in the field of validity of Hooke's law. If we accept that the particle velocity at extremity a) is equal to that of the extremity of the first elastic half-rod, and the velocity of the extremity b) is equal to that of the extremity of the second half-rod, we have:

$$V_{1.2} = \frac{\sigma_{1.2}}{\rho c}$$

in which V is the particle velocity, σ the stress, ρ the density, and c the speed of sound.

It is also true that

$$\epsilon' = \frac{V_1 - V_2}{\ell}$$

where ϵ' is the deformation velocity and ℓ the length of the test-piece.

By integrating this expression with respect to time, we have the total deformation of the test-piece. Thus the complete analysis of the stress-strain diagram can be done with simple measurements of the operating stress carried out with the two semi-conductor strain-gauges. In order to take the restriction of the section into consideration, however, the measurement of the deformation is repeated with a fast camera.

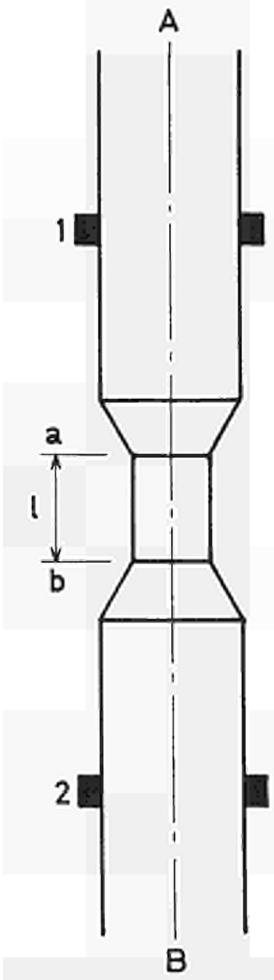

Fig. 2: Principle of the test method.

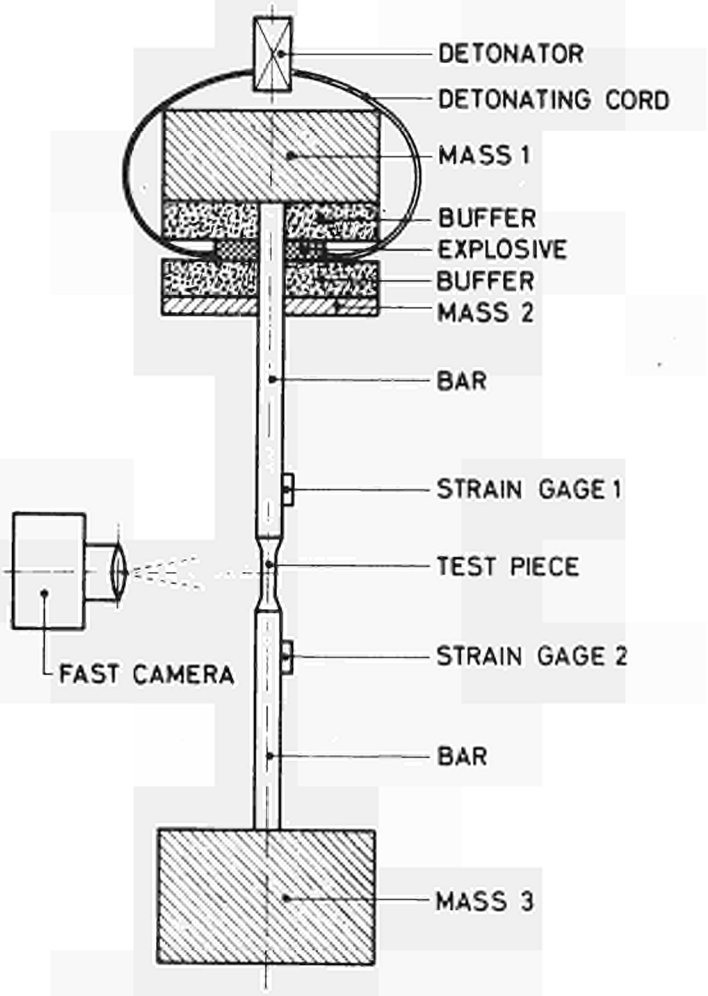

Fig. 3: Device of dynamic tests with explosives.

We said earlier that this method is valid if the velocities of the extremities of the elastic rod are equal to those of the two extremities of the test-piece. This situation can be obtained if the operating pulse is long enough compared with the test-piece, and the value of the pressure sufficiently uniform throughout the entire duration of the test. This condition, which is not easily obtained, given the complexity of the geometry of the test-piece and its attachments and the high deformation velocities required, was achieved by means of a device which will be described in the following paragraph.

An explosive charge (Fig. 3) is detonated between two buffers composed of porous rubber. The buffers serve to cut off the top of the detonation peak and convert it into an even pulse having a lower pressure value and a sufficient duration to fulfil the condition we mentioned above as being necessary to the validity of the experiment. The pulse duration is regulated by the quality and thickness of the buffers, but also by the mass 2, which acts as a moving breechblock. The test proceeds, as already described, with the propagation of the tension wave along the rod. The second half-rod has to be of such a length that the wave reflected from mass 3 will not reach the test section before the test is completed, i.e., before the test-piece breaks. The strain-gauges used are of semiconductor type 1 MP H1E BNr410, 120 Ω, K = 120; there are two of them to each position, mounted opposite one another at 180° and connected in series, so as to compensate for any deflection of the rod.

The strain-gauge values are read on dual-trace oscillographs, 556 TEKTRONIX type. The fast camera used to check the deformation values, is of the CORDIN rotating-mirror type.

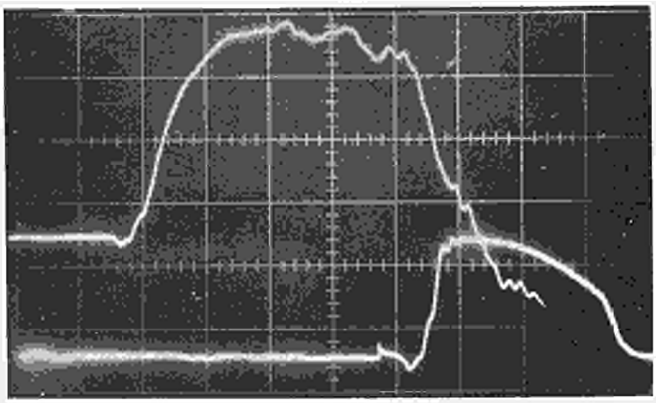

↑ 11,8 kg/mm^2/square
→ 50 μsec/square

↑ 2,36 kg/mm^2/square
→ 50 μsec/square

Strain-gauges records:
- higher trace: strain-gauge 1
- lower trace: strain-gauge 2

Fig. 4: Hopkinson split-rod system.

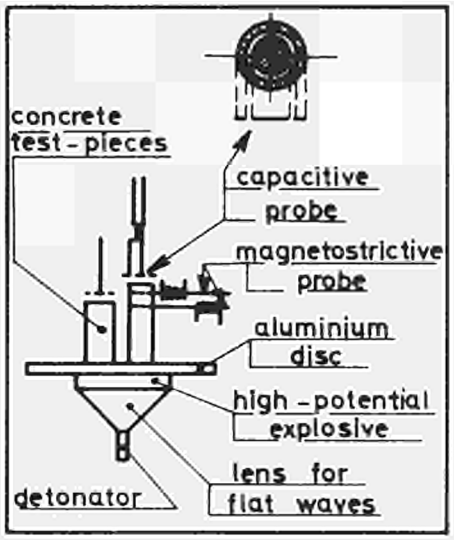

Fig. 5: Device for determining the equation of state of concrete.

Fig. 4 shows the recording of a measurement done on an ARMCO steel test-piece of diameter 3 mm and length 5 mm in the test section.

Since the elastic limit of the material forming the rod is about 100 kg/mm^2, the maximum wave intensity obtainable with the system described is sufficient in theory to achieve deformation velocities of up to 10^5 sec^{-1}. In the tests run to date deformation velocities of $1.5 \cdot 10^3$ sec^{-1} have been attained, as required for our reactor safety experiments.

As it is intended to explore a lower range of velocities (between 10^2 and 10^3 sec^{-1}), a second device is being developed, in which the same principle is applied but the loading system is a shock wave from a shock tube. This device is not described here.

The progress of this research will be reported [7] at the AIAS Conference at Palermo on 4-7 April 1972. The devices have been the subject of an application for patent.

Equations of State of Reinforced Concrete Subjected to High-Intensity Pulse Loading

To ascertain the energy that can be absorbed by the biological shield in the event of a fast-reactor accident, the following (Rankine-Hugoniot) equations are used. They can be solved when the wave velocity U_s and the particle velocity U_p are known:

- conservation of mass
- conservation of momentum
- conservation of energy.

In the experiments to determine the equations of state, the test-piece is stressed by a high-intensity pulse produced by an explosive (Fig. 5) or a high-pressure shock tube (reflected wave pressure 5000 atm), which is now under construction.

The test-pieces, of diameter 50 and height ranging from 150 to 350 mm, are of dimensions similar to those used for the preliminary calibration in the static state.

In the extreme case of an infinitesimal deformation in the event of a shock wave, the following relation is valid:

$$U_p = U_r = U_{sl}$$

in which U_r = velocity of the reflected wave,
U_{sl} = velocity of the free surface.

The velocity of the free surface is measured with the capacitive probe shown in diagram in Fig. 5. The two concentric windings of this probe are applied end-on to the free surface [8]. The movement introduces a change of permeability in the zone traversed by the electric lines and hence a change of capacity. This change is independent of the velocity, so that static calibration can be done.

This system can be applied even to non-conducting materials such as concrete and enables the velocity of the concrete surface to be measured without having to pass through a conducting element.

U_p and U_s can also be measured with strain-gauges, by the following method. The sensitive element is placed in the direction in which the velocity is to be measured, with one of its ends positioned on the point under study. Thus the strain-gauge must be composed of a wire with cross-section and characteristics constant over its entire length so that an element of length dz will have a resistance dR = rdz, in which r = R, where L_O is the length of the strain-gauge prior to the shock and R is its resistance.

At any given instant t at which the disturbance front reaches position Zt with a given distribution of ϵ in the length $0 \div Zt$, the strain-gauge resistance can be written as:

$$R_t = \int_o^{Zt} r(1 + K\epsilon)\, dz + \int_{Zt}^{Lo} r dz = \int_o^{Lo} r dz + rK \int_o^{Zt} \epsilon dz = R_0 + rK\, \Delta L$$

Deriving with respect to time, we obtain:

$$\frac{dR}{dt} = Kr \frac{d\Delta L}{dt} = r K V$$

in which V is the relative velocity of the two ends of the sensitive element.

The expression written here indicates that the time derivative of the resistance of the signal, is proportional to the relative velocity of the two ends of the strain-gauge.

As only one end of the strain-gauge is affected by the passage of a wave, the signal given by the strain-gauge is proportional to the velocity of the other end and hence to the velocities of the particles anchored to it. This system has already yielded satisfactory results, which were communicated [3] to the Conference on Structural Mechanics in Reactor Technology, Berlin, September 1971.

References

1) UKAEA TRG 1062 (C)

2) G. Fratus, M. Montagnani, I. Quirino, Essais de la déformabilité du Zircaloy-2, Paris, 1972. L'Hydrogène dans les métaux.

3) C. Albertini et al., Energy Absorption by the Concrete Biological Shield under Shock Loading. Berlin, 1971 - *Structural Mechanics in Reactor Technology.*

4) B. Hopkinson, 1914, Phil. Trans. Roy. Soc. A 213, 437.

5) R.M. Davies, 1948, Phil. Trans. Roy. Soc. A 240, 375.

6) U.S. Lindholm, Some Experiments with the Split Hopkinson Pressure Bar, Pergamon Ltd., Press 1964.

7) C. Albertini, M. Montagnani, Diagramma Sforzo-deformazione al μ secondo. Conferenza AIAS - Palermo, 4-7 April 1972.

8) V. Andrighetti, L. Verheyden, Trasduttore capacitivo adatto per la misura di spostamento di corpi conduttori e non conduttori, *Ingegneria Meccanica, anno XX,* novembre 71, No. 11.

LIQUID CONTROL RODS

A. Agazzi, A. Broggi, S. Galli de Paratesi

Introduction – Main lines of the EULER PROGRAMME

The fairly recent developments in the nuclear reactor control field concern the design and construction of shut-down systems presenting very simple structure and reliable operation for the safety rods and related mechanisms in the core and the surrounding area. In some water reactors it has proved difficult to find a satisfactory solution for the installation of safety rods because of the lack of available room in spaces above and below the reactor and the intricate configuration of coolant-tube inlets – and – outlets.

To overcome these and other difficulties liquid poison shut-down systems of new conception have been under development at the Ispra JRC since 1966 in connection with the Community Water Reactor programmes. This activity has been given the name of the EULER Programme [1].

The studies began with the evaluation of several possible systems. Mock-ups were erected to test the feasibility and the dynamic performance of the two chosen systems, termed "bubble tube" and "gravity drop". In both of them, the liquid rods consist of empty tubes passing through the core, which are filled with a suitable "neutron poisoning" solution every time an emergency shut-down is required. It is easily seen that this operation is far easier and safer than dropping a solid rod into a guide tube. Liquid rising in a pipe cannot stick to the walls, even if these are rough or corroded. Even a distorted or ovalized tube cannot prevent the correct shut-down. Thus the frequent cause of dangerous troubles with rods simply does not exist in liquid rod systems, and this is a big advantage from a safety stand-point.

In some reactors the free space between the chanels, especially at the channel ends, is so limited that a suitable arrangement of solid rods would be feasible only by removing an equal number of fuel elements. But calculations have shown that this would entail an unacceptable loss of power (e.g., 8% for a 250 MW_t reactor).

Therefore from the designer's view-point liquid rods are attractive on account of the following exclusive properties:

a) easy penetration through intricate primary circuit configurations,
b) flexibility of adjustement to any route inside the core and in the adjacent zones,
c) saving of out-of-core space to a height at least equal to that of the active zone, which would be needed to hold solid rods in readiness,
d) ease of access to the various system components during reactor operation.

The goals of the different stages of the feasibility research were achieved and attractive prospects for applications to specific reactor designs opened up.

In 1968 the design of a 36-rod shut-down system for a 250 MW_e power plant was developed in collaboration with industry, in the context of the ORGEL prototype call for tender. The exploitation of the Euratom patents and related know-how was officially requested by the French CGE – Babcock Atlantique Industrial Group and an agreement to this effect was signed in 1970 with the Commission. In this frame-work a joint project was developed up to the first months of 1971 by the firm GAAA and the Ispra staff, the purpose being to design a liquid rod system for an advanced 600 MW_e thermal power plant.

As far back as 1966 the Italian CNEN and CISE had also confirmed their joint uninterrupted interest in Ispra's work on liquid rod systems. This interest mainly concerns the applications for the CIRENE Project, and the related activities have been financed by the Association Contract CIRENE III-008.

Hence the EULER programme was run during 1971 along both internal and external guidelines, pursuing three definite projects.

"Gravity-Drop" Multi-Rod Project

This full-scale prototype was completely designed and constructed by the Ispra JRC, the reference specifications being those for the liquid rod shut-down system which will actually be installed in the fog-cooled heavy-water-moderated CIRENE reactor. It is a fully instrumented out-of-pile facility of the "gravity drop" type, having a liquid level difference of about 14 m for its 46 mm diam. in-core tubes [4] (see Figs. 1 and 2).

The system is shown in Fig. 3. It is based on the principle of the U-tube in a similar way to the "gas balancing system" introduced into some Canadian reactors to drop the moderator level in the case of emergency.

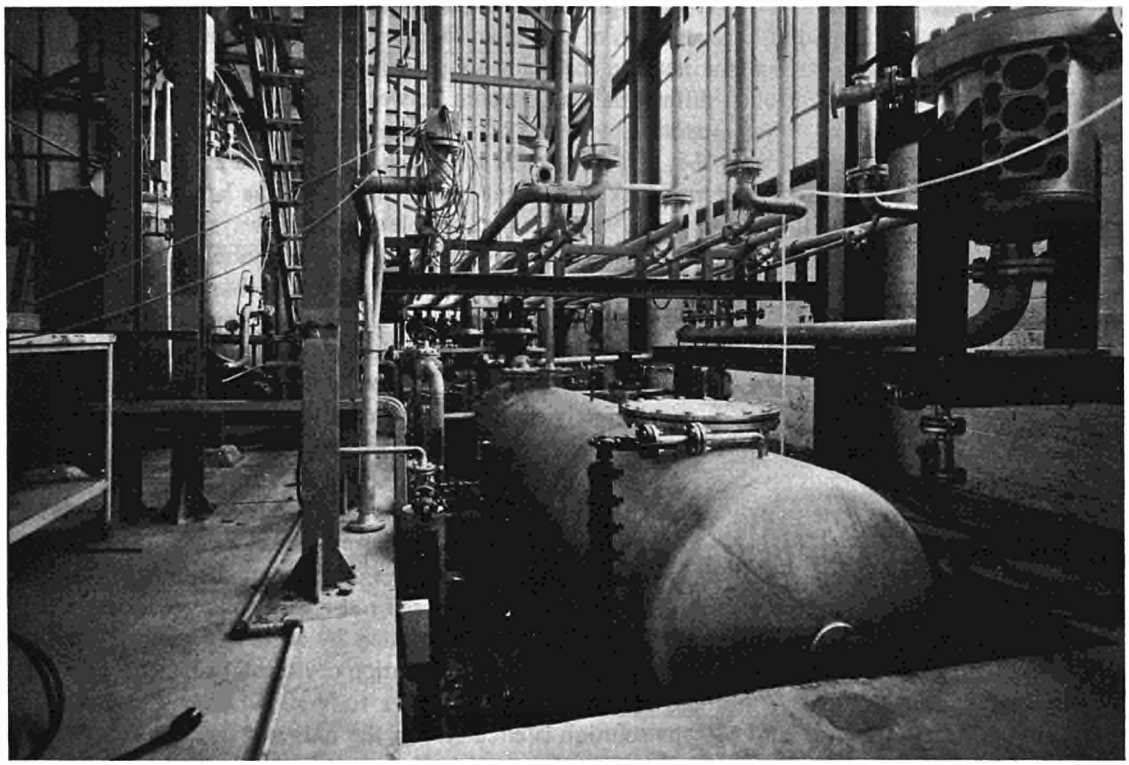

Fig. 1: Gravity-Drop prototype for the CIRENE Reactor.

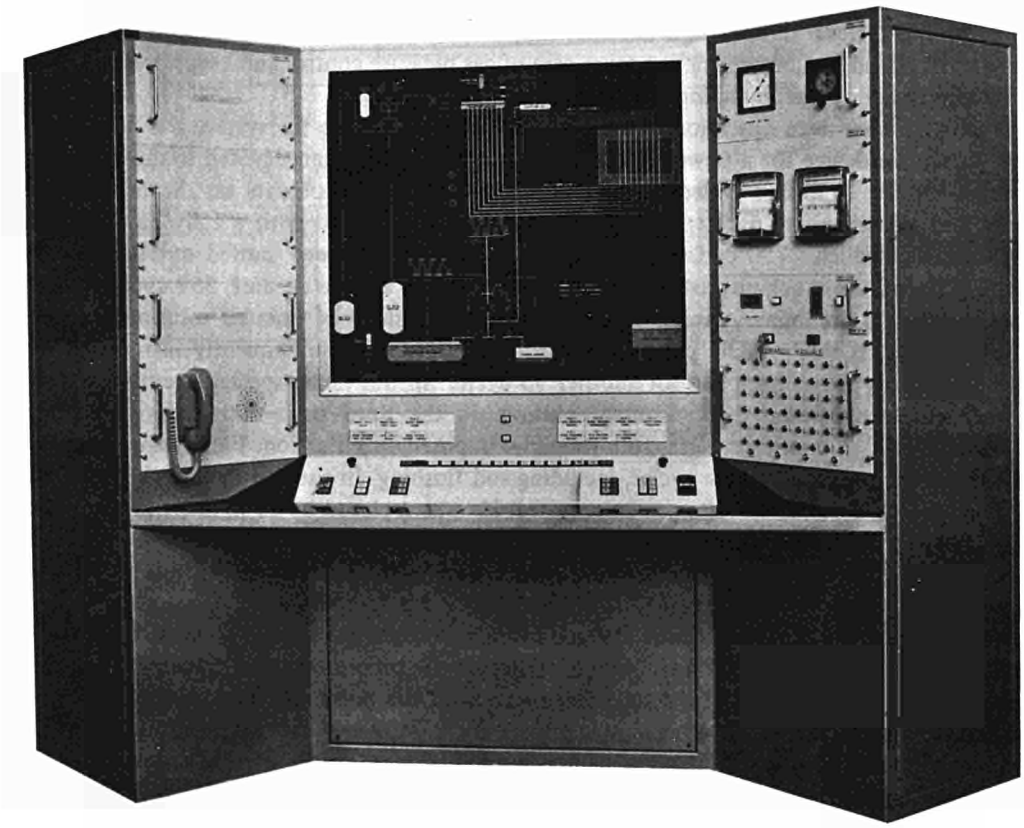

Fig. 2: Control console for automatic operation of the gravity-drop prototype.

In our case the application of that concept concerns small quantities of poisoning solution in independent in-core tubes, instead of large amounts of D_2O in an chamber surrounding the calandria.

During normal reactor operation, the neutron-absorbing solution is held out of the reactor core (at normal level) by means of a controlled differential gas pressure between the header tanks T-1 and T-2. Automatic fast valves V-1 through V-6, operated by means of a 2-out-of-3 logic, are energized and closed.

The level is controlled through valve V-8, in a very simple way. That valve is opened and injects a small quantity of gas into the rod system and into tank T-5 via the header tank T-2. The latter is an auxiliary device, mounted in parallel with the rods in such a way that the liquid level in it is always the same as in the rods. The gas injected through V-8 is continuously transferred from T-5 to T-1, bubbling in the vertical connection pipe. If, owing to system leakage or upset, the pressure in T-2 drops and thus allows the level in the rods and T-5 to rise, the extremity of the bubbling tube closes, so allowing the pressure in the rods to be restored to the set value, and the level will return to normal value. If, on the contrary, a system upset causes the pressure in T-2 to rise, the level in the rods and in T-5 goes down and thereby causes the extremity of the bubbling tube (which is appropriately shaped) to open wider, allowing the discharge of more gas until the normal level is restored. This kind of level control has proven very precise, and extremely reliable because no control loop is involved.

Shut-down action by simple gravity drop is performed by opening valves V-1 to V-6, and the rods are filled with solution up to the header T-2. At the moment of shut-down, valve V-8 is closed.

Each rod is a part of an independent loop. An automatic stop valve is placed at the bottom (i.e., the lowest point) of each loop, valves V-9-1 to V-9-N. The bottom of each rod is also connected to a second, smaller-diameter loop, the purpose of which is to circulate the solution by means of pump P_2 during reactor normal operation in order to prevent any possible deposit formation or irregular concentration. The bottom of the circulation loops is also provided with valves, V-10-1 to V-10-N. After shut-down, by opening valves V-16, V-15, V-12 and V-9 the solution is circulated in the rods and through the solution tank T-3 by means of pump P-1, to prevent it from over-heating by gamma irradiation in the in-core portion of the loop. With all valves closed again, the level controller can be re-energized and the rods withdrawn to their normal working level.

The rods can be flushed out before resetting the system. Of course, this operation requires the reactor to be put in a safe state by other means than the liquid rods, e.g., by lowering the moderator level. The solution is discharged into tank T-3 by opening valves V-9, V-10, V-11 and V-15. Then valves V-11 and V-15 are closed, V-13, V-14 and V-16 opened and demineralized water is admitted to the bottom of the loops and discharged via T-2, V-16 and V-14 as long as is required to clean the residual solution out of the rods. By closing V-13 the system can then be drained, and by closing V-11, opening V-12, and energizing V-1 to V-6 and the level controller it can be refilled with solution by means of pump P-1. Once the normal level in T-1 is reached (level in the rod is automatically controlled) the pump is stopped, all valves closed and the system is reloaded. Compressor C-1 takes care of gas pressure control and keeps pressure in T-1 and T-3 near the atmospheric value, pumping into accumulator tank T-4.

The prototype came into operation at the beginning of 1971. Since the system is a novel fast-acting emergency shut-down device for a power reactor, much attention has been devoted to the different stages of operation. In order to ensure collection of the maximum quantity of data on the behaviour of the components and the assembly as a whole, the prototype was provided with a fully automatic control system by means of which 2750 cycles of operating sequences have been carried out to data. For the general setting up of the mock-up instrumentation and the test automatic unit, 559 cycles without rod flushing were run as a preliminary, using demineralized H_2O instead of borated solution and air as the monitoring gas. The H_3BO_3 - LiOH poisoning solution and N_2 were subsequently introduced into the circuit and the prototype has been run for another 90 cycles. In this phase special attention was given to the instrumentation concerning the poisoning solution. In the third stage 500 automatic cycles were executed with helium as monitoring gas, following the imposed specification. Finally the prototype was satisfactorily run up to 300 complete cycles, including rod flushing. In the end the possibility of using O_2 as monitoring gas was considered. As a preliminary test He was replaced by air in order to approximate as closely as possible to the actual operating conditions with O_2 and 1350 automatic cycles have been performed. Circuit degreasing and operation of the mock-up in the presence of 0_2 will be performed in 1972.

The system has given confirmation of the good dynamic behaviour predicted by the NIAGARA PG digital code, by means of which the optimum selection of the geometrical and physical parameters was determined at the design stage. The total time for insertion of the poisoning solution into the rods, with helium as monitoring gas, is 985 ms using simple gravity for a 4500 mm core height. For shorter insertion times a high-pressure booster at $\sim$ 10 Kg/cm^2 is employed (660 ms). The theoretical displacement vs. time curves agree with experimental results to within 5 %. As a result of the above 1971 operating experience

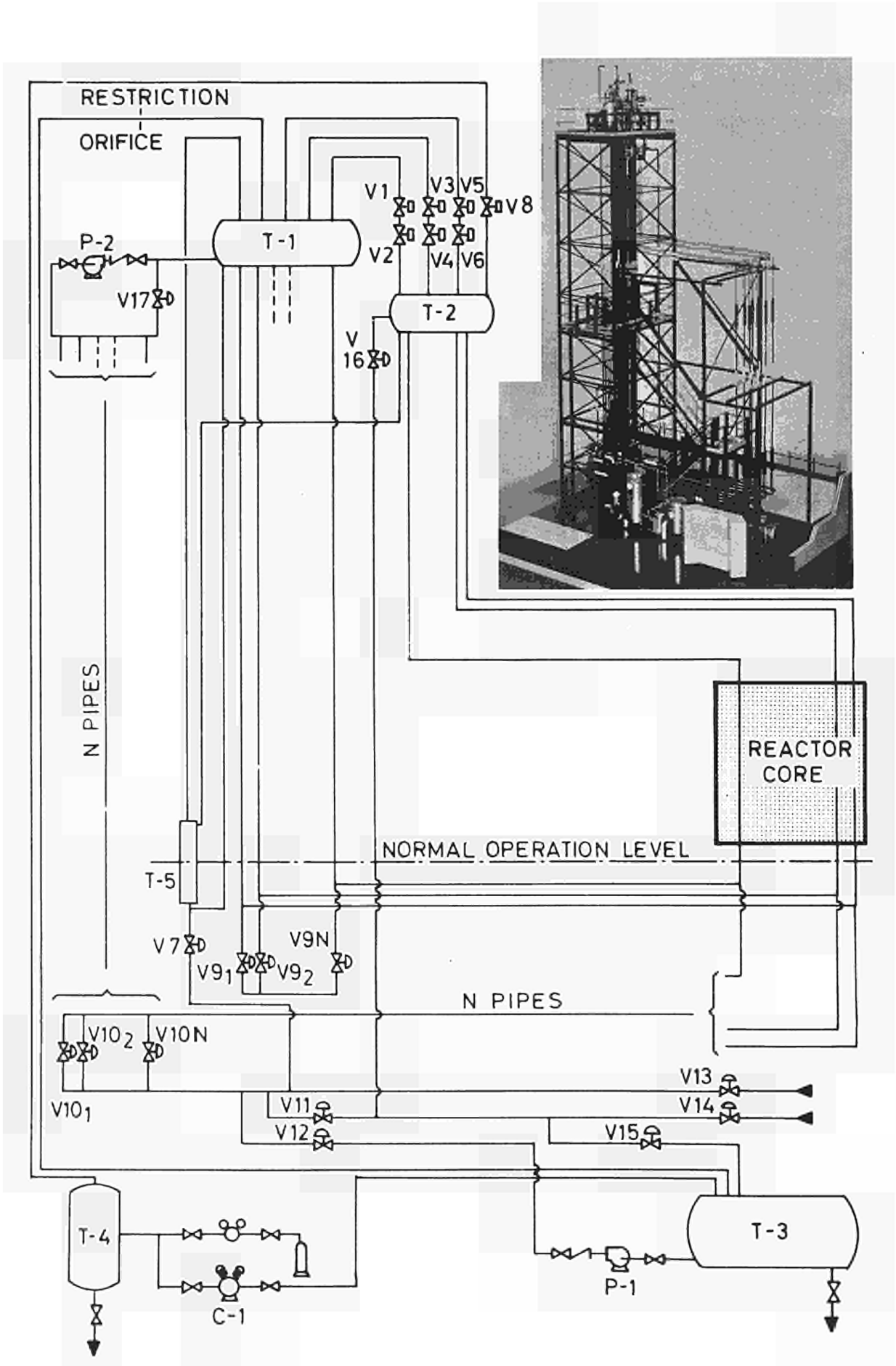

Fig. 3: Flow-sheet of the out-of-pile prototype for the CIRENE Reactor.

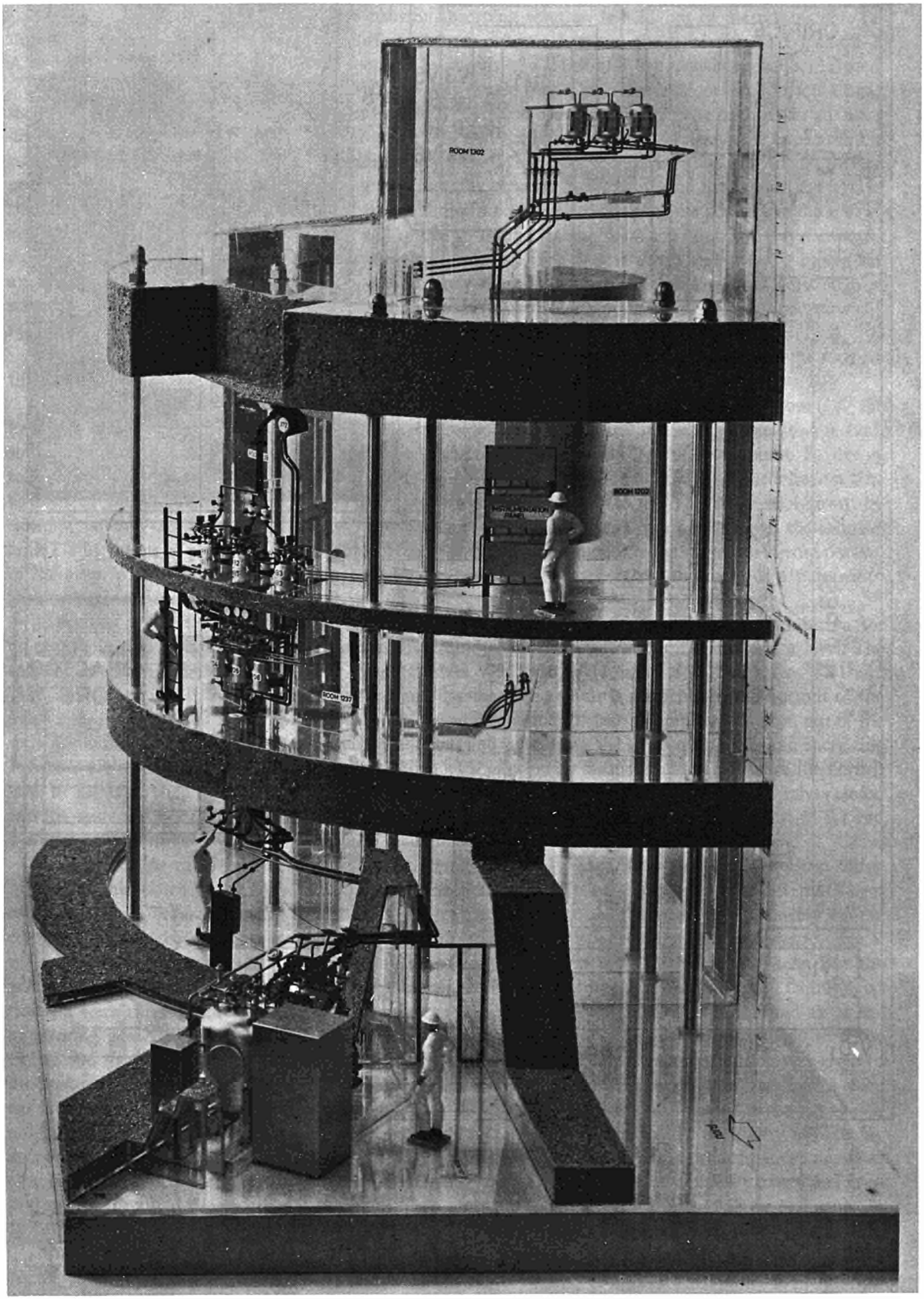

Fig. 4: View of the "bubble-tube" shut-down system in the Essor Reactor.

some useful modifications will be introduced in 1972 for the prototype, mainly concerning flushing, gas and radiolysis-product evacuation circuits and related operation.

CHARLES Project

This project deals with the application of a "bubble tube" system to the ESSOR reactor [3]. The system will be mounted in the core alongside the existing solid rods. Owing to its very fast intervention time it will be possible to intervene before the core fuel elements are damaged by dangerous accidents occurring in connection with particular experiments.

The system, consisting of three circuits of two rods each, will be a major confirmation of the forecast which assigns to liquid rods an indispensable role wher there are problems of bulk, penetration and fitting with already-existing structures (Fig. 4).

In 1971 the electronic control of the system, fully automatic with logical microcircuits, was built and tested by our laboratories. The out-of-pile test loop "OSSO", reproducing the path of the group of liquid rods regarded as the slowest, was succesfully operated during the first six months of 1971. The liquid poison insertion time of 280 ms versus a 230 cm core height confirms the calculations performed by the NIAGARA TB digital code. A special scroll-type hydrodynamic diode has been chosen as a braking device at the rod outflows. The mechanical construction of the loop will be ready by Jan. 1972. Operation of the system will start in the second half of 1972 in accordance with the ESSOR schedule.

CECILE Project

By means of the irradiation loop CECILE, which is being mounted in the Ispra-1 reactor, important data will be gathered on the in-core corrosion behaviour of the Zircaloy stainless steel joints connecting the rod tubes to the rest of the circuit. For this puropose three types of joints, (which are in general located in line with the top and the bottom reflectors) have been proposed: two of metallurgical type obtained by explosion or extrusion, and one of mechanical type, obtained by rolling.

The particular conditions of the contact of the bimetallic welding with a solution of boric acid in water under irradiation will be reproduced in the CECILE loop in order to investigate whether corrosion may arise from the coupled action of electro-chemical and radiation effects.

In 1971 each type of joint was submitted to bench mechanical tests. The experimental circuit, equipped with the instrumentation for fully automatic running, has been constructed and the installation in the reactor is nearly completed. The schedule for the first months of 1972 covers tests on the control system, preparation and introduction of the experimental set of joints into the reactor channel, and the subsequent start-up. The first results are expected in 1973.

References

1) A. Agazzi, A. Broggi, S. Galli de Paratesi "EULER-Liquid Rods for Nuclear Reactor Control" *Eurospectra* V.9 No, 3, Sept. 1970.

2) S. Galli de Paratesi, L. Ghiurghi, H. Musik "Reliability assessment of a Novel Liquid-Rod Shut-down System". 3th CREST Meet. RISO 1969

3) A. Broggi "Reattore ESSOR-Impianto a Barre Liquide" (not available)

4) A. Agazzi, A. Broggi, G. Cordani, S. Galli de Paratesi, L. Ghiurghi "Engineering & Control Characteristics of a Liquid Multi-rod Scram Prototype" to be published in *Nuclear Applications & Technology.*

THERMAL ANALYSIS OF FUEL ELEMENTS

Nijsing, Eifler

General

The studies briefly described here are part of a basic research programme related to flow and heat transfer in liquid-metal-cooled fuel rod assemblies. This research programme centres on the acquisition of fundamental knowledge on turbulent transport mechanism in rod-bundle geometries and on the development of universal hydrodynamic and thermal computation methods in which use is made of this knowledge. The aim is twofold:

a) to make methods available that can be used for accurate thermal analysis pertaining to conditions of normal reactor operation;
b) to acquire information on flow and heat-transfer effects associated with anomalous fuel element behaviour. This anomalous behaviour which may ultimately lead to serious fuel element damage may involve channel deformations (due to swelling), fuel rod bowing and subchannel blockages.

The experimental research on turbulent transport properties is conducted with water as the working fluid. Results of separate experimental studies with liquid metals in simple geometries, carried out outside the Ispra laboratory, are employed for evaluating interactions between turbulent and conductive modes of heat transport.

During 1971 emphasis was on the following subjects of research:

- Two-dimensional velocity and temperature fields in assemblies of bare fuel rods;
- Subchannel thermohydraulic analysis of fuel-rod bundles;
- Flow and heat-transfer effects in rod assemblies with partially blocked subchannels.

A start was also made on the development of computation methods to be used for the determination of three-dimensional temperature fields in rod bundle geometries.

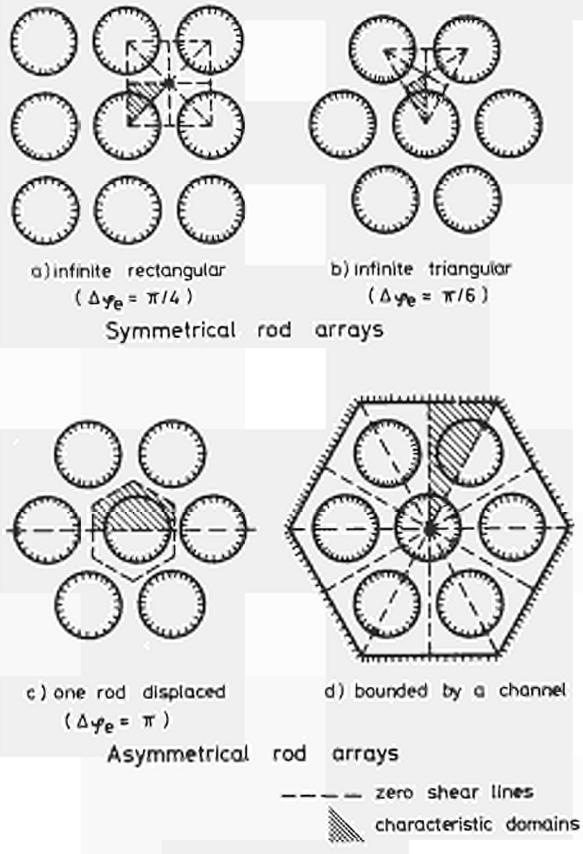

Fig. 1: Typical rod arrays.

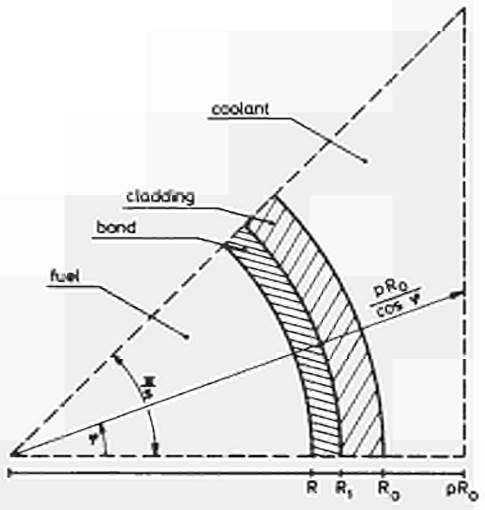

Fig. 2: Characteristic domain of infinite rod array.

Two-dimensional velocity and temperature fields in assemblies of bare fuel rods

Methods have been developed for theoretically predicting two-dimensional velocity and temperature fields in assemblies of smooth fuel rods under conditions of fully developed flow and heat transfer. Typical rod arrays are represented in Fig. 1. Symmetry considerations may be applied to restrict the attention to "characteristic domains" of such arrays. For the case of an infinite array such a domain is represented in Fig. 2. A first step in the analysis is to set up momentum and heat balances on a volume element in the coolant region as is shown schematically in Fig. 3. This leads to momentum-flux and heat-flux differential equations. Making use of experimental knowledge regarding turbulent diffusion and secondary flow, it is possible to find the solution for the momentum flux field and the velocity field by a rapid mathematical procedure. This procedure, of analytical nature, involves the subsequent radial and circumferential integration of the momentum flux equation. The wall shear stress is represented in terms of a Fourier series. The coefficients of this series are then determined by applying the integrated momentum flux expression at a finite number of circumferential positions in the caracteristic domain ("point matching"). The determination of the velocity field then is straightforward [1) 2) 3)], give the details of this procedure. The solution of the heat transfer problem proceeds along similar lines. The already established velocity field is used as input information. Additional account needs to be taken of heat conduction in the solid materials region (fuel, bond, cladding) for which an analytical Fourier-type solution is available. The solution for the temperature field in the entire region is found simultaneously ("multiregion analysis") by applying continuity of heat flux and temperature at the boundaries between the various regions. Details of the method are presented in [1)].

The experimental programme is aimed at acquiring basic information on turbulent transport properties (turbulent diffusivities, secondary velocity) in regular arrays. A typical test section cross-section is shown in Fig. 4. The test sections are mounted vertically in a water circuit and velocity and temperature distributions are measured at the open test-section outlet, using pitot and thermocouple probes. For the heat transfer case, use is made of special heating rods provided with an electrochemically deposited metal layer in which electric current generates the heat.

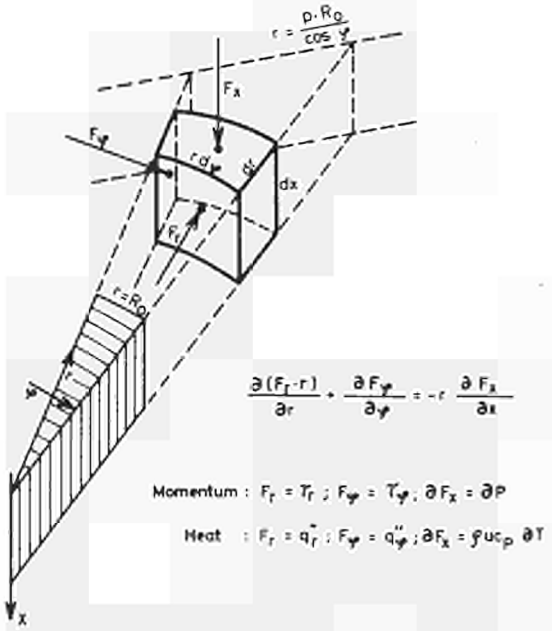

Fig. 3: Momentum and heat balances on a volume element in the coolant region.

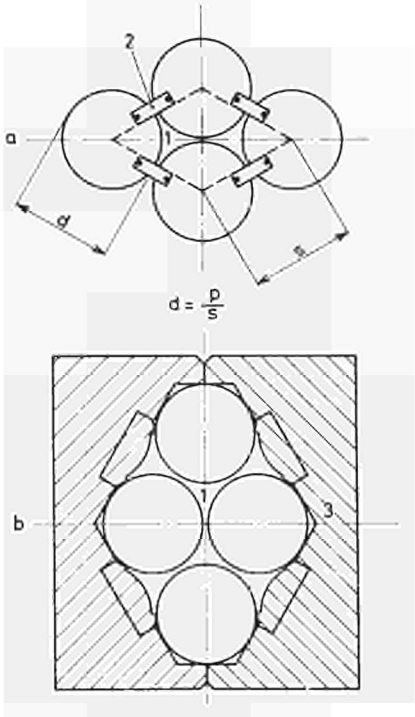

Fig. 4: Cross sections of test sections for hydrodynamic and heat transfer studies.

In the experiments carried out during 1971 the emphasis was on very closely spaced rod assemblies (pitch-to-diameter ratios of 1 and 1.02). One of the reasons for interest in this close rod spacing is connected with the fuel rod bowing phenomenon. A typical result for a circumferential velocity variation in a triangular rod array with a pitch-to-diameter ratio of 1.05 is given in Fig. 5. In the figure η denotes the ratio of a radially averaged coolant velocity (at a given circumferential position) to the bulk coolant velocity. It is seen that the theoretical prediction based on anisotropic turbulence and on the existence of secondary flow closely agrees with the experimental data. A typical result of a theoretically established velocity field in the corner region of a hexagonal fuel channel is shown in Fig. 6. Theoretical heat transfer predictions for liquid-metal-cooled rod assemblies with a triangular array are presented in Figs. 7-10. Fig. 7 deals with the variation of the Nusselt number ($\alpha_{av}\, d_e/\lambda_c$) as a function of the pitch-to-diameter ratio p for a Reynolds number of 100000 and a Prandtl number of 0.0045. It is observed that the heat transfer coefficient for the boundary condition of uniform surface temperature always exceeds that pertaining to the boundary condition of uniform wall heat flux. At rod spacings beyond p = 1.15 heat transfer predictions are almost independent of the thermal boundary condition and they differ only slightly from those based on the simplified "equivalent annulus" approach. Additionally Fig. 7 shows that the "slug flow" heat transfer predictions differ significantly from those for turbulent flow. The effect of turbulent heat transport in the coolant region on circumferential cladding temperature variation is shown in Fig. 8. It is seen that with a liquid metal coolant, turbulent diffusion significantly attenuates circumferential temperature variations. The effect of secondary flow is much less significant. In this connection it is worth noting that the velocity distribution underlying the calculations is very greatly affected by secondary flow. Fig. 9 presents information on circumferential variation of temperatures in the coolant region and at the outer cladding surface. It is seen that for a pitch-to-diameter ratio p = 1.05 the radial temperature variation in the coolant is much less important than that in the circumferential direction. Amplitudes of circumferential cladding temperature variations are given in Fig. 10 as a function of the Peclet number for a triangular array with p = 1.10. Good agreement is observed between the theoretical predictions and the experimental data of Subbotin et al. in the Peclet number range 20 - 600.

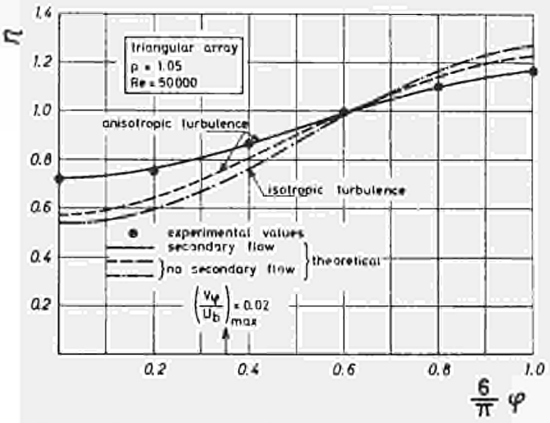

Fig. 5: Circumferential distribution of dimensionless velocity.

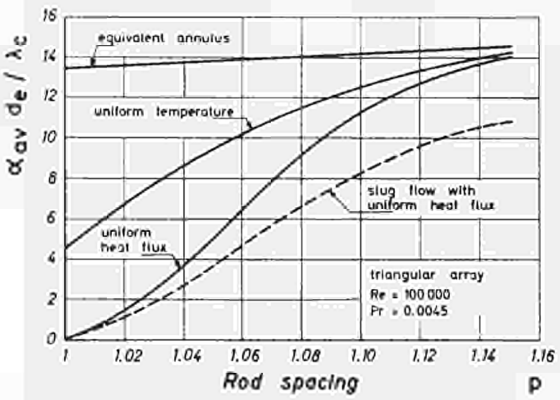

Fig. 7: Variation of nusselt number with rod spacing.

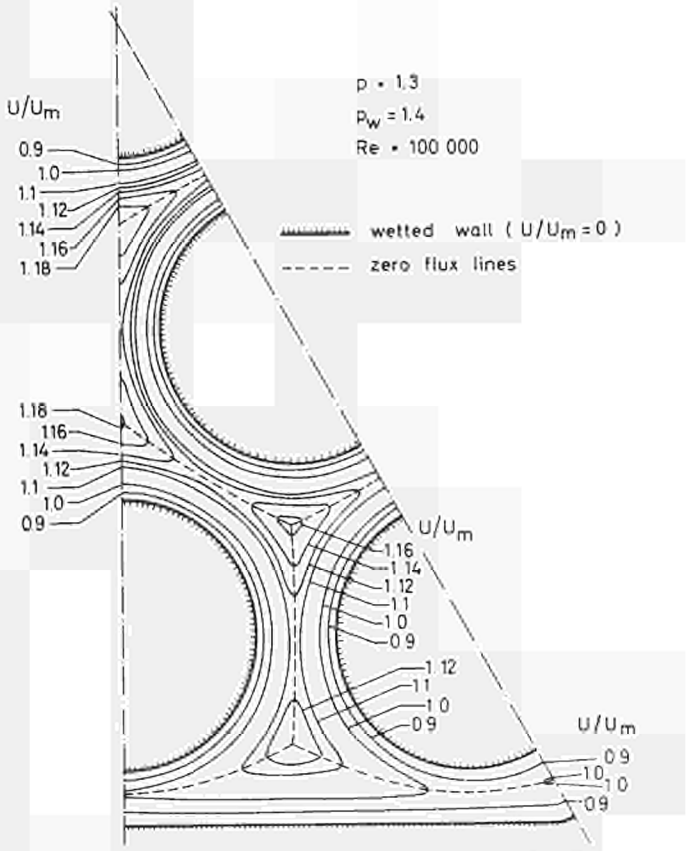

Fig. 6: Velocity distribution in a nineteen-rod bundle, example A.

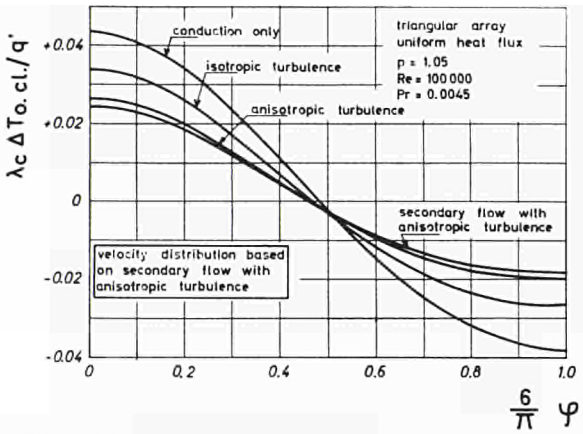

Fig. 8: Effect of turbulent heat transport on circumferential cladding temperature variation.

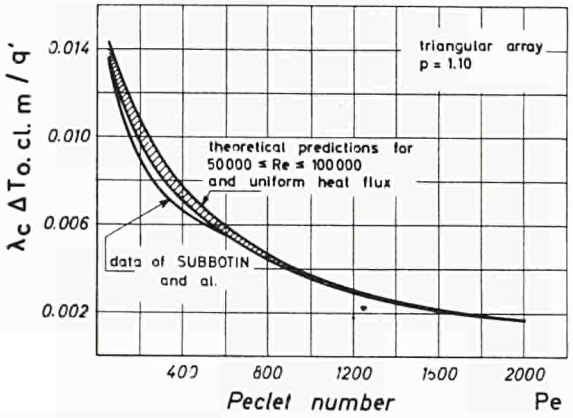

Fig. 10: Etude of circumferential cladding temperature variation.

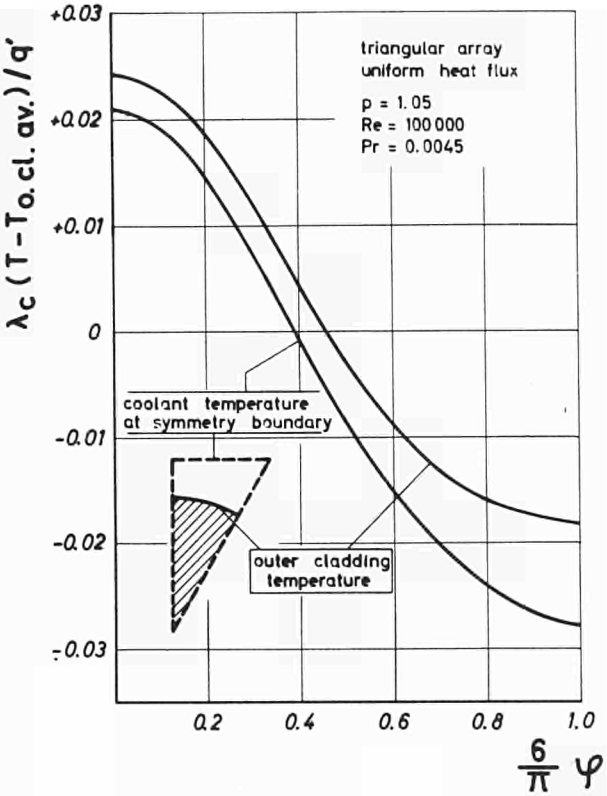

Fig. 9: Circumferential variations of outer cladding temperature and of coolant temperature.

Subchannel thermohydraulic analysis of fuel rod bundles

When fuel channels contain a very large number of rods provided with spacing elements (helical wires or grids) and it is desired to establish the spatial temperature distribution, a convenient computational approach is that based on the subchannel concept. In 1971 a computing method (called "HERA") was completed which is based on such an approach, according to which the bundle flow area is subdivided into a number of subchannels in which hydrodynamic and thermal coolant conditions are characterized by bulk average values. To evaluate the subchannel flow and temperature distribution the momentum and energy conservation principles are applied and appropriate account is taken of hydrodynamic and thermal interactions between subchannels.

The solution for the subchannel coolant temperature distribution is obtained analytically, involving the solution of an algebraic eigenvalue problem. This is an advantageous feature which distinguishes the "HERA" computation method from other thermohydraulic codes based on the subchannel concept. The method has been described in Ref. [4]. In Ref. [4] illustrative calculations are presented dealing with the effect of a strong lateral power gradient on subchannel coolant temperature distribution in a 217-rod hexagonal liquid-metal-cooled fast assembly. Fig. 11 and Table 1 illustrate the conditions considered.

Table 1

Total number of rods	217	Coolant inlet temperature	400°C
Fuel rod length	1 m	Coolant outlet temperature	600°C
Outer rod diameter	6 mm	Av. Reynolds number	63000
Rod-rod spacing	1.8 mm	Av. Prandtl number	0.0045
Rod-wall spacing	2.1 mm	Ratle	1
Number of grids	5	Fraction of flow in outer subchannels	0.134
Dist. between grids	0.2 m	Axial power distribution	sinus type
Dist. 1st grid from entrance	0.1 m	Ratio extrap. to real length	1.5
Coolant	Na	Max. lin. power of rod with max. rating	320 W/cm
Coolant mass flow	17 Kg/s	Radial power variation relative to max. power	5%
Av. coolant velocity	3.69 m/s	Tot. assembly power	4.29 MW

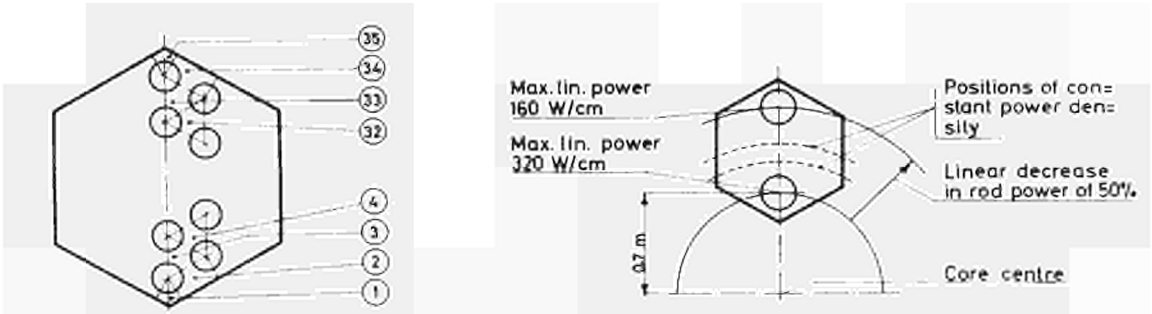

Fig. 11: Reference subchannels referred to in figs. 12-13. Position of hexagonal assembly with respect to core centre.

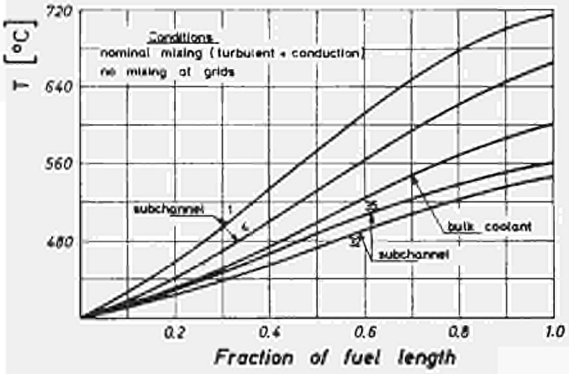

Fig. 12: Axial distribution of subchannel coolant temperatures in hexagonal fuel rod assembly.

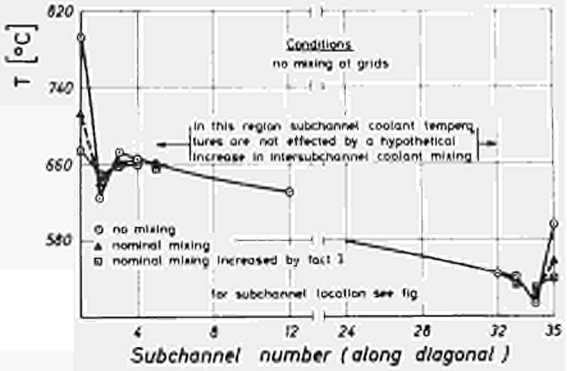

Fig. 13: Lateral variation of subchannel coolant temperature at outlet of hexagonal fuel rod assembly.

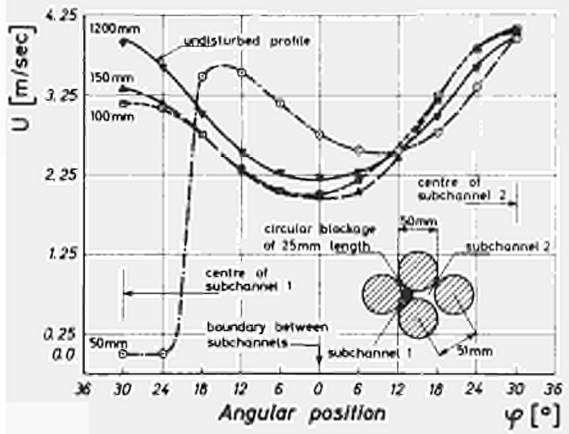

Fig. 14: Velocity profiles along centre line for different axial distances down-stream of blockage.

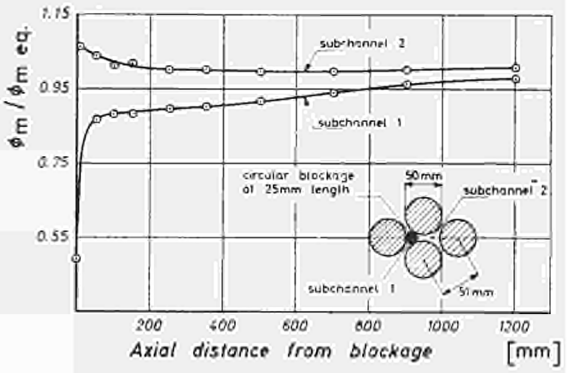

Fig. 15: Dependence of subchannel mass flowrates on axial distance downstream of blockage.

Figs. 12 and 13 show typical results regarding the coolant temperature behaviour in subchannels along the channel diagonal. An important result is that thermal subchannel interactions ("mixing") do not significantly attenuate subchannel coolant temperature differences except in the vicinity of the channel wall. In this region, where very important coolant temperature variations may prevail, the subchannel lumping procedure is a gross oversimplification of the physical situation, and the problem here should be attacked by a more local approach. For this reason much emphasis will be placed in 1972, on the development of computation methods predicting three-dimensional temperature fields in fuel rod assemblies.

Flow and heat-transfer effects in rod assemblies with partially blocked subchannels

An important aim of the rod bundle flow and heat-transfer studies is to acquire basic knowledge on transport phenomena related to abnormal fuel-element behaviour which may ultimately lead to a reactor accident. In this context experimental studies have been started to study flow and heat-transfer effects caused by subchannel blockages. Ref. [5] deals with such a study. Typical results shown in Figs. 14 and 15 deal with the effect of a circular blockage in one of the subchannels of a tightly packed triangular array of smooth rods. Fig. 14 shows velocity profiles along the line between centroids of blocked and adjacent undisturbed subchannels for distances 30 mm, 100 mm, 150 mm and 1200 mm downstream of the blockage. It is observed that the extent of the "stagnant" region behind the blockage amounts to about 50 mm. At this downstream position sharp lateral velocity and pressure gradients exist, giving rise to high mass-and momentum-fluxes which restore the subchannel centre velocity of the "blocked" subchannel to about 70% of its equilibrium value at the 100 mm downstream position. Fig. 15 shows how subchannel mass flow rates (made dimensionless with respect to the subchannel mass flow rate of the undisturbed system) vary with axial distance downstream of the blockage. It is seen that at the 100 mm downstream position the subchannel mass flow rate in the blocked subchannel is already again 90% of its equilibrium value. Predictions on subchannel coolant temperature distributions in assemblies with a partially blocked subchannel have been made with the HERA computation code. For a typical fast hexagonal assembly (pitch to diameter ratio = 1.3, Na coolant, sinusoidal power distribution, max. lin. power 420 W/cm, coolant inlet temperature = 400°C), in which one subchannel is partially blocked along the entire fuel-bundle length so that the residual mass flow rate is 20% of the nominal value, results are presented in Fig. 16. It is seen that mixing has a very significant effect on the coolant temperature distribution. For the case considered here, subchannel blockage leads to an important local increase in coolant temperature which is, however, not high enough to cause boiling of the coolant.

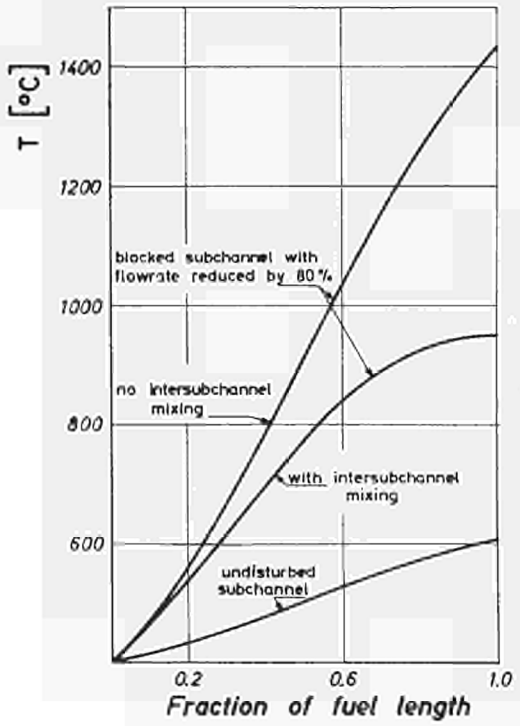

Fig. 16: Axial distribution of subchannel coolant temperatures in hexagonal assembly with single subchannel blockage.

References

1) R. Nijsing, W. Eifler, Temperature Fields in Liquid-Metal Cooled Rod Assemblies, Invited lecture at Int. Seminar on Heat Transfer in Liquid Metals, Trogir (Yugoslavia), 1971, to be published in Progress in Heat Transfer, Pergamon Press (1972)

2) W. Eifler, R. Nijsing, Berechnung der turbulenten Geschwindigkeitsverteilung und Wandreibung in exzentrischen Rign spalten, *Atomenergie 18* (1971), 133-142.

3) W. Eifler, R. Nijsing, Berechnung der turbulenten Geschwindigkeitsverteilung und Wandreibung in asymmetrischen Stabbündeln, *Atomkernenergie 18* (1971) 189-197

4) R. Nijsing, W. Eifler, Thermal Design Aspects of Fuel Rod Bundles with Emphasis on Intersubchannel Mixing, Deutsches Atomforum, Bonn (1971), 126-129

5) R. Nijsing, W. Eifler, Hot Subchannels in Hexagonal Fuel Rod Assemblies of Fast Breeders, *Liquid Metal Boiling Meeting*, Ispra, 15/16 April, 1971

DEPRESSURIZATION STUDIES

G. Friz, W. Riebold

Introduction

The aim of the depressurization experiments is to study the history of:

a) the cladding temperature of the fuel elements
b) the coolant pressure distribution in a PWR cooling channel as consequence of a rupture in the primary cooling circuit.

These data are necessary to test existing computer codes and to develop new ones for safety calculations.

A rupture in a primary reactor cooling circuit leads to a complex superposition of time-varying temperature distributions in the fuel elements and coolant and time-varying hydrodynamical and heat transfer phenomena.

To keep the experimental effort within reasonable limits only one subchannel has been simulated.

The essential parameters have been preserved, however, in order to obtain representative results.

The experiments are executed in the DHT-1 loop, which is a single-channel system with an upper and lower plenum. The length and diameter of the circular test-section correspond to the length and hydraulic diameter of one reactor subchannel. The wall thickness is equal to that offthe fuel rod cladding; this allows an accurate determination of the heat flux into the coolant from the measured values of power input and wall temperature. The power input to the test section can either be varied to simulate the heat flux from the fuel to the cladding in a real fuel element, or controlled in a simple manner more suited to the needs of systematic theoretical analysis.

Experiments on the FORCE installation for the study of two-phase flow dynamics in depressurization conditions were interrupted during 1971. A rubber balloon is to be mounted in the pressure vessel to prevent the dissolution of pressurized air in water. The experiments to be conducted in 1972 should yield information on the influence of air dissolved in water on the dynamic coolant behaviour under depressurization conditions.

During the report period a data acquisition system, purchased for the whole Technology Division, was delivered and put into operation. Two members of the depressurization group together with some members of the Electronics department had been instructed to look after this SMART (System for Measurement and Automation in Real Time), which at first was linked up with the FORCE and DHT-1 installation.

Experiments

In the first test series, concluded during 1971, ruptures in the "hot leg" of the loop were simulated by means of a quick-acting valve, the coolant being initially stagnant.

The varied parameters were:

- the rupture size, from 2 to 4, 6 and 8 mm diameter fo the diaphragm behind the opening valve;
- the time function of power input;
- the positive and negative time delay between power insertion and rupture simulation;
- connection or disconnection of pressurizer.

The initial temperature and pressure were $310 \div 320^{\circ}C$ and $130 \div 140$ bar respectively.

Measured or evaluated parameters were:

- wall temperature as function of time
- heat flux to coolant
- heat transfer coefficient
- time and position of heat transfer crisis;
- time to complete voiding;
- pressure history.

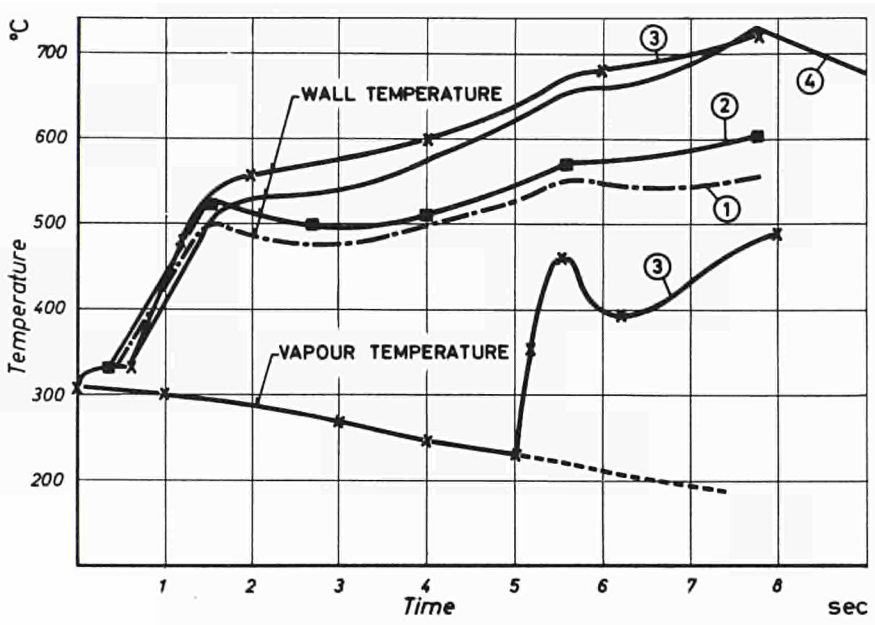

Fig. 1: Wall and bulk temperatures at 22 hydr. diam. upstream testsection outlet.

Results

A typical example of the behaviour of the wall (cladding) temperature vs. time is given in Fig. 1. One observes clearly the onset of the heat-transfer crisis which causes the strong temperature increase at about 0.6 sec. The subsequent breaks in the curve are the consequance of the stepwise power input. The heat flux to the coolant is obtained by the ordinary heat balance equation

$$q_c = q_e - c \cdot \frac{d\delta}{dt}$$

with q_e = electrical heat input, q_c = heat flux to the coolant and $d\delta/dt$ = wall temperature time derivative, c = heat capacity of wall material. An example of these evaluations is given by the points in Fig. 2. The average heat transfer coefficient α can be calculated by taking the equilibrium coolant temperature belonging to the measured pressure. The qualitative results from 90 runs can be summarized as follows [1]:

– The post-crisis heat flux depends on the rupture cross-section: initially (immediately after crisis onset) the heat flux is higher with greater rupture sections, but decreases afterwards more rapidly than in the case of smaller rupture sections.

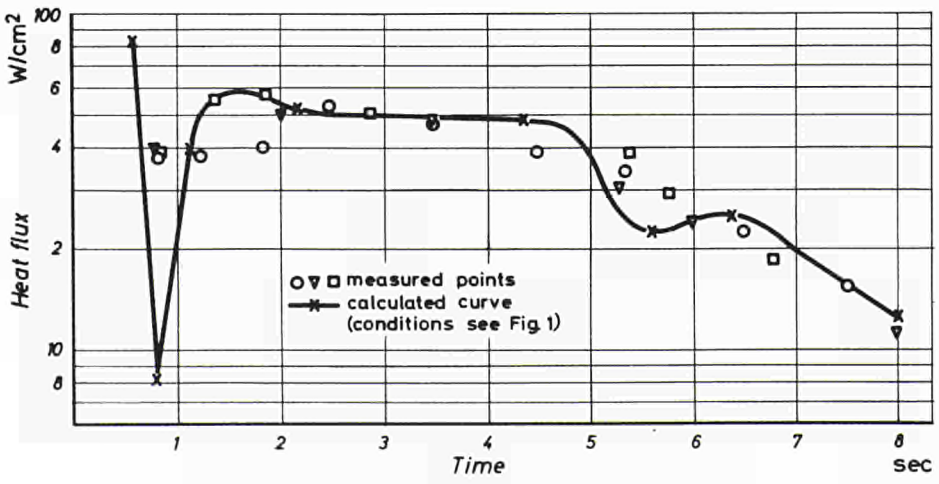

Fig. 2: Heat flux into coolant as function of time.

– Qualitatively similar is the time evolution of the heat transfer coefficient α. A conservative mean value of the experimental curves can be expressed by the equation

$$\alpha = 2{,}4 \cdot n \cdot e^{-1{,}8 \cdot n \cdot t}$$

where n is the ratio between the rupture section and the flow cross-section. Since the half-crest-value time τ_h of the pressure curves is nearly proportional to 1/n, this α-relation could also be expressed in τ_h. This representation holds for the hottest part in the channel (in our case the upper part), which for safety considerations is the most important one. The crisis behaviour in the upstream direction can generally be described as follows: the onset of crisis occurs later, i.e., the limit between crisis region and no-crisis region propagates against the flow direction. This movement, however, is not strongly reproducible, which indicates that it is very sensitive to small variations of the initial temperature distribution.

– With the pressurizeconnected to the circuit, the heat flux is for some seconds higher than in the case of a disconnected pressurizer. This indctes that an additional volume (to that of the test section) has an influence on the heat flux, probably by two effects: the additional water quantity and the additional driving force which in the present case increases the mass flow in the test section. This behaviour, however, must depend on the position of the pressurizer relative to the test section and the rupture position, i.e., in other cases (cold leg rupture, for instance) the effect may be contrary.
– A positive or negative time delay between power insertion and rupture simulation has no essential influence on the post-crisis heat flux and α -coefficient.
– The total amount of heat transferred to the coolant during the blow-down is of the order of two full-power seconds, and is nearly independent of rupture section.
– With smaller rupture sections the scattering of the results increases, indicating higher instabilities which are probably caused by the decreasing velocity in the test section.
– The onset of crisis in the hottest part of the channel after power insertion occurs at about 0.5 sec at full power and at about 0.8 sec at 80% power. These values do not depend very strongly on the rupture section.

The main effort during the last months was concerned with close cooperation with GAAA , Paris, on a theoretical analysis of our experiments, using a computer code developed by Messrs. J.C. Megnin and A. Raynaud of GAAA. This code is designed to calculate the evolution of the pressure and the temperature in the fuel elements and their claddings in several parallel channels, with a rupture at the entrance or exit of the system. The calculated results have been compared with the observed behaviour. After a study of the possible physical hypotheses and heat transfer coefficients used by the theory the following statements can be made:

– the assumption of a slip ratio equal to 1 (s = 1) gives as good or even better results than all other slip correlations;
– the assumption of thermodynamic equilibrium is sufficient for good agreement between calculation and experiment;
– MOODY'S correlation for critical mass flow holds good up to about 50% steam quality in the upper plenum; for higher qualities it yields too small mass flow rates; in this region the simple formula for dry steam gives better results;
– in the post-crisis region the film boiling formula of TONG with the MIROPOLSKY correction term gave satisfactory results.

The two figures provide an example of the comparison between the experimental and calculated results.

The cooperative work will continue along these lines to cover a wide range of conditions. A first joint publication [2] on this object will appear in Spring. The continuation of the experiments will be concerned with the study of the consequences of a "cold leg" rupture.

References

1) G. Friz, W. Riebold. "Experimentelle Untersuchung des Wärmeübergangs wâhrend der Druckentlastung bei Bruch im heissen Strang des Primärkühlkreislaufes eines Druckwasser-Reaktors". Paper presented to the 7th session of the "Working Group of Reactor Emergency Cooling", Cologne, 13 Sept., 1971.

2) G. Friz, J.C. Megnin, A. Raynaud, W. Riebold, H. Wundt. "Experimental investigation and blow-down code calculation of transient heat transfer during depressurization" To be forwarded to Nuclear Engineering and Design.

SODIUM SUPERHEAT BOILING

H.M. Kottowski, K.H. Spiller

General

The phenomena of liquid metal superheat at incipient boiling and the subsequent "steady state" boiling are of interest for fast reactor safety and high-temperature liquid-metal boiling-condensation heat-exchanger systems.

In the activities of 1971 preference was given to the investigation of the following factors influencing the incipient superheat: What is the influence (a) of the O_2-impurity? (b) of the operation history ? (c) of the surface structure?

Theoretical work was done on the mechanism of bubble nucleation and two sets of experiments were performed:

To answer these questions,

1) Loop experiments, with Na of various O_2-content and various operation history and constant heating surface conditions, to investigate the influence of O_2-impurity and operation history on the incipient superheat;
2) Experiments at laboratory level with Na of constant O_2-impurity, to investigate the influence of the heating-surface structure on the incipient superheat.

Theoretical work on nucleation

The nucleation of bubbles in the liquid can arise in two different forms, homogeneous and inhomogeneous, e.g., nucleation on wall cavities or impurities in the liquid.

In cases of homogeneous nucleation, the nucleus arises through local statistical entropy fluctuation, which brings together a number of molecules of high thermal energy which cause defects in the liquid lattice structure big enough for bubbles to form. The energy required to form critical defects in the liquid itself is high

$$A_{Ko} = \frac{4}{3}\,\sigma\pi r^2$$

and therefore the probability of nucleation is small.

$$I \approx \exp\,(-A_{Ko}/KT)$$

σ is the surface tension, r the nucleus radius and K the Stefan-Boltzmann constant.

The nucleation is primarily a problem of the formation of sufficiently large defects and is determined by the energy term A_{Ko}.

The observed Na superheat of 10°C to 400°C cannot be interpreted as a homogeneous nucleation process. Therefore the nucleation has to occur on the heating surface on wall cavities or impurities in the liquid, which reduce the nucleation energy. The dominant factors are the surface tension and the wetting conditions, which seem to depend very much upon the O_2-impurity, and the shape of the cavities in the heating surface. Fig. 1 shows qualitatively the influence of the shape of cavities on the nucleation energy.

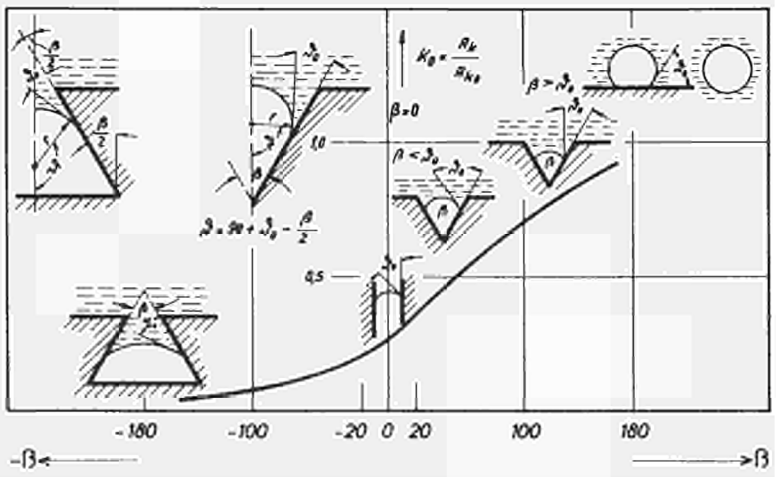

Fig. 1: Influence of shape and contact angle on nucleation energy.

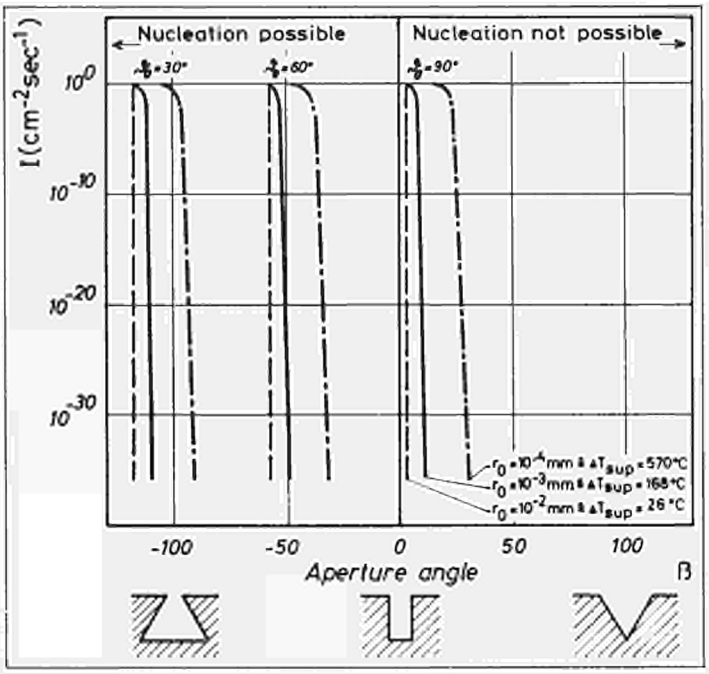

Fig. 2: Probability of nucleation.

The influence of the surface tension, wetting conditions and the shape can be described by the relation:

$$A_K = \frac{1}{3}\,\sigma\pi r^2\,[2\text{-}3\sin(\delta_o - \beta/2) + \sin^3(\delta_o - \beta/2)] + f(\beta)$$

in which δ_o is the wetting angle, β the aperture angle of the cavities and r the curvature radius of the liquid surface in the cavity, $f(\beta)$ the shape correction factor.

The importance of the wetting conditions, the shape of the cavities on the probability of nucleation, i.e. whether nucleation in liquid-filled cavities is possible or not, is shown in Fig. 2 for cavities of various sizes and various wetting conditions. For example, for a wetting angle of $\delta_o = 60°C$, nucleation is only possible in re-entrant cavities with a re-entry angle $< -30°$. In cavities with a reentry angle $> -30°$ nucleation is impossible.

The probability of nucleation per cm^2 of the heating surface per sec is given by the relation:

$$I = 10^{-5}\,N \cdot N_L\,\frac{\rho_L}{M}\,\nu \cdot f(r) \cdot \exp(-A_K/KT)\ [\text{nucleation events/cm}^2\,\text{sec}]$$

in which $N = 10^8$ defects/cm^2, $N_L = 6.023 \cdot 10^{23}$ n/Mol, ρ_L = liquid density, M = molecular weight, $\upsilon = 10^{13}$ Hz (oscillation frequency of the molecules in the liquid), f(r) = statistical density distribution of the size of the cavities, K = Stefan-Boltzmann-constant T = liquid temperature [°K], A_k = nucleation energy.

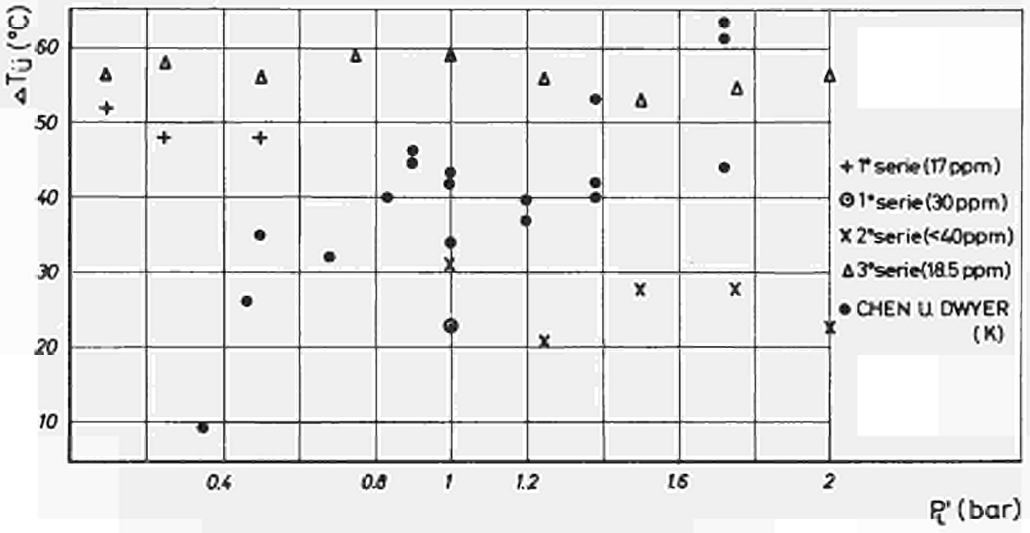

Fig. 3: Statistical mean value of superheating experiments.

Loop experiments

Four series of experiments were performed to study the effect of the O_2 contents in the Na (17 ppm, 18.5 ppm, 30 ppm and 40 ppm) on the superheat, and three series to investigate the importance of the operation time and operation history on the superheat. These experiments were started in 1970. The experiments were performed with a constant O_2-content in the individual experimental series, but with different O_2-contents for the various series (Fig. 3).

The aim of these experiments was to simulate the deactivation of gas- or impurity-filled wall cavities during operation by forced deactivation. The forced deactivation was achieved by the pressure-temperature-history process proposed by Chen and Holtz. All incipient boiling test runs were done at 1 bar system pressure. According to the pressure-temperature process, the liquid temperature was lowered in our experiments to 630°C and the pressure to the value of P_L indicated on the X-axis in Fig. 3 and maintained at this condition for 30 min before starting a new test run. The dots in Fig. 3 represent the statistical mean value of ten test runs. The individual measuring values scatter by about ± 20°C.

To obtain information on the importance of the operation time on the incipient superheat, the loop was run continuously at 1 bar and 300°C 1900 h between the first and the second test series and 1600 h between the second and the third one.

The experiments do not show any definite influence of time or pressure-temperature-history process on the superheat neither on the mean value, nor on the scattering range of the individual measuring values. It can be concluded that after a relatively short operating time most of the cavities are flooded and nucleation occurs in the liquid-filled cavities. The most conspicuous result of these experiments is the strong influence of the O_2-impurity on the superheat.

Laboratory Experiments

The apparatus used in the laboratory simulates a single subchannel of a fast breeder reactor. During the actual measurements the test section works at stagnant conditions. Preheating to 600°C with 50 Hz; heating to simulate the malfunction is with high frequency (4.5 MHz) which is very similar to the reactor heating conditions. The sodium in the apparatus is brought to a desired oxygen content by cold trapping or is highly purified by distillation within the apparatus.

Using a test section, one half of which was left in the original state of the drawn tube, the other half being pickled with 10% HCl, the results shown in Fig. 4 were found.

Both positions 1 and 2 of the untreated test-section yielded – from repetition to repetition of the measurement – highly scattered superheats. Because of the large number and the great differences in size of the cavities in the wall of the drawn tube, the superheat obeys the laws of statistics. In positions 1 and 2 practically the same superheats were found, in both cases augmenting with time. In positions 3 and 4 of the pickled half-tube the scattering of superheat was essentially smaller. Probably the shallow cavities are removed and the finest ones enlarged by the pickling; thus the smallest and the biggest superheats cease. No increase of the superheat with time was observed with the pickled part of the tube.

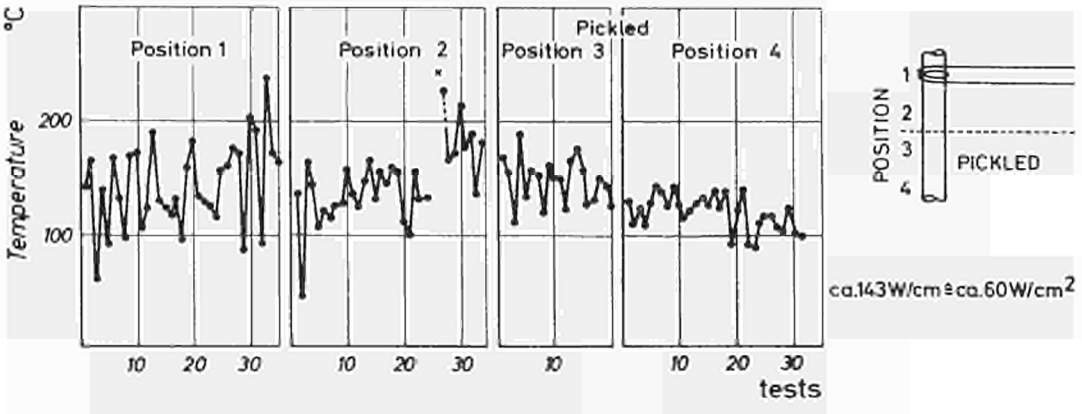

Fig. 4: The influence of pickling of the tube on the superheating of pure Na.

Very many more measurements are necessary before an unequivocal statement can be made, because of the statistical character of the superheat. Consequently the measuring method was modified and the continuous photographing the tube surface with rising temperature was omitted.

The tube is now observed immediately by a photomultiplier. The augmenting temperature is recorded on a Polaroid packfilm as the vertical ascendent light spot of an oscilloscope. Up to 80 single measurements may be given on only one Polaroid picture. In the future a statistic mean value may be formed from several hundred single measurements.

References

1) K.H. Spiller, Some new results on the influences of surface conditions and impurities on the superheat of sodium, Liquid Boiling Group Meeting at Ispra, 15-16 April, 1971

2) K.H.Spiller, Visualization of stagnant sodium superheat and boiling in a channel, International Heat Transfer Seminar, *Heat Transfer in Liquid Metals*, Trogir (Yu), September 6-11, 1971

3) K.H.Spiller, D. Droste, Reinigung von Kalium and anderen Alkalimetallen, *Chemie in Labor und Betrieb 11* (Nov. 71), p. 487-490, and *12* (Dec 71), p. 538-542

4) K.H.Kottowski, The Mechanism of Nucleation, Superheating and Reducing Effects on the Activation Energy of Nucleation, Proceedings *International Heat Transfer in Liquid Metals*, Progir (YU), September, 6-11, 1971

5) H Kottowski, R. Warnsing, R. Kleih, A. Birke, Contribution to the Problem of Remaining Liquid Layer after Ejection, L.M.B.W.G.-Meeting, April 15-16, 1971.

FLUIDISED BEDS

A. Faraoni, J. Flamm, H. Langenkamp, D. van Velzen

Introduction

The high-temperature fluidised bed coating technique as applied to nuclear fuel microspheres has attained considerable empirical standards on relatively small scale, e.g., coating of 3 to 5 kg charges of 800μm diameter UO_2 kernels in 120 to 150 mm diameter fluidised bed columns. Demand and economic aspects call for larger units and throughputs, e.g., to feed a 10,000 MWe power reactor programme sread over five years about 80 to 100 coating units with present-day tested capacities would be needed in continuous operation. Today the capital investment is of the order of $ 20,000 to 25,000 per coating unit. Extrapolation from existing know-how needs further (cumbersome and increasingly expensive) empirical work, which at present lacks the necessary theoretical background. In order to assess the highly complex coating process, appropriate groups of system parameters must be isolated and their relative effects on the coating process and throughput rates established.

Model work can thus considerably contribute to the comprehension and consequently, to the development and scale-up of the process, because only in this way can quantification of paramount process parameters be accomplished and physical laws for adequate mathematical models established.

Hence, the following parameters have to be quantified:

- the gas residence time in the reaction zone,
- the solids transport through the reaction zone, and
- the gas temperature profile in the reaction zone.

The state of fluidization under coating conditions may vary from "spouting" to "bubbling" and "slugging". In a first step JRC model work at room temperature has been concerned with "spouting-type" beds in a column geometry proven for high-temperature coating (standard DRAGON Project 125 mm diam. coater), concentrating on both gas flow and solids transport measurements in this type of bed.

Some prospecting work on an advanced high-temperature system has also provided feasibility data for a direct-resistance heated bed.

Gas flows in spouting beds

A perspex model of the 125 mm ID fluidized bed unit in use at the DRAGON roject for high temperature coating was operated with compressed air at room temperature with three different two-flow nozzles and six types of solids.

Local gas velocities were obtained by means of dynamic gas pressure measurements, using a Prandtl tube arrangement. This system allowed for vertical introduction of the probe from the top of the column with fine positioning control in both radial and vertical directions.

Differential pressures were measured at various axial distances above the nozzle (3, 5, 7, 10, 15, and 20 cm in most cases) and appropriate radial positions. From these data radial pressure profiles were derived for each elevation, which were then converted into gas velocity profiles.

From each gas velocity profile the average gas velocities in the spout and in the annulus are then calculated by numerical integration.

The average gas velocity in the spout (v_{sp}) decreases sharply with axial distance above the gas injector. There is evidence of a strong influence of the nozzle exit velocity as well as the total gas flow, all other parameters being constant. This leads logically to the hypothesis that the momentum introduced into the system by the gas is the governing parameter, which is common knowledge in jet applications. In the present case the momentum is defined as:

$$M = \frac{Q_1 v_1 + Q_2 v_2}{g}$$

It appears that the average upward gas velocity in the spout is clearly dependent on the introduced momentum, irrespective of particle properties. The slopes of the curves decrease with increasing distance above the nozzle exit. This implies that the influence of the momentum is most pronounced in the immediate neighbourhood of the gas inlet and fades out with increasing distance from the gas inlet.

By regression analysis the relation between v_{sp}, M and x has been established as:

$$v_{sp} = \frac{1610}{x + 4.8} \cdot M^{0.018\,(35 - x)}$$

The gas distribution pattern is, however, more relevantly described by volumetric gas flows than by average gas velocities. This is conveniently expressed by the gas transport ratio which is defined as the ratio of the gas flow in the spout to the total gas flow.

It appears that generally the gas transport ratio passes through a maximum at approximately 5 to 7 cm above the nozzle exit and then drops towards zero. The maxima are clearly a function of the quantity of gas injected and the nozzle geometry. In analogy to the findings on the average gas velocity in the spout, the momentum introduced by the gas also governs the gas transport ratio.

Here, too, clear relations exist, irrespective of particle properties. Again the slopes of the curves decrease with increasing distance from the gas inlet, which is in line with the reasoning for the declining influence of the momentum as a function of x.

Regression analysis yields the following equation:

$$TR = 1 - 2.64 \cdot 10^{-2}\, x + f(x)\, M \cdot 10^{-3}$$

where $f(x) = 5.84 \cdot 10^{-2}\, x(10 \cdot 15 - x)$.

The above correlation holds for values of x from 0 to 10 cm. For distances from the nozzle larger than 10 cm the momentum ceases to be the only governing factor, which is also evident from the fact that f(x) becomes zero when $x = 10 \cdot 15$ cm.

To comprehend the gas transport ratio in a spouting bed for values of $x \geqslant 10$ cm, it should be borne in mind that the minimum gas velocity for stable spouting is dependent on the bed height. This means that there exists a maximum spoutable bed depth (L) for any given injected gas quantity, dependent on nozzle geometry, bed geometry and solids parameters. Values for L have been determined experimentally.

Inserting L into a correlation with TR and x, it appears that the best possible representation is:

$$TR = a\,(1 - x/L)^2$$

This equation holds for $7 \leqslant x \leqslant L$, where $x = 7$ forms the continuity link between the two equations for TR.

It follows that:

$$a = (0.815 + 1.29 \cdot 10^{-3}\, M)\,(\frac{L}{L-7})^2$$

In summary, the work described here has led to the finding of hitherto unknown aspects in the fluidization of coarse particles. In the first place the quantity of momentum introduced by the fluidization gases plays a very important part in the gas distribution near the gas inlet. The momentum is a quantity which is very often used in jet technology, but it has, to the investigator's knowledge, never, until now, been considered in fluidization research. In this work it has been shown that with the aid of the momentum, an empirical mathematical description of the gas flow in the vicinity of the nozzle can be obtained. A striking fact is, that the particle characteristics do not enter into the equations, hence it can be concluded that here the gas movement is independent of solids properties.

Further it has been shown that in a spounting bed a considerable recirculation of gas takes place in the surroundings of the nozzle. There is evidence that, depending on the introduced momentum, a high percentage of the injected gas quantity is recirculated, owing to a kind of venturi effect of the jet-type gas inlet. This is a completely new aspect of the spouting bed technique and may be of paramount importance for applications with high rate kinetics, such as the coating process.

For illustration a generalised gas flow pattern is given in Fig. 1c together with one set of experimental data on the gas transport ratio (Fig. 1b) and mean gas velocities in the spout (Fig. 1a).

Solids circulation in souting beds

Knowledge of the solids circulation forms an important part in assessing a process with high rate kinetics. Therefore relevant measuring techniques had to be adapted or developed.

The approach proceeded along two lines:

- acoustical method
- radioactive tracer method.

The *acoustical method* was investigated first. The principle of the method consists in the analysis of the electrical signal (amplitude and frequency) from a piezoelectric crystal coupled to the external end of a metallic probe which is introduced into the bed at a known position. The signal should be a function of the number of impacts of solid particles on the probe. Various signals were indeed obtained as a function of the position of the probe inside the bed, but evaluation and calibration of these signals proved to be extremely difficult, mainly because of an excessive noise level.

For this reason the method was shelved but some preparatory work has been done on embedding a

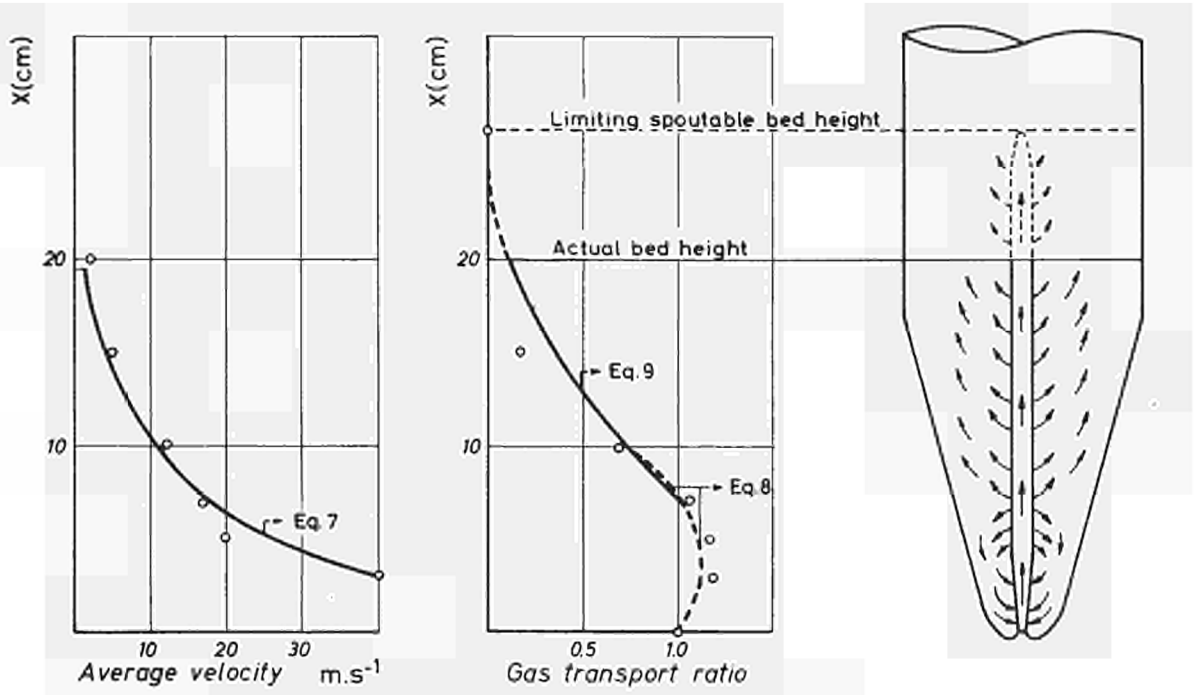

Fig. 1: General gas flow pattern in a spouting bed.

piezoelectric crystal in the probe end, which is immersed in the bed. Proving tests are still outstanding.

The *radioactive tracer method* is based on the intensity of radiation of a particle marked by 24Na isotope (~ 200 microcuries) as a function of the distance of this particle from a 3" NaI scintillation counter.

The radiation intensity was measured by means of a multi-channel analyser, the channels being used successively. The counting time per channel was varied between 10 and 100 ms. With this set-up the axial position of the marked particle is continuously followed and the solids circulation rate can be calculated from the average time passed between two successive passages in the spout.

Several general qualitative conclusions can be drawn at present.

- About 80% of the particles are sucked into the spout at an axial distance of less than 2 cm from the nozzle exit.
- Once a particle is in the spout, it will be transported to or above the bed surface. In all our experiments, the activated particle has never been observed to leave the spout earlier.
- Average residence times of the particle in the spout are 200-500 ms.
- Measured solids circulation rates vary between 500 and 1400 kgh^{-1}, mainly as a function of the gas throughput with little apparent influence of the momentum introduced by the fluidizing gas.

Advanced high temperature technology

Refractory coatings are generally applied to nuclear fuel particles by gas-phase pyrolysis in batchwise-operated high-temperature fluidized beds (1200-2200°C) of cylindrical geometry. The necessary heat is conventionally generated in single or three-phase graphite resistance heaters, surrounding the fluidized bed column and having water-cooled power connectors. In order to avoid decomposition of the reactants before entering the bed the gas distributor is conveniently kept below a critical temperature by water cooling. Thermal gradients are encountered and enhanced with increasing bed diameter and reactant throughput. It becomes invariably more difficult to confine radiation losses with increasing bed size. High-temperature fluidized beds of up to about 150 mm internal diameter are known in operation with installed capacities of the order of 100 - 150 kW, i.e., to allow for conveniently short heating-up cycles.

Economically interesting unit sizes require column diameters in excess of 200 mm, preferably up to 300 mm, invariably enhancing the problems of radiation shielding and transient or unsteady-state heat flow. A basic requirement for scale-up to these coater sizes is to concentrate heat generation in the zone wetted by the fluidized bed and, because of the large quantities of gas to be heated to operating temperature, also in the vicinity of the gas distributor.

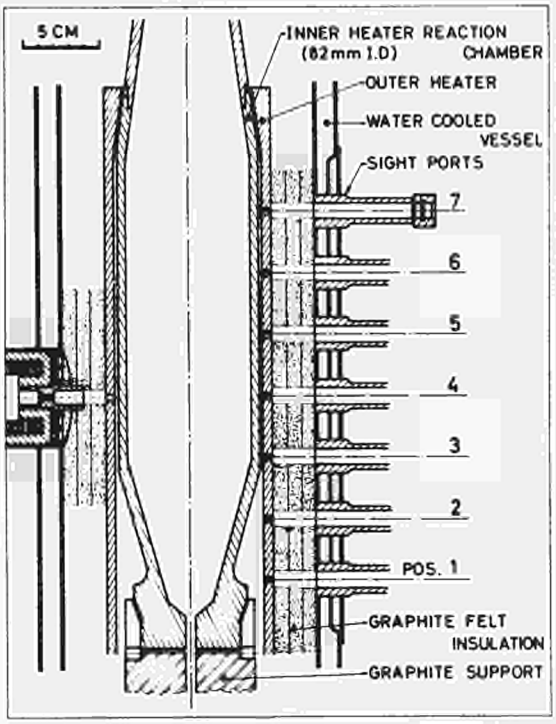

Fig. 2: Geometry of direct-resistance heated bed.

Obviously, the most efficient solution is to employ Joule heating of the reaction chamber. This system has been studied for various coater sizes and thermally tested in a small prototype unit [2]. The thermal performance of an 82 mm ID reaction chamber (Fig. 2) was contrasted to that of a 55 mm ID reaction chamber of conventional design and heating, using the same furnace casing.

Three reresentative sets of axial temperature profiles as measured on the outside walls of heater and reaction chamber of the respective systems are given in Fig. 3, together with the power inputs at thermal equilibrium under stationary conditions.

Although the effective bed cross-section of the directly heated reaction chamber was more than twice that of the conventional bed (52 and 23.6 cm^2 respectively), the power required to heat the reaction chamber to "equivalent" temperatures amounts only to some 50 - 60% of that required for the conventional bed. Further, axial temperature gradients in the reaction chamber are greatly reduced.

Process application and precise formulation of all parameters relevant to the coating process are of potential interest and should be pursued in additional studies.

References

1) D. Van Velzen, H.J. Flamm, H. Langenkamp, Gas Flows in Spouting Beds, DP-Report 785

2) H.J. Flamm, A Direct-Resistance Heat Fluidized Bed: Principles and Thermal Performances of a Pilot Plant, EUR-4699.e (1971)

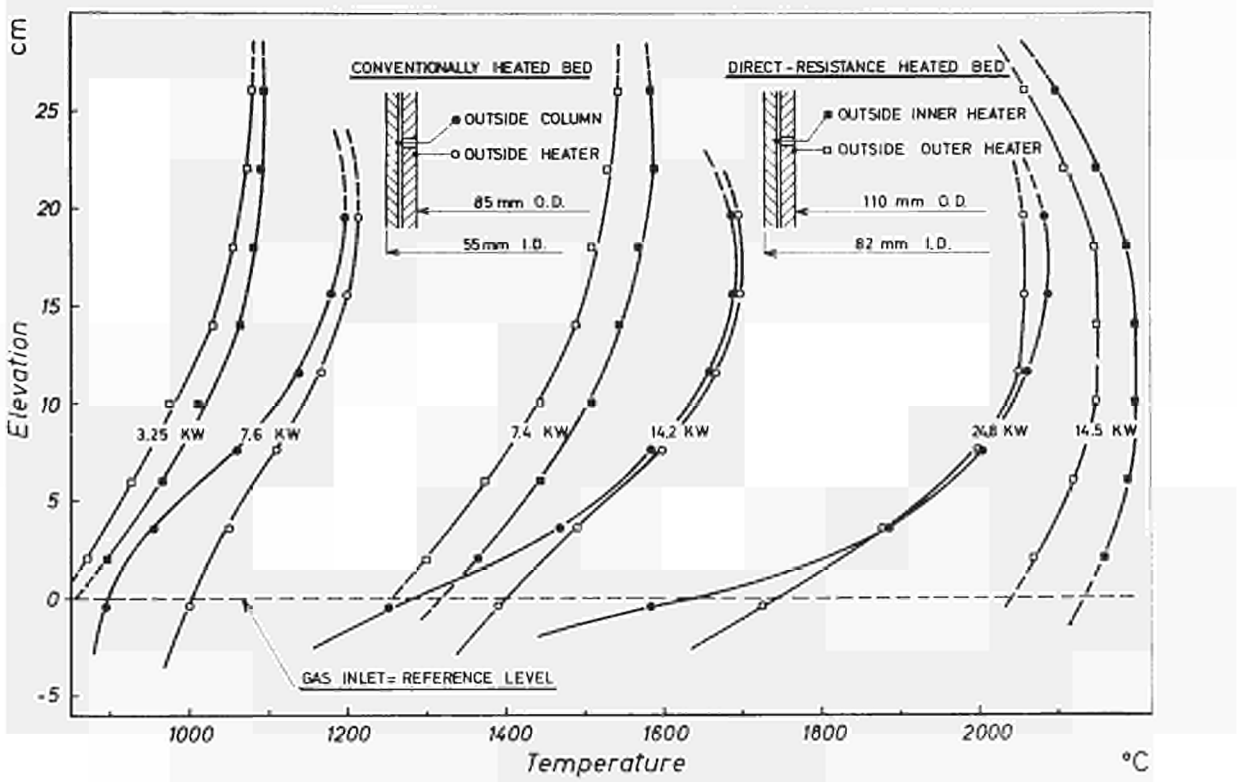

Fig. 3: Temperature profiles (empty beds - Argon 1.1 ata).

RELIABILITY STUDIES

G. Volta, J. Amesz, A. Colombo, R. Richena

General

In recent years there has been a progressive movement towards the control of systems and equipment safety in design and in operation by the use of probabilistic criteria.

These criteria, applied extensively in the early sixties to the electronics and aerospace field, were steadily extended to other fields: – chemical, mechanical and civil engineering.

The strong interest in these criteria is due to their ability to take into account explicitly and quantitatively the variability of the various factors affecting the performance of a system.

The application of such criteria requires on one side the availability of computerized sophisticated methods of assessing the probability of an event concerning the system, given the probability of related events concerning its components; on the other side, the experimental and theoretical assessment of statistical failure models for the components. This last aspect is of greatest importance in the case of mechanical components, brittle materials, and big components for which any statistical analysis may be based on very small samples.

Our activities have dealt with both the aspects mentioned. The development of methods, however, has been done in close connection with specific problems or "pilot cases" in order to obtain, together with the development of new methods, a clear assessment of their practical applicability and value.

Development of codes for system reliability analysis

The first step of the work was a critical analysis of the existing codes and a search for the relationship between codes and logical system presentation.

An inventory was made of all the codes accessible in the open literature and the main characteristics of each one were analysed. The point in the general reliability process at which each of these codes can be applied was defined and the inter-dependence between codes and representations was investigated [1] (Fig.1).

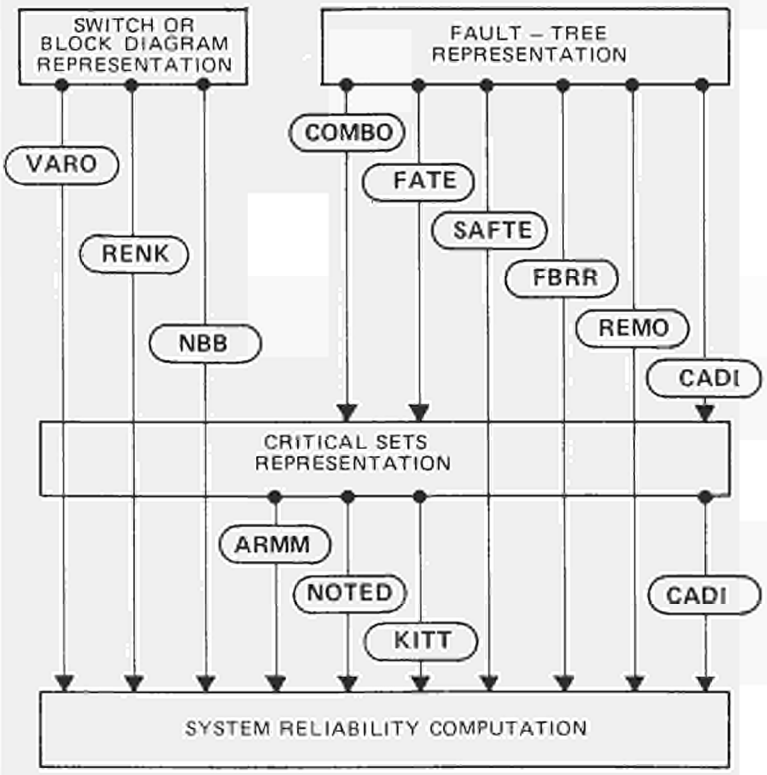

Fig. 1: Reliability analysis of systems composed of elements defined by binary random variables. Codes and representations.

Then, with reference to a typical electrical supply system for a nuclear power station, three different methods of logical representation and reliability computation were compared.

The three methods are:

- fault-tree representation and computation with a COMBO-KITT-type
- block-diagram representation and computation with a NBB-type code
- NOTED code-oriented representation and computation with NOTED-type code.

The evaluation and comparison of the three methods made evident the advantages of the fault-tree representation associated with a two-step code (critical set computation – reliability computation, so the fault-tree representation will be assumed for any future work.

The second step was the development of improved codes.

A simulation code which avoids some limitations of the existing SAFTE code was written. The code, called REMO [2] is formed by a group of algorithms enabling the following types of systems to be treated:

- systems without repair
- systems with repairable components
- systems with stand-by components.

The algorithms were studied with a view to cutting down as much as possible the amount of computer fast memory space needed and the execution time.

The development of a very general two-step analytical code for system reliability analysis based on the kinetic fault-tree theory was then begun. The code is called CADI.

The code will allow the analysis on any type of system, with repair and with sequential gates.

The part of the code written and tested is the solution of the Volterra integral equation which gives the unavailability of a component as a function of the repair pdf and failure pdf.

To allow a continuous reliability measurement of a plant in operation, two codes were written [3]. The first (called OPCHAR) allows the computation of the operational characteristics (failure and repair laws) of the components from the operational data. The second one (called POCHAR) computes for the same components the "posterior characteristics" applying the Bayes theorem in its discrete form.

Pilot plant-reliability analysis

The most complete pilot application of methods, including both the "a priori" and "a posteriori" probability analysis was carried out on the operating in-pile loop CART [3].

The probability of a three-pump loss was evaluated "a priori" by a fault-tree analysis and "a posteriori" through the sequential application of two years' operation data (OPCHAR and POCHAR codes) on the same fault-tree. The "a priori" probability, considering no repair for a period of 1000 hours, resulted as 10^{-14}. This figure was increased to 10^{-7} on the basis of the operating experience. The result, though still acceptable, has drawn the attention of the operators to the components which have proved much less reliable than expected. The collection of data is continuing for the posterior probability of this and of other accidents.

A second complete pilot application carried out consists of a reliability and availability analysis of the PEC reactor electrical supply system (cooperation with CNEN).

The analysis was carried out on a fault-tree of 57 primary events and 66 gates. The first step of the analysis produced the following important finding: the system has just minimal cut-sets of order 2 and 4. As only the cut sets of order 2 are relevant for the reliability of the system, a further quantitative analysis could be limited to these sets, in which only 22 of the 57 components are involved.

In a second step the probability of failure of the electrical supply as a function of time was evaluated quantitatively, assuming various failure and repair laws.

Reliability of loaded structures

The activity was split in two directions, namely the application of the strength-stress interference method to safety devices and containment structures, and the search for material failure laws assuming stochastic failure models.

The statistical behaviour of rupture discs was investigated [4]. Thus the statistical distribution of geometrical and physical parameters measured on 2" discs (radius of curvature, membrane thickness, plastic instability of the constituent material) was fitted into the expression given by a plastic-instability failure model.

The standard deviation of the burst pressure was found to be 6.5%. This figure is in contrast with the limits imposed by certain codes (e.g. ASME):5% max. deviation from the nominal value.

The experimental programme should be pursued with burst tests and fatigue experiments to refine

these preliminary results and to change the standard value.

The probabilistic approach to the design of a containment structure was worked out for the PEC reactor containment. This containment was built some years ago to be used for the PRO reactor (this project was then abandoned and was designed according to the ASME VIII code. A new calculation was done according to ASME III, the code that should be applied now for the specific case. According to ASME VIII the maximum permissible internal pressure is 2.19 kg/cm^2, whilst according to ASME III it is 2.7 kg/cm^2.

The probabilistic approach, in which the variability factors are explicitly considered, yielded results and supported conclusions which appear much less arbitrary than those given by deterministic codes. The probabilistic approach also allowed a unified appreciation of the loads of various nature such as internal pressure due to DBA, seismic load, and loads due to atmospheric phenomena.

The problem of the statistical interference of the failure low from a small sample of rupture tests was treated with reference to steel and graphite [5) 6)]. The approach chosen can be briefly outlined as follows.

If the failure oof a material is caused by a cumulative damage process, the mathematical form of the failure distribution can be deduced from the experimental sample function of damage. The knowledge of the physical form of the distribution also allows the use of the Bayesian inference technique, resulting in the highest confidence level. A comparison in the low probability region (10^{-4} - 10^{-6}) between the gamma (functional) distribution obtained in this way and the usually-adopted distributions such as normal, log-normal, Weibull, shows a discrepancy of various orders of magnitude.

References

1) A. Colombo, R. Ricchena, G. Volta, Survey and critical analysis of programs for system reliability computation, CREST Specialist Meeting on Reliability, Munich, May, 1971, MRR 90 (1971).

2) R. Ricchena, A New Code for System Reliability Analysis Crest Specialist Meeting MRR, 90 (1971).

3) A. Colombo, T. Luisi, G. Proja, G. Volta, Operational Reliability of an In-Pile Loop, Crest Specialist Meeting, MRR 90 (1971).

4) A. Nay, Affidabilità di dischi a rottura per impianti a pressione, ATI, Convegno Nazionale, L'Aquila, Sept. 71.

5) J. Amesz, Statistical inference from Small Samples: Some Experience in Mechanical Reliability Evaluation, CREST Specialist Meeting, MMR 90 (1971).

6) J. Amesz, F. Lanza, G. Volta, Experimental and Theoretical Investigation on Probabilistic Criteria for the Mechanical Resistence of Graphite Structures. 1st International Conf. on Structural Mechanics, Berlin, Sept. 1971.

DEVELOPMENT OF THERMAL ISOLATION SYSTEMS FOR H.T.G.R.

E. Aranovitch, F. Farfaletti-Casali, S. Crutzen

Introduction

Thermal insulation represents an important percentage of the cost of the concrete vessel, of the order of 25% by some estimates. From a reliability point of view, it is an essential component which must retain its integrity during the lifetime of the reactor.

The realization of a satisfactory insulation system involves many different aspects, not only the thermal characteristics but also such problems as compatibility and corrosion of materials, vibrations, transient operating conditions (accidental rapid depressurizations), and the time required to mount it on the vessel, which has a significant incidence on costs.

The nature of the gas coolant has an important influence on the design of the insulation. The solutions optimized for CO_2 cannot be extrapolated directly to helium because of the great differences in density and thermal conductivity between the two gases, and the design should specifically take these differences into account.

Our activities, which have dealt mainly with the multilayer type of insulation (maximum temperature: 700°C), concentrated on the following points:

- design work of new solutions with study of some fabrication aspects concerning welding, mounting problems and thermal tests;
- study of rapid depressurization phenomena in insulation systems;
- mathematical codes for the optimization of geometrical dimensions with basic experimentation in heat transfer;
- a new activity on insulation systems for higher temperatures (1000°C) will be started this year.

Development of an original solution

A new concept of thermal insulation was designed and patented. It consists essentially of layers of thin metal foils 0.2 mm thick, which are stamped into a special modular geometry with two undulations at right angles for absorbing thermal dilatations and increasing the transverse rigidity (Fig. 1). These foils are spot-welded to lateral walls of thin foils surrounding each modulus.

The modular pitch is of the order of 300 to 600 mm, the thickness of the cells about 6 mm and the number of layers of the order of 7 with hot gases at 350°C and heat losses of 0.25 w/cm^2.

In such a solution the thermal dilatations are absorbed locally and not at the boundaries of the insulation structure, with the double advantage of (a) a simpler and more rapid mounting of the panels one beside the other without expansion joints or clearance problems, (b) elimination of the risks of clamping that might arise in solutions requiring the overlapping of layers.

At this stage it is diffucult to make an exact economic evaluation of this type of insulation. A tentative analysis has shown promising results mainly because of three points:

- its lightness ($\sim$ 25 kg/m^2). Optimization calculations have shown that the layers of stagnant gas can be thicker with helium than has been proposed in most solutions. Thin foils can be used because of increased rigidity by stamping.
- The use of large prefabricated panels considerably reduces the mounting time on-site.
- With temperatures higher than 700°C the metal foils need not all be in the same material; for the hotter layers special metals or alloys can be used and for the colder layers conventional metals would be sufficient.

Finally it should be noted that the modular geometry can also be used for a mixed solution in which the stacked foils are replaced by an insulation material such as ceramic fibres.

The thermal characteristics of this insulation structure were measured experimentally in two test facilities up to a temperature of 700°C on the hot side, with the cold side maintained at constant temperature with a cooling system. In the facility shown in Fig. 2 panels of 1200x3000 mm can be tested. The equivalent thermal conductivity of the insulation was determined as a function of different parameters (number of cells, inclination plane, width of cells, emissivity coefficient). The effect of fastening studs on local temperature distribution was investigated. These tests, carried out at atmospheric pressure with nitrogen, are extrapolated, using a GRASHOF similitude, for nominal working conditions with helium under pressure. The insulation was also subjected to 200 thermal cyclings with temperature variations of 300°C.

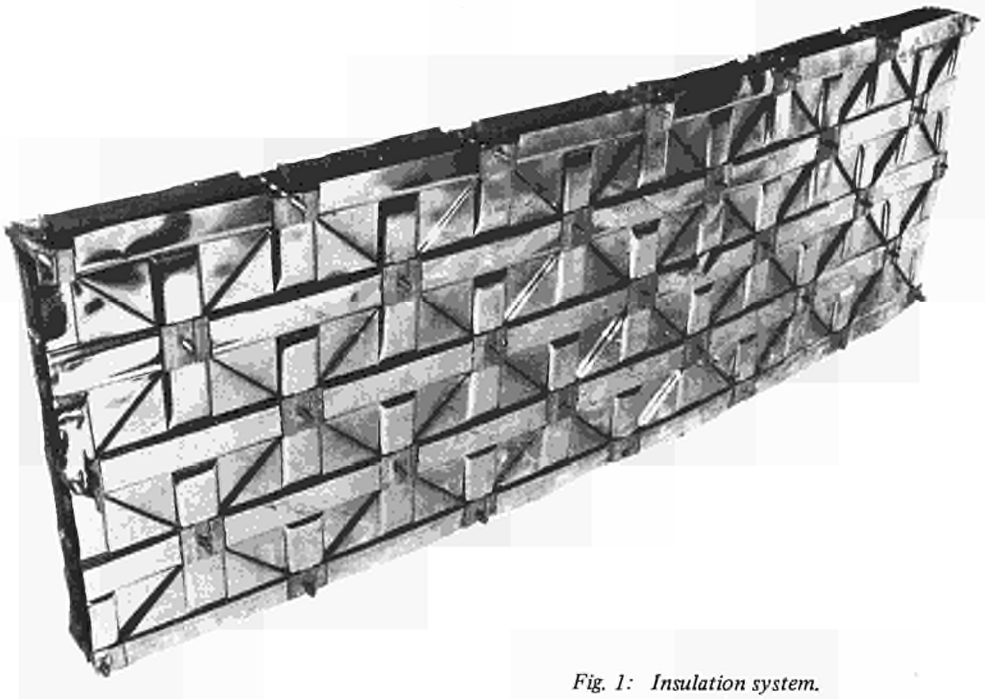

Fig. 1: Insulation system.

Study of rapid depressurization phenomena

The multilayer foil type of insulation is designed to keep the natural convection in the laminar range. In such systems, thermally speaking, it is better to have the individual cells as leaktight as possible in order to avoid macroconvection, but from a safety point of view the insulation must be able to withstand without deterioration accidental rapid depressurization due for instance to pump failure, which in the case of the direct cycle solution could reach the order of 20 atm/sec in the primary ducts. This means that there must be communications between the cells and the outside. A compromise must be found between these two contradictory requirements. The results presented here concern tests of rapid depressurization (up to a 20 atm/sec) performed on insulation bobbins of the DARCHEM type.

A schematic design of the depressurization facility is shown. It consists mainly of a pressure vessel, in which either panels or bobbins can be tested, up to diameters of 560 mm and lengths of 2450 mm, at an initial pressure of 25 kg/cm^2. Different depressurization rates, from 0 to 200 atm/s, are obtained by variation of the diameter of a diaphragm through which the gas escapes into the ambient space after the bursting of a disc system in the upper head of the vessel. The tests are done with non-corrosive gases such as helium and nitrogen. During the tests the absolute pressure in the vessel is measured as a function of time by pressure transducers. The differential pressure between the inside and outside of the insulations is measured with strain-gauge pressure transducers.

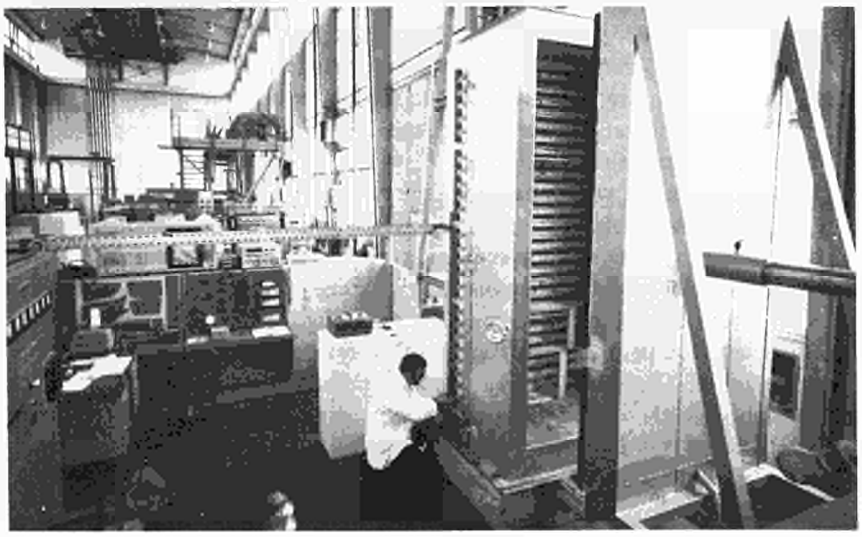

Fig. 2

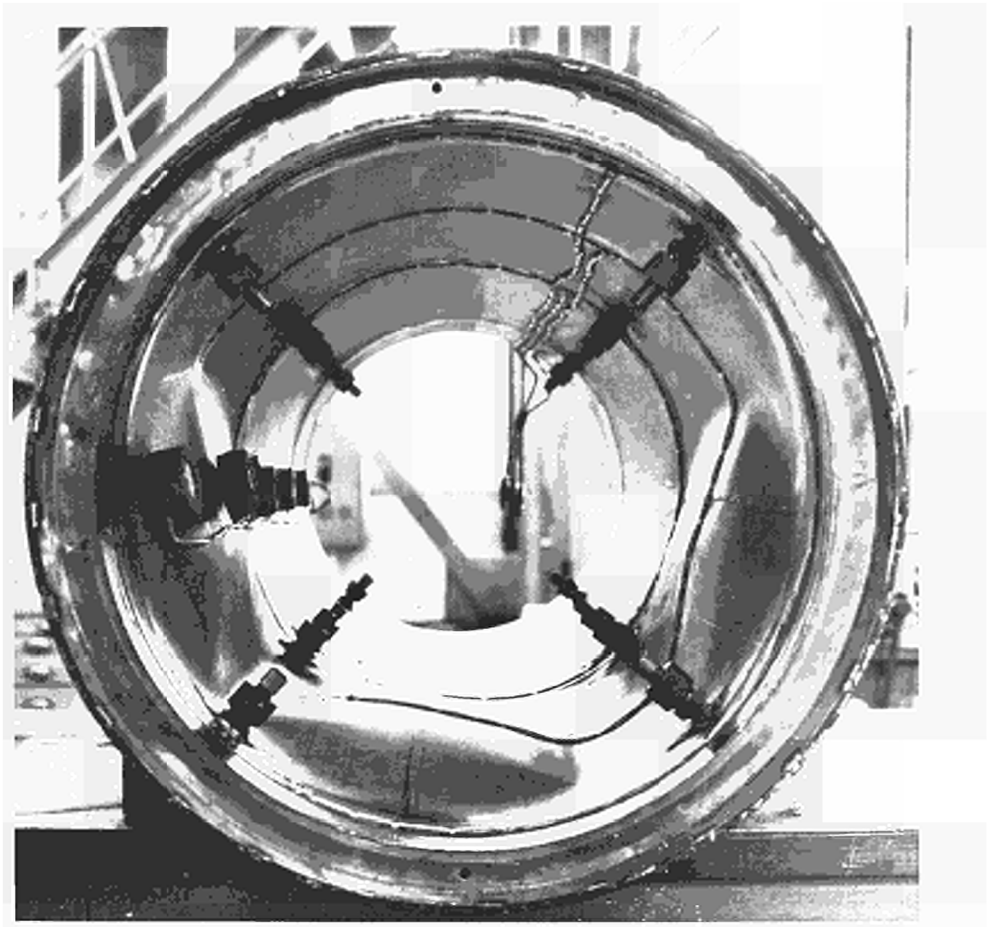

Fig. 3: Insulation coil after buckling.

The test insulations consist of two insulation bobbins (lenght 605 mm, inside diameter 480 mm, outside diameter 540 mm). Each bobbin is composed of 17 layers of stainless steel foils separated from each other by a wire mesh. The layers are enclosed between an inner and outer layer of stainless steel.

By assuming that the depressurization phenomenon in the vessel is isentropic, that the velocity of the gas is sonic at the diaphragm and that the gas is perfect, the pressure $P_A(t)$ in the vessel can be calculated theoretically as a function of time.

The pressure difference ΔP between the inside and outside of the insulation, during the depressurization of the vessel, is measuredd. From the mechanical point of view, one is particularly interested in the maximum value $(\Delta P)_{max}$ and the critical time t_{cr} at which it occours. In order to predict these values, a mathematical model was made.

It is interesting to note that in a reduced system the equations are independent of the molecular weight of the gas and of the initial temperature. In a reduced system, the maximum pressure difference can be expressed as a function of the initial depressurization rate and the critical time at which a comparison was made between the calculated curves and the experimental points.

Two different types of bobbins were tested, with increasing depressurization rates, and between tests various modifications were performed on the bobbins in order to reduce the ΔP. On the first bobbin with an inital depressurzation rate of 16.1 atm/sec (helium under initial pressure of 25 kg/cm^2) a ΔP of 0.85 kg/cm^2 was measured and no damage was observed. Under the same conditions, the second bobbin with a ΔP of 1.63 kg/cm^2 was subjected to severe damage in the form of buckling (Fig. 3).

An important correlation exists between permeability tests (gas flow resistance tests) and the values of (ΔP)max measured during depressurization. Changes in the values of the permeability characteristics after a series of depressurization tests mean that there have been alterations in the internal structures of the insulations.

Other control tests, such as X-ray photographs (to observe displacement of the wire mesh), metrology and leaktests of welds were performed.

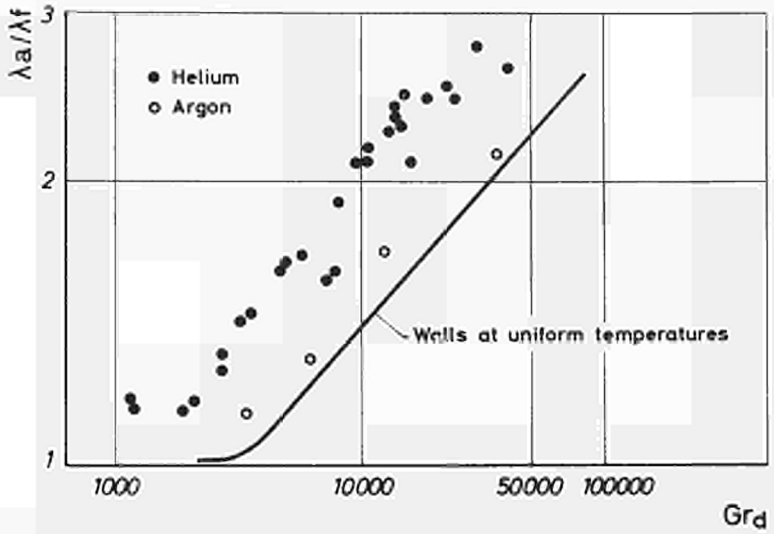

Fig. 4: Influence of vertical temperature gradients.

The tests demonstrated the importance of ascertaining the behaviour of multilayer insulation systems under rapid depressurization conditions, which can be severe in the ducts of the primary circuit. Because of the rather low resistance to buckling of these systems, the pressure difference between the inside and the outside of the insulations should not exceed 1 kg/cm^2. Permeability tests have shown that the gas flow resistance of the inside wire mesh is negligible compared to the gas flow resistance at the boundaries of the insulations. With the help of a mathematical model these permeability tests can also be used to predict the values of the maximum pressure difference in the insulations submitted to depressurization. Agreement with experimental results is fairly good.

This work on depressurization phenomena was performed in the framework of a collaboration contract with KFA Jülich.

Basic studies of heat transfer in multilayer insulation systems

In multilayer systems, heat is transferred from the hot wall to the cold wall by complex modes involving natural convection, radiation and thermal conduction with a relative importance for each mode varying with each layer. These phenomena of heat transfer have been studied theoretically and experimentally in a test model with four layers in series. Tests were done with helium and nitrogen up to GRASSHOF numbers of 1.000.000 with special attention to the influence of vertical temperature gradients or heat transfer by natural convection. In the last period this experimental program was completed. Very good agreement was found with a mathematical model (Fig. 4). Meanwhile a collaboration contract has been signed with the Politecnico di Torino concerning the problem of natural convection in close cells.

Thermal insulation systems for very high temperatures (≅ 1000°C)

An activity on thermal insulation systems at temperatures of the order of 1000°C is being started.

An economic and technological evaluation of special insulating materials such as silicon nitride, carbon foams, etc., will be made. Design aspects concerning fabrications, mounting and assembling will be studied. An experimental programme including thermal tests, thermal cycling and pressure cycling and depressurization tests will be performed on specimens and elementary structures. Two installations (one with a plasma generator and a depressurization facility) are being constructed.

References

1) "Thermal Insulation Systems for Prestressed Concrete Vessels of High Temperature Gas Reactors" *Deutsches Atomforum*, Boon, April, 1971. Aranovitch, E., Crutzen, S., Dufresne, J., Farfaletti, F.

2) "Calculation Methods of Multi-layer Insulation Systems for High Temperature Gas Reactors", First Int. Conf. on Structural Mechanics in Reactor Technology, Berlin, Sept., 1971. Aranovitch, E., Crutzen, S., Dufresne, J., Farfaletti, F.

3) "Rapid depressurization of a multilayer insulation system for High Temperature Gas Reactors" *Deutsches Atomforum*, Hamburg, April, 1972. Aranovitch, E., Van Asselt, D.

4) "Etude thermique d'une structure isolante cellululaire métallique mixte par des méthodes graphiques et statistiques de traitement des données experimentales".

5) "Internal Thermal Insulation Panels for the Prestressed-Concrete Pressure Vessels and the Primary Circuits of Gas Cooled Nuclear Reactors".

ELECTRONICS

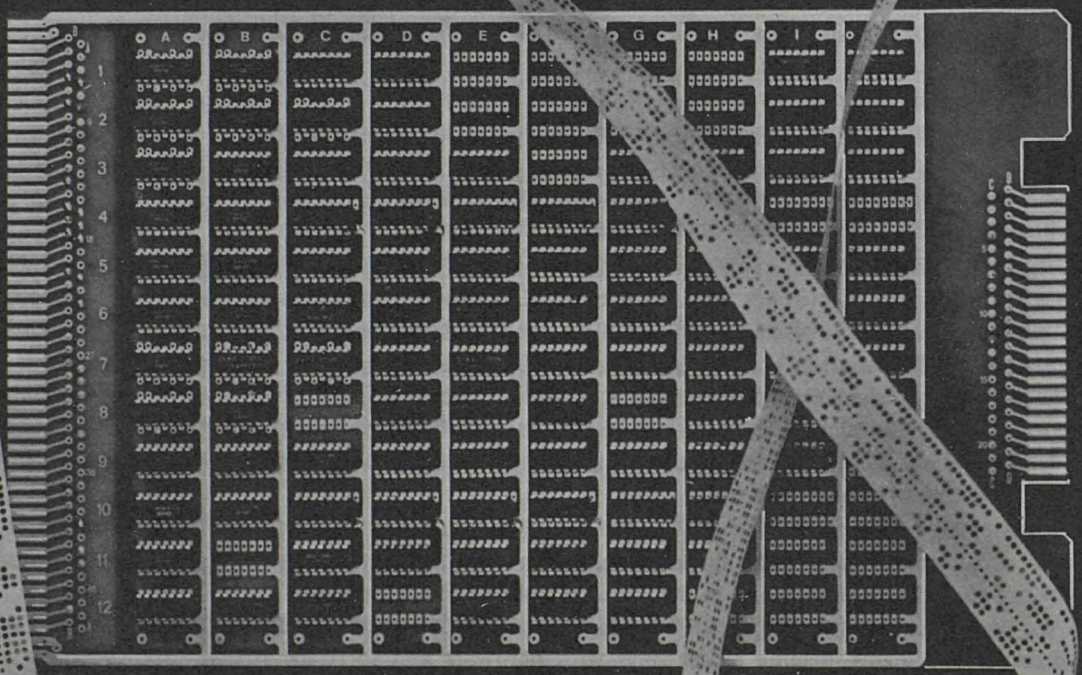

ION IMPLANTATION STUDIES

SMART, A REAL-TIME SYSTEM

DATA TRANSMISSION SYSTEM

DEVELOPMENT OF A SKINMETER

PORTABLE MULTICHANNEL ANALYSER

DERANDOMIZER FOR FAST ACQUISITION

ELECTRONIC UNIT

G. Bertolini

The Electronic department was formally established in August 1970 by combining four laboratories previously belonging to the departments of Engineering, Reactor Physics and Chemistry. These laboratories had been working for many years in nuclear electronics, control instrumentation, data transmission, biomedical electronics and semiconductor detectors development. The present organization of the Service is as follows:

1. Administration. This includes the ESONE-CAMAC Office which acts as Secretary for the ESONE Committee, sends out technical documentation to research laboratories and industries, and collaborates with the DG XIII in the publication of the CAMAC Bulletin.
2. Data Acquisition and Instrumentation Section.
3. Automation and Control.
4. Electron Physics Section (main activity: Ion Implantation Studies).
5. Diversification Section (main activity: Biomedical Engineering).
6. Technical support including a Maintenance Service for the electronic instrumentation of the Centre.

The activity of the Electronics Service can be divided into two parts: support to the programmes of the Centre and its research. The electronics research involves the development of special instrumentation, giving advice on the implementation of complex data acquisition systems, and the development of new methods.

The highlights of these activities are presented in the Selected Topics.

Apart from a great quantity of miscellaneous instrumentation developed for the Ispra JRC laboratories, three types of study were undertaken, chosen in the light of the outcome of extensive discussions with the research laboratories of the Centre.

- Analysis of the characteristics of the available mini-computers (PDP, HP, IBM, LABEN, CII, PHILIPS).
- Study of automatic design of digital circuits. The program foresees the extension to the automatic layout of the printed circuits and to the circuital analysis. Fig. 1 shows an example.
- At the end of the year it was decided to start the development of modular instrumentation in CAMAC Standard. Two teams, dealing respectively with hardware and software aspects of CAMAC, will start operation at the beginning of 1972.

The Electronics department pursued its own research line in the fields of Biomedical Engineering and Electron Physics.

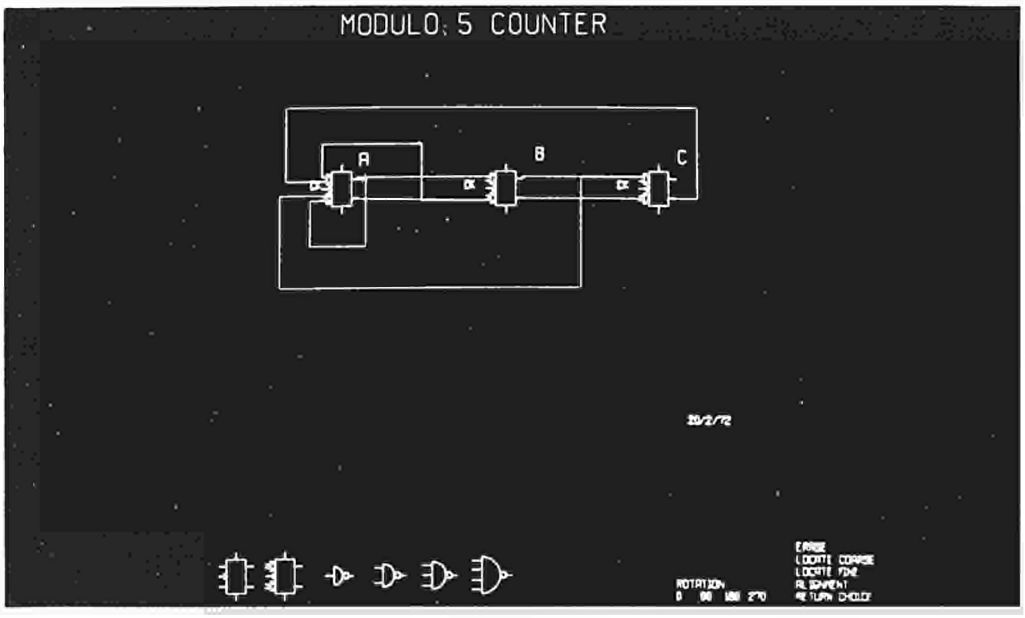

Fig. 1

Biomedical Engineering

This activity was carried on during 1971 by the engineer in charge, together with trainees or personnel of the Electronics department.

At the end of the year two other engineers joined in this research, thus creating the nucleus of a future group.

During the past year a programme was submitted in connection with the "Pollution" project, and was approved by the Advisory Committee.

The principal results obtained can be summarized as follows:

- Improvement of the electronic control of the mechanical hand.
- Increase of the signal-to-noise ratio in the detection of myoelectronic signals.
- Stimulation of nerves by means of a new electrode conception.
- Study of a miniaturized and completely passive pressure transducer.
- Development of a non-irritant electronic skin-impedance meter.

Electron Physics

The activity of this section has evolved from the studies on semiconductor detectors to more general fields of Electron Physics. In this context, taking advantage of the experience previously gained in the field of semiconductors, research on the physicochemical behaviour of ions implanted in semiconductors was undertaken.

At this stage most efforts have been devoted to establishing special techniques like ion implantation and methods of impurity concentration profile analysis.

The work on semiconductor detectors continued with an experiment conducted jointly with the University of Milan on the determination of the half-life of the decay ^{76}Ge $\not\beta\beta\rightarrow$ ^{76}Se. For the neutrinoless transition a value of the order to 10^{22} years was obtained, which represents the highest limit obtained for this type of transition. This experiment also allowed investigation of the ultimate limit and the components of the radioactive background associated with a Ge(Li) spectrometer (IEEE 1971 Nuclear Science Symposium).

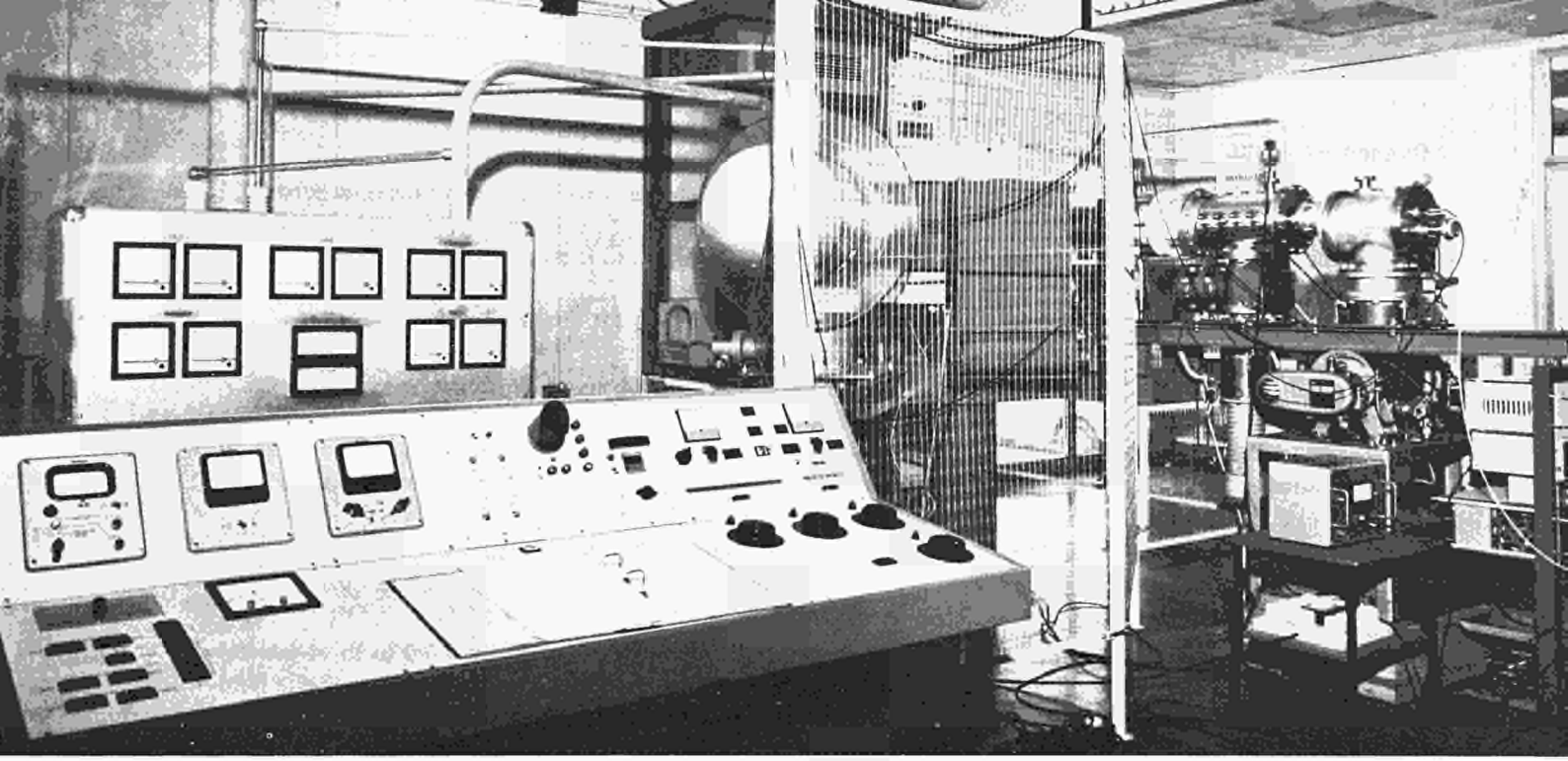

Fig. 1: The 100 KeV heavy ion accelerator.

TECHNIQUES FOR ION IMPLANTATION STUDIES

G. Restelli F. Cappellani

100 keV Heavy Ion Accelerator

In connection with a research project on ion implantation, a 100 keV ion accelerator has been designed and constructed [1) 2)]. The work was started in 1969 and completed during this year. The machine allows acceleration from 0 to 100 keV of almost every ion species with the exception of Au, Pt and Ir.

A view of the machine is shown in fig. 5.1, while fig. 5.2 gives the schematic layout of the accelerator.

The accelerating voltage has been split into two steps: the first one, applied to the source, can be set from 0 to 75 kV in steps of 10 kV each while the second one, applied to the constant field tube, can be continuously adjusted from − 25 to + 25 kV. The ion source potential with respect to the grounded target is given by the algebraic sun of the two voltages. The main advantage of this configuration is the high extraction potential (at least 25 kV) even for the lowest ion energies, thus assuring a good ion extraction yield. The ion source is the DANFYSIK 910 model, with which currents of some μA can be obtained from a broad range of chemical elements and compounds. The extraction and focusing system consists of a three-electrode Einzel lens. The extraction gap, as well as the position of the ion source outlet in the plane normal to the beam axis, can be varied without breaking the vacuum. The configuration of the electrodes was designed according to the results of computer calculations for ion trajectories [3) 4)].

The analysing magnet is of sector type with an aperture angle of 127°, radius 60 cm and a mean gap width of 32 mm; the mass x energy product is equal to 16 amu.·MeV. Double focalization is accomplished by means of diverging poles with hyperbolic shape [5)]; a circular beam of parallel trajectories at the magnet input is focalized in one point at the end of the magnet (ignoring space charge effects) [6)].

Some peaks of the Xe beam mass spectrum (shown in fig. 5.3), as displayed by the beam scanner positioned 25 cm from the magnet output, enable the separation of the peaks and their resolution to be assessed.

The post-acceleration is provided by a set of ten electrodes calculated to give a constant electric field distribution on the beam axis. From the experimental results it appears that the beam dimension at the target is not influenced by the operation of the constant field tube (retardation or acceleration). Uniform irradiation of the target area is ensured by sweeping the beam in X-Y directions [7)]. Beam sweeping over a square of 3 cm side is performed by two sets of electrostatic deflection plates. These are driven by 2000-volt peak-to-peak triangular waves of 20 and 2000 Hz frequency respectively for the X and Y sweep.

The maximum deflection angle results ± 1,5°. A remote control order given by a current integrator connected with the target stops the beam sweeping, positioning the beam out of the bombarded area, when a preset charge has been implanted.

The target chamber consists of a cylinder provided with a terminal flange which can be easily interchanged with other normalized flanges. The room-temperature facility allows implantations on up to eight specimens to be performed consecutively without breaking the vacuum. Using the other flanges, four samples to be bombarded can be cooled by liquid nitrogen down to 100°K or heated up to 800°K by an electron gun. Beam collimators and a secondary electron suppressor are incorporated in the target chamber. A beam viewing facility is provided for the room-temperature implantation flange.

A two-axis goniometer can be fitted to the target chamber for implantation in channeling conditions. The goniometer designed and constructed in the laboratory allows positioning of the specimen with an accuracy of 0.05°. The sample on the goniometer can be cooled or heated during the implantation.

The vacuum system has been designed to reduce to a minimum the surface contamination of the target. Therefore a turbomolecular pump and an ion pump are used in the second part of the accelerator after the magnet. Electrical and vacuum commands, controls, protection circuits and the beam control systems are assembled in a control console.

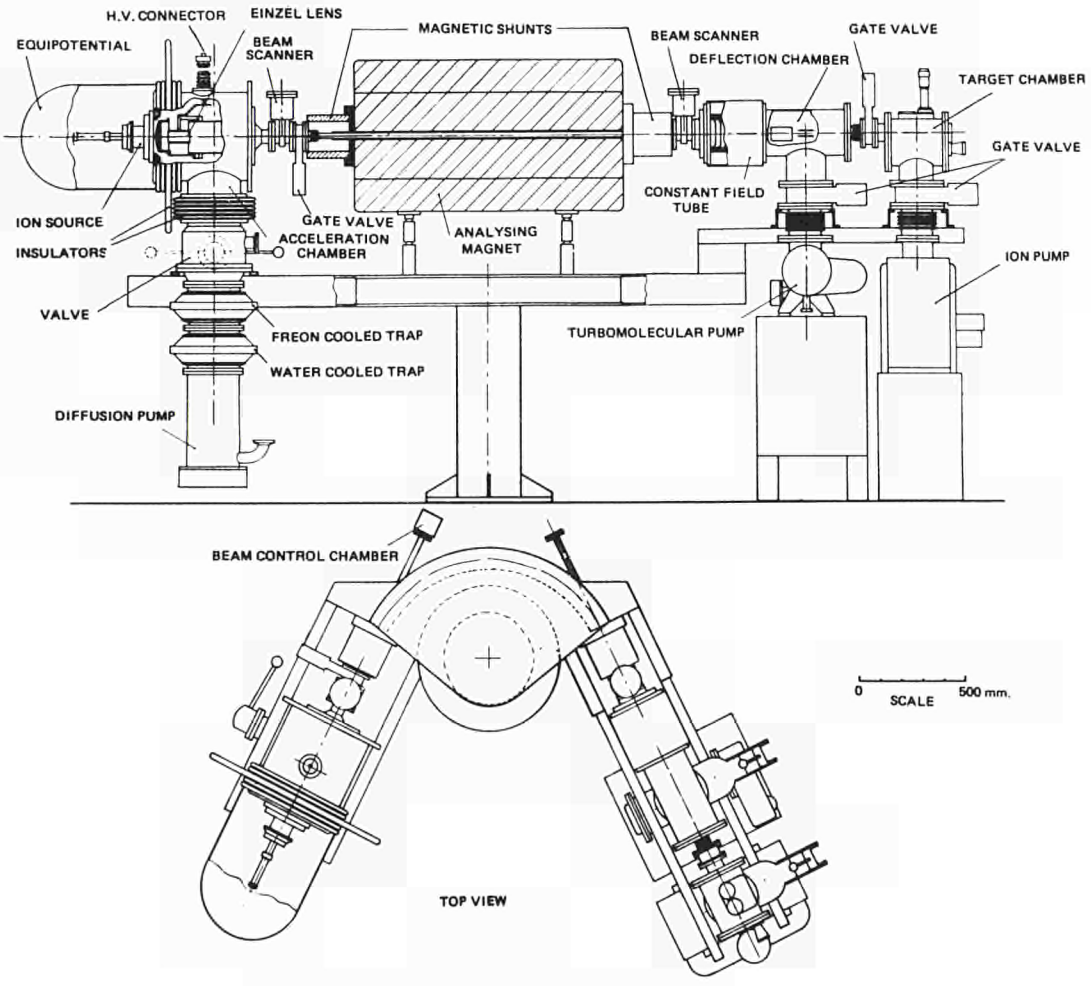

Fig. 2: Schematic lay-out of the accelerator

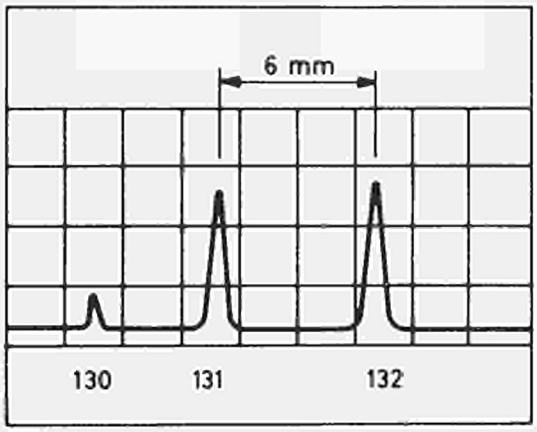

Fig. 3: Mass spectrum of Xe (from M = 130 to M = 132) as displayed with the beam scanner.

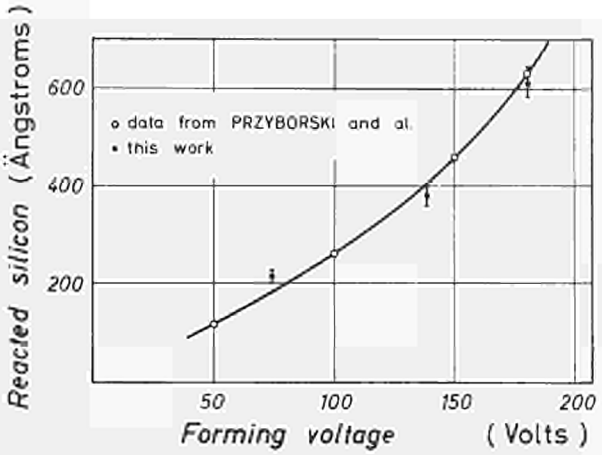

Fig. 4: Reacted silicon vs. forming voltage calibration curve EG – 0.4 % KNO_3 – 10 % H_2O; anodization current 5 mA cm^2.

Anodic Oxidation Studies

The determination of the distribution versus depth of concentration of impurities diffused or implanted in a substrate is one of the most important problems in the field of ion implantation. In fact the study of ion penetration and range, the determination of the electrically active fraction in semiconductors and the understanding of enhanced diffusion phenomena depends on a precise knowledge of the impurity concentration profile. The profile determination is performed by successive removal of thin (20-2000 Å) layers of material in a controlled and reproducible way, measuring by a suitable technique either the impurities removed or those remaining in the sample.

Removal of the layers is most frequently performed by "anodic stripping" [8]. This consists in the electrochemical growth of an anodic oxide on the surface of the specimen to be sectioned.

The oxide is then selectively removed by a reagent which does not dissolve the substrate. The thickness of the oxide and then the thickness of the material stripped can be accurately controlled by the parameters of the electrochemical process.

In spite of the common use of this technique many problems still exist concerning its optimum utilization and the limits of accuracy attainable in the evaluation and reproducibility of the layer removed. This theme has been the object at this laboratory of various studies, begun during 1970 and performed in cooperation with the Physics and Chemistry Divisions:

a) application of anodic oxidation to silicon sectioning [9];
b) design of an automated system for physical profile determination using radioactive tracers;
c) extension of the anodization technique to SiC sectioning.

Here we shall report extensively only on point a), since research on b) and c) is still in progress.

Among the anodization baths reported in literature, the ethylene glycol (EG) 0.4% KNO_3 10% H_2O [10] has been studied. This presents the following advantages over other electrolytes:

a) it allows room-temperature operation;
b) it does not dissolve the silicon;
c) it gives brilliant interference colours;
d) it allows accurate control for the growth of the oxide layer;
e) it gives reproducible results.

Anodization in constant current mode appears definitely preferable and offers through the recording of the forming voltage a more accurate control of the oxide thickness with respect to anodization for preset time. The dependence of the anodic stripping process on parameters such as lattice disorder, and in some cases resistivity, requires the construction of a calibration curve (thickness of silicon removed vs anodizing voltage). An absolute calibration of the silicon removed can be performed by measuring the weight loss or by radiochemical evaluation of the silicon dissolved: both methods are critical. It is proposed to use for this calibration the measurement of the silicon to silicon oxide thickness ratio (Si : SiO_2) to transform the oxide thickness evaluated by optical methods into silicon thickness removed per anodization. This was done in the case of the EG electrolyte and showed the satisfactory agreement of a calibration curve constructed in this way (reacted silicon vs. forming voltage) with that obtained by a radiochemical method by Przyborski et al. [11] (fig. 5.4) and with values obtained by weighing techniques [12].

The limits of accuracy obtainable in the anodic stripping appear to depend on the experimental technique used. If the interference colour of the oxide is visually compared with those of a series of specimens accurately calibrated (e.g. by ellipsometry) the total accuracy that can be expected appears not worse than ± 8%. The error can be greater when the anodization is only controlled by presetting the forming voltage. This is especially true when N+ layers of resistivity lower than $10^{-2}\,\Omega$ cm are sectioned. It has been observed in fact that the calibration curve of oxide thickness versus forming voltage deviates up to 25% for N+ layers of $10^{-4}\,\Omega$ cm. These errors compare unfavourably with those reported in literature [1) 4)]. However it should be noted that both these curves were obtained using silicon slices all of the same resistivity (O.1 and 0.4 Ω cm).

The use of this electrolyte and generally of the anodization process as a silicon sectioning technique appears satisfactory for the removal of silicon layers 150-200 Å thick. For thinner layers the large spread in the Si: SiO_2 ratio observed inhibits the achievement of a reliable calibration.

Consequently the use of the anhydrous diethyleneglycol 0.4% KNO_3 was investigated. The water content was below 0.5%. This electrolyte appears to give less spread in the oxide thickness obtained at a preset forming voltage in constant current operation and should simplify the problem of the variation of the Si: SiO_2 thickness ratio. In fact in nearly anhydrous electrolytes it is generally accepted that the anodic oxide grown on silicon corresponds to stoichiometric SiO_2 (Si: $\overset{\circ}{S}iO_2$= 0.43). Our results are in satisfactory agreement with this hypothesis for oxides thicker than 600 Å but for thinner oxides the Si: SiO_2 ratio differs considerably; a value of 0.6 ± 15% has been observed, in agreement with recent results reported for anodization in N-methylacetamide with 10% H_2O [13)].

It must be concluded that when layers thinner than 150 A of silicon have to be removed it is still necessary to resort to other more critical techniques like vibratory polishing [14)] chemical etching [15) 16)], or R.F. sputtering [17)].

References

1) R. Benoit, G. Bertolini, F. Cappellani, G. Restelli: Nucl. Instr. & Meth 99 (1972) 421.
2) R. Adam et al. EUR-4753 e (1972)
3) C. Mongini-Tamagnini, to be published.
4) G. Gaggero, to be published.
5) L. Stanchi, *Nucl. Instr. & Meth.* 73 (1969) 313.
6) G.Gaggero, EUR report to be issued.
7) R. Benoit, G. Melandrone, EUR 4754 e (in press).
8) J.A. Davies, G.G. Ball, F. Brown and B. Domeji, Can. J. Phys. 42 (1964) 1070.
9) A. Manara, A. Ostidich, G. Pedroli and G. Restelli, *Thin Solid Films 8* (1971) 359.
10) K. M. Busen and R. Linzey, Trans. AIME 236 (1966) 306.
11) W. Przyborski, J. Lipper and L. Sarholt-Kristensen, *Radiation Effects 1* (1969) 33.
12) J.A. Kerr, Wembley Lab. ASM unpublished report (1967).
13) K. Gamo, K. Masuda, S. Namba, S. Ishihara and I. Kimura, *Appl. Physics Letters 17* (1970) 391.
14) J.L. Witton, *J. Appl. Phys. 36* (1965) 3917.
15) I.A. Galaktionova, V.M. Gusev, V.G. Naumenko and V.V. Titov, Coll. Int. sur les Applications de Faisceaux Ioniques à la Technologie des Semiconducteurs, Grenoble (1967) 487.
16) R. Bader and S. Kalbitzer, *Appl. Phys. Letters 16* (1970) 13.
17) D. Gupta and R.T.C. Tsui, *Appl. Physics Letters 17* (1970) r94.

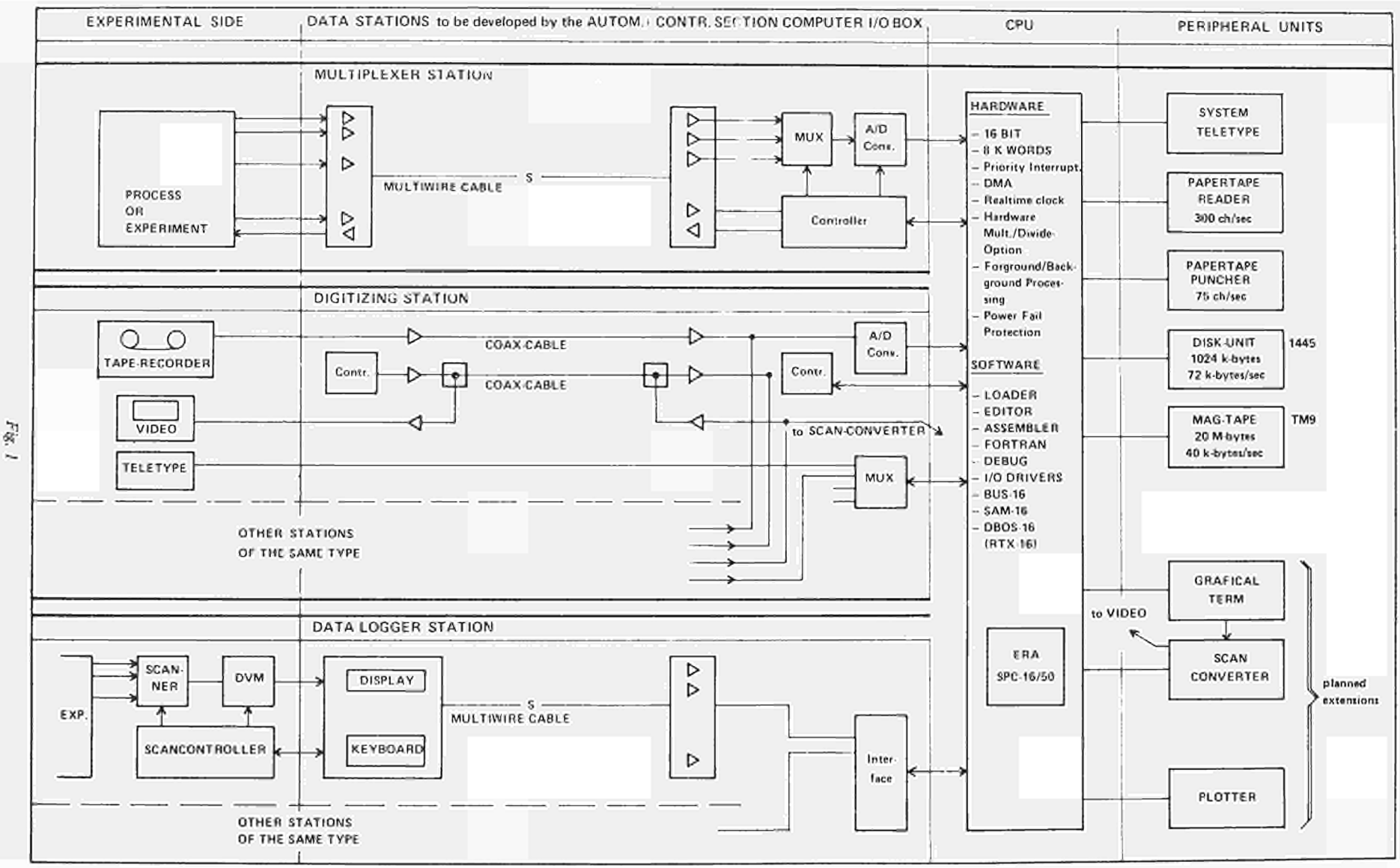
EXPERIMENTAL SIDE
DATA STATIONS to be developed by the AUTOM. CONTR. SECTION COMPUTER I/O BOX
CPU
PERIPHERAL UNITS
MULTIPLEXER STATION
PROCESS OR EXPERIMENT
MULTIWIRE CABLE
MUX
A/D Conv.
Controller
DIGITIZING STATION
TAPE-RECORDER
VIDEO
TELETYPE
Contr.
COAX-CABLE
COAX-CABLE
A/D Conv.
Contr.
to SCAN-CONVERTER
MUX
OTHER STATIONS OF THE SAME TYPE
DATA LOGGER STATION
EXP.
SCAN-NER
DVM
SCANCONTROLLER
DISPLAY
KEYBOARD
MULTIWIRE CABLE
Inter-face
OTHER STATIONS OF THE SAME TYPE
HARDWARE
- 16 BIT
- 8 K WORDS
- Priority Interrupt
- DMA
- Realtime clock
- Hardware Mult./Divide-Option
- Forground/Background Processing
- Power Fail Protection
SOFTWARE
- LOADER
- EDITOR
- ASSEMBLER
- FORTRAN
- DEBUG
- I/O DRIVERS
- BUS-16
- SAM-16
- DBOS-16 (RTX-16)
ERA SPC-16/50
SYSTEM TELETYPE
PAPERTAPE READER 300 ch/sec
PAPERTAPE PUNCHER 75 ch/sec
DISK-UNIT 1024 k-bytes 72 k-bytes/sec
1445
MAG-TAPE 20 M-bytes 40 k-bytes/sec
TM9
GRAFICAL TERM
to VIDEO
SCAN CONVERTER
PLOTTER
planned extensions

Fig. 1

SMART, A SYSTEM FOR MEASUREMENT AND AUTOMATION IN REAL TIME

J. Eder, L. Kobus, W. Riebold, F. Sorel

Introduction

In a big research laboratory environment like that of the Technology Division many functions of measurement and recording, logging and displaying the results and providing outputs for controlling equipment can be simplified and coordinated by a minicomputer, which figures as the central unit of a data acquisition system. Such a system, which can be shared by many experiments, was been purchased by the Technology Division during 1970 and 1971.

During the rather long period of examination and discussion of the different systems which were on the market at that time, the Electronics Department gave advisory support in the search for the system that would best meet the technical requirements (from the application point of view) and simultaneously show the most favourable price performance ratio (from the hardware point of view).

The system chosen consists of the SPC 16/50 minicomputer as the central processor unit (CPU) and the different peripherical units as sketched in Fig. 1.

During 1971 the Electronics Department started, at the request of Technology, on the development of different data stations (Fig. 1) which link the experiments with the CPU. As a first step, therefore, a project study was made on the basis of the then existing system and requirements on the experiments side. Future extensions and the possible need to improve the system with further peripherals were also taken into account.

The brief outline of the design philosophy given below is followed by a description of the first part of the work done. Owing to the lack of specialized personnel in the Technology Division and the large amount of software work to be done, the Electronics Department is also providing software support.

Design Philosophy

Any given experiment - which may be located at distances up to 1 km from the computer - is equipped with a data station which provides for the transmission of the experimental data and the exchange of control signals with the computer. Depending on the nature of the data processing desired, different types of data stations are required.

The jobs foreseen for the minicomputer can be subdivided into three categories:

1. measurement of process data with fast transients and multiple parameters;
2. digitizing with high A/D conversion rates and time synchronization of tape-recorded analog signals;
3. data logging with preliminary calculations to scale the measured results into engineering units.

In a later evolution of the system the automatic control of experiments in response to measured values (digital control-loops) may be envisaged.

The system designed around the SPC 16/50 minicomputer optimally matches the above-mentioned requirements from the hardware and software point of view.

The SPC 16/50 meets the stringent specifications of fast A/D conversion and offers furthermore a broad choice of I/O interfaces and miniprocessors, thus avoiding expensive development of special equipment.

SMART Hardware Requirements

The hardware configuration of the system in shown in Fig. 1. Three types of data stations are provided. The computer can service several stations of each type.

Multiplexer Station

An analog data transmission system on a multiwire cable has been developed, which transmits the measurement signals and some control signals to the computer. The Multiplexer, A/D converter and control circuitry are assembled in the computer I/O-box. The A/D converter is program-controlled whilst the data channel works in DMA (direct memory access) mode in order to achieve high transfer rates. During data input a simultaneous core-to-bulk transfer (magnetic disk or tape) on another DMA channel is possible.

Fast Digitizing Station

At present, tape-recorded analog signals can be digitized via the A/D input of the multiplexer station. This, however, entails transporting the bulky, heavy tape-recorders to the computer room (an identical playback-drive is not available at the computer installation). Consequently, since many labs concerned with digitizing are distantly located, it is planned to install transmission systems with two coaxial cables. At the data station the analog signals will be transmitted sequentially track by track on one cable while the other cable sends timing signals for the synchronisation of the A/D conversion. For this purpose a further A/D converter with a conversion rate high enough to exploit the highest possible rate of direct data transfer to the SPC 16/50 core memory is necessary.

Data-Logger Station

Data input stations are in preparation which serve as a two-way interface between the digital data sources and the transmission system to the computer. The digital data sources consist generally of an integrating digital voltmeter and a scanner which are controlled by the data station. One of the stations will be equipped with a keyboard and a display to input auxiliary data (e.g., job numbers, data) and control commands. Later on the keyboard will be replaced by a teletype. In a final stage every data station will be equipped with a teletype and a video monitor (as shown for the digitizing station in Fig. 1). This final stage has to be taken into account already in the present development work on all data stations. The teletypes are provided for the dialogue with the computer and the exchange of control signals.

Although the teletype can be utilized to list and display results of the measurements, this is only a temporary solution. As soon as a graphic terminal becomes available for the system, each data station will be equipped with a low-cost video receiver. By means of a scan converter, the graphical or alphanumeric information in the graphic terminal is transformed into a video signal, which can then be transmitted on one of the coaxial cables to the various data stations.

In this way any subscriber to a data station terminal has access to a graphic display for inspection of his results without spending the full price of a true graphic terminal.

Software Considerations

The different functions and experiments are divided into tasks, which help to clarify overall program structure. The task is a program or function, which may be written in FORTRAN or Assembly language and separately compiled. The work of writing task programs can be divided among the groups concerned with the experiments.

Tasks can communicate mutually by means of external definitions and references. The writing of programs is supported by an important subroutine library located on the disk storage unit. Multiple files on the disk storage unit are provided for storage of task programs (user library) in source or binary format. At a later date tasks may be taken from that library and modified owing to new experimental requirements.

A disk-based operating system (DBOS-16) is available which simplifies program compilation, assembly, debugging, editing and linking. DBOS incorporates an input/output system which is capable of generating totally device-independent programs. Programs reference I/O operations by logical unit number. Drivers are included which support most standard peripherals. Special purpose user-programmed drivers can be easily incorporated.

A real-time-executive operating system is available which permits the real-time scheduling of up to 255 functional programs (tasks) on a fully priority basis.

Conclusions

At the present time two blow-down experiments with 16 parameters are serviced by SMART via the multiplexer station.

Two versions of data logger stations are planned. The development of the first model is terminated and a prototype will soon be built. The second model is a stripped-down version without keyboard and display.

For the multiplexer input an analog data transmission system on multiwire cable is in preparation.

A conversational program for plotting up to 7 parameters simultaneously on the teletype has been assembled and tested.

DATA TELEPROCESSING SYSTEM 130

S. Amie, M. Combert, S. Colzani, J. Eder, A. Termanini

Introduction

System 130 is designed for online data transmission between several distantly located digital data sources and the peripherical unit of a centralized computer. Any data source is linked via an associated remote station to a central station, which serves as an interface to the peripherical unit. 4 bit (= 1 character) parallel transmission is used.

The transmission speed is generally limited by the data source or by the available communication line and not by the system 130 itself.

The dialogue with the central computer is assured by standard I/O terminals (e.g., teletypes) installed at each remote station.

Main Features

- Central station with up to 36 remote stations
- Transmission speed up to 40000 bit/sec
- 4-bit parallel transmission
- Maximum distance 2000 m
- Photocoupled interface to avoid ground loop problems
- Real time clock at every remote station
- Central station compatible with various computer systems.

The standard configuration of the System 130 includes a central station and six remote stations.

Each System 130-remote station receives data from its associated digital data source. After conversion into 4-bit characters the information is sent in 4-bit parallel mode to the central station, which communicates with the peripheral unit.

The Central Station forms data blocks of length n characters, suitable to the requirements of the peripheral unit and the computer I/O software. It decodes the computer's control signals in addressing and timing commands. If a data source is ready to transmit its data, it informs its remote station by generating a ready flag and a transmit request at the central station. The computer periodically checks the request of each remote station and enables the first station which is ready to transmit. The central station issues a multi-character-input (MCI) signal and initiates the transmission of one data block of the corresponding remote station. The first data transmitted contains the value of a real-time clock, indicating the time at which the data source had terminated its accumulation. This is followed by the source data block. During the transmission of the source data block an increment-channel-pulse (CIP) is created and sent to the data source to ask for the content of the successive analyser channel.

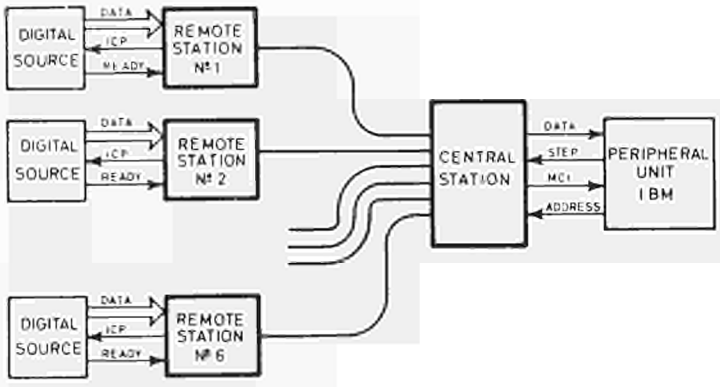

Fig. 1

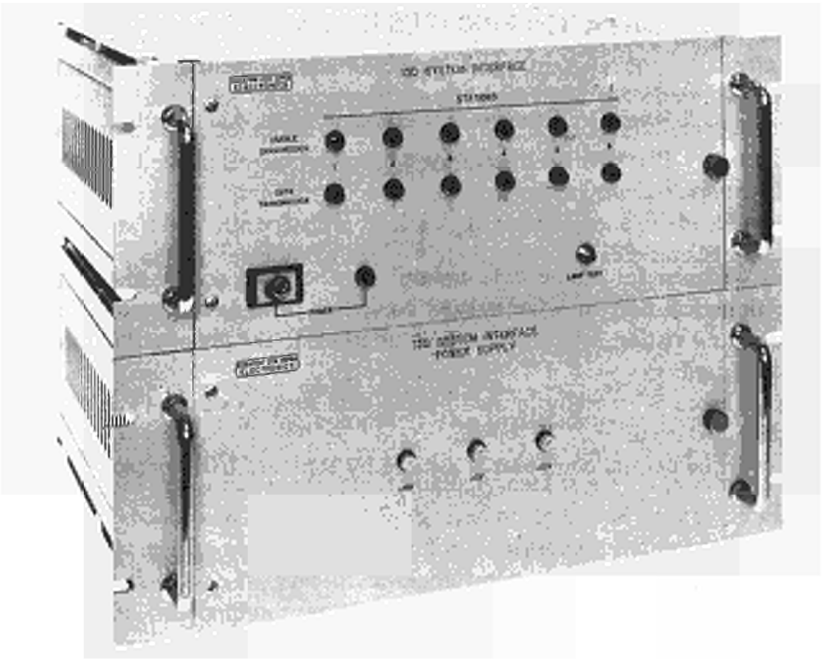

Any data block is terminated by a 4-bit status word which can be end of block (EOB) or an end of transmission (EOT) signal.

EOB signifies that still more data is to be transmitted, whereas EOT terminates the transmission from a data source.

The Central Station controls up to six remote stations It receives the control signals from the peripheral unit which provide addressing and timing of the remote stations, and transfers suitably formatted data blocks to the peripheral unit.

Up to five expansion units can be connected to a central station. Any expansion unit controls six remote stations.

- After the control unit (see Fig.) has received an address the multiplexer opens the corresponding line of the requested remote station, the status of which is then checked. If the called station is not ready the computer removes the address, otherwise the transmission begins.
- The block generator counts the desired length of the data block and issues at the end a 4-bit status word. EOB (0100) is used to signal the end of a data block which interrupts the transmission. The next block is then tranferred. When the last character of a data source is encountered and the data source resets its ready flag an end of transmission EOT (1000) statusword is sent to the computer and the transmission of this remote station is terminated.
- The interfaces to the remote stations and to the peripheral unit are equipped with optical couplers. Thus an ideal decoupling between the central station and the external world is achieved, avoiding tedious problems with ground loops.

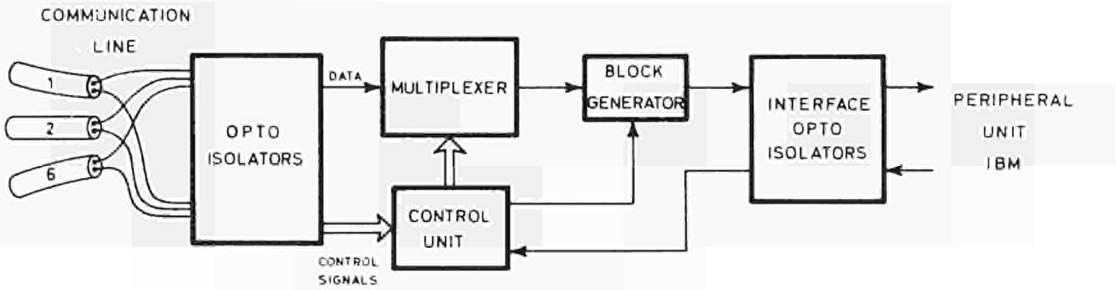

Fig. 2

System 130-remote stations are designed to link digital sources containing memorized data via a system 130 central station to a peripheral unit of a centralized computer system.

- The data transfer between source and remote station is provided for 6 BCD-digits in parallel mode. The transmission to the central station occurs in 4-bit parallel mode by means of a digit serializer.
- A real time clock with 6-digit display (hours, minutes, seconds) is available. The data source advises its remote station with a ready flag that it has terminated its data collection. At that moment the content of the real time clock is transferred to a buffer. This is the first value to be transmitted.
- The control unit generates an "increment channel pulse" (ICP) which automatically transfers the next analyser channel to the remote station after the transmission of the preceding channel is completed.
- During the interruption after an EOB the ready flag remains on and the transmission of the clock value is suppressed for the second and following data blocks. The transmission of data blocks continues as long as the ready flag is on. It is reset after the last analyser channel preselected by the operator.
- The Interface to the central station is equipped with optical couplers, whereas the data source is directly connected with the remote station by means of suitable level adapters.

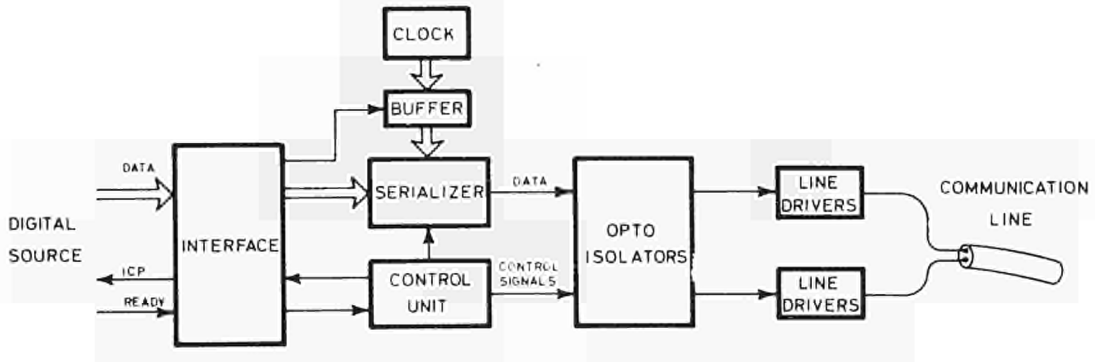

Fig. 3

DEVELOPMENT OF AN INSTRUMENT FOR THE MEASUREMENT OF ELECTRICAL PARAMETERS (U, R, C) OF THE SKIN WITH MINIMUM IRRADIATION INFLUENCES ON THE BIOSYSTEM

W. Becker

The measurement of the electrical skin resistance is a classical method of diagnostic medicine. Furthermore it is reported [1] that the measurement of the so-called Psychogalvanic Reflex (again the conductivity of the skin) is applied to special aspects of industrial medicine, e.g., for emergency crews working under environmental stress, for instance in heavily contaminated ambients. M.W. Johns et al. [2] stated recently that by registration of skin resistance the sleep periods of a patient could be recorded. An elaborate diagnostic method based on the knowledge of the ancient Chinese Acupuncture, has been developed by Voll [3]. Similar methods, all following the same basic idea of measuring the electric skin resistance at the "acupoints" of the different "meridians", have also been developed by many others. For many measurements of biopotentials at the body surface a better knowledge of the skin's resistance behaviour could improve the measuring efficiency. It can be concluded herefrom that these are reasons enough to study more carefully the distribution of electrical skin impedance over the skin surface and the possible relevance of impedance pattern alterations to pathological situations or prepathological tendencies of the organism. It is hoped that such measurements might even in some cases be adapted to the prediction of environmental toxic effects on humans before pathological alterations occur. Because of its easy and noninvasive application this might be achieved through health-screening of local populations. Since the aim of the work described here has not been primarily to do clinical tests but rather to develop an instrument capable of faithfully reproducing results, the falsifying technical influences of the measurement method have to be kept to a minimum.

Because the subcutaneous region has a much higher conductivity then the epidermal one, the impedance measurements referred to here are to be done vertically through the epidermis and the corium, hence between the surface and subcutaneous region. This can be achieved by using one relatively small measurement electrode and one reference electrode with a large surface. Since the current density is much lower at the big reference electrode and the endosomatic region is of good conductivity, in practice only the impedance of the skin area under the measurement electrode is measured. With the developed instrument it is intended specially to study the fine structure of the skin impedance pattern. Therefore a small measurement electrode of 1-3 mm diameter is normally applied. One of the influences on the measured tissue which might alter its characteristics is the mechanical electrode pressure applied to establish contact with the tissue. This influence is usually not negligible if small-surface electrodes are used. It will be very difficult to eliminate this influence however, since with light pressure the skin contact is rather unreliable. There might be also a chemical influence of the electrode material on the tissue if measurements are performed over long periods. The same difficulty might occur if a conductive jelly is used as a contact bridge between the electrode and tissue. So far there is no real answer to this problem. Tests have been made with gold, graphite and moistened fibre bundles as electrode material. The graphite proved to be a rather stable, good contact-making and nontoxic electrode. Silver/silver chloride will also be tested for this purpose. The test answer would be the development of a method for contactless measurement. This seems to be fairly impossible for impedance measurements but hopeful for skin potential. As a first step, towards non-galvanic measurement of tissue impedance, which would avoid the problem of chemical processes at the electrode/tissue interface, capacitive electrodes are being developed. The results are also influenced by the applied measurement current itself. Existing instruments normally use appreciable current densities of d.c. or low-frequency sinusoidal current. To exclude alterations of the tissue properties by the measurement current as far as possible, a bipolar pulse generator is used as the current source in the developed instrument; thus the time integral of the current is zero. Each bipolar pulse is followed by a relaxation interval, the better to ensure original conditions of the tissue at every measurement. An electronic clamp circuit is incorporated in the instrument so that although a current generator is used the applied voltage at the tissue surface does not surge even in the case of bad or initiating contact with the skin. Since this clamp circuit is triggered from the output signal of the operational amplifier following the electrode and blocks the generator, the applied voltages are kept to extremely low values.

By observing the output pulse shape on an oscilloscope or recorder one can also assess the capacitive component of the skin impedance. Provision has been made for this in order to find out during clinical application whether the value of the R/C ratio has any diagnostic significance whatsoever. The instrument can also operate as a sensitive voltmeter with high input impedance, measuring the slow or static bioelectric potentials on the skin. It is very often useful to judge the internal impedance of these bioelectric sources and possibly their energy capacity. For this reason the instrument is equipped with a footswitch (to leave the operator's hands free). Pressing the footswitch will cause a preselectable drop in the input impedance of the voltmeter. The input impedance of the biological battery could be assessed from the resulting drop of the voltmeter reading and its energy capacitance from the time constant of any decay that occurs.

If measurements of the fine structure of the skin impedance or potential pattern are made and contemporarily followed under a microscope (e.g., to distinguish, in the specific measurement, unwanted artefacts either of anatomic origin such as hair follicles or due to microdamage to the skin or small particles on it) the operator cannot watch the meter-reading to establish its correlation with his visual observations. An acoustic generator has therefore been built which converts the measured value into a frequency-modulated audio signal.

The instrument is battery-supplied in order to avoid any trouble due to mains coupling.

The initial applications of a previous less elaborated version of the instrument have already proved its great versatility and good performance in minimizing influences on the tissue during measurement.

References

1) Dr. J. Bessuges, Chef de la Section Médicale et Sociale du Centre de Production de Plutonium de la Hague (France) in:"Emotivité et travail en scaphandre"

2) M.W. Johns et al., Dept. of Surgery Monash Univ. at Alfred Hospital, Melbourne, Australia, in:"Use of Skin Resistance in Monitoring Sleep and Wakefulness" 9th International Conference on Medical and Biological Engineering, Melbourne, 1971

3) Dr. med. R. Voll. Elektroakupunktur, Anderthalb Jahrezehnte Forschung und Erfahrung in Diagnostik und Therapie *Med. Lit. Verlagsgesellschaft*, Uelzen, Germany

PORTABLE MULTICHANNEL ANALYSER

L. Stanchi, N. Coppo

The necessity of a genuinely portable analyser is apparent in many applications where it is primarily important to be able to act independently of any supply and where simplicity is highly desirable. Detailed analysis is in general not requested in such cases, and some precision can be sacrified in favour of robustness. Why develop another multichannel analyser when the market offers so many different types? The reason for the study is that even the portable analysers are in fact quite heavy and require a source of power, i.e., a line of 115 V or 220 V a.c. We had in mind at least two applications where a light, battery-operated analyser would be very useful. One is the control of series of fissile materials where in general single-channel analysers (battery operated) have been used. The second is the health physics monitorizing of air or water in the surroundings of the Centre. A wide territory is in general monitorized under tedious conditions and an auxiliary supply operated with gasoline is required; this is quite cumbersome on the lakes or on the mountains.

Our laboratory developed some years ago [1] a very simple method of analog-to-digital conversion, so the decision to apply it to a truly portable multichannel analyser followed quite naturally. With our method the circuitry required is considerably simpler than it is in traditional ADC's and simplicity in turn gives reliability and low power consumption.

In order to lengthen the operating time (10 h), the integrated circuits are powered only at the proper time during signal processing. The whole instrument is assembled in a suitcase. It contains: NaI integral line – NiCd battery – Battery charger – Core memory – Chart recorder – GaAs display for counting time – Electronic circuitry for signal processing and data acquisition.

Operation with an external detector (GeLi) is also provided for. An internal DC-DC converter supplies the low voltages for circuitry and the high voltage for the photomultiplier.

There are two modes of operation:

1) Multichannel analysis

Five energy ranges adjusted for the internal PM can be selected from 128 to 2048 keV f.s. An upper and a lower threshold discriminator can select part of the energy range. Analysis is performed on 256 channels which can be split into two groups of 128 or four groups of 64 channels. Spectra stored into the memory can be printed on the chart recorder or displayed on a conventional scope. Print-out on teletype via an external driver is also feasible.

2) Single channel analysis

The counting inside the preselected energy window is performed on the 1st channel. When the preset count ($2^6 - 2^{16}$) is reached the operation is stopped and the counting time can be read on the six-digits GaAs display.

The figure shows the first prototype built in the laboratory. The circuitry for measuring and reading the time was not included in that instrument. It is to be noted that in the new instrument the display is not continuously energized but can only be observed during the operation of a push-button.

Reference

1) G. Colombo, L. Stanchi, A New Method of ADC for Improving Resolution, IEEE Trans. on Nuclear Science 15, 291 (Feb. 1968)

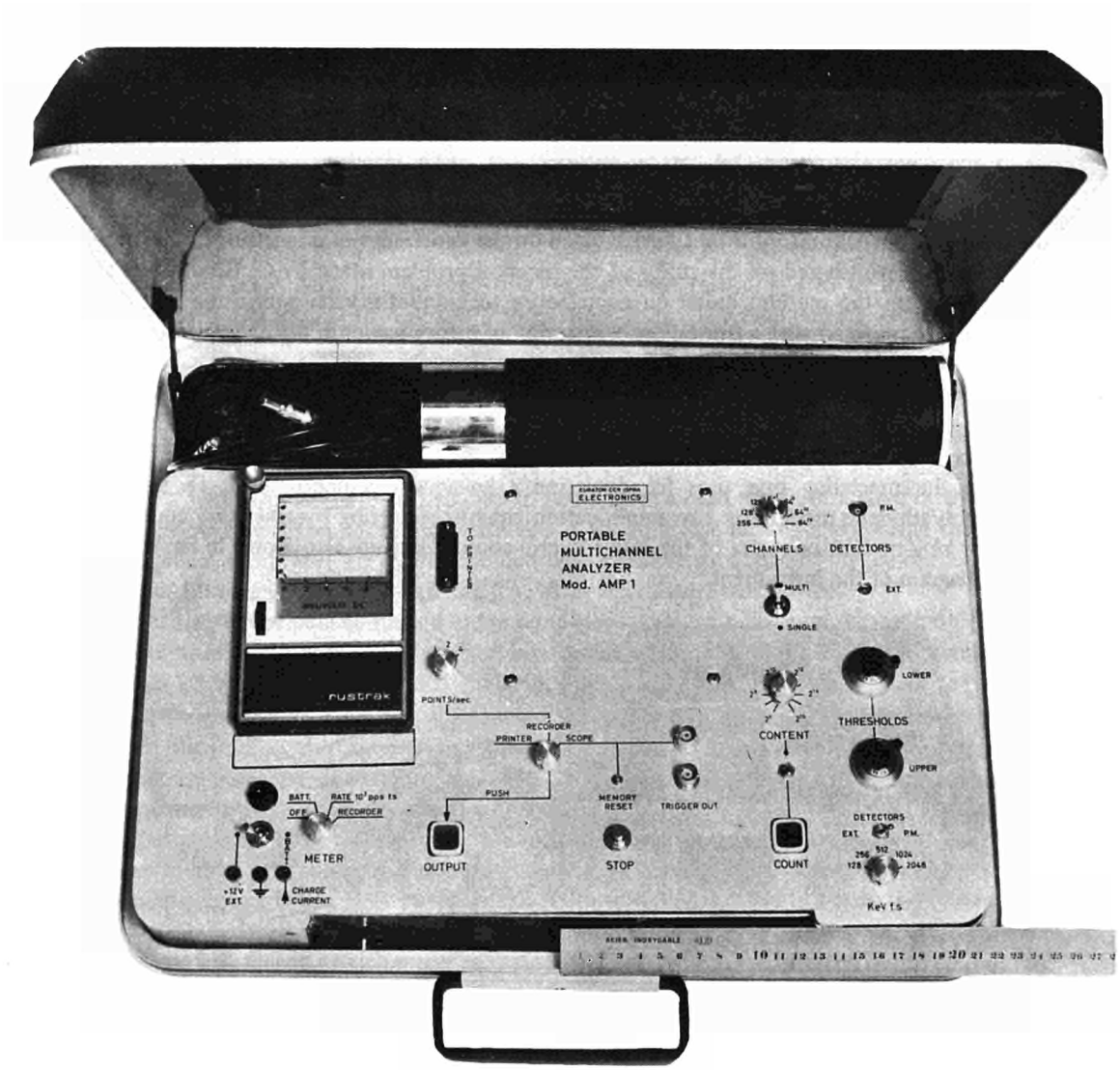
ELECTRONICS
PORTABLE
MULTICHANNEL
ANALYZER
Mod. AMP 1
CHANNELS
DETECTORS
P.M.
MULTI
SINGLE
Ext.
LOWER
THRESHOLDS
UPPER
CONTENT
POINTS/sec
RECORDER
PRINTER
SCOPE
PUSH
MEMORY
RESET
TRIGGER OUT
BATT.
OFF
RATE
RECORDER
METER
+12V
EXT.
CHARGE
CURRENT
OUTPUT
STOP
COUNT
DETECTORS
Ext.
P.M.
Kev f.s.
rustrak

Fig. 1

DERANDOMIZER FOR FAST ACQUISITION INTO A SMALL COMPUTER

L. Stanchi

Introduction

A correct evaluation of neutrons emitted by spontaneous fissions in a fissile material can lead to the identification of the radioisotopes present in the sample. For that purpose it is necessary to realize a device by which the neutrons due to spontaneous fissions can be distinguished from the neutrons generated by α, n reactions. Instruments of this type are based on the fact that neutrons due to α, n reactions are emitted one at a time, whilst each fission produces simultaneously several neutrons the mean number of which is a characteristic constant of the isotope.

We developed in our laboratory a first device based on the experience of an instrument constructed at Brookhaven. The work was based on the study of the physical problem made by G. Birkhoff et al. It has been demonstrated that the method based on coincidence techniques is valid and in the first device the coincidence time was prefixed with a frontal panel selection of binary values in the order of the life time of neutrons in the moderator.

A second improved device shown in fig. 1 uses simultaneously four different times of coincidence. The total count of incoming pulses and the number of pulses which are not in the coincidence time in respect of a preceding one, are used for the determination of the isotope responsible for the fissions. This instrument, like the preceding one, uses for detection a hexagonal geometry with 18 He^3 counters immersed in a polyethylene moderator. Six amplification chains connecting together two counters of the inner six-counter ring or four counters of the outer twelve-counter ring are also shown in fig. 1, together with the block diagram of the instrument.

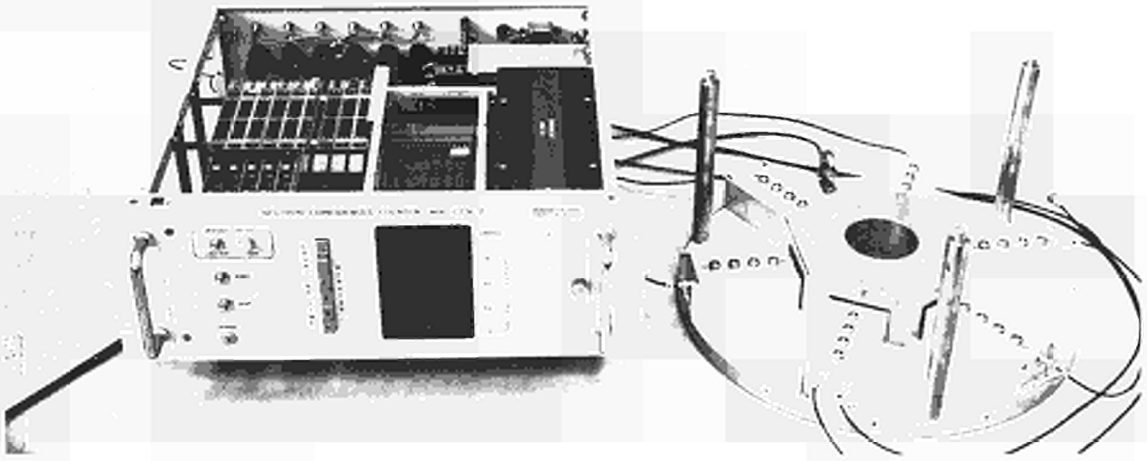

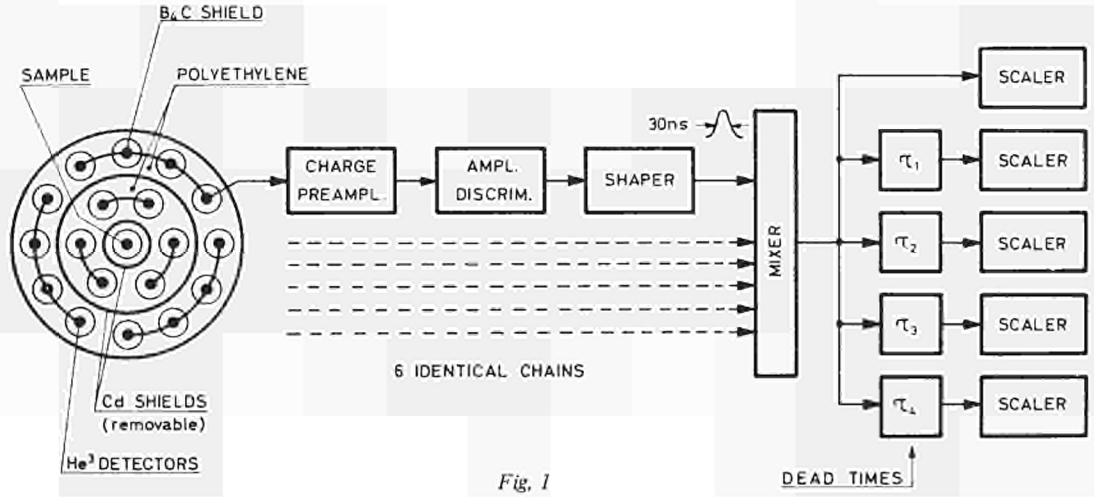

Fig. 1

A third device has been constructed for use with a process computer (Laben 70). The purpose of this instrument is the acquisition of the arrival time of all the neutrons in real time in order to process them with the computer instead of recording them with a coincidence counter with fixed dead time.

The instrument is designed for working with very high neutron fluxes and is controlled by a 10 MHz clock with the purpose of realizing a dead time of 100 ns. As this resolution greatly exceeds the capability of computers, a solid-state temporary memory has been introduced. The registers of this memory are filled by the incoming neutrons and emptied by computer control so that the instrument acts as a derandomizer.

Eight 28-bit registers are controlled by an 8-bit ring shift register and constitute a temporary memory. Each pulse corresponding to an incoming neutron forces the shift register to advance by one step. This in turns activates a line of the temporary memory. A synchronous 20-bit counter is running with a 10 MHz clock and is always connected in parallel, bit per bit, to the eight lines of the memory. When a pulse arrives, a line of memory records the real time of occurrence. Delicate problems of phase had to be solved in order to have control of the memory when the counter is set. All the writing logic has therefore been synchronized and the statistical occurrence of the events has been properly phased. The remaining 8 bits of the memory registers are used to give a label to each pulse in order to memorize in which of the eight inputs the pulse occured.

This writing logic does not prevent the possibility of recording two or more simultaneous pulses occurring in different inputs. In this case a single time with more than one label is written in one memory register. This allows for an exactly "zero" dead time for pulses coming from different counters. The equipment has eight different inputs although in the present application the connection has been made with six lines of neutron counters.

The instrument is designed for work up to very high rates. Nevertheless, in cases of very low rates it can happen that no pulses at all will occur in a time equal to the content of the counter, that is $2^{20} \times 100$ ns, roughly a tenth of a second. In this case the computer would not have a trace of the elapsed time. To avoid this inconvenience an additional ninth line is added at the input for recording the overflows of the counter. If there is no label for a zero recorded time it will be processed by the computer only as a time. If there is a label it means that a pulse arrived just when the counter overflowed.

The reading of the data contained in the temporary memory is done by the computer at its own speed. As the computer has a word length of 16 bits a double word reading has to be accomplished for each datum. The 28 bits stored in one row of latches is normally sent to 28 flip-flops in the interface and connected via appropriate gates to the data bus of the computer. Suitable positions are assigned to each bit. In addition one bit is kept to zero or to one in order to identify first and second word. Two bits are free for other uses.

A ring shift register equivalent to the one used for writing is controlled by a pulse synchronized with the internal clock of the computer. Each output of the ring shift register controls a row of AND' s connected to the 28 outputs of a memory register. A wired OR is used at the outputs of the 8 AND's corresponding to one of the 28 bits read in the 8 rows. The 28 bits are sent to the interface card where a synchronized clock transfers the datum to the output of the flip-flops.

The logic is arranged in such a way that if at least one datum is present on the temporary memory a dc level is sent to the computer which begins to read. The ring shift register proceeds step by step until the temporary memory is emptied.

Thus the dc level is removed and any other request reading by the computer is prevented. The position in which the computer stops reading is exactly the last which was written and the immediately next one will be filled by the first incoming event. The two ring shift registers run a sort of race where the reading will always reach the position of the writing but will never overpass it because it is forced to stop when the temporary memory is empty. The mean time between pulses in the writing operation must be higher (but statistically some intervals are shorter) than the time elapsing between two readings.

The interface is assembled on a single big card mounted directly into the computer and containing about 100 integrated circuits. The acquisition unit with the temporary memory is assembled in a six-unit crate mounted in a standard 19" rack.

The general logics of the dialogue with the computer is imposed by the computer itself. Some special solutions were adopted for this instrument. Certain problems had to be solved, first of all the fact that it is impossible to call the computer with a pulse because the peripheral unit can send only a dc level which must be kept present till one datum is present on the temporary memory. The end of the "data in" pulse causes the switching of a particular flip-flop "Clear flag f.f." which is set to zero at the beginning of the whole operation and thereafter continues to switch for every input of data. At the same time the end of the "data in" pulse resets the "Bus flip-flop" which prepare the bus for reading the second word. A second "data in" pulse sends the second word to the bus. The end of this pulse does not modify the bus flip-flop, which stays at zero, but resets the " clear flag" flip-flop which in turns clears the flag. So a neutron is

recorded with a double word into the computer. At this point the operation stops if only one datum was present in the temporary memory and waits for the next events. But if more than one event was written in the temporary memory, the complete operation is repeated. The circuits are so arranged that they can work with program interrupt mode or with direct memory access. The software can select the mode of operation in the hardware. A word counter and an address counter will decide the number of locations used and the starting address. If, for example, the number 4000 is written in the word counter the operation is repeated 2000 times for 2000 double words, filling 4000 locations. At the end of this sequence the word counter overflow stops the operation. A read status will give appropriate information on the status of the peripheral unit. Afterwards the computer begins to process the data.

The equipment is used for a succession of data inputs and processing; after processing only reduced data are kept and the memory is used for another accumulation of data. Fig. 2 shows the derandomizer is shown.

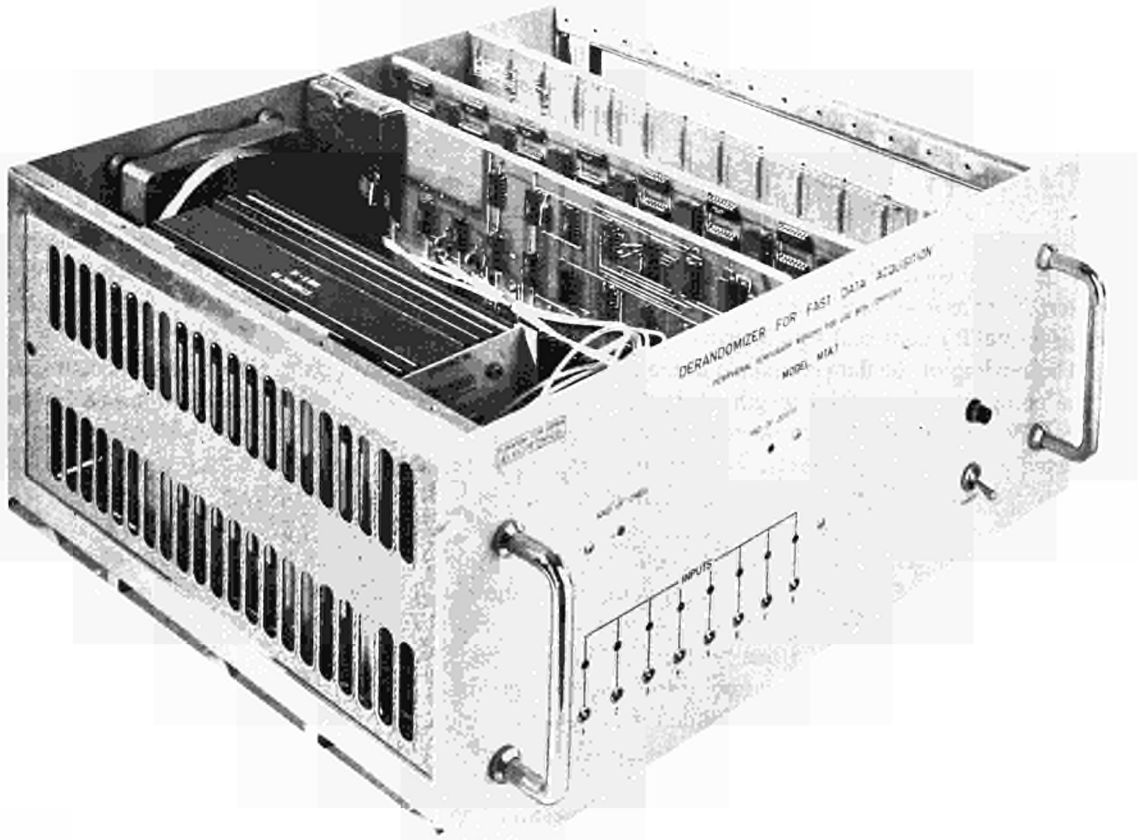

Fig. 2


MATERIALS
BURNABLE POISONS
COMPOSITE MATERIALS
IDENTIFICATION SEALS
WATER SPLITTING
COATED PARTICLES
IN-PILE VISCOSITY
HEAT PIPES
CERAMICS IMPREGNATED GRAPHITE

MATERIALS DIVISION

C. Marchetti

The CCR activity on materials development, originally scattered between various divisions at Ispra and Petten, has been merged into one single administration unit, the Materials Division. This partly explains a certain amount of dispersion in the research objectives, and the frequent traces of canceled projects.

The Division has been subdivided into 9 sections, according to fields of interest, with an average of around 20 people each.

The sections are:

- General Metallurgy
- Physical Metallurgy
- Structural Analysis
- Ceramics
- Applied Physical Chemistry
- High Temperature Technology
- High Temperature Compatibility
- Irradiations and Fuels
- Nondestructive Control

The reasons for this form of organization are the following:

1. When working on a project the tasks can be divided between sections without any need to reorganize the Division according to the size of the tasks and their fluctuations in time.
2. The disciplinary homogeneity stimulates a better scientific standing.
3. It is more appropriate to the basic and long-term research which, according to the Council of Ministers, should constitute the backbone of our future research.

The drawbacks are typical of any system organized by tools and not by purpose; i.e. a strong tendency to form closed groups which find it difficult to communicate and which tend to get stuck in a routine.

To compensate for this, the importance of personnel and money as status symbols has been de-emphasised, and the build-up of personnel discouraged. The section heads have been encouraged to become in a sense entrepreneurs, and to them has been left most of the work of maintaining contacts inside and outside the institution; organising collaboration and contracts; of preparing conferences and meetings. Time will show the validity of this policy.

The most important research subjects are described in the following pages. Only one of them merits a particular explanation because it does'nt belong to the category of items usually dealt with by a Materials Division, the: "Direct Production of Hydrogen with Nuclear Heat". It is in fact an interdisciplinary project with the ambitious objective of extending the use of nuclear energy into the nonelectrical energy market. Its inscription under the Materials Division heading is due to the fact that the project did originate there, and that research at the moment pivots around the physico-chemical properties and behaviour of materials'

Now a word about the future. It is very difficult to make forecasts due to the numerous and diverse boundary conditions, which our programs must fit. However, it is clear that:

1) Materials play a key role in any branch of technology.
2) The Community is not very well placed in this field.
3) We are certainly competent and well equipped to do such research.
4) The Council of Ministers recommend concentration upon basic and long-term research.

Assuming that the role we will be called upon to play may be a reasonable one we are basing our actual policy upon the following points:

- Concentrating on a few items of broad consequence. The mechanical behaviour of materials (e.g. deformation and fracture); the development of materials with special properties (e.g. for high temperature use) could be examples. This oriented research could reasonably account for 50% of the potential of the division.
- Preparing or preserving the competences that would be of use for solving materials problems for projects and objectives of the CCR. This may account for 30% of our potential.
- Extending our contractual relationships with industry and external institutions under the label of technical services and public service. This may cover 20% of our potential.

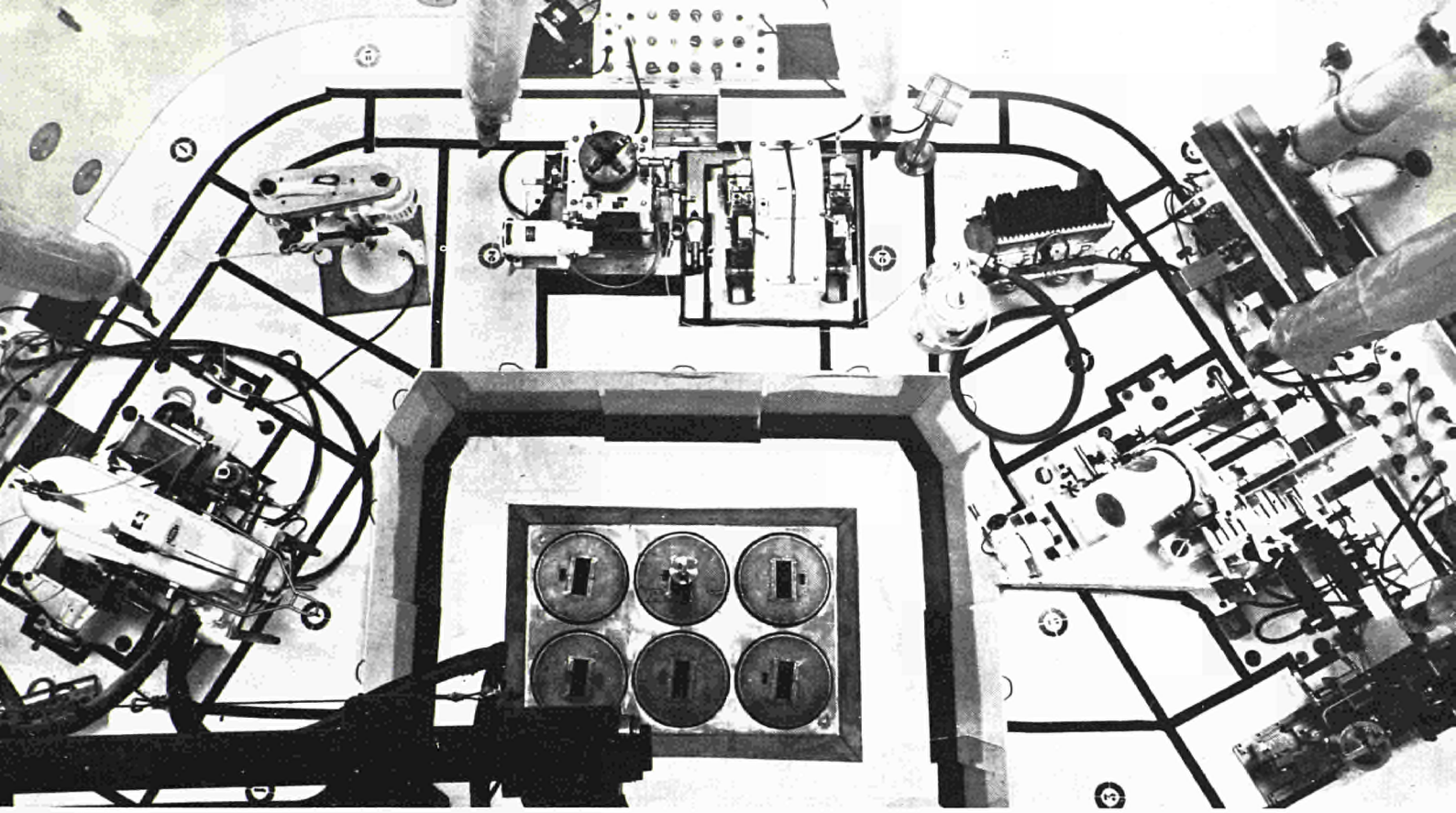

IRRADIATION BEHAVIOUR OF FUEL WITH BURNABLE POISON

R. Klersy, O. Simoni, A. Schürenkämper

Introduction

The addition to reactor fuels of parasitic neutron-capturing elements in small amounts may be of great advantage to reactor design and control. The depletion of these elements, usually designed as burnable poisons, during the reactor operation compensates for reactivity losses due to fuel depletion and accumulation of stable fission products. The concentration and geometrical shape of the burnable poison must be so calculated that its consumption rate follows the fuel depletion and that no poison residue remains at the end of the reactor core life. These requirements could be satisfied by the use of self-shielding poisons consisting of microsphere of various diameters.

The present work describes the irradiation behaviour of UO_2 fuel containing microspheres of gadolinium oxide. These microspheres are prepared by a sol-gel process and then coated with a 30 μ molybdenum layer which acts as a diffusion barrier between UO_2 and Gd_2O_3. The microspheres are incorporated in the UO_2 powder and sintered together in the form of fuel pellets.

Nine fuel rods have been irradiated in the DIRCE organic loop of the Ispra I reactor at burnups of 6,500 MWd/t, 9,400 MWd/t and 14,000 MWd/t.

The linear power was about 500 W/cm and the central temperature of the fuel varied from 2,000 to 2,600°C. The concentration of burnable poison in the fuel varied from 200 to 4,000 ppm, the diameter of the microspheres was 300 and 500 microns.

Results

The post-irradiation examinations of the fuel revealed the following:

a) the external dimensions of the fuel rods did not show any various after irradiation to 14,000 MWd/t U;
b) the metallographic examination of the fuel pellets which contained the Gd_2O_3 microspheres showed that the microspheres remained intact in the temperature range below 1500-1600°C. Above this temperature the molybdenum coating is more or less destroyed and the reaction between UO_2 and Gd_2O_3 takes place.

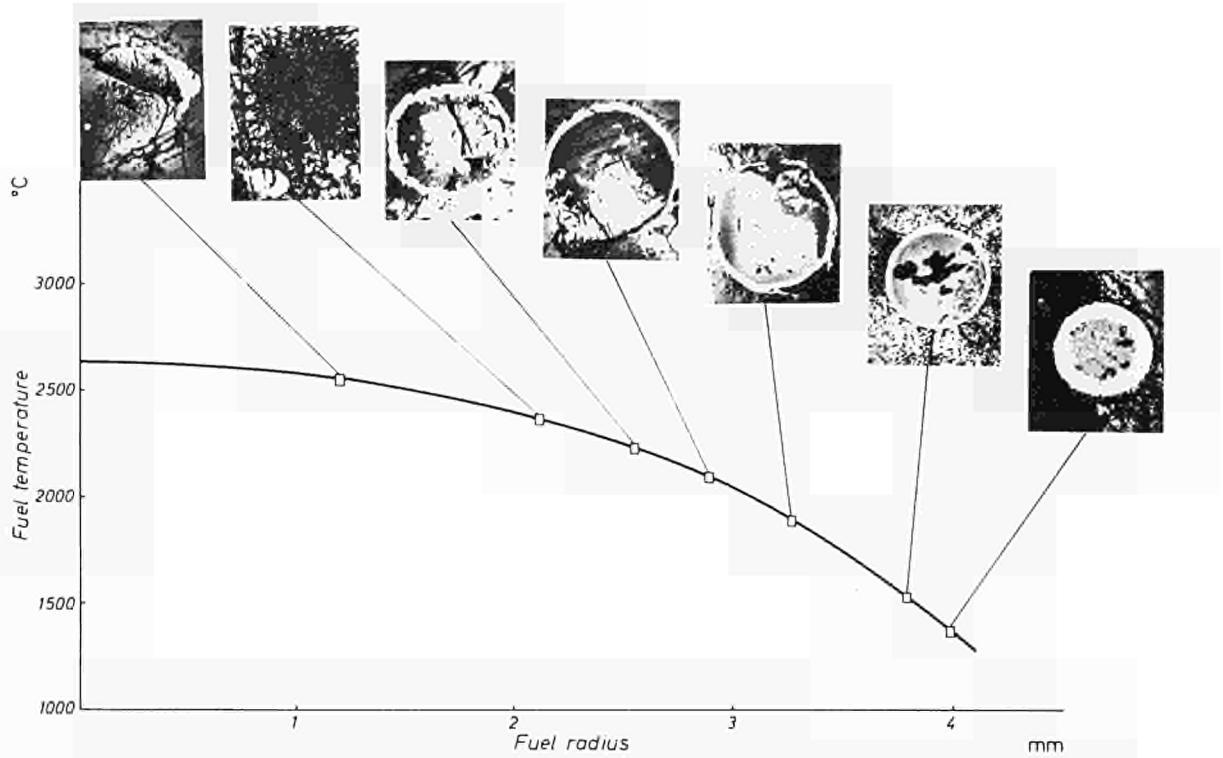

Fig. 1: Metallographic aspect of microspheres in different radial positions of the fuel rod 1C (b.up: 6500 MWD/T_U).

(25 x)

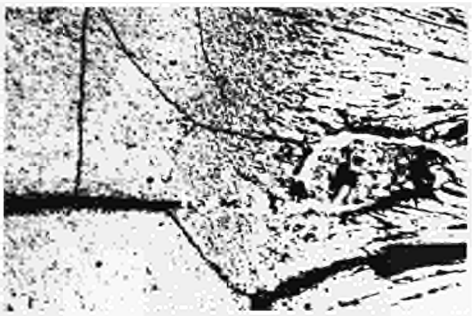

(64 x)

Fig. 2: Macroscophic and micrographic aspect of a deformed microsphere in the columnar grain zone of UO_2 (burn-up 14.000 MWD/T_U, temperature 1770°C).

(27 x)

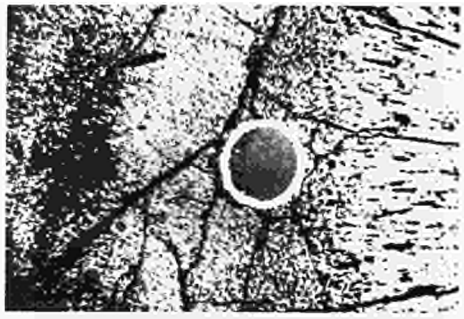

(100 x)

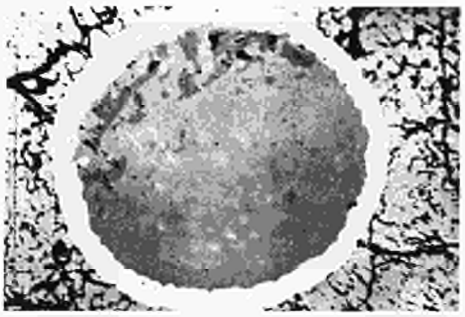

Fig. 3: View of a microsphere located at the boundary of the columnar grain zone (burn-up 14.000 MWD/T_U, temperature 1460°C).

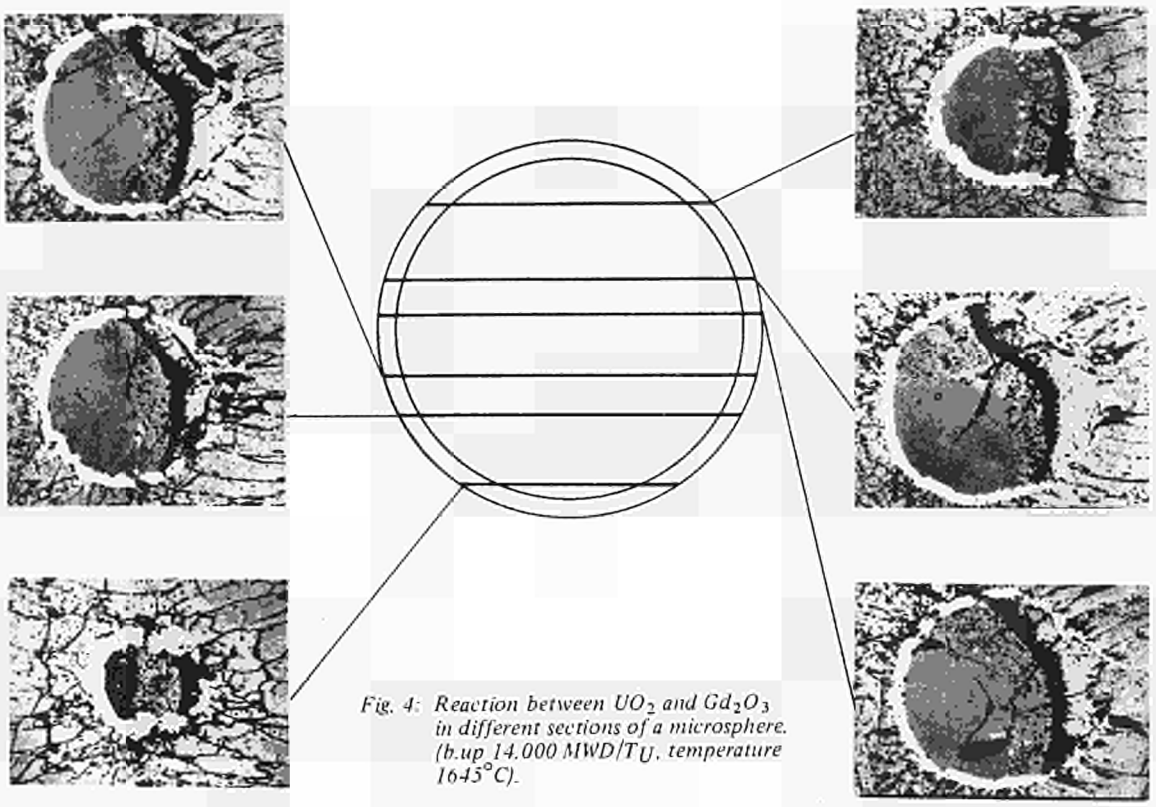

Fig. 4: Reaction between UO_2 and Gd_2O_3 in different sections of a microsphere. (b.up 14.000 MWD/T_U, temperature 1645°C).

Fig. 1 shows the metallographic aspect of microspheres as a function of their radial position in the fuel pellets.

The same figure shows the radial temperature distribution, which enables the mean irradiation temperature for each microsphere to be determined.

In most cases the spherical shape of the gadolinium oxide remains and one can assume that the self-shielding effect of the poison spheres is not suppressed. In some cases the microspheres are deformed when they are located in the zone of the columnar grains of UO_2. It may be that the mechanical deformation of the microspheres due to the grain growth of UO_2 contributes to the rupture of the molybdenum coating.

Fig. 2 shows an example of deformed microspheres in the zone of columnar grains.

Fig. 3 shows a microsphere located at the boundary of the columnar grain zone. The undulating appearenace of the molybdenum surface seems to indicate the beginning of a reaction between the constituents.

Fig. 4 illustrates this reaction in different sections of a microsphere. A large number of small metallic inclusions (probably Mo) can be observed in the ceramic material.

In Fig. 5 the total number of intact and defective microspheres observed are plotted as a function of their irradiation temperature and of the burnup of the fuel elements. The influence of the temperature on the reliability of the microspheres appears very clearly, while the burnup does not seem to have any influence.

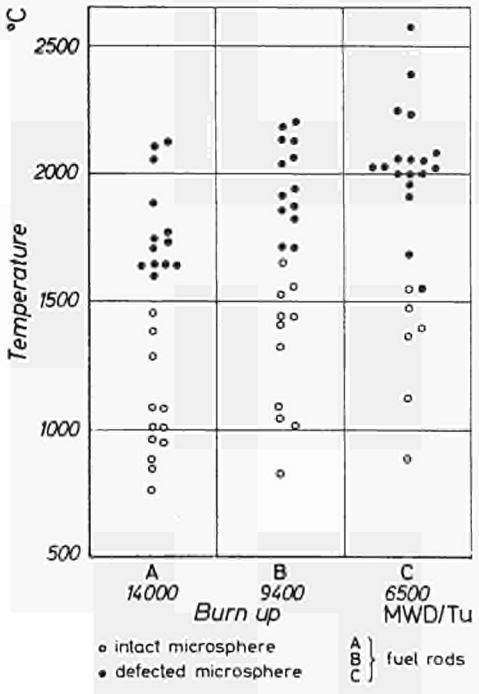

Fig. 5: Influence of temperature and burn-up on the integrity of the microspheres.

COMPOSITE MATERIALS. EUTECTIC UNIDIRECTIONALLY SOLIDIFIED ALLOYS.

D. Boerman, J. Dejace, R. Matera, G. Piatti

Introduction

There have been many different definitions of composite materials according to the field of interest of the scientist concerned (magnetic properties, electrical characteristics, mechanical strength, etc.). Broadly speaking, a composite material may be said to be a material consisting of at least two chemically distinct phases, with a definite separation interface and characteristic properties which are not to be found in the separate constituents.

The criteria on which classification is based also vary, but they usually relate to the morphology of the material. Besides structures made up of alternate layers of different constituents, various dispersions in a matrix and impregnated frameworks, there is the fibrous structure, which is considered typical. Materials described as fibre-reinforced are those in which one phase is present in the form of filaments (or lamellae) with diameters (or thicknesses) ranging from fractions of a micron to several microns and with values of concentration by volume ranging from a few percent to as much as 70%; moreover, these filaments or fibres usually lie in one direction.

At this point it is worthwhile recalling a particular characteristic displayed by many materials in the fibrous state, namely a considerable increase in their strength properties compared with the normal solid state. The mechanical properties of materials with a whisker structure, i.e., single crystals a few microns in diameter and virtually free from the imperfections found in ordinary crystal structures, are even better.

With fibrous composites, the high strength of the fibre can be exploited; the basic principle here involves the use of the deformation of the matrix to transfer the stress applied to the composite, via the interface, to the constituent fibres, which can withstand a heavy load. The resistance of the composite in this way comes close to that of the fibres.

The possibility of using strong but brittle composite materials means that ceramics and refractories can also be considered as possible constituents, so that fibres made from substances maintaining their good properties even at high temperature are conceivable. Composite materials have thus an attraction when very good high-temperature mechanical properties are required, since they offer a means of overcoming the limitations imposed by high temperature on all types of material. The impetus in this direction stems from the requirements of advanced technology in connection the developments in the field of space, high temperature reactors, gas turbine technology, etc.

Unidirectional solidiffication of eutectics

There are numerous techniques for the production of composites, all consisting of two main stages, namely production of the fibres and their incorporation in the matrix.

A method for the production of composites which differs from the others in one particular respect is known as the unidirectional solidification of eutectics; with this technique the fibres can be formed in situ, since they are grown directly in the matrix in a single operation.

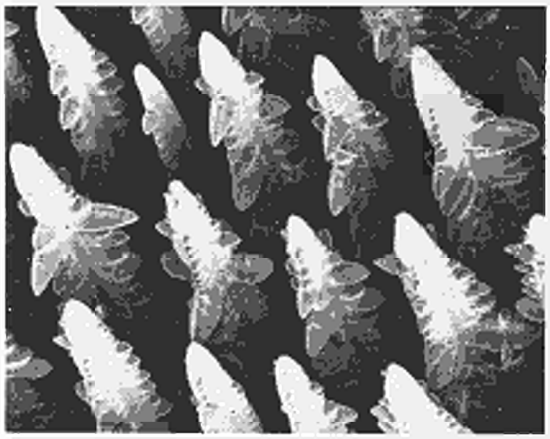

Fig. 1: Electron scanning microscope picture of dendrite structure Ni base system produced by unidirectional solidification.

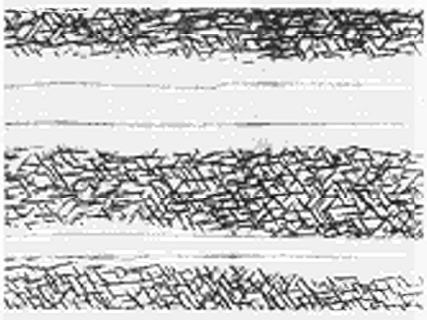

Fig. 2: Longitudinal section of unidirectionally Ni-Ni_3 Ta eutectic exibiting fine precipitates in the matrix interlamellae space, (865 x)

The conditions in which the two phases are produced are close to equilibrium, thus giving a structure with high thermal stability at high temperatures – very important for purposes of practical application.

Not all eutectic alloys can be used to obtain structures of the composite type defined above. There is not as yet a complete theory to explain the phenomenon. Only experiments can provide direct information on each system; with the data obtained from phase diagrams it is impossible to predict whether the structures obtained will be fibrous or lamellar.

Moreover, in certain cases dendritic structures are produced (fig. 1) which depend on the various parameters involved and on the type of system. This proves that, in the case of eutectic systems, oriented (fibrous or lamellar) structures can be obtained by unidirectional solidification only if the various parameters involved are strictly controlled.

The very nature of the system has a great bearing on the production of composite material. For instance, the volumetric fraction of fibre, which must be high in order to ensure that the composite has the desired mechanical properties, naturally depends on the eutectic composition. This composition can obviously not be regulated at will, so not all eutectic systems lend themselves to the production of composites. It should, however, be noted that similar structures can be obtained even in the case of systems which are not strictly eutectic.

In the last years different alloys were developed in the Materials Division Laboratories at Ispra by the unidirectional solidification technique [1) 5)]. They can be divided into two types: aluminium base eutectic alloys (Al-Al_4Ce, Al-Al_4Ca, Al-Al_3Y, Al-AlSb, Al-Al_3Pd, Al-Al_2Au, Al-Al_3Pt) and heat resistant alloys (Ni-Cr, Ni-Ti, Ni-Ta, etc.). The previous work [5)] on the structure and mechanical properties of a series of Ni-based eutectics solidified under a thermal gradient at constant rate, emphasized the possibility of obtaining a good mechanical behaviour at elevated temperature in the case of the system Ni-Ni_3Ta. Starting from these results a larger study on this system was undertaken in 1971 in order to specify the influence of the different structural parameters on the mechanical properties of the composite.

Commercial purity Ni(99,5) and Ta(99,8) were used in the fabrication process, which involved arc melting of the elements under argon and vacuum casting of the alloy in rods. These rods were subsequently unidirectionally solidified in a vertical alumina crucible withdrawn from a platinum resistance furnace through a cooling water spray. An argon flux prevented contamination by the atmosphere. Details of solidification apparatus are given elsewhere [6)].

Structure and mechanical properties

The microstructure of this system solidified under a thermal gradient of 150°C/cm at a constant rate of 0.5 cm/h consists of lamellae of Ni_3Ta, partially oriented transversely to the growth axis, in a solid solution of Ni, as can be seen from Fig. 2. Radiocrystallographic analysis has not yet made clear which one of the two equilibrium modifications of Ni_3Ta, the orthorhombic phase stable at low temperature or the body-centred tetragonal high temperature allotrope, is present. The question is still under investigation. The volume fraction of the fibres is assumed to be about 8%, according to the equilibrium phase diagram [7)]. Extensive precipitation of Ni_3Ta occurs in the matrix, as a consequence of the large decrease of solid solubility of Ta in Ni with cooling. These precipitates have a morphology of fine plates, not thicker than one micron, aligned in three different directions (fig. 3). The aligment of the reinforcing intermetallic phase presents variations as high as 30° at this stage of composite development. A much steeper thermal gradient and lower impurity content of the alloy could reduce this phenomenon.

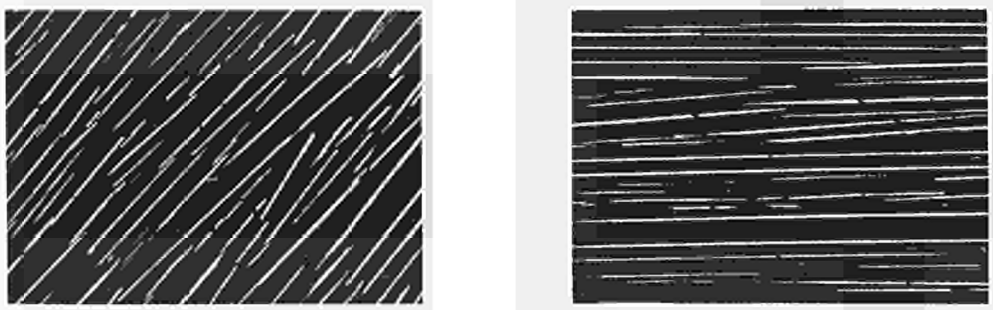

A – Transverse section *B – Longitudinal section*

Fig. 3: Microstructure of unidirectionally solidified Ni-Ni_3 Ta exibiting lamellar structure. (94 x)

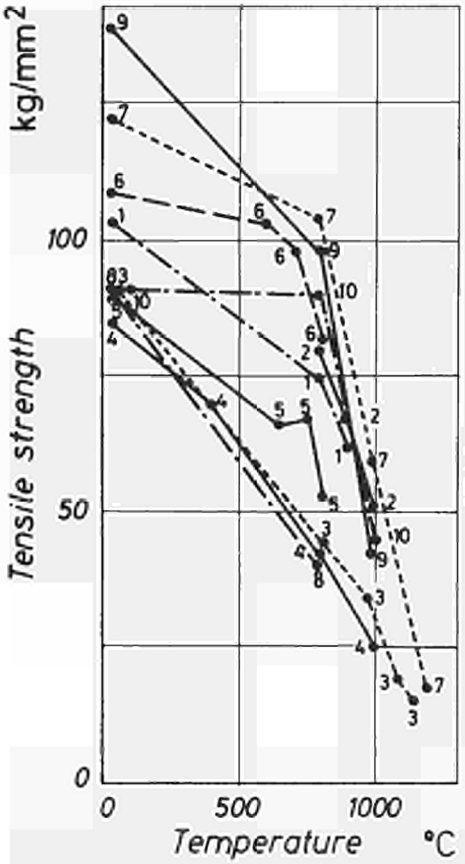

1) Ni-Ni_3Ta R = 1 cm/h
2) Ni-Ni_3Ta R = 1 cm/h treated 100 Hours at Testing Temperature
3) Ni-NbC from F.D. Lemkey and E.R. Thomson Metall Trans. Vol. 2 p. 1537, 1971
4) Ni-Ni_3Nb R.T. Quin, R.W. Kraft, R.W. Herzberg Trans. ASM, Vol. 62, p. 38, 1969 and W.R. Hover and R.W. Herzberg Vol. 2 p. 1283, 1971
5) *Ni + (NiBe) (+) (Cr) matrix fibers
6) *Ni + (Cr + Al - Mo + W) + (NiBe) matrix fibers solut. treated + aged

*from Yuan-Shou Shen and L.B. Griffiths Metall. Trans. Vol. 1, p. 2305, 1970

7) Ni + NiMo from Thomson, AFML-TR-67-228, p.214, 1967 and Paris University these 1970 Annarumma, p. 9
8) Ni + Ni_3Si from A.R.T. de Silva and G.A. Chadwick Metal Science Journal, Vol. 3 p. 168, 1969
**9) Udimet-700 wrought Ni superalloy
**10) Mar-M-200 cast Ni superalloy

** ASTM-Data Series DS-7-S1 (properties of selected superalloys)
Aerospace and Structural Metals Handbook of 1971.

Fig. 4: Elevated temperature tensile strength (Su) of Ni-Ni_3 Ta and several Ni superalloys.

Other microstructural defects such as voids and oxide inclusions are occasionally present. As we shall see later, these defects greatly affect the fracture mode and the resistance of the composite.

Tensile properties of Ni-Ni_3Ta composite have been tested on round specimens, 4 mm in diameter and 30 mm in gauge length, machined from the unidirectionally solidified rods in a direction perpendicular to the solidification front. Tests were performed in an INSTRON-TT-CM-5 ton electromechanical machine equipped with a vacuum chamber and a resistance furnace. Tests were carried out in air at room temperature and in a vacuum of about 10^{-5} Torr at 800°C, 900°C and 1000°C. Some of the tensile specimens were soaked in vacuum at 800°C, 900°C and 1000°C for periods of 100 and 1000 hrs prior to test in order to verify the thermal stability of the coupled structure.

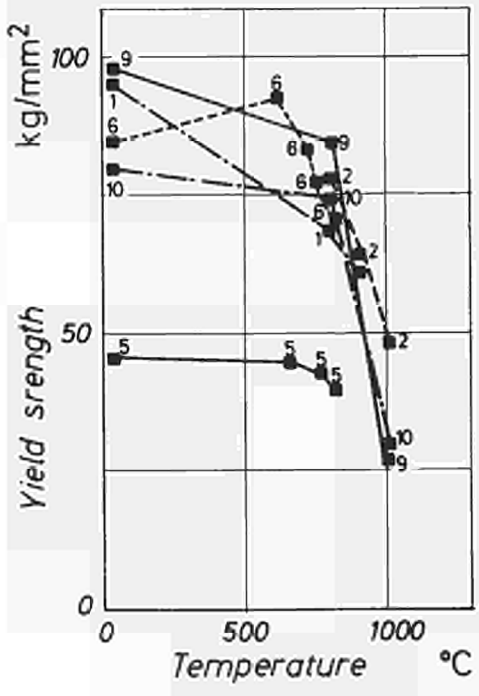

1) Ni-Ni_3Ta R = 1 cm/h
2) Ni-Ni_3Ta R = 1 cm/h treated 100 Hours at Testing Temperature
3) Ni-NbC from F.D. Lemkey and E.R. Thomson Metall Trans. Vol. 2 p. 1537, 1971
4) Ni-Ni_3Nb R.T. Quin, R.W. Kraft, R.W. Herzberg Trans. ASM, Vol. 62, p. 38, 1969 and W.R. Hover and R.W. Herzberg Vol. 2 p. 1283, 1971
5) *Ni + (NiBe) (+) (Cr) matrix fibers
6) *Ni + (Cr + Al - Mo + W) + (NiBe) matrix fibers solut. treated + aged

*from Yuan-Shou Shen and L.B. Griffiths Metall. Trans. Vol. 1, p. 2305, 1970

7) Ni + NiMo from Thomson, AFML-TR-67-228, p.214, 1967 and Paris University these 1970 Annarumma, p. 9
8) Ni + Ni_3Si from A.R.T. de Silva and G.A. Chadwick Metal Science Journal, Vol. 3 p. 168, 1969
**9) Udimet-700 wrought Ni superalloy
**10) Mar-M-200 cast Ni superalloy

** ASTM-Data Series DS-7-S1 (properties of selected superalloys)
Aerospace and Structural Metals Handbook of 1971.

Fig. 5: Elevated temperature yield strength ($S_{0.2}$) of Ni-Ni_3 Ta and several Ni superalloys.

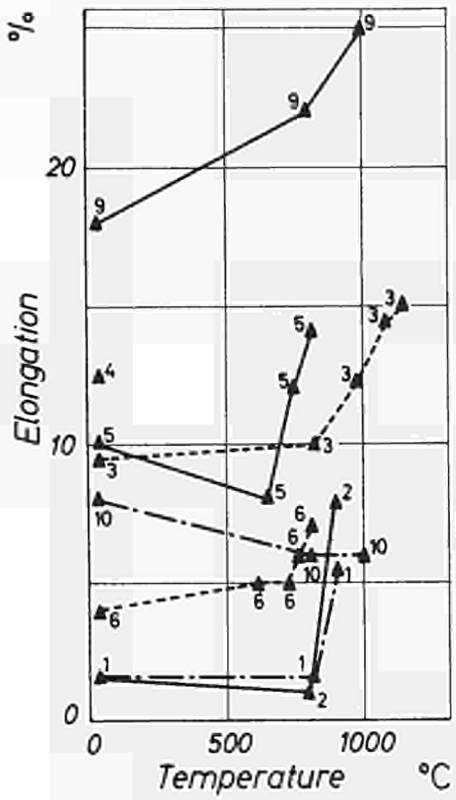

1) Ni-Ni_3Ta R = 1 cm/h

2) Ni-Ni_3Ta R = 1 cm/h treated 100 Hours at Testing Temperature

3) Ni-NbC from F.D. Lemkey and E.R. Thomson Metall Trans. Vol. 2 p. 1537, 1971

4) Ni-Ni_3Nb R.T. Quin, R.W. Kraft, R.W. Herzberg Trans. ASM, Vol. 62, p. 38, 1969 and W.R. Hover and R.W. Herzberg Vol. 2 p. 1283, 1971

5) *Ni + (NiBe) (+) (Cr) matrix fibers

6) *Ni + (Cr + Al - Mo + W) + (NiBe) matrix fibers solut. treated + aged

*from Yuan-Shou Shen and L.B. Griffiths Metall. Trans. Vol. 1, p. 2305, 1970

7) Ni + NiMo from Thomson, AFML-TR-67-228, p.214; 1967 and Paris University these 1970 Annarumma, p. 9

8) Ni + Ni_3Si from A.R.T. de Silva and G.A. Chadwick Metal Science Journal, Vol. 3 p. 168, 1969

**9) Udimet-700 wrought Ni superalloy

**10) Mar-M-200 cast Ni superalloy

** ASTM-Data Series DS-7-S1 (properties of selected superalloys)
Aerospace and Structural Metals Handbook of 1971.

Fig. 6: Elevated temperature elongation of rupture (epb) of Ni-Ni_3 Ta and several Ni superalloys.

A considerable degree of scatter is associated with the tensile data. However, optical microscope observations on the longitudinal section of the fractured specimens and scanning electron microscope observations of the fracture surface enabled the lower values to be imputed to the presence of one or more of the structural defects described above.

In all cases the tensile strength retention is superior to that of conventional Ni base superalloys and comparable to that of Ni base composites, as can be seen from Figs. 4, 5 and 6. The symbols used have the following meaning:

$S_{0.2}$ = engineering 0.2% offset yield-stress

S_u = engineering maximum tensile stress

e_{pb} = engineering plastic strain at breaking point

The stress-strain curves can be described in terms of classical composite behaviour. There is an evident change in slope of the curve with increasing stress when passing from a region in which both fibres and matrix deform elastically to a region in which, while the fibers remain elastic, the matrix yields and deforms plastically. The fibres show extensive mechanical twinning (Fig. 7) and have broken into segments, the shorter one being nearer to the fracture surface. Most of the fibre cracks are independent of one another, indicating the good toughness properties of the Ni matrix (Fig. 8). Break-up of fibres extends over several millimetres from the surface.

Fig. 7: Optical micrography of a specimen showing mechanical twinning in the Ni_3 Ta fibers. (100 x)

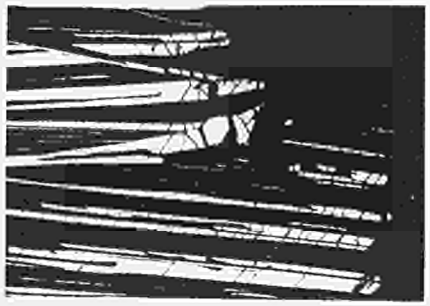

Fig. 8: Optical micrography of a specimen in the rupture zone. (100 x)

Fig. 9: Scanning electron microscope picture of the rupture zone Ta specimen with the broken lamellae of intermetallic Ni_3 Ta. (450 x)

Fig. 10: Scanning electron microscope image of composite with very fine fibers obtained by unidirectional solidification of complex Ni system. (450 x)

A complete examination of the fracture surfaces of all the tensile specimens with a scanning electron microscope is being performed. Representative pictures are shown in Fig. 9. They confirm the brittle behaviour of the fibres, even at more elevated temperature, and the good bonding between fibres and matrix, demonstrated by the absence or small amount of fibre pull-out from the surface. To sum-up, the evaluation of the mechanical characteristics of the composite Ni-Ni_3Ta at elevated temperature is good.

Development

At present the new composite obtained by unidirectional solidification and based on the Ni-Ta binary eutectic is under development also from more practical points of view (weldability, machinability, etc.) in order to consider applications of composites in which properties other than mechanical are of primary importance.

In continuation of previous programs on the Ni-Ta binary eutectic alloys solidified by extracting the heat in one direction, a certain effort has been directed towards spreading research work into ternary systems, particularly Ni-Ta-X, or more complex systems, in order to achieve improvement of mechanical properties (resistance and ductility) and corrosion resistance (impure helium or oxydising atmosphere). Fig. 10 shows a picture obtained by scanning electron microscope of a Ni base composite structure unidirectionally solidified. The addition of different elements enables a very fine structure to be obtained. The fibre dimensions are of the order of one micron.

Further research is planned for the future in this direction.

References

1) K.N. Street, C.F. St.John and G. Piatti, The structure of unidirectionally solidified binary eutectics Al-Ca, Al-Ce and Al-Y, *J. Inst. Metals 95* (1967) p. 326

2) G. Beghi, G. Piatti and K.N. Street, The structure of unidirectionally solidified Al-Sb binary eutectic *J. Metals Sc. 6* (1971) p. 118

3) K.N. Street, R. Matera and G. Piatti, Resistenza meccanica degli eutettici binari Al-Ca, Al-Ce e Al-Y solidificati unidirezionalmente, XIV Convegno A.I.M., Trieste, Italy, 1-3 June 1970

4) G. Beghi and G. Piatti, Morfologia degli eutettici binari Al-Au, Al-Pt e Al-Pd solidificati unidirezionalmente, XIV Convegno A.I.M., Trieste, Italy, 1-3 June 1970

5) G. Beghi, D. Boerman and G. Piatti, Valutazione preliminare di un materiale composito Ni-Ta ottenuto per solidificazione unidirezionale, XIV Convegno A.I.M., Trieste, Italy, 1-3 June 1970

6) G. Beghi, D. Boerman, R. Matera and G. Piatti, Mechanical properties at high temperatures of a Ni-based eutectic: Ni-Ni_3Ta, to be presented at "Verbundwerkstoffe", Konstanz (Germany), 16-17 March 1972 (Deutsche Gesellschaft für Metallkunde)

7) F.A. Shunk, Constitution of binary alloys, Second supplement, Mc Graw-Hill Book Co., New York, 1969

IDENTIFICATION TECHNIQUES IN THE CONTROL OF FISSILE MATERIALS

P. Jehenson and S. Crutzen

Introduction

A simplified scheme of the nuclear fuel cycle may be the following:

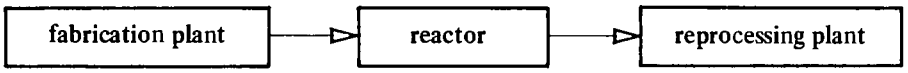

- the fissile materials flowing from the fabrication plant to the reprocessing plant are contained in *fuel elements;* they are "confined".
- the fissile materials circulating in the fabrication and reprocessing plants may often be "confined" when they are not being processed: e.g., raw materials during storage, or scraps.

Therefore, a means of guaranteeing the "confined" fissile materials would considerably reduce the effort needed for the circulation control of these materials and also simplify the application of other control methods.

In order to guarantee the integrity of the "confined" fissile materials, the container must be tamperproof and have a unique and unreproducible identity.

It is important to underline here the difference between a unique numeration which is never tamperproof and a unique identification which when properly designed is tamperproof.

In order to identify the "containers", we adopted the "fingerprint" principle, using either "natural marks" (unique and unreproducible) due to the container fabrication process e.g., weldings or "artificial" marks (unique and unreproducible) added on or in the container, e.g., inclusions added within the cladding of a fuel element.

Identification based on the "containment" calls necessarily for bookkeeping of the fissile materials; the fact of having in library an "identity card" e.g. for a fuel element, permits an easy verification on theft or substitution tampering.

The identity of a "container" being recorded, the scheme of the identity control is the following:

- classification of the identity cards (library)
- new recording of the container identity, at a storage point
- comparison of the two identity records of that container.

Each identity card in the library remaining uncalled during a verification indicates a theft or at least the absence of the corresponding "container". Any identity reading not matched in the library, i.e., all erroneous identity, indicates tampering.

Identification method

The method is based on:

- the natural or artificial marking of the piece to be identified; this marking is done by inclusions or defects randomly dispersed in a matrix. The choice of the marking place is specially important to ensure the validity of the identification.
- the identity reading; it is carried out by means of ultrasonics. The output signals are electric analog signals. Other detection methods have been tested, eddy currents and X-ray fluorescence, but up to now the ultrasonic method has given the best results.

The problems of achieving a unique identification system are:

- Choice of the marking systems
- Fabrication of the seals
- Choice of the identity measurements system and of the recording chain
- Study of the feasibility of the complete system

Since 1970, different cases of application of the unique identification method have been studied. Ref.[1] mentions some of them, namely MTR fuel element plates and seals. In 1971, we considered other means of marking MTR plates (e.g. marking the box on the edge plate) and different means of applying seals (e.g., on LWR fuel element).

Often we have difficulty in complying with the severe criteria imposed or in applying the identification method. Ultimately we reached the general conclusion that INSTEAD OF USING NATURAL OR ARTIFICIAL MARKS PRINTED IN THE CONTAINER, IT IS PREFERABLE TO APPLY SEALS ON THE CONTAINER.

This principle offers the advantages of not modifying the characteristics and the qualities of the container, permitting the identity measurement of the seal before it is positioned on the container, and permitting the identity verification either on the container or on the removed (but no longer usable) seal. This method permits a *centralization* of controls, increases the reliability of the system of measurement and control of identity, and decreases the tampering possibilities.

Seals

Fabrication

The general characteristics for the fabrication of marked seals were already described in the reports in references 1 and 2. The main characteristics of the seals (composition, geometrical forms, types of inclusions) depend on their practical applications. Different methods, using the *powder metallurgy techniques* have been set up for different types of seals:

- with a light matrix (plexiglass, aluminium, SAP) containing inclusions (bronze, tungsten, etc.)
- with a heavy matrix (stainless steel) containing inclusions (W, etc.) or without inclusions but identified by their own particular structure.

System of identity measurement by ultrasonics

Using industrial ultrasonic apparatus, the signals obtained by scanning of the seals were very satisfactory as was shown by the parametrical studies [3].

The general method used is based on reflection owing to the great difference in acoustical impedance existing between the matrix and the inclusions. The transducers utilized are standard but all focalized in order to select the explored zone correctly [4].

The mechanical part of the installation has to position the transducer with great reproducibility and to rotate the seal regularly around its mechanical axis. The mechanical tolerances of the transducer positioning system and the different characteristics of various transducers of the same type and fabrication serial can be defined after a parametrical study to be performed for each application case. The effect of the most important parameters is suppressed by calibrating the installation with a standard which is an artificial defect made in the seal.

The identity, which is given by the ultrasonic response (Fig. 1) can be codified without losing its character of unique identity: to each maximum amplitude response is assigned a confidence interval due to the imperfect reproducibility; knowing the maximum and minium values of amplitude response, the number of discrete values which one inclusion can give is calculated. To each of these values one character is assigned. The chosen characters (alphabel Q) and the number of detected inclusions (format I) define a codification language. This language contains $L = Q^I$ (1) words [3].

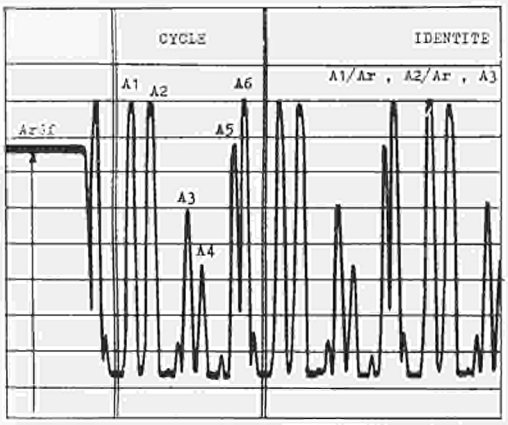

Fig. 1: Identity of a seal.

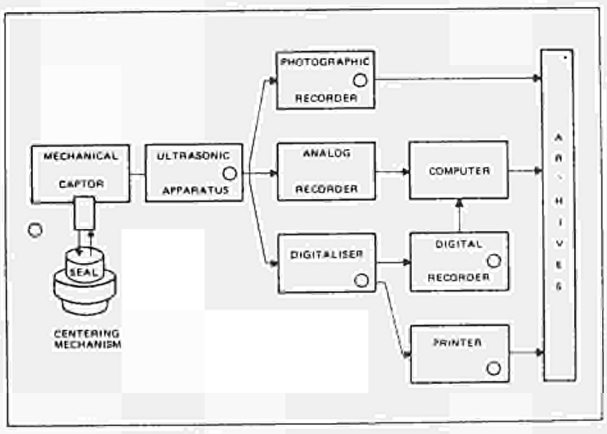

Fig. 2: Scheme of the identification chain.

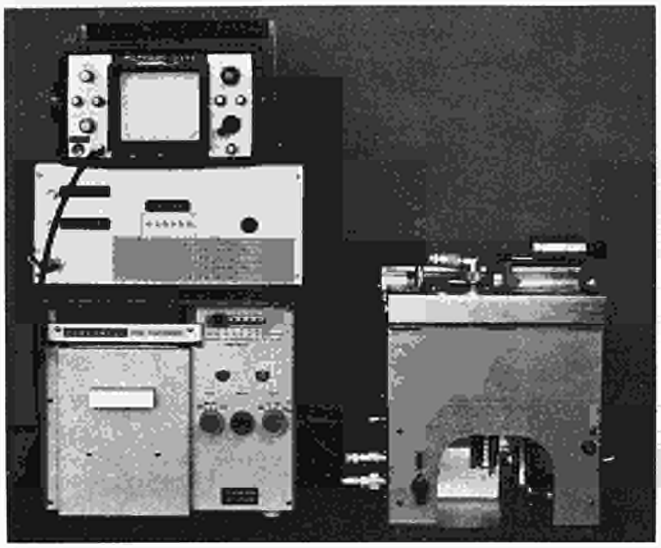

Fig. 3: Prototype identification chain.

Registration of the identity

The registration of the electrical output signals is made in analog form (by pen or photographic recorder). The readouts obtained are easy to interpret and may be used integrally or partially as an identity card. These analog data can be coded in digital form for automatic storage and checking. The method is described in detail in [1]. Figs. 2 and 3 illustrate the control chain showing different alternatives. By using the complete chain one can, at any time and without difficulty:

- bring the library up to date,
- print the results,
- have the general situation of the fissile materials under control.

Moreover, with the data centrally stored in a computer, all other information obtained by other control methods can be added in.

Specific application of seals

Usual seals

The usual seals are composed of a box and a cap, both made of a sintered material (plastics, aluminium composites, stainless steel) containing metallic inclusions randomly dispersed.

The seal is closed by simply pressing these two parts together, an internal clip providing an irreversible closure.

Reopening is impossible without destroying the internal marking, which completely surrounds the locking system (Fig. 4).

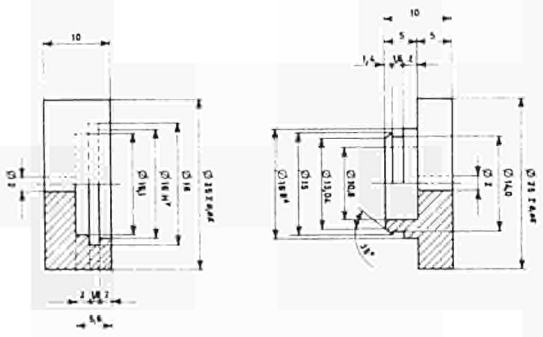

Fig. 4 a: Scheme of the usual seal.

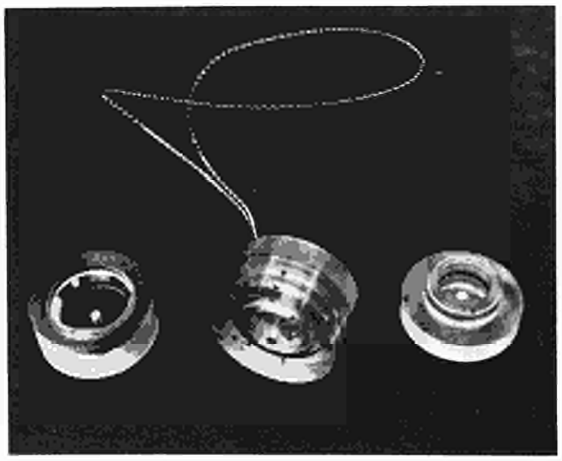

Fig. 4 b: Usual seal with wire.

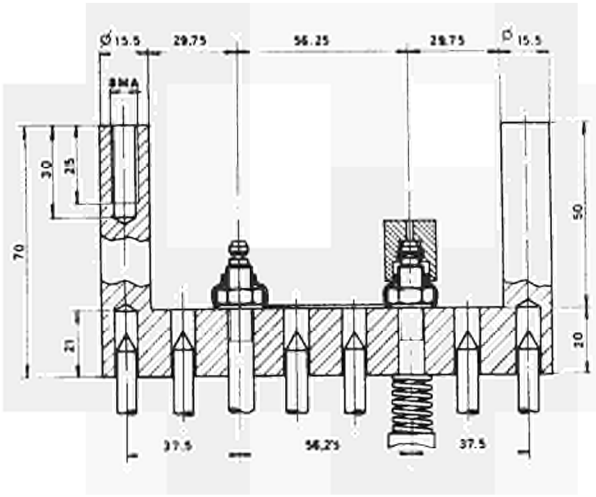

Fig. 5a: Cap seal used for LWR fuel element identification.

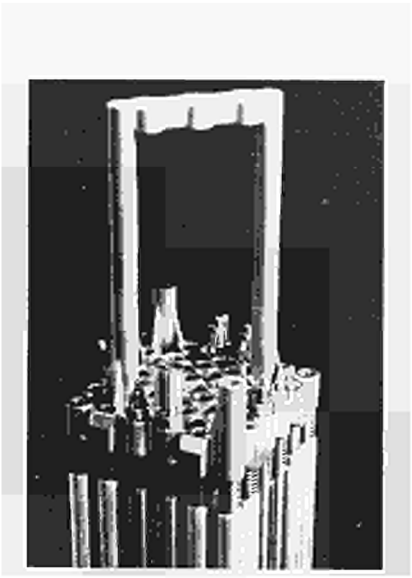

Fig. 5b

These seals have to be used with tamperproof wires [1)]

These seals can be applied, for example, on:

containers used in fabrication and reprocessing plants (particles, plates, scraps), for transportation or for storage.

critical assemblies: in these experimental installations, a great quantity of strategical raw material is in circulation. The control by means of physical measurements and bookkeeping may be simplified by applying seals on the containers (bird-cages).

pebble-bed reactor: seals may be used to safeguard exits, and to prevent tampering with particle-counting instruments, burnup checking equipment and irradiated-particle containers.

Cap seals

This type of seal was designed for the identification of light water reactor fuel elements. The seal is a cap made of stainless steel which, following the general principle, contains randomly distributed inclusions. The sealing is done by applying a marked "cap seal" on one or more tie-rods, in order to lock the screws. The practical details of application are described in [5)] and Fig. 5. The seal is designed to enable these long-life (5 years) fuel elements to be dismantled if necessary (to change failed fuel pins); it can be taken off without destroying the marks, but remains unusuable for a new sealing.

Rivet seals

This type of seal was designed and fabricated for use on the box of MTR fuel elements; the seal rivets the nozzle on the edge plate of the fuel (Fig. 6) so that the element cannot be dismantled and plates cannot be pulled off.

Only the disc of the seal is marked with inclusions; the cylindrical foot is destroyed by removal of the seal, which remains unusable for a new sealing.

Uncertainties and Tamperproofness

The proposed identification principle provides theoretical tamperproofness. The method uses certain random properties related to the seal fabrication process.

Three practical aspects:

a) the physical or technological process used to detect this property which bestows unique identity,
b) the data processing system, and
c) the mode of application of the method in each particular case are imperfect and introduce doubts as to the practical tamperproofness of the method.

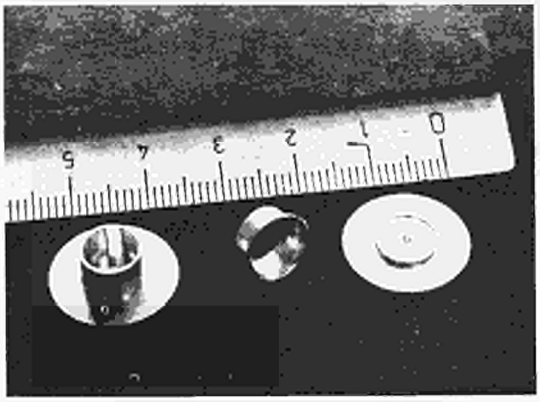

Fig. 6 a: Rivet seal before and after use.

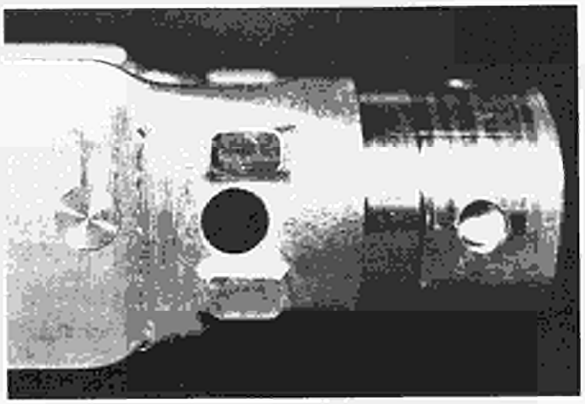

Fig. 6 b: MTR fuel element (HFR PETTEN) with rivet seal.

An elementary analysis can be made in order to appreciate the influence of the three parameters given above on the tamperproofness of the identity for particular application [3].

Uncertainties due to the identity detection

Guided by the results of the parametrical study and helped by the standard, some tests simulating the real working conditions were performed concerning the reproducibility of the response of each inclusion detected.

Let us consider the compound event which consists in the occurence of one at least of the events: "error for one inclusion response" (Ai); this composed event is the error on the identity of the seal.

The probability of error on the identity (p) is the sum of the probabilities of the events Ai. If the correlation (c) existing between the variables A_i, assumed to be gaussian is taken into account, the probability p is:

$$p = c\, I\, (2),$$

I being the number of detected inclusions.

Using the equations (1) and (2), the number of inclusions I to be put in the K elements to be identified can be calculated, as can the confidence interval to be associated with each response of inclusion (number of discrete values for one inclusion: H). In Fig. 7, ϵ is the probability of error on the response of one inclusion.

Example

An example is reported here for the case of plastic seals with bronze inclusions [8].

The diagram in Fig. 7 gives the solution (I, H) for different values of K and two cases of calibration of the installation:

- usual case: calibration of
  - a) the position of the seal,
  - b) the electronic gain of the measuring chain.
- exceptional case: adjustment of the whole installation on the spot using only the standard for calibration of the transducer, gain, positions.

The results of the statistical tests show that, in some exceptional cases, the number of discrete values of response for one inclusion can be very low; the possibility of tampering with the identity has then to be considered.

Fig. 7: Number of inclusions needed in for the identification of K.

SEALS		
K	H	
	usual	exception
10^2	45	27
10^3	37	22
10^4	21	12

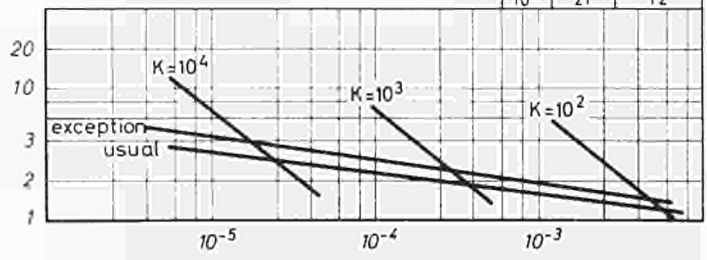

If I is very high, the method is no longer tamperproof.

In order to preserve the inviolability of the identity, the value of K has to be limited; the maximum value of K depends on the particular case of application of the method.

Influence of the data treatment chain

The complete chain is as shown in Fig. 2. Each element of this chain introduces an uncertainty.

The first studies of the method were done with the reduced chain and the results given above take into account the lack of precision of each element of this chain.

A reliability analysis has to be done for the complete chain.

Influence of the complexity of the method in use

The marking system is always localized and weak points may subsist where cutting, substitution of part of the fissile material and rewelding is possible; therefore, the principle of identification described will be applied one, two or three times depending on the design of the element to be identified.

The total identity is then composed of several partial identities. For p_t, total probability of error, *remaining the same,* the confidence intervals associated with each partial response must increase and the number of distinct possible responses for one inclusion decreases. As was seen, for big values of I, the possibility of tampering with the method would then exist (Fig. 7).

In conclusion our method, as others, presents an optimum in the application of the principle. The parameters of practical application have to be predetermined as far as the following points are concerned:

- the number of seals to be identified (K);
- the number of inclusions to be put into each seal (I).

Final remarks

The unique identification based on the "containment" can ensure the control of fissile materials from the fabrication plant up to the reprocessing plant. The identification can realize the union between these two plants where the control, based on physical measurements and bookkeeping, has to be intensified.

If the identity-reading system is simple enough and if the checking of this identity is automated, the library can at all times give the position of the controlled fissile materials in the zone of the considered fuel cycle. The application of tamperproof seals is the most convenient way to identify containers; it allows easy compliance with the severe criteria imposed, simplified identity-reading and checking processes and good centralization of the controls, increasing the reliability of the control system and diminishing the danger of tampering.

References

1) P.S. Jehenson, S.J. Crutzen, E.E. Borloo, J.C. Jansen, "Procédés d'identification à preuve de fraude en vue du contrôle de la circulation des matières fissiles par la technique du "Containment". *IAEA-SM-133/26. July 1970*

2) W. Bürgers, Fabbricazione dei sigilli a prova di *"Fraude"* (not available)

3) S. Crutzen, Uncertainties and tamperproofness of a unique identification method using a natural or artificial marking system". *International meeting on nondestructive measurement and identification techniques in nuclear safeguards. 20.9.191971 (Euratom JRC Ispra).*

4) E. Borloo, Relevé par ultrasons, de l'identité de sceaux à preuve de fraude" *(not available)*

5) P.S. Jehenson, Application des sceaux à l'identification des éleménts combustibles du type LWR *(not available)*

6) Euratom Patent *"System zur Kennzeichnung von Gegenständen"* P 1935 686.6 - 10.7.1969 - Germany - S.J. Crutzen, M. Warnery, J. Faurè. Euratom Patent *"Siegel zur Kennzeichnung von Gegenständen"* 61.143 - 16.6.1970 - Luxembourg - W. Bürgers, S. Crutzen, J. Jansen, P. Jehenson.

7) P. Jehenson, Methods of unique identification, for the control of the flow of fissile materials. International Meeting on Nondestructive Measurement and Identification Techniques in Nuclear Safeguards. 20-21-22 Sept. 1971 (Euratom JRC Ispra).

8) S. Crutzen, C. Francocci, Etude paramétrique et statistique de sceaux en matière plastique pour le contrôle des stocks de matières fissiles, *(not available)*

HYDROGEN PRODUCTION FROM WATER USING NUCLEAR HEAT

G. Beghi, G. De Beni

Introduction

The energy market of the European Economic Community is strongly dependent on imports of primary sources, principally oil.

The advantages of nuclear fuel as a primary energy source suggest nuclear power as a means of reducing this dependence of the EEC. From this point of view, a wider use of nuclear reactors for the overall energy requirements is an important objective, more especially if both electricity and thermal energy can be economically generated from the nuclear fission heat.

Electricity generation problems are well known and industrial capacity is growing continuously.

But only about 25% of today's total primary energy requirement in Europe is used to generate electricity; hence it appears that a very large market remains for nuclear energy, if it can supply heat at appropriately high temperatures and competitive prices. Up to now the process heat needed for chemical plants, oil refineries, metallurgical processes and domestic heating has been generated by burning fossil fuels.

In view of the growth rate currently estimated for the energy market, and of the rising costs of natural gas, mineral oil and coal, the idea of using nuclear reactors as pure heat sources is increasingly attractive. The next step now is to find high-temperature processes which will directly consume nuclear heat or can be used to "package" this energy in convenient chemical forms for distribution over long distances and to small-scale users.

Hydrogen may be considered an interesting "packaged energy" carrier for its versatility, feasibility of transport and distribution, various uses and finally its "clean" combustion, a very important factor for the reduction of environmental pollution [1].

Hydrogen is now industrially produced by steam-reforming of light hydrocarbons (mainly methane) and by partial oxidation of hydrocarbon fractions (from methane to heavy residues). The production from water by conventional electrolysis is uneconomic at the present time. A new possibility of producing hydrogen is the decomposition of water by chemical processes, with various reactions in a closed cycle which needs only heat. If the temperature level is suitable for nuclear reactors, this method is particularly convenient for an extended utilization of nuclear heat.

Requiring only uranium and water as primary raw materials, and consuming neither oil nor natural gas, these water decomposition processes using nuclear heat would help to decrease the dependence of the Community in the energy market and make for better conservation of natural resources.

Research at Ispra

In the light of the foregoing, the aim of the research done at Ispra is to investigate the feasibility of developing chemical cycles for the decomposition of water, a step-by-step water-splitting process using a series of recycled chemicals to form intermediate compounds and having thermal energy input requirements which lie within the foreseen capabilities of the High Temperature Gas-cooled Reactors.

The stages in the work are the following:

a) a search for chemical cycles which are theoretically feasible, according to the thermodynamic data;
b) study of the unknown reactions in the selected cycles;
c) development of the most promising cycles, under steady-state conditions, on the laboratory-bench cale, to determine all the data concerning the reactions, concentrations, and separations;
d) studies on the coupling of the chemical process to the nuclear reactor.

The purpose is to collect all the data necessary for demonstration of the technological feasibility and for the design of a pilot plant; this will be the basis for economic evaluations and comparisons of the most promising processes.

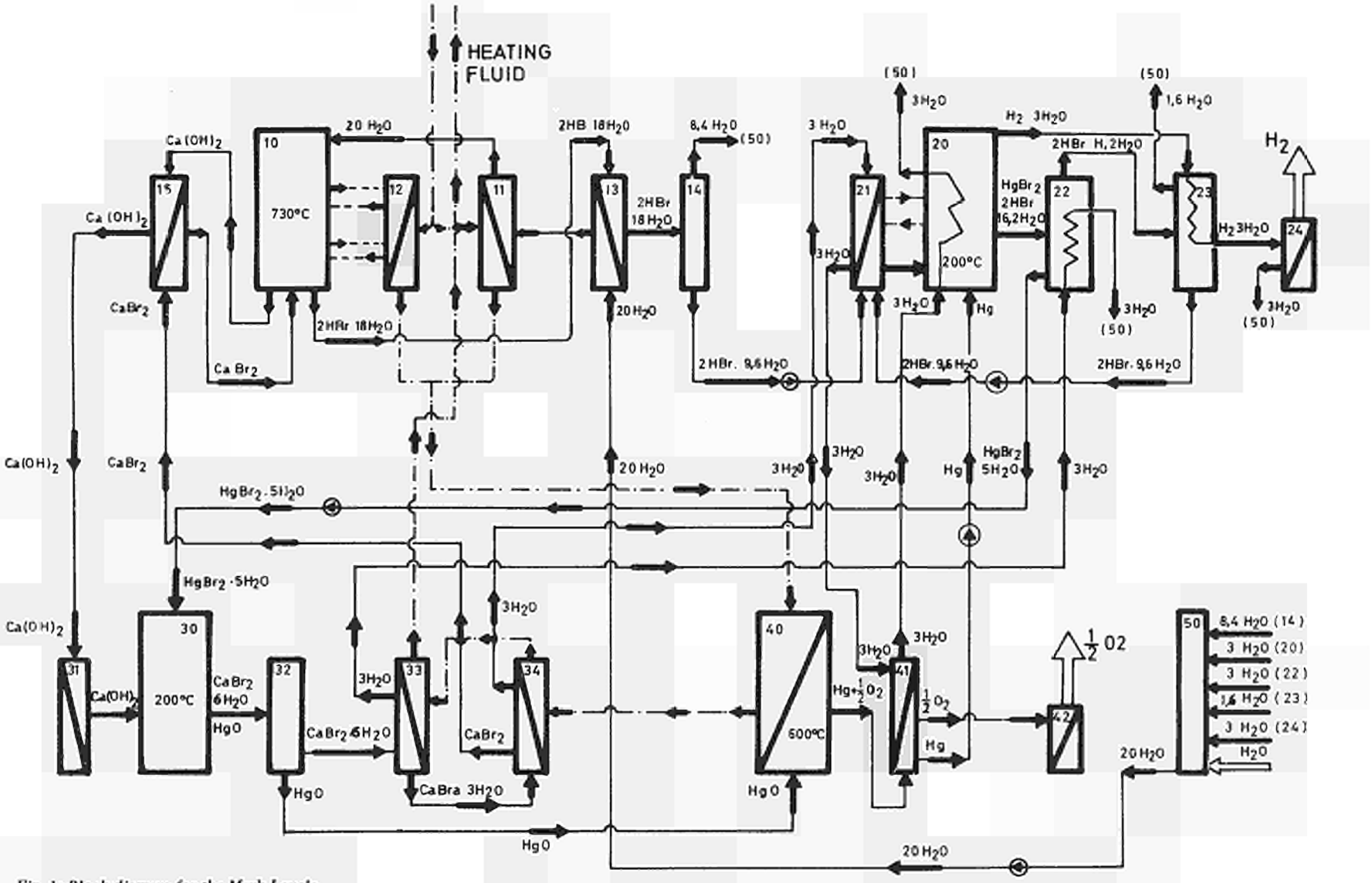

Fig. 1: Block diagram for the Mark I cycle.

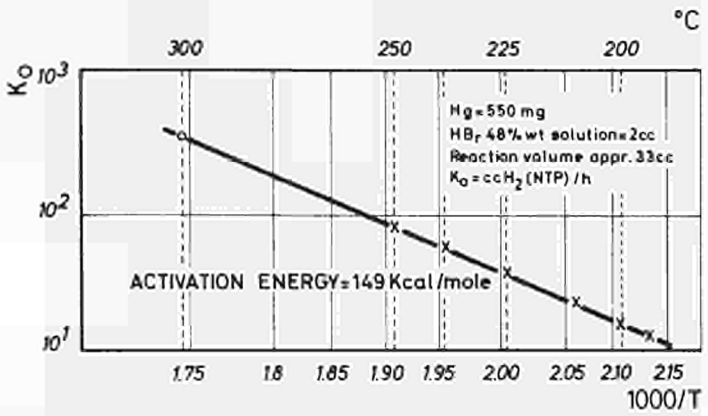

Fig. 2: $Hg + 2HBr \rightarrow HgBr_2 + H_2$ Temperature dependence of rate constant.

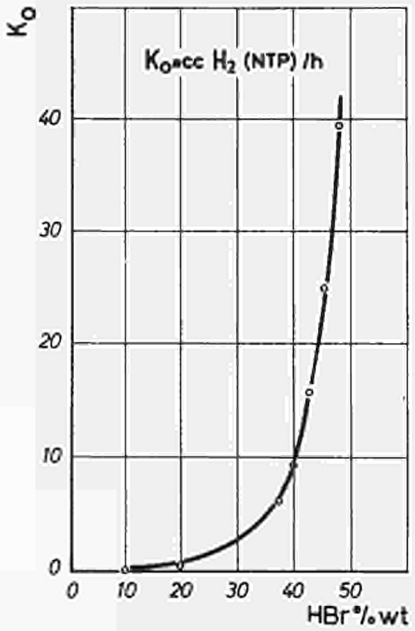

Fig. 3: $Hg + 2HBr \rightarrow HgBr_2 + H_2$ Hydrogen formation rate at 200°C influence of HBr concentration.

Work is in progress in these directions; various chemical cycles have already been defined, although the knowledge of each has so reached various levels. At the end of 1971 the chemical cycles under study were the following:

- Mark-I cycle, and its possible modifications;
- manganese cycles;
- vanadium chloride cycle;
- chlorine-iron cycle.

The Mark-I cycle

The Mark-I cycle was the first of the chemical cycles to be found, and was patented by G. De Beni [2]. It is a four-step cycle which uses compounds of mercury, bromine and calcium. The set of reactions is the following:

1) $Ca\,Br_2 + 2H_2O \xrightarrow{730°} Ca(OH)_2 + 2HBr$ — water splitting
2) $Hg + 2\,HBr \xrightarrow{250°} HgBr_2 + H_2$ — hydrogen switch
3) $HgBr_2 + Ca(OH)_2 \xrightarrow{200°} CaBr_2 + HgO + H_2O$ — oxygen shift
4) $HgO \xrightarrow{600°} Hg + 1/2\,O_2$ — oxygen switch

Whose sum is: $H_2O \longrightarrow H_2 + 1/2\,O_2$.

A preliminary block-diagram of this cycle is shown in Fig. 1; mass flows refer to the production of 1 mole H_2.

The experimental results of the work in progress are the following:

1) The hydrolysis reaction of calcium bromide (reaction 1) has been realized in steady state conditions with experimental set-ups; alumina has been utilized as construction material for the high temperature zone. Preliminary experiments were carried out at atmospheric pressure, with injection of water vapour into liquid calcium bromide; these first experiments showed that pure alumina withstands corrosive conditions well for several hundreds of hours. Even though thermodynamic calculations predict low values, sufficient $CaBr_2$ conversion ratios were obtained with a HBr concentration of about 25%; on the basis of these preliminary results an apparatus consisting in a column is being constructed for complete determination of all the important parameters: reaction rate, conversion ratio, concentrations, etc.
2) The reaction of hydrobromic acid with mercury was studied to determine the best conditions for the reaction rate. The parameters which have been examined are temperature, hydrobromic acid concentration, mercury surface area and catalysts.
   From the reaction rates at temperatures between 197°C and 250°C the activation energy for the reaction has been calculated to be about 15 kcal/mol (Fig. 2). Extrapolating the reaction rate at 300°C we can expect a hydrogen formation rate of about 700 cc (NTP)/h cm^2.
   A strong influence of the hydrobromic acid concentration on the hydrogen formation rate was found at 200°C (Fig. 3). At the same temperature, the addition of iridium-black grown on tungsten powder increased the hydrogen evolution rate by a factor of 2.3.

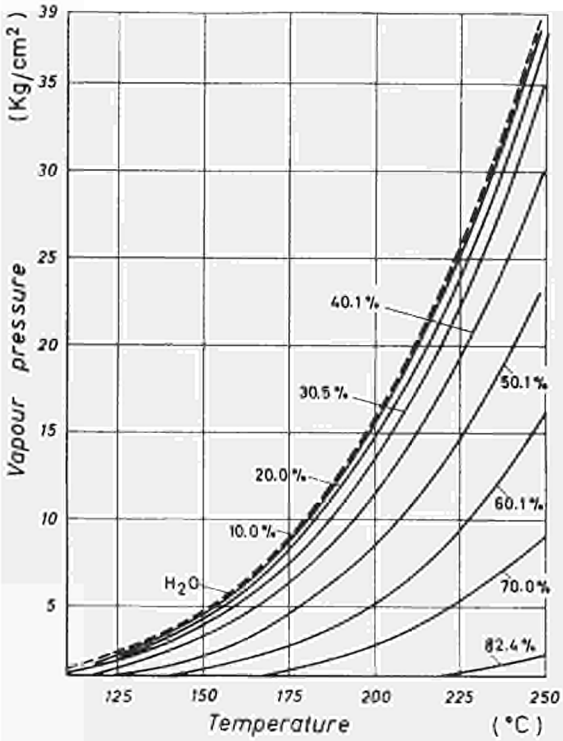

Fig. 4: Boiling temperatures of $CaBr_2$ solutions

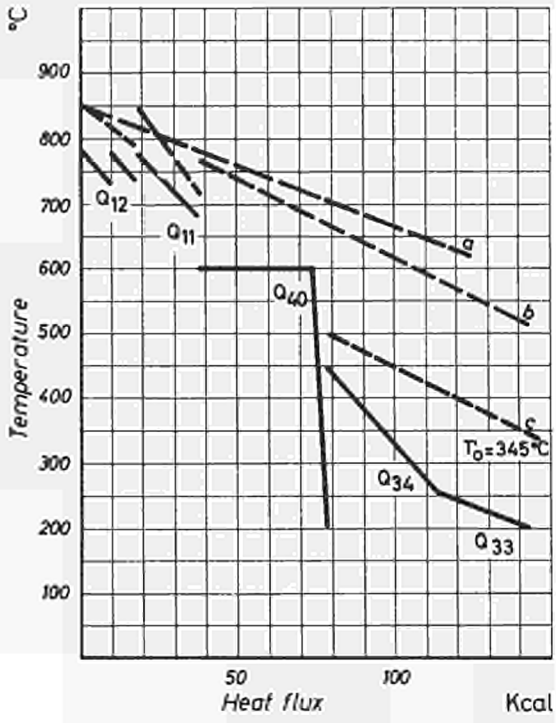

Fig. 5: Example of process thermal coupling using 850°C helium gas as primary heat carrier.

3) Among the physical properties measurements which are in progress, the determination of the boiling temperatures of calcium bromide solutions, up to 250°C, as a function of pressure and concentration has been accomplished (Fig. 4).
4) Structural material problems were examined for a preliminary evaluation. The more corrosive conditions are due to hydrobromic acid, at various concentrations and temperatures. Exploratory corrosion tests in concentrated (48 wt%) and diluted (30 wt%) HBr are in progress. Tests have been performed at temperatures up to 300°C and for durations of up to 2000 hours; the best resisting materials are tantalum, molybdenum, Zr-2.5Nb alloy, Zircaloy 2, with depth of attack of the order of the micron.

Some preliminary observations can be made regarding the coupling of the cycle to the HTGR nuclear reactor.

The cycle Mark-1 draws heat at different temperatures, the maximum temperature being 730°C. These quantities can be plotted in a diagram, with the temperature in °C as ordinate, and the quantity of heat (Kcal/mole H_2) as abscissa.

We can draw in the same diagram a similar plot for the heat carrier, and the distance between these lines will represent the ΔT in the heat exchangers. The amounts of heat represented by these lines are indexed according to the flow-sheet in Fig. 1. We can see in Fig. 5 how the quantities Q_{12}, Q_{11}, Q_{40}, Q_{34} and Q_{33} fit in the diagram. The heating fluid is represented with dashed lines. The figures refer to the production of 1 mole of H_2.

With the initial temperature of the fluid at 850°C and a minimum ΔT of 40°C we obtain the line a), with a mass-flow corresponding to a heat capacity of 540 cal/deg. C.

If we put heat exchangers 11 and 12 in parallel, as shown in figures 1 and 5, we obtain line b). As can be seen, the splitting of the heat carrier into two streams in the high temperature region permits a lower final temperature for the heat carrier. This is also the temperature of re-entry into the reactor, a fairly critical value owing to the material problems it involves for the base of the reactor core.

Another possibility is that of bleeding off part of the heat carrier (line c, Fig. 5) to produce mechanical or electrical energy for operating the auxiliaries of the plant and reactor.

Some modifications of the temperature levels may be foreseen, to give better match between the heating fluid line and the Q lines, with a lower mass-flow rate and lower final coolant temperature.

A very interesting point is that most of the heat produced by the nuclear reactor is correctly utilized in the chemical plant, so that the system is inherently a single-purpose one.

Still in the context of the Mark-I process, evaluations are in progress for some modifications of the cycle, principally:

- a different path for the $HgBr_2$ decomposition in order to avoid the formation of the $HgBr_2$ complex;
- the substitution of another element instead of mercury.

Manganese cycles

Alkali hydrides can be reacted with manganese metal to give the oxide MnO_2 and hydrogen [3].

With MnO_2 as the manganese oxide, stable in molten sodium hydroxide, it is possible to construct this cycle for hydrogen production:

1) $Mn_2O_3 + 8NaOH \longrightarrow 2\,(MnO_2 \cdot 2Na_2O) + 3H_2O + H_2$ at 600°C
2) $2\,(MnO_2 \cdot 2Na_2O) + \text{water} \longrightarrow 8NaOH_{acq.} + 2Mn(OH)_4$ at 100°C
3) $8NaOH_{acq.} \longrightarrow \text{water} + NaOH$ to 400°C
4) $2Mn(OH)_4 \longrightarrow Mn_2O_3 + 4H_2O + 1/2\,O_2$ at 700°C

Some tests were run to verify the reaction between Mn_2O_3 and NaOH. In spite of the results given by Williams, no reaction was observed; even the substitution of KOH for NaOH did not give better results.

A modification of the chemical cycle was tried, using alkali carbonates for the hydroxides.

The modified cycle becomes:

1) $Mn_2O_3 + 4Na_2CO_3 \longrightarrow 2(MnO_2 \cdot 2Na2O) + 3CO_2 + CO$ at 800°C
2) $2(MnO_2 \cdot 2Na_2O) + \text{water} \longrightarrow 2Mn(OH)_4 + 8NaOH_{acq.}$ at 100°C
3) $CO + 3CO_2 + 8NaOH \longrightarrow 4Na_2CO_3 + H_2 + 3H_2O$ at 400°C
4) $2Mn(OH)_4 \longrightarrow Mn_2O_3 + 4H_2O + 1/2\,O_2$ at 800°C

In the first reaction it would be possible to benefit from the higher free energy of formation of carbon monoxide at high temperature.

The reaction between Mn_2O_3 and the alkali carbonate was tested at the maximum temperature allowed by the volatilization of carbonates (800°C) with various stoichiometric ratios, but again no reaction was observable. Other experiments are planned.

Vanadium chloride cycle

The study of the halides of the transition metals led to the construction of a cycle working with vanadium and chlorine; the same set of reactions were independently described by researchers of the Allison Division of General Motors Co. among a group of four cycles, working with chlorine.

The reactions are the following:

1) $Cl_2 + H_2O \longrightarrow 2HCl + 1/2\,O_2$ at 700 ÷ 800°C
2) $2HCl + 2VCl_2 \longrightarrow 2VCl_3 + H_2$ at 100°C
3) $4VCl_3 \longrightarrow 2VCl_2 + 2VCl_4$ at 700°C
4) $2VCl_4 \longrightarrow 2VCl_3 + Cl_2$ at 100°C

The first reaction of this cycle is well known in industry. The available thermodynamic data for the vanadium chlorides allow the calculation of an acceptable yield for each reaction at the indicated temperatures. Some experimental work was done at the Allison Division on reaction 2. In spite of the expected favourable equilibrium they did not find any evidence of reaction under those conditions.

Some experiments on reactions of vanadium chlorides are planned, to find more favourable new conditions.

Chlorine-iron cycle

Continuing the investigation of four-step processes, a new cycle involving chlorine, sulphur and iron compounds was found [4].

The four reactions of this cycle are the following:

1) $Cl_2 + H_2O \longrightarrow 2HCl + 1/2\,O_2$ at 800°C
2) $2HCl + S + 2FeCl_2 \longrightarrow 2FeCl_3 + H_2S$ at 100°C
3) $H_2S \longrightarrow H_2 + 1/2\,S_2$ at 800°C
4) $2FeCl_3 \longrightarrow 2FeCl_2 + Cl_2$ at 350°C

Again reaction 1 is the well-known reaction. Laboratory work has been started on reaction 2 which appears the most difficult to achieve owing to the expected fairly unfavourable equilibrium concentrations of reaction products, and to the possibility of side reactions (formation of FeS). For reaction 3, too, some experimental work is in progress to find a practical way by which extraction of hydrogen and elemental sulphur could be obtained in a continuous operation.

Another possibility has been envisaged for the H_2S decomposition. This decomposition could be obtained by a two-reaction cycle, whose reactions are:

1) $H_2S + FeS \longrightarrow H_2 + FeS_2$ at 300°C

2) $FeS_2 \longrightarrow FeS + 1/2\ S_2$ at 800°C

Thermodynamic calculations show good possibilities for the two reactions. In fact reaction 2 is well known in industry; it is simply the thermal decomposition of pyrite.

References

1) C. Marchetti, Hydrogen, master-key to the energy market. *Eurospectra*, Vol. X, No. 4 (1971) p. 117.

D.P. Gregory, D.Y.C. NG, G.M. Long, Electrolytic hydrogen as a fuel. In: *The Electrochemistry of Cleaner Environments Plenum Press*, New York (1971).

W.E. Winsche, T.V. Sheenan, K.C. Hoffman, Hydrogen, a clean fuel for urban areas. *1971 Intersociety Energy Conversion Engineering Conference Proceedings*, Boston, Mass., August 3-6, 1971, SAE Paper No. 719006.

G.A. Mills and J.S. Tosh, Non-energy uses for fuels. Paper ASME-NAFTC-4, *North-American Fuel Technology Conference*, Ottawa, Canada, May 31-June 3, 1970.

2) G. De Beni, French Patent No. 2.035.558, Febr. 17, 1970.

3) D.D. Williams, J.A. Grand and R.R. Miller, The Reactions of Molten Sodium Hydroxide with Various Metals, J.A.C.S. 78, 5150-5 (1956).

4) C. Hardy, Process for Hydrogen Production – Patent pending.

CESIUM MIGRATION IN SILICON CARBIDE

V. Coen, D. Quataert, H. Hausner

Introduction

In the coated particle fuel for High Temperature Gas Cooled Reactors a silicon carbide layer is frequently used to decrease the release of solid fission products Cs, Sr and Ba. Since the release of fission products from pyrolytic silicon carbide coatings is very small, considerable uncertainty exists in regard to the diffusion coefficients for these metals, the transport mechanism and its dependence on the structural properties of the silicon carbide. It is the purpose of this investigation to obtain information in this field which may contribute to a better understanding of the release process and perhaps lead to an improvement in the retention properties of silicon carbide. At the present time special emphasis is placed on the investigation of the cesium migration.

Experimental

The silicon carbide samples are prepared in a fluidized bed from methyltrichlorosilane-hydrogen mixtures. Different structures, compositions, and densities are obtained by variation of the deposition conditions. Characterization of the samples is done by density measurements in a density gradient column, by metallography, chemical and spectrographic analysis and by examination with the scanning electron microscope.

Selected samples are being heat-treated inside a tantalum container up to 2000°C under a controlled cesium vapour pressure (Fig. 1). Cesium filling is done in a vacuum glove box under purified argon, before the tantalum container is closed by electron beam welding. For the analysis of the heat-treated silicon carbide, the ion-microanalyser, the scanning electron microscope and activation analysis are used.

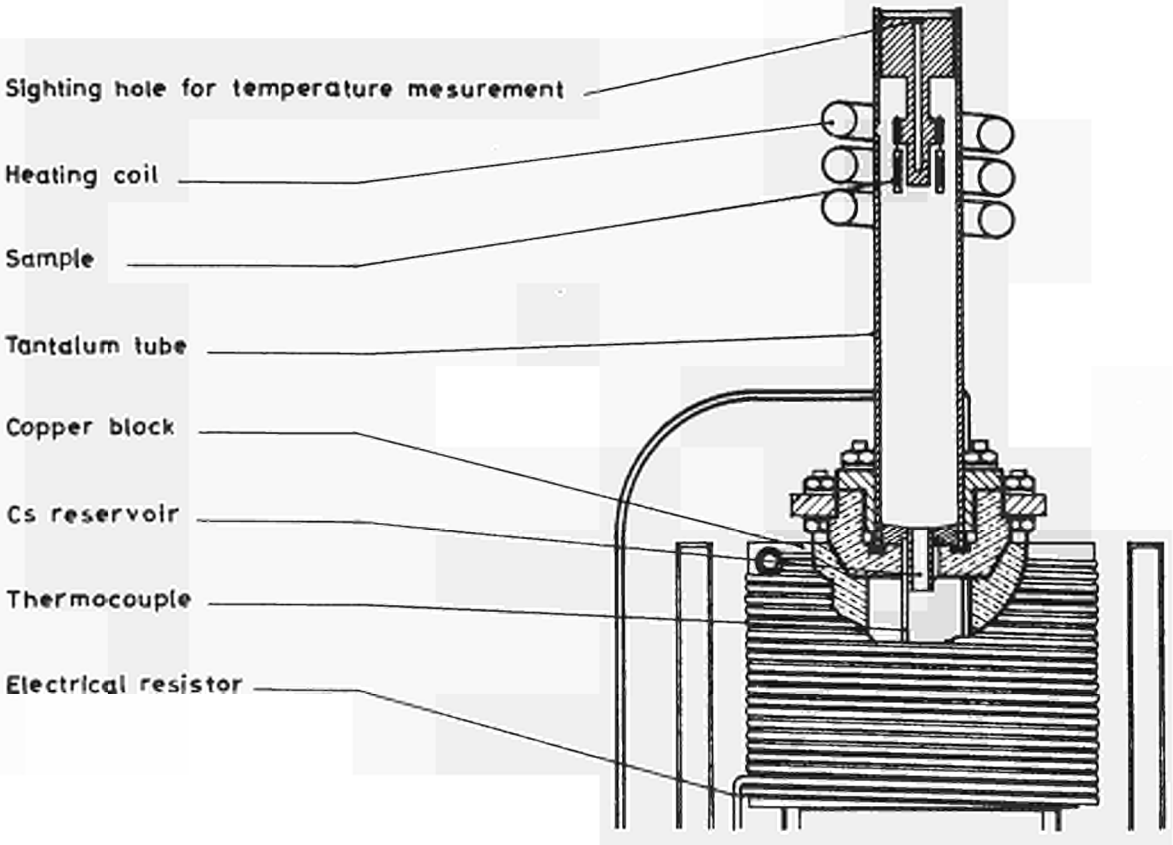

Fig. 1: Experimental set-up for heat treatments in cesium.

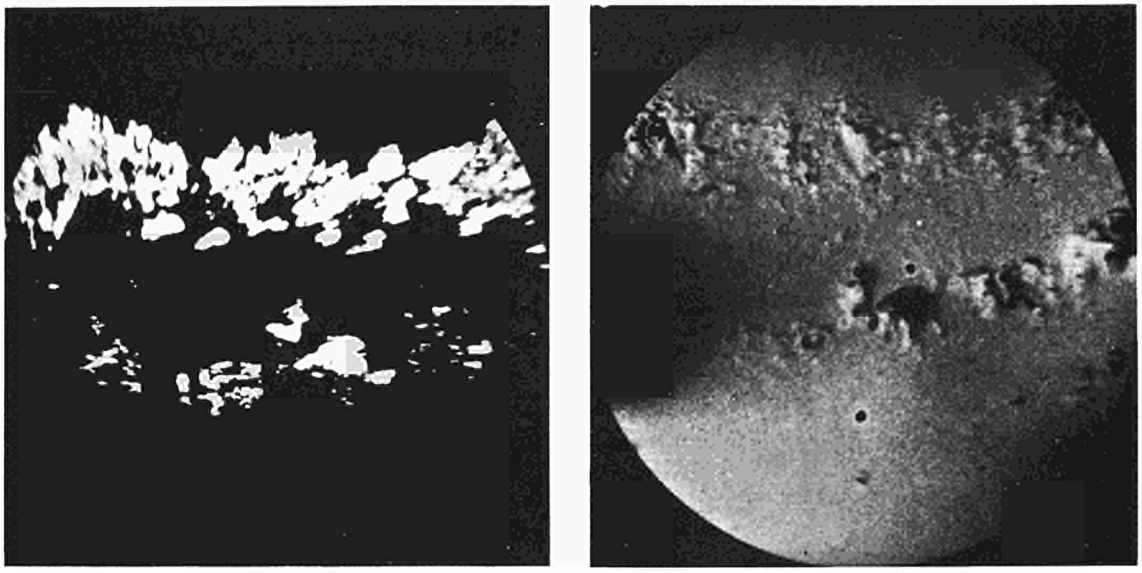

Cs^+-emission *Si^+-emission*

Fig. 2: Porous zone in silicon carbide. (ϕ image 200 μm)

Results

The results obtained to date indicate that the distribution of cesium in the samples is not homogeneous. The transport of cesium seems to take place mainly via microdefects in the silicon carbide. The following photographs (Figs. 2-4) show the Cs distribution as observed by the cesium emission in the ion-microanalyser. The difference in the Si emission from the silicon carbide indicates defects in the samples and the correspondence between these defects and the localized cesium concentration is evident. In addition it has been observed that the structure of the silicon carbide has a significant influence on the cesium penetration. Whereas samples with a fine crystalline structure did not reveal any cesium migration under the experimental conditions (1500°C, 20 mm Cs), samples with a striated structure showed an intensive penetration of cesium along these striations (Figs. 5 and 6).

These results support the assumption that defective particles, especially particles with a defective silicon carbide layer, are mainly responsible for the cesium release from particles in high temperature reactors.

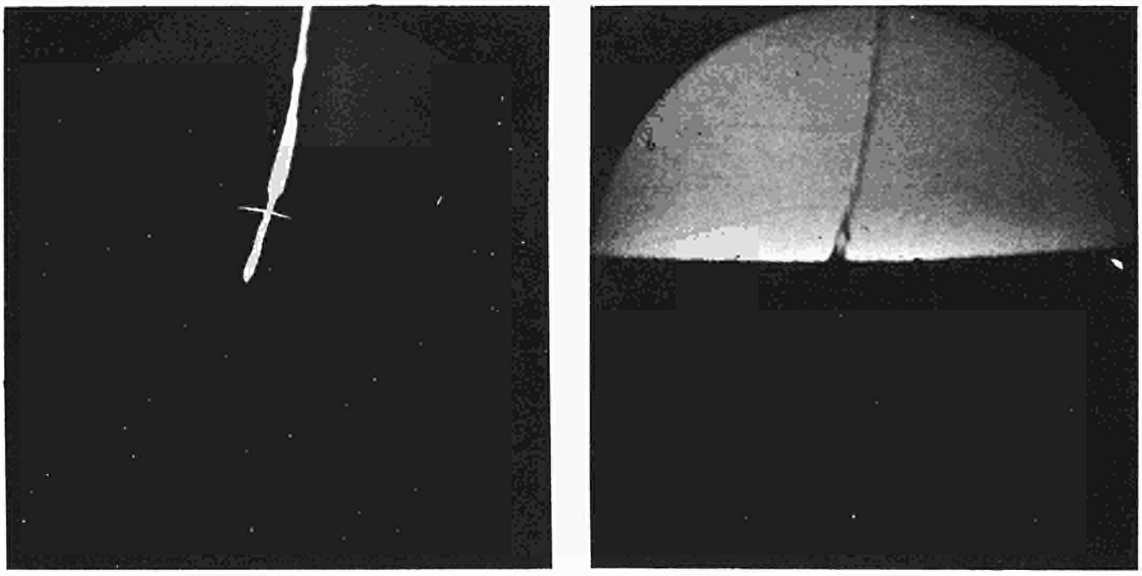

Cs^+- emission *Si^+- emission*

Fig. 3: Crack in silicon carbide. (ϕ image 200 μm)

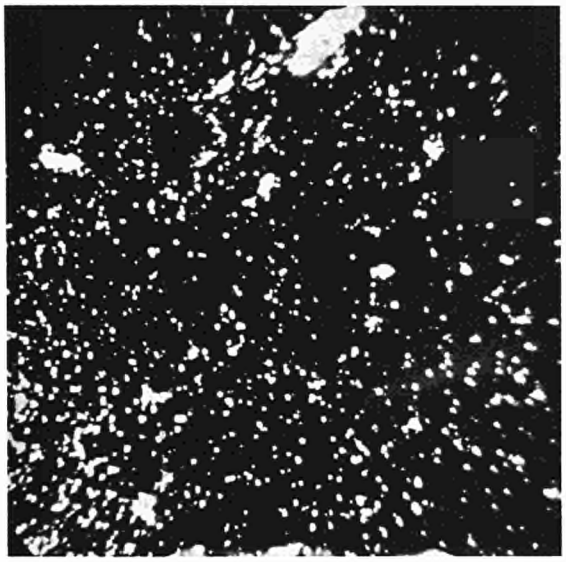

Cs^+ - emission

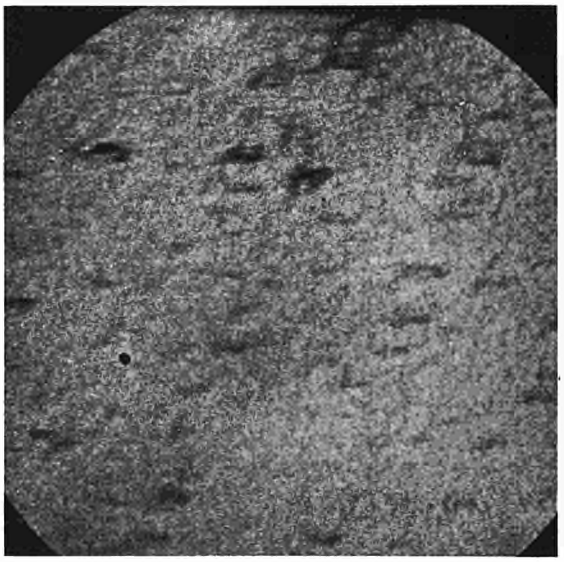

Si^+ - emission

Fig. 4: Microdefects in silicon carbide. (ϕ image 200 μm)

Fig. 5: Striated structure in silicon carbide. (ion-etched)

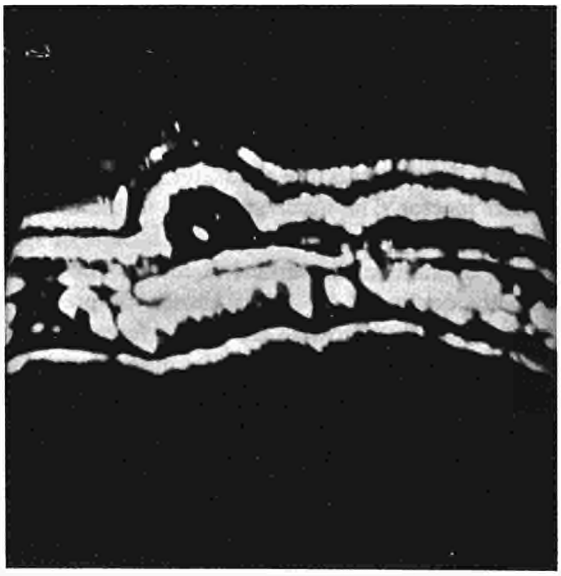

Fig. 6: Cs penetration in striated structure. (ϕ image 200 μm).

VISCOSITY MEASUREMENTS UNDER IRRADIATION

A. Schneiders, P. Schiller

Introduction

The problem of investigating the change of viscosity of acqueous suspensions during neutron irradiation arose in our laboratory. These measurements must be carried out in a nuclear reactor. It becomes necessary, therefore, to choose a measuring procedure which can transmit the experimental data out of the reactor by means of electrical signals. The necessity of working in a nuclear reactor strongly limits the choice of measuring procedures. An additional difficulty lies in the fact that the material to be investigated is in a suspension form. The measuring device must therefore allow a means of keeping the suspension homogeneous during the measurements. In view of these limitations a viscometer which works on the following principle was developed. The sealed capsule containing the acqueous suspension is excited to vibrate mechanically and the logarithmic decrement of the resulting oscillations is measured.

Description of the apparatus

The class of viscometers with vibrating systems uses the drag forces of a liquid on a solid wall to damp the oscillations of the system.

For such viscometers one must solve the following points.

1) In general it is quite difficult to calculate directly the influence of the viscosity on the oscillation. It is therefore necessary to calibrate the apparatus with a known liquid.
2) The proper geometry for the system must be chosen very carefully so that the apparatus is sufficiently sensitive in the viscosity range in which where one wants to measure.
3) Finally one has to develop a device to measure the mechanical vibrations. For this, the existing apparatus developed specially for solid state physics was used.

Fig. 1 represents the apparatus developed for viscosity measurements in acqueous suspensions in the nuclear reactor. The numbers, which in the following are indicated in parenthesis, refer to various parts of Fig. 1. The capsule (2) is suspended by sets of springs (3) and (5) in a heavy container (1). The capsule is free to oscillate in the vertical direction. The combination of helical springs (5) and of the flat springs (3) specially developed by us, is chosen to prevent torsional and horizontal motions of the capsule. The electromagnet (8) provides the driving force that sets the capsule in oscillation.

A plate capacitor (6) and (7) constitutes the pick-up system for the oscillations. In the capsule a float (4) is elastically attached to it by flat springs (3). The springs allow a motion of the float only parallel to the axis of the capsule. The remaining cavity in the capsule is partially filled with the liquid whose viscosity is to be measured while leaving room for expansion. The up-and-down motion of the float with respect to the capsule creates, by means of the liquid layer in the gap between capsule and float, a drag force on the capsule and this force damps the oscillation of the capsule.

The apparatus used to measure the viscosity of acqueous suspensions up to 300°C had the following characteristics:

– Amplitude float movement	:	1.2	mm peak to peak
– Amplitude capsule movement	:	2	mm peak to peak
– Mass of float	:	256	g
– Mass of capsule	:	955	g
– Float capsule gap	:	0,4	mm
– Measuring frequency	:	17	c/sec
– Volume of the suspension	:	13.5	cm^3
– Viscosity range for this suspension	:	0.09	..... 2 centipoise
– Precision	:	± 5%	

Fig. 2 gives the block diagram of the electronic section of the measuring equipment. The signal of the low frequency oscillator is amplified and then fed to the excitation coil of the viscometer and to one of the beams of a double-beam oscilloscope. The oscillations of the measuring capacitor in the viscometer are transferred by a device to an alternating voltage and then fed to a level recorder, a frequency counter and a dual beam oscillograph.

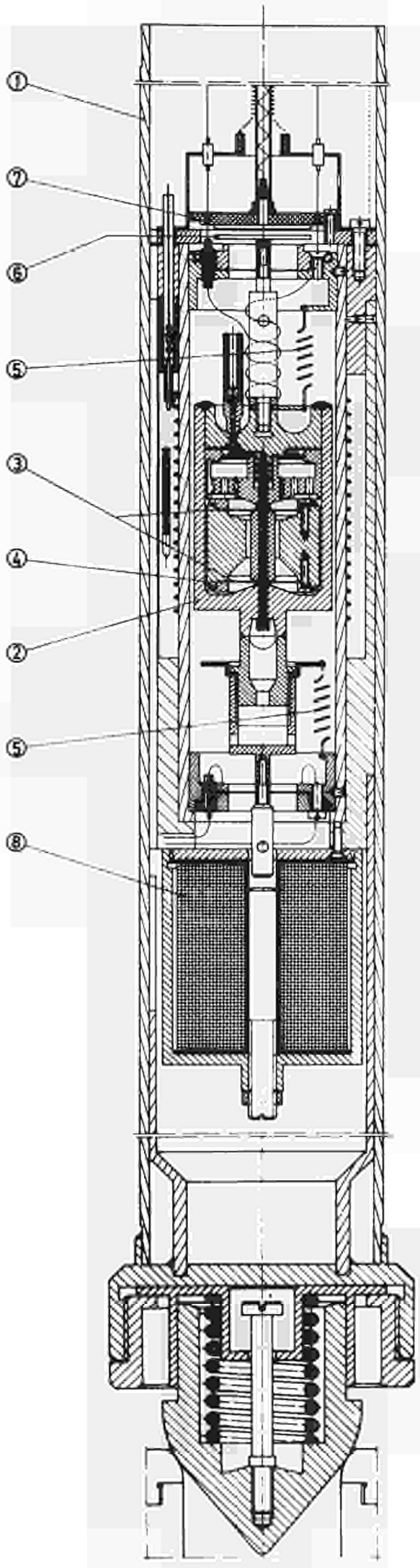

Fig. 1

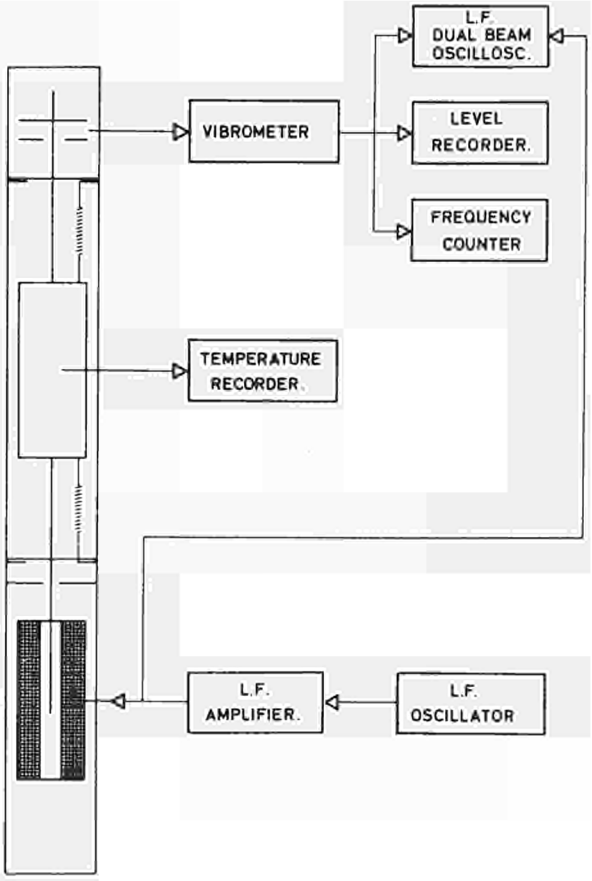

Fig. 2: Block diagram of measuring apparatus.

Temperature registration can be established in the case of measurements in furnaces or nuclear reactors.

Results

The apparatus described above has been used to measure the influence of neutron irradiation on a suspension of a mixture of thorium oxide and enriched uranium oxide in water. The suspension contained 200 g powder in one litre of water. The powder had particles of 5 μm and was composed of 98.5% ThO_2 and 1.5% UO_2; the uranium was enriched to 90%. The total fluence was $0.9 \cdot 10^{20}$ neutrons/cm^2. The temperature at which the measurements were done was 300°C.

Fig. 3 represents the measured viscosity as a function of irradiation time. The irradiation was not continuous because it was interrupted several times. The longest interruption took place after 220 hours of operation when the rig was removed from the reactor in order to be modified and then placed in position 6 EV. This interruption lasted for 80 days. A second interruption occurred after 880 hours of irradiation and lasted three days. All other reactor shut-down periods, which were much shorter, are considered to be part of the irradiation time.

Fig. 3 shows that the viscosity increases with irradiation time. One can observe that the viscosity remained fairly constant during the first 300 hours of irradiation while a marked increase took place between 300 and 800 hours. After 800 hours the viscosity value did not change so markedly. It is noticeable that as soon as the viscosity increases the dispersion of the data increases also. The dispersion can be traced to the fact that with increasing irradiation time the behaviour of the fuel suspension differs increasingly from that of a pure Newtonian liquid.

Conclusions

It has been shown, that a viscometer without rotating parts can be built. By changing the constants of the apparatus the range of the viscometer can be shifted to higher or lower values. In the particular case of a suspension the range will be restricted at the lower end by the time of sedimentation.

The VISIR-2 experiment has shown that it is possible to do viscosity measurements in a nuclear reactor. More specifically it was found that the proper functioning of the developed viscometer is not affected by radiation damage when it is exposed to radiation flux for a period of time that can be as long as a few months.

During the experiment the measured viscosity of the fuel suspension increased as a function of the neutron fluence. At the beginning of the experiment the viscosity corresponded to that of pure water (0.1 centipoise at 300°C), while at the end the value had more than doubled to about 0.25 centipoise.

It is thought that this increase in the viscosity is due to a change of the fuel particles under irradiation.

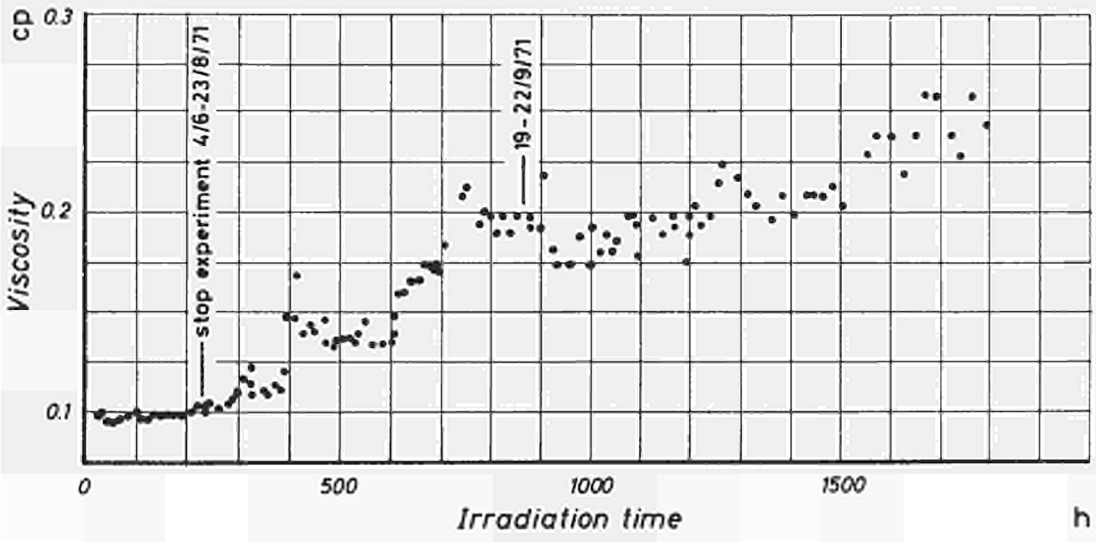

Fig. 3: Viscosity versus irradiation time.

HEAT PIPES

C.A. Busse, F. Brossa, F. Geiger, D. Quataert

Introduction

During recent years there has been a growing interest in heat pipes, mainly in the USA, Europe and the USSR. The rate of publications in this field has increased to about 200 a year. In order to improve access to the rather scattered information a two-day Round Table Discussion on heat pipes was organized at Ispra in November 1971, in which experts from 12 laboratories in the Community participated, as well as representatives from 5 laboratories in the UK, CSSR, Sweden and Switzerland.

Heat pipe work at Ispra was concentrated in 1971 on two subjects:

- the heat pipe mechanism,
- corrosion.

The studies on the heat pipe mechanism were executed in close collaboration with the University of Stuttgart, Institut fur Kernenergetik (doctorate theses).

Studies on the heat pipe mechanism

Work was done on the ultimate limit of axial heat transfer, which is not yet well understood, and the gas plug effect, which is the basis for a number of interesting heat pipe applications.

Ultimate limit of axial heat transfer

The axial heat flux in heat pipes is limited in principle for two reasons: insufficient return flow of condensate and vapour flow limitations. If the liquid return flow is guaranteed by a suitable wick design, the axial heat flux is ultimately limited only by vapour flow effects. One can distinguish several vapour flow regimes depending on the relative magnitude of the inertia and viscous forces in the vapour. When the inertia forces dominate ("inertia flow regime"), the vapour flow is limited by the well-known choking phenomenon. In choked flow the vapour leaves the evaporator with sonic speed. Therefore the related heat transfer limit is usually called the "sonic limit". In the regime of dominating viscous forces ("viscous flow regime") choking does not occur. The axial heat flux increases steadily with decreasing pressure at the evaporator exit and is finally limited by the fact that the vapour pressure can not be smaller than zero. We call this the "viscous limit" of heat transfer.

In previous analytical work only the sonic limit of heat transfer was considered; the analytical problem was simplified by neglecting the radial variation of the velocity, and the resulting one-dimensional flow problem was solved essentially by numerical analysis.

A theoretical study was therefore done, in which the ultimate limit of heat transfer was analysed taking into account both the axial and the radial variation of the vapour velocity; the resulting two-dimensional compressible flow problem was solved by an analytical approximation method, both for the sonic and the viscous limit of heat transfer [1]. The analysis showed that the radial variation of the axial velocity is decisive in the viscous flow regime, while in the inertia flow regime its influence is limited to a 5% decrease of the ultimate limit of heat transfer. For the average axial heat flux density at the sonic and the viscous limit of heat transfer ($\bar{q}_S$ and $\bar{q}_V$ respectively) the following relations were obtained:

$$\bar{q}_S = 0.474\, h_{fg}\, (\rho_o\, P_o)^{1/2} \tag{1}$$

$$\bar{q}_V = \frac{d^2\, h_{fg}}{64\, \eta\, l_{eff}}\, \rho_o\, P_o \tag{2}$$

(h_{fg} = specific heat of vaporization of the working fluid, ρ_o P_o = vapour density and pressure at the evaporator end of the heat pipe, d = diameter of the vapour channel, η = vapour viscosity, l_{eff} = effective heat pipe length).

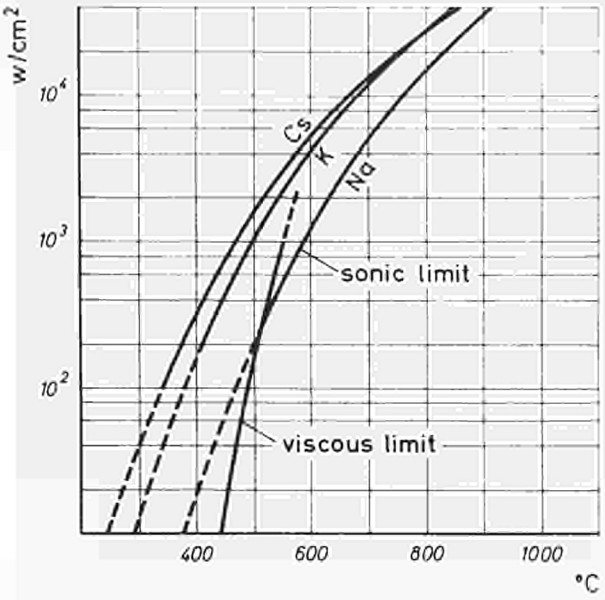

Fig. 1: Ultimate heat transfer limit of heat pipes (curves: theory; dots: experimental data of Kemme; Los Alamos).

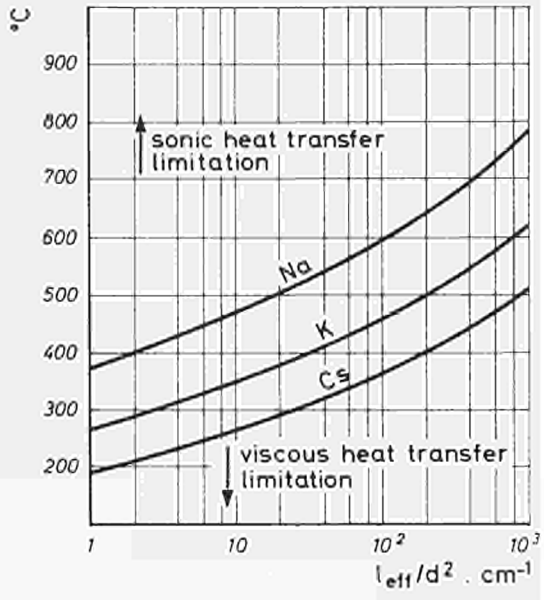

Fig. 2: Transition from viscous to sonic heat transfer limitation.

Fig. 1 shows the excellent agreement of these formulae with experimental data. An important conclusion from equations (1) and (2) is that for every heat pipe below a certain temperature T_{ot} (which depends on the working fluid utilized, the geometry of the heat pipe and the relative distribution of heat sources and sinks on the heat pipe wall) the ultimate heat transfer limit is of the viscous and not of the sonic type. This viscous limit can lie much below the sonic limit, a fact which needs attention in the analysis of heat pipe start-up. Fig. 2 shows a plot of the transition temperature T_{ot} versus l_{eff}/d^2 for some alkali metals.

Equation (1) predicts that for most working fluids the sonic heat transfer limit at a pressure $P_o = 10$ atm has a value of the order of 100 kw/cm². Practically, however, it has not yet been possible to reach heat fluxes of this order of magnitude. What happens is that latest at heat fluxes of the order of 10 kw/cm² the heat transfer breaks down because of insufficient return flow of condensate to the evaporator, in spite of the fact that the theoretical pumping power of the wick is not yet exceeded. The reasons for this lack of condensate back-flow are not yet well understood. Therefore an experimental study of the problem was started in the reference period (thesis work). A method of fabricating capillary structures with a very high pumping power was developed and a flow-type calorimeter for measurement of the heat transfer capacity of heat pipes at high axial heat fluxes was set up.

Studies of the gas plug effect

During the reference period the results of a study were published, which deals with temperature stabilization by gas-controlled heat pipes under strongly varying thermal loads (thesis work). In these papers [2)3)] the rules are summarized for the design of heat pipes with an inert gas plug for maximum temperature stabilization. It is shown that the temperature-load characteristics can be derived from a simple model. An important conclusion is that the temperature which is to be stabilized is essentially influenced by variations of the gas plug temperature. This influence increases with the partial pressure of the working fluid in the gas plug. It is therefore also necessary to stabilize the gas plug temperature. One solution of this problem is to cascade two gas-controlled heat pipes, the second heat pipe stabilizing the temperature of the gas plug in the first heat pipe. A radiator was designed with such an arrangement to keep a surface close to a temperature of 1000°K. With a 100% increase of the power to be dissipated, the increase of the surface temperature was about 2.5%.

Besides many applications which the gas plug effect may find in the field of measurement and control of temperatures or vapour pressures, a potential use is in the separation of gases. With a Mo/Li heat pipe and using H_2 as a buffer gas it was demonstrated that at temperatures above 1000°C H_2 is separated from Li (Fig.3). This effect may be of interest in fusion reactor technology for the recovery of tritium from Li.

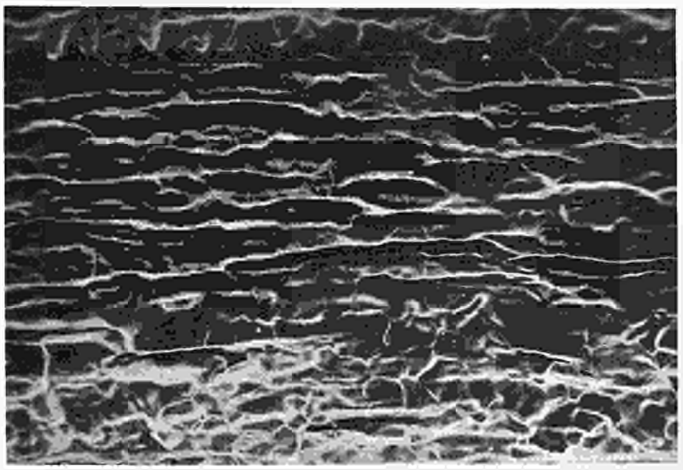

Fig. 5: W-26 Re/Li heat pipe after 721 hours of horizontal operation at 1800°C, average heating rate 120 w/cm². Oblique view into one of the grooves serving as liquid flow channels (x 135).

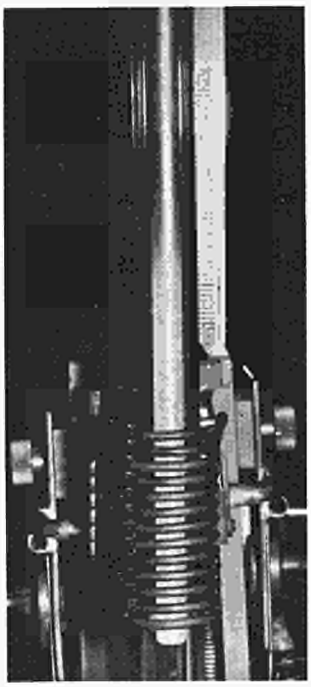

Fig. 3: Separation of hydrogen (cold region of the pipe) from lithium (hot region, 1500°C) in a molydenum heat pipe, operated under vacuum with RF-heating.

Corrosion studies

W-Re/Li systems

Corrosion studies with heat pipes were started in 1965 with the aim of finding materials for heat pipes capable of at least 10,000 hours of operation at 1600°C and having good mechanical properties and a high heat transfer capacity. This aim was reached for the first time during the reference period, after having tested many different material combinations including Nb, Ta, W and their alloys as wall materials and Bi, Pb, Ba, Tl and Li as working fluids [4)5)]. The heat pipe was made of W-26Re as wall material with Li as working fluid. It was tested in high vacuum in the horizontal position for 10,000 hours at 1600°C with a heating rate of 120 w/cm² (RF heating). Fig. 4 shows the heat pipe after the test. There is practically no corrosion. A very slight mass deposit was found in the heating zone. It contained about 50 wt% Re and indicated preferential dissolution of Re in the cooling zone. However, no Re concentration gradients were observed in the wall of the cooling zone. This may be due to the presence of the intermetallic σ-phase (containing about 50% wt of Re) which was found in the wall material and which acts as a Re source when Re is removed from the wall material by diffusion.

In order to establish the temperature limitations of the W–26Re/Li system two heat pipes (identical to the 1600°C test) were built and life-tested at 1700°C and 1800°C with heating rates of 120 w/cm². The 1700°C heat pipe has reached, at the end of the reference period, a total operation time of 5183 hours and shows no signs of deterioration. The 1800°C test was terminated at 721 hours, when a leak occurred in the cooling zone. First inspection after cutting open the heat pipe showed an unusual corrosion pattern consisting of axially running narrow slits all over the surface of the liquid flow channels (Fig. 5). One of the slits was so deep that it penetrated through the heat pipe wall.

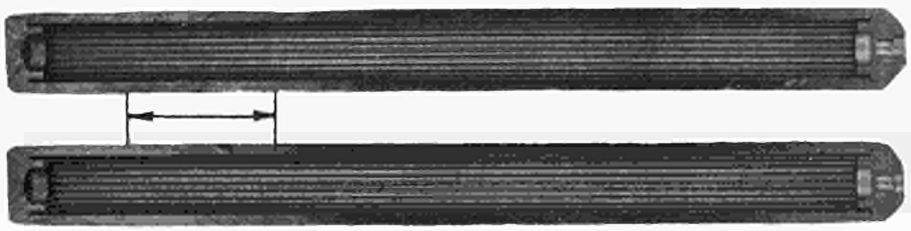

Fig. 4: W-26 Re/Li heat pipe (116 mm long) after 10,000 hours of horizontal operation at 1600°C, average heating rate 120 w/cm². The flash indicates the heating zone. Vertical cut, Li removed.

In order to reduce the fabrication costs of W-Re heat pipes an installation was set up for making grooved tubes by chemical vapour deposition. The apparatus was tested first with pure W, using as reaction the reduction of WF_6 by H_2. The deposits were made in a quartz chamber on a rotating horizontal madrel heated by RF. A uniform thickness of the deposit was obtained by use of multiple gas inlets and outlets. A study of the parameters which influence the W-deposition gave the following results:

- mandrel temperature: deposits can be achieved in the temperature range of 500°C to 900°C. The higher the temperature the more complete is the reaction;
- pressure: the best results were obtained at a total gas pressure of 4–6 mm Hg. Raising the pressure increases the grain size and therewith the brittleness of the deposit; reducing the pressure leads to a more complete reaction but also to a smaller deposition rate;
- ratio H_2/WF_6: a complete reaction is obtained if there is a large H_2 excess, in practice 10 parts of H_2 for one part of WF_6;
- mandrel material: both Mo and Fe gave satisfactory results. There is a slight interaction between Fe and W, and no apparent interaction between Mo and W;
- ratio between diameters of chamber and mandrel: the bigger the chamber, the more uniform is the deposit.

Fig. 6 is a section through the wall of a W tube of 1.7 mm wall thickness deposited on a grooved Fe mandrel with a deposition rate of 0.09 mm/h and a mandrel temperature of about 800°C. In order to obtain complete filling of the grooves of the mandrel with W, as shown in this figure, it is necessary to avoid over-low mandrel temperatures and, in consequence, over-low deposition rates.

Fig. 6: Deposit of CVD-W on a grooved Fe mandrel (deposit thickness 1.7 mm).

First deposits of W-5Re were made, using the reduction of WF_6-ReF_6-mixtures with H_2. The alloys had the desired composition but proved to be very brittle. It is suspected that this is due to impurities in the ReF_6.

a) Section through the wall perforation in the evaporator zone.

b) Section in 14 mm distance from the wall perforation (transition evaporator - condensor).

c) Section in 24 mm distance from the wall perforation (condensor section).

Fig. 7: Grain growth in a SGS-Ta/Li heat pipe after 890 hours of operation at 1600°C.

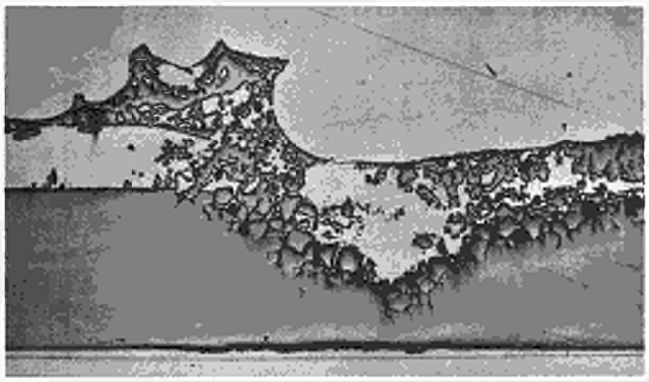

Fig. 8: Longitudinal section through the wall perforation of a SGS-Ta/Li heat pipe (221 hours of operation at 1600°C).

Fig. 9: Detail of Fig. 8 showing the intergranular Ta-Li-Y-O corrosion phase and Ta-O platelets in the grains.

Ta/Li system

Heat pipes are much less expensive than boiling loops; they can be built and operated under close control of impurities. Compared to classical pool-boiling refluxing capsules, heat pipes have the advantage of being more sensitive to impurities and permitting a better interpretation of the results, since they can be operated without fluctuations at practically isothermal conditions and with laminar liquid flow. The heat pipe therefore is an interesting device for basic studies on the corrosion by boiling liquids [6].

In the reference period the heat pipe was used to study the mechanism of the corrosion of Ta by boiling Li at 1600°C. For this purpose two heat pipes were built from SGS-Ta (a Ta which contains only about 10 ppm wt of O and which is grain-stabilized by traces of Y) and filled with Li under very clean conditions. The heat pipes were operated with RF heating in ultra-high vacuum in order to eliminate the possibility of impurity pick-up from the outside. Both heat pipes failed after several hundred hours of operation by wall perforation in the evaporator section. The heat pipes were analysed with an ion-analyser developed by Slodzian and Castaing and built by CAMECA. The following conclusions were drawn [7].

SGS-Ta recrystallizes at 1600°C completely in less than 15 minutes. There is precipitation of Y_2O_3 and marked coalescence after 15 hours. O and Y diffuse out of the inner surface of the wall into the Li condensate. As a result an Y_2O_3- depleted zone is created on the inside of the heat pipe wall, which increases rapidly in thickness going from the evaporator to the condenser section. The Y_2O_3 depletion causes strong grain growth in this zone (Figs. 7a, b, c). O and Y are carried with the backflow of the condensate to the evaporator and locally enriched by the evaporation process. The enrichment causes the wall perforation (Fig. 8) owing to dissolution of Ta in a Ta-Li-Y-O "corrosion phase", which is liquid at the operating temperature of 1600°C and which is found between the grains (Fig. 9) and as deposit on the outside of the heat pipe near the wall perforation. Platelets of a pure Ta-O-phase (presumably Ta_2O_5) inside the grains in direct contact with the corrosion phase (Fig. 9) indicate that in the zone of wall perforation no Li-phase can have existed any more.

References

1) C.A. Busse, Theory of the ultimate heat transfer limit of cylindrical heat pipes, will appear in the *Int. Journal of Heat and Mass Transfer.*

2) R. Schlitt, Temperaturstabilisierung durch Wärmerohre, *Forsch. Ing.-Wes.* 37(1971) 91.

3) R. Schlitt, Temperaturstabilisierung mit Wärmerohren bei wechselnden Wärmeströmen, EUR 4634d (1971).

4) C.A. Busse, F. Geiger and D. Quataert, Status of emitter heat pipe development at Ispra, *IEEE Conference Record of 1970 Thermionic Conversion Specialist Conference,* October 26–29, 11970, pp. 550–555.

5) C.A. Busse, Heat pipes for thermionic space power supplies, presented at the *Third International Conference of Space Technology,* Rome, May 3-8, 1971.

6) C.A. Busse, Werkstoffprobleme bei Hochtemperatur-Wärmerohren, Forsch. Ing.-Wes. 37 (1971) 48.

7) D. Quataert, Investigation of the corrosion mechanism in tantalum-lithium high temperature heat pipes by ion analysis, *Forsch. Ing.-Wes.* 37 (1971) 37.

CERAMIC IMPREGNATED GRAPHITE

F. Van Rutten

Introduction

The object of this study was to develop a composite material, impregnating graphite with a glass or a ceramic, to be used as a canning material.

The principal aim was to obtain a material impervious to fission products, with a good stability under radiation, easily brazed and having acceptable mechanical properties.

Preparation of this material, and in particular how to obtain impervious material, is the main subject of this report. The brazing question has been practically resolved by using an ZrBe alloy as a brazing material. An irradiation test is going on in the HFR reactor to study the irradiation effect.

Mechanical properties are to be studied.

The study will be concluded by a careful economic study in connection with an appropriate design of a fuel element.

Glasses and ceramics preparation

The main glasses and ceramics which have been prepared up to now are listed in table I. The preparation involves oxide powder mixture and heating up to 1600°C in a furnace under an argon atmosphere.

In this work reference will be made to the different glasses and ceramics by their number only.

Table I

Ph. state	No.	P.F.	Density	σ macr.	Composition %				
					SiO_2	MgO	CaO	Al_2O_3	ZrO_2
Crystall	6	1391	3,195	0,00672	55,56	18,62	25,82	–	–
Glassy	32	1460	2,70	0,00460	51,35	13,79	–	34,86	–
Glassy	44	1300	2,834	0,00567	54,51	17,41	19,36	8,72	–
Glassy	45	1320	2,740	0,00518	53,30	16,08	12,82	17,30	–
Glassy	46	1420	2,722	0,0049	52,40	15,00	6,45	26,15	–
Glassy	63	1420	2,73	0,00474	50,63	13,65	5,87	23,87	6,00
Crystall	65	1345	2,981	0,00981	–	6,7	41,5	51,8	–
Glassy	68	1440	2,600	0,00609	49,91	5,59	21,85	25,65	–
Glassy	69	1420	2,744	0,00486	51,53	14,33	6,16	24,98	3,00
Glassy	70	1460	2,5739	0,00426	53	15,34	–	31,66	–
Glass	72	1470	2,634	0,00443	48,44	17,12	–	34,44	–
Glass	&3	1350	2,546	0,00431	50,77	14,72	5,89	21,62	6,00

Impregnation

The impregnation is done by placing the sample and the impregnating materials (broken in small pieces) in a cylindrical crucible closed by a piston rod. The crucible is heated in a vacuum furnace. Around 1500°C the piston is pushed by means of a hydraulic system up to the chosen pressure: generally at 30 kg/cm^2 all the intergranular porosities are filled and operation is stopped. The samples subjected to impregnation were made of 3780 grade graphite produced by Carbone Lorraine. The imperviousness was tested using a helium leak detector. The graphite impregnated with materials 32, 46, 63, 69 is generally impervious; the impregnated porosity is between 65 and 81% of the open porosity. Other materials such as No. 6 give a very poor impregnation, while No. 44 gives no impregnation at all.

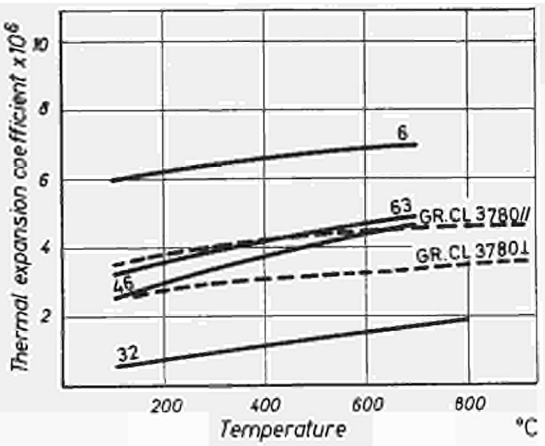

Fig. 1

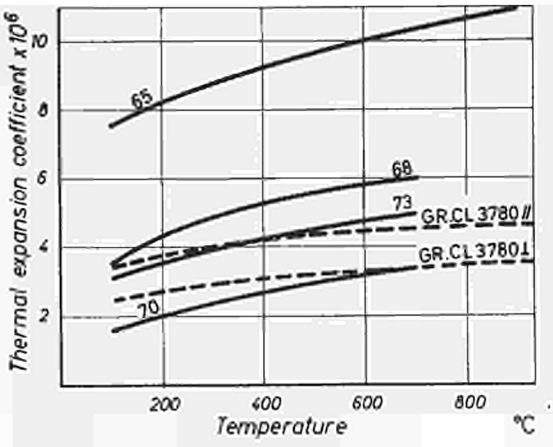

Fig. 2

Nrs. 65 and 68 give good impregnation results with an impregnated porosity of between 80 and 90%, but the resultant material is not impervious.

If we take into consideration the thermal expansion coefficient of the impregnating materials (Fig. 1, 2) it is clear that in order to obtain an impervious material the t.e.c. must be equal to or lower than that of the graphite.

At 1500°C under vacuum (10^{-1} torr) the silica of the silicates began to react with the graphite, giving carbon monoxide, silicon carbide and also metallic silicon which sublimates and which is found afterwards in the coldest part of the furnace. As the SiC has a surface tension higher than that of graphite its formation on the pore walls must facilitate the wetting by the impregnating material. This wetting is essential to the imperviousness; as a matter of fact impregnations performed under a pressure of 150 torrargon in order to decrease the kinetics of the silica-graphite reaction are unable to produce impervious materials.

A pretreatment of graphite in order to cover the pore walls with SiC was developed, starting from an aqueous solution of sodium silicate. The impregnations performed after this pretreatment give rise to more constant values of impregnated porosity, which is always higher than 81%.

Even starting materials having a t.e.c. higher than that of graphite, such as Nos. 65 and 68, give an impervious product after the pretreatment.

Materials 70 and 73, used only after pretreatment, also give an impervious material, while 71 and 72 do not.

Thermal annealing and cycling

In order to examine the stability at high temperature, samples were annealed under argon at temperatures from 875 to 1100°C. After annealing no changes of weight or dimensions were detected; but many samples showed a loss of imperviousness (Table II).

Table II

Impregnating material No	Annealing time	Temperature	Leak test
32	168 h	875°C	impervious
	150 h	1000°C	leak 10^{-4} torr l/s
46	168 h	875°C	impervious
	150 h	1000°C	leak 10^{-4} torr l/s
65	820 h	1000°C	impervious
	160 h	1000°C	impervious
	820 h	1000°C	impervious
69	150 h	1000°C	impervious
	160 h	1100°C	impervious
	820 h	1000°C	leak $2\ 10^{-6}$ torr l/s
73	340 h	1000°C	impervious
	200 h	1100°C	impervious

Table III

Impregnating material No	No of cycles	Temperature	Leak test
46	50 50	750°C 800°C	Impervious Leak = 10^{-6} torr l/s
63	50 50	800°C 900°C	Impervious Leak = 4,4 10^{-7} torr l/s
65	50	1000°C	Impervious
73	50 20	1000°C 1100°C	Impervious Leak = 10^{-6} torr l/s

Only graphite impregnated with material 65 stays impervious after 800 h at 1000°C. Long-term tests of No. 73 are under way.

Thermal cycling is conducted between 20 and 1000°C. In this case the cycle is completed in 40 minutes. The sample is heated to between 20 and 500°C in a minute is then stabilized at the temperature of 1000°C in 15 minutes. The cooling from 1000 to 500°C takes 15 sec. but ambient temperature is only reached after 15 minutes.

Weight and dimensional variations are not significant. As seen for annealing, most of the materials are no longer impervious (Table III).

Irradiation effects

Eight samples of glass-impregnated graphite have been irradiated in the DIRCE loop in the ISPRA-I reactor. They were exposed to a thermal flux of 5.6 10^{20} n/cm^2 and to a fast flux of 2.8 10^{19} n/cm^2 (nickel dose) at 300°C. The dimensional variations were lower than 2% which was the sensitivity of the measure. No distortion or chipping was detected.

A rig to be irradiated at higher flux at the HFR reactor (Petten Centrum, the Netherlands) has been prepared, and the irradiation will be performed in 1972.

Table IV – Impregnated graphite corrosion in water at 350°C after 720 h.

Material number	Leak test (*)	$\frac{\Delta l}{l}$	$\frac{\Delta \phi}{\phi}$	$\frac{\Delta P}{S}$	$\frac{\Delta P}{St}$
		%	%	(mg/cm^2)	μg/cm^2 h
32	I	1.30	1.01	10.59	14.71
65	L	1.12	0.87	8.80	12.22
46	I	1.39	1.05	13.87	19.27
69	I	0.59	0.48	8.20	11.39
63	I	0.62	0.58	8.38	11.64
70	I	1.29	0.87	9.29	13.90
72	L	1.02	0.71	5.97	8.29
72/a	I	− 2.88	0.79	−6.08	− 8.44
73	I	0.49	0.50	7.29	10.13

* I = Impervious L = Leakage after corrosion

Results are the mean of the results obtained on two samples, except materials 69, 63, 72 and 72/a where only one sample was used.

Table V – Impregnated graphite in superheated steam at 600°C, 50 kg/cm².

Material No	Impregnated porosity	Exposure time h	Leak test	$\frac{\Delta l}{l}$ %	$\Delta\phi/\phi$ %	$\Delta P/s$ mg/cm²
65 C/L	79.25	761	I	0.54	0.50	9.13
		1469	L	1.35	0.94	14.77
		2230	L	1.49	1.23	14.22
63 G/L	82.7	761	I	0.00	0.00	1.50
		1469	I	0.12	0.07	1.55
		2230	I	0.21	0.07	1.48
46 G/L	80.8	761	I	0.26	0.14	2.02
		1469	I	0.26	0.14	1.84
		2230	I	0.32	0.14	1.54
32 G/I	80.4	720	L	0.01	0.025	0.56
		1564	L	0.05	0.015	0.73
6 C/L	63.4	761	L	0.00	0.15	4.74
		1469	L	0.03	0.14	3.38
46 G P/L	82.7	708	I	0.15	0.15	1.18
		1416	I	0.30	0.27	1.34
		2136	I	0.33	0.22	0.22
69 G P/L	82.1	708	I	–	0.07	0.27
		1416	I	0.07	0.14	0.96
		2136	I	0.07	0.07	0.20

Notation: C = Ceramic; G = Glass; P = Pretreated; L = Leakage after corrosion; I = Impervious.
For each condition only one sample was tested.

Water and superheated corrosion

The samples are exposed to deareated water at 350°C or to superheated steam at 600°C in autoclaves. Dimensional variations, weight variation and possible leaks are measured after each exposure. The water extracted from autoclaves is analysed after each test. Table IV and V give a summary of the results obtained.

Water is a corrosive agent stronger than steam, so that the amount of silica found in the water is higher when the tests are conducted under water.

Weight increase is due mainly to hydration of the silicates used. Tests for longer periods, restricted to the more promising materials, are necessary to evaluate the long-term corrosion rate.

Conclusions

Two parameters are important to obtain a good and reproducible impregnation producing an impervious material: thermal expansion coefficient and wetting. Of these two the last one is the more important. Material 65, even if it has an high t.e.c. (see Fig. 2), allows the production of an impervious material when the graphite is pretreated.

Materials impregnated with 65 and 73 are the only ones giving a material stable at 1000°C. Devitrification and phase transitions are the reason for the leaks encountered in the other materials. During corrosion by water and steam ZrO_2-containing ceramics are the most promising impregnating materials.

CHEMISTRY

FUEL
ELEMENT
REPROCESSING

POST
IRRADIATION
ANALYSIS

WATER
CHEMISTRY

RADIOCHEMICAL
ANALYSIS

NEW
ANALYTICAL
DEVELOPMENTS

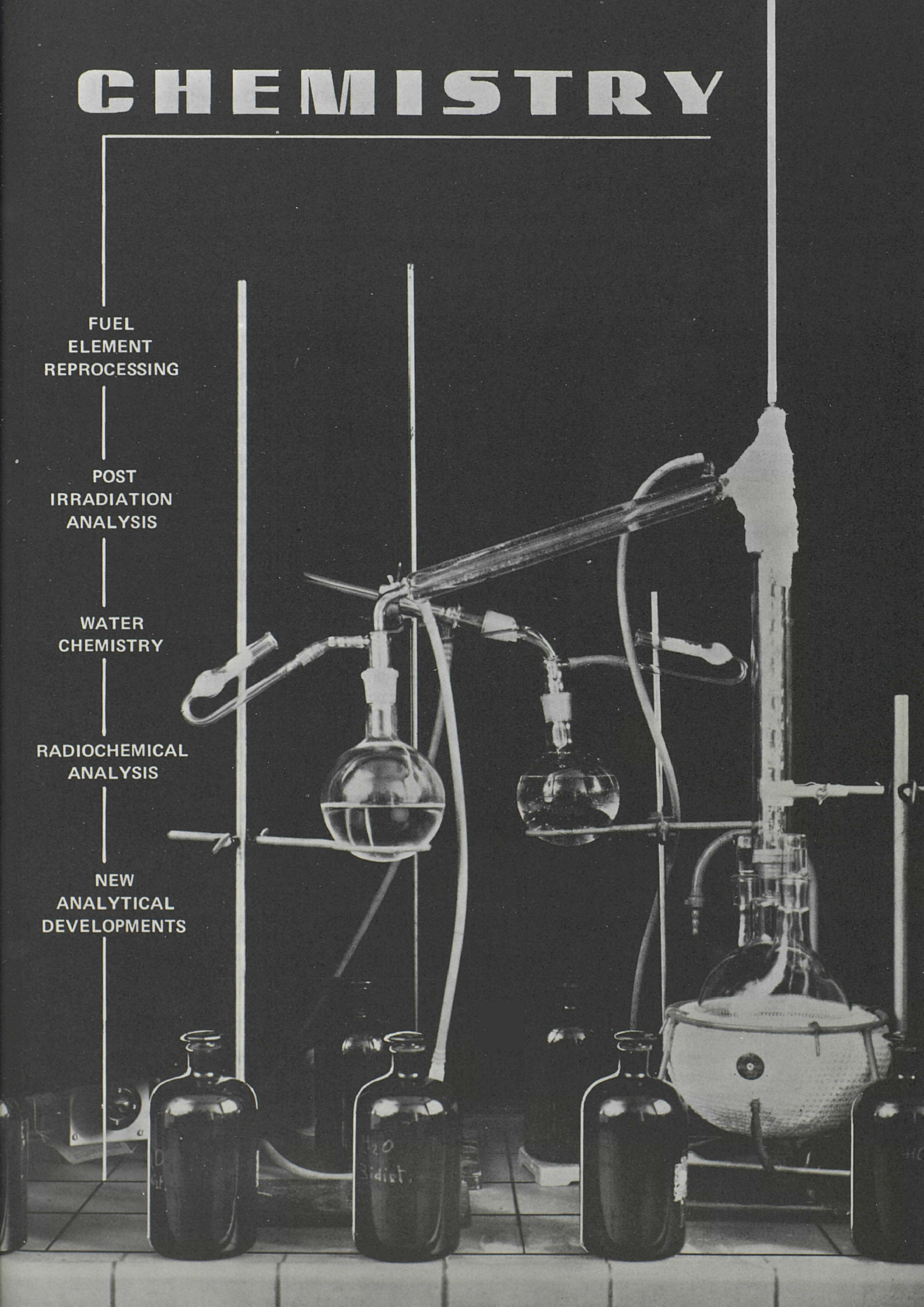

CHEMISTRY DIVISION

H. Hannaert

The Chemistry division consists of one administrative, one technical and ten scientific units.

The first unit, which forms the infrastructure of the division, deals with the management of the budget, the acquisition of scientific material and the inventory of instruments.

The task of the second unit is to give technical assistance to the different scientific units. This help comprises glass-blowing, the work of the mechanical and plastic workshop, and electronic assistance.

The scientific units are distinguished by their special subjects as well as by their instruments and the techniques used.

The Organic Analysis Unit

The Organic Analysis Unit is in possession of very good instruments and uses such techniques as liquid chromatography, gas chromatography and thin layer chromatography. It also employes optical techniques such as infrared, ultraviolet and Raman spectroscopy. Lastly, there are two mass spectrometers, one of which is of high resolution. In addition to this there is also a very well equipped organic synthesis laboratory.

The Inorganic Mass Spectrometry Unit

This unit is highly specialised and has available very sensitive instruments, which are mainly used for the determination of isotopic fractions and for fuel-element burnup measurements. These instruments are equipped with small computers by means of which the percentage composition of the analysed samples can be determined.

The X-Ray Unit

This unit has instruments for X-ray fluorescence and X-ray diffraction, as well as an instruments able to determine the smallest quantities of gas dissolved in metals. The principal advantage of X-ray fluorescence is the possibility of analysing all the elements with an atomic number higher than 12 without destroying the sample, whereas X-ray diffraction is essentially used for the identification of the crystalline phases.

The Applied Chemistry Unit

This unit primarily works in the field of kinetic measurements and interpretation of reaction mechanisms by determination of the necessary thermodynamic quantities. This unit is also in charge of the maintenance and operation of a 2 MeV Van de Graaff accelerator. In addition to this its personnel participates in the preparation of the irradiation experiments for the other scientific divisions.

The Wet Chemistry Unit

It has the task of carrying out delicate analyses for which physical techniques are not yet in existance or recognized, or for which no standards are available. In these laboratories the ppm level of water, boron, chlorine and sulphur and total ash content of a sample are determined. Electrochemical techniques are likewise used and more particularly potentiometry, polarography, colori- metry, and spectrophotometry. The more classical methods like gravimetry and titrimetry are in everyday use.

The Gamma Spectrometry Unit

It is equipped to perform radiochemical precision measurements. It has radiochemical devices (e.g. hot cells and glove boxes) for the treatment of irradiated fuel elements.

The samples, appropriately prepared are analysed by means of a gamma spectrometer with a Ge(Li) semiconductor or a NaI(Tl)scintillator. These instruments are connected on one side with an analyser and on the other side with a computer. This unit has also devised and developed new techniques along with the corresponding instrumentation.

The Applied Nuclear Chemistry Unit

This unit is in charge of all the activation analyses and radiochemical separations which are demanded. Their work includes the production and the utilisation of radiotracers; for this they can use a fully automatic installation which finally supplies the percentage composition of the samples. The laboratory is connected with the computing Centre (CETIS) by a teleprocessing system and with the reactor by a multiple pneumatic tube system. A neutron generator of 14 MeV is used for activation analyses, where fast neutrons are required. This unit likewise has a counting room, where gamma spectrometers, 4000-channel analysers and a 8 K computer are available.

The Optical Spectroscopy Unit

It is equipped with numerous high-precision spectrometers and uses the techniques of atomic absorption, emission spectroscopy and atomic fluorescence. These techniques enable the unit to carry out complete analysis of very complex and varied samples.

The High-Temperature Chemistry Unit

This unit is particularly well equipped for carrying out pyrochemical studies on fuel elements, metallic deposition by means of high-frequency plasma, and the preparation of single crystals. It also has a team of scientists capable of determining the thermodynamic quantities and the phase diagrams of ceramics, using a quadruple mass spectrometer.

The Decontamination Unit

This unit is in charge of the chemical treatment of the Centre's radioactive effluents and solid waste. A purification plant is available to process the contamined water. The controlled use of polyelectrolytes has contributed to a very noticeable improvement of the treatment.

The remaining concentrated sludge as well as the solid waste is packed in barrels under bitumens. The high-activity waste is wrapped in concrete. A combustion installation allows the destruction of organic waste (polyphenyls and all the other contaminated organic products).

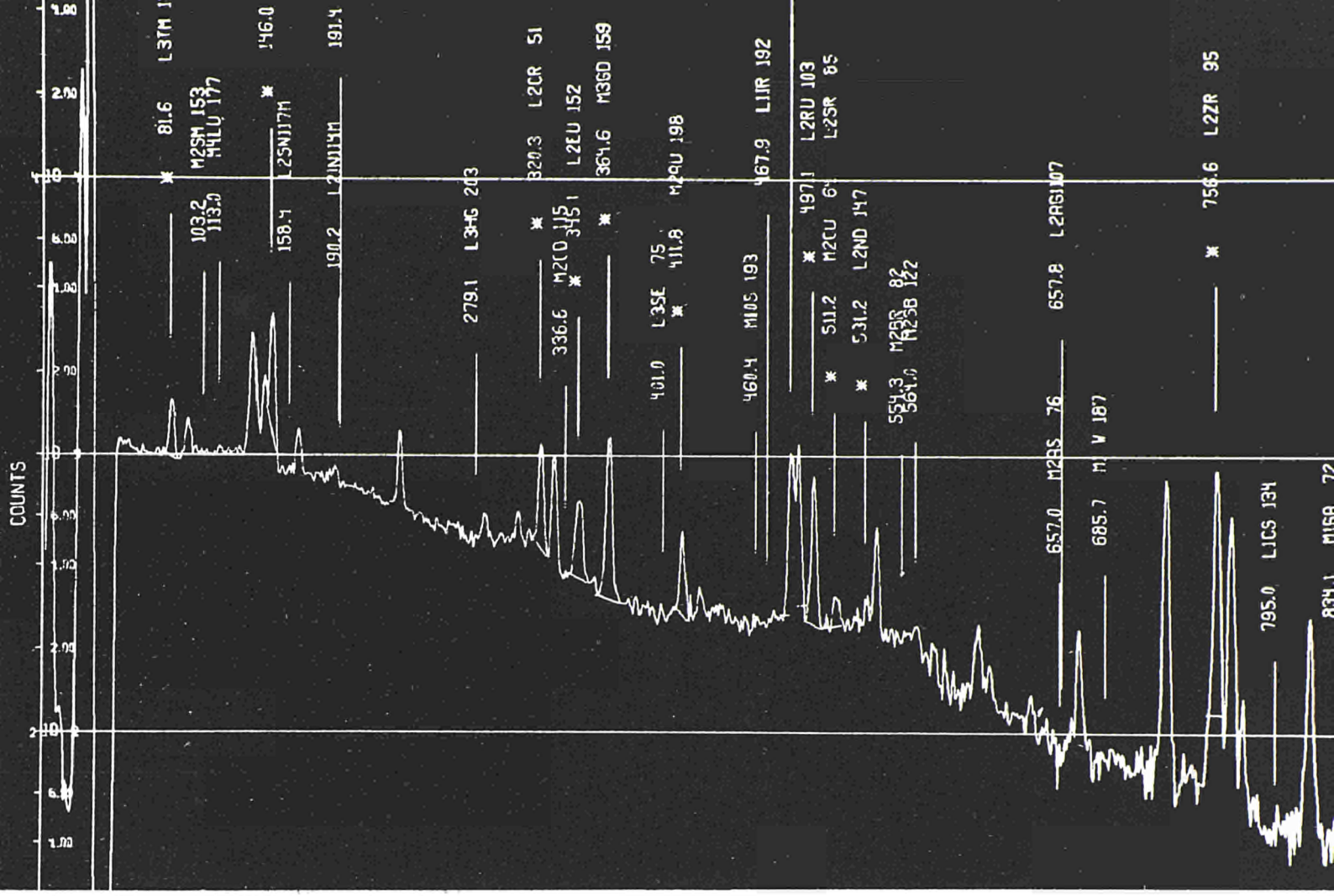

Fig. 1

RADIOCHEMICAL ANALYSIS CONTROLLED BY COMPUTERS

F. Girardi, G. Guzzi, G. Bertozzi

Introduction

In recent years, the possibilities of automated chemical analysis carried out with the aid of electronic computers have greatly increased. Three different working schemes are now technically feasible for various analytical methods, including radiochemical ones:

1. Automated acquisition of the raw analytical data on punched or magnetic tapes and "batchwise" treatment of the data.
2. On-line connection of the analytical equipment to a large centralized computer by means of a teleprocessing system, possibly time-shared among different users.
3. Use of a small computer located in the analytical laboratory and directly interfaced to the analytical equipment, for immediate calculation of data while they are being obtained.

Since these systems have become available at Ispra for radio-chemical applications including gamma ray spectroscopy and activation analysis, a special effort is being made to provide efficient and reliable software packages for the users of the three systems, and also to evaluate their relative performances.

A short outline of the three systems, showing their present state of development is given here.

Scheme 1: Batchwise use of a large computer

The raw analytical data from the gamma spectrometers are collected on punched tapes. Automatic sample changers allow the acquisition of data from various samples overnight. The tapes are then processed at the Scientific Information Processing Centre by the IBM 360/65.

The programs which were previously used were reorganized and completed in 1971 in order to meet the requirements of different users. The scheme of the main program is the following. A check specimen is run as the first spectrum. In our activation analysis application this specimen is a metallic alloy wire used as a flux monitor during irradiation. Gamma spectrometry of this wire allows the energy calibration of the spectrometer, the determination of the neutron flux and a rough check on the correctness of the irradiation, decay and counting times manually assigned by the operator. Then the unknown spectra are analysed, following the instruction of special "oriented" libraries which are prepared by the analyst for each particular problem. These libraries make it possible to obtain the final results in parts per million for the various elements, and the detection limits for undetected elements. Table 1 shows an example of results obtained by non-destructive analysis of high-purity silicon.The results were obtained by counting the sample at three different decay times after a seven-day activation in the Ispra 1 reactor. A computer program was also prepared to obtain an analog output (CALCOMP drawing) which shows the way in which the raw data have been processed (peaks found, energy assigned, interpolation of data for background subtraction etc.) Fig. 1 shows a portion of a typical "processed" spectrum. These analog outputs were found to be of great help in practical application, because they show at first glance if the spectrum has been correctly analysed.

Table 1 – Final results of non-destructive activation analysis of high-purity silicon carried out with computerized gamma ray spectrometry.

Element	At/cc	ppm
Ag	$< 2.2 \times 10^{12}$	$< 1.64 \times 10^{-4}$
As	$< 3.9 \times 10^{13}$	$< 2 \times 10^{-3}$
Au	2.32×10^{11}	3.2×10^{-5}
Br	$< 4 \times 10^{12}$	$< 2.2 \times 10^{-4}$
Cd	$< 1.2 \times 10^{13}$	$< 9.5 \times 10^{-4}$
Ce	1.35×10^{12}	1.3×10^{-3}
Co	2.10×10^{14}	8.5×10^{-2}
Cr	1.99×10^{11}	6.8×10^{-5}
Cs	$< 5.90 \times 10^{10}$	$< 5.40 \times 10^{-7}$
Eu	$< 7.40 \times 10^{15}$	$< 7.60 \times 10^{-3}$
Fe	1.84×10^{14}	7.05×10^{-4}
Ga	$< 1.60 \times 10^{15}$	$< 7.7 \times 10^{-4}$
Gd	$< 1.50 \times 10^{12}$	$< 1.65 \times 10^{-2}$
Hf	$< 2.20 \times 10^{11}$	$< 2.74 \times 10^{-7}$
Hg	$< 8.30 \times 10^{13}$	$< 1.15 \times 10^{-5}$
Ho	$< 3.20 \times 10^{12}$	$< 3.60 \times 10^{-2}$
In	$< 1.45 \times 10^{9}$	$< 1.15 \times 10^{-1}$
Ir	$< 9.80 \times 10^{12}$	$< 9.60 \times 10^{-6}$
La	$< 6.90 \times 10^{10}$	$< 6.60 \times 10^{-3}$
Lu	$< 6.00 \times 10^{10}$	$< 7.00 \times 10^{-4}$

Element	At/cc	ppm
Mo	8×10^{13}	5.2×10^{-4}
Nd	$< 2.10 \times 10^{12}$	$< 2.10 \times 10^{-2}$
Os	$< 3.90 \times 10^{15}$	$< 5.20 \times 10^{-1}$
Pt	–	–
Rb	$< 4.30 \times 10^{12}$	$< 2.50 \times 10^{-5}$
Ru	1.77×10^{10}	1.23×10^{-3}
Sb	$< 5.80 \times 10^{13}$	$< 4.86 \times 10^{-7}$
Sc	$< 1.07 \times 10^{12}$	$< 3.3 \times 10^{-6}$
Se	$< 5.90 \times 10^{14}$	$< 3.20 \times 10^{-5}$
Sm	$< 6.60 \times 10^{15}$	$< 6.60 \times 10^{-8}$
Sn	$< 3.90 \times 10^{12}$	$< 3.20 \times 10^{-2}$
Sr	$< 6.90 \times 10^{11}$	$< 4.10 \times 10^{-3}$
Ta	$< 2.60 \times 10^{10}$	$< 3.20 \times 10^{-2}$
Tb	$< 3.10 \times 10^{14}$	$< 3.30 \times 10^{-5}$
Te	6.3×10^{12}	5.52×10^{-4}
Tm	$< 1.60 \times 10^{15}$	$< 1.80 \times 10^{-4}$
W	$< 4.60 \times 10^{12}$	$< 5.80 \times 10^{-4}$
Zn	$< 7.60 \times 10^{15}$	$< 3.40 \times 10^{-2}$
Zr	5.07×10^{13}	3.1×10^{-1}

Scheme 2: Time-shared teleprocessing system connected with a large computer

The working scheme of our system is shown in Fig. 5. Six spectrometric installations placed in five different buildings are connected with a central station which is in turn connected to an IBM 1070 Terminal. Details on the hardware of the teleprocessing system are given in the Electronics section. Computer programs for this system which are now in preparation will allow the transfer to the IBM 360/65 at a rate of 130 characters per second of the analytical data from the gamma spectrometers, which are sequentially scanned at every 30th second. Auxiliary data and instructions for data elaboration are sent by the operators of the different spectrometric stations by means of teletypewriters (IBM 2741) directly connected to the IBM 360/65 via telephone cable. The final results are also directly sent to the IBM 2741. The instruction message of the operator is stored after analysing the spectrum, and all successive spectra are processed according to the same instructions, unless a change is made by the operator. The stations can therefore operate unattended for routine work on batches of samples.

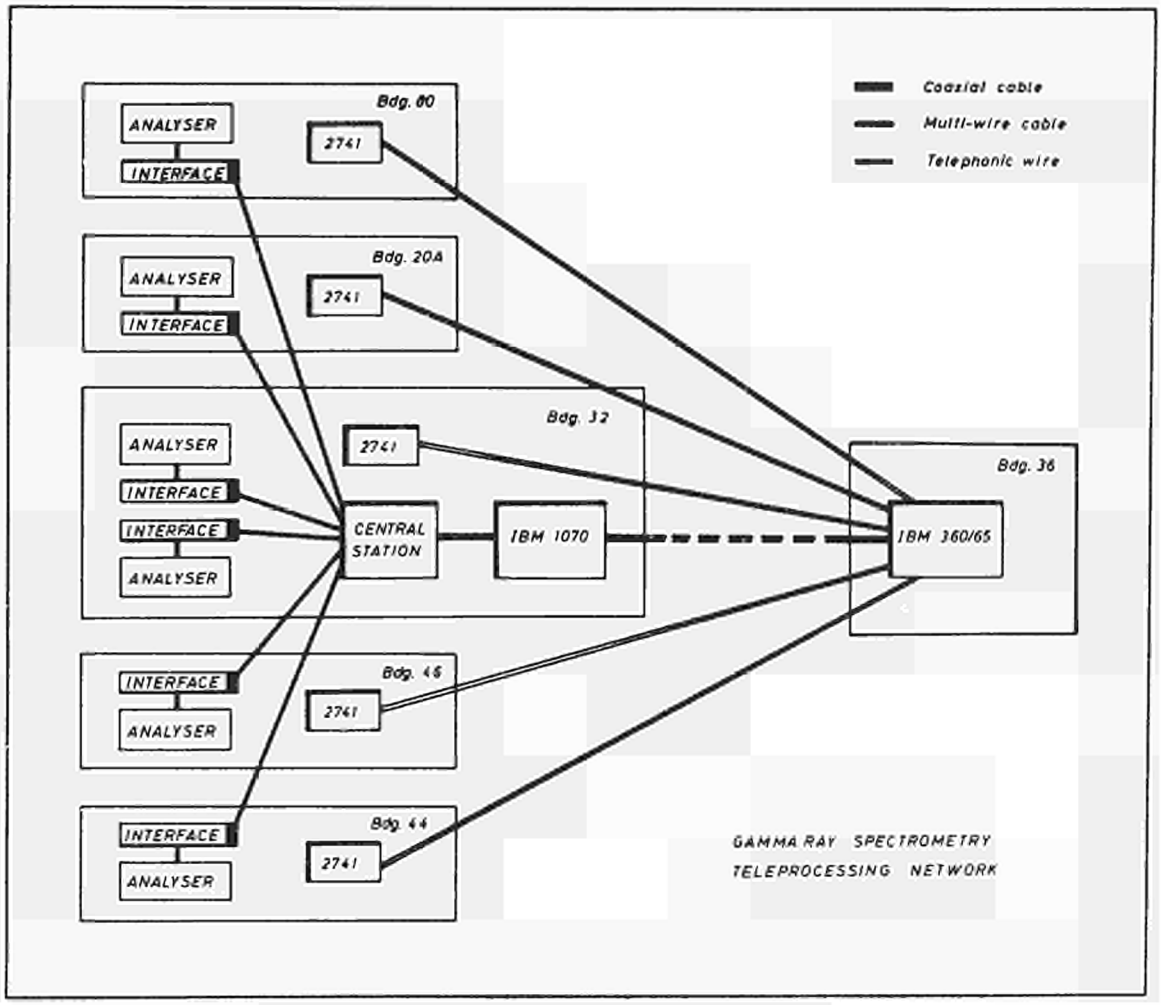

Fig. 2: Gamma ray spectrometry teleprocessing network.

By keeping the fast input messages and the slow return messages on separate lines (13 characters/second), the system should work with the necessary efficiency, in spite of the great number of users connected on to a single input dataway. The software package for gamma spectrometric analysis uses the same basic routines which were developed for system 1. The routines are organized in a modular scheme, which simplifies the addition of new routines whenever they become available.

Scheme 3: Use of a small computer for data acquisition and processing

The use of a small computer (LABEN 70) for both data acquisition and processing is being studied.

Our central processor is equipped with an 8 K memory (words of 16 bits). By using as peripherals an analog-to-digital converter, a display unit and a teletypewriter, the computer can be used as a multi-channel analyser. The memory capacity is large enough to allow the acquisition of spectra containing up to 4096 channels. Storage of the spectrometric data is obtained through a tape puncher.

At present, the operator must provide the computer with the necessary instructions for the acquisition and storage of each successive gamma spectrum. The punched tape can afterwards be processed on the same computer, after the change of the operating programs, which can be done in a couple of minutes. Since the computer can also be used for equipment control, it is possible to operate it as a fully automatic gamma-ray spectrometer, and work is under way to provide the necessary hardware and software.

By limiting the acquisition of each spectrum to a maximum of 2048 channels, sufficient memory space should be left to allow the immediate analysis of the spectrometric data, when results are needed with a minimum of delay after acquisition. The software used to process the gamma spectrometric data utilizes the same basic routines which were developed for system 1, and which have been translated into the Laben assembler language.

POST-IRRADIATION ANALYSES OF THE FUEL ELEMENTS OF THE TRINO VERCELLESE REACTOR

A.M. Bresesti, M. Bresesti, S. Facchetti, M. Mannone,
P. Barbero, C. Cerutti, J. Evans, F. Marell, A. Peil, R. Pietra (Chemistry Div.)
R. Klersy, A. Schürenkämper, A. Frigo, E. Ghezzi,
J. Meerschman, A. Pollicini (Materials Div.)

Introduction

Under the joint EURATOM-ENEL research contract No. 071-66-6 TEEI, the aim of which was the collection of technical information on the behaviour of a large PWR reactor, post-irradiation analyses were performed at the Ispra Joint Research Centre on fuel samples from the Trino Vercellese power plant.

The objective of the post-irradiation analyses was the provision of experimental data on burnup and isotopic compositions of uranium and plutonium in order to perform a comparison with theoretical predictions.

The theoretical analysis was performed by FIAT NUCLEARE under the joint EURATOM-FIAT research contract No. 098-66-6 TEEI.

Some fuel samples were also analysed at the Transuranium Institute, Karlsruhe, in order to provide a check on the experimental results obtained at Ispra.

In the present paper the experimental techniques are briefly described and only the most important results are given. Complete information on the experimental and theoretical work can be found in [1) 2)].

Characteristics of the Fuel Samples

The Trino Vercellese nuclear power plant, operated by ENEL, is equipped with a pressurized water reactor. The reactor fuel is uranium oxide with stainless steel cladding.

At the end of the first operating cycle (core average burnup: 11,590 MWd/t(U), three fuel assemblies were selected, one from each of the three different core enrichment regions, for post-irradiation analyses.

The fuel assemblies were transported to Ispra and dismantled in the pool of the ESSOR reactor. Eight rods were removed and subjected to gross gamma scanning and gamma spectrometry measurements. At selected positions the fuel rods were cut and 10 mm thick samples were prepared for destructive analyses.

Fuel samples subjected to different irradiation conditions were selected in order to study the effects of initial fuel enrichment, burnup level and neutron spectrum on the final isotopic compositions of the uranium and plutonium.

The analyses were performed on 26 samples taken from 21 different positions. The characteristics of the fuel elements and the locations of the fuel samples are reported in Table 1.

Table 1 – Fuel samples

Assembly	Average Burnup MWd/t(U)	Initial Enrichment %	Rod Number	Axial Locations (numbered fr. top)
G-7	12,380	2.719	1 2 3	1 – 4 – 9 1 – 4 – 7 – 9 1 – 7 – 9
H-10	14,170	3.130	4 5 6	1 – 4 – 7 – 9 4 – 7 – 9 7
L-7	8,660	3.897	7 8	7 1 – 7

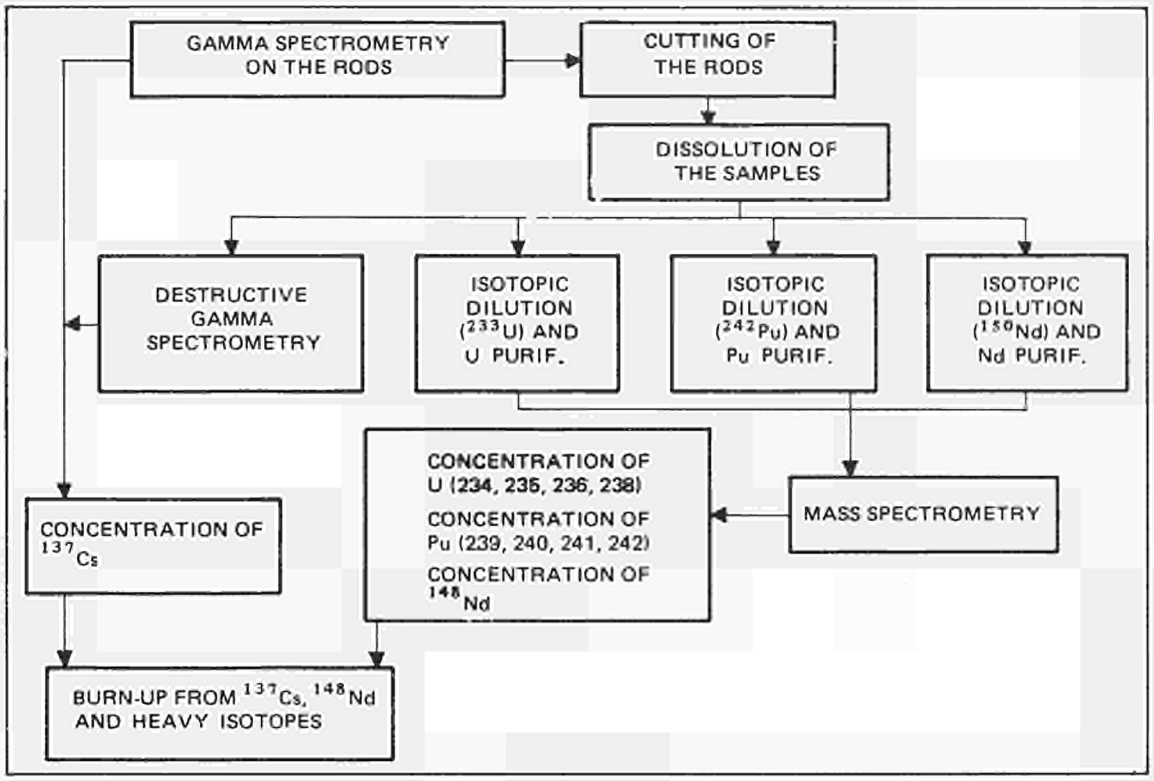

Fig. 1: Sequences of the post-irradiation analyses.

Post-Irradiation Analyses

The sequence of the analyses performed on the fuel samples is illustrated in the flow diagram in Fig. 1.

The experimental techniques utilized at the Ispra Joint Research Centre are shortly described in this section. The experimental techniques utilized at the Transuranium Institute are described in [3].

After the non-destructive measurements the fuel rods were cut in the selected positions. The fuel samples were dissolved in nitric acid in a hot cell and the solutions were diluted so that they could be handled outside the cell.

Aliquots of these solutions were then subjected to gamma and mass spectrometry. Gamma spectrometry was used to determine the activity of ^{137}Cs from which the burnup was derived; mass spectrometry was used to determine the concentrations of heavy isotopes and ^{148}Nd. The concentrations of heavy isotopes and ^{148}Nd were then utilized for separate evaluations of the burnup.

Non-Destructive Gamma Spectrometry

A gross gamma scanning in the energy range 50 keV to 2500 keV was performed on 8 fuel rods using a NaI(Tl) detector. The rods were rotated and displaced automatically in order to obtain activity measurements in steps of 0.5 mm in the axial direction. A typical gross gamma activity distribution along a rod is shown in Fig. 2. The narrow depressions in the activity distribution correspond to the interfaces between two pellets. Larger depressions and peaks which occur at nominal intervals are due to stainless steel grids which displace water in the coolant channels.

The gross gamma activity distribution was a useful tool to identify and to select for the destructive analyses the fuel fuel samples located in the unperturbated position.

Each fuel rod was also analysed by means of a Ge(Li) detector in six positions corresponding to the positions chosen for the destructive analyses. The relative activities of the ^{137}Cs, ^{134}Cs, ^{106}Ru and ^{144}Ce fission products were determined. Only the activity of ^{137}Cs (662 keV gamma-photopeak) was utilized for the burnup determination. The activities of the other fission products were used for isotopic correlation studies. Reproducibility measurements have shown a standard deviation of about 1.5% for each single rod. The error in the relative measurements between different rods is probably higher because the measurements were made over a long time period.

The relative measurements on the ^{137}Cs activity were normalized on the basis of the results of the destructive gamma spectrometry in order to obtain absolute values of burnup.

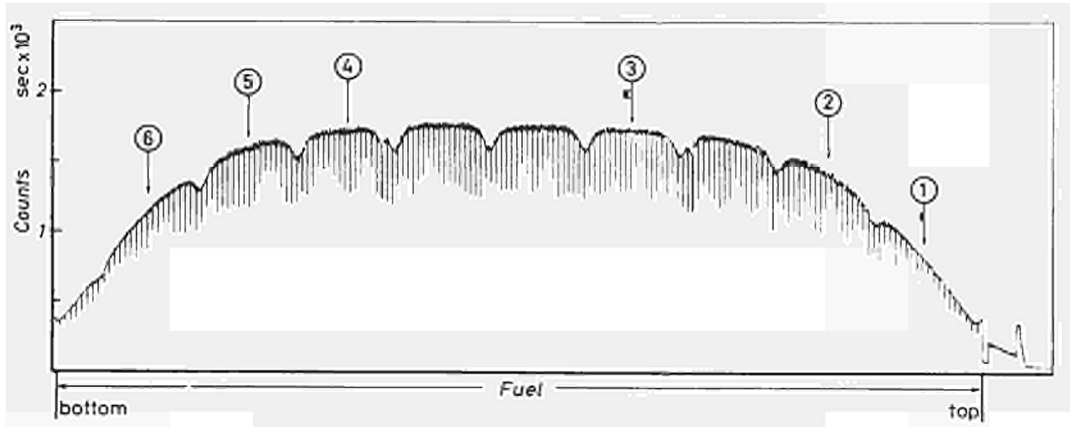

Fig. 2: Typical gross gamma-scanning activity distribution.

Destructive Gamma Spectrometry

Known aliquots of the diluted fuel solutions were measured by means of a Ge(Li) detector. A typical gamma-ray spectrum is shown in Fig. 3. The absolute activities of the fission products ^{137}Cs, ^{134}Cs, ^{106}Ru and ^{144}Ce were determined by comparison with reference sources of known activity supplied by the Radiochemical Centre, Amersham. The values of the uranium concentrations, determined by isotopic dilution and mass spectrometry, were used in order to calculate the ^{137}Cs specific activity expressed as dis/sec. gU.

The quadratic combination of the errors in the reference source, in the gamma spectrometry measurements and in the uranium concentration of the fuel solution, gave the total error in the measurements of the ^{137}Cs specific activity (standard error about 2%).

Isotopic Dilution and Purification of Uranium, Plutonium and Neodymium

The concentrations in the fuel solution of uranium and plutonium nuclides and ^{148}Nd were determined by isotopic dilution and mass spectrometry analyses.

Spikes of ^{233}U, ^{242}Pu and ^{150}Nd were utilized. The radiochemical procedures adopted for the purification of uranium, plutonium and neodymium are the following:

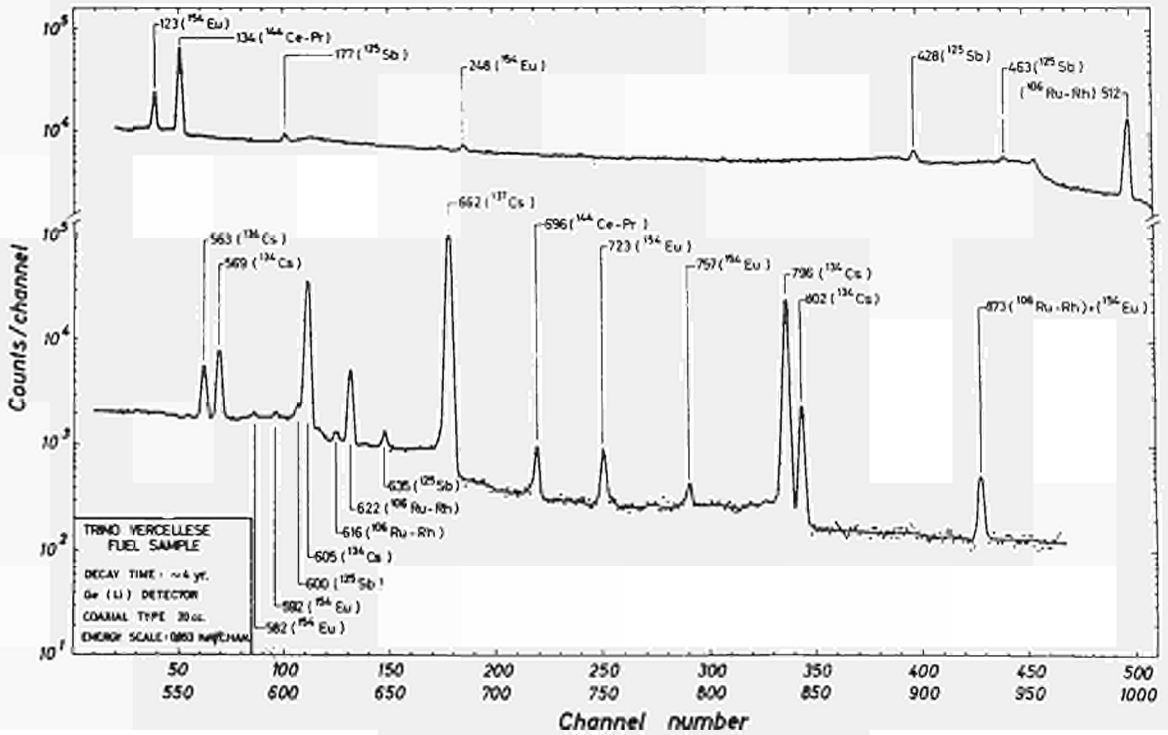

Fig. 3: Gamma-ray spectrum of fission products.

Uranium: Known aliquots of the diluted sample solution (about 10μg. of uranium) and of the spike solution (about 5μg of ^{233}U) were mixed and evaporated to dryness. After addition of 1 M nitric acid, the plutonium was reduced to the trivalent state by hydroxylamine hydrochloride and stabilized by ferrous sulfamate. The uranium was purified by solvent extraction from an aluminium nitrate solution with 10% TBP in isooctane and by stripping with a 0.9 N sulphuric acid and 0.1 N nitric solution.

Plutonium: Known aliquots of the diluted sample solution (about 1μg of plutonium) and of the spike solution (about 0.25μg of ^{242}Pu) were mixed with concentrated nitric acid and carefully evaporated to dryness. After addition of 0.5 M nitric acid, the plutonium was reduced to trivalent state by hydroxylamine hydrochloride and then oxidized to tetravalent state by sodium nitrite in order to ensure the valence homogeneity of the plutonium isotopes. Plutonium was purified by solvent extraction from 1 M nitric acid solution with TTA 0.5 M in xylene and by stripping in 8 M nitric acid. The solution was then evaporated twice to dryness, the second time after addition of concentrated perchloric acid in order to destroy traces of organic compounds.

Neodymium: Known aliquots of the sample solution (1-2μg of ^{148}Nd) and of the spike solution (about 1 μg of ^{150}Nd) were mixed with 40% HF in order to have a 6 M nitric and 6 M hydrofluoric acid solution. This solution was loaded on an anhydrous manganese dioxide (AMD) column. Uranium, plutonium and fission products (except rare earths were eluted with 6 M HF; rare earths were then eluted with 8 M HNO_3. To separate cerium from the rare earths, the nitric solution was percolated through an anion exchange resin mixed with PbO_2. Cerium and traces of plutonium were retained. The selective separation of the neodymium from its neighbouring rare earths and ^{241}Am was made by absorption on a cation exchange resin and fractional elution with 0.25 M α-hydroxyisobutyric acid. The fractions containing neodymium were then purified from α-hydroxyisobutyric acid using a cation exchange resin in nitric acid solution.

Mass Spectrometry

The isotopic compositions of the uranium, plutonium and neodymium samples have been measured by the mass spectrometers Varian Mat CH_4 and AEI MS 503, equipped with thermal-ionization double filament sources.

For all the fuel samples three spiked and three unspiked independently purified solutions were prepared. A minimum of two mass spectrometric runs were carried out for each fuel sample, the third solution being in general analysed only in case of poor agreement in the results. For each run the number of scans was at least ten.

The precision of the measurements of the isotopic ratios depends on the abundances of the different nuclides. Standard deviations of about 0.5% were obtained in the measurement of the ratios $^{235}U/^{238}U$ and $^{240}Pu/^{239}Pu$.

Corrections were introduced for mass discrimination effects as determined by means of isotopic standards of the National Bureau of Standards. Corrections were also introduced to take into account the presence in the fuel of natural neodymium.

The ^{233}U and ^{242}Pu spike solutions were calibrated against standards of the National Bureau of Standards with an error in the concentration values between 0.3 and 0.5%. The ^{150}Nd spike solution was calibrated against a standard of natural neodymium supplied by the Central Bureau of Nuclear Measurements of Euratom in Geel. The error in the calibration was between 0.6 and 0.8%.

Consistency of the Experimental Values

The reliability of the experimental data can be checked through the comparison of the burnup values obtained by means of different techniques and in different laboratories. In fact the burnup values can be calculated from the concentrations of ^{137}Cs and ^{148}Nd and from the isotopic compositions and mass ratio of uranium and plutonium.

The calculations of the burnup values from the experimental data were performed by FIAT NUCLEARE, utilizing the BURNUP code [4].

The experimental burnup values MWd/t (U) obtained with the various techniques in the laboratories of Ispra and Karlsruhe are reported in Table 2.

For the five pairs of adjacent pellets examined at Ispra and Karlsruhe the agreement of the results is satisfactory (within 4%) with the exception of the samples G-7-3-1. For these samples a disagreement in the same sense was observed also for the measurements of isotopic compositions and plutonium/uranium ratio. This fact supports the opinion that the deviations do not derive from experimental errors but from a real difference in the burnup of the adjacent pellets.

Table 2 – Burnup values MWd/t(U) obtained with different experimental techniques.

Assembly	Rod	Axial location	Cs 137 non–destr.	Cs 137 destr.		Heavy elements		Nd 148	
			Ispra	Ispra	Karlsruhe	Ispra	Karlsruhe	Ispra	Karlsruhe
G–7	1	1	8078	7822	–	7677	–	–	–
		4 *	14295	14099	13883	14193	14411	14178	14728
		9 *	11127	10478	10444	10200	10544	–	10352
	2	1	8636	8307	–	8897	–	8745	–
		4	14650	14644	–	15730	–	–	15405
		7	15040	–	15007	–	15731	–	15405
		9	10617	–	11142	–	11410	–	11108
	3	1 *	8566	8879	7716	9103	8052	8839	7956
		7 *	16057	16146	15740	16648	16460	–	15733
		9	11194	11860	–	12065	–	12066	–
H–10	4	1	7475	7415	–	7932	–	7270	–
		4	14345	15156	–	15680	–	15384	–
		7	14862	15477	–	16616	–	15895	–
		9	11937	11226	–	11457	–	11556	–
	5	4	16233	–	16400	–	16624	–	16804
		7	16388	17064	–	17132	–	17428	–
		9	12213	12219	–	12837	–	12380	–
	6	7	18002	17715	–	18697	–	17961	–
L–7	7	7 *	12392	12035	12242	12381	11906	11936	12383
	8	1	3642	3717	–	3211	–	3489	–
		7	7462	7411	–	7152	–	7689	–

*Pairs of adjacent fuel sections.

The burnup values obtained with different techniques were also in close agreement. In fact, if the averages of the different experimental determinations are taken and the standard deviations are calculated, these latter range from 1.5% to 4% for all the samples with the exception of the samples H-10-4-7 and L-7-8-1, which have standard deviations of 5% and 6% respectively. These differences are within the limits of the errors of the different methods which are 4% and 5% for destructive and non-destructive ^{137}Cs measurements, 2% for ^{148}Nd measurements and 4% for heavy element measurements. A very good agreement between Ispra and Karlsruhe has also been observed for the experimental data of depletion and production of uranium and plutonium nuclides.These data were obtained by the processing with the BURNUP code [4] the experimental results of isotopic compositions and uranium/plutonium ratios. The data of depletion and production of the heavy nuclides are reported in Tables 5 and 6.

The agreements between different laboratories and between different techniques promote confidence in the experimental results and in the estimated errors of the measurements.

A different way to check the consistency of the experimental data is through their analysis by isotopic correlation techniques. It has been observed that linear correlations exist between heavy isotopes and fission products in irradiated fuel [3]. The consistency between independently obtained sets of data can be proved by the observation of these correlations.

An example of linear correlation, between the $^{134}Cs/^{137}Cs$ activity ratio and the Pu/U mass ratio, is shown in Fig. 4. The average deviation of the points from the least-square straight line is 2.5% (neglecting the point with the lowest burnup). This deviation is within the experimental errors of the measurements.

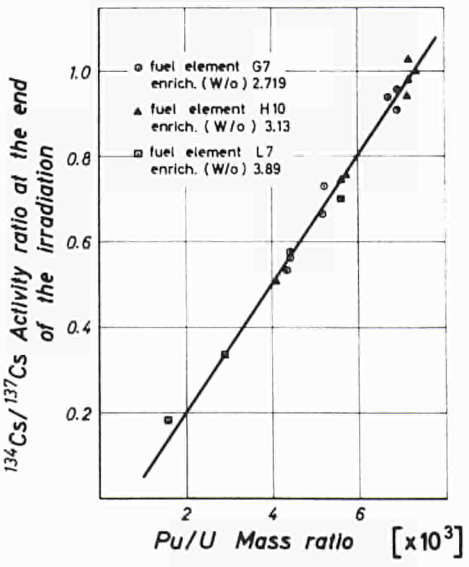

Fig. 4: $^{134}Cs/^{137}Cs$ activity ratio versus Pu/U mass ratio for the fuel of the Trino Vercellese reactor.

This correlation indicates that the gamma-ray measurements on ^{134}Cs and ^{137}Cs are consistent with the mass spectrometry measurements on uranium and plutonium. This correlation also suggests the possibility of measuring the plutonium content of irradiated fuels by means of non-destructive measurements of the $^{134}Cs/^{137}Cs$ activity ratio.

Comparison between Experimental Data and Theoretical Predictions

The detailed evaluation of burnup and isotopic inventory characteristics within the core was performed by FIAT NUCLEARE [1)2)] using:

- a full core representation in X,Y geometry in order to obtain the average characteristics of the fuel assemblies and of the fuel rods under examination,
- a simplified multichannel synthesis technique for the estimation of the axial shapes along the fuel assemblies or fuel rods under examination and of the local burnup and isotopic inventory at the sample positions.

Three basic computer codes were used for the detailed spatial burnup evaluation.

- PHANTOM-3 [5)], a unit cell spectrum-dependent burnup evaluation code,
- CONDOR-3 [6)], a two-dimensional 20,000 mesh diffusion-theory pointwise depletion code,
- SQUIRREL [7)], a one-dimensional diffusion-depletion code.

Table 3 – Comparison between experimental and theoretical burnup values MWd/t(U). The experimental values are the average of the results obtained with different techniques.

Assembly	Rod	Axial location	Exper. value	Theoret. value	Difference %
G–7	1	1	7859	8091	− 2,9
		4	14255	14034	+ 1,6
		9	10524	11049	− 4,8
	2	1	8646	8727	− 0,9
		4	14945	15137	− 1,3
		7	15296	15358	− 0,4
		9	11069	11826	− 6,4
	3	1(Ispra)	8847	8997	− 1,7
		7	16131	16307	− 1,1
		9	11796	12653	− 6,8
H–10	4	1	7523	8801	−14,5
		4	15141	15098	+ 0,3
		7	15712	15492	+ 1,4
		9	11544	12392	− 6,8
	5	4	16515	16381	+ 0,8
		7	17003	16809	+ 1,1
		9	12412	13251	− 6,3
	6	7	18094	17916	+ 1,0
L–7	7	7	12182	11903	+ 2,3
	8	1	3515	3000	+ 14,7
		7	7428	7500	− 1,0

The comparison between experimental and theoretical burnup values is shown in Table 3, where the experimental values are the average of the results obtained with different techniques. The agreement is extremely good for all the samples with the exception of the samples in the extreme positions 1 and 9. In fact, for the samples taken from the other positions the maximum deviation between theoretical and experimental values is 2.5%. The difference of 14% for the sample H-10-4-1 can be explained by the presence of the neighbouring control rod. The difference of 15% for the sample L-7-8-1 can be explained by a poor representation of the water reflectors. In fact, the rod L-7-8 is located at the periphery of the core.

Table 4 shows the comparison between experimental and theoretical values of the rod average burnup. The observed agreement demonstrates that the differences between experimental and theoretical data observed for the extreme positions of the rods have little influence on the average burnup of the rods.

Table 4 – Rod average burnup. Comparison between experimental and theoretical values MWd/t(U)

Rod number	Experimental values	Theoretical values	Differences %
1	12,930	13,239	− 3,4
2	11,996	12,274	− 2,3
3	13,475	14,057	− 4,3
4	12,913	13,353	− 3,4
5	14,372	14,488	− 0,8
6	15,550	15,442	+ 0,7
8	6,288	6,073	+ 3,4

Table 5 – Comparison between experimental and theoretical values of U 235 depletion and U 236 production (kg/t(U)).

Assembly	Rod	Axial location	D 25 exp.	D 25 calc.	Diff. %	P 26 exp.	P 26 calc.	Diff. %
G–7	1	1	7,47	7,84	−5,0	1.430	1.519	− 6,2
		4 (I)	12,05	12,22	−1,4	2.240	2.285	− 2,0
		4 (K)	12,28	12,22	+0,5	2.220	2.285	− 2,9
		9 (I)	9,64	10,22	−6,1	1.915	1.928	− 0,7
		9 (K)	9,84	10,35	−5,2	1.847	1.950	− 5,6
	2	1	8,65	8,75	− 1,2	1.583	1.604	− 1,3
		4	13,29	12,92	+ 2,8	2.306	2.332	− 1,1
		7	13,33	13,09	+ 1,8	2.371	2.435	− 2,7
		9	10,56	11,01	− 4,3	1.942	2.034	− 4,7
	3	1	8,71	9,38	− 7,6	1.570	1.606	− 2,3
		7 (I)	13,85	13,71	+ 1,0	2.475	2.497	− 0,9
		7 (K)	13,67	13,71	− 0,3	2,484	2.497	− 0,5
		9	11,04	11,73	− 6,3	2.027	2.087	− 3,0
H–10	4	1	8,01	8,81	− 10,0	1.434	1.732	− 20,8
		4	14,02	13,70	+ 2,3	2.636	2.623	+ 0,5
		7	14,69	14,02	+ 4,6	2.541	2.647	− 4,2
		9	11,13	11,82	− 6,2	2.304	2.254	+ 2,2
	5	**4**	**14,58**	**14,56**	**−0,1**	**2.786**	**2.758**	+ 1,0
		7	14,99	14,86	+0,9	2.832	2.805	+ 1,0
		9	12,41	12,63	− 1,7	2.214	2.363	− 6,7
	6	7	16,28	15,64	+ 3,9	2.907	2.867	+ 1,4
L–7	7	7 (I)	12.56	12.06	+ 4.1	2.528	2.355	+ 6.5
		7 (K)	12,13	12,06	+ 0,6	2.558	2.355	+ 8,6
	8	1	3.948	3,45	+14,4			
		7	8.09	8,80	− 9,2			

Table 5 shows the comparison between experimental and theoretical values of the ^{235}U depletion and ^{236}U production. The maximum differences are again observed for the samples H-10-4-1 and L-7-8-1. If the values of these two sections are neglected, the average difference between experimental and theoretical values is about 3.5% for the ^{235}U depletion and 2.5% for the ^{236}U production.

Table 6 shows the comparison between experimental and theoretical values of the production of ^{239}Pu, ^{240}Pu and ^{241}Pu. For the production of ^{239}Pu the agreement is within 10% with the exception of the samples H-10-4-1 and L-7-8-1. If the values of these samples are neglected, the average difference is about 6%. The calculated values of the ^{239}Pu are normally higher than the experimental values. If the average of all the determinations is considered, the calculated value is 3.5% higher than the experimental value. The same overestimation is observed for the ^{240}Pu production. This difference could be due to an overestimation of the effective fuel temperature and to a consequence of the Doppler effect.

Table 6 – Comparison between experimental and theoretical values of the production of Pu 239, Pu 240 and Pu 241 (kg/t(U)).

Assembly	Rod	Axial location	P 49 exp.	P 49 calc.	Diff. %	P 40 exp.	P 40 calc.	Diff. %	P 41 exp.	P 41 calc.	Diff. %
G–7	1	1	3.608	3.972	−10,1	0.515	0,577	−12,1	0,204	0.185	− 9,0
		4(I)	5.041	5.248	− 4,1	1.123	1.101	+ 2,0	0.596	0.584	+ 1,9
		4(K)	4.991	5.248	− 5,1	1.118	1.101	+ 1,5	0.609	0.584	+ 4,0
		9(I)	4.072	4.548	−11,7	0.719	0.853	−18,7	0.329	0.351	− 6,9
		9(K)	4.159	4.588	−10,3	0.746	0.869	−16,5	0.346	0.363	− 5,1
	2	1	3.606	3.952	− 9,6	0.560	0.630	−12,6	0.228	0.205	+10,2
		4	4.769	5.220	− 9,5	1.160	1.202	− 3,6	0.615	0.646	− 5,1
		7	4.926	5.154	− 4,6	1.196	1.220	− 2,0	0.637	0.651	− 2,3
		9	4.134	4.505	− 9,0	0.802	0.923	−15,1	0.371	0.382	− 3,0
	3	1	3.537	3.410	+ 3,6	0.585	0.644	−10,2	0.248	0.188	+23,9
		7(I)	4.806	4.532	+ 5,7	1.251	1.292	− 3,3	0.679	0.642	+ 5,5
		7(K)	4.889	4.532	+ 7,3	1.254	1.292	− 3,0	0.683	0.642	+ 6,1
		9	4.141	3.978	+ 3,9	0.840	0.986	−17,4	0.404	0.383	+ 5,2
H–10	4	1	3.483	4.158	−19,4	0.442	0.580	−31,1	0.171	0.197	−15,4
		4	5.266	5.479	− 4,0	1.118	1.101	+ 1,5	0.614	0.617	− 0,5
		7	5.234	5.426	− 3,7	1.137	1.129	+ 0,7	0.618	0.635	− 2,8
		9	4.418	4.824	− 9,2	0.775	0.890	−14,9	0.369	0.400	− 8,4
	5	4	5.172	5.457	− 5,5	1.211	1.205	+ 0,5	0.676	0.682	− 0,8
		7	5.234	5.404	− 3,2	1.247	1.237	+ 0,8	0.694	0.702	− 1,2
		9	4.446	4.765	− 7,2	0.834	0.959	−15,0	0.409	0.429	− 4,8
	6	7	4.968	4.620	+ 7,0	1.297	1.313	− 1,2	0.697	0.66	+ 4,4
L–7	7	7(I)	4.647	4.549	+ 2.1	0.723	0.676	+ 6.5	0.350	0.305	+14,8
		7(K)	4.525	4.549	− 0,5	0.710	0.676	+ 5,0	0.345	0.305	+13,1
	8	1	1.464	1.22	+20,0						
		7	2.525	2.540	− 0,6						

Concluding Remarks

The comparison of the results of the post-irradiation analyses with the theoretical data has shown that the burnup evaluation methods utilized by FIAT NUCLEARE are quite satisfactory for the predictions of burnup and plutonium production. The programmed post-irradiation examination of one spent fuel assembly, discharged at the end of the second cycle of the Trino Vercellese reactor, will give other interesting results to confirm the reliability of the theoretical prediction. The work performed on the fuel of the Trino Vercellese reactor has also given us complete confidence in our experimental techniques through a comparison between the results obtained with different methods and in different laboratories and through an analysis of the experimental data by the isotope correlation technique.

References

1) A.M. Moncassoli et al., Post-Irradiation Burnup Analysis of Trino Vercellese Reactor Fuel Elements. Comparison with Theoretical Results. Paper presented at the Panel on Reactor Burnup Physics, Vienna, 12-16 July 1971. (to be published in the Proceedings of the Panel)
2) Post-Irradiation Analyses of the Fuel Elements of the Trino Vercellese Reactor. EUR-Report in preparation.
3) A. Ariemma et al., Experimental and Theoretical Determination of Burnup and Heavy Isotope Content in a Fuel Assembly Irradiated in the Garigliano Reactor. EUR 4638 (1971)
4) G.Aroasio, The BURNUP Code, EUR-Report in preparation.
5) L. Criscuolo, V. Paterlini, The PHANTOM Code (unpublished), FIAT Nuclear Energy Laboratory
6) E. Salina, CONDOR-3, A Two-Dimensional Reactor Lifetime Program with Local and Spectrum Dependent Depletion. EUR-4539 (1970)
7) E. Salina, The SQUIRREL Code, FIAT Report FN-E-96 (1969) and EUR-Report in preparation.

WATER CHEMISTRY

Introduction

The studies on the corrosion and mass transport phenomena in the high-temperature circuits of nuclear power plants require accurate monitoring of the high-purity water for metal impurities at the ppb level.

The analysis of such extremely diluted solutions represents a cumbersome and complicated problem, because the application of currently-used analytical methods is hindered by difficulties connected with a lack of sensitivity.

The problem is further complicated by the fact that the impurities concerned may be present in ionic form as well as in the form of suspended particles whose nature is not yet sufficiently known. No straightforward procedure for determining the total quantity of these impurities was available. Among the other elements the concentration of Fe, Ni, Cu, Cr, Mn and the composition of the particulate matter are of particular significance in the establishment of valid theories on corrosion and mass transport processes. Hence different analytical techniques have been used and various methods have been studied with a view to obtaining the following information:

a) the ionic concentration of certain impurities
b) the chemical form of the suspended particles
c) the total concentration of typical impurities.

As far as possible such methods have been investigated involving little or no chemical treatment of the sample, in order to avoid the risk of contamination or blank values higher than the concentrations sought.

X-Ray Measurements

N. Toussaint, W. De Spiegeleer

The detection and the quantitative determination of dissolved matter (cations) were performed by using a preconcentration step by ion exchange (a high molecular weight copolymer sulphonated in order to give ion exchange properties and supplied in the sodium form) followed by X-ray fluorescence analysis. At present the analytical procedure for the determination of Fe, Ni and Cr in the concentration range 0 to 1000 μg/l has been established. The precision is about ±5% and ±2% at the 5 μg and the 50 μg levels respectively, the limit of detection being 0,05 μg. The sample volume required ranges from 50 to some 200 ml depending on the concentration level of the impurities, A typical working curve established for Cr in the concentration range 0 to 10 μg is shown in Fig. 2.

Preliminary investigations were carried out by X-ray spectroscopy for the detection and quantitative determination of the suspended particles collected on millipore filters. These tests revealed the presence of Fe, Ni, Zn, Cr, Pb and Cu and showed that a linear relationship exists between the weight of the collected matter and the corresponding line intensity measured in the range from 0,05 to 2,0 mg/cm^2.

Crystallographic analysis of the compounds present in the suspended matter, by X-ray diffraction on several samples from the K.R.B. Gundremmingen nuclear power plant, revealed the presence of α Fe_2O_3 and Ni-Fe oxydes.

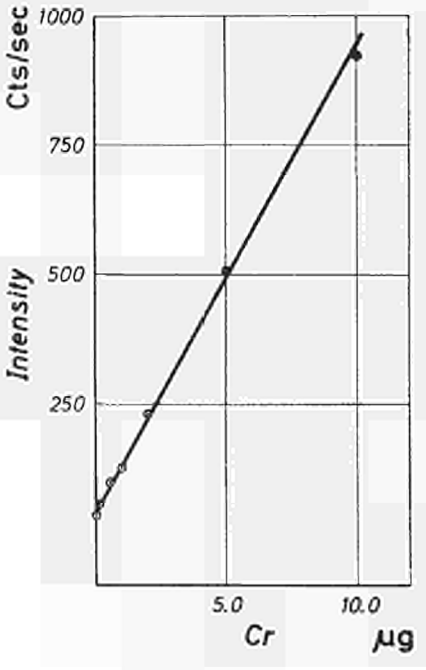

Fig. 1

Wet Chemistry Analysis

J. Collin, G. Serrini, G. Serrini-Lanza, H. Muntau, G. Renaux, W. Leyendecker

In order to evaluate the composition of the iron oxides suspended in water, the particles collected on a 0,45 μm millipore filter were examined. The collected material (ferrous hydroxide, ferric hydroxide, magnetite) was analysed for the content of ferrous and ferric iron before and after an oxidation step.

The filter, containing some 1000 μg of total iron, is kept under air-free atmosphere in order to prevent oxidation of the ferrous hydroxide, and is divided into two equal parts. The first is analysed immediately, while the second is processed after being kept in an oven at 120°C for 24 hours.

The ferrous iron contained in the first half of the filter originates from the ferrous hydroxide and – as to one third – from the magnetite. The value of the percentage of the ferrous iron before and after the oxidation can easily be related to the contents of the ferrous hydroxide, the ferric hydroxide and the magnetite by the analytical procedure described by C. Reban and J.P. Berge ("Magnetic deposits in boilers from iron in solution". Paper presented at the American Power Conference in Chicago on April 21, 1970).

The determinations of the ferrous iron were performed by a microspectrophotometric method, taking into account the interference from the ferric iron.

Several checks of the contents of total and soluble silica at the level of 10^{-5} – 10^{-6} % in pure water were also performed. The values given by the microspectrophotometric procedure were found to fit excellently with those obtained by the official UNIPEDE method.

Atomic Absorption Analysis

G. Rossi, Ch. Pickford

The determination of the total (ionic and particulate) concentration of some metal impurities was achieved by using a flameless atomic absorption procedure. The method set up allows for the automatic and simultaneous determination of up to five elements with the required sensitivity; moreover it is both quick and accurate and avoids any chemical pre-treatment of the sample. A special instrument has been designed and constructed for this purpose.

The apparatus essential to the analysis consists of six main sections, i.e., primary light source and supply, automatic sample injection system, furnace and power unit, program control unit, detection system, and polychromator. A sketch of the experimental set-up is shown in Fig. 3. The light emitted by a hollow cathode and containing the resonance frequencies of the elements under investigation, is focused, after modulation, within the graphite cell and subsequently on the entrance slit of a polychromator. After evaporation of the solvent at low temperature, a fast evaporation of the residue is achieved by heating the graphite cell to a high temperature of up to 2600°C. Absorption signals due to the atomic species generated in the cell are monitored by the photomultipliers, integrated and converted into a digital read-out signal expressed in concentration. A supplementary photomultiplier monitors a non-resonance frequency from the hollow cathode lamp and is used as reference line.

This mode of signal treatment, which is schematically presented in Fig. 4, was considered necessary in order to eliminate possible interference due to spurious absorption signals from fumes or solid particles in the cell. Moreover, integration of the absorption minimizes the differences between the evaporation rates corresponding to the different chemical forms under which each element is likely to be introduced into the cell. For the sake of simplicity only the cases of a single measuring channel and a reference channel are represented in Fig. 3 and 4.

In order to program the sample injection, furnace, integrator and read-out system, a multiposition telephone-type electromagnetic switch is used. This provides the possibility of switching over control to the program control unit of the furnace power supply and back again, using a switch operated by an eccentric rotary cam. In this way up to five injections of each sample prior to analysis can be performed in order to step up the sensitivity by a corresponding factor.

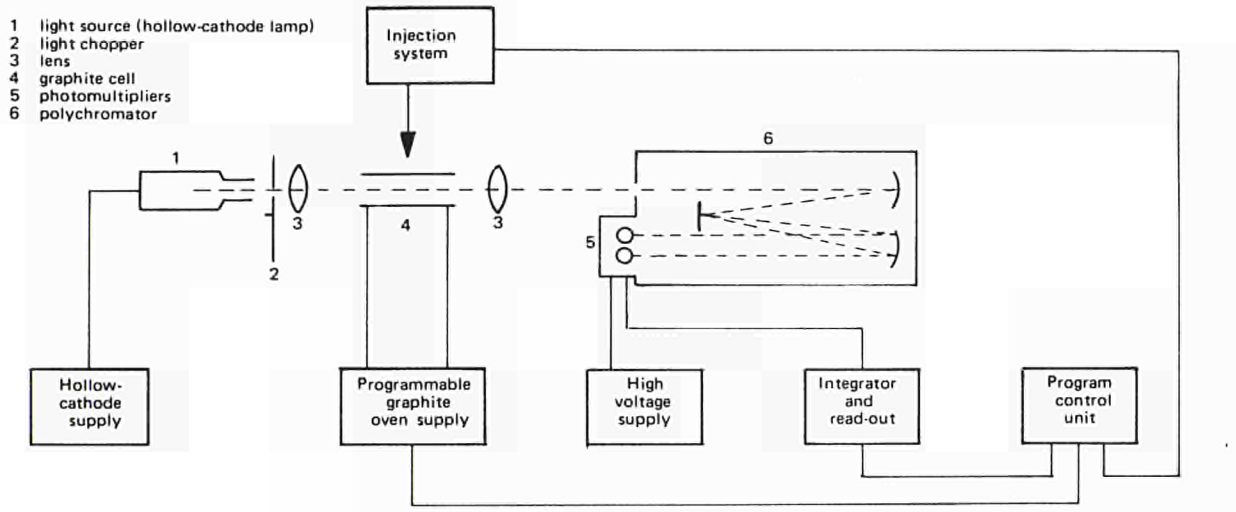

Fig. 2

Table 1.

Element	Sensitivity	
	absolute (Wt/1%)	relative (ppm/1%)
Pb	40.10^{-12}	0.0004
Ni	70.10^{-12}	0.0007
V	500.10^{-12}	0.005
Cd	$0.25.10^{-12}$	0.0000025
Ag	5.10^{-12}	0.00005
Mn	9.10^{-12}	0.00009
Co	30.10^{-12}	0.0003
Cu	40.10^{-12}	0.0004
Fe	60.10^{-12}	0.0006
Cr	150.10^{-12}	0.0015
Al	1000.10^{-12}	0.01
Sb	1500.10^{-12}	0.015

A series of elements were investigated with the described instruments, the achieved sensitivities (for 0,1 ml sample single injection and for 1% absorption), being listed in Table 1. The reproducibility was evaluated at different concentration levels. The results show that the reproducibility is unusually high, and is achievable irrespective of the weight of the element introduced into the cell.

Typical figures range from 1.7% for 0.003 ppm Mn to 1% for 0.01 ppm Cu and 1.1% for 0.25 ppm Fe. This technique has also been widely applied to a large variety of actual samples including heavy water, drinking water, distilled water, and solutions of air pollution monitoring filters.

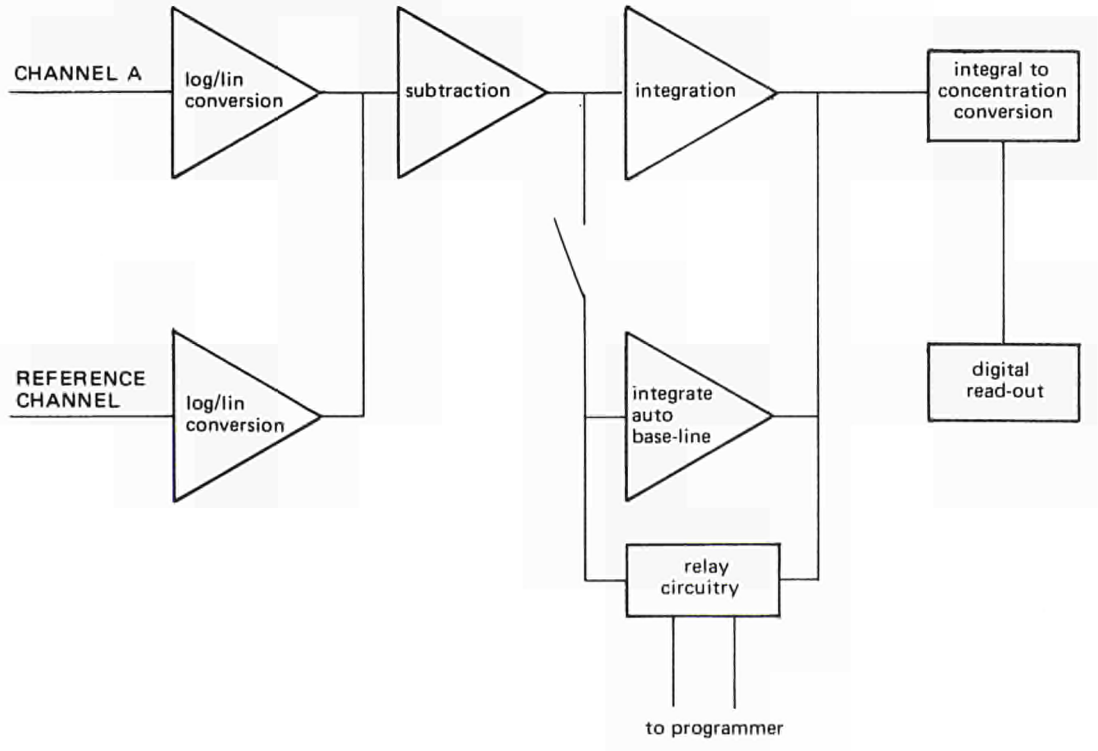

Fig. 3

PYROCHEMICAL HEAD-END TREATMENT FOR FAST REACTOR FUEL ELEMENTS

A. Avogadro, A. De Plano, G. Mutzbauer

Introduction

The problems encountered during the transport, handling and reprocessing of fast reactor fuel elements have a very marked influence on the overall fuel-cycle cost for power reactors of this type. As a matter of fact, owing to the large quantity of fissile material present, the out-of-core fuel inventory is a major cost-determining factor, hence the obvious need to reduce the time taken by the different operations in the fuel cycle. The demand for utmost speed in reprocessing raises numerous severe problems owing to the high burnup and specific power densities characteristic for fast reactors.

Furthermore, attention has to be paid to the handling and criticality problems arising from the presence of large amounts and high concentrations of plutonium.

For these reasons the existing conventional reprocessing plants cannot be employed economically in this case without modifications.

A potential way of overcoming these difficulties consists in the application of pyrochemical methods in the head-end treatment of the fuel elements, in order to facilitate the subsequent operations. By combining pyrochemical methods with the classical solvent extraction cycle one could make use of the typical advantages of both methods whilst avoiding their inherent drawbacks.

The work carried out at the Ispra JRC in the field of pyrochemical processing is oriented towards this philosophy and is centred on the development of typical unit operations for the head-end treatment of spent fuels.

Our work has been directed towards three specific topics:

a) liquid-metal decanning of spent stainless-steel-clad fuels (Solinox process)
b) oxidative pulverization by fused salts and extraction of volatile fission products (Saltex process)
c) pyrochemical separation of plutonium from the bulk of the fuel.

It should be noted that these operations can be considered individually or consecutively.

Liquid metal decladding (Solinox process)

Decanning of fuel material by liquid-metal dissolution of stainless-steel-clad elements offers many potential advantages, particularly for highly irradiated fuels. This decanning process can be performed directly without dismantling the fuel elements, therefore the complex mechanical operations are avoided. Also the difficulty of removing the sodium adhering to a fuel assembly can be overcome and so the head-end steps are minimized.

The fundamental aspects of liquid metal decanning were evolved at the Ispra JRC [1) 2)], the conceptual design studies and scaling-up of this process are being performed at S.C.K./CEN-Mol in connection with Belgonucléaire and Euratom [3) 4)].

Optimum dissolution of the stainless steel and other high nickel alloys could be obtained with an Sb/Cu (10 to 23.5 wt.% Cu) solvent alloy at 900-1000°C as seen in Figs. 1, 2 and 3.

Attempts were made to find ternary solvent alloys in order to reduce the price and to improve some dissolution parameters (temperature, fluidity). Partial substitution of aluminium for the antimony in the Sb-Cu alloy was tried. The results obtained show that Al reacts with Sb forming an Al-Sb intermetallic compound with a high melting point (Fig. 7). The formation of this compound increases the temperature of primary solidification, changes the Sb-Cu ratio and therefore seems not to be favourable for this process.

The dissolution of sodium in Sb-Cu solvent alloy at an operating temperature of 1000°C was investigated. The Sb-Na phase diagram shows that Na will be dissolved in any quantity in Sb. Moreover the existence of $Sb\text{-}Na_3$ and Na-Sb intermetallic compounds indicate a strong affinity between Sb and Na. No phase diagrams for Na-Cu, Na-Fe, Na-Cr and Na-Ni are available. The affinity of Na for these metals has been ignored.

Exploratory EMF measurements of the Na/Sb-Na (1%) couple were performed. From 0.7 V at 670°C an activity coefficient of $3 \cdot 10^{-2}$ was derived. At 1000°C this activity coefficient can be extrapolated to $7 \cdot 10^{-2}$. Since the vapour pressure of Na over liquid Na at 1000°C amounts to about 2.5 atm, it is possible to calculate that the vapour pressure of Na over Sb-Cu-Na (1 wt.%) alloy at 1000°C will be as low as 1 mm Hg.

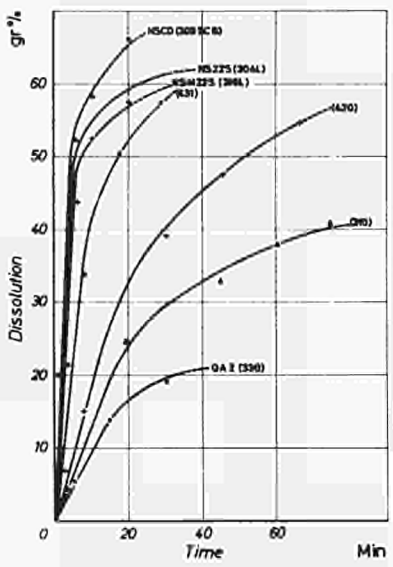

Fig. 1: Dissolution rates of different s.s. in solvent alloy Sb/Cu 10 Wt % temp. 1000°C.

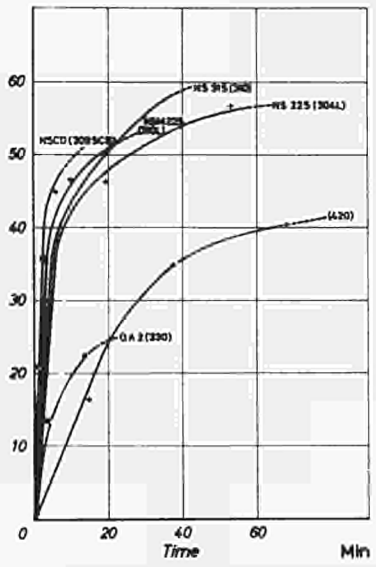

Fig. 2: Dissolution rates of different s.s. in solvent alloy Sb/Cu 15 Wt % temp. 1000°C.

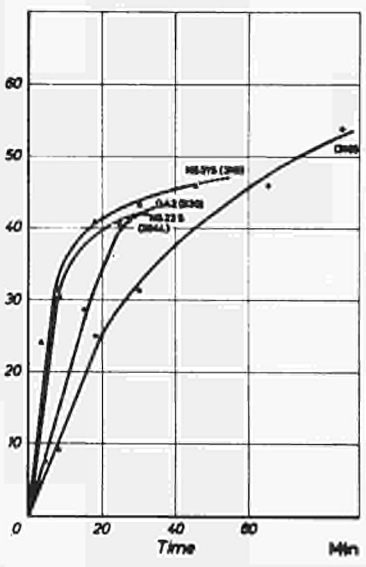

Fig. 3: Dissolution rates of different s.s. in solvent alloy Sb/Cu 23,5 Wt % temp. 1000°C.

The dissolution method therefore comprises in a single operation several of the consecutive steps scheduled in the conventional flow sheet, such as cleaning (sodium removal), dismantling of the element and decladding.

Oxidative fuel pulverization in molten nitrates (Saltex process)

The preparation of fast breeder fuel for solvent extraction is more difficult than that of thermal reactor fuel because of larger amounts of troublesome fission products (such as I^{131}, Kr^{85}, Xe^{133}, Tritium) and the presence of PuO_2 which is difficult to dissolve in nitric acid. Moreover it is necessary to dispose of tritium and other volatile fission products prior to the acid dissolution, in order to avoid the risk of releasing liquid and gaseous contamination to the environment.

The Saltex process developed at the Ispra JRC [5) 6)] involves an oxidative breakdown of fuel material with molten nitrates; by this method tritium and other volatile fission products will be isolated and the fuel converted into the uranate and plutonate form easily soluble in nitric acid.

As compared to the oxidizing treatment with oxygen at 900°C, as currently scheduled in the Oak Ridge flow sheet [7) 8) 9)], the breakdown process with molten nitrates has the following advantages:

- The fission gases are set free undiluted by other gases, thus facilitating their final disposal.
- More effective breakdown of the fuel, hence smaller fuel losses and easier dissolution.
- Lower working temperature (about 450°C as against 900°C in the American flow sheet).
- The melted nitrate can be easily recycled.

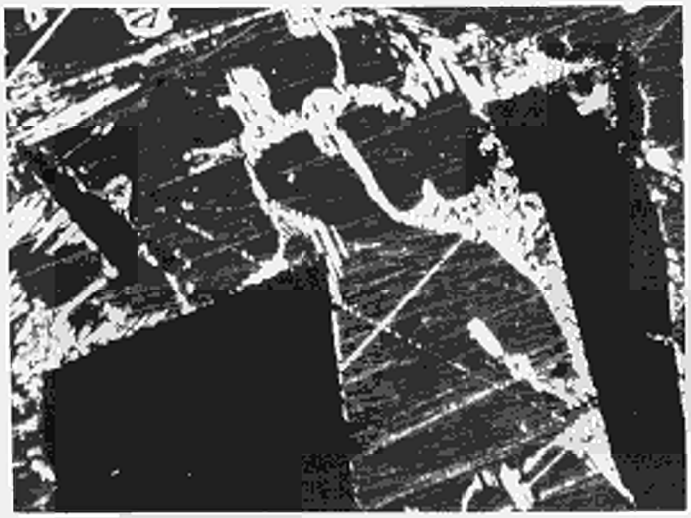

Fig. 7: Metallography of Sb - Cu - Al alloy (85 - 10 - 5 Wt %); back phase = Sb-Al crystals.

Uranate formation studies

The structure of the anhydrous uranates obtained by reaction between UO_2 and fused alkali nitrates at 45°C was investigated [10]. The isomorphous substitutions between the alkali metals and the crystalline structure were determined. Partial solubility of Li, K and Cs in the $Na_2U_2O_7$ structure exists and depends upon the cation ratio in the melt. The solubility limits within the original Na diuranate structure were found to be:

$$Li = 1\%; \qquad K = 3\%; \qquad Cs = \text{less than } 0.5\%$$

Therefore when nitrate mixtures are used for fuel breakdown, the composition of the formed uranate will depend upon the melt composition. To be able to reestablish the right composition of the melt before recycling takes place, the chemical formula of the uranate must be known.

Thermal and radiolytic stability of nitrates

Studies were done on the thermal and radiolytic decomposition of pure alkali nitrates and their mixtures.

At temperatures below 500°C, the thermal nitrate decomposition is essentially

$$NO_3^- \rightleftharpoons NO_2^- + 1/2\ O_2$$

The nitrite concentration in the melt is a function of time and temperature.

In Table 1 gives typical equilibrium conditions at 480°C for pure nitrates in a closed system.

Table 1

Experimental conditions	KNO_3	$NaNO_3$
Volume fraction of the melt (%)	38	40
Time for equilibrium attainment (hrs)	24	22
Nitrite concentration (%)	0.033	0.2
Oxygen pressure (mm Hg)	35	290

In open systems, the thermal decomposition follows a $y = bt^a$ time law, where y is the nitrite content in the melt and a, b are characteristic temperature dependent coefficients.

In a practical case, these parameters are

$$a = 0.9729; \qquad b = 92.62 \qquad [y \text{ in ppm}]$$

for a $NaNO_3 - KNO_3$ mixture (70-30 mole ratio) at 480°C.

Radiolytic experiments on nitrates were done with capsule irradiations at dose rates of 1 to 7 watts/h/g, using of the Van der Graaff accelerator. The samples were heated at 480°C and cooled down rapidly at the end of irradiation. In Fig. 4 the radiolytic behaviour of $NaNO_3$ at 480°C is plotted and compared to the thermal decomposition.

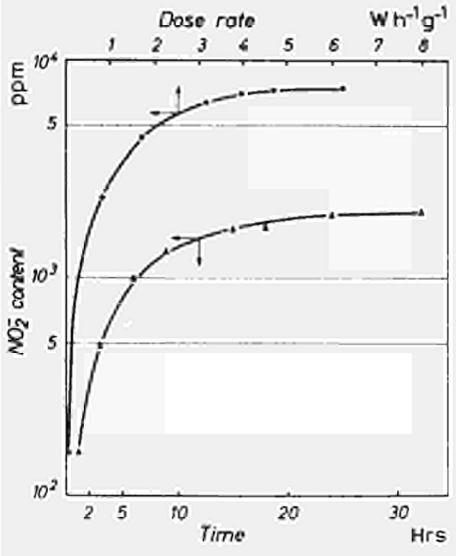

Fig. 4: Thermal and radiolytic stability of fused $NaNO_3$ at 480°C.

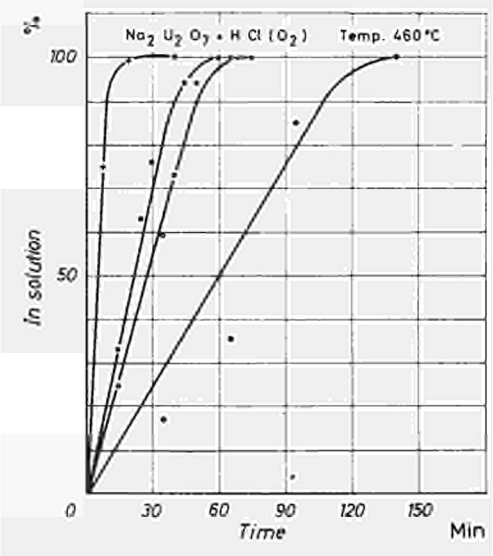

Fig. 5: $Na_2U_2O_7 + H\ Cl\ (O_2)$. Temp. 460°C.

Nitrate melt regeneration

After each fuel breakdown the molten nitrates must be regenerated before being recycled. Preliminary experiments show that oxygen can completely oxidize the nitrite present if an overpressure is employed. At 500°C, without any special precautions for gas-liquid contact, a melt of pure nitrite is completely oxidized to nitrate in 6 hours with an oxygen overpressure of 400 mm Hg, while at normal pressure the reaction is only completed as to 50%.

Pyrochemical extraction of plutonium

Following on the oxidative pulverization of the fuel as described above, the Saltex process provides for selective dissolution of the uranium in a molten chloride medium and extraction of the insoluble plutonium dioxide which is left behind in suspension.

This separation is at present carried out at 450-500°C in a $MgCl_2$-NaCl-KCl or KCl-LiCl eutectic.

Two separation methods have been developed:

a) selective dissolution of uranium with a HCl + O_2 gaseous mixture as chlorinating agent. In these conditions the uranate is dissolved in the melt as uranyl chloride whereas plutonium is left behind in the form of PuO_2 (higher oxygen partial pressure results in lower plutonium solubility). We chose an 80% O_2 concentration to carry out the U-Pu separation tests. Two tests performed with 20% of plutonium confirmed the total solubility or uranate after a 90 min oxychlorination, whilst the plutonium solubility in the salts was found to be less than 500 ppm. Fig. 5 shows the dissolution rate of uranate versus increasing O_2 amounts in the gaseous mixture.

b) Total solubilization of uranium and plutonium in the melt followed by selective precipitation of Pu with MgO. The fuel oxidated by nitrate breakdown is easily soluble in molten chlorides at 450-500°C with the use of gaseous hydrogen chloride. From this solution the Pu is selectively precipitated by addition of Magnesium oxide to the melt. Two typical laboratory experiments in Pu precipitation at 490°C are reported in Table 2.

PuO_2Cl_2 in sol. (mg) MgO added to the melt (mg)	190 28		190 56	
Contact time (min)	U % in sol.	Pu % in sol.	U % in sol.	Pu % in sol.
0	100	100	100	100
5	–	–	100	10
10	–	–	100	5
15	100	13	–	–
20	100	$\leqslant 3$	100	$\leqslant 3$

After addition of MgO powder, the melt was kept in agitation with an inert gas and the samples were taken by filtration, dissolved in water and counted by gamma spectrometry with a Ge (Li) detector.

Technological developments

Technological work was focused on the development of equipment and demonstration of the different processes on a pilot-plant scale. The Solinox process is already transferred to the industrial scale at CEN, Mol (Belgium) in collaboration with the Belgonucléaire Soc. [3].

For the technological demonstration of the Saltex process a furnace was designed in collaboration with CEN, Mol, and is now in construction. This furnace (Fig. 6) offers the possibility of making several heterogeneous reactions (gas-liquid, solid-liquid) with molten salts, followed by filtration and recycling of the salts. The use of the gas-lift system allows of employing a "one-pot" way and reduces the corrosion problems.

Fig. 6: Graphite furnace for pilot plant experiments.

1. Gas inlet
2. Gas liquid separator
3. Interchangeable filter
4. Gas outlet
5. Furnace

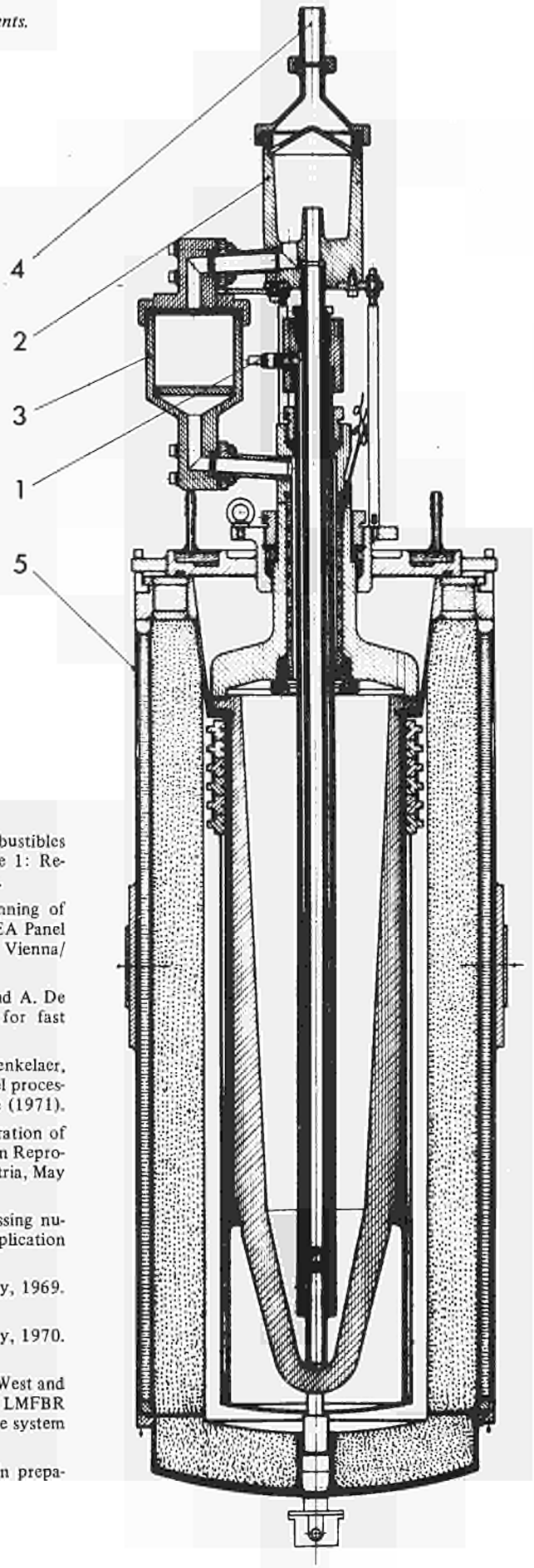

References

1) M. Payrissat, J.G. Wurm, Dégainage des combustibles UO_2-PuO_2/inox par les métaux liquides; partie 1: Recherche d'un alliage solvant; EUR-4229 f (1969).

2) J.G. Wurm, M. Payrissat, Liquid metal decanning of hyghly irradiated UO_2-PuO_2/SS clad fuels; IAEA Panel on Reprocessing of Highly Irradiated Fuels, Vienna/Austria, May 1969.

3) J.G. Wurm, P.R. Heylen, R.C. De Benkelaer and A. De Coninck, Pyrochemical head-end conception for fast breeder fuel processing; EUR-4614 e (1971).

4) J.G. Wurm, C. David, P.R. Heylen, R.D. De Benkelaer, A. De Coninck and R. Verbeke, Fast Breeder fuel processing pyrochemical head-end study; EUR-4615 e (1971).

5) A. Avogadro, J.G. Wurm, A pyrochemical separation of plutonium from irradiated fuels; IAEA "Panel on Reprocessing of Highly Irradiated Fuels", Vienna/Austria, May (1969) and EUR-4242 f (1969).

6) A. Avogadro, J.G. Wurm, A method of processing nuclear fuels; Euratom patent: Netherlands Application No. 68.15301 filed 25 Oct. 1968.

7) Chem. Technol. Div. Annu. Progr. Rep. 31 May, 1969. ORNL-4422 p. 67.

8) Chem. Technol. Div. Annu. Progr. Rep. 31 May, 1970. ORNL-4572 p. 54.

9) C.D. Watson, R.S. Lowrie, W.S. Groenier, G.A. West and S.D. Clinton, Head-end processing of spent LMFBR Fuel; Proceedings of 16th Conference on remote system technology (1969).

10) A. Avogadro, N. Toussaint: Euratom report in preparation.

DEVELOPMENT OF NEW TECHNIQUES

Mercury Monitor

G. Rossi, E. Orthman-Römer

A simple low-cost apparatus has been developed for the determination of Mercury at the ppb level in various matrices by a flameless atomic absorption procedure.

A simplified diagram of the apparatus is sketched in Fig. 1.

A resonance monochromator is used for isolating the 2537 nm Hg radiation from the light emitted by a low-pressure Hg vapour discharge lamp. This radiation is simultaneously monitored by two photomultipliers; the first measures the light intnsity transmitted through the 30 cm long, 15 mm diam. absorption cell, the second – in the opposite direction – is used for providing the unabsorbed reference signal. Both signals are amplified and the ratio displayed on a 0-10 V strip chart recorder. According to the nature of the sample, a chemical tratment is performed in such a way as to obtain a form of Hg in the solution that can be reduced by $SnCl_2$.

After the additon of the reducing solution an argon flow of about 3 litres/min is directed into the reaction flask. All the Mercury in the solution is swept and transferred into the absorption cell in the form of metal vapour.

A linear relationship is established between the absolute quantities of Hg in the solution and the corresponding absorbance values in the range 5 to 100 ng of Hg, the limit of detection (1% absorption) being 0.8 ng.

Depending on the Hg level in the sample, a precision of 5 to 10% is normally obtained.

Tests performed on actual samples added with known quantities of Hg showed that a recovery ranging from 80 to 100% is achieved. Several samples including water, plants, fish tissues, human tissues, and flour were analysed on a routine basis.

The most striking features of the procedure consist in the easiness of its operation, the extremely high sensitivity and selectivity, the rapidity and the very broad applicability.

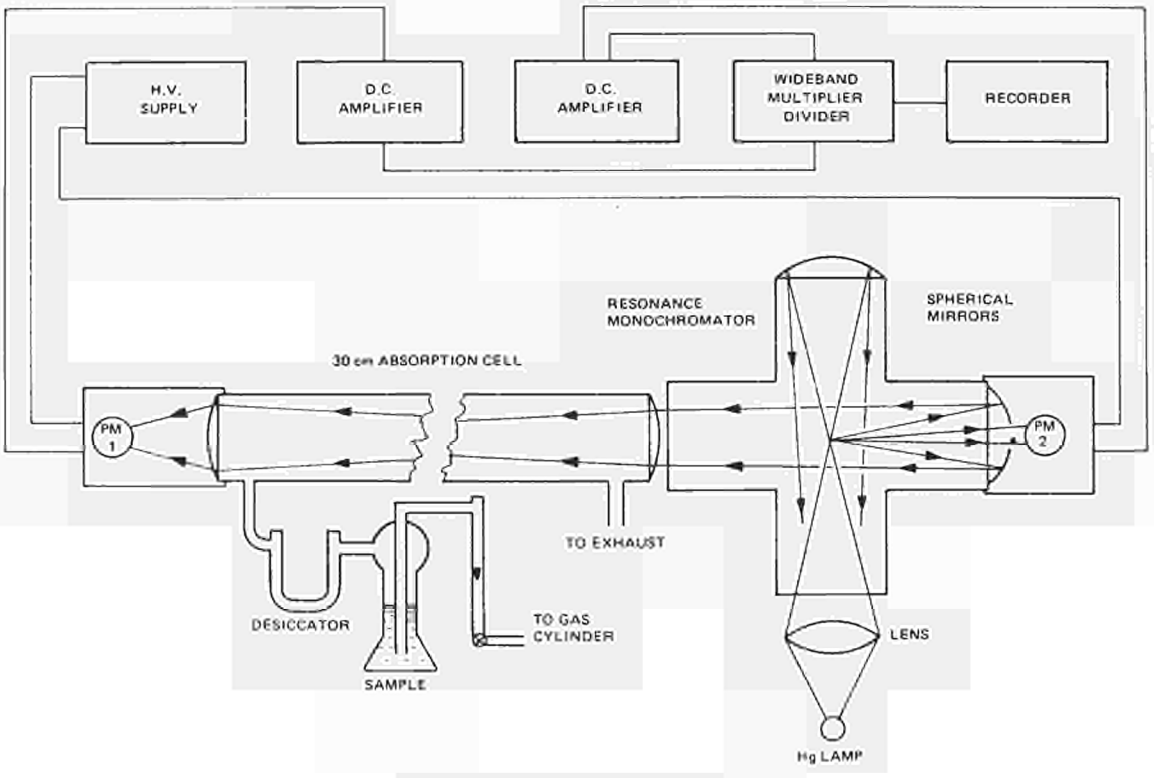

Fig. 1: Sketch of the Mercury monitor.

New X-Ray Diffraction Analysis Method

N. Toussaint, M. Ooms

A quantitative X-ray diffraction analysis method has been developed using the basic equation relating the intensity of the diffracted X-rays to the absorptive properties of the compound in a multi-component system. By introducing into this equation the total mass absorption coefficient μ_T, a simple equation

$$I_1/(I_1)_o = \frac{x_1 \mu_1}{\mu_T}$$

is derived where $I_1 / (I_1)_o$ = the ratio of intensity diffracted at a definite Bragg angle of component 1 in a mixture to that of component 1 in the pure state.

x_1 = the weight fraction of component 1

μ_1 = the mass absorption coefficient of the pure component 1

and μ_T = total mass absorption coefficient of the sample, including component 1

This total mass absorption coefficient is determined from the MoKα Compton diffused radiation on an X-ray fluorescence arrangement. The average relative error for the mass absorption coefficient determination was found to be about 5% (Table 1). Analyses of synthetic mixtures gave a relative error of 1-8% (Table 2) depending on the concentration.

This method can replace the internal standard technique in most cases, because it eliminates the difficulties of finding a suitable internal standard, dilution of the sample, and homogeneity problems in the mixing procedure.

Table 1 – Comparison between calculated and found values of mass absorption coefficients.

Sample no.	μ Mo Kα calculated	μ Mo Kα found	Sample no.	μ Mo Kα calculated	μ Mo Kα found
1	3,69	3,6	8	17,61	19,0
2	7,11	7,2	9	19,30	19,5
3	8,91	9,3	10	20,25	18,9
4	9,70	10,2	11	24,78	25,2
5	12,42	13,3	12	25,89	26,0
6	14,89	13,8	13	34,48	35,5
7	17,20	18,2	14	34,30	35,5

Table 2 – Analysis of text mixtures

Matrix	Composition (%)		Found (%)
CuCl	NaCl	10,0	10,8
CuCl	NaCl	20,0	19,1
CuCl	NaCl	40,0	39,5
C	Fe	10,0	9,4
C	Fe_2O_3	10,0	9,2
Fe_2O_3+C	Fe	20,0	21,5
Fe_2O_3+C	Fe	30,0	31,4
Fe+C	Fe_2O_3	10,0	9,3
Fe+C	Fe_2O_3	40,0	38,2

Reference

Quantitative X-ray diffraction analysis by a diffraction-fluorescence technique. *Anal. Chim. Acta, 57* (1971) 289-293.

Trace and Ultramicro-Level Determination of Oxygen in C-H-O Organic Compounds

A. Colombo

The method was developed for the trace level determination of oxygen in organic coolants, after modifications of the Schütze method had proved to be unsuccessful. Briefly explained it consists in vaporizing the sample (weight less than 30 mg) in a stream of hydrogen which flows over a quartz-wool cracking catalyst at 950°C, followed by a nickel hydrogenation catalyst at 375°C, thus converting the oxygen of the sample into water which is measured by a commercial Keidel electrolytic hygrometer. Rather surprisingly the final apparatus proved to be successful without any modification, in the ultramicro analysis of oxygen-rich compounds weighing less than 0.5 mg. The typical results obtained as average of at least three determinations were the following:

Table 3 – Analysis of organic coolants

Sample	0 ppm	0 ppm (Activation Analysis)
Terphenyl mixture 1	415	205
Terphenil mixture 2	375	235
Terphenil eutectic mixture	460	320
Hydrogenated terphenyls	2515	2905
Mixture 1	1535	1325

Table 4 – Analysis of oxygen-rich compounds

Sample	0 % found	0 % theor.–(weight)
Benzophenone	8,72	8,78
Diphenilene oxide	9,59	9,51
β–naphthol	11,36	11,10
2–2' di-hydroxybiphenyl	16,75	17,18
Citric acid	58,87	58,29

The discrepancies between this and the activation analysis method are, for the moment, unexplained. Although not thoroughly tested, it seems that small and simple variations of the apparatus or of the analytical procedure should be sufficient to adapt the method for the determination of the oxygen in organic substances containing atoms other than carbon and hydrogen.

Molecular Weight and Structure Determination of Thermally Unstable Molecules

H. Knoppel, H. Schauenburg

The work on Field Desorption (FD) mass spectrometry, initiated in 1970, was continued in 1971 in order to study the detection of molecular weight and structure of thermally unstable molecules, which cannot be measured by classical MS techniques.

The method consists in dipping a very thin, specially prepared wire (tungsten, 10 μm dia.) into a solution of the substance under investigation. Inside the ion source of a MS the adsorbed molecules are desorbed as ions by the simultaneous action of a high electric field and temperature.

After a series of modifications of the combined FI/EI ion source of the CEC 21-110 mass spectrometer and improvements of the emitter introduction system, we succeeded in measuring the FD mass spectrum of a mono-nucleic acid (thymidine-5'-phosphoric acid). The protonated (quasi-) molecular ion gave rise to the most intense ion current in the upper mass range. This was the first time that the molecular ion of a nucleic acid has been detected mass-spectrometrically. The most intense of the numerous mass lines of the spectrum appeared at m/e = 99 and m/e = 127, the first of which corresponds to the ion $[P(OH)_4]^+$, i.e., to the protonated phosphoric acid ion, whereas m/e = 127 represents the protonated base (thymine). Both fragments are characteristic constituents of the molecule.

Further experiments and the experience gained from a visit to the laboratory of Prof. Beckey (Bonn University) led to the conclusion that for FD measurements the combined FI/EI ion source should be replaced by a much simpler pure FI source, in order to suppress sparking, which destroys the thin emitter wires.

Dual Flame Photometric Detector

B. Versino, G. Rossi, J. Poelman

The aim of this work was to construct and set up a dual flame photometric detector (DFPD) which allows the simultaneous selective determination of P-, S-, and Cl-containing compounds eluted from a GC Column (see Fig. 2) by "three-channels" operation. For P- and S-containing compounds, the molecular emission bands HPO and S2 at 526 nm and 394 nm respectively are measured; for Cl-containing compounds, after reaction with In, the InCl band at 360 nm is recorded.

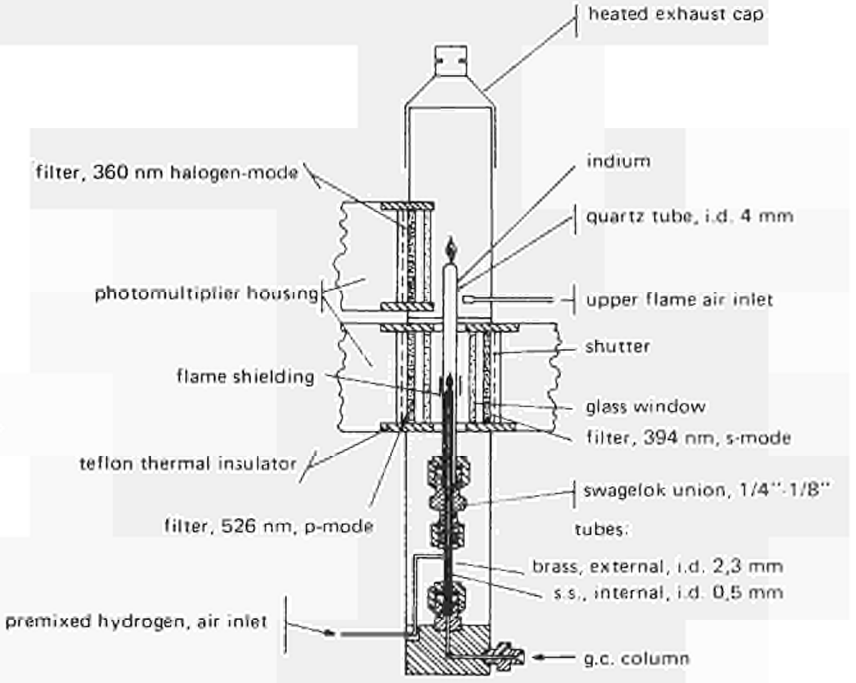

Fig. 2: Dual-flame photometric detector (DFPD).

Results

The data and characteristics of the DFPD are summarized in Table 5 in which a comparison is made with two "classic" GC % detectors: the thermionic (TID) and the electron capture (ECD). The DFPD is a selective detector allowing rapid quantitative determinations; the lack of sensitivity for Cl-containing compounds is counterbalanced by better linearity and specificity, the latter drastically reducing the number of interfering substances and thus allowing more concentrated samples to be used.

The detector seems to be particularly well suited for rapid pesticide analyses owing to the fact that it reduces the need for clean-up procedures.

The work has been fully published in CHROMATOGRAPHIA 4, 331 (1971).

Table 5 – Characteristics of the Dual-Flame Photometric Detector (DFPD)

Parameters	P-Mode	S-Mode	Halogen-Mode	TID(CsBr)	ECD (^{3}H)
Photomultiplier Dark Current (amps)	4.10^{-9}	4.10^{-9}	4.10^{-9}	—	—
Background Current (flame on amps)	6.10^{-8}	2.10^{-8}	3.10^{-7}	3.10^{-9}	3.10^{-8} standing curr.
Baseline Noise (flame on, amps)	5.10^{-10}	2.10^{-10}	1.10^{-8}	3.10^{-12}	8.10^{-12}
Detectability (gm/sec)	$1.1.10^{-13}$ methyl parath	8.10^{-12} methyl parath	$1.1.10^{-11}$ aldrin	$2.5.10^{-14}$ methyl parath	1.10^{-13} gm/ml aldrin $\cong$ 5.10 gm/sec aldrin
	$1.3.10^{-13}$ atomic P	9.10^{-12} atomic S	6.10^{-11} atomic Cl	3.10^{-14} atomic P	$\cong 3.10^{-14}$ atomic Cl
Linearity (slope of the log-log plot response vs. concentration)	10^5 (slope 1.01)	nonc. calibration straight line only (slope 1.1)	5.10^3 (slope 1.01)	$\sim 10^3$	$\sim 5.10^2$
Specificity	Response to P-compounds ~150 times that for S-compounds. No response for halogenated compounds	Response to S-compounds ~40 times that for P-compounds. No response for halogenated compounds	Response to halogenated compounds (Cl) ~100 times the interference signals from S and P-compounds	Response to P-compounds ~1000 times that for S-compounds, N-compounds and halogenated compounds	Response to all electroncapturing compounds
Gas Flows (ml/min) N_2 (GC-column carrier)	35			40 (He)	40
H_2	~220	premixed, lower flame		20	–
Air	~200	premixed, lower flame		160	–
Air	~500	upper flame only		–	–
Flame extinguishing (sample injection)	> 10 µl			> 10 µl	–

Thin Layer Chromatography

F. Geiss, H. Schlitt

The aim of this work was to use our experience gained in the field of liquid-solid chromatographyin the last ten years, proposing the Thin Layer Chromatography (TLC) which is a very dynamic, but less efficient separation technique for selecting the separation conditions for the more static but highly efficient Column Chromatography (CC). Moreover, the CC allows easy recovery of separated compounds for further identifications and offers the possibility of using detectors for quantitative determinations. There is no lack in the literature of proposals for transfer formulae, but already their number and different results show that there is still some want of clarity in this field.

Therefore, starting with well defined separation conditions in TLC and taking identical stationary phases as the basis for TLC and CC, we developed a transfer formula whose validity has been checked by using a separation of six dyes in TLC under two different conditions and transferring the respective results to a column.

The agreement of the values precalculated from TLC with those measured in CC is shown in Fig. 3. At the same time we noted the decisive influence of the column wall material. Only the use of glass columns permits the separation of dyes on Kieselgel 60 as the stationary phase with good resolution. The influence of the column wall was less important when using stationary phases with other characteristics. This work will be published in the Journal of Chromatography.

Fig. 3

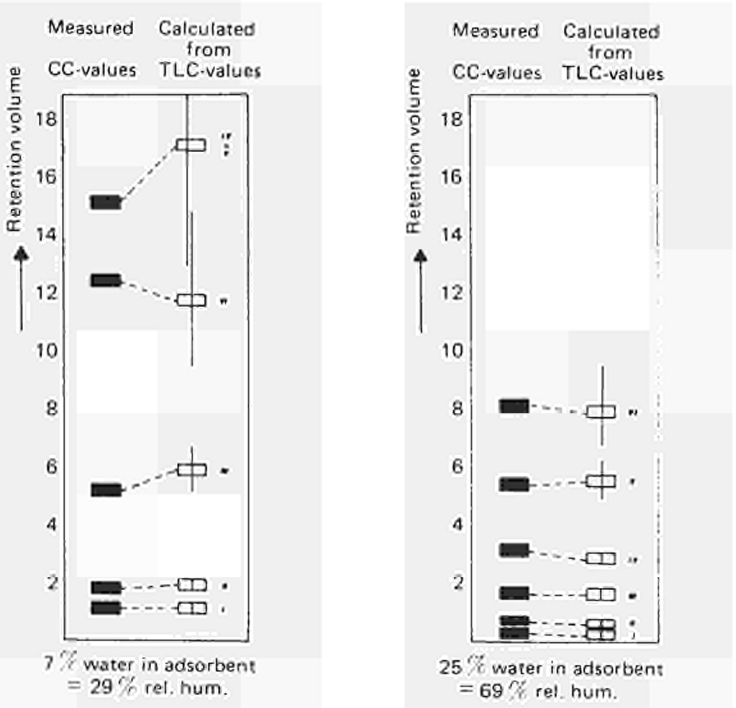

Pulse Polarography, Voltametry and Electrodialysis Developments

H. Muntau, R. Cenci

Separation and identification of the physicochemical forms of heavy metals in natural waters

In order to predict the migration of heavy metals along the "ecological chain", information about their physicochemical state in the aquatic environment is needed. The aim of the study is to collect information concerning several heavy metals that show poisoning effects on aquatic organisms, for example, Co, Zn, Cd, Pb and Cu.

The following results have been obtained:

Electrodialysis

The prototype electrodialysis cell equipped with the ion-exchange membranes purchased recently from Water Softeners Ltd. has been constructed. As the determination of Co in the different fractions presents considerable difficulties owing to the extremely low concentration level (< 0.1 ppb), Zn was chosen as a test element, for which a rapid and simple pulse polarographic method has been set up. From the first series of experiments a separation factor of about 42% was calculated.

Determination of "ionic" lead in natural waters

The total and the "ionic" lead present in the water of Lake Maggiore were determined by pulse polarography after enrichment of the "ionic" lead with the aid of the chelating ion-exchange resin "Chelex 100". The total lead was determined with evaporation of the unfiltered water in quartz containers, mineralization of the residue with perchloric acid, and pulse polarography. Water samples from 24 sites were analysed. The "ionic" lead values vary between 2.0 and 14.0 μg/l.c; values for total lead reach 100 μg/l.c. in a few extreme cases. [1]

Determination of Cu, Pb, Zn and Cd in plants

The concentration factors for the enrichment of Pb, Cu, Zn and Cd in several species of subaquatic plants collected from heavily and slightly polluted sites of Lake Maggiore are to be determined.

The principle of the method is the mineralization of the organic matter at 300°C with the aid of sulphuric acid, and the pulse polarographic determination of Pb, Cu, Zn and Cd in the ash after the removal of silica. Each step of the procedure was checked for losses.

The method was applied to the analysis of four different species originating from both the heavily and slightly polluted sites. The results demonstrate the unequivocal dependence of the metal contents on artificial pollution, for example by galvanoplastic industries. The different plant species behave in a variable manner. The distribution of the metals is not uniform throughout the single plant specimen. [2]

Development of a sessile-drop technique in anodic-stripping voltammetry (ASV)

Conventional electrodes used in ASV suffer from diffusion of amalgam species, formed by the reduction of the depolarizer at the surface of the mercury electrode, into the bulk of the electrode, thus decreasing the sensitivity of the method and causing a "memory" effect of the electrode. The aim of the study was the construction of an electrode from which the amalgams can be readily stripped off and which will not suffer from leakage effects.

A microcell consisting of a sessile drop electrode attached to a smooth platinum micro-contact has been constructed. The contact is sealed into a pedestal-like glass support, which is sealed to the bottom of the micro-cell. Stirring is effected by a constant stream of argon bubbles, and the contact to the reference electrode by the usual micro-salt bridge. The equipment has been used for a direct determination of Cu, Pb, and Zn in water from Lake Maggiore. [3]

Site	Metals found μg/L		
	Cu	Pb	Zn
Angera	5,6	11,2	54,9
Ranco	7,8	6,2	68,3
Ispra	9,6	13,1	107,8
Monvallina	12,4	7,1	233,0

References

1) H. Muntau, M.A. Castiaux, "The determination of "ionic" lead in natural waters", in preparation.

2) H. Muntau, R. Gommes, "The distribution of heavy metals in the subaquatic flora of Lake Maggiore, in preparation.

3) H. Muntau, "Die Direktbestimmung einiger Schwermetalle in natürlichen Wässern mit Hilfe der "Sessile-Drop-Technique", in preparation.

BIOLOGY


ENVIRONMENTAL CONTAMINATION
RADIATION BIOPHYSICS
BIOCHEMICAL EFFECTS

BIOLOGY DIVISION

K. Gerbaulet

Under the Commission's established programme the biological research done in 1971 at the Joint Research Centre, Ispra, was conducted along the following three lines:

1. Comprehensive studies of risks arising from environmental comtamination by radioactive and other pollutants, based on the knowledge of the mechanisms involved in their transfer in both the food chain and ecological systems.
2. Studies on the biochemical effects of ionizing radiations and/or chemical products on isolated systems of fundamental biological importance.
3. Experimental and theoretical studies in the field of radiation biophysics and microdosimetry.

The corresponding activity reort covering the research carried out during the reference period is published separately by the Commission's Biology Division of the Directorate General for Industrial, Technological and Scientific Affairs.

Nevertheless, it was deemed worthwhile to add to the annual report of the Joint Research Centre three selected topics typical of the work various scientists are involved in and describing the facilities available in the Division.

The biological work was flexibly organized using the multiple scientific competence of the various staff members, together with the technical facilities in specific time-limited projects which – in their present state – are schematically presented in the following organization chart:

Biology Division Functional Organization chart

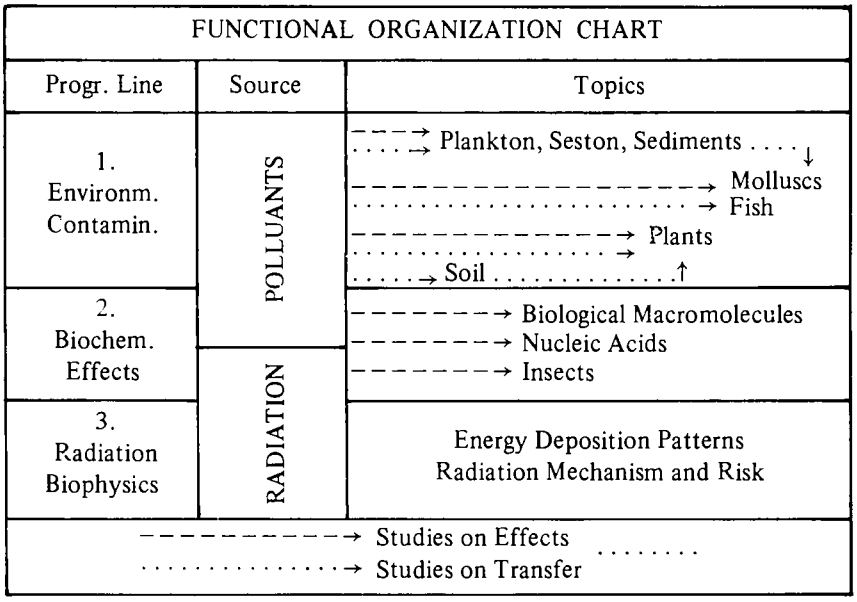

It should be emphasized here that the biological research is considerably assisted by the close collaboration with the multidisciplinary Divisions of the Joint Research Center and by the availability of fellowships and student grants. As to the latter, an average of 14 students and 14 post-graduate Fellows, from Five Member States, worked in Biology in 1971, for training and secialization purposes. Six of them obtained their doctor's degree.

Part of the research work was carried out in collaboration with the EURATOM/ITAL Association (Netherlands), under a subcontract with the French Atomic Energy Commission (CEA), and within the context of the European Dosimetry Program.

During 1971, the Third Symposium on Microdosimetry was organized at Stresa, Italy, with the aid of the Brussels Headquarters, and was attended by experts from over 15 different countires. Another Workshop Meeting in the domain of "Radiosensitivity and Repair" was held at the Joint Research Centre.

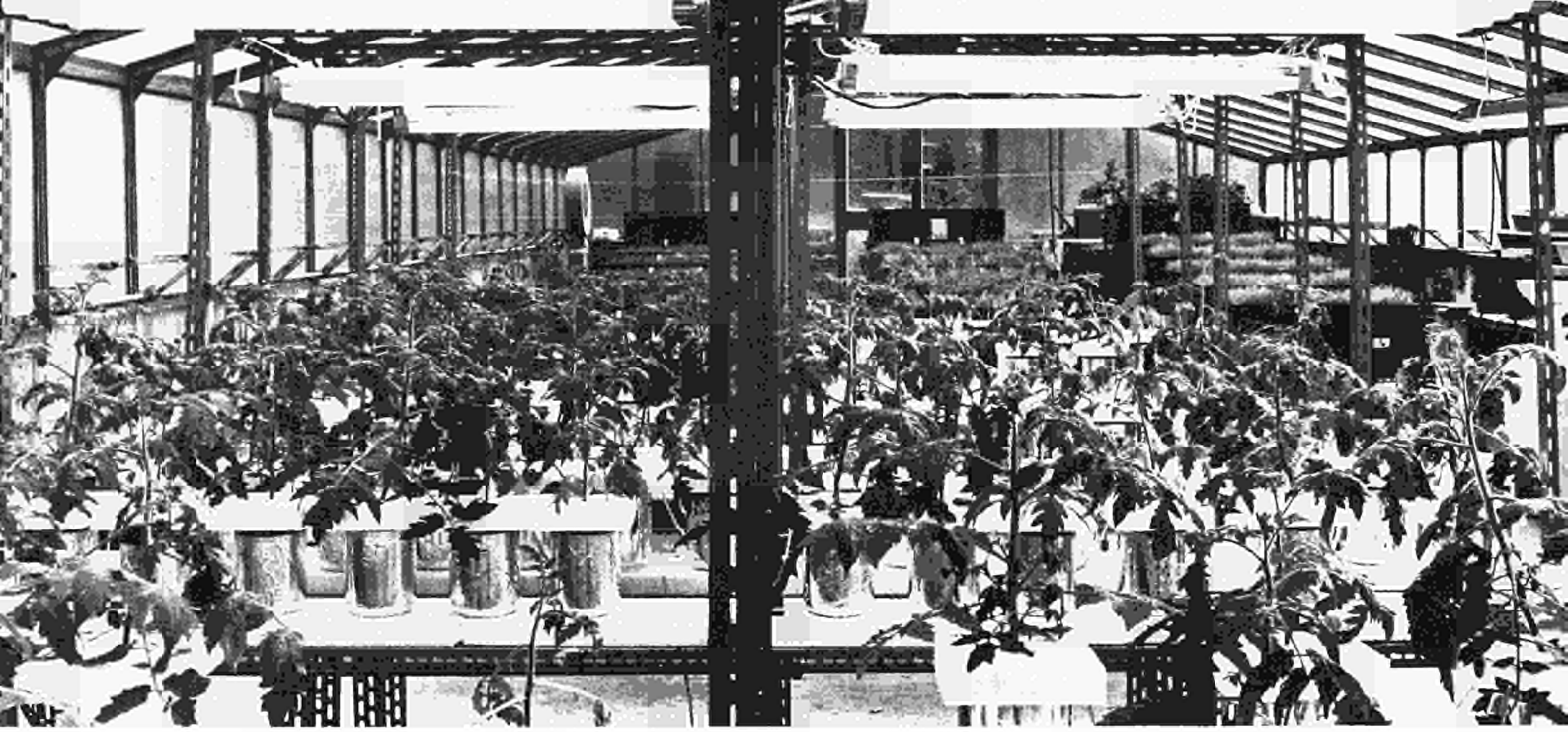

INTERACTIONS OF FOREIGN COMPOUNDS WITH MACROMOLECULES OF FUNDAMENTAL BIOLOGICAL IMPORTANCE

N. Bertazzoni, K. Gerbaulet, H. Ott, J.F. Scaife, P. Scoppa

Introduction

There is little doubt that many diseases hitherto regarded as spontaneous are caused by chemical products. This fear is heightened by the rapid and progressive increase in human exposure to new synthetic chemicals, which in general are inadequately characterized toxicologically, quite apart from ecological effects. It is therefore indispensable to develop methods for anticipating and detecting hazards.

A new line of research in modern toxicology is the study of interactions of foreign compounds with biological macromolecules. Toxicological research on pollutants and new synthetic chemicals is generally performed under the pressure originating from immediate need to solve particular problems. This approach does not usually provide principles valid for general application. At present, the number of chemicals which are a potential hazard to man is increasing at an alarming rate. Every problem is studied individually by applying tests of traditional toxicology to a large number of animals and for a sufficiently long period of time. Valid extrapolation to man can be done only if there is the basic knowledge of mechanisms by which the normal pathways of biochemical processes occurring in the organism are altered. The need, then, is for a direct approach to the mechanisms by which foreign compounds interact with simple biological systems, such as macromolecules of fundamental biological importance.

The occurrence of interactions with plasma proteins extends over a wide range of substances. The binding of small molecules to the blood vehicles modifies the diffusibility of bound chemicals and consequently impedes their exchange through haemato-tissular barriers. The biological activity of a foreign compound is related to its plasmatic concentration in unbound form. The plasma proteins may have one or more binding sites for the same substance, which may be independent or interact with each other. Pharmacological studies have shown the tremendous importance of competition between one drug and another, and between drugs and foreign compounds, for the binding with plasma proteins. Thus the magnitude of biological effects depends largely on the quantitative and qualitative characteristics of the binding.

Interactions with enzymatic systems have a particular importance, mainly for the effects on nucleic acids synthesis and metabolic detoxification processes. Impaired synthesis of genetic material may result in carcinogenic, mutagenic and teratogenic effects. Alterations of drug-metabolizing enzyme systems modify pharmacokinetic parameters and induce non negligible risks in the case of therapeutic treatments.

The studies on the interactions of foreign compounds and their metabolic products with nucleic acids provide preliminary information on the potential hazards resulting in genetic effects. This type of research, up to now performed mainly with alkylating agents and antibiotics, shows that foreign compounds may interact with DNA, binding themselves on several sites of the DNA molecule. The occurrence of interaction and the parameters which characterize the binding are therefore useful information for deciding whether further studies, expensive and of long duration, on more complex biological systems will be needed. On the other hand, the knowledge of the sites of interaction and the chemical groups involved may provide basic information for the introduction of suitable modifications in the structure of the foreign compound, in such a way that the derivative obtained can no longer interact with the DNA molecule.

Such preliminary "in vitro" studies are in line with Recommendation 621 of the Consultative Assembly of the Council of Europe, on the problems arising out of the use of live animals for experimental and industrial purposes.

Work performed

A pilot study was done on the interactions of aflatoxin B_1 with macromolecules of fundamental biological importance. The aflatoxins, metabolic products of some strains of Aspergillus flavus, are among the most potent carcinogenic and toxic agents. These mycotoxins were chosen for the pilot study since they are implicated as contaminants in human and animal foodstuffs. Their great importance is shown by more than 2000 reports published since the discovery of aflatoxin in 1962.

Preliminary work consisted in a careful examination of the recent literature on aflatoxins [1], establishment of the most suitable materials for handling aflatoxin solutions without losses by adsorption [2], development of a sensitive fluorometric method for quantitative determination of aflatoxin B_1 in aqueous solutions [3], and biosynthesis of carbon-14 and tritium labeled aflatoxins [4].

In the course of the studies on the interactions of aflatoxin B_1 with serum albumin and with deoxyribonucleic acid, the following techniques were applied: low-shear viscosimetry, equilibrium and dynamic dialysis, ultrafiltration and diafiltration, differential spectrophotometry, fluorescence quenching and polarization, zonal, frontal, equilibrium and affinity chromatography.

Effects on the activity and induction of microsomal drug-metabolizing enzymes of rat liver were tested with three different substrates: hexobarbital (hydroxylation of aliphatic side chain), benzopyrene (hydroxylation of aromatic ring), aminopyrine (N-demethylation). Indicators of induction, such as cytochrome b_5 and cytochrome P-450, were determined by differential spectrophotometry.

Results

The occurrence of interaction between aflatoxin B_1 and serum albumin was shown by differential spectrophotometry [5] and frontal elution chromatography [6]. An apparent association constant of 10^4 litre $mole^{-1}$ was calculated from data obtained at 25°C in 10 mM phosphate buffer at pH 7.4. Increases of temperature and/or ionic strength result in a lower value of association constant. Binding occurs rapidly and does not require preliminary incubation: it is fully reversible, as shown by exhaustive dialysis and zonal chromatography on Sephadex columns.

Biliary excretion of aflatoxin B_1 and its metabolites [7], as studied in the rat, accounts in 6 hours for about 25% of the dose administered (60 μg/kg, i.p.): the maximum excretion rate occurs 90 minutes after dosing. After this time, the excretion rate decreases slowly, propably because a certain amount of aflatoxin is bound to plasma proteins and not readily available for metabolic transformations. This hypothesis is in good agreement with the results obtained from further studies on hepatic metabolism of aflatoxin, performed in isolated and perfused rat liver [8]. The existence of a weak binding between aflatoxin B_1 and serum albumin suggests that transport, metabolism and biological activity of this mycotoxin can be easily modified by other foreign compounds competing for the binding sites of plasma proteins.

Aflatoxin inhibits only slightly the metabolism "in vivo" of hexobarbital. In rats pretreated with a sublethal dose of aflatoxin B_1 (3 mg/kg, i.p.), there is no significant change at 12 and 24 hours, whereas the prolonged hexobarbital narcosis at 24 hours shows the existence of impairment of hepatic function. The opposite temporal pattern was observed in animals induced by treatment with phenobarbital: the induction phenomenon is inhibited at 12 and 24 hours, and not affected 48 hours after administration of sublethal doses of aflatoxin B_1. These results of "in vivo" experiments suggested more detailed biochemical studies to measure the concentration of indicators of induction and the levels of some drug-metabolizing enzymatic activities. Investigations were performed on the microsomal fraction of rat liver: the concentrations of cytochrome b_5 and cytochrome P-450 were determined, as well as the levels of hexobarbital hydroxylase, benzpyrene hydroxylase and aminopyrine demethylase. The results obtained [9] show that aflatoxin,

administered at the same time as the inducing agent, markedly inhibits the neosynthesis of drug-metabolizing enzymes. The effect is of limited duration: after 48 hours, when most of the mycotoxin has been metabolized and excreted, the induction phenomenon is not significantly altered. The inhibitory action could then be due to a blockage of the synthesis of enzyme protein, resulting from interaction of high concentrations of aflatoxin wwith the DNA molecule. The strict similarity between the behaviour of actinomycin D and aflatoxin B_1 (interaction with DNA, inhibition of DNA - and RNA - polymerases etc.) suggests that the inhibition of induction of drug-metabolizing enzymes occurs at the level of RNA synthesis.

To investigate the effects of aflatoxin on nucleic acid synthesis, the interaction of the mycotoxin with DNA was studied by gel filtration methods[10]. In fact, the primary effect on nucleic acid synthesis is the formation of an association product with the DNA molecule. The structural modification of DNA results in the inhibition of DNA-dependent RNA synthesis, and then frmation of DNA - and RNA - polymerases is inhibited by this mechanism. Several investigations "in vitro" on the aflatoxin-DNA system have been performed, but there does not exist good agreement between the results obtained by different authors. Recently a marked effect of light on the extent of interaction between aflatoxin and DNA has been observed. The photodecomposition of aflatoxin B_1 occurs relatively rapidly in aqueous solutions and the resulting products can interfere in the measurement of the association constant for the aflatoxin-DNA complex. The use of equilibrium methods, based on gel filtration on Sephadex columns, allowed the experiments to be carried out in a short time, avoiding exposure to light. The apparent association constant, calculated from the data obtained at 25°C in 10 mM phosphate buffer at pH 7.4, is 234 litre mole;1 [11]. This value is in good agreement with that obtained by improved fluorometric methods and much lower than those previously calculated from dialysis and differential spectrophotometry. Increases of temperature and/or ionic strength result in lower values of the apparent association constant. Magnesium ions, at millimolar concentration, markedly reduce the extent of the interaction. These effects are probably due to structural modifications of native DNA, resulting in stabilization of the double helix and changes of hydration characteristics. The approximate values of some thermodynamic parameters of the interaction were calculated and the following conclusions were reached. The interaction between aflatoxin B_1 and DNA is weak and readily reversible; it is characterized by an apparent association constant much lower than those calculated without avoiding exposure to ambient light. It is therefore assumed that photodecomposition products of aflatoxin B_1 interact to a higher extent with DNA. Increases of ionic strength and presence of magnesium ions inhibit the interaction. The association reaction is exothermic and it is then favoured by lowering the temperature. The evaluation of enthalpy change, despite severe limitations, suggests that hydrophobic bonds are involved in the formation of association products.

Further studies on the effects of light on the aflatoxin-DNA system were performed [12]: preliminary results show that after exposure to UV light the association constant is increased and a small fraction of photodecomposition products or unmodified aflatoxin is linked to DNA by covalent binding.

The effects of aflatoxin B_1 on DNA were investigated by enzymatic methods [13] with the aid of the terminal deoxynucleotidyltransferase isolated from calf thymus. The unprimed and primed reactions catalysed by the terminal deoxynucleotidyltransferase were studied. The presence of aflatoxin in the unprimed reaction results in a reduction of the normal lag period, making the polymerization start earlier than in the control. The effect is proportional to the concentration of aflatoxin. The priming activity of native DNA preincubated with aflatoxin is not modified after short incubation and is highly increased after 6 and 24 hours of incubation. The information obtained with the unprimed reaction experiments would suggest that aflatoxin does not impair the mechanism of the poly-dA synthesis, whereas other mutagenic drugs which bind strongly to DNA are known to inhibit completely the process of polymer formation without the presence of an initiator. This means that aflatoxin does not act by intercalating between successive base pairs of the double helix. The effect on the terminal transferase primed reaction is difficult to explain. The highly increased initiating activity of the native DNA incubated for prolonged periods of time with aflatoxin should stand for the production of new 3'-OH initiating sites resulting from breakage of the phosphodiester bond. From this aspect the drug appears to be radiomimetic. These data are confirmed by the studies on the effect of aflatoxin on DNA viscosity, as measured by rotating low-shear viscosimetry. At very low ionic strength, incubation of native DNA with aflatoxin brings about a drop in viscosity of about 20-40%. The effect is produced only after prolonged incubation and is strictly dependent on the ionic strength; in 10 mM buffer it is not detectable at all.

The cytotoxic mode of action of aflatoxin was evaluated in mammalian cell cultures [14]. Prolonged exposure of synchronized cell cultures to aflatoxin B_1 results in retarded passage through the S-phase and decreased rate of DNA synthesis. Consequent to this, mitosis is also inhibited. Rat liver cells are very sensitive to aflatoxin: "in vivo" synthesis of RNA is 74% inhibited 30 minutes after administration of aflatoxin B_1 (0.5 mg/kg, i.p.).

Conclusions

The pilot study on the interactions of aflatoxin B_1 with some macromolecules of fundamental biological importance allowed the establishment in our laboratories of several physico-chemical and enzymatic techniques for evaluating the characteristics of interactions. Gel filtration methods for studying reversible binding have been automated. [15] Further developments and improvements of methodology are in progress.

The results obtained show that aflatoxin interacts with serum albumin and with DNA, but does not affect to a large extent the activity of drug-metabolizing enzymes. Induction by foreign compounds, resulting in "de novo" synthesis of these enzyme systems, is however inhibited by sublethal doses of aflatoxin B_1. Both the concentration of free mycotoxin in the animal organism and its transport and biological activity can be easily modified by changes of physico-chemical parameters, as well by the administration of other foreign compounds. These latter can act by different mechanisms: they can displace the weakly bound aflatoxin from plasma proteins or affect the rate of its metabolism by inducing or inhibiting drug-metabolizing enzymes. Since aflatoxin is inactivated in the organism by hydroxylation and O-demethylation, competition phenomena by other foreign chemicals will result in a prolonged action of the toxin. At high dosage the inhibition of specific protein synthesis, i.e., the induction of drug-metabolizing enzymes, shows that it is impossible to accelerate the metabolism of aflatoxin by administration of inducing chemicals; such a treatment can be effective only when the toxin is present in low concentrations. The occurrence of interaction with DNA provides an explanation for the well-known carcinogenic effect and for the inhibitory action on nucleic acids and protein syntheses.

The conclusions reached from these studies are in good agreement with those originating from research performed on more complex biological systems, such as cell cultures, perfused liver, whole animals.

The pilot study on aflatoxin is now accomplished and final reports are in preparation. The experience acquired and the techniques established will be applied to further research on the interactions of the heavy metals involved in nuclear technology and in environmental pollution with plasma proteins, nucleic acids, and drug-metabolizing enzymes.

References

1) Scoppa P.: Selected papers on aflatoxin (1968-June 1971), with special reference to biological effects. EUR/c - IS/789/71e

2) Scoppa P., Marafante E.: Uptake of aflatoxin by plastic materials. Experientia, 27, 414, 1971.

3) Scoppa P., Marafante E.: Fluorometric determination of aflatoxin B_1 in aqueous solutions. Ann. Microbiol., in press.

4) Ott H., Pirrwitz D.: Preparation of labelled aflatoxin. Activity Report on Aflatoxin, 30 Oct. 1970.

5) Scoppa P., Marafante E.: Interaction of aflatoxin B_1 with albumin: spectrophotometric studies. *Boll. Soc. Ital. Biol. Sper.*, 47, 198, 1971.

6) Scoppa P., Borlè W.O.: Interaction of aflatoxin B_1 with albumin: chromatographic studies. *Boll. Soc. Ital. Biol. Sper.*, 47, 201,1971.

7) Scoppa P., Marafante E., Rodighero L.: Biliary excretion of radioactivity from 14 C-aflatoxin in the rat. *Boll. Soc. Ital. Biol. Sper.*, 47, 475, 1971.

8) Gerbaulet K., Gerber G.B., Brohee H., Roumengous M.: Biliary excretion and subcellular distribution of 14C-aflatoxin B_1 in the isolated perfused rat liver. In preparation.

9) Scoppa P., Marafante E.: Effect of aflatoxin B_1 on induction of microsonal drug-metabolizing enzymes of rat liver. *Boll. Soc. Ital. Biol. Sper.*, 47, 198S, 1971.

10) Scoppa P., Marafante E.: Gel filtration methods for studying interactions between DNA and organic compounds of low molecular weight. *Boll. Soc. Ital. Biol. Sper.*, 46, 249S, 1970.

11) Scoppa P., Marafante E.: Chromatographic studies on the interaction between aflatoxin B_1 and DNA. *Boll. Soc. Ital. Biol. Sper.*, 47, 197S, 1971. (Ital.)

12) Ott H., Scoppa P., Marafante E.: Effect of UV light on the interaction aflatoxin B - DNA. *Boll. Soc. Ital. Biol. Sper.*, 47, 162S, 1971. (Ital.)

13) Bertazzoni U.: Effect of aflatoxin on DNA: results obtained with enzymatic methods. Activity Report on Aflatoxin, Oct. 1970.

14) Scaife J.F.: Aflatoxin B_1: cytotoxic mode of action evaluated by mammalian cell cultures. FEBS Letters, 12, 143, 1971.

ENVIRONMENTAL CONTAMINATION STUDIES

E. Levi, C. Myttenaere, P. Reiniger

The release into the atmosphere or water of radioactive and chemical pollutants has extended the studies on terrestrial and aquatic ecosystems. Early studies aimed at determining concentrations from deposits occuring beyond man's control; later studies were designed to assess and attempt to forecast hazards and danger levels in the various components of a cyclic chain, itself formed of a number of smaller chains: the ultimate interest being not only man but also his environment.

In both terrestrial and aquatic ecosystems, studies involve not only the uptake and distribution of a pollutant by the fauna and flora as well as its behaviour in water and soils, but also the influence the environment has on these processes.

Studies in terrestrial ecosystems: Behaviour of radiocesium

Introduction

The terrestrial ecosystem studies carried out at the Joint Research Centre considered the fate of substances reaching the vegetation or the soil from the atmosphere or through irrigation, whether of the surface or spray type. Thus the studies performed can be subdivided broadly into foliar uptake and root uptake of a pollutant, including in these two groups the absorption in the first case by all the above-ground parts and in the second case by all the underground parts of plants. In both cases the physico-chemical characteristics of the substance in water and soil have to be considered.

Among the radioactive pollutants studied, cesium is typical, its stable form being present in nature in very low quantities while its radioactive isotopes were introduced into the environment by the action of man. It has been chosen here by attempt to summarize some of the results obtained so far and to describe the methods and facilities available at the Joint Research Centre for such studies of pollutants in ecological systems.

In assessing the hazards to man from contamination by cesium, studies are made in the field, under semi-controlled (greenhouse) or well-controlled environmental conditions. Samplings from the field are usually made as part of large national or international survey programmes. They are indicative of levels present in the collected samples; but in order to extrapolate, estimate or predict other situations in an efficient and reliable fashion, controlled investigations had to be carried out. These considered the total retention of cesium, its penetration and subsequent distribution in whole plants including the edible parts.

Foliar Uptake Studies

Aerial parts of plants in any ecosystem invariably come into contact with chemical substances in the atmosphere. When not penetrating as gases, these are deposited on all surfaces and may or may not subsequently penetrate into the tissues and react within the plants. If cesium in the form of dust or as a solution reaches any aerial organ of a plant, it is deposited on its surface and is retained at different rates depending particularly on the characteristics of the surfaces. These differ in their retention ability and penetrability because of morphological and/or genetical traits inherent to the species considered, and also because of the environment in which the plants grow.

Bean plants were used as indicators for a large number of dicotyledonous crops in a number of tests carried out in controlled conditions. Plants were grown in a constant optimum environment in individually aerated glass jars containing a standard nutrient solution. Treatment consisted briefly in applying a set volume of a solution of constant composition and surface tension to specific areas of leaves at definite growth stages. At set times after treatment, the fraction of the isotope not retained by the plant was washed off and measured. The plants were then harvested and separated in a number of fractions indicative for the purpose of the experiment, and the radioactivity present was measured.

Much information is now available from a large number of individual experiments. It can be pieced together and summarized as follows. The foliar uptake process can be broadly subdivided into three steps, namely, penetration, retention and transport beyond the area treated with the applied element. Cs

penetrates almost totally, with time, and more rapidly in the presence of K^+ or at high relative humidity of the air. Penetration is adversely affected by changes of air or root temperatures away from optimum growth conditions, by the presence of Na^+ or Rb^+ or by senescence of leaves. Retention in the treated area is relatively constant in proportion to the amount taken up by the plant and varies with the metabolic activity, which allows or disallows translocation to other plant parts and even root losses. Transport away from the treated area was observed by autoradiographic and analytical methods and found to have definite cycling patterns, at least in the bean, affecting only part of the plant. Generalized distribution following leaf uptake occurs much later. In general, conditions favouring an active metabolism enhance downward transport and cycling of Cs that has penetrated the leaf surfaces. Extrusion of this elment by the roots occurs even before the generalized distribution mentioned above has been completed and was found, so far, to be positively affected only by increased root temperature. Using two different isotopes of Cs, the kinetics of simultaneous foliar and root uptake of this element was determined. No interference whatever was noted.

A typical study performed was designed to ascertain the kinetics of Cs uptake by bean leaves and its fate over a one-week period. Some of the results are shown in Table 1.

*Table 1 – Distribution of Cs*Cl following its deposition in solution on a beam leaf under constant controlled conditions. Values are averages of 5 replicates and expressed in percentage of the total radioactivity applied.*

Hours after treat.	Wash in water	Wash in carrier	Penetrated in plant	Retained in tra-ted area	Found in rest of plant	Lost from roots
1	96.7	0.1*	3.2	2.3	0.2*	0.7*
2	67.8	1.0*	30.2	30.1	0.7*	0.4*
3	35.6	1.1*	63.3	61.1	1.8	0.4*
4	35.4	0.6*	64.0	61.7	2.0	0.3*
5	24.3	0.7*	75.0	71.7	3.0	0.3*
6	20.8	0.4*	78.8	74.7	4.0	0.1*
24	7.6	0.3*	92.1	76.4	13.6	2.1
48	5.2	0.1*	94.7	70.3	20.4	4.0
72	9.2	0.1*	90.7	62.6	21.5	6.6
168	1.1	0.3*	98.6	65.6	23.2	9.8

*: Not significant

Using an installation designed and built at the Joint Research Centre at Ispra, it is possible to carry out under semi-controlled conditions artificial contaminations of crops by simulating a steady rain of variable characteristics or a spray irrigation. In an experiment, for example, a crop of wheat grown in containers of 1 m^2 surface area was "spray irrigated" with water containing Cs*Cl. The treatments were carried out during different periods of the crop's life cycle. Results showed that only a very small fraction was actually retained by the whole plant material. The fraction detectable in the mature grains was less than 0.5% of the Cs* sprayed on the seeding plants. Removing the seed coats (husk) from the grains removed more than half of the measurable radioactivity. The crop in this experiment, which was treated only until flowering, had a very low concentration of Cs in its grains, accumulating there at the end of its movement within the plant after leaf and/or root absorption from the Cs* which had reached the soil by direct contamination or run-off from the plants.

Soil studies and Root Uptake Studies

The transfer of radiocesium from the soil to the plant is largely dependent on the nature of the soil. Cesium, like other cations, is present in soils in various states: in solution, adsorbed on the cation exchange sites of clay minerals and of organic matter and "fixed" at special exchange sites in the lattice of clay minerals.

Equilibrium is established rapidly and reversibly between the Cs in solution and that adsorbed; and the quantity of Cs* present in these two forms will determine that taken up by the plant. "Fixed" cesium which is adsorbed on preferential sites is not readily released to the soil solution and thus remains largely unavailable. Accordingly, the uptake of radiocesium by plants will be relatively important from sandy soils and organic soils poor in clay minerals with a high Cs "fixing" power, but it will be of secondary importance from soils with a high clay content. Other soil factors which influence the "fixation" of Cs on clay minerals are the potassium or ammonium content and possibly also the soil water regime.

Whenever present in the soil solution, an element is available for root uptake and the quantity taken up is commonly expressed in terms of percentages or so-called "concentration factors" or "transfer coefficients" representing the ratio of the element/g of plant material to the element/g of substrate. These studies, again, can be carried out under very exactly controlled conditions, or under partially controlled greenhouse or lysimeter conditions or even derived from field plots. As regards experiments in controlled or partially controlled environmental conditions, these are carried out by supplying to part or to the totality of the root system the element to be studied. The growth medium can be a well-defined soil, or again a nutrient solution containing all the essential elements in their correct or purposely altered concentrations. By using lysimeters, also available at the Joint Research Centre at Ispra, one can grow crops, including rice, under open air conditions while controlling the soil and water regime more accurately than possible in the field.

When soils are used as media for plant growth, a number of methods are available for evenly distributing the studied chemical substance in the whole mass, the main purpose being to make available to the whole root system, as uniformly as possible, the ions under investigation. One such method adopted was the spraying of a solution onto the soil and mixing it throughly before weighing out constant amounts to fill pots in which plants were grown in a greenhouse.

A number of experiments were carried out to determine transfer coefficients for cesium and their dependence on various soil factors. A crop of rye grass was first considered and a number of representative soils of the Community previously studied from their physical and chemical aspects were used as growth media. They differed widely in clay and organic matter content and the transfer coefficient for Cs-134 was shown to vary inversely with the clay content, as can be see in Table 2. At the same time a rapid soil extraction method using $Mg(NO_3)_2$ was developed, permitting a good indication of the Cs transfer coefficient as shown.

Table 2 – Uptake of Cs-134 by ryegrass from different soils of the European Community.

Soil type	Location	Organic matter %	Clay %	Cs-134 Mg-extractable %	Transfer coeff.
Terra fusca	Corato, Italy	2.9	56.5	0.42	0.020
All. Gley	Porto Tolle, Italy	2.4	41.4	0.71	0.024
Pseudogley	Ahrweiler, W. Germany	2.7	23.4	0.53	0.38
Braunerde	Allonville, France	2.9	20.4	0.92	0.046
Rendzina	Allonville, France	3.9	12.7	1.28	0.052
Podzol	Hannover, W. Germany	7.9	4.2	2.28	0.15
Fen	Emmen, Netherlands	23.3	3.0	4.31	0.30

Later work using beans as test plants gave coefficents of transfer of 0.008 for the Terra Fusca, 0.013 for the Braunerd and 0.58 for the Podzol, confirming on a dicotyledonous crop the previous findings on the influence of clay content on Cs uptake. Other studies considered the uptake of Cs by plants from soils containing different quantities of this element. The age and development of the plants were also considered. Results available show that for example in a Podzol, a tenfold increase in Cs concentration causes a doubling of the transfer coefficient. At low levels of Cs in the same soil no effect on transfer coefficients could be noted. The development of the test plant is an important factor particularly because of the limited volume of soil it can scavenge. On the same Podzol, for instance, the coefficients measured varied by a factor of two depending on the stage at which plants were harvested.

In studies of root uptake, the composition of the medium is of prime importance; but when using radioactive isotopes, the so called carrier concentration as well as the concentration of the isotope in the solution have to be considered. A typical experiment carried out on tomatoes gave results some of which are summarized in the following table.

Table 3 – Uptake of radiocesium by tomato plants from a nutrient solution containing or devoid of stable cesium. (Values expressed in nCi/g dry matter and in relative percent in plants).

Cs-137 Ci/l	0.2	0.2	0.2	0.2	10.0	10.0	10.0	10.0
Stable Cs added, ppm	–*	–	1.0	1.0	–	–	1.0	1.0
	nCi	%	nCi	%	nCi	%	nCi	%
Roots	8.6	23.7	62.1	23.5	561.0	24.3	2087.0	17.5
Stems	1.8	8.2	11.1	7.1	1o6.6	6.8	575.0	8.2
Leaves	5.8	58.5	33.3	55.2	338.0	57.6	1617.0	58.1
Fruit	1.1	9.7	7.3	14.3	50.7	11.2	360.0	10.4

*-6×10^{-5} ppm

It thus appears that, although the relative distribution in the various plant parts did not differ, the addition of "cold" cesium allowed a greater uptake.

While normal land plants require aerobic conditions for their root system, rice, through its specific anatomy, is able to thrive in flooded conditions. This is particularly interesting to consider since absorption from soil and irrigation water can occur simultaneously by the roots and the leaf bases. This was, among other reasons, why a number of investigations were carried out with this plant, and a special installation set up. It enables rice plants to be grown and treated under semi-controlled greenhouse conditions. Root absorption, base-leaf, or both or a differentiation between the two uptake possibilities through double labelling of the soil and the supernatant solution are thus possible.

Results available so far indicate the distribution of Cs in the various parts of developing rice plants. Concentration factors noted in an experiment are shown in the following table.

Plant part	Concentration factors	
	Plant/Soil*	Plant/Water+
Roots	0.572	63
Leafy shoots	0.052	111
Panicle minus grains	0.019	70
Hull	0.010	45
Caryopsis	0.005	20
	* cpm/g dry matter / cpm/g dry soil	+ cpm/g dry matter / cpm/ml irr. water

The secondary importance of the soil factors in these studies was ascertained and the concentration factors obtained between plants and supernatant water were found to be definitely higher than those obtained between the same organs and soil. The chemical composition of the water appears to play an important role here. The importance of base-leaf uptake was clearly demonstrated. Here again by using a double labelling technique it was possible to differentiate between root and base-leaf uptakes. Two isotopes of Cs were used, and results available showed that no equilibrium could be obtained between them under the experimental conditions adopted. This point is being further investigated.

Thus combining the teste'd method available it is possible, using the various facilities, to study accurately and relatively speedily the fate of an element or a substance reaching the above-ground parts of plants, the soil, or the water it is irrigated with. Experimenting in a well-controlled environment allows one additionally to reduce the number of major variables to one at a time, to repeat an experiment whatever the season, and to vary as required one or the other factor influencing the process studied.

Further experiments are in progress to determine possible constants in order to admit an extrapolation to field conditions of results thus obtained.

SPECTRAL ENERGY TRANSFER OF FAST NEUTRONS TO SMALL SPHERES OF BIOLOGICAL SIGNIFICANCE

J. Booz, M. Coppola

Abstract

Spectra of the energy imparted to spherical tissue-equivalent volumes of cellular and subcellular size (up to 6.5 μm) were measured and calculated for fast neutrons between 0.6 and 6 MeV.

The experimental spectra were obtained by irradiating a 2" Rossi-counter with monoenergetic fast neutrons of 0.62 MeV, 1.02 MeV, 2.01 MeV, 3.45 MeV, 4.44 MeV and 5.85 MeV. Two effective diameters were chosen of 6.5 and 1.0 μm respectively.

For the calculation, a Monte Carlo-program was set up and executed for the same experimental parameters by an IBM 360/65 computer.

Good correlation between experimental and calculated spectra was obtained at the selected volume sizes at least in the single event region above 5 KeV/μm. There is, however, strong disagreement in the region of smaller event sizes. This is partially due to the gamma-contamination of the neutron beam which was not considered in the calculations.

In a second step a routine was added to the original Monte Carlo-program to take into account the effect of the energy straggling of protons and alpha particles both in the counter wall and in the inner gas.

The results show that the influence of the energy straggling is already important at 1.0 μm effective diameter, mainly in the region below 5 keV/μm, and increases with decreasing diameter.

The theoretical spectra were calculated using energy-dependent W-values. Spectra which were evaluated with a constant W-value showed a greater deviation from the measured spectra.

Introduction

The radiobiological effect of a given radiation may be related to the spectral distribution of energy transferred by the radiation to small sensitive volumes in the irradiated material. The probability distribution of energy transfer by a single charged particle crossing the volume can be determined experimentally ("single event spectrum"). In these measurements the sensitive volume is simulated by the tissue-equivalent counting gas of a proportional counter with tissue-equivalent walls. The diameter of the counter is the same as the diameter of the sensitive volume to be simulated if both are measured in g/cm^2.

Several measurements of single event spectra have been made, mainly by Rossi and co-workers [1)-5)] for the special case of the irradiation of spherical tissue equivalent volumes with neutrons and gamma-rays.

These measured spectra do not yield the correct information about the energy transfer of the radiation to real tissue, owing to the following facts:

- the measured spectrum is the distribution of ionization, not of deposited energy, [9)]
- the measured spectrum is influenced by errors, which are intrinsic to the method (wall effects),
- the tissue-equivalent materials which are normally used do not have exactly the same chemical composition and consequently the same stopping power and macroscopic cross-section as the tissue itself [6)-8)].

A mathematical analogue can overcome these difficulties, if the calculation is sufficiently accurate. For this purpose a Monte Carlo-calculation can be used, taking into account all possible types of neutron reactions within the counter and determining the energy deposition of each reaction product.

In order to test the appropriateness of this procedure the ionization spectra may be calculated and compared with the measured distributions.

This report illustrates the results of measurements and calculations made at Ispra for six neutron energies between 0.62 MeV and 5.85 MeV and effective sphere diameters from 6.5 μm down.

Experimental method

Neutron production

The beam of monoenergetic neutrons was produced by a 3 MV Van de Graaff-accelerator. Neutrons of the three upper energies 3.45 MeV, 4.44 MeV and 5.85 MeV were obtained by means of the exothermic ^{2}H(d, n) ^{3}He-reaction, which has a Q-value of 3.268 MeV. In order to produce neutrons of the remaining three energies, that is 0.62 MeV, 1.02 MeV and 2.01 MeV, the endoergic ^{3}H(p, n) ^{3}He-reaction was used, having a threshold value of 1.019 MeV in the laboratory system.

The irradiation room was separated from the accelerator by a concrete wall of 90 cm thickness. The neutrons passed through a collimator with an opening angle of 1.0°. No gamma-ray filter was used at the end of the collimator. The counter was placed at a distance of 155 cm from the neutron producing target and at 46 cm from the collimator end.

Proportional counter

For the simulation of the tissue volume a spherical 2" Rossi-counter was used. The counter wall consists of a tissue-equivalent plastic material as developed by Shonka [10]. The chemical composition of this plastic is given in Table 1. The counting gas is supposed to be a mixture of 64.4% CH_4, 32.4% CO_2 and 3.2% N_2, by volume percentage, as proposed by Rossi and Failla [11].

An analysis of the actual gas gave a composition of 64.5% CH_4, 32.2% CO_2 and 3.2% N_2 with an accuracy of 0.1%.

Fig. 1 shows the design of the proportional counter. The helical wire, which serves as a guard electrode in order to ensure a uniform cylindrical field along the counting wire, is held at about 25% of the positive potential of the collecting wire.

The gas pressure is manually adjustable by means of two needle valves. During the time of irradiation the reading of the aneroid pressure gauge was continuosly minitored by means of a television camera. In addition the constancy of the gas multiplication factor was checked before and after each measurement by means of the built-in calibration source (see Fig. 1). Further details of the experimental set up are described in [9].

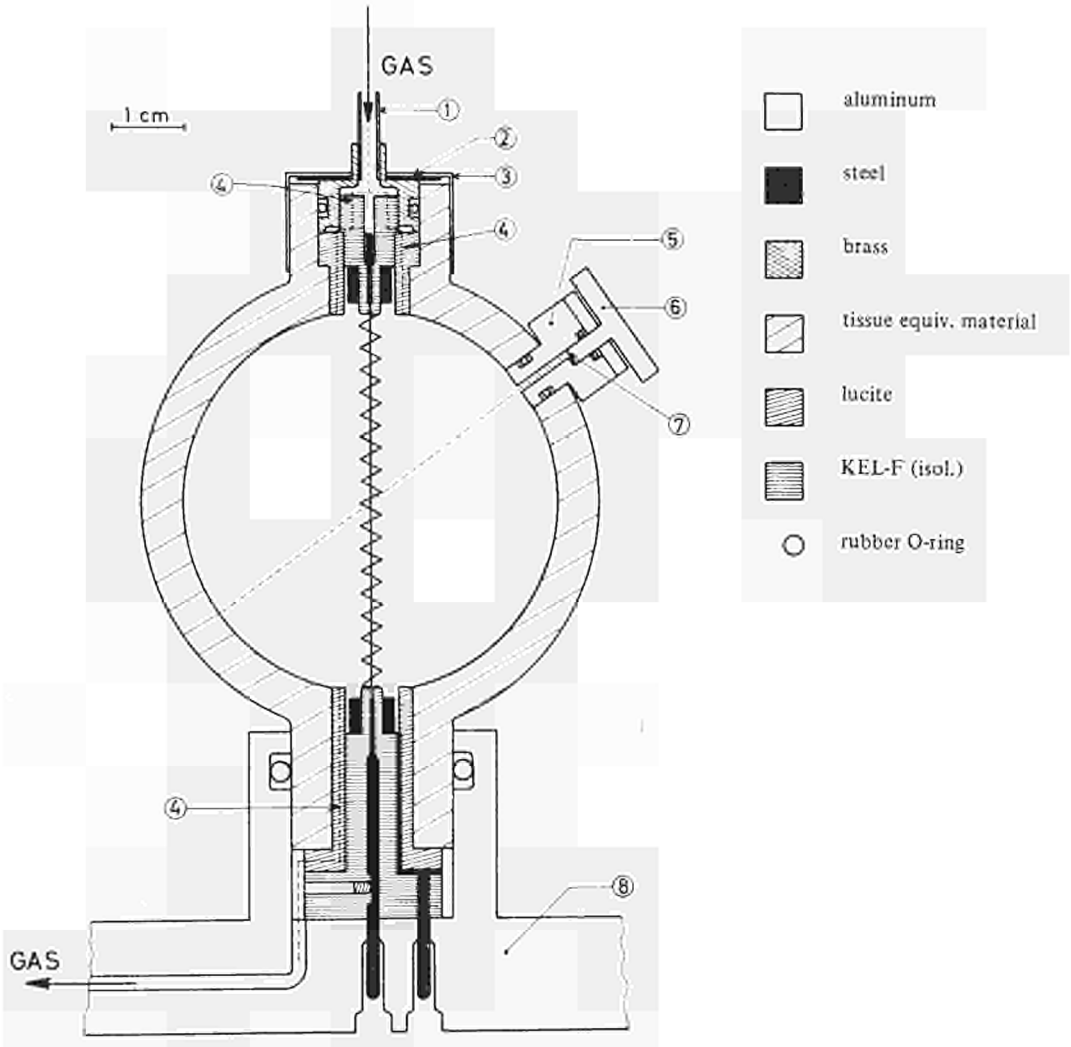

Fig. 1: Design of the proportional counter.
1: gas inlet (aluminium); 2: spring washer (steel); 3: aluminium cover; 4: these parts are slit to enable gas flow; 5: built-in alpha-source; 6: pivot; 7: ^{241}Am-preparation; 8: counter socle.

Linearity of electronics

The linearity of the complete electronical chain was tested with a ramp-mode pulse generator. The results proved the system to be linear within statistical errors between channels 26 and 999. The information stored in the channels up to 25 was discarded in all measurements.

Energy Calibration of Spectra

The proportional counter yields a spectrum linearly dependent on the ionization produced by an ionizing particle passing through the counting volume. The counter, however, does not measure directly the energy deposited by the particle in the gas volume. In order to calibrate the spectrum in terms of energy, a built-in collimated ^{241}Am-source was used. This emits alpha particles of 4.725 MeV, after preabsorption of about 14% by the gold coating. The alpha particles deposit only a small fraction of their initial energy within the counter, e.g., about 90 keV along 1.0μm and about 670 keV along 6.5 μm [7]. Therefore, for the conversion between ionization and deposited alpha energy, it is necessary to use the differential W-value of the alpha particles of the given energy.

The energy spectrum obtained by this kind of calibration is not necessarily identical to the spectrum of absorbed energy. The two spectra would be identical only if the Fano-fluctuation could be neglected, and if the differential and the absolute W-value for all types of charged particles of various velocities were equal to the differential W-value of alpha particles of 4.725 MeV.

This holds generally for electrons [11) 12)], possibly also for protons and alpha particles of sufficiently high velocity [13)] ($v \geqslant 10\, v_0$, $v_0 = e^2/h \approx 2.2 \cdot 10^8$ cm/s), but normally it does not hold for velocities smaller than $10\, v_0$ (see Leake [14)]).

Calculations

Monte Carlo-Program

For the calculation of the energy absorption in spheres a Monte Carlo-program was set up in FORTRAN IV [9)]. The program - hitherto called ENSFERA-0 - used the techniques of statistical weights and importance sampling and simulated all radiation-induced processes within the counter. Table 1 gives a survey of the possible neutron reactions in the counter wall and in the counter gas.

The history of a neutron is ended either by an absorption reaction or when its statistical weight falls below a fixed value.

The primary result of the calculation is the spectral distribution of the energy, which is deposited in the gas-filled counting volume by the neutron-produced secondary ionizing particles. In order to obtain an ionization spectrum, which can be compared with the measured one, the deposited energy has to be converted into ionization. This conversion is done for each single event using an energy-dependent W-value (formula of Neary et al. [15)]). The details of the conversion are analysed and discussed in [9)].

To proceed with the calculations a second version, ENSFERA-1, of the Monte Carlo program was established. This version differs from the previous one mainly by taking into account the energy straggling of the secondary produced charged particles both in the counter wall and in the counting gas. In fact this procedure was limited to protons and alpha particles since on the one hand they are by far the most numerous contributors to the energy transfer process, and on the other hand the heavier ions are significant only above 100 keV/μ [17)], where the influence of energy straggling is small. The relative variance $\tau\epsilon/\epsilon$ is about 2% at $\epsilon \approx 600$ keV (see Fig. 8).

Table 1 – Neutron reactions with the atoms of the counter (X signifies that the corresponding reaction is considered in the calculation; – means that the reaction is not possible below 5.85 MeV).

Element	Number of atoms per cm. barn	(n, n)	(n, γ)	(n, p)	(n, t)	(n, α)	(, n'γ)
H	$6{,}56\ 10^{-2}$	x	x	–	–	–	–
C	$4{,}08\ 10^{-2}$	x	x	–	–	–	x
N	$1{,}61\ 10^{-3}$	x	x	x	x	x	x
O	$2{,}06\ 10^{-3}$	x	–	–	–	x	–
F	$6{,}64\ 10^{-4}$	x	x	x	–	x	x
Si	$2{,}28\ 10^{-4}$	x	x	x	–	–	x
Ca	$3{,}32\ 10^{-4}$	x	x	x	–	x	x

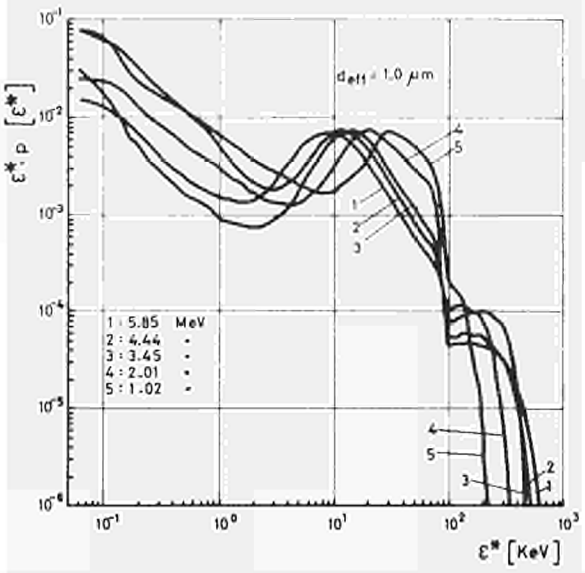

Fig. 2: Probability p (ε) of energy deposition as function of the deposited energy ε* for 1.0 μm effective diameter.*

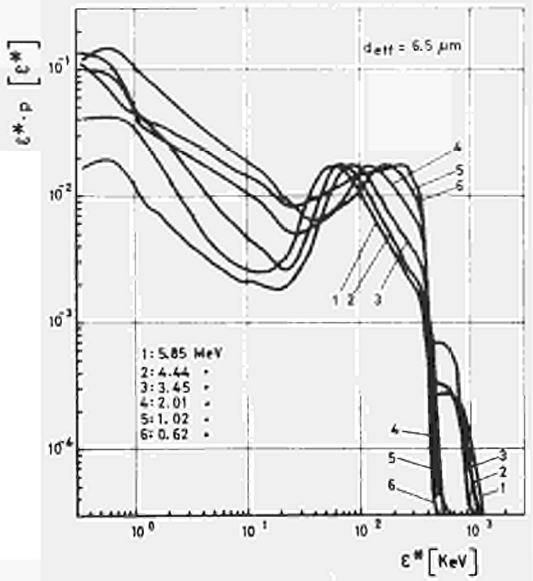

Fig. 3: Probability p (ε) of energy deposition as function of the deposited energy ε* for 6.5 μ effective diameter. Probability in relative units.*

Energy Straggling

It is well known that the energy straggling phenomenon is quite complex and therefore it is rather difficult if not impossible, to describe in a precise way this effect for particles which can lose anything from zero percent up to a hundred percent of their initial energy. In the region of small energy losses, the so-called stochastic region, the particle energy spread can at first be neglected and the effect can be formally described using the laws of statistics for independent events. In the region of higher energy losses, the so-called bulk region, the effect is strongly influenced by the shape of the probability distribution of the events themselves.

The consequence is that in the stochastic region it is possible to give a mathematical expression for the shape of the energy spectrum and the spread, while in the bulk region the theory [23) 24)] gives at most numerical values of energy spread and distribution skewness, each value depending on the particular charged particle, incoming energy and final energy loss.

To overcome such a difficulty it was decided to simplify the problem, first by disregarding the asymmetries of the straggling affected energy spectra, and second by using a kind of semi-empirical law which would satisfy with a reasonably small inaccuracy the behaviour of the increasing energy spread with increasing energy loss. The first simplification is justified by the fact that for small energy losses (Vavilov parameter $\kappa \ll 10$, see, e.g., [21)]) the straggling has practically no influence on the shape of the measured distributions, while the theoretical calculation shows that for very large energy losses the asymmetry of the distribution stays small [24)].

Neutron Reaction Data

The main source of data concerning neutron reaction parameters, such as reaction cross-sections and elastic angular distributions, was the data library of the GAM II-code of General Atomic [18)].

The angular distributions after reactions other than elastic scattering were assumed to be isotropic, in the centre of mass system.

Results and Discussion

Experimental Spectra

Figs 2 and 3 show the measured probability distributions for the two effective diameters of 1.0 and 6.5 μm. The independent variable ε* is proportional to the ionization and is not identical to the deposited energy ε, as explained earlier. For comparison, the curves are normalized to the same value of the maximum above 10 keV.

The maximum of each curve is mainly influenced by the protons. The sharp decline of the spectrum at about 90 keV/μm is due to protons of maximum LET. In the region above 90 keV/μm only the heavier ionizing particles (e.g., alpha particles, C-, N-, O-recoils) contribute to the spectrum [17)].

Table II: Ratio $N_g : N_n$ (number of gamma rays per number of neutrons) for different neutron energies.

Nuclear reaction for neutron production	$^2H(d,n)^3He$			$^3H(p,n)^3He$
neutron energy (MeV)	5.8	4.2	3.5	1.0
$N_g : N_n$	3 : 1	1 : 1	1 : 3	> 20 : 1

Control measurements made with a liquid scintillator in order to check the portion of gamma-rays indicated a relatively high gamma contamination of the used neutron beam. Table II shows the ratio of the number of photons N_{ph} and the number of neutrons N_n for different neutron energies.

The photons may either set electrons in motion by photoelectric effect or produce compton scattering. These electrons produce events in the low energy region. The electron range in tissue amounts to 1 μm at an energy of 5.5 keV and to 6.5 μm at an energy of 16.9 keV (Cole [19]). The maximum energy deposition of electrons lies, therefore, in this order of magnitude.

Consequently, in the region of small values of ϵ^* (about 3-6 keV/μm) the experimental curve shape is not representative for neutron single event spectra.

Calculated Spectra

Figs 4-6 show some of the normalized experimental single event spectra (straight line) and the corresponding ionization spectra calculated with ENSFERA-O (histogram). The ordinate of the calculated spectra is multiplied by a constant, which is chosen in such a way that calculated and measured spectra have the same total event probability in the supposed region of correspondance (that is, above a boundary energy which is marked by an arrow in the figures). One sees that in the range of small event sizes the measured event probabilities are considerably higher than the calculated ones. This difference is to be expected qualitatively, because the Monte Carlo-program simulates an irradiation with monoenergetic neutrons only, and does not take into account the influence of the gamma-ray contamination, or the low energy tail of the primary neutron spectrum, which is due to the presence of the collimator. In fact, at low values of ϵ^* the spectra calculated with ENSFERA-O are mostly due to delta-ray events. In the region of higher energies, above about 5 keV/μm, there is satisfactory agreement between calculated and measured spectra. In this energy region, therefore, the results of the Monte Carlo-calculation are believed to be valid.

The remaining difference at the high energy end between experimental and calculated spectra is at maximum about 10% (see Fig. 5). This deviation is possibly due to incorrect mass stopping power values of the heavy ions. It cannot be excluded, furthermore, that the neutron cross-sections and the used

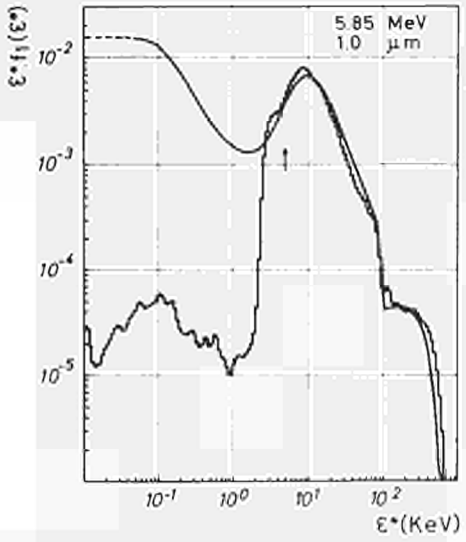

Fig. 4: Calculated (histogram) and measured event probability f_1 (ϵ^*) for 5.85 MeV neutron energy and 1.0 μm effective diameter. Both spectra have the same total event probability above the energy denoted by an arrow. Calculation without energy straggling.

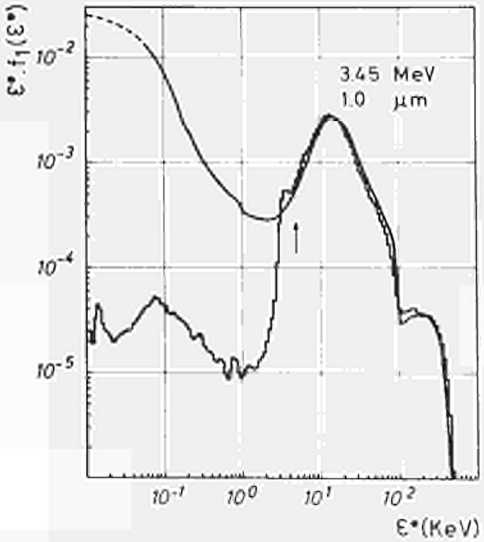

Fig. 5: Calculated (histogram) and measured event probability f_1 (ϵ^*) for 3.45 MeV neutron energy and 1.0 μm effective diameter. Both spectra have the same total event probability above the energy characterized by an arrow. Calculation without energy straggling.

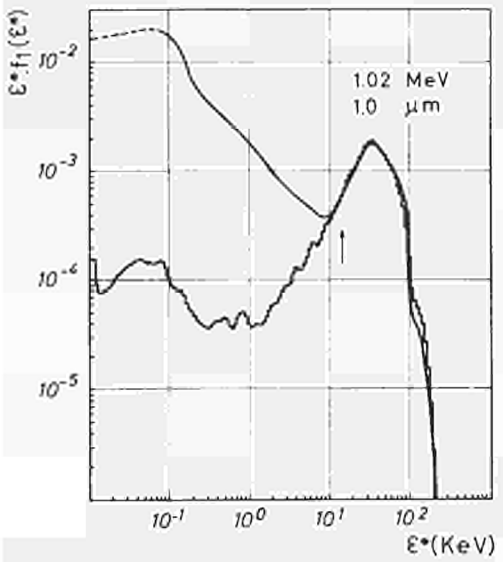

Fig. 6: Calculated (histogram) and measured event probability f_1 (ϵ^*) for 1.02 MeV neutron energy and 1.0 μm effective diameter. Both spectra have the same total event probability above the energy characterized by an arrow. Calculation without energy straggling.

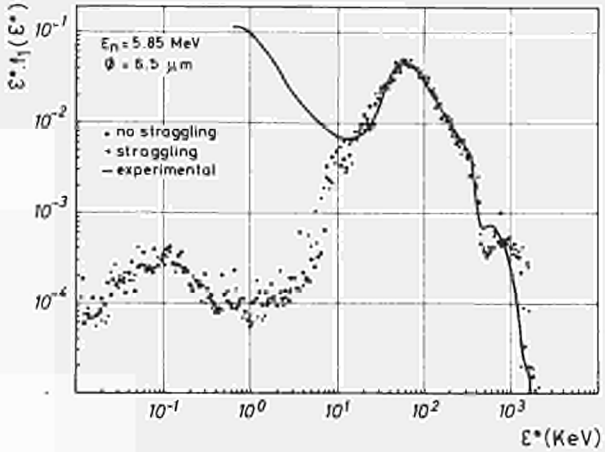

Fig. 7: Measured and calculated distributions of ionizations for 5.85 MeV neutron energy and 6.5 μm effective diameter. The calculated spectra (circles without and crosses with energy straggling) are normalized. The experimental spectrum has the same total event probability as the calculated spectra above the energy characterized by an arrow.

dependence of the W-value [15] are perhaps not quite correct and contribute to this deviation. The energy straggling, however, is negligible in this region, as has already been explained. Also the counter resolution and the ionization fluctuation (about 0.8% at $\epsilon^* = 500$ keV [22]) is smaller than the channel width of 3% and cannot account for the observed difference.

The comparison between the results of the calculations made with the two versions of the Monte Carlo program described is shown in Figs 7-9. It is evident that the influence of the straggling on the shape of the ionization spectrum is negligible at an effective diameter as large as 6.5μm. It is still not too relevant at 1 μm, except in the region below 3 keV/μm. This region, however, could not be explored in the present measurement owing to the reasons mentioned before. At effective diameters below 1.0 μm the influence of the energy straggling becomes larger with decreasing diameter, and changes considerably the overall shape of the distribution of the ionization events.

As to the comparison with the experimental results, the shape of the 1.0μm spectrum including straggling appears, as expected, in better agreement with the measured distribution than the spectrum without straggling (see Fig. 8).

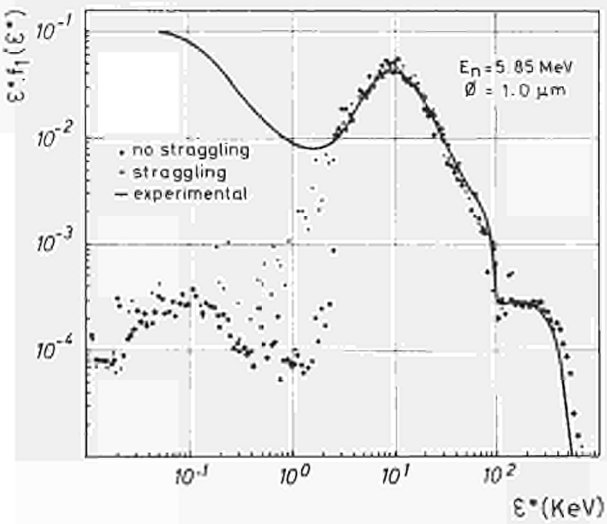

Fig. 8: Comparison of ionization distributions as in Fig. 7, but for 1.0 μm effective diameter.

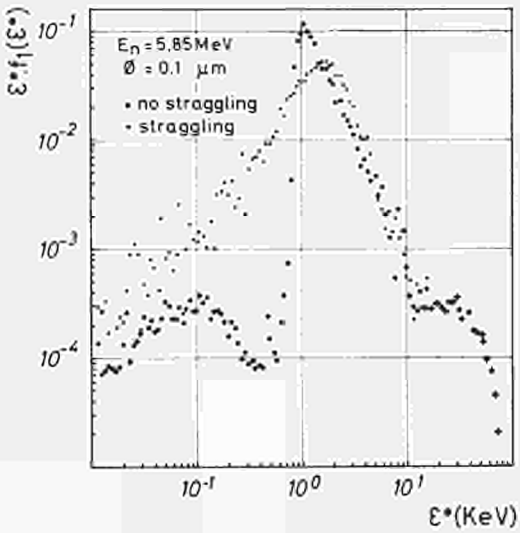

Fig. 9: Comparison of calculated distributions of energy absorption for 5.85 MeV and 0.1 μm effective diameter.

Conclusions

The good agreement between the experimental and the calculated spectra above 5 keV/μm proves that the established Monte Carlo-program works with satisfactory accuracy.

In order to obtain this agreement we have abandoned the hypothesis of a constant W-value for all charged particles and used instead an energy dependent W-value for the recoil ions.

Moreover, the influence of secondary charged particle energy straggling appears to be relevant with protons and alpha-particles for effective diameters equal or less than 1.0 μm.

A certain difference in the region of the higher energy shoulder is probably due to uncertainties in the mass stopping powers of the heavy ions and in the neutron cross-sections, and also to the possibility that the formula used for the energy dependence of the W-value of ions is not fully correct.

References

1) H.H.Rossi, G. Failla, Tissue-equivalent Ionization Chamber, *Nucleonics*, Febr. (1956), pp. 32-37
2) H.H.Rossi, Spatial Distribution of Energy Deposition by Ionizing Radiation, *Rad.Res. Suppl. 2* (1960) pp. 290-299
3) H.H.Rossi, Annual Report on Research Project, Report NYO-2740-1; 2; (1964,1965)
4) H.H.Rossi, Microscopic Energy Distribution in Irradiated Matter, in: Attix, Roesch, Tochilin (Eds.): Radiation Dosimetry. I. (1968) 43-91
5) D. Srdoc, Experimental Technique of Measurement of Microscopic Energy Distribution in Irradiated Matter Using Rossi Counters, *Rad. Res. 43* (1970), 302-319
6) J. Booz, U. Oldenburg, M. Coppola: Das Problem der Gewebeäquivalenz für schnelle Neutronen in der Mikrodosimetric, Proc. Symp. Neutron Dosimetry, Munich, 1972
7) U. Oldenburg, J. Booz, Mass Stopping Power and Pathlength of Neutron-Produced Recoils in Tissue and Tissue Equivalent Materials. I. Neutron Energy 6 MeV, EURATOM-report, EUR 4786, e (1972)
8) U. Oldenburg, J. Booz, Improvement of Tissue-Equivalent Materials for Fast Neutrons and Ions, (in preparation)
9) U. Oldenburg, J. Booz, Calculation and Measurement of Neutron-Produced Single Event Spectra, *Rad. Res.*, in press
10) F.R. Shonka, J.E. Rose, G. Failla, Conducting Plastic Equivalent to Tissue, Air and Polystyrene, Proc. Sec. Un. Nat. Intern. Conf. on Peaceful Uses of At. Energy, 21 (1958) 184-187
11) J. Booz, The Relation Between Energy Absorption and Ionization in Tissue-Equivalent gas for gamma Quanta of Low Energy, Proc. of Symposium on Microdosimetry, Ispra, 1967, pp. 331-351
12) J. Booz, One The W-value of gamma-Quants and Electrons of Very Low Energy, in preparation
13) J. Booz, Th. Smit, A. Waker, Energy Dependence of the Differential W-value of alpha-Particles in Tissue Equivalent Gas, *Phys. Med. Biol.*, June 1972
14) J.W. Leake, The Measurements of W, the Average Energy to Produce an Ion Pair, Report AERE-R 5130 (1967)
15) G.J. Neary, R.J. Munson, R.H. Mole, Chronic Radiation Hazards, London (1957) 73
16) U. Oldenburg, Mikrodosimetrische Untersuchungen zur Energieübertragung schneller Neutronen an weiches Gewebe, Report EUR 4787, d (1972)
17) U. Oldenburg, J. Booz, A Monte Carlo Analysis of Neutron Produced Single Event Spectra, *Biophsik 8* 71 (1971)
18) G.J. Joanou, J.S. Dudek, GAM-II, a B" code for the Calculation of Slowing down Spectrum and Associated Multigroup Constants, Report GA-4265 (1963) (Last corrections in data library: 1966)
19) A. Cole, Absorption of 20 eV to 50,000 eV Electron Beams in Air and Plastic, *Rad. Res.* 38 7 (1969)
20) E.D. Cashwell, C.J. Everett, Monte Carlo Method for Random Walk Problems, London (1959) 128-133
21) H.D. Maccabee, M.R. Raju, C.A. Tobias, Fluctuations of Energy Loss by Heavy Charged Particles in Thin Absorbers, *Phys. Rev. 165* No.2, 469 (1968)
22) J.L. Campbell, K.W.D. Ledingham, Pulse Height Distributions from Proportional Counters, *Brit. J. Phys. 17* 769 (1966)
23) C. Tschalär, Straggling Distributions of Large Energy Losses, *Nucl. Instru. Meth. 61*, (1968) 141
24) C. Tschalär, Straggling Distributions of Extremely Large Energy Losses, *Nucl. Instr. Meth. 64* (1968) 237

OPERATION OF THE BIG INSTALLATIONS

ISPRA-I REACTOR

ECO REACTOR

ESSOR REACTOR

I.D.T. GROUP

COMPUTING CENTRE

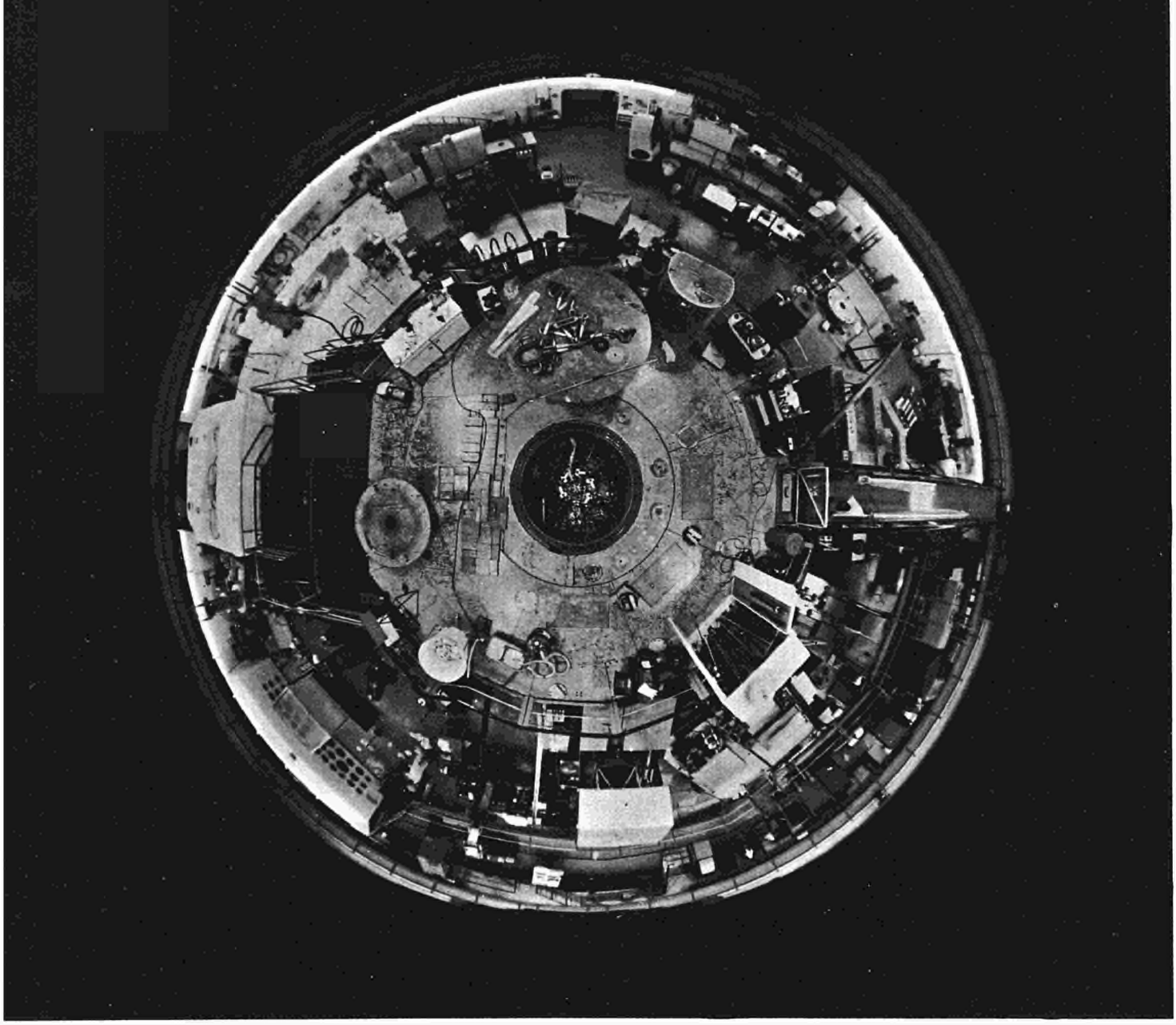

THE ISPRA-1 REACTOR

H. Hasenjaeger, R. Gritti, G. Neisse,
M. Corbellini, G. Dal Bon, R. Henkès

The task of the Ispra-1 section is the operation of the reactor itself and of the organic-liquid irradiation loop DIRCE, the execution of the associated maintenance work, and certain hot operations on irradiated experiments.

General use of the reactor

The Ispra-1 reactor, a D_2O cooled and moderated tank-type reactor, rated thermal capacity 5 MW, was originally planned mainly for beam-tube experiments. By 1963-64 the reactor was adapted to accept additional in-core experiments of technological interest and contained at certain times three organic liquid loops and several rig experiments.

At the end of 1971 one organic loop was in operation and several rigs were under irradiation.

In addition to the neutron physics beam tube experiments, the thermal/fast neutron converter for shielding experiments should be mentioned. Detailed information on these experiments is given in the activity reports of the different scientific divisions of the CCR.

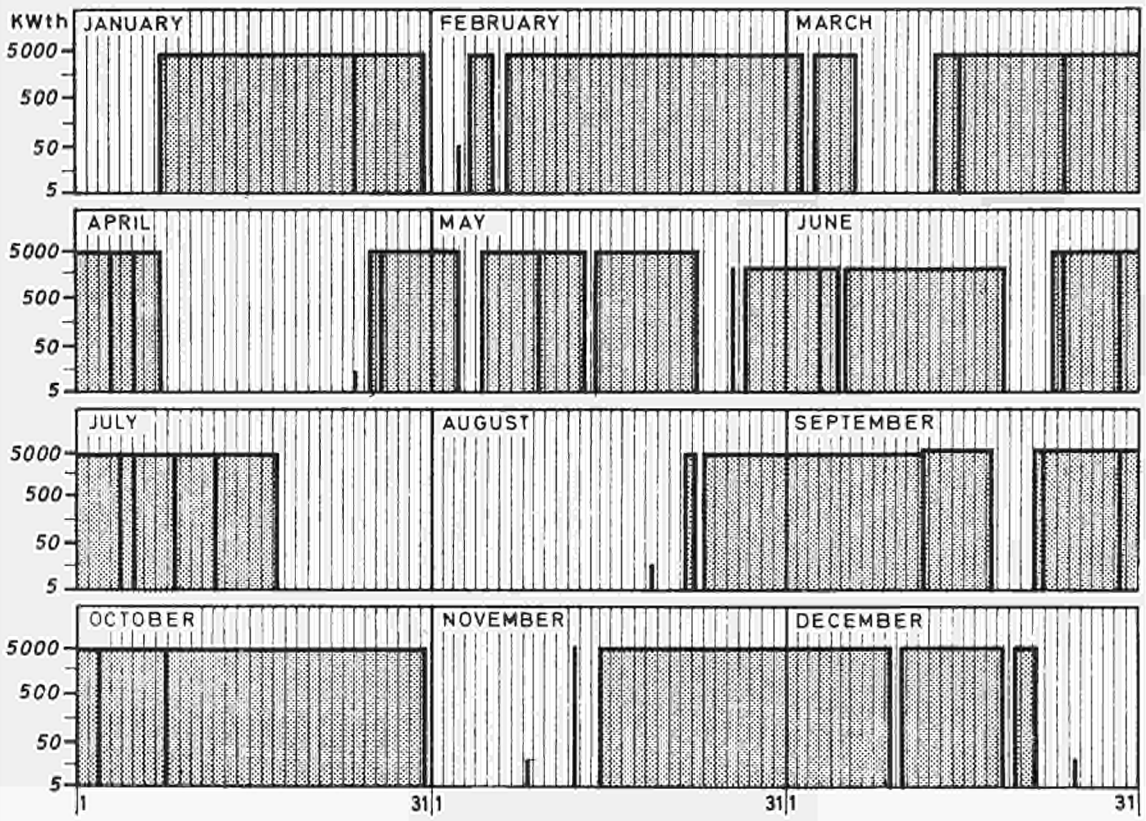

Fig. 1: Power – diagram of Research Reactor ISPRA-1 in 1971.

Operation of the Ispra-1 reactor

The total operating time in 1971 amounted to 253 days (70% efficiency), the total dissipated thermal power to 264 days' operation at nominal power (5 MW).

As can be seen in Fig. 1, the reactor operated mainly at nominal power. In the course of the year 35 events of unscheduled reactor shutdown occured, corresponding to a loss of 14.5 days' reactor operation (18 events equal to 8.6 days lost were caused by experiments; 10 events equal to 3 days are attributed to the reactor, 5 events equal to 0.8 days were due to main electric power outage and 2 events equal to 2 days resulted from strike actions).

During recent years the duration of the reactor operating cycles was gradually raised from about 11 days in 1963 up to 25-35 days in 1971. This became possible mainly by raising the uranium content in a single element from 200 g to 250 g U^{235}.

Electric main power outages, which were rather frequent in previous years owing to short line interruptions (less than 1 sec in time) were drastically reduced by introducing 1 sec delay in the "electric power outage" scram signal and using natural flow inertness or construction of supplementary fly-wheel drives in order to assure sufficient cooling flow in the reactor or experimental circuits.

The radial neutron flux distribution in the vessel is kept fairly homogeneous since the installation of six in-core flux monitors (electron emission type). By this means the different burnup of fuel elements or of control rods can be compensed by individual control-rod level adjustment.

Maintenance

The reactor ha been operated since 1959 and furnished energy corresponding to about 2300 days operation at nominal power. In order to ensure efficiency of the reactor, maintenance during recent years was directed towards substitution of worn parts and, for elements of the nuclear circuits, providing complete spare units where the substitution of worn parts would necessitate too long a shutdown. By the end of 1971 all non-fixed core components had been replaced at least once and the control-rod drives renewed and improved. The efficiency of the absorber elements is regularly measured to determine the cadmium burnup. The aluminium vessel itself was visually inspected in Summer 1971 and no significant sign of corrosion or wear was found. The original tube-type electronic instrumentation was mostly replaced by improved transistorized equipment.

DIRCE loop activities in 1971

Various AMOEBA elements were placed in the DIRCE loop in 1971.

The loop operating characteristics were as follows:

- liquid employed: HB 40
- liquid temperature: 300°C for AMOEBA 1
  250°C for AMOEBA 2
- pressure at in-pile section inlet: 10 kg/cm^2 for AMOEBA 1
  1.7 kg/cm^2 for AMOEBA 2

The irradiation of AMOEBA1 was termined according to schedule on 14 March 1971.

The AMOEBA 2 element was placed in tthe reactor on 14 April 1971 and had to be removed on 14 May, owing to the loss of a capsule weld which allowed organic liquid to get into the capsule.

The loop operated empty until 18 July, when the long annual reactor shutdown began. During the shutdown the various loop maintenance jobs were done (overhaul of values and instrumentation, calibration of measuring instruments, etc.).

On 12 August samples of graphite impregnated with ceramic material were placed in the loop. The operating conditions were then: main flow: 5 m^3/h with a coolant temperature of 200°C and 8 kg/cm^2 pressure at the in-pile section inlet.

In the course of 1971 the DIRCE loop affected reactor operation as follows:

- 25 August 1971: reactor power reduced for 1 hr 50, for repair of a solenoid valve acting on the plant pressurizing circuit;
- 15 November 1971: scram, causing a 1 hr reactor shutdown, due to inconect action on the instrumentation.

The other effects on reactor operation were due to the removal of the two elements AMOEBA 1 and 2.

At the end of the year circulation troubles arose, owing to aging of the liquid (fouling on the in-pile section walls); consequently both the loop and the in-pile section had to be cleaned during the Christmas shutdown.

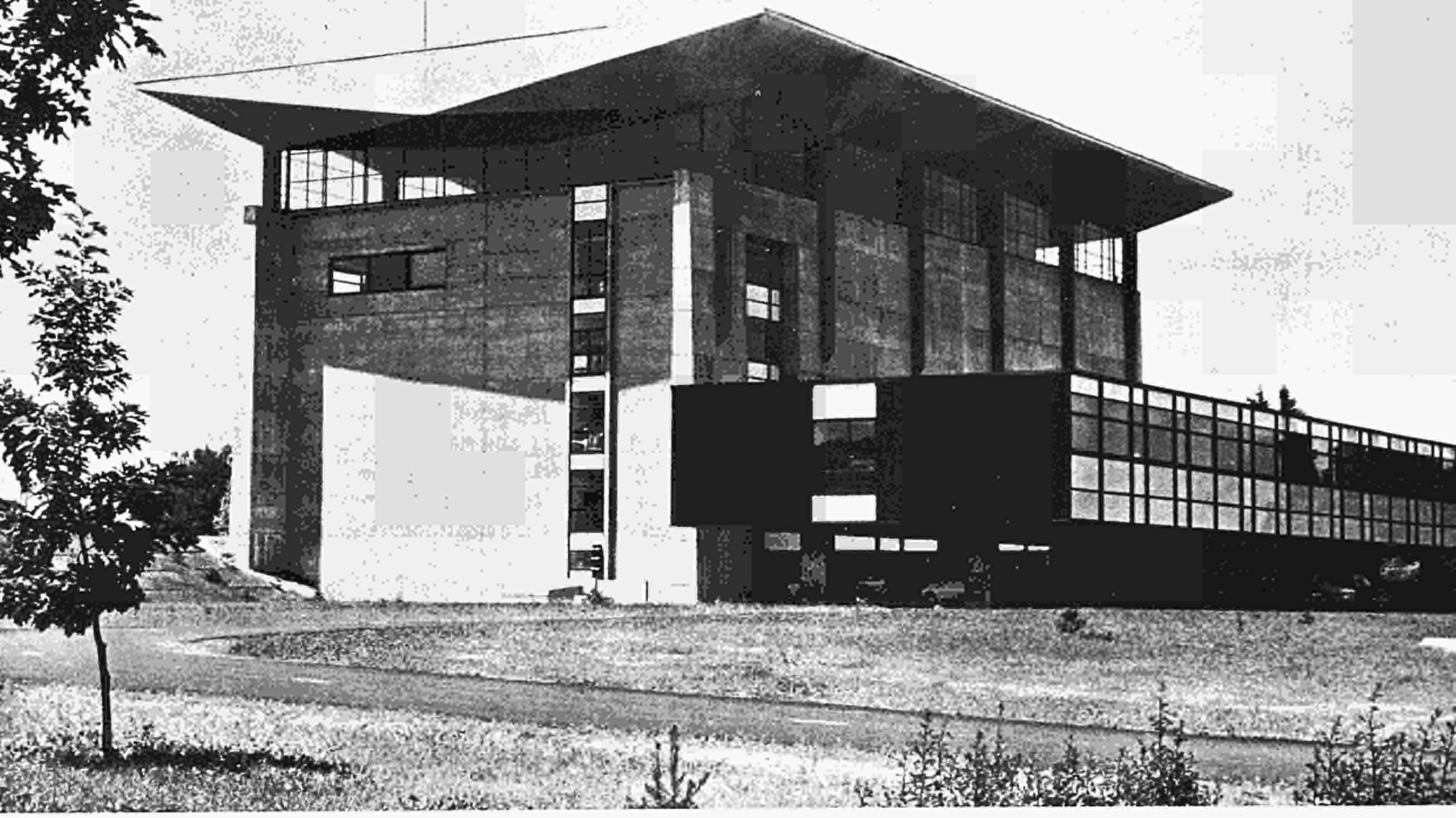

ECO REACTOR

F. Toselli

Introduction

The critical facility ECO was constructed for the experimental determination of the lattice parameters of ORGEL, a heavy-water-moderated, organic-liquid-cooled reactor.

ECO became critical in December 1965 and was utilized in the frame of the ORGEL project for buckling measurements and evaluation of other important neutron parameters such as temperature coefficients, reactivity change as a function of the burn-up, neutron spectrum, etc.

Since the end of the ORGEL project the activity of the ECO facility was more oriented towards the physics problems of thermal reactors than to specific requests of heavy water reactor projects.

This action obtained the complete approval and support of our partners in the Community countries who actively shared in the experimental programme and the interpretation of the results (in particular CEA, SIEMENS, CNEN, CISE). We give here a short survey of the type of experiments performed in ECO from criticality up to 1971:

- material buckling measurements by the method of progressive substitution for fuel elements of different geometry (37, 19, 7, 4 rod cluster) and composition (U, metal, UC, UO_2, ThO_2).
- Detailed cell parameter measuremnts using the activation and oscillation technique (e.g., thermal spectrum indices, initial conversion ratio, Doppler effect up to 1600°C, burn-up, etc.).
- Reactivity temperature coefficient measurements up to 350°C by means of progressive heating of progressive heating of 1 to 9 special fuel elements supplied by a suitable loop.
- Reactivity void coefficient measurements by producing homogeneous and heterogeneous void in the coolants of different fuel element types. These experiments were of interest for basic reactor studies as well for ORGEL, CIRENE, MZFR and the CNEN thorium reactor project.

ECO Activity 1971

The activity of the ECO facility during 1971, as well as for the past years, was established in agreement with the national experts in D_2O reactor physics.

The main activities (chronologically shown in table 1) were:

- reactivity temperature coefficient measurements of MZFR-type fuel elements consisting of 22 UO_2 rod clusters with D_2O as coolant. The variation of the critical height was measured for coolant temperatures of 20-200°C, heating progressively 1, 5 and 9 fuel channels. The aim of these experiments was the determination of B_2/T.
- Resonance integral and Doppler effect measurements in different UO_2 fuels for HTR, up to 900°C.
- Reactivity temperature coefficient measurements in Pu containing lattices using the same technique as for the MZFR experiments. Single and three-rod elements were investigated with D_2O and H_2O as coolants. For single-rod elements reaction rates were also determined by foil actions. During this year only the first phase of the irradiation programme was performed and will be completed in 1972.
- Reactor noise measurements, for establishing methods for reactor safety studies. The interesting results led to the porposal of further detailed investigations in ECO in the future.
- Reactivity void coefficient measurements in Pu-containing fuel elements.

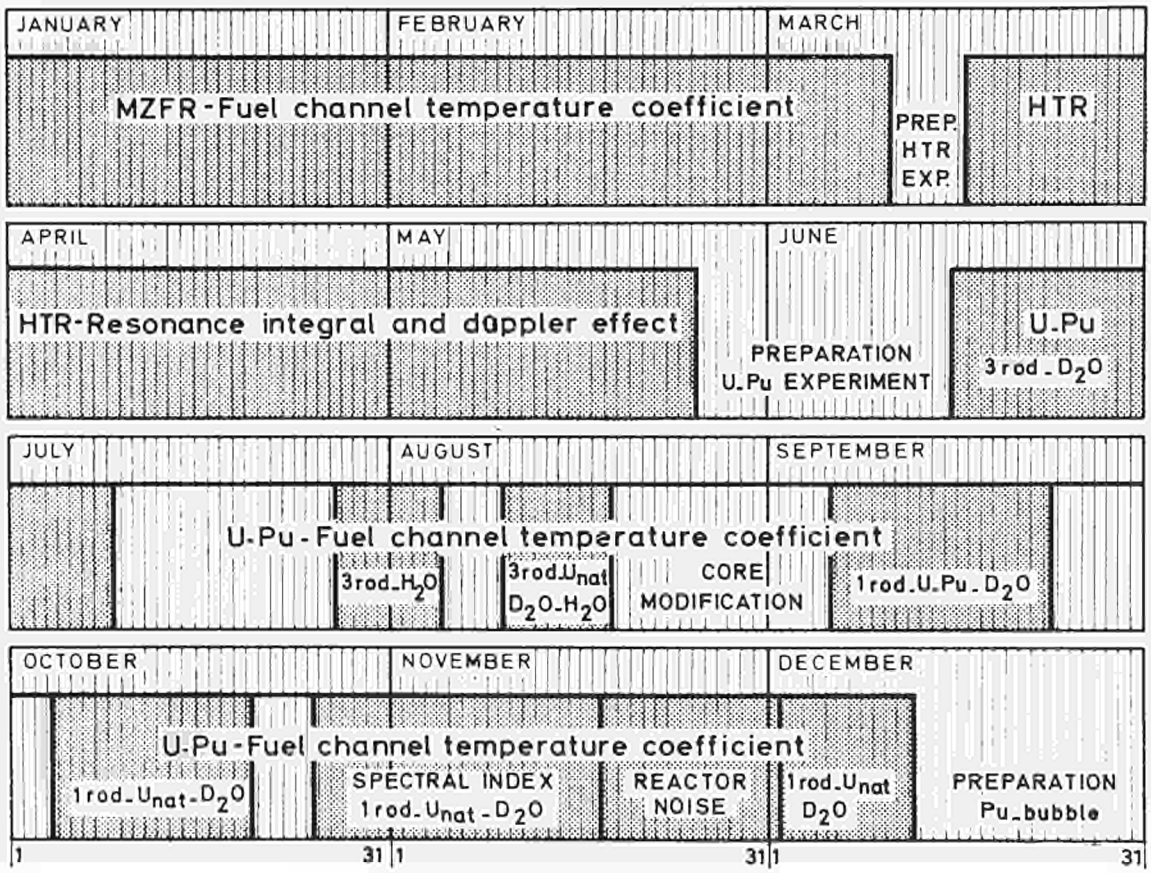

Table 1 – ECO experiments 1971.

ECO operation 1971

During 1971 the reactor ECO was operated for the work mentioned in the preceding paragraph.

For the execution of experiments ECO ran on 130 of the 233 working days of the year, corresponding to a utilization of about 56%. It should be mentioned, moreover, that although the ECO staff is sufficient only for one-shift operation, during 34 days the reactor was operated 24 hours a day and on about 30 days a two-shift operation was necessary to fulfil the experimental requirements. This shows that the utilization of ECO during 1971 was excellent. The rest of the time was spent on fuel-element and core modifications, installation of new experiments tests and maintenance work, which are frequent operations in critical facilities and require a lot of time.

A brief summary of the 1971 ECO operation is given: channel temperature coefficient measurements with MZFR-type fuel elements.

The installation of a new stainless steel loop to replace the organic one, performance tests, mounting of the nine fuel clusters and connection of the channels with the loop, loading of buffer and driver core zones and calibrations of the reactor were finished by the end of 1970.

Up to mid-March 9171, six complete series of fuel-channel temperature coefficient measurements at three lattice pitches and two moderator temperatures were performed, as well as measurements of the total core temperature coefficient between 20 and 60°C. During this experiment some trouble was caused by the coolant circulation pump, but the repair time was utilized for important maintenance work and some reactor calibrations.

HTR fuel irradiations

The experimental time scheduled for this activity was one month, but the first interesting results justified an extension of the programme to two months. All measurements were performed at one lattice pitch with a constant number (120) of fuel elements in the core. The central fuel element only was equipped with samples to be irradiated.

The experiments consisted in 33 irradiations for resonance integral measurements (16 with UO_2 pellets, 17 with UO_2 coated particles) and 18 irradiations for Doppler effect measurements (six at room temperature and 12 at 900°C).

Owing to the time required for preparing the special fuel element, heating the fuel section and removing the irradiated fuel, two irradiations a day were only possible in exceptional cases.

Channel temperature coefficient and reaction rate measurements in Pu-containing lattices

Between June and December 1971 a series of channel temperature measurements with natural U and U-Pu metal fuel elements up to 200°C were performed.

Table 2 shows the experimental programme executed with exception of the total core temperature coefficient measurements between 20 and 60°C.

The preparation and manipulation work during these experiments (mounting and test of fuel channels, assembling and loading of buffer and driver elements, preparation and test of the loop, change of coolant and fuel, rearrangement of core, etc.) lasted for about two months. Besides the temperature coefficient measurements, eight irradiations for reaction rate measurements in single-rod natural U fuel were performed at 20°C.

Reactor noise analysis

A series of noise measurements in ECO was performed as part of the programme "Failure detection by noise analysis". Fuel element vibrations were generated by forced coolant circulation; the correlation of the resistered noise with the radial and azimuthal position of one fuel element was investigated.

Reactivity void coefficient measurements in Pu-containing fuel elements

The preparations for this experiment, including core loading and mounting of the special central bubble element and bubble circuit, was finished in December 1971. Thus the experiments were able to start at the very beginning of 1972.

Table 2 – Experiments in ECO 1971.
Fuel channel temperature coefficient measurements in 3-rod and 1-rod elements.

Lattice pitch (cm)		17.5		18.8		20.5		23.5		28.5		
Type of Coolant	Tm (°C) / Fuel	20	60	20	60	20	60	20	60	20	60	
D_2O	U_{nat}	1	1	–	–	1	1	1	1	–	–	
		–	–	3	3	–	–	3	3	3	3	*)
	U – Pu	1	1	–	–	1	1	1	1	–	–	
		–	–	3	3	–	–	3	3	3	3	
H_2O	U_{nat}	–	–	3	–	–	–	3	–	3	–	*)
	U – Pu	–	–	3	3	–	–	3	3	3	3	

*) only the central fuel channel heated.
1 = 1-rod fuel element
2 = 3-rod fuel element

ECO experiments: preparation and maintenance

Electronic instrumentation

To improve ECO's nuclear instrumentation performances, the programme of replacing electronic tubes with solid-state circuits was pursued during 1971.

This activity included:

- designing manufacturing and mounting new transistorized nuclear instrumentation (Lin channel with linear and deviation applifiers, CIC power supply; Log channel with log and period amplifiers; doubling time meter with linear automatic range change amplifier).
- Designing wiring and testing new control-room interblock circuits, following the modification of the nuclear channels.
- Designing and constructing a new instrument, the "Magnet coupled indicator amplifier", for the safety and control rods of the Ispra 1 reactor.

Convertional instrumentation

A new experimental facility was developed for reactivity void coefficient measurements with Pu-containing fuel. This work includes a loop for the bubble generation in the test element, the test element itself, and the out-of-pile void calibrations with dummy and test element.

General maintenance

All the preventive maintenance operations following the periodic (daily, weekly, monthly and quarterly) controls were carried out in accordance with the Nuclear Safety prescriptions for the ECO Facility.

In particular, periodic maintenance jobs were done on the most important components of the Safety System safety rods, safety valves, level meters, emergency electric power supply etc.

The electronic instrumentation of the reactor, health physics and conventional instrumentation were checked according to a fixed programme. The efficiency of the ECO facility was also checked by the CNEN Safety Division inspector on 27 May, 11 November and 18 November 1971.

The maintenance of the experimental equipment (stainless steel loop, bubble circuit, hot cell, etc.) was performed periodically to ensure the currect execution of experiments.

ECO Safety Committee

During 1971 te ECO Safety Committee analysed and authorized the execution of the following experiments:

- measurements of teperature coefficients with UO_2/22/10 fuel elements.
- Measurements of temperature coefficients with Pu-containing elements.
- Measurements of void coefficients in Pu-containing elements.

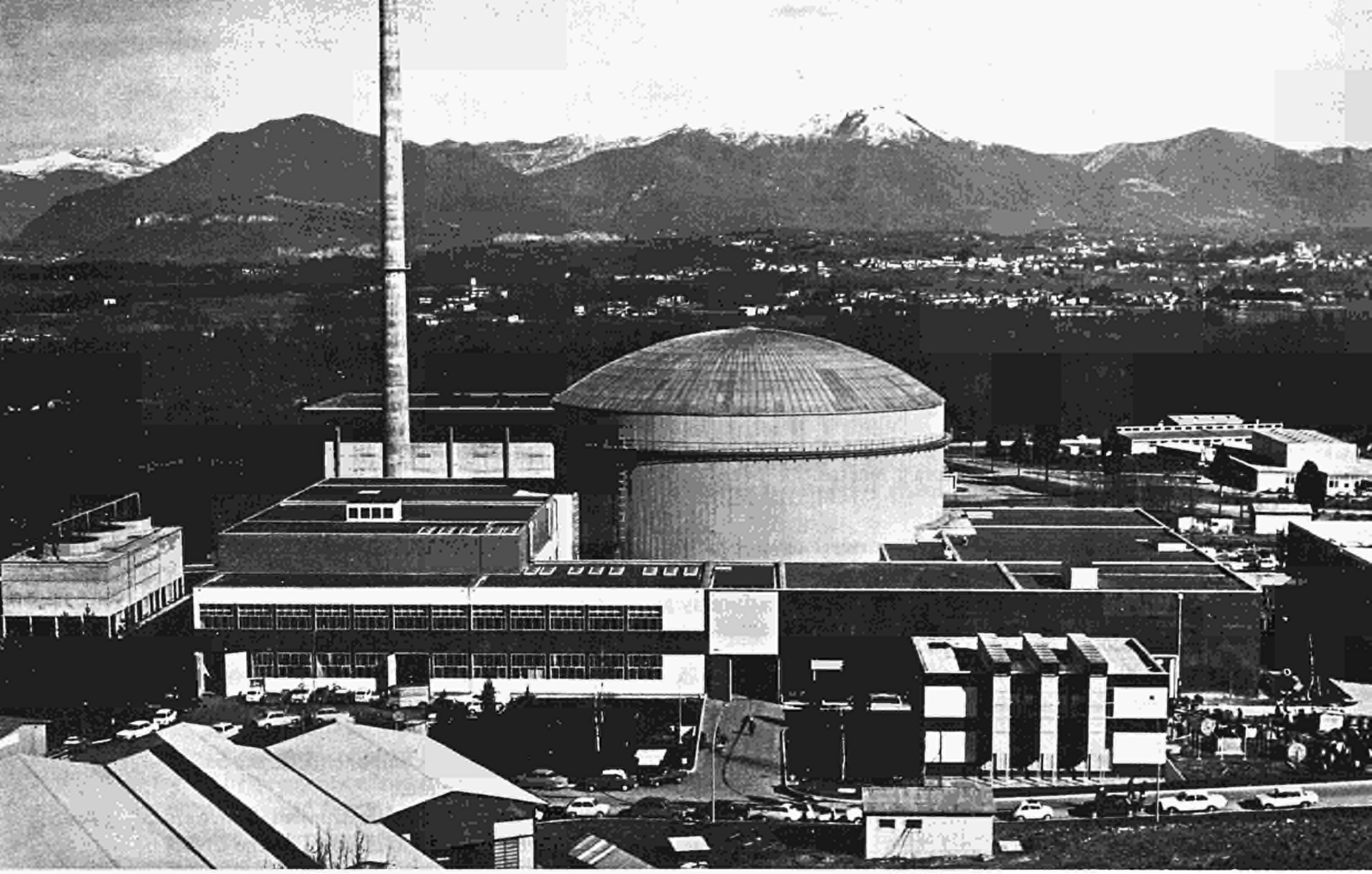

ESSOR PLANT ACTIVITIES 1971

J.P. Lecoq

Introduction

General context

In May 1971 was concluded, as scheduled, the study regarding the conversion of the ESSOR reactor into a test facility for HWR and LWR fuel elements.

This study, carried out in close collaboration with the nuclear industry, was followed up with a market analysis providing a survey of European industry's requirements as regards LWR fuel elements over the next 20 years and a review of present technical know-how and development prospects [XII/234/71]. The conclusion reached was that full-scale industrial operation might be backed up by a development and irradiation programme, of which the main points capable of clarifying the questions raised were defined [III/736/71].

Both documents were discussed during the meeting held in Brussels (2 June 1971) with 36 representatives of 19 reactor and fuel manufacturers, together with six reactor utilities representatives.

The technical soundness of this study was recognized by the HWR and High Flux Reactors Programme Management Advisory Committees which, however, advised the Commission and the Council of Ministers against the construction of pressurized or boiling water loops, on grounds of economy and time.

The time required between ordering and the completion of preoperational tests has been estimated at 36 months and the cost of building each circuit at 4/5 MUC.

Nine months after these contrasting opinions, it should be noted that the French CEA has now decided to build the CAP reactor, a multipurpose marine propulsion facility which will also permit high-performance testing of LWR fuel elements from 1975 onwards, a date similar to the one claimed for the ESSOR loops with identical aims.

In the meantime, the decision to build pressurized loops in MZFR was postponed, while the USAEC released 57 documents to the National Intervenors, most of them showing high concern about the design criteria used for ECCS, the poor knowledge of the channel accident conditions, the irrelevance of experimental tests conducted so far to the large reactors now being built, the crudeness of the LOCA codes, the lack of ability to define the margin of safety with confidence, etc.

In view of these events which underline the good sense of its former proposals, the ESSOR Division endeavoured during the second half-year to develop various irradiation devices on a lesser scale intended to ensure the best utilization of the reactor during the water-loops construction phase, should any private or public concern take over the ESSOR reactor. The main characteristics of these devices were described in a memorandum sent to the Italian CNEN at its request as well as to the industrial firms consulted during the inquiry and to the High Flux Reactors Programme Management Advisory Committee during its meeting of 25 January 1972.

Lastly, the draft of a common enterprise status was discussed with the legal advisers of the Commission in view of a possible takeover of ESSOR by a private or public concern.

The ESSOR Division contributed directly to a comparative study on pricing methods and irradiation cost evaluation in several reactors, particularly HFR, BR-2 and ESSOR. The results of this study were submitted to the High Flux Reactors Programme Management Advisory Committee (14 January 1971) which consequently forwarded to the Council of Ministers and to the Commission a recommendation on the pricing policy to be applied in working out and applying irradiation tariffs. This study showed that the operation costs of the ESSOR reactor are comparable with those of the other facilities of equivalent performance; moreover, owing to the considerable irradiation volume available inside the moderator, ESSOR can claim the cheapest costs per volume unit and per thermal integrated flux unit, i.e., for thermal reactor fuel-element testing.

Plant operation

In 1971 the ESSOR reactor operated for 142 days at full power in order to carry out the programme of irradiation of the CART C2 test section.

The main difficulties concerned the control computer which provoked several undue shutdowns or power reductions, and the fouling of the secondary (light water) side of the heat exchangers.

Various experiments provided confirmation of the reactor's intrinsic safety in natural convertion cooling, the tightness of the container and the ability of the MK 5 multiple loop to operate in the flow and temperature ranges required for operating the neutron converters.

The hot laboratories unit carried out the CART TS 1 post-irradiation examination and the conditioning of 20 driver zone fuel elements (fuel cutting and packing, recuperation and decontamination of the plugs).

The fitting up of the examination cells was continued, with the installation of the SAMES accelerator in the neutrography cell, gamma-scanning acceptance tests, mock-up tests of an optical dimensional measurement device, out-of-cell acceptance tests of the fission-gas sampling device (puncture test), completion and operation of the defects printing method.

Management difficulties

The state of uncertainty as to ESSOR's future entailed on one hand considerable delays in the orders as well as work to be carried on inside the JRC. and on the other hand the non-replacement of specialized staff necessary for the reactor operation shifts.

Moreover, the management of a large nuclear installation on an annual programme basis raises many budgetary and regulation difficulties when modifications of the installations and fuel element supplies are concerned.

Reactor and experimental circuits operation

Reactor operation

The governing factor of ESSOR reactor operation during 1971 was the irradiation of the CART loop, which since 1970 was loaded with the C2-A experimental fuel element. The irradiation of the C2-B fuel element started at the end of 1971.

The reactor was operated for 142 days at the nominal power required for the C2 fuel element, corresponding to 20 MW on the driver-zone for the C2-A and to 13 MW for the C2-B (see Fig. 1).

The integrated reactor power during 1971 amounts to 2365 MWd.

19 scrams and 14 power reductions were recorded, essentially due to troubles in the data processing system (T.I.S.).

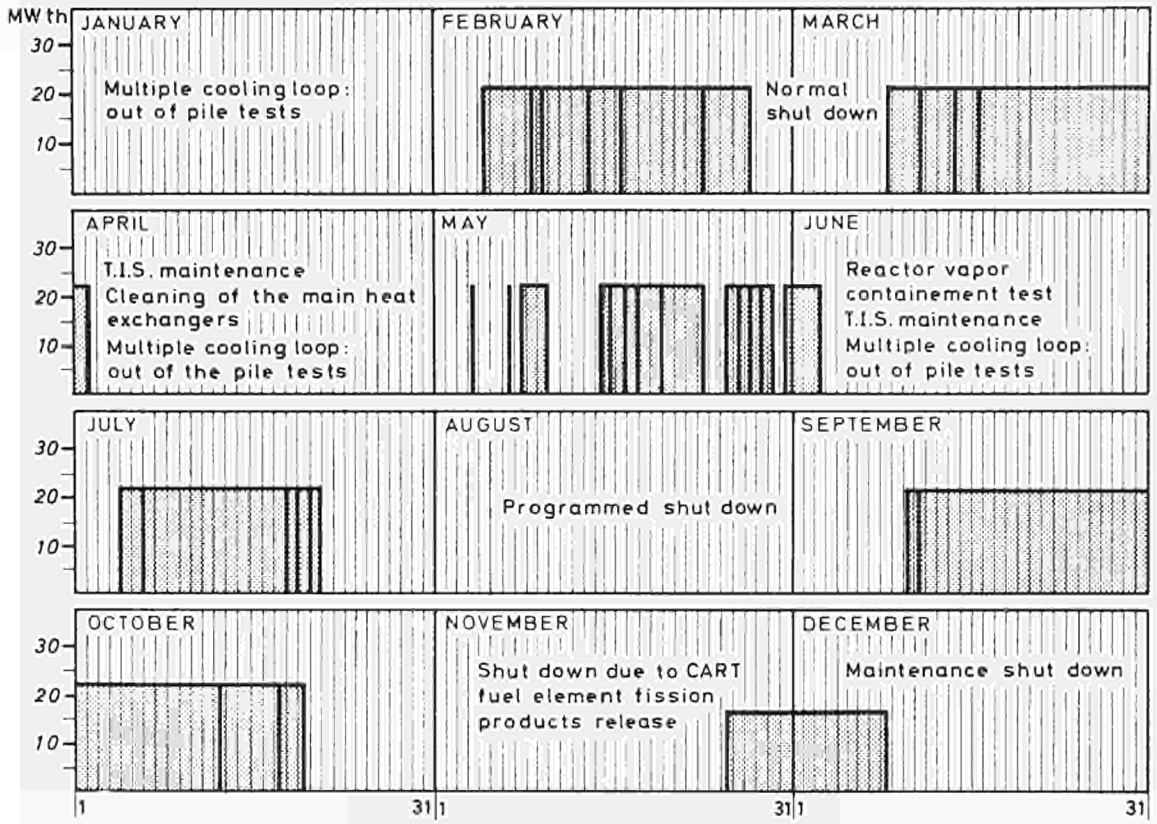

Fig. 1: ESSOR Reactor. Load diagram during 1971.

From the third reactor cycle onwards, the average burn-up of the driver-zone fuel elements was increased to 40% - the upper limit agreed by the Safety Report. Thus the operating period was increased by about 20%. Moreover, the average cycle burnup was doubled (20% of initial U^{235} content instead of 10%) by loading eight fresh fuel elements at the beginning of each operating period, instead of four as previously. This allowed a more homogeneous neutron flux distribution which led to a more even burnup.

Neither degradation of the heavy water concentration nor significant presence of corrosive radicals was observed:

driver-zone circuit: 99.69 mole % D_2O
moderator circuit: 99.72 mole % D_2O

The tritium concentration increased from $0.836 \cdot 10^{-4}$ Ci/g to $1.57 \cdot 10^{-4}$ Ci/g in the driver-zone circuit, and in the moderator zone from $0.585 \cdot 10^{-3}$ Ci/g up to $1.272 \cdot 10^{-3}$ Ci/g.

The periodical check of the reactor containment tightness yielded good results. The measured leakage rate was found to be 0.178% volume per day at 100 g/cm^2 internal overpressure, as against 1% volume per day allowed by the Safety Report.

Technical difficulties

The efficiency of all the heat exchangers using light water as secondary coolant had been decreasing since 1970. When the shells were opened, it was found that this was due to deposition of mud and fine sand on the outer surface of the tubes. The cleaning was done by drying with hot air and flushing with clean water. The heat exchange coefficient returned to the original value. In future the light water system will be fed with filtered and decanted water (see Fig. 2).

The fan of the south atmospheric cooling tower has been shut off nearly all the time, owing to the cracks that appeared on the reinforced girder. Vibration measurements revealed a resonance between the frequency of the three-bladed fan and the eigen frequency of the girder.1A new four-blade fan rotor is being assembled.

Short circuits due to wear and tear occured on the supply to the electromagnet of safety rod no. 3.

The lift mechanisms of all the safety rods are to be replaced.

Experience has shown that after 1.5 years the D_2O level safety device is no longer operative, owing to corrosion and fouling of the floats. The device has been replaced.

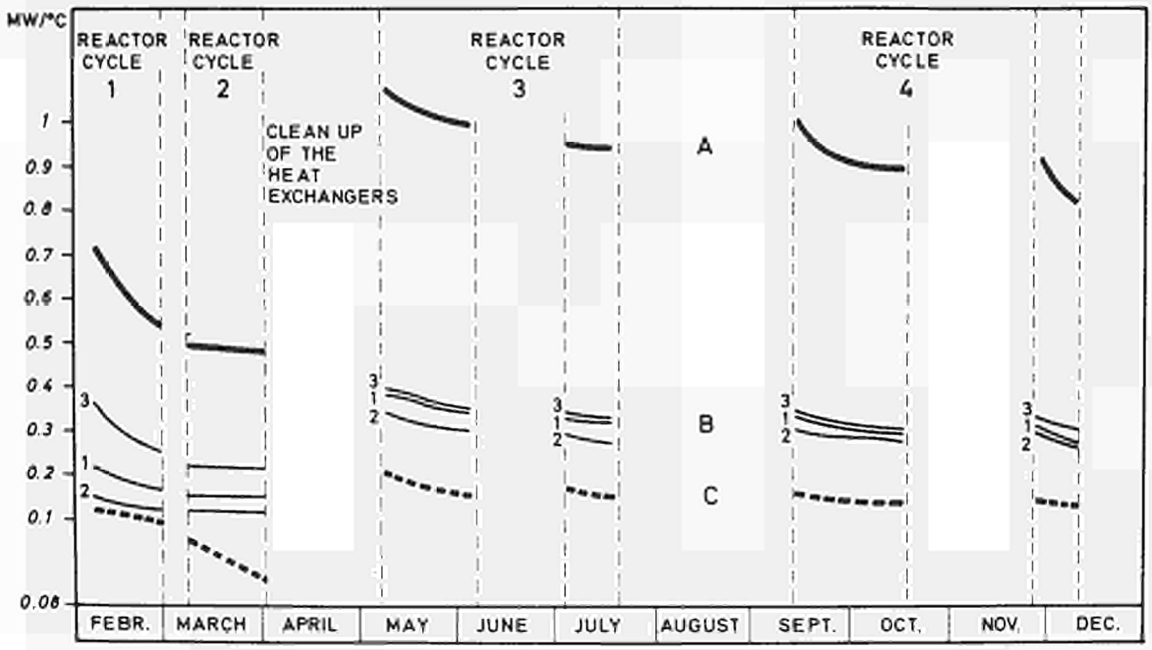

Fig. 2: Feeding and moderator zone. Heat exchange coefficients during 1971.

——— feeding zone total heat exchange coefficient

——— feeding zone heat exchanger 1, 2, 3: heat exchange coefficients

▪▪▪▪▪▪▪ moderator zone total exchange coefficient

Routine checks of the driver-zone heat exchangers revealed the presence of heavy water in the intermediate space. So far the leakage is small enough to be allowed.

Some technical troubles occurred in the data processing system (T.I.S.). Owing to the complexity of the system, the causes have been very difficult to find out.

In some cases, the troubles were due to aging of circuit components or to incorrect commutation between the two central units.

Improvements in reactor operation and experiments feasibility

A difficulty, when removing partially burn driver-zone fuel elements from the decay pool for a new core loading, is that light water retained in the fuel assembly is carried into the heavy water circuit. After non-conclusive tests with air-drying inside the handling machine, it was decided simply to rinse the fuel element by immersing it in a small quantity of heavy water before loading. This solution was found quite satisfactory.

The D_2O/H_2O heat exchanger tube-rupture detection system was modified in order to reduce its response time and increase its sensitiveness and selectivity. It used to monitor the total gamma activity of the secondary circuit light water. Now, a small booster pump draws off a small quantity of light water which is monitored for the presence of N 16.

Gamma irradiation tests on polymer gaskets were carried out in the decay pool, enabling the choice of the gaskets for use on the handling machines to be optimized.

In 1970 tests confirmed that the decay heat of the driver-zone fuel elements can be removed by natural convection cooling. Using two fuel elements instrumented with thermocouples, it was furthermore verified that the fuel elements can be unloaded with all pumps shut off.

The organic-cooled experimental loop was operated on its bypass in order to check the condition of the equipment, to carry out some thermal-hydraulic tests and to check the feasibility of cooling the planned neutron converters. The following test were performed:

- loop operation at 340°C on primary circuit;
- start-up of the purification system;
- cooling by natural convection of both primary and secondary circuit;
- fast depressurization of the primary circuit.

Results were satisfactory and only minor adjustments are necessary to put the loop in good condition for in-pile operation.

During the first reactor cycle some neutron noise measurements were performed with a Statistical Dynamic Analyser. The results are being interpreted.

CART loop operation

The light water fog-cooled loop CART is used by the CISE for fuel element development for the Italian CIRENE project.

The irradiation of the C2-A fuel began in 1970 and was interrupted on 20 October 1971. The total burn-up reached is 2505 MWd/tU. The average thermal power was kept constantly at 1080 KW (see Fig. 3).

Owing to a release of fission products into the cooling circuit, several tests were performed before unloading in order to determine approximately the amount of release and the size of the canning defect. For this purpose supplementary instrumentation was installed on the primary circuit-ionisation chambers close to the primary surge tank, scintillation counter on the main channel outlet line.

First, with the reactor shut down, several pressure and temperature cycles were performed, after which the reactor was brought critical up to 10% of the C2-A nominal power (100 kW).

The following radionuclides were detected: I^{131}, Xe^{131}, Xe^{133}, Ce^{141}, Cs^{137}.

Meanwhile, the C2-B fuel element was assembled and then loaded at the end of November 1971. In accordance with the first phase of the irradiation programme, the average power of this fuel was kept constantly at 750 kW. At the end of 1971, the accumulated burnup was 138 MWd/tU.

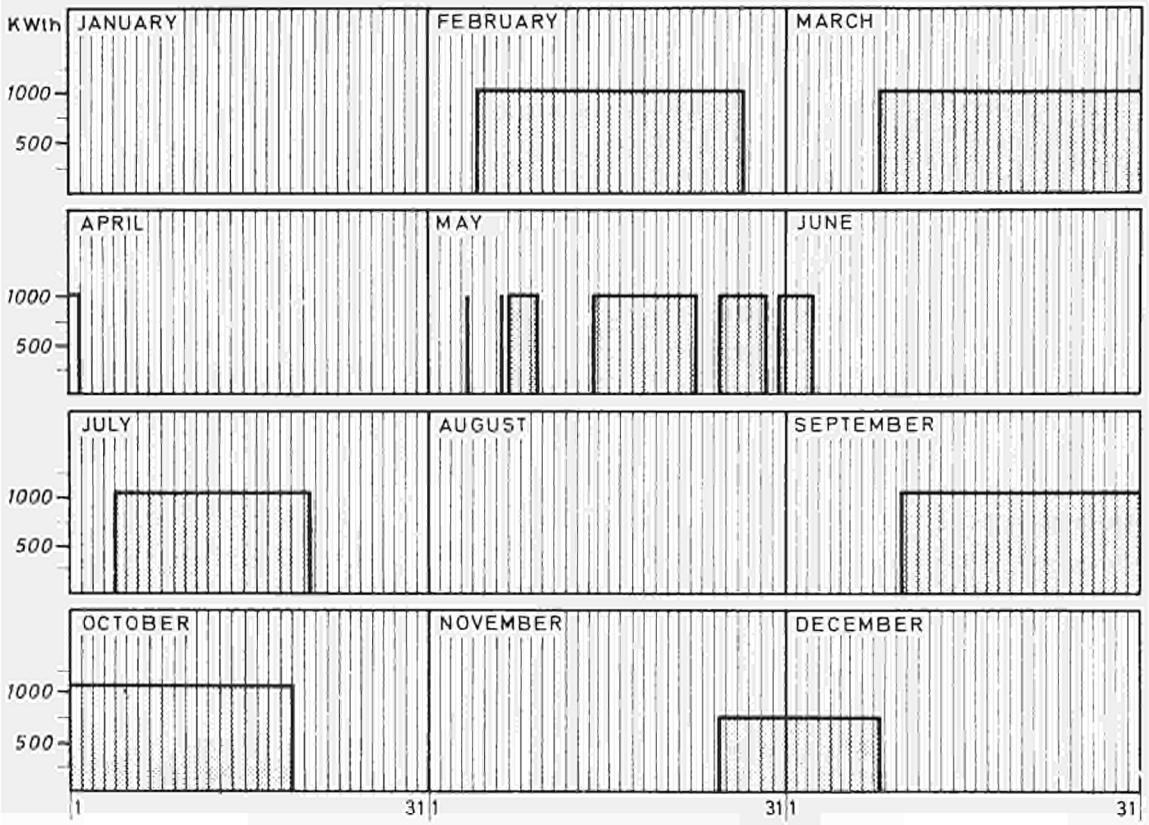

Fig. 3: Cart experimental loop. Load diagram during 1971.

Hot laboratories operation

Work at the hot laboratories in 1971 was centred on:

- post-irradiation examination of the C1 fuel element irradiated in the CART loop;
- conditioning of burnt driver-zone fuel elements;
- reception and testing of hot cell equipment.

The main assistance work consisted in decontamination and chemical treatment of some expensive reactor components with a view to their re-utilization.

CART-1 post-irradiation examination

In January and February 1971, metrological, visual and photographic examinations were carried out on 36 active rods from the last two C1 bundles; prints of some of these rods were subsequently taken. Eleven of them were packaged and sent to CNEN's Casaccia hot laboratory for metallographic examination; one was sent to the Ispra LMA. Results were reported in report 9.7621.A.021 (classified).

Conditioning of driver fuel elements

20 driver zone fuel elements from the reactor were cut up. The first run of 12 elements was preceded by testing and improvement of methods. Each run was followed by conditioning and waste disposal, which entailed tests conducted jointly with the Ispra Waste Disposal Department. The upper parts of these assemblies were dismantled and decontaminated by the ultrasonic method and, after chemical treatment, returned to the cold workshop. Residual contamination was nil.

Cell equipment

Neutrography cell

The SAMES generator was tested after installation of the ion-getter pump and the beam-viewer. At the same time design and manufacturing studies were done on the moderator, the rod presentation system and the screen transfer system, and were subsequently sent to the manufacture-shop.

Gamma scanning

The mechanical part was adjusted; the INa detector, the 400 channel analyser and the teletype printing machine were assembled and tested.

Optical measurement device

Preliminary tests were carried out on a real mock-up and the specifications of the compound lens and the measurement system were determined.

Puncture test system

The cold tests of the bench and the modifications allowing for cell introduction were completed.

Defect measurements by print method

At the request of the CISE, we studied and improved the printing and defect-measuring methods, with a view to examining the deformation of the rod ends, the welding cracks and the fretting of the grids. Deformations were measured with a profile projector and defects with a rugosimeter. A preliminary internal report was drawn up.

Technical support activities

The activities of the technical support unit can be divided into three main types. They include design and project work, which is generally assigned to the Project Office, technical developments, instrumentation and control operations assigned to the laboratories, and some tasks performed for private industry using the competence of the above specialized groups.

Design and project work

The Project Office has orientated its main efforts towards direct technical backing for the reactor and the hot laboratories, and towards the preparation of several experimental systems.

One should mention in the first area, the detailed design of a remotely-operated neutron radiography system and of a photographic bench to be installed in the ADECO hot cells, the study of a major modification of the reactor auxiliary vacuum station and a conceptual design of advanced driver fuel elements.

Besides this, an order for a new fabrication of standard driver fuel elements was prepared and an invitation to tender for the reprocessing of the irradiated fuel was sent to the European reprocessing facilities.

As regards the experimental systems to be introduced into ESSOR, the main objectives were:

- final lay-out of the liquid safety rods in the reactor containment building and installation of the out-of-pile circuits;
- study, in collaboration with the industry, of a reference design of large pressurized and boiling water loops for ESSOR; the final report contains a cost and time estimate for these loops;
- furthermore, the compatibility of these loops with the reactor was studied in order to define their mutual behaviour in the event of transients simulating power reactor accidents. On this basis, the technical specifications were established in readiness for an invitation to tender.

Besides these main projects, more specific applications were studied, including a PWR physics test fuel element now being manufactured, a neutron converter for the organic-cooled loop, and various devices to be installed either into driver fuel elements or into the heavy water moderator.

Laboratories

The primary purpose of the laboratories is to work in direct support of the reactor and the experiments with particular reference to the clean workshop (ATEN). Acting as the main control gate before the loading of components into the reactor core, the ATEN has dealt with the pre-irradiation assembly and testing of about 90 in-core components and tools and the acceptance of 140.

The chemistry laboratory was responsible not only for analysis of the heavy water and light water used for the reactor itself, but also for the monitoring of the CART loop primary circuit. Moreover, this laboratory has two heavy-water reconcentration columns which were used in 1971 to reconcentrate 13 tons of D_2O for the ECO facility and to make high purity D_2O standards (99,999 mole %) at the request of the IAEA.

Assistance to other concerns

All these groups shared in the preparation and performance of two on-site inspections of nuclear power reactors at the request of the utilities: in March, remote visual inspection of the Dodewaard reactor vessel; in November, remote inspection of the steam generator and pressurizer at the RB-3 power station.

ACTIVITY REPORT OF IDT GROUP

G. Fontaine, J.M. Junger, J. Vaccarezza

This group, attached to the Chemical Division during 1971, has continued with the same work as in the past:

- decontamination in-situ of nuclear plants and laboratories (S. Barbieri);
- decontamination of materials (S. Barbieri);
- treatment of solid and liquid waste (Sentoll - Vannuzzi);
- temporary storage of active materia (Sentoll);
- Study of new plants (Mosselmans);
- Laboratory studies (Vaccarezza-Gillot).

Decontamination (local and in-situ)

The personnel of this group is divided into three shifts.

This personnel is provided with standard material (marks, respiratory apparatus, special clothes) placed in two special trucks. The decontamination of material is done in special rooms (Block 40) or directly in the laboratory.

Radioactive solid waste treatment

Low-level radioactive waste

Low-level radioactive wastes are treated with bitumen and placed in 200-litre drums.

High-level radioactive waste

According to the contamination and activity level, these wastes are stored in pits or placed in standard concrete containers and then filled with cement.

Liquid waste treatment

Radioactive contaminated water

The liquids of the first group ($< 10^{-6}$ μCi/ml) are remote filtered. The liquids of the second group (10^{-6} to 10^{-3} μCi/ml $\beta\gamma$) are decontaminated by a chemical process or by ion exchange.

Fig. 1

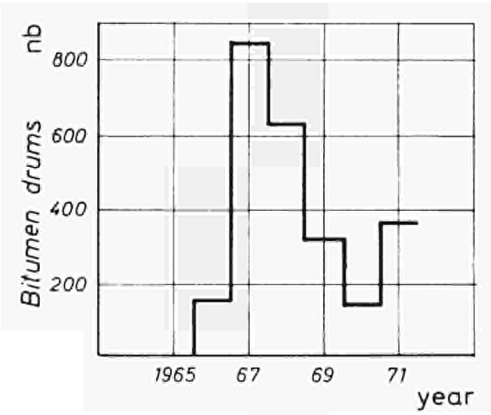

Fig. 2

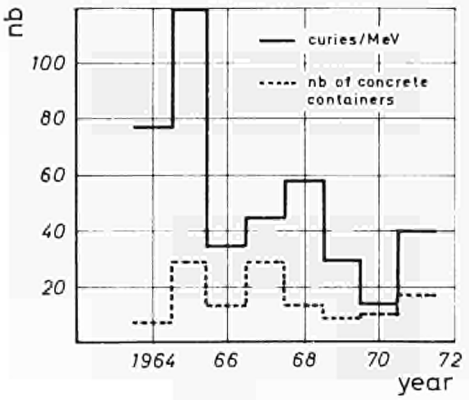

Fig. 3

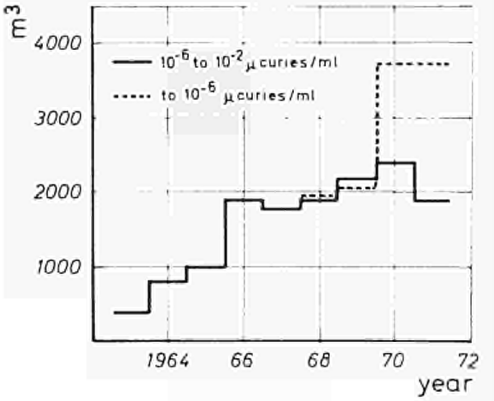

Fig. 4

High-level radioactive liquid waste (water)

Because of the small amount of this liquid produced annually in the Centre we have, after different laboratory experiments, adopted the method of solidification with concrete including certain mineral absorbers.

Organic liquids

For the destruction of active or inactive organic liquids we have a submerged combustion evaporator.

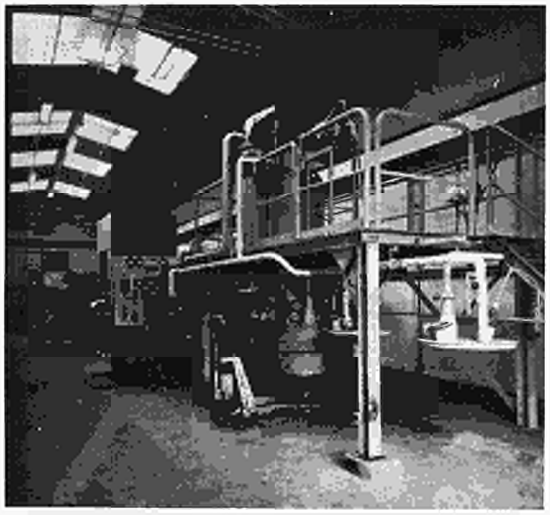

Fig. 5: Low-level radioactive solid waste plant

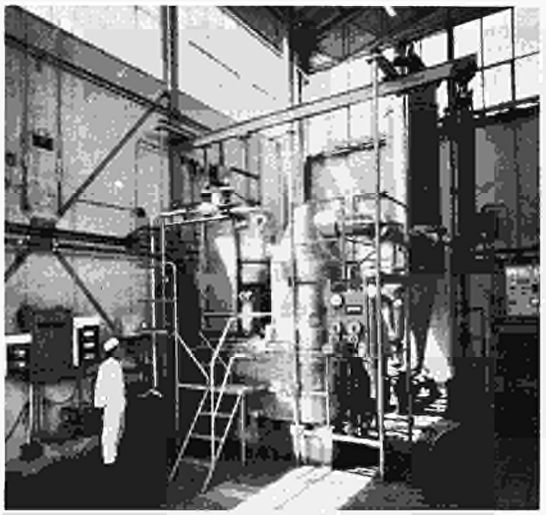

Fig. 6: Submerged combustion evaporator.

Laboratory studies for the treatment of radioactive effluents at the Ispra JRC

Although direct activities were drastically limited due to illness (accident), documentation studies and preparation of new programmes were pursued during this period. Laboratory experiments comprised checks of the physicochemical properties (zeta potential and sedimentation measurements) of radioactive effluents treated in the Station, followed by tests for the optimum flocculation conditions.

Research comprised tests with various flocculants on one standard solution, and optimization of decontaminant addition by zeta potential measurement and adjustment towards the isoelectric point.

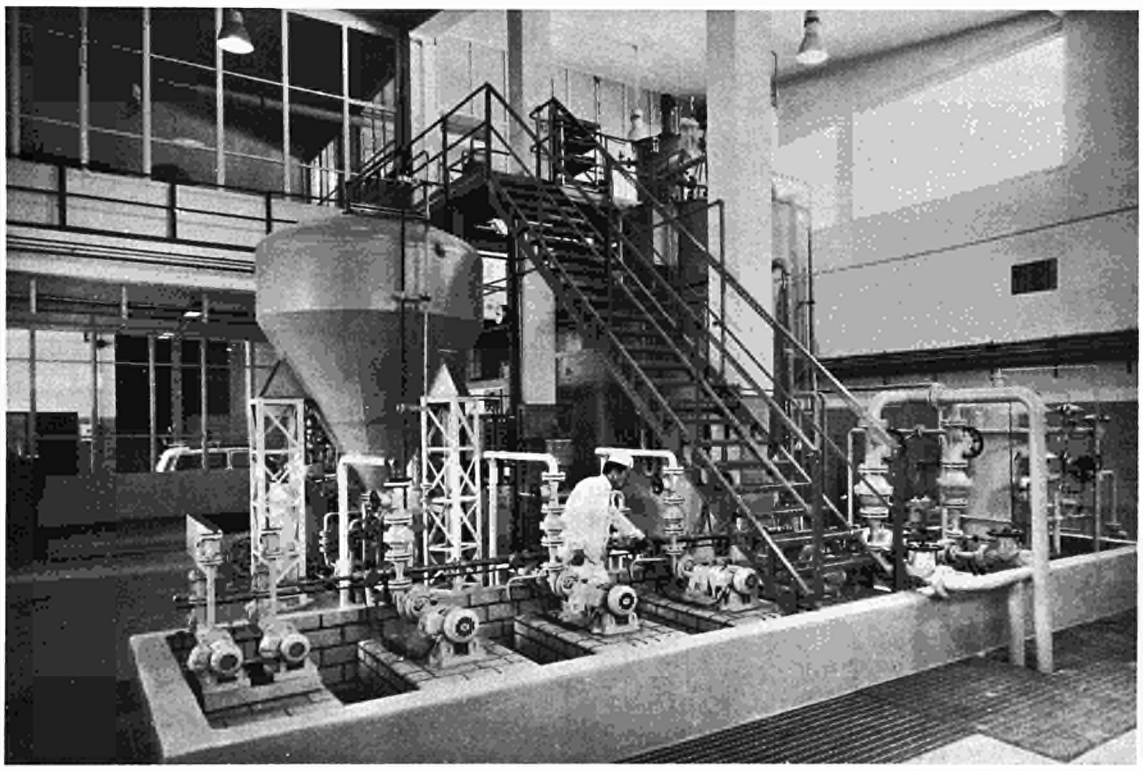

Fig. 7: Radioactive contaminated water treatment plant.

COMPUTING CENTRE

J. Pire

The JRC Computing Centre is administered as part of the CETIS Division and comprises, in addition to the computers and their operators, a "system support" unit and a "User Support" unit for questions of programming.

I. The Computers

A. The 360/65

The actual computing work is at present done with an IBM 360/65 machine which has a central storage capacity of 768 K* bytes. The main peripheral units consisted at 1 January 1971 of:

a) a 2301 drum with a capacity of about four million bytes; the average access time is 8 msec and the transfer speed is 1,200,000 bytes/sec;
b) two removable disk units, type 2314, each comprising eight disk drivers with a capacity of about 28 million bytes per disk pack, providing a direct-access mass storage of about 450 million bytes;
c) seven 800 cpi magnetic tape drivers including one with seven tracks and six with nine tracks.
d) two fast printers;
e) a fast card reader and punch.

In addition to these general-purpose units there are:

f) a 2250 graphic video unit for processing interactive programs;
g) four 2260 conversational alphanumeric units used for interrogating and updating files;
h) a 1050 unit limited to keyboard and printer, used chiefly to debug and time the conversational teleprocessing and desk computer system;
i) the requisite support equipment for connections to two laboratories and a remote job entry (RJE) teleprocessing station.

*) K = 1024

During 1971 development work centred on two main points: teleprocessing development in general, and enlarging the mass storage capacity.

The RJE connections rose from one to five in the first six months. The extensions included the installing of a 2780 unit at the Materials Division and the connecting up of the CBNM, Geel; moreover, at the end of the year, a 2770 terminal was tested at CETIS and will be installed at the ESSOR premises in 1972.

The conversational stations increased from seven to ten and then to 21 during 1971 (the last terminals were actually made available to the users in the second fortnight of January 1972), with the connecting up of four new laboratories and the addition, at the end of the year, of ten 2741 (teleprinter) units.

The direct-access mass storage was increased, according to plan, to 672 million bytes by the addition of a third 2314 unit in October. This increase was made necessary by the growing numbers of programs stored on-line and of both administration and scientific library data. Of the 24 disk drivers available, 20 are permanently occupied by disk packs containing programs to be constantly accessible for special purposes; four drivers are available for particular packs to be put on at users' request.

The 360/65 computer was operated in two eight-hour shifts a day, except during the period from 5 July to 5 September when operation was reduced to one normal shift extended by supplementary hours. Thus it was operable for about 3600 hours. The total use time during the year amounted to 3492 hours, of which 3440 were paid to IBM (52 hours being deduced for recongnized errors). The invoiced output, minus the time necessary for system management and production time (internal conversational teleprocessing) charged to the operating management, came to 3,201.17 hours, to which are to be added111.84 hours chargeable under the heading of peripheral operations; this brings the net invoice time to 3313.01 hours, with an efficiency rate of 96.5%.

The invoiced utilisation represents the execution of 72,323 jobs including, apart from the computing work, the following peripheral operations:

punched card readins	42,6 million
cards punched	3.8 million
lines printed	156.9 million

The amount of work supplied was substantially higher than in 1970.

Number of jobs	+ 40%
Number of cards read	+ 18%
Number of lines printed	+ 11%.

Only the number of cards punched fell slightly, by 5%. The equipment could still tolerate a slightly higher load, but not another surge of growth like the one recorded between 1970 and 1971.

The following table gives some idea of the turn-around time, i.e., from the time when a job is read into the reader to the completion of the last peripheral operation concerning that job:

15'	30'	1 h	2 h	4 h	8 h	1 day	longer
33%	16%	14%	12%	9%	7%	5%	4%

Obviously the turn-around time depends on the actual length of the job requested; for jobs taking no more than a minute to perform, a turn-around time of less than 15 min is obtained in over 50% of the cases; as to the 4% which took more than a day, mots of these were from RJE stations which do not come back until several days after sending in the work, or else jobs read in and stored just before a weekend or holiday period, so that the results are not delivered until work is resumed.

B. The 7090 Computer

The IBM 7090 installed in August 1961 is now ten years old. It was not used very much in 1971 and its reliability has become very uncertain. In view of the high maintenance costs (60,000 u.a. a year), it was running at a complete loss and was finally put out of service on 20 December 1971.

C. The 360/30 Computer

This machine has a storage capacity of 16 K bytes and is equipped with a card reader/punch, an interchangeable-chain printer, six magnetic tape units (four 30,000 bpi and two 60,000 bpi), a punched tape reader, a tape punch and a graph plotter. With the operating method developed by CETIS in 1966 and 1967 it can, if necessary, process three different jobs in parallel.

This computer, installed in 1966, is still used for various administrative jobs and for special peripheral work such as driving the plotter, converting punched tapes to and from magnetic tapes, and printing special documents.

It is employed in two shifts a day. Naturally, the system of use of this computer is in no way comparable to that of the 360/65; nevertheless, the invoiced operations still provide an efficiency of about 80%.

Computer Management

The computers are in charge of a team of 14 operators.

The program and data punching work dealt with 799,000 cards and was done by three keypunch operators, backed up by a service contract with IBM representing roughly the work of five people.

The System Support

The 360/65 computer worked for 10 months under version 18 of the operating system, generated at the end of 1970, and two months under version 20.1 generated in 1971.

It became necessary to generate version 20.1, first to include the new material installed in October, and secondly to take advantage of new facilities, more especially multi-tasking. At the same time version 3 of HASP II (spooling program) was generated. By simultaneously introducing the new OS and HASP versions it was possible, using the dynamic assignment of priorities, to cut out the time-slicing process which was accounting for something like 3% of the total time.

In addition the necessary developments were completed to link in the 2740 types of conversational terminals and the job entry terminals, types 2780, 2770, 1130 and 360/30.

The system support is operated by a staff of three.

User Support

This activity is covered by a staff of five specialists in the use of control and programming languages, who have enough experience to give their colleagues efficient assistance.

The aid to programmers in along three lines: first, advice and direct aid regarding the use of programming languages, control coards, error detection; this work also included the acquisition and distribution to users of the requisite technical manuals. Secondly, designing general-interest programs, inserting these programs in the general libraries, generally testing them and making them available to the users or specialists in the fields covered by the programs. And thirdly, the developement of general-interest routines.

An exhaustive list of the last-named would take up far too much space; we will only mention

a) the conversion, for the 2250 unit, of the graphic routines used for the CALCOMP plotter; these routines form the basis of all the programs using the 2250 unit;
b) the implementation of new versions of the Project Management System (PMS), the General Purpose Simulation System (GPSS), and the DYNAMO simulation program, the Mathematical Programming System (MPS), the conversion for use in conversational mode of the Continuous System Modelling Program (CSMP) of the LICE-compiler executor, etc.

Users

The JRC science departments enganged in direct Research & Investment projects account for 75% of utilization of the Computing Centre. The remaining 25% relate in part to certain contributions to the indirect action (more especially Fusion in Biology) and, for the rest, to work done by CETIS on behalf of JRC administrative departments, other Commission departments (notably DG Energy, DG Agriculture), and outside contractors.

The table which follows gives an idea of the user breakdown by objective; the last column of the table evaluates the trend for each objective in relation to 1970.

CETIS computing equipment: use % per objective.

Objective or activity	% of annual total		index 71 base 70
	1970	1971	
012 – Fast reactors	1,51	1,73	1,27
021 – Heavy water reactors - ESSOR	4,03	3,45	0,95
022 – Heavy water reactors - multipurpose research	2,70	1,93	0,78
023 – Heavy water reactors - research on reactor types	0,91	0,68	0,83
032 – High temperature gas reactors	4,31	1,27	0,32
041 – Reactor safety	2,44	2,66	1,20
042 – Control of fissile materials	0,61	1,47	2,65
060 – Reactor physics	15,72	14,01	0,98
070 – Condensed state physics	11,52	16,55	1,58
080 – Materials	0,83	1,26	1,67
090 – Direct conversion	0,02	0,49	
100 – Thermonuclear fusion and plasma physics	1,29	2,28	1,95
111 – Biology and health physics, radiation protection	5,41	4,55	0,92
120 – CETIS - Data processing	25,51	24,51	1,06
130 – Nuclear standards and measurements	0,22	0,62	3,10
150 – H F R	---	0,16	
180 – Instruction and training	0,18	0,18	1,10
------ – JRC administrative depts.	7,29	7,65	1,16
------ – JRC technical and general depts.	0,93	1,50	1,77
------ – Commission depts. other than JRC	2,24	3,28	1,61
------ – External	12,33	9,77	0,87

$$\text{index} = \frac{\text{time used 1971}}{\text{time used 1970}}$$

SUPPORTING ACTIVITIES

ADMINISTRATION AND PERSONNEL DIVISION
FINANCE AND SUPPLY DIVISION
PUBLIC RELATION OFFICE
ORGANISATION AND INFORMATION SYSTEM SERVICE

DESIGN AND FABRICATION DIVISION
INFRASTRUCTURE DIVISION

HEALTH PHYSICS DIVISION
MEDICAL SERVICE

SECURITY SERVICE

DIRECTORATE OF GENERAL, TECHNICAL AND ADMINISTRATIVE DIVISIONS

P. Herrinck

Administration and Personnel
Finance and Supply
Public Relations
Organization and Information Systems

Design and Fabrication
Infrastructure

Health Physics
Medical
Security

During 1971 the General, Technical and Administrative Divisions continued to provide the requisite support to the scientific activities and also tackled the reorganization and rationalization problems stemming from the restructuring of the J.R.C. with its new independence.

First, this entailed the reorganizing of the Finance and Supply and the Administration and Personnel Division so as to extend their activities to cover the other three Establishments at Karlsruhe, Geel and Petten. Secondly, rationalization of the work involved computerizing the practical management of the administrative and technical divisions. This twofold aim was successfully achieved in the course of the year, without delaying or detracting from everyday management operations, and at the same time the scientific divisions continued to receive the aid they were entitled to expect.

It can now be stated that whatever direction the J.R.C. programmes may take in the future, the General, Technical and Administrative Divisions will be in an even better position than before to carry out their work efficiently and discreatly, thus enabling the scientific divisions to pursue their work unharassed.

ADMINISTRATION AND PERSONNEL

P. Blaes

The scope of the Administration and Personnel Division was increased during 1971 to include all the J.R.C. Establishments. On the 31st December 1971, the staff of the four J.R.C.'s, totalled 1988 (staff and personnel of the Establishments) of which 1442 were at Ispra: the number of locally employed personnel and auxiliary staff totalled 364, of which 307 were at Ispra: the final total is therefore 2,352 individuals.

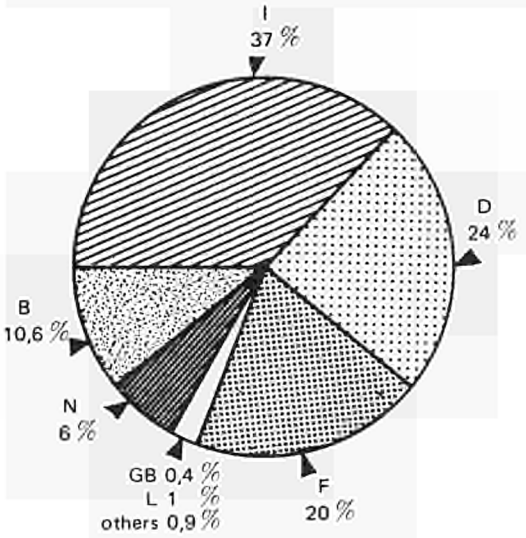

Distribution by nationality (excluding A.E. and supernumeraries)

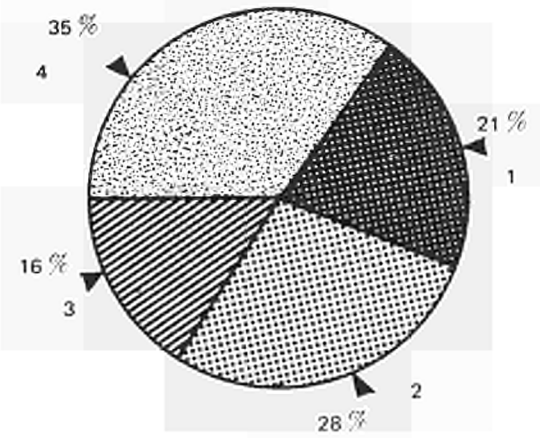

1 Scientists and engineers
2 Technical staff
3 Administrative staff (including supernumeraries)
4 Craftsmen, guardians, fireman and service personnel (including supernumeraries)

Distribution of personnel at the JRC's Ispra Establishment.

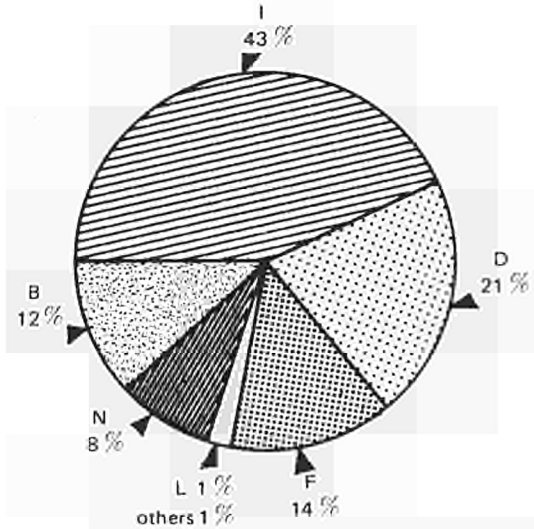

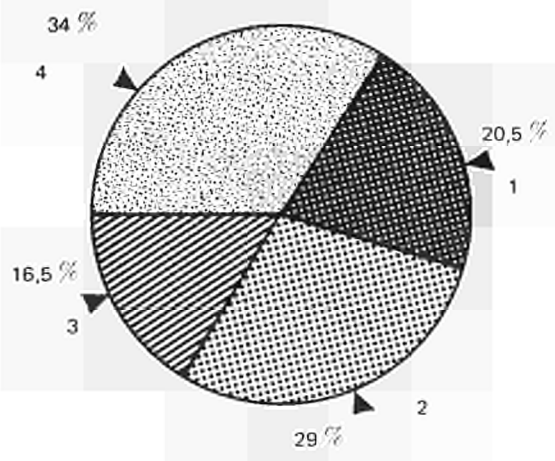

Distribution of JRC personnel (including A.E. and supernumeraries).

Personnel distribution by Services and by categories (Administrative and Scientific), (including personnel recruited but not yet working). Situation at 31st December 1971.

Service	A	B	C	Total (1+2+3)	Establ. Staff	Total (4+5)	Locally Empl. staff	Scholarship-holders Graduates	Scholarship-holders Students	General Total
	1	2	3	4	5	6	7	8	9	(6+7 8+9)
Direction	17	5	7	29	5	34	1			35
Programme Management	12	1	2	15	3	18	1			19
Security	1	5		6	24	30	17			47
Direct. General Serv. Adm./Tech.	2	3	1	6		6				6
Administr. and Personnel	7	19	10	36	38	74	65			139
Finances and Supply	4	20	6	30	27	57	20			77
Design and Fabrication	10	47	39	96	76	172	35			207
Infrastructure	3	10	2	15	40	55	11			66
Protection	12	20	1	33	39	72	22			94
Medicine	4	11		15	3	18	4			22
Biology	2	1		3		3	1			4
C.E.T.I.S.	30	42	6	78	12	90	2			92
Chemistry	44	39	5	88	15	103	22			125
Heavy water	9	6	3	18	1	19	1			20
Nuclear studies	42	19	2	63	5	68				68
Materials	46	68	4	118	17	135	15			150
Physics	33	19	4	56	4	60	1			61
Research reactors	9	33	1	43	23	66	7			73
Technology	60	97	14	171	42	213	20			233
Essor	19	77	4	100	46	146	5			151
Local staff Association		1		1		1	1			2
Personnel waiting to start work	1			1	1	2				2
	367*	543*	111*	1.021*	421*	1.442*	251*	*	*	1.693*

Social Affairs

During 1971 some organisational changes were made in this section: in july the canteen (mensa) and Club House were added to its responsibilities whilst the Sick Insurance Office was transferred to another section of the Division. Later, in October, the administration of visitors, Fellows and other students remaining temporarily in the Centre was transferred to this section.

Housing

The year 1971 showed a 95% occupation of all housing either run or owned by the Institute. The transfer of a number of officials from other units to Ispra in a very short period caused considerable difficulties in finding adequate furnished accomodation. Generally the housing problem remains one of the main difficulties for the personnel as the rents go up continually and have reached a very high level, especially in the towns. A number of unfurnished appartments (about 200) specially constructed by the Italian Government for our personnel are in great demand, owing to the fact that the rents are fixed at the 1965 level.

Social Assistance

This service continues to deal with an ever-increasing number of individual problems which are probably aggravated by the uncertain work climate of the last couple of years. The Infant Day Care Centre is operating under very difficult working conditions and is always fully occupied (about 45 children per day).

Mensa and Club House

The two canteens serve between 15,000 and 21,000 meals a month. It has not been necessary this year to raise the price of meals, in spite of the rising price levels of most materials and services. The Club House showed more activity towards the end of 1971, which expressed itself is a small profit margin at the end of the year.

Visitors, students, Fellows (paid or unpaid)

During the year there were, as in other years, about 120 students, of various levels, present in the Centre. Efforts were made to improve the administration of this activity.

This group of people presents particular difficulties, as they need furnished accommodation for sometimes short periods.

This type of accommodation becomes more difficult to find, a fact which is explained by the constantly improving standard of living of the local population.

General Services

Transport

After a period of stability (1968 and 1969: 15,800 travellers) a considerable increase already noticeable in 1970 (18,059 travellers) was observed in 1971, when 24,842 people were transported in hired cars. This increase has been mainly due to an increase in the number of meetings in connection with the installation at Ispra of the General Management of the J.R.C. A lesser reason for the rise in numbers has been the transport of "shift" workers.

- The normal transport of staff members to and from work has not changed much: every morning and evening 13 coaches serve a network covering about 380 Km.
- The number of vehicles in use for internal services has not varied, except for the addition of a new fire service vehicle (a "Schnorchel" which has a gondola for fire extinguishing work which can be raised to 26 metres above the ground).
- The shortage of funds which has made it possible to replace worn out vehicles, has led to a rather high number of large-scale repairs (reconditioning of motors, clutches, gear boxes, and repainting (bodyworks).
- The restructurisation of the Establishment has led to a very high number (more than 600) of removals and heavy transports: more than 1,500 tons of various materials have been transported by a staff whose numerical inadequacy has now become chronic.

Communications

The work of the Post Office has not varied much. Nevertheless, a high degree of absenteeism has made the collection and distribution work more difficult than it need have been.

Although the organization of the "diplomatic bag" service has been considerably modified, 5 weekly services between Linate and Ispra have been guaranteed.

Following a serious crisis, due to shortage of personnel, the telephone switchboard was able to improve its situation by taking on new staff: although it was impossible to satisfy all demands during the first six months of the year, the outgoing traffic put through 65,000 calls.

It should be noted that the Internal Switchboard in Milan now manages to establish international communications with a delay that rarely exceeds 30 minutes. This is already a great improvement.

Telex traffic is on the increase: there have been about 7,300 messages in both directions. The work load is increasing noticeably, because of the increasing length of the majority of telexes transmitted, and because of the greater number of copies to be distributed on the arrival of a message (DG, CCR, CIP syndicates, and various committees).

Cleaning

The conventional cleaning work, together with nuclear cleaning, has been carried on as in the past, in spite of a rather troubled socio-psychological atmosphere.

The cleaning activities involved about 90,000 m^2 (conventional cleaning) and nuclear cleaning has been done over a total surface equivalent to about 28,000 m^2.

Typewriter maintenance

The systematic preventive maintenance of typewriters and calculating machines continues to give spectacular results.

In spite of the age of many machines (replacements cannot be afforded) the number of repairs has fallen to 195 (as against 727 in 1967 and 483 even in 1969).

The introduction of a "Copy Service" system as a substitute for the "obsolete" photocopying machines belonging to the Establishment, has made it possible to improve the quality of the copies produced considerably, and at a lower price per copy: 1,700,000 copies were produced in 1971 (number converted to format DIN A4).

Training and Education

Training courses and scholarships (bursaries).

Tables 1 and 2 give the number of trainees and scholarship-holders present at Ispra in 1971, with their distribution by country of origin and by Division.

Table 1 – Number of traines and scholars.

	student trainees	scholars	apprentice trainees	total
Present at 1.1.71	21	20	6	47
Arrived during the year	53	22	3	78
Total	74 [1])	42 [2])	9 [3])	125
Left during the year	56	10	4	70
Present at 31.12.71	18	32	5	55

Table 2 – Distribution by origin and Division, of the trainees and scholars.

	B		D		F		I		L		N		Others		Total	
	s	b	s	b	s	b	s	b	s	b	s	b	s	b	s	b
BIO	1	5	1	3	–	1	9	4	–	–	–	2	2	2	13	17
CET	1	1	–	–	1	–	6	2	–	–	–	–	–	–	8	3
CHI	–	2	–	–	–	–	2	1	1	–	1	–	–	1	4	4
ETN	–	–	–	–	–	–	3	4	–	–	–	–	–	–	3	4
MAT	–	1	2	1	–	–	1	–	–	–	1	–	1	1	5	3
PHY	1	–	–	3	–	–	5	–	–	1	–	–	–	1	6	5
TEC	3	–	–	2	1	–	10	3	1	–	19	–	–	–	34	5
EFA	–	–	–	–	–	–	–	–	–	–	1	–	–	–	1	–
MED	–	1	–	–	–	–	–	–	–	–	–	–	–	–	–	1
	6	10	3	9	2	1	36	14	2	1	22	2	3	5	74 (1)	42 (2)

(1) Of the 74 student trainees, 35 are preparing study termination papers (Graduation or Diploma theses) and 22 are carrying out some obligatory phase of their studies.

(2) 23 scholarship holders are preparing a Doctorate thesis, or the experimental part of a post-university course: 4 others work within the framework of a collaboration programme between the Ispra Establishment and Universities.

(3) The best students of the Apprentices' School (which is attached to the Central Workshop), can follow practical training courses as traineee apprentices in various laboratories within the Establishment.

Table 3 – Number of students present in 1971, expressed in man-months, corresponding to credit consumption.

	B	D	F	I	L	N	Others	Totals
Student trainees	26	13,5	6	245,5	4,5	95,5	10	401
Scholarship holders	98,5	85,5	7	90	12	24	42,5	359,5

	BIO	CET	CHI	ETN	MAT	PHY	TEC	EFA	MED	TOTALS
Student trainees	84	54	18,5	14	30	36	162,5	2	–	401
Scholarship holders	148	22	43	29	26,5	43,5	42	–	5,5	359,5

Remarks

The normal course of the "training and scholarships" activity was disturbed by an unexpected break in the rhythm of engagements, which were practically stopped during the second quarter of 1971: about 35 candidates (of whom a third were scholars) who should have started work before the end of 1971 have been kept waiting in suspense. This situation becomes even more regrettable by the fact that for a great majority of these candidates their work at Ispra would have been integrated with their studies.

Our reputation with educational institutions and their professors has certainly not been improved by this.

Technical Improvement Courses for Staff Members

During the academic year 1970-71, eight courses were organised at Ispra, according to the programme of the National Conservatory of Arts and Crafts in Paris. At the end of the corresponding final examination, 41 certificates were obtained by Ispra Staff members, of whom 7 were German-speaking, 15 French-speaking, 6 Italian-speaking, and 12 Dutch-speaking (Table 4).

The Preparatory Physics Course was continued (optical elements and heat), and was followed with success by 4 students, 2 staff members also succeeded in the preparatory mathematics examination.

Remarks

Three years of collaboration have led to a very cordial and efficient relationship with CNAM, which benefits both pupils and teachers. This initiative has now proved its viability, and could certainly be formalised and expanded with great profit.

The problem of practical work has been partially solved. The cooperation of CETIS has made it possible to organise an adequate programme of practical work in the field of information and programmation: in addition, a "made to measure" programme has been developed for a specific field (Electronics).

It is deplorable, on the other hand, that of the four rooms reserved for these courses (still not very suitable at that), three have been "occupied" and reconverted into offices, with the result that some of the lessons have had to be cancelled because of lack of space.

Table 4 – CNAM examinations

	Number of CNAM certificates		Number of CNAM certificates
General Mathematics A	3	Practical work on Numerical Analysis	4
General Information A	7	Numerical Analysis B2	4
Practical General Informatics work	10	Mathematical Machines B1	5
Basic Electronics	1	Practical work on Radioelectricity	1
Numerical Analysis A	6		

Professional Training of the Staff

A Fortran Programming Session, given by a Professor of the Bocconi University of Milan, was attended by about 50 people, (half of the total number of applicants). The Course will therefore have to be repeated as soon as there is enough money and man-power available to make this possible. In addition, a course for training radioprotection experts (according to Italian law) has been organised. Finally, secretarial re-education is also the object of training sessions held at Ispra.

Participation in external training activities

During the past year staff members participated in 111 activities: i.e.:

- 7 training sessions in laboratories for the acquisition of specific new knowledge
- 3 general correspondence courses
- 101 specific courses in various fields.

One staff member enrolled during 1971 in 3 courses, 12 enrolled in 2 courses, and the rest (84 individuals) in only one each.

In addition to the above list 23 members took part in small local training programmes.

Normal study programmes should also be mentioned. By this we mean the courses which form part of the regular educational systems organised by educational networks, and which terminate in diplomas (for example secondary technical studies, university studies).

A mixed working party (representing both the personnel and the Institution) has decided upon the criteria, which, based upon our financial limitations, should be applied to repayment demands.

A total of 27 demands have been dealt with according to these criteria, and have been the subject of a proposal: no decision has yet been taken.

FINANCE AND SUPPLY DIVISION

W. Metzger

As far as this Division was concerned, the year 1971 has had a rather transitory character.

During the year, changes caused both by the internal structural organisation of the J.R.C. and the introduction of a new type of budget planned for 1972 were made.

The restructurisation of the J.R.C. has led to one central budget combining the activities of the four Establishments – Geel, Ispra, Karlsruhe and Petten – takes into account both the programmes decided upon and the money set aside for them.

The introduction of a new type of budget known as a "Functional Budget" has necessitated a revision of the entire accounting system, because each different type of activity is related, by credit or by debit, to the remaining whole.

This double objective has been achieved during 1971, but its realisation makes very extensive demands upon the powers of electronic computers.

In spite of this transitory climate, the Division has continued to manage the current budget of the Ispra Establishment, as well as the other activities which are entrusted to it, of which one might mention, amongst others, the survey of markets for general supplies, the administration of contracts signed with outside firms, risk insurance coverage, the running of a central storehouse and the distribution of its goods, customs and excise problems created by the shipment of goods, the keeping up to date of a permanent inventory, the payment of bills, legal disagreements etc.

Budget

In 1971 the expenses of the salaries and other remunerations of the ISPRA Establishment staff have been taken from the research and investment budget, and organised by the Head Offices at Bruxelles. The expenses due to salaries and remunerations of other personnel employed by the Establishment are given below in millions UC.*

	ISPRA	J.R.C.
Establishment Staff	2,763.8	3,636.3
Locally employed personnel	1,275.4	1,488.0
Auxiliary Staff	9.5	49.2
	4,048.7	5,173.5

Investment and operating credits engaged in 1971 for the ISPRA Establishment have been reported in the following Table (in millions of UC).

*) 1 UC (accounting unit of the European monetary agreement) = 3,66 DM = 5,554 FF = 50 FB = 3,62 FlH = 625 lires.

Operation	ISPRA	J.R.C.
Property, material and various administrative operation expenses	2,916.4	4,262.9
Apparatus, and small supplies of fissile material and consumable material	1,962.8	3,954.7
Maintenance and siting of scientific materials	2,166.3	2,573.5
HFR Reactor exploitation	–	2,754.0
ISPRA 1	212.5	212.5
ESSOR	1,417.4	1,417.4
ECO	310.2	310.2
Further exploitation of BCMN	–	213.2
HTGR radiation	–	250.0
Automatic scientific information	84.5	84.5
Professional or personnel information	59.9	59.9
Investments		
Buildings	579.0	1,037.0
SORA construction	721.2	721.2
Large scientific apparatus	192.7	365.2
	10,622.9	18,216.2

Current financial and accounting operations

Each decision to spend money is the object of a financial commitment, and usually at some later date, of a payment.

During the year 1971, the commitments and payments carried out for the Ispran Establishment totalled about 78,000, which represents increases of 7,000 operations over the total for 1970, and 23,500 over that of 1969, and 17,600 over that of 1968.

During the same period 1968/1971, the number of staff occupied on this work has been reduced from 12 to 10.

The graph reproduced below illustrates the development of these data.

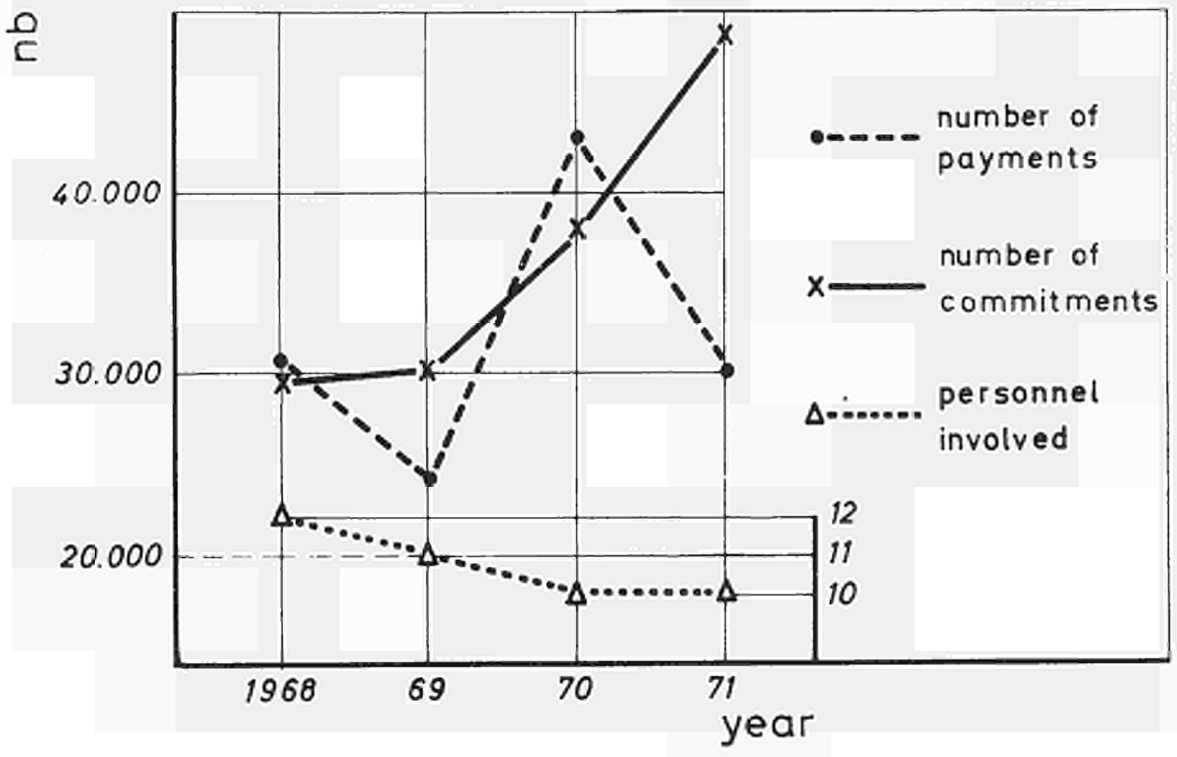

Supplies

For simplicity, supplies for the Ispra Establishment are subdivided into two distinct types.

- the first category involves materials to be used by specific users or Services.
- the second category covers general supply, i.e. articles of common use throughout the Establishment, or at least to a certain number of its Services.

In the first case the Services themselves are responsible for surveying the markets and passing orders to the suppliers which they consider to be most suitable. This Division only enters the picture at the level of accounting the commitments, freeing the goods from customs, inscribing them on to the inventory, distributing them to the user-Services, and liquidating the corresponding bills.

In the second case, in addition to the operations described above, the Division itself carries out the market surveys, as well as passing the orders, mostly by means of contracts or by price agreements. After delivery, the goods are kept in a central store, where users can withdraw them personally, or have them delivered, according to their requirements.

The following sketch illustrates these supply mechanisms.

There is also a Purchasing Office (not included in the sketch) in Milan: its purpose is to take care of, as quickly as possible, small urgent purchases requested by any of the various Services. Some idea of the volume of work involved is given by the following figures: the Office in charge of customs work freed more than 6,000 consignments during 1971, and nearly the same amount during 1970.

The Inventory Office recorded in 1971 the entry of 1,682 inventoriable articles, 1,882 in 1970, and 1,356 in 1969.

The efforts of the customs - freeing/delivery/inventory/storage/distribution chain were coordinated up to the end of 1971 by a total staff of 32 people, which is 19 less than the total staff employed at the end of 1969.

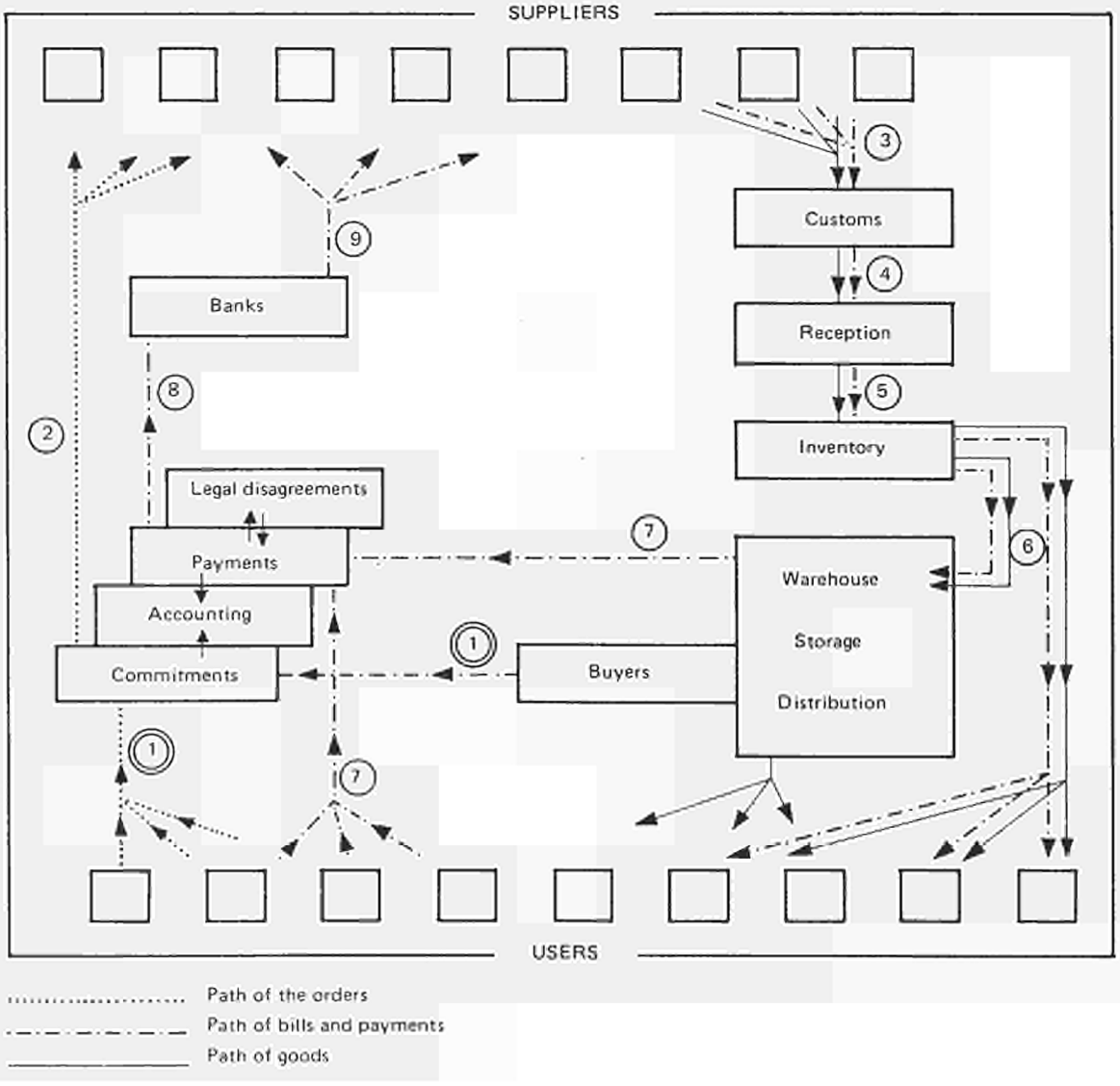

PUBLIC RELATIONS

G.L. Faa di Bruno

The main task of the Public Relations Service is to inform the public at large about activities at the Ispra nuclear research establishment and also to prepare and carry out meetings and congresses.

This essentially implies the distribution of folders, leaflets and assorted printed matter, presence at meetings and exhibition, and looking after visitors and participants at conferences.

Film shows play an important part in Public Relations activity at Ispra. With visiting groups, they aptly round off introductory talks and also illustrate sections of the establishment which for lack of time or opportunity it would not be possible to visite. For this purpose a 35 mm colour-film (title: "From an old world to a new one" by Robert Paul Dagan) produced several years ago had to be adapted to the present-day situation. It tells the story of the birth, growth and life of the Research Centre in recent years.

In 1971 the flow of visitors was so intense that at times only groups booking their visiting-date far ahead could be taken into consideration.

Records for the year show a total of 3,029 visitors, with the following breakdown:

1)	Secondary schools	801	persons
2)	Universities and higher institutions	464	persons
3)	Political and scientific personalities, businessmen	145	persons
4)	Firms and industries	213	persons
5)	Participants at meetings and scientific conferences	1.236	persons
6)	Individual visits	155	persons
7)	Press, radio and TV	15	persons
		3.029	persons

Foremost among prominent visitors in 1971 was Prof. Dr.Ing. Hans LEUSSINK, Minister for Education and Science in the German Federal Republic, who came to Ispra on July 22, accompanied by Dr. SCHUSTER, Director in his Ministry.

On 16 and 17 February we were also able to greet Mr. W.P. SHOVELTON, British undersecretary of Trade and member of the Delegation negotiating the entry of Great Britain into the Common Market.

Among major meetings of the year under report one should mention the Post-Geneva Conference on "Non-destructive measurements and identification technique in nuclear safeguards" held at Ispra on 21-23 September, with 100 participants, and the 3rd Symposium On Micro-Dosimetry held at Stresa on 18-22 October, with about 150 participants.

During the year the Ispra Establishment was also present at the German Industries Show at Berlin (5-14 November) with a well-equipped and much-visited stand.

About 5,000 cuttings from European and other publications (daily and periodical) were distributed among colleagues in the Centre.

Furthermore the Public Relations Service had to take care of about 540 inter-establishment conferences.

Also during 1971, there was pleasant cooperation with the Cultural Committee; with our assistance it was able to carry out a rich and interesting programme of concerts, lectures, etc. The high spot was a lecture by Prof. Hubert Beuve-Mery, founder and editor of the French daily, "LE MONDE".

Ispra, 22 July 1971: Visit of Western German Science Minister, Prof. Dr. Ing. Hans Leussink.
Left to right: *Dr. P. Caprioglio, Director-General of Joint Research Centre*
Prof. Dr. Ing. Leussink
Half-hidden: *Dr. H.W. Schleicher*
Dr. G. Schuster, Director in the Federal Ministry for Education and Science.

ORGANIZATION AND INFORMATION SYSTEMS

F. Sciuto

The Organization and Information Systems Service (OSI) was formed at the beginning of 1970 just before the big changes in organization and structure imposed on the JRC by the Council of Ministers in December of the same year. These changes can be summarized as follows:

- larger autonomy of the JRC and, as a result, increased authority of the Director-General;
- creation of a General Consultative Committee on programmes and of a Scientific Committee;
- transfer from Brussels to Ispra of the Directorate-General of the JRC.

NB. We should also add the introduction of a budget by "objective" instead of the old-type budget by "nature" of expenditure. This will eventually lead to big changes in the organization.

As a result 1971 must be considered as a year of transition from the stand point of organization. Instead of looking at the long-term problems, the OSI Service had to devote its efforts to solving a series of urgent problems.

We shall confine ourselves to mentioning a few examples chosen from among the more important:

in the field of personnel management

- new organization chart of the four Establishments of the JRC (down to the group level);
- codification of the activities of the personnel of grade "A";
- rules related to shift work, stand-by at home and at work, onerous work, etc.;
- critical review of the administrative procedures for the processing of the "ordre de mission" (Official Trip form);
- study of the distribution of administrative personnel among the various scientific divisions;
- review of the procedures of the health insurance scheme.

in the financial field

- organization chart of the Finance Division;
- review of the supply procedure and new definition of the function of the various shops;
- review of the rules relating to the inventory.

We should also mention the study – not yet finished – on the future use of the IBM2750 System. In the first phase it is intended to use this machine as:

- a telephone exchange with automatic billing of personal calls;
- an alarm detection system for the conventional installations at the Establishment and as a data collection unit for preventive maintenance.

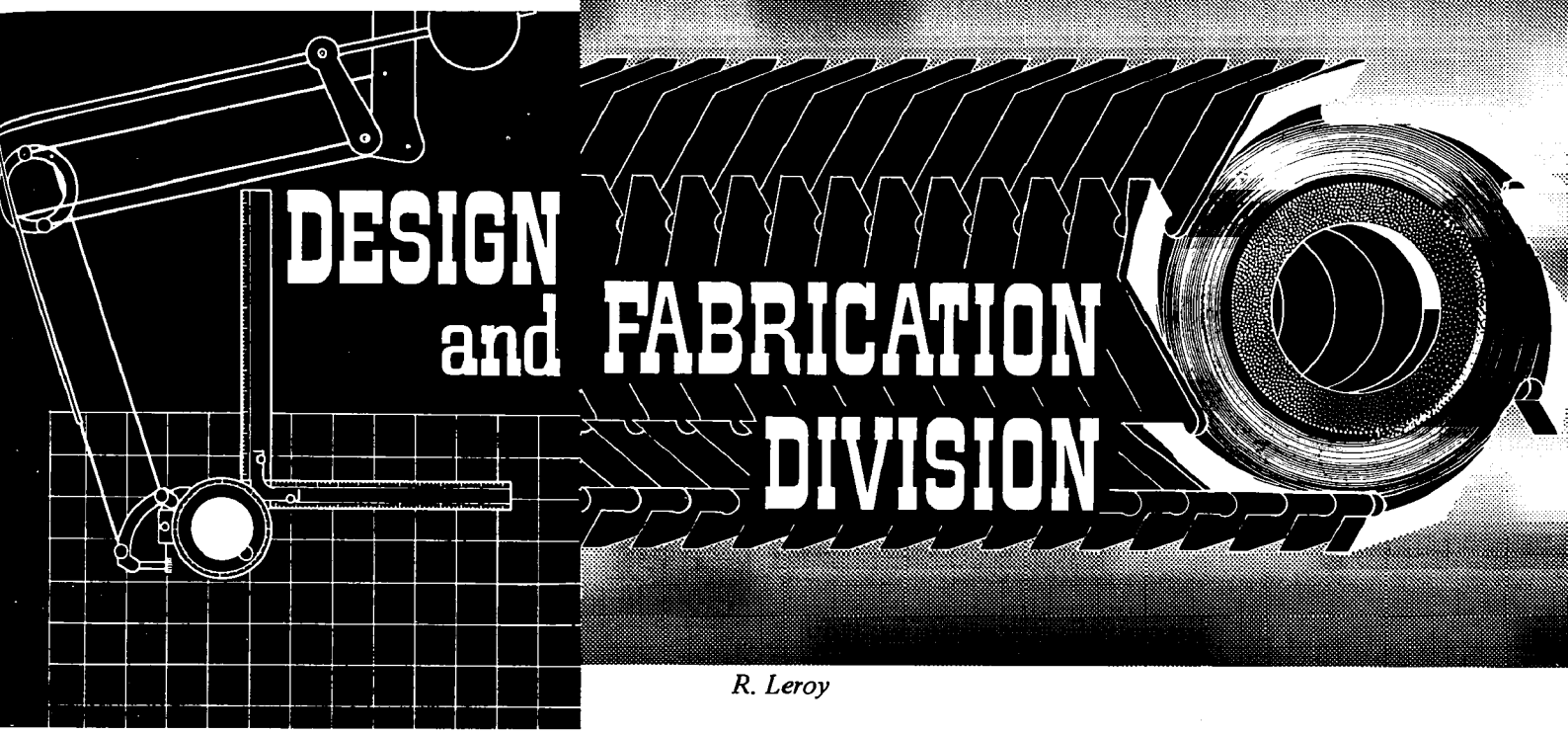

DESIGN and FABRICATION DIVISION

R. Leroy

The aim of the Design and Fabrication Division is to give technical and scientific assistance to all research programs carried out by the different laboratories, by seeing the design and fabrication of the experimental, mechanical and electromechanical devices they need.

The Division organization revised in 1970, expanded in 1971 to include the Raw Materials Store.

The Division can rely upon:

- a Design Office for general purposes, including the document reproduction office of the Establishment;
- a Main Workshop with the management and supervision of the joint Raw Materials Store;
- a number of industrial firms outside the Establishment which carry out all surplus work or jobs requiring particular equipment;
- 15 joint workshops located in the main laboratories and immediately available to the researchers;
- an apprentice training school.

All these different units whose activities are strictly interrelated, were grouped together for the following reasons:

- to reduce the number of offices researchers have to contact in order to obtain the realization of an experimental device, and at the same time to simplify the administrative procedure;
- to coordinate all such activities as necessary for the tasks to be accomplished;
- to facilitate the team work between the design staff and the workshop staff;
- to provide a supply of raw materials fully complying with the guaranteed standards of quality and quantity required, from the project stage onwards;
- to give the Reproduction Office the assistance of the Design Office in carrying out any technical schemes for the issue of scientific reports;
- to enable the Training School apprentices to avail themselves of the facilities offered by the Main Workshop installations, and of the assistance of skilled technicians from the Workshop and the Design Office;
- to establish a standardized management policy for personnel working on common programmes.

The technical management of the Design and Fabrication Division has been worked out in collaboration with the experts of the computing Centre of the Etablishment (CETIS). It makes use of several programmes elaborated by the CETIS computers, which at present persuit:

a) computerized management of the work load (Design Office and Workshop) and its development in relation to the execution times calculated beforehand after a careful examination of the work schedules. With this system one can plan the jobs, ascertain their progress at any time, and determinate the most suitable utilization of the personnel working on different engagements.

b) Computerized management of the Store stock by means of continuous supervision, taking into due account any best possible and the supply requirements. In the near future the stock situation is to be regularly notified to each Scientific Department of the Establishment for the information of all those interested. Such information, involving an intimate contact between the management and the users, will enable supplies to match their specific requirements.

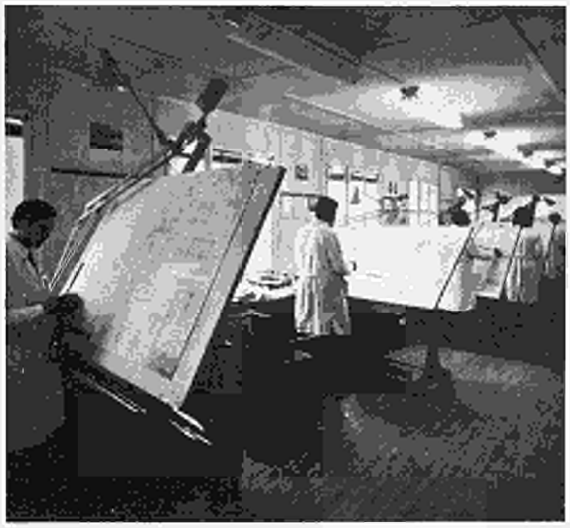

Fig. 1: Draughtsmen room.

Fig. 2: Reproduction workshop.

DESIGN OFFICE

The Design Office and Reproduction Office constitute a unit also known as "General Studies and Radioactive Engineering".

It has to deal with widely varying requests to meet the needs of the different scientific branches of the Establishment.

Essentially it consists of four specialized teams:
General Design, Radioactive Engineering, Special Installations and Electricity, Reproduction Office.

Design

The senior engineers, engineers and draughtsmen avail themselves of the support of the Standards Bureau and the technical documentation office which put their information at the disposal of the whole Joint Research Centre.

The Technical studies that are new in character are dependent upon experimental verifications; these tests are carried out in a small electromechanical laboratory.

For conferences and scientific reports, drawings of curves and diagrams as well as graphic visualizations are needed. This work is done by the Design Office when necessary with outside help.

In addition to the customary calculations of stress analysis, fluid, mechanical and thermal, the Engineering have developed some methods of computer calculation including:

a) stress analysis calculations by with the method of finite elements,more specifically to decide upon the best materials and most favourable shape for devices rotating at high speed;
b) radiation of protection calculations. In particular the Office, jointly with the Nuclear Studies Division, did the shielding calculations for the Sora reactor and for containers for the transport of radioactive materials.

During 1971 the Design Office received 91 requests for new studies and 187 requests for curves and graphs.

Among the various general mechanical, chemical and hydraulic engineering studies, containers under pressure, circuits, etc., rotating devices, radioactive engineering, installations for air conditioning and service fluids, should be mentioned:

The study of a collimator with a small angle of collimation

The problem was to obtain thin collimation walls that are quite parallel. It is difficult to obtain thin metallic foil partitions having the desired accuracy of flatness. With the collaboration of the physicist concerned, the Engineering Office desegned a collimator whose partitions are made of long-fibre paper sheets. These sheets are stretched by applying a special varnish and then coated with a varnish containing boron in order to increase their neutron absorption characteristic. The central workshop built six collimators of that model. Each one has 65 partitions, each thinner than 0.1 mm and 500 mm long. The corrugations were smaller than the thickness of the sheets. This collimator model is protected by an application for a patent.

Study of a flight track for the measurement of neutronic diffraction

This device consists essentially of three vacuum-tight conical channels. Each channel has a neutron counter bench fixed to its extremity. Each channel is about 3 metres long. The three-channel unit forms a sector which can be moved in a vertical plane. The whole device is strongly shielded against the surrounding radiations.

During the measurements the angle formed, by the channels and the incident beam of neutrons must be adjusted. This is done by means of a hydraulic mechanism able to support the 5 ton weight of the whole apparatus and to bring it into the right position with an angular precision of 15 minutes. The whole device was made by the Central Workshop which had to resolve such problems as complexity of forms, large size, diversity of materials and vacuum tightness.

Project of the Sora reactor pulsation device

This project was used as a reference for the more detailed study made by private industry.

The problem was to position a rotor, working inside a helium-filled container, very close to the reactor core. This rotor carries the movable reflector which has to be closer than 20 mm from the nearest fuel element. The rotating speed is 3000 rpm and the circumferential velocity 300 m/sec.

Study of a measurement device for prompt and delayed neutrons

This device, used to check the fissile materials, consists of a set of concentric tubes. When in working position, a fuel-element pin, surrounded by an activated antimony source and a tungsten ring, moves into the centre of these tubes. The most difficult problem was to provide an accurate remote assembly of the set, on account of the presence of the active source. Moreover, the fuel element pin had to reach in four-tenths of a second the upper part of the apparatus where the counters are located. At the same time, the tungsten ring moves downwards.

Study of a cold-neutron monochromator

The Design Office also works under research contracts for outside organizations.

A contract was received for the study of a cold-neutron monochromator for the firm Sorin. The device has a 230 kg rotor which rotates in vacuum with a circumferential velocity of about 300 m/sec. In order to be able to select neutrons with very different wavelengths, the eleven discs bearing the selective helicoidal shots must be able to be moved or changed easily. For this purpose, the discs are not fixed rigidly on the shaft but are axially compressed by means of flexible crossbars, between two flanges.

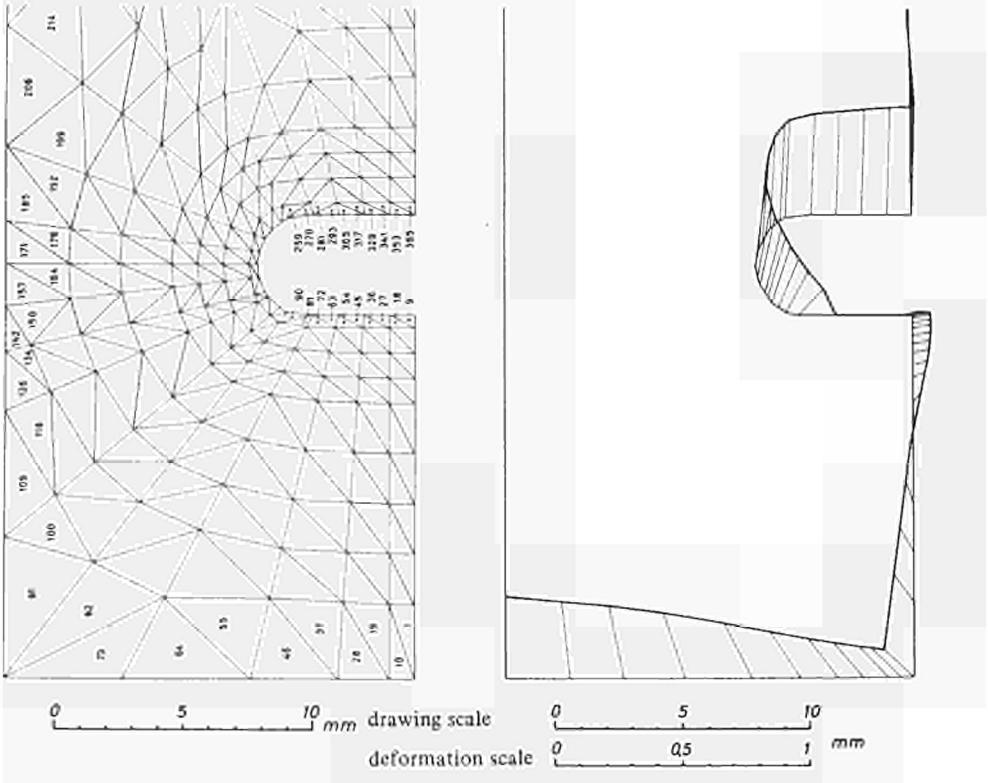

Fig. 3: Calculation of deformation by finite elements method for a SORIN rotor plate (N = 10,000 rpm).

Reproduction

The Office carried out their usual programme:

- The reproduction of documents by duplicator, off-set machines and photocopy;
- heliography reproduction of drawings;
- taking and printing of photographs.

The screen technique for reproduction of pictures which have to be printed was developed.

Slides of curves and diagrams are realized with white lines on a blue background. This process gives a sharper projected picture than the white-on-black process, as sharp as those of a negative (white lines on black background) but more restful for the eye and less disturbed by a surrounding lighting.

The Reproduction Office did the following service work during the year 1971 (in numbers of copies):

photocopies	65.181
off-set interior	1.184.242
photographs, inside	11.463
heliography copies	91.166
duplicator	2.134.670
off-set, exterior	534.570
photographs, exterior	1.979

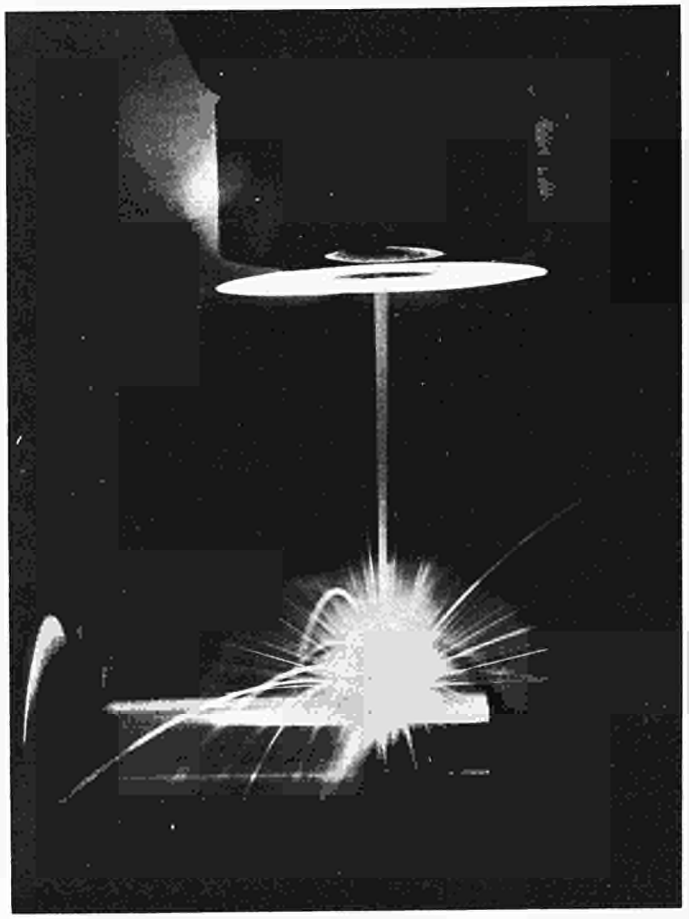

Fig. 4: Part of electron beam welding installation.

MAIN WORKSHOP

The Main Workshop contains the Centre's most important machine tools as well as some special machines. It has to cope with a wide range of very different jobs according to the various scientific requirements of the Centre.

It therefore comprises several departments or skilled units, namely:

- precision mechanics;
- general mechanics;
- boiler work and welding;
- coverings and surface treatments;
- lead and paraffin melting;
- graphite machining;
- checks and inspections.

A specialized Workshop provides for the maintenance of tools and machine tools of the Centre. A "ready execution workshop" carries out a number of simple jobs, according to a simple procedure and very rapidly (1505 applications were dealt with in 1971). Materials supply workshop located in the warehouse provides the Laboratories with items having the dimensions requested and thus avoids the accumulation or waste of material.

Certain technologies complying with specific needs, on which the Workshop technicians have bestowed their best attention have been set up and developed along side these installations.

It is enough to mention:

- the electron beam welding installation, complemented by an original and patented regulating device for electron beam focusing, as well as a welding cycle scheduling system (see picture on left side page);
- electroerosion machining for which a study was done of the influence of the dielectric temperature on the efficiency of the process, which was thereby greatly improved.

During 1971 the Main Workshop carried out 400 job applications.

The most interesting achievements included:

a) *Liquid control rods* consisting of three channel-type assemblies 7 m long and of an average diameter of 120 mm. Since this involved three Zr-2 tubes concentric with three stainless steel tubes twisted together helicoidally, it was technically difficult to provide for their straightness (the measured total camber proved to be less than 1 mm) and to achieve the preset final length.

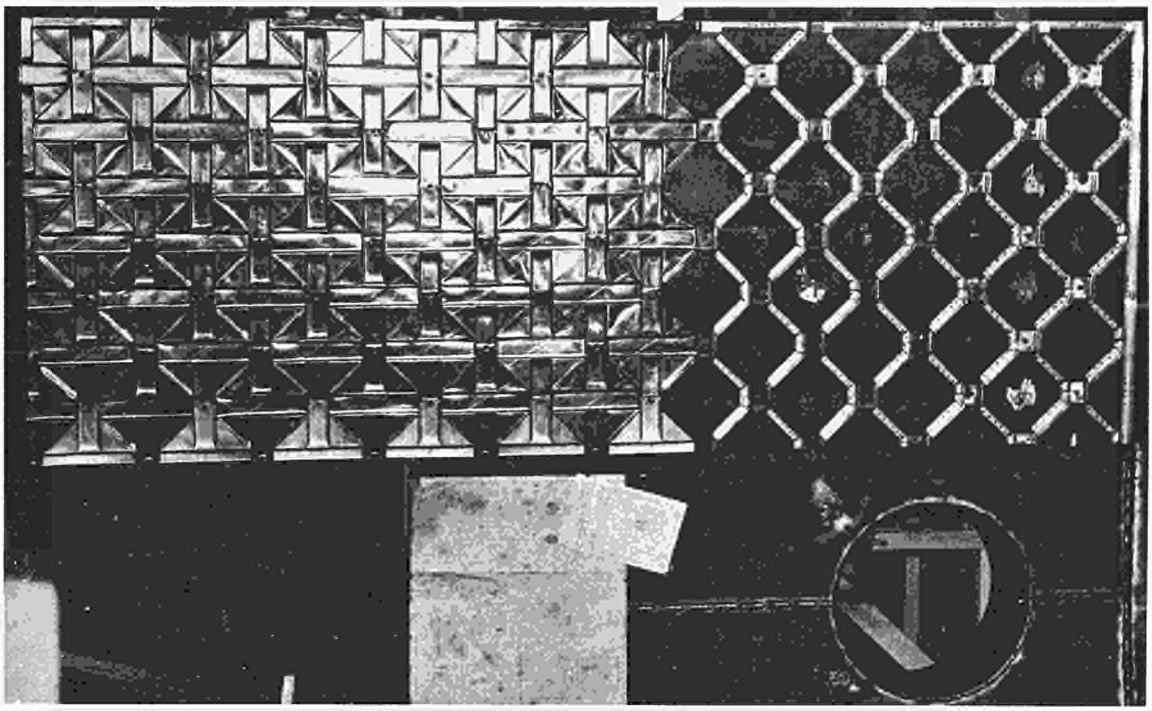

Fig. 5

b) Test panel, thermal scream for HTGR.This involved the construction and assembly of a "honeycomb" on a mock liner of insulation cells (300 x 300 mm) in stainless steel 2/10 thick. Since the standard technique does not comply with nuclear cleaning requirements, several problems of execution had to be solved in order to develop suitable tools for shaping and fixing thin sheets on thick plates by means of hollow-pin welding. (fig. 5).

c) Test section for sodium boiling. Here small-diameter holes had to be drilled for a considerable distance through bars of refractory material (Fluginox). (Holes of 6 and 9 mm diameter were drilled on a length of 1500 mm). A horizontal machine tool was manufactured, having a machining head working by electroerosion while the bar and electrodes, carefully lined up, were rotating in the opposite direction. The precision obtained on the diameter was 5/100 mm with a resulting concentricity of 4/100 mm.

d) Fluidized-bed test injector. This machining, carried out on a Plexiglas block, showed very close tolerances on a very complex shape as illustrated by the picture. (fig. 6).

The Workshop is also active in research program contracts for outside organizations, and fabricated the following:

- a Zr-2 safety tube, 2 mm thick, 6 mm long and having an average diameter of 110 mm, for the 2 CART channel. This tube, which required six welding operations by electron beam, showed a total camber of only 9/10 mm on completion;
- some prototypes of fuel-element anchoring grids for the PEC project. These one-piece grids were entirely fabricated by electroerosion since the standard machining technique did not allow the execution of a cylindrical section of the small hooking bars.

Private Industry

The Workshop in 1971 relied on 70 outside firms in order to meet the different requests of the Laboratories and to carry out the surplus work requested of it. 442 job orders were filled in this way.

A number of these job orders are met through "open contracts", i.e., a price agreement previously established with different firms, which allows a great simplification of the administrative procedure. The number of these job orders increased from 52 in 1970 to 142 in 1971.

The execution of work by local industry generally gives rise to problems concerning the raw materials (supply, conformity, etc.). To avoid these problems the raw materials are supplied by the workshop warehouse.

It is worth mentioning that in 1972 a part of the warehouse supply of common raw materials is to be obtained under agreement from local suppliers in order to simplify the procedure and to reduce the stocks.

Joint Workshops

The situation of these workshops, 15 in number, has remained unchanged since 1970. Having each a small staff, they constitute the ancillary units of the Laboratories or big installations and deal with all maintenance operations and immediate tool jobs of limited importance. The personnel team closely with the researchers. These workshops are under supervision of the Main Workshop which provides the materials supply and any special tooling they need.

Their present staff is too reduced to meet all requirements. (The same can also be said for the clerical staff of the Centre, as well as for the Main Workshop.). The distribution of these workshops is to be re-examined in 1972, however, for better adjustment to the new features of the Scientific Divisions.

Apprentice Training School

The aim of this school is to give young people a professional training as workers or technicians according to the needs of a Research Centre.

The teaching consists of two cycles:

- the first, lasting three years, is carried out at the Main Workshop. The courses are mainly held by technicians working in the Studies or Workshop Departments and consist of: theoretical instruction (mathematics, physics, technology), general culture (languages: German, French, Italian, and legislation) and practical instruction (industrial draughtsmanship, workshop, electricity).
- The second allows the best qualified young men to do a two years' training course in some of the scientific departments. This enables them to practise and develop in the Laboratories the background knowledge they received at school.

As of 31 December 1971 the School was attended by 33 boys in the first cycle, 5 young men on probation in four scientific Laboratories.

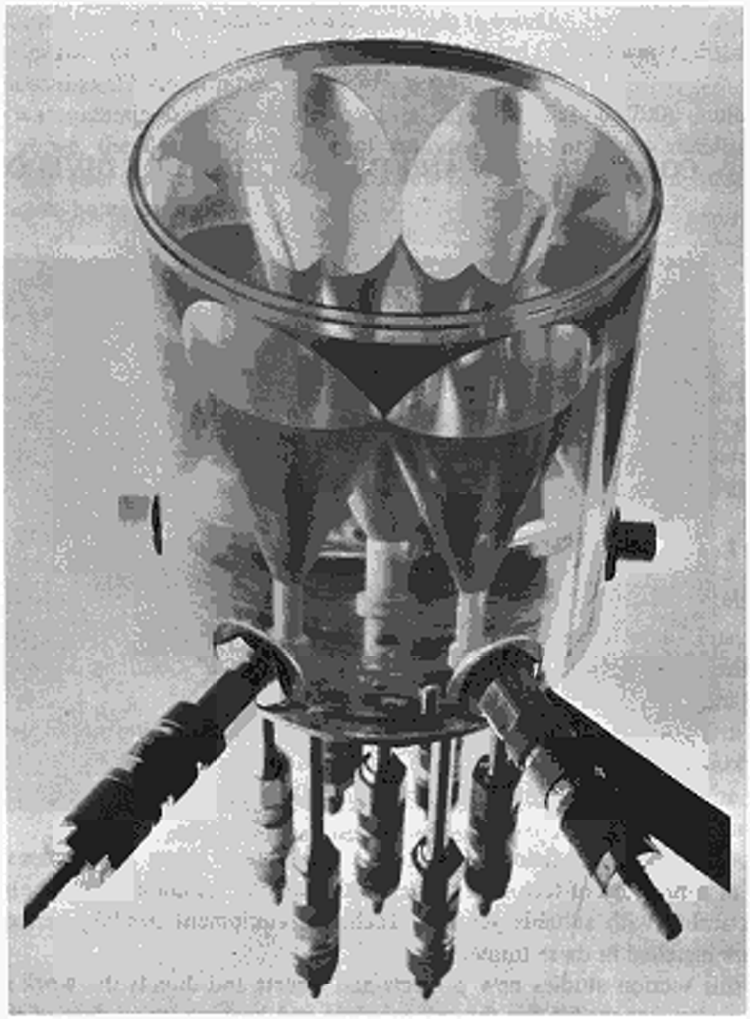

Fig. 6: Fluidized bed injector.

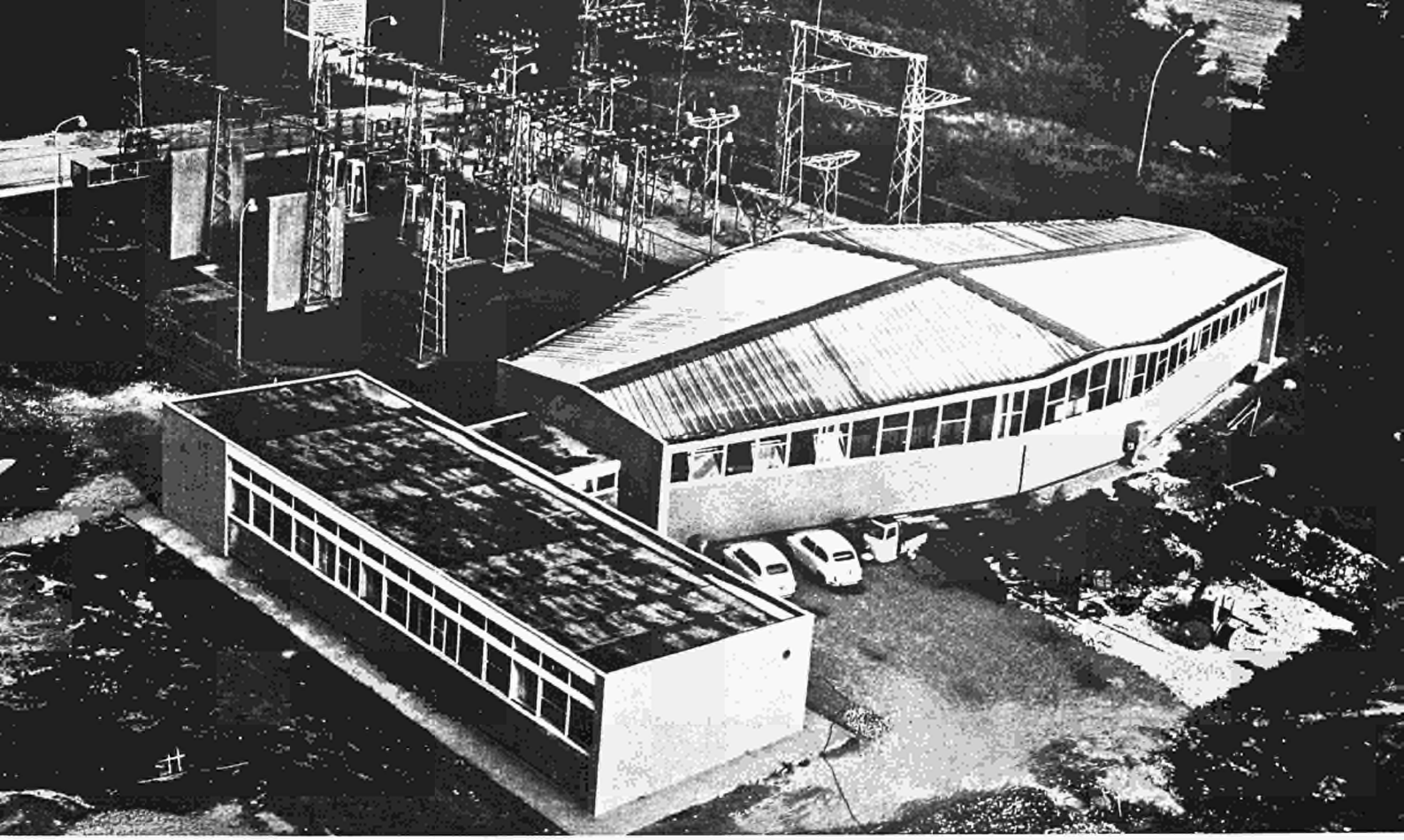

Airview of the electrical power station 50/12 kV.

CONSTRUCTION AND INFRASTRUCTURE DIVISION

E. Pomar

The task of the Construction and Infrastructure Division is to ensure the perfect functioning of the Centre, in its role as supporting the Scientific Divisions in carrying out their research.

This task involves many sectors and requires a vast range of knowledge in highly diversified specialised fields. This fact is illustrated very clearly in the following chapters.

Design and Civil Engineering Works

These include:

- Maintenance and, if necessary, modification of the 259 buildings of the Centre, according to the demands of the research work being carried out in them. These buildings have a total volume of about 750,000 m^3, and cover a total ground surface of about 100,000 m^2.
- To maintain in a good state of repair, and, if necessary, to extend and modify the roadways, the open areas and parking areas (total asphalted surface 200,000 m^2 approximately);
- Maintenance and operation of the waste water purification plant (in collaboration with the Thermal Fluids Section).
- The upkeep of the woods and fields which cover a total area of about 160 hectares.
- Maintenance of a network of technical tunnels which extend for about 5,500 meters, and most of which are also practicable with suitable vehicles. Technical equipment needing periodical maintenance and surveillance are installed in these tunnels.
- In addition, this section studies new projects and directs and directs the work which comes under its influence. It is also responsible for the safeguarding and keeping up to date of the central filing system for designs (blue prints) of buildings and plant.

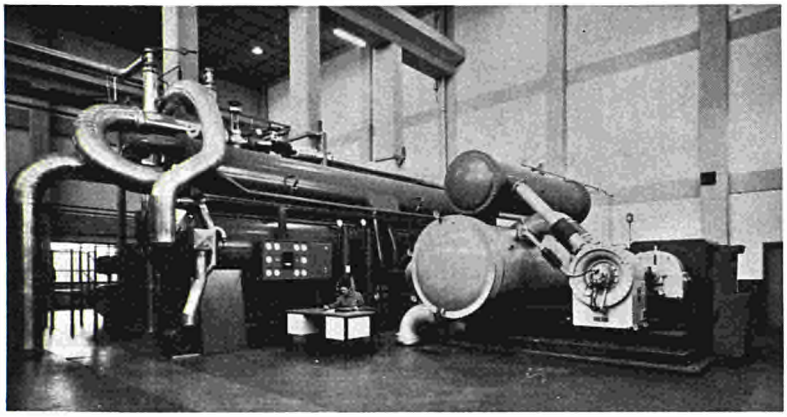

Central rifrigerating plant for airconditioning (3.200.000 frig./h).

Thermal-Fluids Section

This involves:

- The operation and maintenance of the Heating Installation, consisting of three boilers, who together produce a maximum total of 60 metric tons of steam per hour. They also supply the residential area outside the boundaries of the Centre.
- The operation and maintenance of the Main Refrigeration Installation, which consists of two groups of refrigerators, with a freezing power of 3.200.000 fg/h (12,700,000 BTU/hour).
- The operation and maintenance of the Water Plant, which involves the collection, processing and distribution network of water (37 km of pipes). The water is taken from Lake Maggiore at a rate of 2700 mc/hour, and distributed throughout the Centre.
- Operation and maintenance of the superheated (140°C) and cooled (+5°C) water, distributed through a network covering more than 27 km of pipes.
- Maintenance of the water storage tanks, which have a total capacity of about 7000 cubic meters.
- In addition to the above, the Section takes care of studying plans for new installations, directs their construction work, ans also carries out the modifications and modernisation of existing installations, whenever this appears to be necessary.

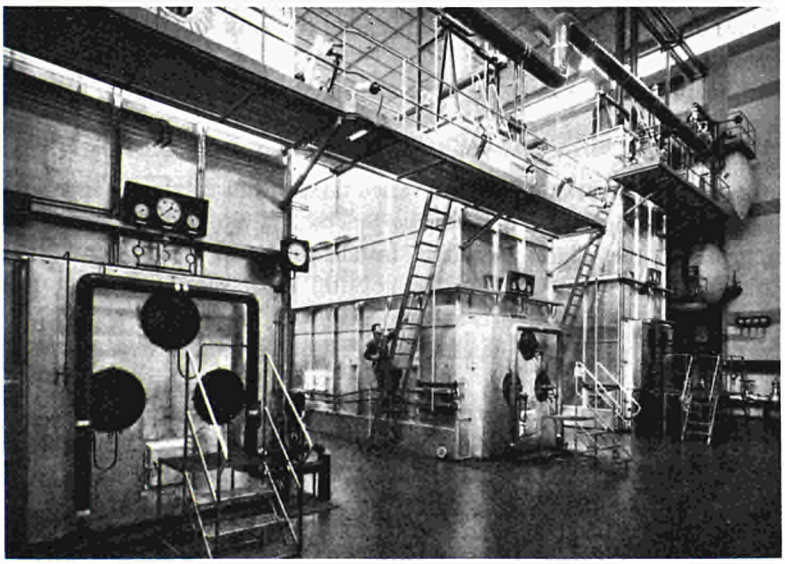

Steam plant for heating and airconditioning (60 t/h).

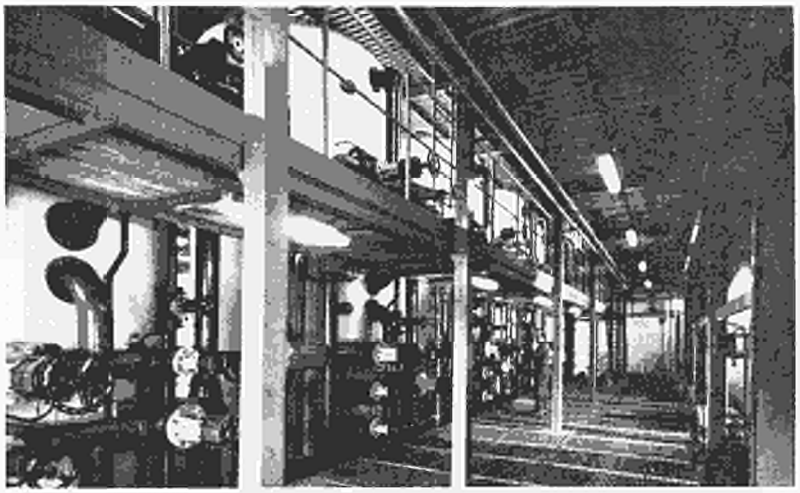

Filtering plant for industrial and drinking water (1650 m³/h).

Development of consumption during the years 1967-1971.

Description	1967	1968	1969	1970	1971
Drinking water and industrial water, (in thousands of cubic metres)	9919,00	10117,00	10234,00	9915,00	10682,00
Steam (thousands of tons.)	109,00	93,00	114,00	112,00	121,00
Electrical energy (thousands of kVA/h)	31800,00	32790,00	33380,00	31580,00	25000,00
Staff employed A-B-C	16	14	13	13	15
Staff employed AE-AL	47	55	55	52	52
Contracts for operation of the general installations of the buildings	62	62	62	58	58

Electricity and Telephones

This section takes care of:

- An electricity transformation Station, of 45/12 kV, which takes electric current from the national network, and transforms it by means of two transformers, with an installed power of 10 MVA each.
- A medium voltage network, which extends over about 1,640 km twin conductors.
- 23 transformer cabins of 12/0,38 kV, with a total installed power of 40 MVA.
- A low voltage network.
- A telephone switchboard, with 24 outgoing lines and 1200 internal numbers, to which are attached a total of 1800 telephones.
- An internal telephone network.

In addition to the already rather complex and varied tasks of this Section, it is also responsible for the operation, maintenance, and modification of both the general and indoor electrical energy installations, as well as the management of the allarm signalling installations (for fire, control, load speakers, data transmission) and the technical supervision of the hoisting apparatures (of which there are 87 units, including gantries (transveyors), monorails, lifts and goods-hoists).

New plant is also designed by this Section, as and when it becomes necessary.

Technical Secretariat

This Office looks after the centralisation and coordination of the technical-administration activities of the various Sections, and more particularly:

- Management of of the funds available to the Divisions for satisfying the various needs of the Centre.
- Sending out the requests for offers, ordering materials and equipment, and making contracts with outside firms.
- Technical-administrative control of the requests for work received from the various Services, and the collection and filing of all documents relative to each individual job.
- Cataloguing and stocking the materials necessary for carrying out work and maintenance services, as well as the organisation of the Stores with index cards for the minimum stocks in hand.
- Dealing with Customs formalities, and with invoices and all correspondence sent by the suppliers of materials.

HEALTH PHYSICS DIVISION

A. Malvicini

Health Physics Control in Reactors and Laboratories

In all control areas of the laboratories and reactors of the Establishement periodic contamination inspections and measurements of the radioactivity of the air are performed regularly. The radioactivity levels observed are within permissible limits. In consequence, even rather hazardous operations, like the decontamination of the Hot Cells, had absorbed doses well below the maximum permissible doses and hardly measurable internal contaminations.

The activity concentrations of possibly-contaminated gaseous effluents from the various nuclear installations were continuously measured with monitors located in the ventilation outlets with the result that the measured values remained within the emission limits established for the Establishment.

On behalf of the Directorate of Safety Control, the Section started to organize the health physics control by inspectors, by preparing regulations, making sure that the health physics instruments used by them are calibrated and in good condition, and by providing personnel dosimeters.

Personnel Dose Control

The average number of persons per month (checked for absorbed dose during the current year was about 2800 (this number includes employees of contractors and visitors). No overexposures were noted. Less than 0.5% of the persons controlled have absorbed doses of about 1.5 rem, less than 2% doses higher than 0.5 rem. In the same period 750 internal contamination checks with the human body counter were performed; the measurements revealed no incorporations.

One member of the Dosimetry Group spent three months as an expert of the International Atomic Energy Agency (IAEA) at the Laboratorio de Dosimetria of the Comissao Nacional da Energia Nuclear in Rio de Janeiro, Brazil, in order to advise the laboratory on its thermoluminescence dosimetry programme and to train local personnel.

A research programme, in the field of thermally stimulated exelectron emission (T.S.E.E.) was initiated with the aim to learn more about the dosimetric properties of ceramic BeO. Up to now the experiments have yielded information on the reproducibility, tha fading characteristics, the dose-linearity of the material under investigation and its usefulness for measuring tritium in solutions and for surface contamination checks.

Site Survey and Meteorology

The radioactivity surveillance outside the installations and in the environment has been carried on mainly through the following activities:

- monitoring of atmospheric radioactivity (air and rainwater) by means of the stations located along the boundary of the Establishment;
- check of the radioactivity of the liquid effluents, performed directly at the source before release as well as at the monitoring station on the Novellino brook;
- measurement of the radioactivity of water (Lake Maggiore, river Ticino, underground water), soil, vegetation and foodsteffs.

The normal meteorological observations concerning the main parameters which characterize the local microclimate have been carried on regularly. Two FORTRAN programs have been developed, for processing the data concerning the vertical thermal gradient and determining the atmospheric stability categories.

The documentation concerning the general data on the release of radioactive effluents from the Ispra Establishment has been prepared, in accordance with art. 37 of the Euratom Treaty.

A study has been carried out, in cooperation with the Laboratorio Radioattività Ambientale of the CNEN (Casaccia Nuclear Centre) and with the Istituto di Igiene of the University of Pavia on the natural radioactivity (^{226}Ra and ^{210}Po) of some Italian mineral waters.

During 1971 some measurements for the monotoring of non-radioactive pollutants in the atmosphere were begun. Since July the following determinations have been carried out regularly on a daily basis: concentration of sulphur dioxide and dust in the air, rainwater acidity and dissolved and undissolved matter in rainwater.

MEDICAL SERVICE

C. Vigan

The work of the Medical Service is summarized in the Table.

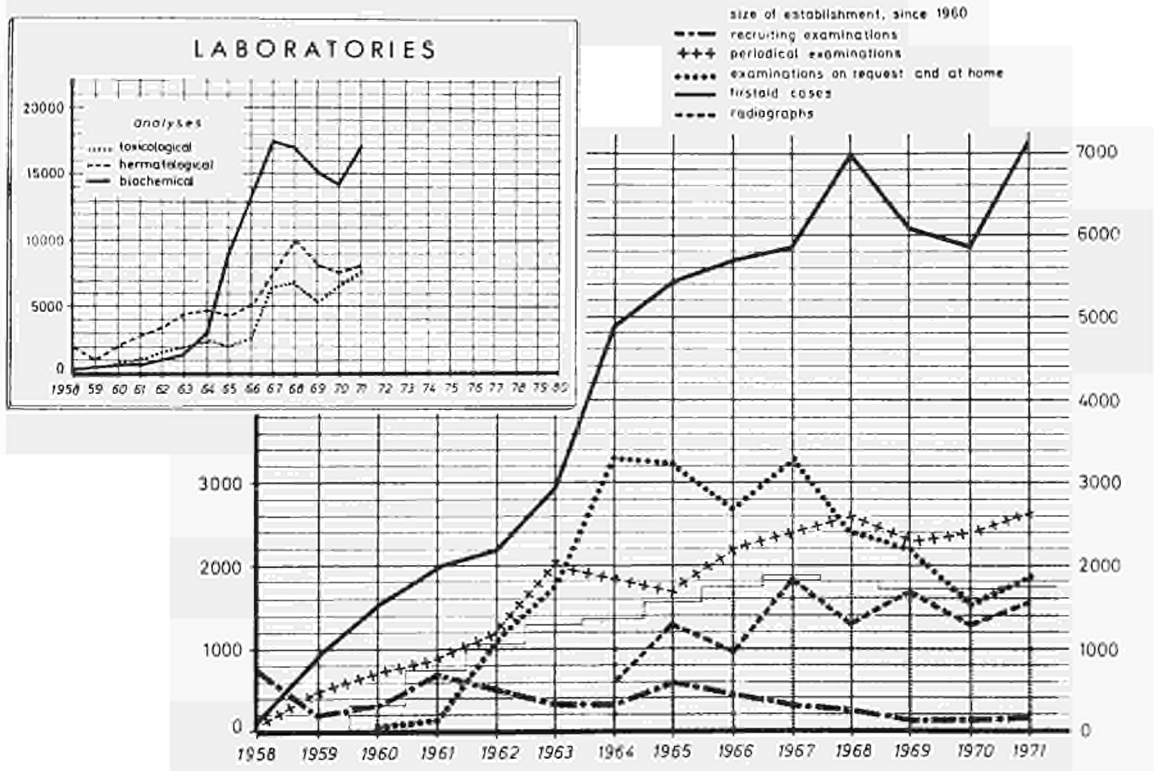

The number of accidents at work fell off considerably during 1971 (152) as compared with the previous years 1970 (226) and 1969 (215). The table gives a breakdown of the accidents by nature of impury and by month.

Accidents at work - 1971 - Euratom Personnel.

1971	J.	F.	M.	A.	M.	J.	J.	A.	S.	O.	N.	D.	TOTAL
Contusions, simple strains, torn muscles	1	3	2	4	2	5	6	1	3	4	6	2	39
wounds	9	5	9	5	11	5	3	7	3	5	3	4	68
burns	–	1	–	2	–	1	1	1	–	2	1	1	10
eye lesions	–	2	3	6	–	3	1	5	3	3	4	1	31
fractures	–	1	1	–	–	–	–	–	–	–	–	–	2
electrocutions	–	–	1	–	–	–	–	–	–	–	–	–	1
road accidents	1	–	–	–	–	–	–	–	–	–	–	–	1
TOTAL	11	12	16	17	13	14	11	14	9	14	13	8	152

SECURITY

H. Kilb

In additio to the routine surveillance work at the Establishment, the Security office also issued entry passes to visitors.

Over the period from 1964 to the present day, 5,764 permanent passes were issued, some of them renewable from year to year, whilst temporary passes valid for one or more days totalled 187,411 working days.

1964	31,998
1965	32,645
1966	32,305
1967	33,669
1968	19,582
1969	11,213
1970	12,964
1971	13,035

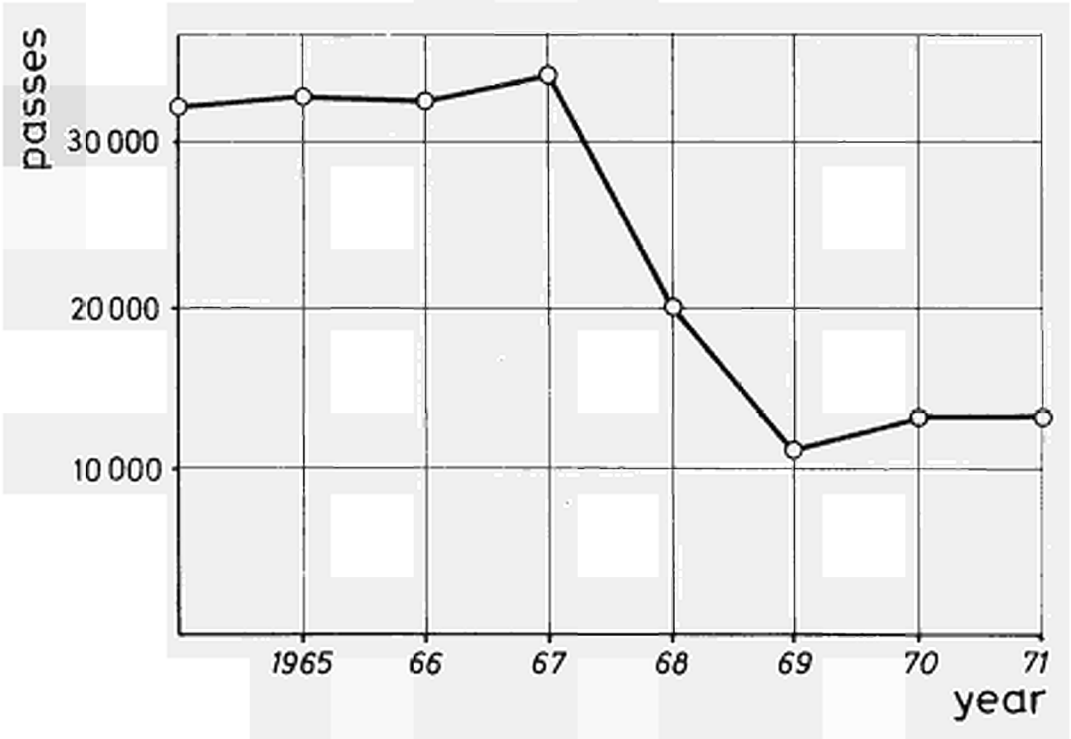

Appendix

CCR-ISPRA – PUBLICATIONS 1971

A. EURATOM REPORTS

EUR 4414 i — F. RUSTICHELLI. *Studio di cristalli monocromatori per neutroni aventi un gradiente della distanza reticolare. Vol. II*

EUR 4505 f.e — J.C. LENY, S. ORLOWSKI. *Le Projet ORGEL – 1959-1969.*

EUR 4544 i — E. IOVACCHINI. *Studio sperimentale del film liquido in un condotto durante l'espulsione di una bolla.*

EUR 4562 f — M. LECLOUX. *Mode d'emploi du code COMET.*

EUR 4592 e — J. RANDLES. *A thermo-hydrodynamic model for the theoretical study of the boiling and ejection of the coolant from a reactor channel due to a direct contact with hot molten fuel.*

EUR 4597 e — D. VAN VELZEN, H. LANGENKAMP, G. SERRINI. *The effect of various impurities on the electrical conductivity of organic coolant liquids.*

EUR 4598 e — G. ROSSI, P. BENETTI, N. OMENETTO. *A versatile burner for flame spectrometry.*

EUR 4599 e — K. KREBS, D.J. WINFIELD, *DOCHAP, a fortran IV program for the correction and calibration of neutron inelastic scattering data.*

EUR 4601 e — T. ASAOKA. *JN-METD1 a fortran IV programme for solving neutron transport problems with isotropic scattering in bare spheres and homogeneous slabs by the J_N method.*

EUR 4602 i — G. SERRINI, W. LEYENDECKER. *Determinazione per via chimica dei prodotti risultanti dalla reazione del mercurio con acido bromidrico (H_2, H_gBr_2, HBr, Hg e Hg_2Br_2).*

EUR 4603 e — G. FORTI. *XBWR – a one-dimensional Xenon transient programme for boiling nuclear reactors.*

EUR 4607 e — H.I. DE WOLDE, J.W. BRINCK. *The estimation of mineral resources by the computer program "IRIS".*

EUR 4608 e — H.I. DE WOLDE, J.W. BRINCK. *A slide rule for the evaluation of geochemical and mineral survey data.*

EUR 4609 e — H.I. DE WOLDE, J.W. BRINCK. *The optimization of mineral exploration investments with imposed targets by the program "EXIST".*

EUR 4620 e — G.C. IMARISIO. *Thermosiphon loops for corrosion measurements in high-temperature terphenyls.*

EUR 4621 e — R. LOPES CARDOZO, H. NORDMEYER, H. LANGENKAMP, C. CERUTTI. *MINOX, a catalytic deoxygeneation process for irradiated organic reactor coolants.*

EUR 4623 i — P. FASOLI-STELLA, L. GUERRI. *Applicazione del metodo MIG alla risoluzione di un problema fluido-dinamico in due dimensioni.*

EUR 4629 f — J. DONEA, S. GIULIANI. *Comportement mécanique de structures complexes en présence de fluage, d'un champ de température et de variations de dimension dues à l'irradiation.*

EUR 4631 e — L. NOBEL. *The analytical determination of the heat transfer coefficient between the free surface of a river and the atmosphere.*

EUR 4634 d — K.R. SCHLITT. *Temperaturstabilisierung mit Wärmerohren bei wechselnden Wärmeströmen.*

EUR 4637 e — C. CAPPELLETTI. *Laboratory guide for the selection of brazing materials.*

EUR 4671 e (MF) — O. GAUTSCH, L. KESTEMONT. *Some experimental results on the fission. Induced losses of uranium from surfaces of UO_2 and U in presence of H_2O and liquid Na.*

EUR 4673 i — E. VINCENTI, A. CLUSAZ. *Costanza (R, Z).*

EUR 4674 e — J. DONEA, S. GIULIANI. *A simplified visco-elastic analysis of graphitic bodies subjected to external loads, temperature gradients and neutron irradiation.*

EUR 4675 i — V. CAMERA, G. BARASSI, J.J. LEGROS. *Metodo rapido e semplice per la determinazione di radioattivitá alfa globale nelle urine.*

EUR 4676 e — T. ASAOKA. *Analysis of critical experiments on the SORA mockup by the S_N method.*

EUR 4677 f — F. COEN, B. HENRY, B. HUBER. *Cinétique de l'hydruration dans le terphényle, hors pile, des jonctions Zr-Nb2,5 %/ acier au carbone soudées par explosion.*

EUR 4678 e — W. MATTHES. *Monte Carlo simulation of the adjoint transport equation.*

EUR 4679 e — W. MATTHES. *Power pulse fluctuations in the SORA Reactor.* Part I: Theory.

EUR 4682 i — A.G. COLOMBO. *Considerazioni sui criteri per l'analisi di sequenze di numeri pseudo-casuali.*

EUR 4683 e H. HERKENRATH, P. MOERK-MOERKENSTEIN. *The pressurized and boiling water loop of the Technology Division at Ispra.*

EUR 4684 e A. ANGELINI. *HTRCP high temperature reactor for chemical purposes. (An application for the steel-making industry).*

EUR 4689 e S. GREGOLI, R. MEELHUYSEN, A. BERTINCHAMPS. *Computer analysis and reconstruction of ESR Spectra of γ- irradiated DNA.*

EUR 4699 e H.J. FLAMM. *A direct-graphite-resistance heated fluidized bed: principles and thermal performance of a pilot plant.*

EUR 4704 e (MF) L. FARESE, C. STOPPA. *Computer implementation of a technique for p.p.s. sampling derived by R.J. Jessen.*

EUR 4709 e G. GRAZIANI. *TRACE: a fuel cycle computer code for fast reactor analysis.*

EUR 4710 i G. BOLLINI, C. GANDINO. *XII° Annuario Meteorologico 1970.*

EUR 4711 e H. HAUSNER, R. KLERSY, A. SCHUERENKAEMPER, O. SIMONI. *Irradiation of an emitter element for a thermionic converter. Experiment DICO M-01.*

EUR 4713 f L. JULLIEN, B. SAVORNIN (CERCA); C. DUMONT, M. GRIN (EURATOM). *Etude du procédé de soudage par friction-diffusion du SAP.*

EUR 4715 d K. DITTERICH. *Korrelationsmethoden und adaptive Systeme. (Vergleich, Tendenzen und Anwendung bei Kernkraftwerken).*

EUR 4740 e G.F. DE BENI, O. GAUTSCH, G. HODAPP. *Some experimental results on the sorption of Cs by submicron W-10 % Ta and Ta powders.*

EUR 4801 e G. BIRKHOFF, F. BONDAR, N. COPPO. *Variable dead time neutron counter for tamper resistant measurements of spontaneous fission neutrons.*

B. PAPERS PUBLISHED IN SCIENTIFIC PERIODICALS AND CONFERENCE PROCEEDINGS

AIELLO, V., MARACCI, G., RUSTICHELLI, F., *Transmission of U^{235} fission fragments in solid media.* The Physical Reviews B 4: *11*, 3812 (1971).

ALBERTINI, A., ANDRIGHETTI, V., MONTAGNANI, M., VERHEYDEN, L., VERZELETTI, G., *Contributo allo studio del contenimento del massimo incidente credibile nello schermo biologico in cemento armato.* Estratto da "Atti del Convegno Nucleare di Pisa", September 21-26, 1971, *I*, (1971)

ARANOVITCH, E., *A method for the determination of the local turbulent friction factor and heat transfer coefficient in generalized geometries.* Journal of Heat Transfer, February 1971, 61.

BECKER, W., *Biomedical Engineering: Quo Vadis,* Euro Spectra, *Vol. X*, 4, 98 (1971)

BEGHI, G., SCHAUER, G., *Esame di saldature per esplosione di lega Zr-2,5Nb con acciaio al carbonio e con acciaio inossidabile.* Energia Nucleare, *Vol. 18* ,7/8, 421 (1971).

BEGHI, G., CAZZANIGA, E., *Il coefficiente di orientazione preferenziale (texture coefficient) nella caratterizzazione dei tubi in leghe di zirconio – Alcune determinazioni sperimentali.* Energia Nucleare, *Vol. 18*, 6, 346 (1971).

BEGHI, G., PIATTI, G., STREET, K.N., *The structure of the unidirectionally solidified Al-AlSb binary eutectic.* Journal of Materials Science, *Vol. 6*, 118 (1971).

BEGHI, G., SCHAUER, G., *Esame di saldature per esplosione di lega Zr-2,5Nb con acciaio al carbonio e con acciaio inossidabile.* Energia Nucleare, *Vol. 18*, 7/8, 421 (1971)

BERNSTEIN, H.H., *Some organizational prerequisites for the introduction of electronic data processing in libraries.* Libri *Vol. 21*, 1-3, 15 (1971).

BUSSE, C.A., *Werkstoffprobleme bei Hochtemperatur-Wärmerohren.* Symposium über Wärmerohrprobleme, Stuttgart (Germany), June 25-26, 1970. Forschung im Ingenieurwesen, *Vol. 37*, 2, 38 (1971).

CHIOCCHIO, O., DIERCKX, R., MARACCI, G., *Measurement of fast reactor type neutron spectra by foil activation techniques.* Nuclear Instruments and Methods 91, 45 (1971).

DIERCKX, R., MARACCI, G., CHIOCCHIO, O., *Measurement of fast reactor type neutron spectra by foil activation techniques.* Nuclear Instruments and Methods *91*, 45 (1971).

DIERCKX, R., MARACCI, G., RUSTICHELLI, F., *Measurement of the 140La fission product yield for fissions in ^{238}U in a thermal reactor type spectrum.* Journal of Nuclear Energy *Vol. 25*, 85 (1971).

EIFLER, W., NIJSING, R., *Berechnung der turbulenten Geschwindigkeitsverteilung und Wandreibung in exzentrischen Ringspalten.* Atomkernenergie, *18*, 2, 133 (1971).

EIFLER, W., NIJSING, R., *Berechnung der turbulenten Geschwindigkeitsverteilung und Wandreibung in asymmetrischen Stabbündeln.* Atomkernenergie, *18/3*, 189 (1971).

FANTECHI, R., HELCKE, G.A., *A CNDO/2 calculation of the radical formed on electron irradiation of mesitylene.* Molecular Physics, *Vol. 22*, 4, 737 (1971).

GAGGERO, G., *Monte-Carlo calculations for the photofractions and energy loss spectra of Ge(Li) semiconductor detectors.* Nuclear Instruments and Methods, *94*, 481 (1971)

GAGLIONE, P., DE BORTOLI, M., VAN DER STRICHT, E., *Predictions of 90Sr levels in milk on the basis of deposition values.* Health Physics, *Vol. 21*, 217 (1971)

GHEZZI, C., MERLINI, A., PACE, S., *Effect of temperature on the anomalous transmission of X-rays in copper and zinc.* Physical Review *B 4*, 6, 1833 (1971).

GIRARDI, F., MERLINI, M., BIGLIOCCA, C., POZZI, G., *A radiotracer technique for the study in vivo of the biological pathway of heavy metals in aquatic organisms.* International Atomic Energy Agency, Nuclear Techniques in Environmental Pollution, Vienne 1971, p. 721

GIUBILEO, M., STRAMBI, E., *Il giudizio di idoneità al alvoro con rischio da radiazioni ionizzanti: contributo casistico su 7835 candidati all'assunzione.* La Medicina del Lavoro, *Vol. 62*, 1, 1 (1971)

GRASS, G., HERKENRATH, H., HUFSCHMIDT, W., *Anwendung des Prandtlschen Grenzschichtmodells auf den Wärmeübergang an Flüssigkeiten mit stark temperaturabhängigen Stoffeigenschaften bei erzwungener Strömung.* Wärme und Stoffübertragung, *4*, 113 (1971).

GRIN, M., MONTAGNANI, M., VERZELLETTI, G., *Die Impulsschweissung.* Schweissen und Schneiden, *Vol. 23*, 12, 493 (1971).

HAUPT, J., VAN STEENWINKEL, R., *Experimental effects of R.F. irradiation on N.M.R. lines in solids.* Zeitschrift für Naturforschung, *Vol. 26*, 2, 260 (1971).

HAUPT, J., *Einfluss von Quanteneffekten der Methylgruppenrotation auf die Kernrelaxation in Festkörpern.* Zeitschrift für Naturforschung, *Vol. 26a*, 10, 1578 (1971).

HUBEAUX, A. *Are there critically-evaluated data in geology?* Reprint from Geoscience Documentation (3/1), February 1971.

HUBAUX, A., *Scheme for a quick description of rocks.* Mathematical geology, *3*, 3, 317 (1971).

JUPPE, G., *Wege zum idealen Implantat-Organ.* Selecta, *3*, 196 (1971).

KISTNER, G., RUBIN, R., SOSNOWSKA, I., *Anisotropic diffusion of hydrogen in niobium single crystals.* Physical Review Letters. *Vol. 27*, 23, 1576 (1971).

KRUEGER, G.J., SPIESECKE, H., *Nuclear relaxation and diffusion in nematic liquid solutions.* Berichte der Bunsen-Gesellschaft für Physikalische Chemie, *Vol. 75*, 3/4, 271 (1971).

KRUEGER, G.J., MUELLER-WARMUTH, W., *Self diffusion of liquid ^6Li and ^7Li as measuredby nuclear magnetic resonance.* Zeitschrift für Naturforschung, *Vol. 26*, 1, 94 (1971).

LANDAIS, E., *Absorption du béryl dans le proche infra-rouge. Sa contribution à la distinction entre émeraudes naturelles et synthétiques.* Bulletion de l'Association Française de Gemmologie, 28, 11-15 Sept. 1971.

MANARA, A., OSTIDICH, A., PEDROLI, G., RESTELLI, G., *Anodic oxidation as sectioning technique for the analysis of impurity concentration profiles in silicon.* Thin Solid Films, 8, 359 (1971).

MATTHES, W., *Calculation of reactivity perturbation with the Monte Carlo method.* Nuclear Science and Engineering 47, 234 (1972).

MONTAGNANI, M., VERZELETTI, G., *L'applicazione della saldatura con esplosivi ai componenti del reattore.* Metallurgia Nucleare 2, 44 (1971).

MONTAGNANI, M., ALBERTINI, C., G. VERZELETTI, *Esame a ultrasuoni dei difetti della saldatura di un elemento combustibile per reattore veloce.* La Metallurgia Italiana, *8*, 1971.

MUELLER-WARMUTH, W., VAN STEENWINKEL, R., YALCINER, A., *Intermolecular nuclear electron interaction and scalar spectral intensities in solutions of 1,3,5 – trifluorobenzene and substituted fluorobenzenes containing free radicals.* Molecular Physics *21*, 3, 449 (1971).

MUELLER-WARMUTH, W., YALCINER, A., *Kern-Elektronen-Doppelresonanzuntersuchungen über zwischenmolekulare Wechselwirkungen in Lösungen von freien Radikalen in substituierten Fluorbenzolen.* Berichte der Bunsen-Gesellschaft für physikalische Chimie, 8, 763 (1971).

NAJ, A., SCHILLER, P., *On the deformation mechanisms in SAP single crystals.* Journal of Nuclear Materials *41*, 2, 161 (1971).

NICKS, R., PENKUHN, H., *Today's approaches to reactor shielding problems.* Nuclear Engineering and Design *15*, 294 (1971).

OHLMER, E., KADLEC, J., *On the rproducibility of the parallel flow induced vibration of fuel pins.* Nuclear Engineering and Design, 3, 355 (1971).

PERLINI, G., *Tabella delle costanti di attivazione da neutroni veloci.* Ingegneria Nucleare *18*, 7/8, 421 (1971).

PIATTI, G., KELLERER, H., GEEL, C., *Nucleation and growth of strain-induced voids during the high-temperature creep of Al-Al_2O_3.* Journal of the Institute of Metals, *Vol. 99*, 283 (1971).

RIEMER, G., SCHERFF, H.L., *Plutonium diffusion in hyperstoichiometric mixed uranium-plutonium dioxides.* Journal of Nuclear Materials *39*, 183 (1971).

ROSSI, G., BENETTI, P., OMENETTO, N., *A new optical system for flame spectroscopy with special reference to thermally assisted anti-stokes fluorescence applications.* Applied Spectroscopy, *Vol. 25*, 1, 57 (1971).

ROSSI, G., *Spettrofotometria di fiamma: principi generali e stato attuale della tecnica.* La Rivista dei Combustibili, *Vol. XXV*, 5, 191 (1971).

RUEDL, E., *Quantitative transmission electron microscopy of bubbles in Al and Al-Al_2O_3 alloys.* American Society for Testing and Materials, *484*, 300 (1971).

SABBIONI, E., CLERICI, L., CAMPAGNARI, F., GIRARDI, F., BARTOLINI, P., *Microdetermination of nucleic acid phosphorus by neutron activation analysis.* Biochemistry, *Vol. 10*, 23, 4185 (1971).

SCHERFF, H.L., HENNECKE, J.F.A. *Carbon monoxide equilibrium pressures and phase relations during the carbothermic reduction of uranium dioxide.* Journal of Nuclear Materials *38*, 285 (1971).

SCHINS, H.E.J., VAN WIJK, R.W.M., DORPEMA, B., *The heat-pipe boiling-point method and the vapor pressure of twelve metallic elements in the range 10-104 Torr.* Zeitschrift für Metallkunde, *Vol. 62*, 4, 330 (1971).

SCHINS, H.E.J., OOMS, M.C., VAN WIJK, R.W.M., *Work funtions of some emitting and collecting refractory metal single crystals.* Proceedings of the 1971 Thermionic Conversion Specialist Conference, I.E.E.E., San Diego (California), October 4-6, 1971, 199.

SCHLITT, R., *Temperaturtabilisierung durch Wärmerohre.* Forschung im Ingenieurwesen, *Vol. 37*, 3, 1 (1971).

SCHWALM, D., *Identification of multiple-input multiple-output linear systems by correlation methods.* International Journal Control, *Vol. 13*, 6, 1131 (1971).

SCHWALM, D., *Parameter estimation of coupled reactors by correlation methods.* Atomkernenergie *Vol. 17*, 2, 140 (1971).

SCHUELE, W., FRANK, W., SEEGER, A., *Evidence for static crowdions in electron-irradiated Au-15 at%Ag alloys.* Radiation Effects *10*, 123 (1971).

SCOTTI, A., *Asymptotic equivalence of equilibrium ensembles of classical statistical mechanics.* Journal of Mathematical Physics, *Vol. 12*, 6, 933 (1971).

SERRINI, G., *Separazione di tracce di terre rare da materiali a base di alluminio. Esame critico di alcuni metodi.* Alluminio *10*, 493 (1971).

SPILLER, K.H., DROSTE, D., *Reinigung von Kalium und anderen Alkalimetallen.* Chemie für Labor und Betrieb *11*, 12 (1971).

TOUSSAINT, C.J., *Excitation efficiencies of different X-ray tube targets for some low energy X-ray spectral lines.* Analitica Chimica Acta *57*, 2, 289 (1971).

TOUSSAINT, C.J., *A high-temperature X-ray diffraction study of the NiO-Li_2O system.* Journal of Applied Crystallography *4*, 293 (1971).

TOUSSAINT, C.J., *Quantitative X-ray diffraction analysis by a diffraction-fluorescence technique.* Analytica Chimica Acta, *57*, 289 (1971).

VAN DER VOORT, E., GUYOT, P., *On the electrical resistivity by scattering on metallic grain boundaries.* Physica status solidi, *47*, 465 (1971).

VAN STEENWINKEL, R., *Experimental effects of R.F. Irradiation on N.M.R. lines in solids. Dynamics of the equilibrium establishment.* Zeitschrift für Naturforschung *11*, 26a, 1825 (1971).

VAN WAMBEKE, L., PANDAITE, *Baddeleyite and associated minerals from the bingo niobium deposit, Kivu, Democratic Republic of Congo.* Mineral Deposita (Berl.) *6*, 153 (1971).

VAN WAMBEKE, L., *The uranium-bearing mineral bolivarite: new data and a second occurence.* Mineralogical Magazine *38*, 418 (1971).

VAN WAMBEKE, L., *The problem of cation deficiencies in some phosphates due to alteration processes.* American Mineralogist, *56*, 1366 (1971).

VAN WAMBEKE, L., *Hinsdalite and corkite: indicator minerals in Central Africa.* Mineralium Deposita (Berl.) *6*, 130 (1971).

VERHEYDEN, L., KLEIN, K., KIND, H., *Direkte Kieselglas-Metallverbindung durch Lötung mittels eines aktiven Metalls – Derzeitiger Stand der Technik.* Glastechnische Berichte, *Vol. 44*, 1, 20 (1971).

VERHEYDEN, L., ANDRIGHETTI, V., *Trasduttore capacitivo adatto per la misura di spostamento di corpi conduttori e non conduttori.* Ingegneria Meccanica *20*, 11, 45 (1971).

VERHEYDEN, L., KLEIN, K., *New metallic seals for high and ultra-high vacuum – description and performances.* Vacuum, *21*, 9, 401 (1971).

VERHEYDEN, L., KLEIN, K., CROUE, C., *Measurement of helium leaks 10^{-5} times better than the sensitivity of a mass spectrometer leak detector.* Vacuum Science and Technology *11*, 545 (1971).

VERSINO, B., ROSSI, G., *Dual-flame photometric detector (DFPD) for the simultaneous G.C. determination of P-S-Cl-containing organic compounds.* Chromatographia *4*, 3, 331 (1971).

C. PARTECIPATION ON SCIENTIFIC CONFERENCES

ALBANESE, G., GHEZZI, C., MERLINI, A., PACE, S., *Application of the Mössbauer effect to the study of inelastic scattering of γ-rays in silicon crystals.* 8th Annual Solid State Physics Conference, Manchester (UK) January 5-7, 1971.

LANDAIS, E., *Absorption du béryl dans le proche infra-rouge. Sa contribution à la distinction entre émeraudes naturelles et synthétiques.* Riunione mensile della Società Francese di Mineralogia e Cristallografia, Paris, January 14, 1971.

GISSLER, W., *Inelastic Neutron Scattering by amorphous selenium.* French-German Discussion Meeting on Amorphous Materials, Saint-Nizier, Grenoble, March 12, 1971.

MULLER-WARMUTH, W., *Neuere Ergebnisse über zwischenmolekulare Hyperfeinwechselwirkungen in Lösungen freier Radikale.* Tagung des Fachausschusses "Hochfrequenzphysik" der Deutschen Physikalischen Gesellschaft, Giessen, 15-19 March, 1971.

BIRKHOFF, G., BONDAR, L., *Application of heterogeneous method for the interpretation of exponential experiments.* EACRP-Meeting on Heterogeneous Methods for Reactor Calculation, Paris (France), March 17-19, 1971.

GEISS, F., *Aspects modernes de la C.C.M.* Colloque sur la Chromatographie sur couche mince, Paris, March 19, 1971.

RUEDL, E., *On the formation of voids by quenching or deformation of metals.* British Nuclear Energy Society Conference on "Voids formed by Irradiation on Reactor Materials", Reading (UK) March 24-25, 1971.

MATTES, W., *Some Monte Carlo applications at the Euratom Research Centre Ispra.* New Developments in Reactor Mathematics and Applications, Idaho Falls (USA), March 29-31, 1971.

VERHEYDEN, L., KLEIN, K., *New metallic seals for high and ultra-high vacuum. Description and performances.* 2nd Vacuum Congress, Tel-Aviv (Israel), March 30 – April 1, 1971.

ARANOVITCH, E., CRUTZEN, S., DUFRESNE, J., FARFALETTI-CASALI, F., *Internal thermal insulation for prestressed-concrete vessel of high temperature gas cooled reactors.* Reaktortagung 1971, Bonn (Germany), March 30 – April 2, 1971.

GRAEBER, H., RIEGER, M., *Experimentelle Untersuchung des Wärmeübergangs an Flüssigmetalle in parallel durchströmten Rohrbündeln.* Reaktortagung 1971, Bonn (Germany), March 30 – April 2, 1971.

HAGE, W., HETTINGER, H., HOHMANN, H., STURM, B., TOSELLI, F., *Messung und Interpretation des Kühlmittel-Void-Koeffizienten in D_2O-Gittern.* Reaktortagung 1971, Bonn (Germany), March 30 – April 2, 1971.

MATTHES, W., RIEF, H., *Monte-Carlo Störungsrechnungen in multiplizierenden Medien.* Reaktortagung 1971, Bonn (Germany), March 30 – April 2, 1971.

NIJSING, R., EIFLER, W., *Evaluation of mixing for thermal design of rod bundles.* Reaktortagung 1971, Bonn (Germany), March 30 – April 2, 1971.

PENKUHN, H., *Eine numerische Integration der Gammatransportgleichung mit azimutal abhängiger Quelle.* Reaktortagung 1971, Bonn (Germany) March 30 – April 2, 1971.

RIESCH, G., *Bestrahlungseinrichtungen am ESSOR-Reaktor.* Reaktortagung 1971, Bonn (Germany), March 30 – April 2, 1971.

VERHEYDEN, L., KLEIN, K., *The metallic four-lip seal. Description and analysis of the performance at different working conditions of this new static seal.* 5th Int. Conf. on Fluid Sealing, Cranfield (UK), March 30 – April 2, 1971.

VINCENTI, E., *A two dimension code "Costanza (R,Z)" for the study of dynamic transient, xenon operational transient and xenon stability.* Reaktortagung 1971, Bonn (Germany), March 30 – April 2, 1971.

MERLINI, A., *Applicazione della diffrazione dei raggi X in trasmissione allo studio delle dislocazioni nei cristalli.* Convegno informativo sullo stato delle ricerche nel settore della preparazione e caratterizzazione di mono-cristalli e strati epitassiali. Parma (Italy), April 5 – 6, 1971.

KRUEGER, G.J., *Electron spin relaxation in solutions of organic free radicals.* 8th Colloquium on NMR-Spectroscopy, Aachen (Germany), April 14-20, 1971.

GANDINO, Cl., *La determinazione dell'altezza delle ciminiere, limitatamente all'inquinamento radioattivo.* XIX Assemblea della Soc. It. Geofisica e Meteorologia, Genova (Italy), April 15-16, 1971.

KOTTOWSKI, H., WARNSING, R., KLEIH, R., BIRKE, A., *Controbution to the problem of remaining liquid layer after ejection.* Third Liquid Metal Boiling Meeting, Ispra, April 15-16, 1971.

NIJSING, R., EIFLER, W., *Hot subchannels in hexagonal fuel rod assemblies of fast breeders.* 3rd Liquid Metal Boiling Meeting, Ispra (Italy), April 15-16, 1971.

SPILLER, K-H., *Some new results about the influence of surface conditions and impurities on the superheat of sodium.* 3rd Liquid Metal Boiling Meeting, Ispra (Italy), April 15-16, 1971.

FLAMM, J., *Principles and practice in fluidized bed coating of nuclear fuel particles.* 1st Colloquium on Fluidized Bed Coating of Nuclear Fuel Particles towards Industrial Scale Operations, Ispra (Italy), April 29, 1971.

BUSSE, C.A., *Heat pipes for thermionic space power supplies.* Third International Conference of Space Technology, Roma (Italy), May 3-8, 1971.

KLEIN, K., *Der metallische Dichtungsring, angewandt in UHV.* Seminar "UHV Physik und Technik des Ultrahochvakuums", Wuppertal (Germany), May 3-4, 1971.

RIEBOLD, W., FRIZ, G., *Die Anwendung einer Korrelationsmethode bei der Untersuchung von Zweiphasen-Strömungen.* Arbeitssitzung des VDI-Ausschusses Mehrphasenströmung, Düsseldorf (Germany), May 7, 1971.

FACCHETTI, S., *Impiego di molecole marcate nell'indagine con la spettrometria di massa.* Corso Teorico Pratico di Spettrometria di Massa, Milano (Italy), May 13, 1971.

KOTTOWSKI, H., *Siedeprobleme bei Flüssigmetallen.* Seminar des Instituts für Reaktortechnik der Technischen Hochschule Aachen (Germany), May 14, 1971.

DONEA, J., *GOLIA: A computer code for the stress analysis of complex structures in presence of creep dimensional changes and a thermal field.* Joint Euratom-Central Electricity Generating Board Meeting on Stresses in Graphite Structures related to HTG Design, Berkeley (UK), May 17-19, 1971.

DONEA, J., REYNEN, J., *Survey of finite element codes at Common Research Centre Euratom, Ispra.* Joint Euratom-Central Electricity Generating Board Meeting on Stresses in Graphite Structures Related to HTG Design, Berkeley (UK), May 17-19, 1971.

ALBERTINI, C., MONTAGNANI, M., VERZELETTI, G., *Esame ad ultrasuoni dei diffetti delle saldature di un elemento combustibile per reattore veloce.* VII. Seminario Nazionale per le Prove non Distruttive e Mostra di Apparecchiature, Trieste (Italy), May 20-22, 1971.

AMESZ, J., *Statistical inference from small samples. Some experience in mechanical reliability evaluation,.* CREST Meeting "Applicability of Quantitative Reliability Analysis of Complex Systems and Nuclear Plants in its Relation to Safety", München (Germnay), May 26-28, 1971.

COLOMBO, A.G., LUISI, T., VOLTA, G., PROJA, E., *Operational reliability evaluation of an in-pile loop.* CREST Meeting "Applicability of Quantitative Reliability Analysis of Complex Systems and Nuclear Plants in its Relation to Safety", München (Germany), May 26-28, 1971.

COLOMBO, A.G., RICCHENA, R., VOLTA, G., *Survey and critical analysis of programs for system reliability computation.* CREST Meeting "Applicability of Quantitative Reliability Analysis of Complex Systems and Nuclear Plants in its Relation to Safety" München (Germany), May 26-28, 1971.

ENDRIZZI, A., *C.S.M.P. versione grafica interattiva.* Convegno Interazione Uomo-Macchina, Sorrento (Italy), May 31 – June 2, 1971.

GAGGERO, G., *Procedure di colloquio T.P. del sistema informativo in dotazione al CETIS.* Interazione Uomo-Macchina, Congresso AICA, Sorrento (Italy), May 31 – June 5, 1971.

PIRE, J., BOLOGNANI, M., *LICE: an incremental compiler and executor.* Congresso AICA, Interazione Uomo-Macchina, Sorrento (Italy), May 31 – June 5, 1971.

CASINI, G., *Reactor Physics Activity at CCR from July 1970 to June 1971.* European American Committee on Reactor Physics, Stockholm, June 7-11, 1971.

BAEHR, A., *Influence of heating wall properties on the heat transfer to droplets.* European Two-Phase Flow Group Meeting, RISO (Denmark), June 9-11, 1971.

BAEHR, A., HERKENRATH, H., MOERK-MEORKENSTEIN, P., *Development of the heat transfer crisis as function of the entrance conditions.* European Two-Phase Flow Group Meeting, RISO (Denmark), June 9-11, 1971.

BENETTI, P., OMENETTO, N., ROSSI, G., *Alcune considerazioni sui parametri che influenzano le misure di intensità effettuate con un monocromatore.* XVI Seminario Spettrochimico della Ass. Italiana di Metallurgia, Sirmione (Italy), June 9-12, 1971.

OMENETTO, N., BENETTI, P., ROSSI, G., *Misura della temperatura di fiamma mediante la fluorescenza assistita termicamente.* XVI seminario Spettrochimico della Ass. Italiana di Metallurgia, Sirmione (Italy), June 9-12, 1971.

VERSINO, B., ROSSI, G., POELMAN, J.A.M., *La fotometria di fiamma nella gas-cromatografia come rivelatore selettivo per prodotti organici contenenti S, P, a Cl.* XVI Seminario Spettrochimico della Ass. Italiana di Metallurgia, Sirmione (Italy), June 9-12, 1971.

OBERHOFER, M., *New developments in TSEE-Dosimetry. TSEE = Thermally Stimulated Exoelectronemission.* 2nd Congress of the European Association of Radiology, Amsterdam (NL), June 14-18, 1971.

BENCO, A., *Considerazioni sugli aspetti normativi e criteri tecnici per l'immissione degli influenti radioattivi nell'ambiente.* Convegno sugli "Aspetti comuni degli inquinamenti convenzionale e radioattivo", Minalo (Italy), June 24-25, 1971.

DE BORTOLI, M., GAGLIONE, P., *Criteri di controllo (capacità dell'ambiente, gruppi critici, campioni rappresentativi).* Convegno sugli "Aspetti comuni degli inquinamenti convenzionale e radioattivo", Milano (Italy), June 24-25, 1971.

FREUND, A., GUINET, P., MARESCHAL, J., RUSTICHELLI, F., VANONI, F., *Cristaux à gradient de maille.* Int. Conf. on Crystal Growth, Marseille (France), June 1971.

BERTOZZI, G., GUELLA, G., GUZZI, G., *"LABEN 70", A new tool for gamma ray spectrometry.* 2nd Symposium on the Recent Developments on Neutron Activation Analysis, Cambridge (UK), June 28 – July 1, 1971.

CUYPERS, M., QUAGLIA, L., WEBER, G., *Study of the influence of the surface treatment of the superficial oxygen content of metals using the nuclear reaction* $O^{16}(d,p)O^{17}$. 2nd Symposium on the Recent Developments in Neutron Activation Analysis, Cambridge (UK), June 28 – July 1, 1971.

CUYPERS, M., GIRARDI, F., BARRET, A., *Fissile material analysis in solution and scrap materials using the delayed neutron technique.* 2nd Symposium on the Recent Developments in Neutron Activation Analysis, Cambridge (UK), June 28 – July 1, 1971.

DONEA, J., GIULIANI, S., *GOLIA – A computer program for the stress analysis of complex structures in the presence of creep, dimensional changes and a thermal field.* Meeting on the Application of Finite Element Methods to Nuclear Engineering Problems, Ispra (Italy), June 30 – July 1, 1971.

REYNEN, J., BLANCKENBURG, J., DE WINDT, P., PUTZEYS, J., *MESHGEN and MESHREF, computer codes for the automatic generation of triangular finite element meshes.* Meeting on Application of Finite Element Methods to Nuclear Engineering Problems, Ispra (Italy), June 30 – July 1, 1971.

REYNEN, J., BLANCKENBURG, J., DE WINDT, P., PUTZEYS, J., *MESHPLOT and STRESSPLOT, computer programs for the plotting of mesh grids and stresses related to triangular finite element codes.* Meeting on the Application of Finite Element Methods to Nuclear Engineering Problems, Ispra (Italy), June 30 – July 1, 1971.

BENCO, A., *Possibilità e opportunità di ampliamento del campo di attività del fisico sanitario ad altri tipi di radiazioni (laser, microonde, ecc.).* IV Riunione della Sezione Fisici Sanitari Operativi presso il CNEN, Bologna (Italy), July 2, 1971.

GLODEN R., *Intégration d'un système différential du premier ordre.* 90ème Congrès de l'AFAS, Chambéry (France), July 5-10, 1971.

KRUEGER, G.J., *Spin diffusion in Lysozyme Studied by Nuclear Magnetic Relaxation.* The Fourth International Symposium on Magnetic Resonance, Rehovot (Israel), August 24-31, 1971.

BRESESTI, A.-M., BRESESTI, M., *Development of gamma-spectrometry techniques for safeguards at the Euratom Joint Research Centre Ispra.* Research Coordination Meeting on Development of Gamma Spectrometry Instrumentation for Safeguards, Wien (Austria), August 30 – September 3, 1971.

FACCHETTI, S., MARELL, A., *La ionizzazione di superficie applicata ad alcuni materiali di interesse nucleare.* 2. Convegno di Spettrometria di Massa, Ispra, (Italy), September 1-3, 1971.

PERSCHKE, S., *SCL-II one more software to resolve linguistic problems.* 1971 Int. Meeting on Computational Linguistics, Debrecen (Hungary), September 4-7, 1971.

BONI, M., CAMAGNI, P., *Effects of plastic deformation on the production and reactions of colour centres.* 1971 Itern. Conf. on Colour Centres in Ionic Crystals, Reading (UK), September 6-10, 1971.

GRAEBER, H., RIEGER, M., *Experimental study of heat transfer to liquid metals flowing in-line through rod bundles.* 1971 International Seminar "Heat Transfer in Liquid Metals", Trogir (Yugoslavia), September 6-11, 1971.

KOTTOWSKI, H., *Mechanism of nucleation and influence of the microstructure of the boiling surface and impurities in sodium on superheating and flow patterns.* 1971 International Seminar "Heat transfer in Liquid Metals", Trogir (Yugoslavia), September 6-11, 1971.

NIJSING, R., EIFLER, W., *Temperature fields in liquid-metal-cooled rod assemblies.* 1971 International Seminar "Heat Transfer in Liquid Metals", Trogir (Yugoslavia), September 6-11, 1971.

SPILLER, K.H. *Visualization of stagnant sodium superheat and boiling in a channel.* 1971 International Seminar "Heat Transfer in Liquid Metals", Trogir (Yugoslavia), September 6-11, 1971.

CAPRIOGLIO, P., SCHLEICHER, H.W., *Synopsis of the activities of the Joint Research Centre of the Commission of the European Communities.* 4th International Conference on the Peaceful Uses of Atomic Energy, Genève (Switzerland), September 6-16, 1971.

RUEDL, E., GAUTSCH, O., *Electron microscopic study of the behaviour of very small bubbles in irradiation environments.* Conference on "Microscopy of Cluster Nuclei in Defected Crystals", Chalk River (Canada), September 8-10, 1971.

FRIZ, G., RIEBOLD, W., *Experimentelle Untersuchung des Wärmeübergangs während der Druckentlastung bei Bruch im heissen Strang des Primärkühlkreislaufes eines Druckwasserreaktors.* Sitzung des Arbeitskreises des VDI "Reaktor-Notkühlung", Köln (Germany), September 13, 1971.

GIARDINA, M.D., SCHUELE, W., FRANK, W., SEEGER, A., *Static crowdions in an Au-15% Ag alloy.* First European Conference on the Physics of Condensed Matter, Firenze (Italy), September 14-17, 1971.

ALBERTINI, C., ANDRIGHETTI, V., MONTAGNANI, M., VERHEYDEN, L., VERZELETTI, G., *Energy absorption by the concrete biological shield under shock loading.* First International Conference on Structural Mechanics in Reactor Technology, Berlin (Germany), September 20-24, 1971.

AMESZ, J., LANZA, F., VOLTA, G., *Experimental and theoretical investigation on probabilistic criteria for the mechanical resistance of graphite structures.* First International Conference on Structural Mechanics in Reactor Technology, Berlin (Germany), September 20-24, 1971.

ARANOVITCH, E., CRUTZEN, S., DUFRESNE, J., FARFALETTI-CASALI, F., *Study and development of thermal insulation systems for prestressed Concrete vessels for HTGR's.* First International Conference on Structural Mechanics in Reactor Technology, Berlin (Germany), September, 20-24, 1971.

BERNARD, J., DUFRESNE, J., FARFALETTI-CASALI, F., PUTZEYS, J., *Design criteria for calculation code of a hot channel in a pressure tube nuclear reactor.* First International Conference on Structural Mechanics in Reactor Technology, Berlin (Germany), September 20-24, 1971.

DONEA, J., GIULIANI, S., *Analyse des contraintes dans des structures complexes en présence de fluage, de variations de dimensions et d'un champ de température.* First International Conference on Structural Mechanics in Reactor Technology, Berlin (Germany), September 20-24, 1971.

FASOLI-STELLA, P., GUERRI, L., HOLTBECKER, H., *Pressure vessel loading due to a channel rupture in a pressure tube reactor.* First International Conference on Structural Mechanics in Reactor Technology, Berlin (Germany), September 20-24, 1971.

REYNEN, J., BLANCKENBURG, J., DE WINDT, P., PUTZEYS, J., *Stress analysis of a graphite fuel element, including radiation creep and dimensional changes.* First International Conference on Structural Mechanics in Reactor Technology, Berlin (Germany), September 20-24, 1971.

REYNEN, J., BLANCKENBURG, J., DE WINDT, P., PUTZEYS, J., *Stress analysis of a bimetallic cylindrical joint.* First International Conference on Structural Mechanics in Reactor Technology, Berlin (Germany), September 20-24, 1971.

NAJ, A., *Affidabilità di dischi a rottura per impianti a pressione: indagine preliminare.* XXVI Congresso Nazionale della Ass. Termotecnica Italiana, L'Aquila (Italy), September 21-25, 1971.

RUEDL, E., GAUTSCH, O., STAROSTE, E., *Studio sulla formazione e risoluzione di bolle contenenti gas inerti nel platino durante l'irraggiamento.* Ottavo Congresso Italiano di Microscopia Elettronica, Milano (Italy), September 23-25, 1971.

RUEDL, E., *Applicazione di TEM, SEM e microanalisi a raggi X allo studio di corrosione di leghe Ni-Mo.* Ottavo Congresso Italiano di Microscopia Elettronica, Milano (Italy), Septembre 23-25, 1971.

STANCHI, L., *Preliminary report on a fast neutron acquisition for spontaneous fissions.* 6th International Symposium on Nuclear Electronics, Varsavia (Poland), September 23-30, 1971.

CLERICI, L., SABBIONI, E., CAMPAGNARI, F., GIRARDI, F., SPADARI, S., *Determinazione del peso molecolare degli acidi nucleici per valutazione diretta del rapporto fosforo totale/fosforo terminale.* XVII Convegno della Società Italiana di Biochimica, Palermo (Italy), September 27-30, 1971.

HELCHE, G.A., FANTECHI, R., *Observation of the hydrazyl radical during fast electron irradiation of hydrazine adsorbed in a zeolite.* Autumn Meeting of the Chemical Society, York (UK), September 27-30, 1971.

BOHDANSKY, J., *Plasmaphysikalische Probleme bei der Thermionischen Energiewandlung.* Physikertagung 1971, Essen (Germany), September 27 October 1, 1971.

MUELLER-WARMUTH, W., KRAEMER, F., DUTZ, H., *Nuclear magnetic resonance studies on motional processes in glasses.* IXème Congrès International du Verre, Versailles (France), September 27 October 2, 1971.

OMENETTO, N., BENETTI, P., ROSSI, G., *Flame temperature measurements by means of atomic fluorescence spectrometry.* 3ème Congrès Int. de Spectrométrie et de Fluorescence Atomique, Paris (France), September 27 October 1, 1971.

PIRE, J., GAGGERO, G., *Type of applications of the conversational extension in HASP.* SEAS XVI, Pisa (Italy), September 29 October 1, 1971.

MOINIL, P., *Conversational extension in HASP.* SEAS XVI, Pisa (Italy), September 29 October 1, 1971.

DIETTRICH, O., *Neuere Arbeiten über Abschirmprobleme im CCR Ispra.* Herbstsitzung der Arbeitsgruppe für Bautechnischen Strahlenschutz, Geesthacht (Germany), October 1, 1971.

BOHDANSKY, J., *A simplified model for the Cs-low voltage arc at electron rich conditions,* 1971 Thermionic Conversion Specialist Conference. San Diego, California (USA), October 4-6, 1971.

SCHINS, H.E.J., OOMS, M.C., VAN WIJK, R.W.M., *Work functions of some emitting and collecting refractory metal single crystals.* Thermionic Conversion Specialist Conference, San Diego (USA), October 4-6, 1971.

ROTA, A., FACCHETTI, S., FARESE, L., HALL, A., ILARDI, S., MANNONE, F., *EUREX Control Experiment (ECE) Interim Report.* Working Group on Quantitative Data and Results of Systems Analysis and Integral Tests, (IAEA), Wien (Austria), October 4-8, 1971.

BREUER, F., DE BORTOLI, M., *Comportamento del radioiodio nell'ambiente e nell'uomo.* XVII Congresso Nazionale della Ass. Italiana di Fisica Sanitaria e Protezione contro le Radiazioni (AIFSPR), Monteporzio Catone, Roma (Italy), October 5-8, 1971.

DANIAULT, J., BEUCHERIE, P., *Applications of a new radio frequency inductive plasma sputtering process.* 5th International Vacuum Congress 1971 International Conference on Solid Surfaces. Boston Mass. (USA), October 11-15, 1971.

MUELLER-WARMUTH, W., *DNP-Untersuchungen über intermolekulare Hyperfeinwechselwirkungen und Molekülbewegungen in Lösungen freier Radikale.* Herbstschule über "Untersuchungen dynamischer Prozesse in molekularen Systemen", Binz/Rügen (Germany), October 17-27, 1971.

PENKUHN, H., *CINNA A neutron shielding code with high-energy resolution.* Winter Meeting,(American Nuclear Society), Miami Beach, Florida (USA), October 17-21, 1971.

BOOZ, J., GIGLIO, G., WAKER, A., GAGGERO, G., *Spectral energy transfer of ions to thin layers of tissue-equivalent matter.* 3rd Symposium on Microdosimetry, Stresa (Italy), October 18-22, 1971.

FANGMEYER., H., *Stand der Entwicklungsarbeiten für die automatische Indexierung bei der Europäischen Forschungsanstalt Ispra.* Deutscher Dokumentartag 1971, Bad Herrenalb (Germany), October 18-22, 1971.

FLAMM, H.J., *Effort analysis and preliminary aspects of programme orientation for fluidized bed coating of nuclear fuel particles.* Second Colloquium on Fluidized Bed Coating of Nuclear Fuel Particles towards Industrial Scale Operations, Ispra (Italy), October 26-27, 1971.

MERLINI, A., GHEZZI, C., ALBANESE, G.F., *Determinazione dello scattering anelastico dei raggi gamma nel KCl per mezzo dell'effetto Mössbauer: contributo dello scattering a più fononi.* 57° Congresso della Società Italiana di Fisica, L'Aquila (Italy), October 26-30, 1971.

ANTONINI, M., CORCHIA, M., NICOTERA, E., RUSTICHELLI, F., *Cristalli curvi di Si come monocromatori per neutroni.* 57° Congresso della Società Italiana di Fisica, L'Aquila (Italy), October 26-30, 1971.

BONI, M., CAMAGNI, P., *Meccanismi di colorazione in alogenuri alcalini deformati.* 57° Congresso della Società Italiana di Fisica, L'Aquila (Italy), October 26-30, 1971.

FREUND, A., RUSTICHELLI, F., VANONI, F., *Monocristallo Cu-Ge quasi perfetto.* 57° Congresso della Società Italiana di Fisica, L'Aquila (Italy), October 26-30, 1971.

FREUND, A., RUSTICHELLI, F., VANONI, F., *Monocristallo Cu-Ge con gradiente del parametro reticolare.* 57° Congresso Società Italiana di Fisica, L'Aquila (Italy), October 26-30, 1971.

GALGANI, L., SCOTTI, A., *Planck-like distribution in classical non-linear mechanics.* 57° Congresso della Società Italiana di Fisica, L'Aquila, October 26-30, 1971.

RUSTICHELLI, F., *Considerazioni sulla deviazione dalla legge di Bragg in cristalli perfetti.* 57° Congresso della Società Italiana di Fisica, L'Aquila (Italy), October 26-30, 1971.

FIEBELMANN, P., *Bestimmung der radialen Wärmeleitfähigkeit von Mehrschichtrohren für Thermionik-Konverter.* 2. Symposium über "Thermophysikalische Eigenschaften fester Stoffe", Stuttgart (Germany), October 28-29, 1971.

SCHINS, H.E.J., *Thermionic electrodes technology.* 2. Symposium über "Thermophysikalische Eigenschaften fester Stoffe", Stuttgart (Germany), October 28-29, 1971.

BERTOLINI, G., CAPPELLANI, F., RESTELLI, G., FIORINI, E., PULLIA, A., *Investigations on the background of a Ge(Li) Detector.* Nuclear Science Symposium (IEEE 1971), San Francisco, Calif. (USA), November 4, 1971.

CANALI, U., *Methods for the calculation of reactor shields in use at Euratom Ispra. Calculations for the upper shield of the Swiss Reactor DIORIT.* Piccolo Seminario sulla Protezione dei reattori, Würenlingen (Switzerland), November 4, 1971.

ARDENTE, V., PIERINI, P., RICCOBONO, G., ROSSI, G., *Decadimento non esponenziale di impulsi neutronici in Berillio a bassa temperatura.* Convegno in Fisica dei Neutroni Applicata su "Il Ruolo degli Acceleratori nella Fisica dei Neutroni Applicata", Legnaro/Padova (Italy), November 9-10, 1971.

GIRARDI, F., CUYPERS, M., *Alcune applicazioni analitiche dei neutroni prodotti da macchine acceleratrici.* Convegno su "Il Ruolo degli Acceleratori nella Fisica dei Neutroni Applicata", Legnaro/Padova (Italy), November 9-10, 1971.

ROSSI, G., *Decadimento non esponenziale di impulsi neutronini in moderatori coerenti.* Ruolo degli Acceleratori nella Fisica dei Neutroni Applicata, Legnaro/Padova (Italy), November 9-10, 1971.

MOSCHINI, G., RICCHENA, R., SARTORI, L., TORNIELLI, *Misure pulsate di reattività in sistemi fortemente sottocritici.* Convegno su "Il Ruolo degli Acceleratori nella Fisica dei Neutroni Applicata", Legnaro/Padova (Italy), November 9-10, 1971.

VERHEYDEN, L., KLEIN, K., *Riassunto delle caratteristiche delle guarnizioni statiche per ultravuoto, con particolare attenzione alla guarnizione "AX".* 3° Congresso Italiano del Vuoto, Torino (Italy), November 18-20, 1971.

VINCENTI, E., CLUSAZ, A., *A two dimensional dynamics code for HTR's with tubular fuel elements.* Colloquium on the Safety Aspects of High Temperature Reactor Systems, Paris (France), November 24-25, 1971.

FIEBELMANN, P., *Stand der Entwicklung von out-of-core Thermionik-Reaktoren.* Seminar über Elektrizitätserzeugung aus nuklearen Energiequellen für Sonderzwecke, Düsseldorf (Germany), November 30, 1971.

FACCHETTI, S., *Isotopic determination by spark source - Comparison with surface ionization technique.* Colloque sur les méthodes analytiques dans le cycle du combustible nucléaire, Wien (Austria), November 29 - December 3, 1971.

Detailed list of publications see Annual Report 1971 "Programme Biology - Health Protection". EUR 4830, pp. 774-781.

KEYWORDS

A. FAST REACTORS
BREEDER REACTORS
FUEL PINS
THERMODYNAMICS
HYDRAULICS
LIQUID METALS
BOILING
SUPERHEATING
MECHANICAL VIBRATIONS
REPROCESSING
EXPLOSION WELDING
BUDGET
EURATOM

B. HEAVY WATER MODERATED REACTORS
TEMPERATURE COEFFICIENT
VOID COEFFICIENT
ZIRCONIUM ALLOYS
THERMODYNAMICS
BUDGET
EURATOM

C. HTGR TYPE REACTORS
FUEL CYCLE
SHIELDING
FUEL ELEMENTS
GRAPHITE
SEALS
THERMAL INSULATION
PROCESS HEAT REACTORS
BUDGET
EURATOM

D. REACTOR SAFETY
BLOWDOWN
URANIUM DIOXIDE
SODIUM
CHEMICAL REACTIONS
CRITICALITY
RELIABILITY
FRACTURES
ACOUSTIC EMISSION TESTING
BUDGET
EURATOM

E. SAFEGUARDS
NON-PROLIFERATION TREATY
BUDGET
EURATOM

F. BUDGET
EURATOM
ISPRA-1 REACTOR
MAGNETIC RESONANCE
RADIATION EFFECTS
NEUTRONS

G. SORA REACTOR
REACTIVITY
REACTOR SAFETY
PROGRAMMING
COMPUTER CALCULATIONS
PLANNING

H. EURATOM
BUDGET
INFORMATION SYSTEMS

J. EURATOM
BUDGET
NUCLEAR FUELS
ISPRA-1 REACTOR
RADIATION EFFECTS
FUEL ELEMENTS
FRACTURES
HYDROGEN

K. FINITE DIFFERENCE METHOD
DIFFERENTIAL EQUATIONS

L. SNR REACTOR
CIRENE REACTOR
SHIELDING
MOCKUP
DATA

M. NEUTRON BEAMS
PULSES
BERYLLIUM MODERATORS
LOW TEMPERATURE
DATA
COMPUTER CALCULATIONS

N. SORA REACTOR
PLANNING
REACTOR KINETICS
ANALYTICAL SOLUTION

O. CAPTURE
CROSS SECTIONS
REACTOR MATERIALS
DATA
RB-2 REACTOR

P. REACTOR KINETICS
THERMODYNAMICS
HYDRAULICS
COMPUTER CODES
TWO-DIMENSIONAL CALCULATIONS
EQUATIONS

Q. POWER PLANTS
ELECTRICITY
EUROPEAN COMMUNITIES

R. NUCLEAR FUELS
COST
NUCLEAR SHIPS
PROPULSION REACTORS
COMPUTER CALCULATIONS

S. RADICALS
RADIATION EFFECTS
ELECTRON SPIN RESONANCE
MOLECULAR ORBITAL METHOD
ORGANIC COMPOUNDS
DATA

T. CROWDIONS
RADIATION EFFECTS
ELECTRONS
GOLD BASE ALLOYS
SILVER ALLOYS

U. QUASI-ELASTIC SCATTERING
NEUTRONS
HYDROGEN
NIOBIUM
MONOCRYSTALS

V. PLASTICITY
DEFORMATION
COLOR CENTERS
POTASSIUM CHLORIDES
POTASSIUM BROMIDES
SODIUM CHLORIDES
LITHIUM FLUORIDES

W. FISSION NEUTRONS
CORRELATIONS
SAFEGUARDS
DATA PROCESSING
INSPECTION

X. RESOLUTION
FOCUSING
NEUTRON SPECTROMETERS
QUASI-ELASTIC SCATTERING
NEUTRON BEAMS
PLANNING
PERFORMANCE

Y. VOID COEFFICIENT
DATA
REACTOR LATTICES
URANIUM DIOXIDE
FUEL ELEMENTS
HEAVY WATER

Z. EXPLOSIONS
CONTAINMENT SHELLS
FAST REACTORS
EXCURSIONS
CRITICALITY

1. MATERIALS TESTING
TRANSIENTS
DEFORMATION
STRAINS
STRESSES
EQUATIONS OF STATE
ZIRCONIUM ALLOYS
RUPTURES
EXPLOSIONS
REINFORCED CONCRETE
MEASURING METHODS

2. CONTROL ELEMENTS
LIQUIDS

3. FUEL ELEMENTS
THERMAL ANALYSIS

4. SODIUM
BOILING
SUPERHEATING
NUCLEATION

5. COATED FUEL PARTICLES
FLUIDIZED BED

6. HTGR TYPE REACTORS
THERMAL INSULATION

7. ION IMPLANTATION
HEAVY IONS
ACCELERATORS

8. RADIATION EFFECTS
URANIUM DIOXIDE
BURNABLE POISONS
GADOLINIUM OXIDES

9. COMPOSITE MATERIALS
EUTECTICS
SOLIDIFICATION
MECHANICAL PROPERTIES

10. SEALS
CONTROL
FISSILE MATERIALS

11. HYDROGEN
PRODUCTION
WATER
PROCESS HEAT REACTORS
CHEMICAL REACTIONS

12. CESIUM
SILICON CARBIDES
DIFFUSION
DATA

13. RADIATION EFFECTS
VISCOSITY
SUSPENSIONS
WATER
THORIUM OXIDES
URANIUM OXIDES

14. HEAT PIPES
HEAT TRANSFER
CORROSION

15. GRAPHITE
CERAMICS
CORROSION
RADIATION EFFECTS

16. RADIATION CHEMISTRY
CHEMICAL ANALYSIS
COMPUTERS
DATA ACQUISITION

17. RADIATION EFFECTS
FUEL ELEMENTS
SELNI REACTOR
DATA

18. WATER
CHEMICAL ANALYSIS
NUCLEAR POWER PLANTS

19. FAST REACTORS
SPENT FUEL ELEMENTS
CHEMICAL DECLADDING
HEAD END PROCESSES

20. MERCURY
MONITORING
MEASURING INSTRUMENTS

21. X-RAY DIFFRACTION
MEASURING METHODS

22. TRACE AMOUNTS
OXYGEN
ORGANIC COOLANTS
MEASURING METHODS

23. PHOTOMETERS
FLAMES
PLANNING

24. THIN-LAYER CHROMATOGRAPHY

25. PULSES
POLAROGRAPHY
VOLTAMETRY

26. AFLATOXIN
THIAMINE
DRUGS
BIO ASSAY
BIOCHEMICAL REACTIONS KINETICS
ENZYMES
AUTOMATION
DNA
BLOOD SERUM
ALBUMINS
BIOCHEMICAL ACTIVITY
BIOSYNTHESIS
INHIBITION
QUANTITY RATIO
RATS
LIVER
TOXINS
LABELLED COMPOUNDS
CARBON 14
TRITIUM COMPOUNDS
TRACER TECHNIQUES
QUALITATIVE CHEMICAL ANALYSIS
QUANTITATIVE CHEMICAL ANALYSIS
STRUCTURAL CHEMICAL ANALYSIS
MICROSOMES
METABOLISM
HEXYL RADICALS
BARBITURATES
BENZOPYRENE
AMINES
PYRIDINES
CYTOCHROMES

27. POLLUTION
CONTAMINATION
RADIOACTIVITY
RADIOECOLOGICAL CONCENTRATION
ENVIRONMENT
WATER
AIR
AQUATIC ECOSYSTEMS
TERRESTRIAL ECOSYSTEMS
HAZARDS
MAN
ANIMALS
PLANTS
SOILS
BEHAVIOUR
CESIUM ISOTOPES
CESIUM COMPOUNDS
LEAVES
ROOTS
SEEDS

28. FAST NEUTRONS
NEUTRON SOURCES
NEUTRON BEAMS
ENERGY SPECTRA
ENERGY LOSSES
BIOLOGY
TISSUES
MONTE CARLO METHOD
MEASURING METHODS
MEASURING INSTRUMENTS
MOCKUP
PHANTOMS
COMPUTER CALCULATIONS

EUR 4842 e

JOINT RESEARCH CENTRE — ISPRA ESTABLISHMENT — ANNUAL REPORT 1971

Commission of the European Communities
Joint Nuclear Research Centre - Ispra Establishment (Italy)
Luxembourg, October 1972 - 388 Pages - 147 Figures - B.Fr. 500.—

This report is a comprehensive review of the work carried out during 1971 in the Ispra establishment of the Joint Research Centre. The first part is devoted to a description of the activity carried-out in the frame of the so-called "objectives" of the 1971 research programme. In the second part are described, from the viewpoint of the Scientific Divisions of the Centre, some of the most relevant scientific and technical achievements. In the third part the operation of the big installations is reported. The fourth part treats both the technical and administrative support activities. A bibliography of reports, contributions to conferences, seminars and meetings etc. is given at the end.

—

EUR 4842 e

JOINT RESEARCH CENTRE — ISPRA ESTABLISHMENT — ANNUAL REPORT 1971

Commission of the European Communities
Joint Nuclear Research Centre - Ispra Establishment (Italy)
Luxembourg, October 1972 - 388 Pages - 147 Figures - B.Fr. 500.—

This report is a comprehensive review of the work carried out during 1971 in the Ispra establishment of the Joint Research Centre. The first part is devoted to a description of the activity carried-out in the frame of the so-called "objectives" of the 1971 research programme. In the second part are described, from the viewpoint of the Scientific Divisions of the Centre, some of the most relevant scientific and technical achievements. In the third part the operation of the big installations is reported. The fourth part treats both the technical and administrative support activities. A bibliography of reports, contributions to conferences, seminars and meetings etc. is given at the end.

—

EUR 4842 e

JOINT RESEARCH CENTRE — ISPRA ESTABLISHMENT — ANNUAL REPORT 1971

Commission of the European Communities
Joint Nuclear Research Centre - Ispra Establishment (Italy)
Luxembourg, October 1972 - 388 Pages - 147 Figures - B.Fr. 500.—

This report is a comprehensive review of the work carried out during 1971 in the Ispra establishment of the Joint Research Centre. The first part is devoted to a description of the activity carried-out in the frame of the so-called "objectives" of the 1971 research programme. In the second part are described, from the viewpoint of the Scientific Divisions of the Centre, some of the most relevant scientific and technical achievements. In the third part the operation of the big installations is reported. The fourth part treats both the technical and administrative support activities. A bibliography of reports, contributions to conferences, seminars and meetings etc. is given at the end.

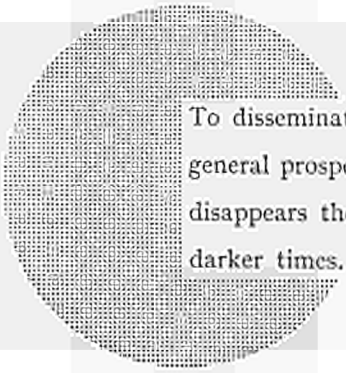

To disseminate knowledge is to disseminate prosperity — I mean general prosperity and not individual riches — and with prosperity disappears the greater part of the evil which is our heritage from darker times.

Alfred Nobel

SALES OFFICES

The Office for Official Publications sells all documents published by the Commission of the European Communities at the addresses listed below, at the price given on cover. When ordering, specify clearly the exact reference and the title of the document.

GREAT BRITAIN AND THE COMMONWEALTH

H.M. Stationery Office
P.O. Box 569
London S.E. 1

UNITED STATES OF AMERICA

European Community Information Service
2100 M Street, N.W.
Suite 707
Washington, D.C. 20 037

BELGIUM

Moniteur belge — Belgisch Staatsblad
Rue de Louvain 40-42 — Leuvenseweg 40-42
1000 Bruxelles — 1000 Brussel — Tel. 12 00 26
CCP 50-80 — Postgiro 50-80

Agency :
Librairie européenne — Europese Boekhandel
Rue de la Loi 244 — Wetstraat 244
1040 Bruxelles — 1040 Brussel

GRAND DUCHY OF LUXEMBOURG

Office for official publications
of the European Communities
Case postale 1003 — Luxembourg 1
and 29, rue Aldringen, Library
Tel. 4 79 41 — CCP 191-90
Compte courant bancaire : BIL 8-109/6003/200

FRANCE

Service de vente en France des publications
des Communautés européennes
26, rue Desaix
75 Paris-15e — Tel. (1) 306.5100
CCP Paris 23-96

GERMANY (FR)

Verlag Bundesanzeiger
5 Köln 1 — Postfach 108 006
Tel. (0221) 21 03 48
Telex ; Anzeiger Bonn 08 882 595
Postscheckkonto 834 00 Köln

ITALY

Libreria dello Stato
Piazza G. Verdi 10
00198 Roma — Tel. (6) 85 09
CCP 1/2640

Agencies :
00187 Roma — Via del Tritone 61/A e 61/B
00187 Roma — Via XX Settembre (Palazzo Ministero delle finanze)
20121 Milano — Galleria Vittorio Emanuele 3
80121 Napoli — Via Chiaia 5
50129 Firenze — Via Cavour 46/R
16121 Genova — Via XII Ottobre 172
40125 Bologna — Strada Maggiore 23/A

NETHERLANDS

Staatsdrukkerij- en uitgeverijbedrijf
Christoffel Plantijnstraat
's-Gravenhage — Tel. (070) 81 45 11
Giro 425 300

IRELAND

Stationery Office
Beggar's Bush
Dublin 4

SWITZERLAND

Librairie Payot
6, rue Grenus
1211 Genève
CCP 12-236 Genève

SWEDEN

Librairie C.E. Fritze
2, Fredsgatan
Stockholm 16
Post Giro 193, Bank Giro 73/4015

SPAIN

Libreria Mundi-Prensa
Castello, 37
Madrid 1

OTHER COUNTRIES

Sales Office for official publications
of the European Communities
Case postale 1003 — Luxembourg 1
Tel. 4 79 41 — CCP 191-90
Compte courant bancaire : BIL 8-109/6003/200

OFFICE FOR OFFICIAL PUBLICATIONS OF THE EUROPEAN COMMUNITIES
Case postale 1003 — Luxembourg 1 5903

CDNA04842ENC